Copy Number Two

A Thesis Entitled

# THE TRANSMISSION AND RADIATION CHARACTERISTICS OF VIBRATING PLATES

By

PETER A. FRYER B.Sc. D.I.C.

Submitted for the Degree of

DOCTOR OF PHILOSOPHY

IMPERIAL COLLEGE LONDON

ACOUSTICS GROUP

March 1972

## SUMMARY

The Thesis is largely devoted to holographic techniques and their use in analysing the modal vibrations of circular gear-like plates and Loudspeakers of paper and 'sandwich' construction. Using a small reverberation room measurements leading to the sound power output could be taken practically 'simultaneously' with a scanned hologram of each plate mode in turn. These measurements gave an indication of the relative radiation efficiencies of the various plate modes, and showed that not only do some radiate more strongly than others, but also that there is a transition from low to high radiation efficiency in the neighbourhood of the 'coincidence critical frequency' for the material of the plate.

The specially developed scanning techniques were used in the study of Loudspeaker cone 'break-up' leading to improved cone designs. The method of 'Single Scan III' was developed to show only those fringes due to subharmonics after these had been observed together with those of the fundamental in the fringe systems of 'Single Scan I'. The complicated fringe systems seen on Loudspeaker reconstructions were classified into distinct groupings which then pointed to ways to improve Loudspeaker cone designs - sandwich cone improvements being the most notable.

Finally, in the appendices, related topics and experiments are discussed with radiation theory being emphasised, and an attempt is made to calculate the Sound Pressure Level and the Radiation Resistance due to a circular plate in a manner analogous to existing 'coincidence' radiation theory for a rectangular plate.

GENERAL CONTENTS


| | | | |
|---|---|---|---|
| Summary | | | iiii |
| Contents | | | iv |
| SECTION | I | INTRODUCTION | 2 |
| SECTION | II | HOLOGRAPHY ITS TECHNIQUES & VARIATIONS | 11a |
| | | Contents | 11b |
| | | Introduction | 12 |
| | 1) | Holography In General | 13 |
| | 1.1) | Theory of Single Exposure Holography | 13 |
| | 1.2) | General Holographic Techniques | 15 |
| | 1.3) | Holographic Recording Media | 20 |
| | 1.4) | Techniques for maximum light utilisation | 24 |
| | 2) | The Stroboscopic Method | 29 |
| | 2.1) | Theory | 30 |
| | 2.2) | Basic Stroboscopic Method | 31 |
| | 2.3) | Live and Frozen Fringe Techniques | 35 |
| | 2.4) | Strobing Techniques | 38 |
| | 2.5) | Advantages and Disadvantages | 42 |
| | 3) | The Time Averaged Method | 43 |
| | 3.1) | Theory | 44 |
| | 3.2) | Advantages and Disadvantages | 46 |
| | 3.3) | Modifications | 47 |
| | 4) | Alterations in Sensitivity | 53 |
| | 4.1) | Increasing the Sensitivity | 54 |
| | 4.2) | Reducing the Sensitivity | 56 |

| | | | |
|---|---|---|---|
| SECTION III | | EXPERIMENTS ON CIRCULAR PLATES | 63 |
| | | Contents | 63a |
| | | Introduction | 64 |
| | 3.1) | Development of a Plate Excitor | 65 |
| | (i) | Introduction | 65 |
| | (ii) | Impulsive Excitor | 66 |
| | (iii) | Continuous Wave Exeitor | 73 |
| | 3.2) | The Reverberation Room | 74 |
| | (i) | Discussion | 74 |
| | (ii) | Reverberation Room Criteria | 75 |
| | (iii) | Reverberation Room Construction | 80 |
| | (iv) | Measurements | 82 |
| | 3.3) | Apparatus Used | 87 |
| | (i) | Overall Layout | 87 |
| | (ii) | Details of the Apparatus | 88 |
| | 3.4) | Experimental Method | 99 |
| | (i) | Stroboscopic Method | 99 |
| | (ii) | Simple Scanning Method | 102 |
| | (iv) | Upper Frequency Limit of a Disc Stroboscope | 104 |
| | (v) | Time Averaged Method | 105 |
| | 3.5) | Results and Calculations | 107 |
| | (i) | Power Level Calculations | 107 |
| | (ii)-(v) | Results Tables | 110 |
| | (vi) | Average Radiated Acoustic Power | 113 |
| | 3.6) | Conclusions | 115 |
| | | Suggestions for Further Work | 116 |

SECTION IV EXPERIMENTS WITH LOUDSPEAKERS 117

Contents 117a

Introduction 118

4.1) Holographic Methods Applied to Loudspeakers 120

(i) Live and Frozen Stroboscopic Fringes 120

(ii) Basic Scanned Holography 122

(iii) Single Scan I 123

(iv) A Phemonenon Observed with Single Scan I 123

(v) Single Scan II 126

(vi) Single Scan III 127

4.2) Theory of Scanned Holography 128

(i) Double Exposure Holograms 128

(ii) Basic Scanned Holography 129

(iii) Single Scan I 131

(iv) Single Scan II 132

(v) Single Scan III 132

(vi) Possible Explanations for 'Blanking Fringes' 133

4.3) Experimental Points 141

(i) Treatment Given to Loudspeakers 141

(ii) Vibration Isolation Speakers and Hum 142

(iii) Experimental Layout 144

(iv) Photography of the Reconstructions 144

4.4) Experimental Method 146

4.5) Typical Features in the Holograms of Loudspeakers 147

(i) Hypothetical Ideal Loudspeaker 147

(ii) Real Loudspeakers - Fringe Classifications 148

4.6) Discussion of Results - Paper Cones 152

4.7) Sandwich Bass and Treble Units 157

(i) Introduction 157

(ii) Discussion of Results 159

(iii) Relation between Modal Patterns and Radiated Sound 163

4.8) Conclusions 166

(i) Mid Range Paper Cones 166

(ii) Sandwich Units 166

(iii) General 167

4.9) Suggestions for Further Work 167

APPENDIX I OTHER METHODS OF MODE VISUALISATION 169

Contents 169a

Introduction 170

A I.1) General Methods 170

A I.2) Methods Utilising a Laser 177

(i) Speckle Patterns 178

(ii) Laser Scanning 183

APPENDIX II MODES AND RADIATION 187

Contents 187a

Introduction 188

A II.1) Modal Frequencies 188

A II.2) Excitation of Modes and Surface Displacement 195

A II.3) Radiation from a Modal Piston 202

(i) Discussion of Radiation Theory 202

(ii) Treatment of Objects to Reduce Sound Radiation 204

(iii) Theory Applied to Rectangular Plates 209

(iv) Theory Applied to Circular Plates 214

(v) Some Standard Results for Comparison 229

APPENDICES (III)(IV) & (V) 231

A III PRELIMINARY DUCT EXPERIMENTS 232

A IV FACTORS INFLUENCING GEAR NOISE 234

A V A FURTHER SCANNING PHENOMENON 238

REFERENCES 240

List of Symbols 249

Glossary 252

Acknowledgements 255

Papers Cited in support of this Thesis: Number (1) 256

Number (2) 261

Number (3) 262

Number (4) 265

Number (5) 308

Number (6) 321

Total Number of Pages: Thesis 363

Papers 94

Sections - Found on their Contents Pages.

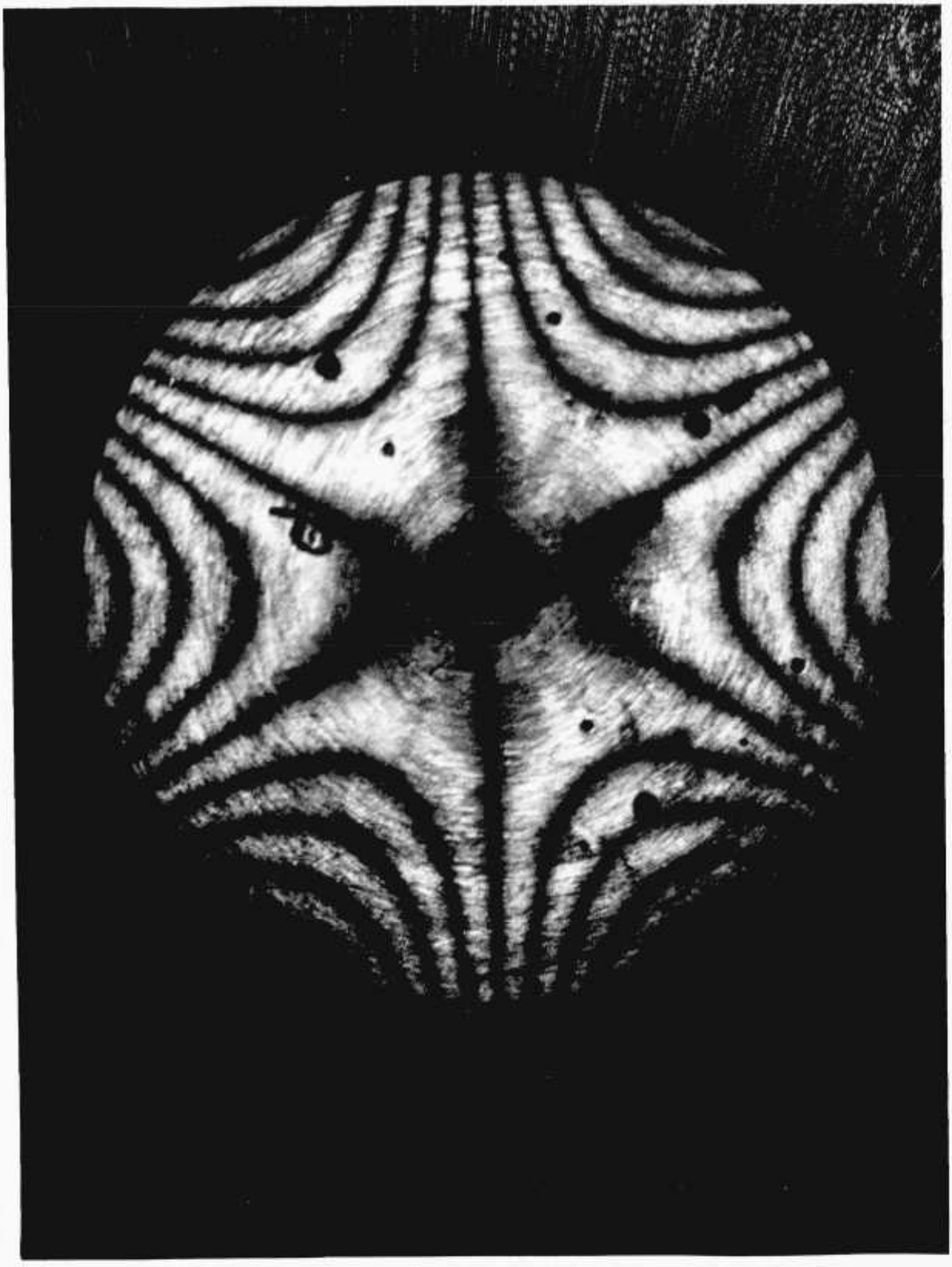
Figures 84

Plates 17

## List of Plates


| | | |
|---|---|---|
| Plate Number 1 | Stroboscopic Double Exposure Disc 1 at 1200 Hz | 1 |
| Plate Number 2 | Stroboscopic Double Exposure Disc 1 at 1200 Hz | 11c |
| Plate Number 3 | Time Average Exposure Disc 1 at 5700 Hz | 11c |
| Plate Number 3a | Illustration of 'map-like' nature of fringes | 31a |
| Plate Number 4 | Stroboscopic Double Exposure Disc 1 at 3380 Hz | 63c |
| Plate Number 5 | Time Average Exposure Disc 1 at 1200 Hz | 106b |
| Plate Number 6 | Time Average Exposure Disc 1 at 5700 Hz | 106c |
| Plate Number 7 | Stroboscopic Double Exposure Disc 1 at 2050 Hz | 106d |
| Plate Number 8 | Scanned Hologram Speaker 1 at 2.2 KHz (max.ampl.) | 117c |
| Plate Number 9 | Scanned Hologram Blanking Fringes-phase 1 | 124b |
| Plate Number 10 | Scanned Hologram Blanking Fringes-phase 2 | 124b |
| Plate Number 11 | Time Average. Sandwich Bass with Stiffeners.5.4 K | 158a |
| Plate Number 12 | Time Average. Sandwich Bass at 5 KHz | 158a |
| Plate Number 13 | Time Average. Sandwich Bass at 3 KHz | 158b |
| Plate Number 14 | Time Average. Sandwich Bass at 1.3 KHz | 158b |
| Plate Number 15 | Time Average. Sandwich Treble at 15 KHz | 162a |
| Plate Number 16 | Time Average. Sandwich Treble at 10 KHz | 162a |
| Plate Number 17 | Time Average. Sandwich Treble at KHz | 162b |
| Plate Number 18 | Time Average. Sandwich Treble at 12.5 KHz | 162b |
| Plate Number 19 | Stroboscopic Double Exposure Disc 1 at 2050 Hz | 239a |
| Plate Number 20 | Stroboscopic Double Exposure Disc 1 at 2050 Hz | 239a |
| Plate Number 21 | Apparatus for Loudspeaker Study | 249 |
| Plate Number 22 | Scanned Hologram Disc 1 at 3180 Hz | 249 |

Plate Number One



Stroboscopic Double-Exposed Hologram. Plate (1) at 1200 Hz

2

## SECTION ONE

## INTRODUCTION

## INTRODUCTION

The first section of the work described in this thesis was sponsored by the Admiralty as part of their gear wheel noise programme. The second part was sponsored by Rank Leak Wharfedale as a research project into Loudspeaker 'break-up' phenomena. Experimental techniques developed during the gear wheel study were then applied to the study of Loudspeakers. The essential aim of the first part of the work was to find out the basic sources of noise in the operation of gear wheels and thence to help prevent this noise generation. A large amount of work has already been carried out on the various parameters affecting the generation and propagation of gear wheel noise and the methods whereby the noise may be reduced are well known - the most obvious being to increase the accuracy of manufacture and alignment of the wheels, some of the others are tabulated in appendix ( IV ).

The gear noise chain is as follows: excitation - propagation and standing waves in the gearing and associated panels - radiation. The phenomenon can be studied at any of these stages and the main object of the first part of the work was to study stage two with particular reference to standing waves modes and radiation from gear-like plates. A measure of the power radiated was gained with the aid of a small reverberation room in which the experiments were conducted, and the vibration modes were made visible using the specially developed technique of scanned holography.

The actual mechinism whereby the noise is initially excited is not fully understood but there are many contributary factors. Assuming that all the errors of manufacturs and alignment have been removed we are left with several mechanisms of generation such as stick-slip, pitch-line schock, rolling and sliding friction, deformation under load leading to impact noise of mating teeth, variations of

stress during the mating cycle producing various types of waves, lubricant squirting and cavitation and many others. Any one of these could be the major cause or they could all be equally relevant. A characteristic common to many of these methods of generation is that they are impulsive in nature, especially pitch line shock and impact noise.

With so many variables it was felt desirable to simplify the system and consider one form of impulsive excitation which may model many of the other causes. Many methods of excitation were considered such as the solid carbon dioxide method but they were dismissed as they were not at all impulsive neither did they have the capability of being adapted to excite continuous tones in a controlled manner. So it was finally decided to develop a ball bouncing device based on a paper in Electronics Letters (Anon 1966). This device was also modified and used as the excitor for single mode investigations.

The physics of the dropping ball is quite well understood: coefficients of restitution, energy lost during impact and the surface waves generated are all well covered in the literature. Papers by Y.M.Tsai (1966), Tokita (1961) and Tillet (1954) to some extent cover the theory of surface waves generated by a bouncing ball and the shape of the propagated pulses, but do not deal with rapidly repeated pulses which set up standing waves in finite plates. Many papers deal with impacts on elastic half spaces (eg Tsai and Kolsky (1967)), and Tokita (1961) takes it one stage further to deal experimentally with the actual radiation from the plate. The dynamic response of plates due to moving loads which may be likened to the rolling part of gear meshing and to the contact point moving round the gear circumpherence has been discussed by Raske and Schlack (1967).

A Fourier analysis of the repeated pulses assuming that they were half sine waves was carried out. This showed that the spectrum consists of a series of equal amplitude harmonics covering the whole audio-band but tailing off at the high frequency end of the spectrum. The upper frequency limit depends on the duration of the pulse, which itself is a function of the impact velocity according to the Hertz law (1881). If one of these harmonics coincides with a plate partial (the harmonics of discs are not integer related) this will be excited more strongly.

The theory of plate modes is well covered in the literature though the gear-like plate is not so well covered. The gear can be likened to a plate supported rigidly at the center and simply supported at one point (which is variable) on its circumference. Mary Waller (1961) did a great deal of experimental work on the excitation of modes in circular plates supported at the center, and it is to be expected that those modes involving one or more nodal diameters will be preferentially excited in the gear-like system. Frequencies of plates supported by a ring of variable radius are tabulated by Bodine (1967) and the first few modes of thick plates are capable of reasonably accurate calculation, but thereafter calculation and experiment always seem to diverge. The mathematical treatment of plate modes is fully covered in

Having excited the plate either in an impulsive manner or at one particular frequency, ways of visualising the modes produced were then considered (Appendix I). There are many ways of investigating wave systems and standing waves in plates one of which - the holographic method - has been extended and used in these experiments on discs and later in the investigation of loudspeaker vibrations. Strain gages were rejected as they only give information about a small area of the plate (as do transducers such as crystals, electro-

static pickups and fibre-optic light beam devices) though they are useful for determining the shapes of passing pulses. The Schlieren method was rejected as was multiple beam interferometry because special plates would have had to be made. Photoelastic coatings are used extensively in engineering for the measurement of stresses. This method enables the magnitude and direction of the principal stresses to be determined at any point but there is quite a large amount of analysis involved. What is really required is information about the movement of the surface of the plate as this is what determines the sound which is radiated. The classical method as used by Chladni, Waller and other workers is the use of powders (lycopodium and 'bomb dust') to show up the nodal lines of vibrating plates. This is not the most sensitive of methods and gives no indication about the movement of large areas of the plate or of local amplitude variations so this method was rejected.

Three methods are now left: One which is too complicated to be set up - at least initially - is the laser scanning technique as described by Korpel of the Zenith Radio Corporation (1968). This utilises the deflection of the accurately parallel laser beam on reflection from the wave train or modal structure on the plate. What is seen with this method, which can be adapted for stroboscopic use, is the pattern of the wave train against the background of physical features on the plate surface. This method can be made sensitive to a few angstroms of movement of the plate.

The second method utilises the Moire fringe technique. This technique in any of its several forms can be made to show up angular variations of the plate surface. In its simplest form, as initially described by Ligtenberg (1955) and also by Nicola (1966) only one diffraction grating is used. The plate object is specularly polished

and a grating with a small hole in the middle is placed a short distance from it. A picture of the grating reflected in the object is then taken with a camera looking through the hole. The plate is then distorted and a second exposure taken. Moiré fringes then occur between the two exposures giving a measure of the point by point distortion of the plate. The method is most useful when the light for the second exposure is strobed at the same rate or frequency as the vibrating plate. For single frequency excitation this enables the deflection of any part of the plate at any point in the cycle to be derived with a sensitivity depending on the pitch of the grating and its distance from the plate. The moire fringes in fact depict lines of constant surface slope. There are many papers describing refinements to the basic technique notably by P.S. Theocaris in a book (1969) and very many journals. Moire fringes are also combined with holography when two sets of contour fringes taken during different object states will produce moire fringes. There are good papers describing the theory of the formation of the fringes themselves notably Oster et al (1964). The most adaptable, relevant and easily applicable method, however, is the method of Stroboscopic Holographic Interferometry.

The method utilises coherent light from a laser and enables a three dimensional image of the undistorted object to be produced. On looking through the resulting photographic plate (the hologram) illuminated with laser light an image of the object localised at the object is seen. If the plate is then vibrated or distorted, interference fringes are then seen between the altered object and its unaltered image.

The basic holographic system is as follows. A beam of coherent light is split into two separate beams, one of which is diverged and shone directly onto the photographic plate - this is

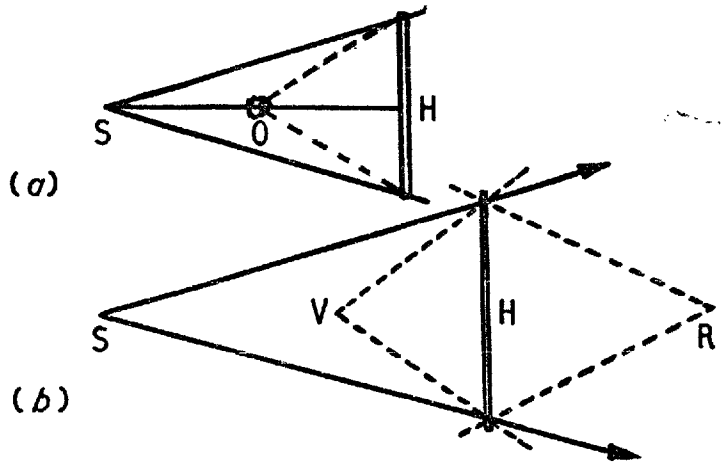



Figure (1) Gabor's original transmission system

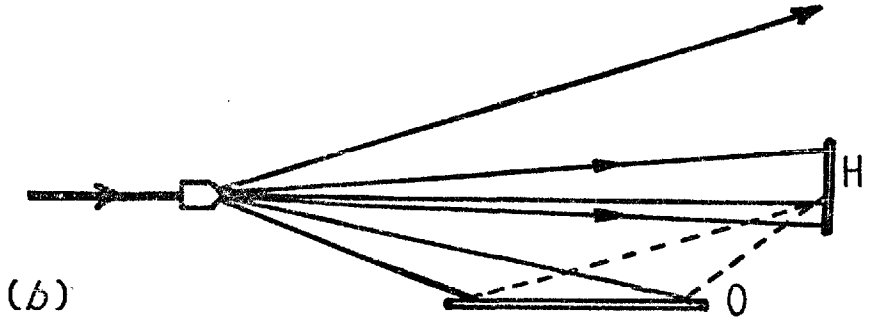



Figure (2) Simplest possible reflection system

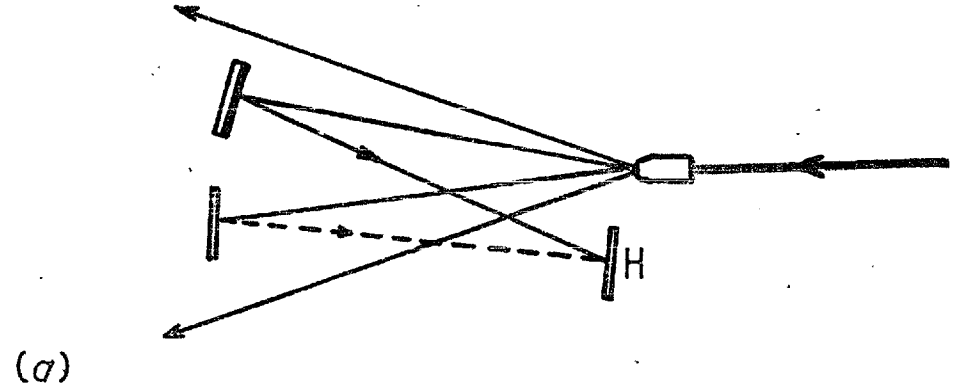



Figure (2) Simple reflection system

the reference beam and effectively acts as a carrier onto which the signal information is modulated. It places the signal with its phase information intact on the correct part of the transmittance-exposure curve for the photographic plate. The other beam is also diverged and shone onto the object plate which should not be specularly reflecting but preferably coated with something similar to 'Scotch-Lite'. The light reflected from the object - the signal - falls on the photographic plate together with the reference beam, where the fine interference pattern caused by the interaction between the two beams is recorded in the plane of the photographic emulsion. When the laser beam is diverged and shone onto the developed plate the emulsion acts as a complicated diffraction grating causing two images of the original object to be reconstructed - a virtual image located on the object (if the photographic plate is accurately located in the original position and the reference beam is used for reconstruction) - and a real image hanging in space in front of the hologram. If the object plate was vibrating at the time of the exposure, fringes are seen on the reconstruction which not only give information about the nodes of the vibration, but also give information about the amount of movement of each part of the object plate. These fringes are known as 'time averaged' or 'Powell and Stetson' fringes (1965).

When using the stroboscopic technique a hologram is first taken of the stationary object and after developement is returned exactly to its former position. Interference then occurs between the light coming from the actual object and that coming from the virtual image. If the illuminating light is stroboscopically interrupted at the same frequency as the vibrating object, fringes are now seen which map relative object movement in steps of half the wavelength of light used. The stroboscopic technique has several advantages over the basic time averaged technique which are fully described in Section II.

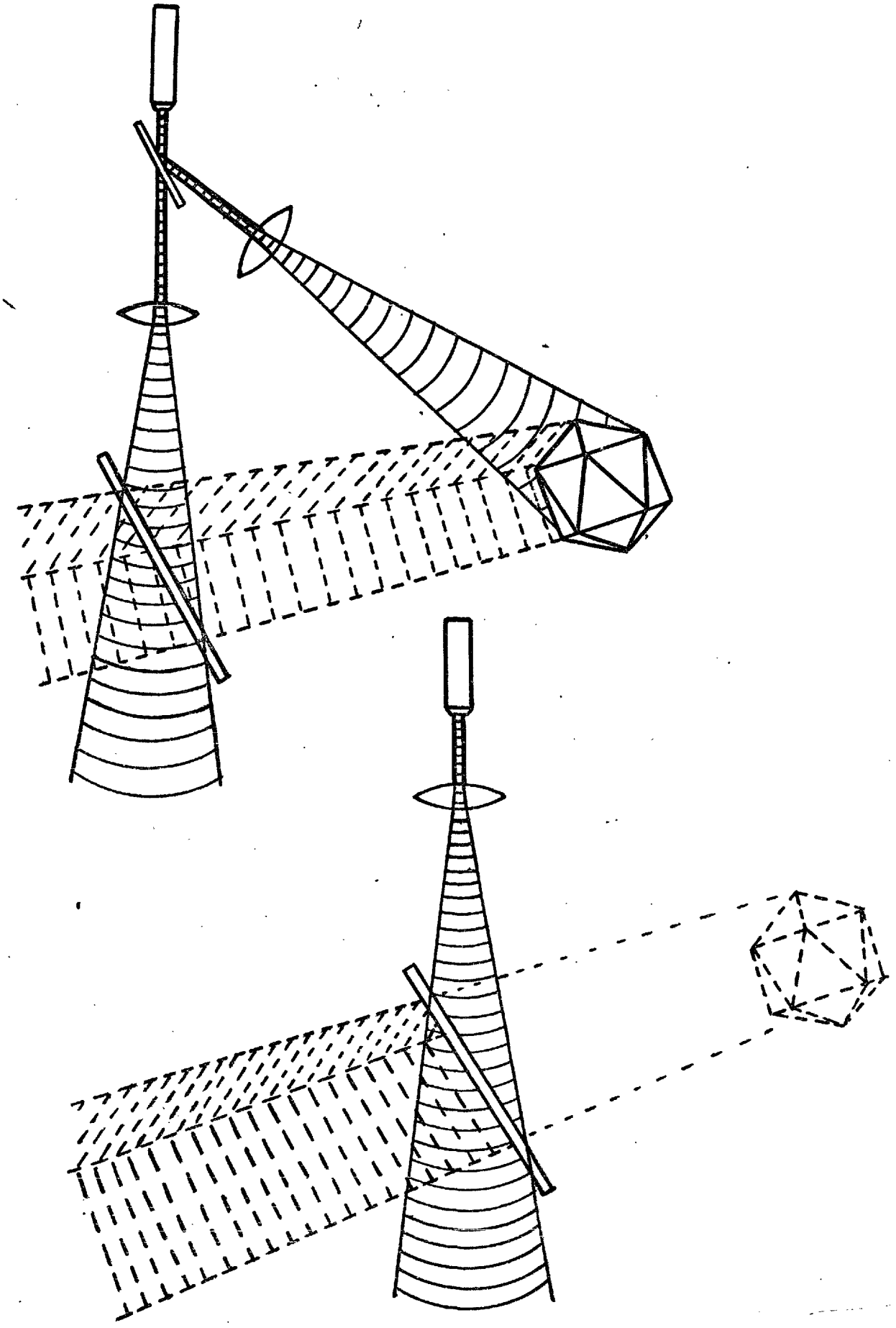


Figure 2a Simple System showing recording and reconstruction

A further extension of the stroboscopic technique has been developed by the author which has several advantages over the more commonly used technique. This system removes the need for a live hologram to set the phase for the stroboscopic exposure because it can store fringe systems corresponding to all phases of the object vibration on one hologram. The fringes corresponding to the desired object phase can be seen by moving the eye along the hologram until the desired section is reached. This experimentally simple and more convenient method still requires two exposures on the one photographic plate, so the technique was developed further to enable both exposures of the stroboscopic method to be taken 'simultaneously' in one longer exposure. This technique has an interesting side effect whereby information about subharmonics is given on the same hologram without interfering unduly with the basic fundamental frequency information. Fringes showing only the subharmonic may be produced by a simple modification of this method. These techniques and their theory are described fully in Sections III and IV.

Having developed several interesting techniques for the study of vibrations these were put to work firstly for the study of gear-like plates, and secondly for the study of paper-cone and 'sandwich' loudspeakers. The results gained have proved to be very useful to loudspeaker designers giving clear pointers to modifications which will result in better loudspeakers. The most notable result being the well behaved 'nodal' form of the break-up patterns in the sandwich type cones allowing damping materials to be placed at the antinodes and so completely remove troublesome resonances.

The studies of gear-like plates were carried out in a small reverberation room which, though falling short of the ideal, allowed rough power output figures to be gained for each of the plate modes

studied at the same time as a hologram, showing the amplitude of movement of each part of the object, was taken. These experiments showed that some modes radiated far more sound power for a given amplitude of movement than others (as would be expected from theoretical considerations involving the coincidence critical frequency, implying that damping and support conditions could be deployed most effectively in preventing these modes.

The studies of Loudspeakers were carried out under the sponsorship of Rank-Leak Wharfedale Ltd. Stiffly suspended mid-range speakers were relatively simple to investigate holographically as they were less sensitive to air currents and structure borne vibrations. In general live fringe holography was ruler out because unfortunately paper cone Loudspeakers are not intrinsically stable to the order of a few wavelengths of light, and in the time taken to develop, fix and dry the photographic plate the cone shifts in a random manner. This results in a system of fringes resembling wood grain being seen over the surface of the cone. Time averaged holograms, doubly exposed frozen fringe techniques, and especially the several systems of scanned holography enable good pictures to be taken of mid-range and treble loudspeakers (Section IV).

Bass units need not be studied holographically at low frequencies as simple stroboscopic methods using stroboflash units give a satisfactory idea of the very large movements involved. However, at high frequencies where the bass unit cones 'break-up' (i.e. all parts of the cone no longer follow the movements of the voice coil, and modal systems of vibration are set up superimposed on the ideal piston motion) the only method of investigation is that of holography.

The fundamental resonance of bass units lies close to that of the isolating bench, and furthermore the amplifier hum, though

small, has a large effect on the magnitude of the cone vibrations (since for a given electrical input voltage the cone amplitude increases fourfold for each halving of the frequency) rendering holography of these units difficult. These problems were solved however, and the interesting results about the break-up patterns of the sandwich bass unit were consequently obtained.

A brief study of radiation from modal systems was then undertaken to try to find the theoretical power output expected from discs and loudspeakers. The coincidence critical frequency ($f_c$) is the single most important parameter followed closely by the material homogeneity and isotropy for frequencies below $f_c$. Expressions for the radiation restance of square plates above and below $f_c$ were found using existing theory and an expression for the sound pressure at a distance R and also the radiation resistance of a baffled modal piston were derived. Theory also points to which treatments given to objects to remove the modal radiation are likely to be the most effective depending on wether the frequency is above or below $f_c$.

## SECTION TWO

## HOLOGRAPHY ITS TECHNIQUES AND VARIATIONS

CONTENTS - Section 2 - Holography its Techniques and Variations


| | | |
|---|---|---|
| Introduction | | 12 |
| 1) | Holography in General | 13 |
| 1.1) | Theory of Single Exposure Holography | 13 |
| 1.2) | General Holographic Techniques | 15 |
| | (i) Stability Requirements | 15 |
| | (ii) Long Objects | 16 |
| | (iii)Focussed Image Holography | 17 |
| | (iv) Scanned Reference Beam | 18 |
| | (v) Polarisation of the Reference Beam | 18 |
| | (vi) Reference Beam Strength | 18 |
| 1.3) | Holographic Recording Media | 20 |
| | (i) Theory of Recording Media | 20 |
| | (ii) Dichromated Gelatin | 21 |
| | (iii)Thermoplastics | 22 |
| | (iv) Lithium Niobate | 22 |
| | (v) Ferroelectric | 22 |
| | (vi) Photoelectrochemical | 23 |
| | (vii)Magnetic | 23 |
| | (viii) Others (new materials are used every month !) | 24 |
| 1.4) | Techniques for Maximum Light Utilisation | 24 |
| | (i) Choice of Materials | 24 |
| | (ii) Object Treatment | 27 |
| 2) | The Stroboscopic Method | 29 |
| 2.1) | Theory | 30 |
| 2.2) | Basic Stroboscopic Method | 31 |
| 2.3) | Live and Frozen Fringe Techniques | 35 |
| 2.4) | Strobing Techniques | 38 |
| | (a) Laser Emitting Pulses | 38 |
| | (i) Q Switched | 38 |
| | (ii) C.W. Switching | 39 |
| | (b) Interupting the Laser Light | 40 |
| | (i) Pockles Cell | 40 |
| | (ii) Bragg Cell | 40 |
| | (iii) Strobe Disc (N.P.L.) | 41 |
| | (iv) Strobe Disc (Synchronous Motor) | 42 |
| 2.5,6) | Advantages and Disadvantages of the Stroboscopic Method | 42 |
| 3) | The Time Averaged Method | 43 |
| 3.1) | Theory | 44 |

3.2) Advantages and Disadvantages of the Time Averaged Method 46

(i) Advantages 46
(ii) Disadvantages 46

3.3) Modifications to the Basic Method 47

(i) Phase Modulated Reference Beam 48
(ii) Combination Modes 49
(iii) Subfringe Technique 51
(iv) Large Amplitude Phase Modulation 51
(v) 180° phase shift of Reference Beam 52

4) Alterations in Sensitivity 53

4.1) Increasing the Sensitivity 54

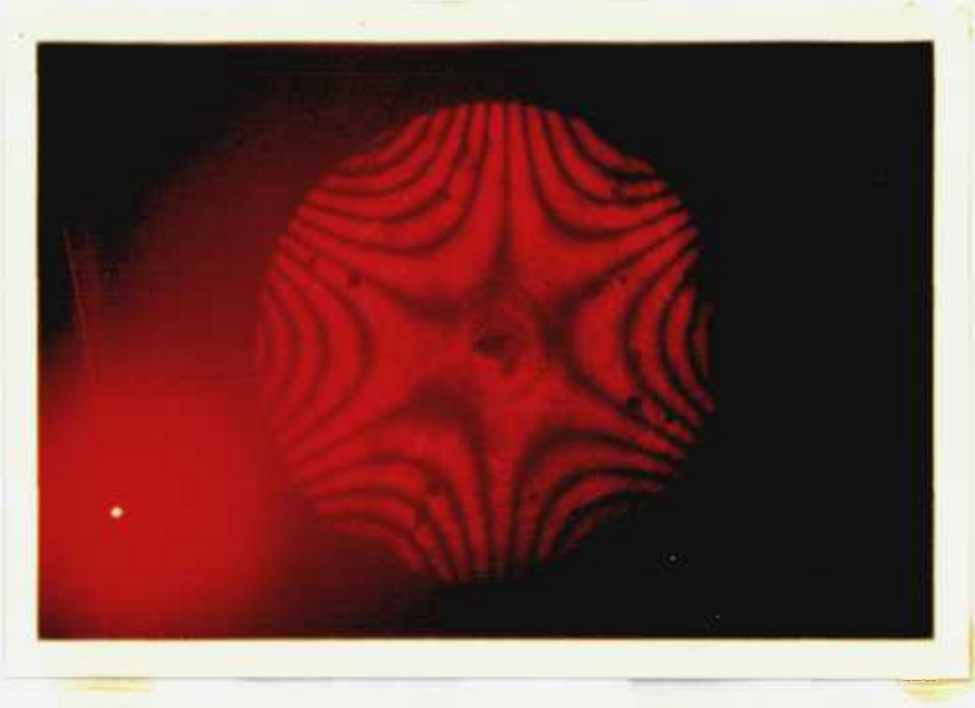
(i) Subfringe Technique 54
(ii) Temporally modulated Holography 55
(iii) Ultra Violet Holography 56
(iv) Use of Multiple Beams 56

4.2) Reducing the Sensitivity 56

(i) Temporally Modulated Holography 56
(ii) Oblique Illumination and View 57
(iii) Non Holography 58
(iv) Moire Techniques - to (viii) 58


Total Number of Pages : 69

Plate Number 2



Stroboscopic Frozen Fringe Hologram, 1200 Hz

Plate Number 3



Time Averaged Hologram, Plate (1) , 5700 Hz

## HOLOGRAPHY ITS TECHNIQUES AND VARIATIONS

### Introduction

The chief advantages of holography for vibration analysis are its simplicity, sensitivity, and the possibility of viewing, and measuring with high accuracy, how the whole surface of the object is vibrating. This may be carried out in real time, using live fringes, or at leisure, utilising cine films or frozen fringe holograms either simple or scanned. Holography can be used, in general, without special object treatments such as polishing, coating or the making of models, but some object surface treatments will facilitate the process. Measurements can be carried out in the field, especially where pulsed lasers are used, and the technique does not affect the vibrations or movements being observed. It may also be carried out remotely - even with distorting media between the apparatus and the object - this is an important consideration in some applications and industrial situations. The sensitivity of the basic technique is however, too high for many industrial situations - even after it has been reduced using one of the methods described below, but the sensitivity is approximately correct for the plates and speakers investigated in the present experiments using unmodified holography. Although holography is used in many applications, from the determination of the size of particles in sprays (Thompson and Parrent 1967), through the deblurring of photographs (Stroke and Halioua 1970) to the measurement of the growth of cacti over 20 minute periods, the greatest potential use is, however, likely to be in the field of vibration detection and measurement.

Many workers have contributed ideas to the practice of basic holography, the time averaged method and the stroboscopic method, and this section will cover some of the useful developments and related topics in four main parts. Part 1 deals with holography in general with

particular reference to techniques for maximum light utilisation, some of which were developed for, and used in, the present experiments; materials other than the basic silver emulsion which can be used as holographic recording media are also described. Part 2 deals exclusively with stroboscopic holography, its theory, practice and some variations in the basic technique pointing out particularly the scanning method and comparing it with other variations of the basic technique. Part 3 covers time averaged holography in similar detail pointing out some of the ingenious modifications to the basic method which have been devised to counter its weaknesses. Finally Part 4 describes some techniques for altering the basic sensitivity of the two methods which will be useful in extending the frequency range of plate and speaker investigations since the main limitations are lack of sensitivity at high frequencies andtoo much sensitivity at low frequencies.

## 1) Holography In General

### 1.1) Theory of Single Exposure Holography

Photographic plates are sensitive only to intensity, i.e. to the square of the amplitude of the light waves, so that ordinarily phase information is lost. Gabor et al (1965) have shown that not only amplitude but also phase information about the light wave must be recorded if a three dimensional image is to be reconstructed. The emulsion may be made to record phase as well as amplitude information by shining onto it another beam, called the reference beam, together with the object beam. Both beams are usually derived from the same laser.

The two beams interfere and the resulting interference pattern is effectively a complicated diffraction grating or (Ferrier 1969 , Rogers 1950) a collection of zone plates. When either of the two beams is directed on to the developed emulsion, part of it is diffracted to

reconstruct the other beam. In practice the reference beam is usually more intense than the object beam to ensure that it is linearly reconstructed. Mathematically the recording process may be expressed as follows:

The intensity I of the light source may be expressed as the amplitude 'a' times its complex conjugate a*, i.e.

$$I = aa^* \quad (\text{also } I = |a|^2) \tag{1.1}$$

If r denotes the reference amplitude and o denotes the object beam amplitude, then the intensity at the holographic plate is

$$I_p = (r + o)(r^* + o^*) \tag{1.2}$$

$$= rr^* + oo^* + or^* + ro^* \tag{1.3}$$

Now oo* and rr* are the object ($I_o$) and the reference ($I_r$) beam intensities respectively. Hence (1.3) may be written as

$$I_p = I_r + I_o + or^* + ro^* \tag{1.4}$$

But $r = r\exp(i\phi) = r(\cos\phi_r + i\sin\phi_r)$

and $r^* = r\exp(-i\phi) = r(\cos\phi_r + i\sin\phi_r)$ (1.5)

Thus (1.4) may also be written as

$$I_p = I_r + I_o + 2or\cos(\phi_o - \phi_r) \tag{1.6}$$

Again if the reference beam of amplitude r illuminates the developed plate, then the transmitted ~~intensity~~ AMPLITUDE is

$$T = rI_p = rI_r + rI_o + rro^* + rr^*o \tag{1.7}$$

$$= rI_r + rI_o + rro^* + I_ro \tag{1.8}$$

The term $I_ro$ is the reference intensity modulated by the object amplitude and this is identical to the original object wavefront. For a collimated reference beam, the term rro* represents the real conjugate - pseudoscopic image which is in focus at the same distance in front of the hologram as the object and virtual image are behind it. The theory of double exposed holograms will be developed in Part 2 from this basis, and that of time averaged holography in Part 3 while that of single scan systems will be found in Section IV.

## 1.2)General Holographic Techniques

The practical aspects of holography are well known (Lehman 1968 Rogers 1966) but one or two techniques will be outlined below which have been used in the present experiments or which have been useful to bear in mind when conducting the experiments.

The simplest possible optical layout is shown in fig ( 2 ) where one beam-expanding lens provides both the object illumination and the reference beam. Each worker in the field of holography has his own variations on the same theme. Fryer (1970) has an arrangement shown in fig ( 3 ) which has a minimum of components in the object beam path and the strength of the reference beam is altered by means of a simple 'zoom lens' system.

When taking reflection holograms, and not using a pulsed laser, if the beam splitter, object and reference beam lenses, hologram and stationary parts of the object are not maintained relative to one another to within 1/8 of a wavelength of light, then extraneous fringes or time average effects will result. It is to be noted that the laser itself need not be included in the stable part of the system, a fact which was used in the experiments on loudspeakers Section IV. The desired stability may be achieved by mounting the components on a rigid massive worktable which is isolated from floor borne vibrations by a suitable set of mounts. Commercially available components do the job expensively, and a concrete slab on rubber does the job effectively and cheaply.

The object and reference beam path lengths should not differ by more than the coherence length of the laser which in most simple helium-neon lasers is roughly equal to the length of the laser and possibly with recurring coherence at multiples of twice the length of the laser (Rose and Pruet 1967). The coherence length may be extended by placing a Fabry-Perot etalon within the laser cavity or by using

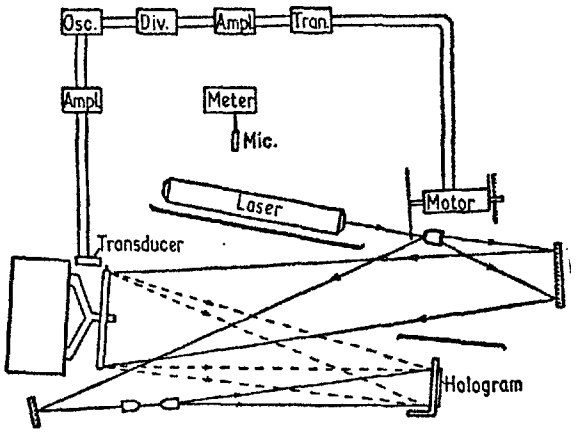



Figure 3 A practical holographic system (after Fryer 1970 a).

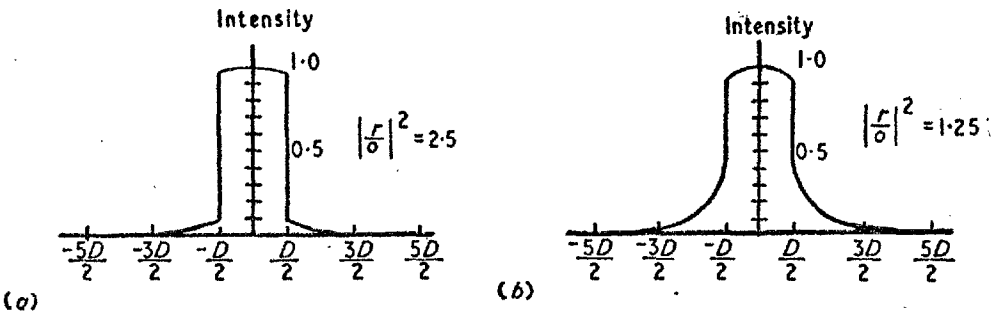



Figure 5. Image blur for two difference reference-object beam ratios (after Goodman and Knight 1968).

various mode locking techniques (Bradley 1970). Wherever possible the temperature of the system should be maintained within fairly close tolerances if any prolonged work is to be done, this is because fringes may occur as a result of differential expansions in the system. Hot air currents may also cause fringe blurring.

ii When very long objects must be analysed, the limited coherence length of lasers that may be available, or the effective coherence length of a ruby laser giving a short pulse (see page 39 ), necessitates the use of a device described by Lyman Orr (1968) and by Abramson (1968 and 1969) who calls it 'the Holodiagram' fig ( 4 ).

The laser and photographic plate are placed at the foci of a system of ellipses. If a point object and a mirror are placed anywhere on one of these ellipses ( both reflecting light onto the hologram) the path difference between the two beams is zero. If we now consider two of the ellipses and arrange for the distance between them to equal the coherence length of the laser, the diagram will aid in finding the best position for a long object. If the object can be manoevred so that it lies between these two ellipses the whole length of it will be recorded on the hologram.

If the object is too long to allow this technique to be used, many object beam splitters may be used to illuminate different parts of the object (Melroy 1967), the path differences to each part of the object being then arranged separately to be within the coherence length of the laser. The object plates used in the first part of the work are sufficiently shallow not to warrent the use of these techniques, but assemblies of speakers and large speaker cabinet studies may cause their use in future experiments.

The holodiagram also has another application when double exposure techniques (dealt with more fully in Part 4) are adopted. as

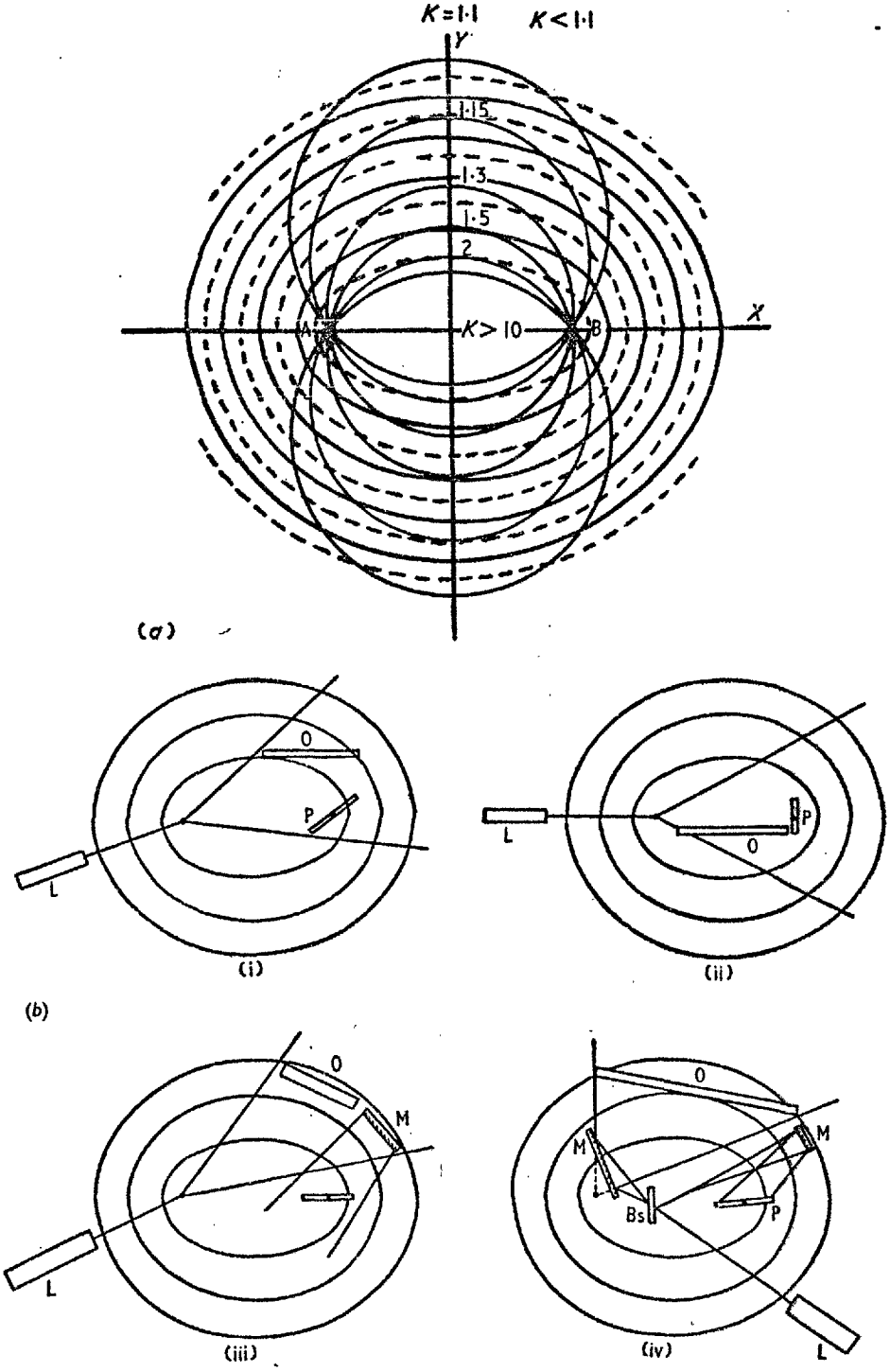



Figure 4 (*a*) The holodiagram (after Abramson 1970). (*b*) Some ways in which the holodiagram facilitates choosing a holographic layout (after Abramson 1970): (i) no mirror for reference beam, (ii) one position for a long object, (iii) hologram with mirror for reference beam, (iv) using a beam splitter and two mirrors. L, laser; O, object; P, photographic plate; M, mirror; Bs, beam splitter.

it may be used to help determine the amount of movement that each fringe appearing on the object represents. Briefly, the system of ellipses is drawn so that they are separated by half a wavelength of light where they intersect the line joining the foci. When a point object is moved normal to the ellipses, each time one is crossed a complete cycle of light intensity variation occurs at the hologram. The greatest number of cycles, i.e. fringes, for a given object movement occurs along the line joining the foci and to the right side of the hologram, the minimum number occurs when the movement is normal to this line at the center of the diaphragm.

(iii) When taking large numbers of holograms it may prove useful to be able to see at a glance, using white light, which holograms have useful information in them. The technique of 'image holography' allows this to be accomplished and involves an image of the object being formed on the photographic plate with the reference beam added in the usual way. The resulting hologram (of the image) will be capable of reconstruction by white light. If a double exposed hologram is made in this way, the resulting image will still keep its interferometric properties, and fringes will be seen on the reconstruction. The image may be formed only on part of the photographic plate, leaving the rest for normal holographic use, and the white light reconstruction may be used for selection purposes.

It must be remembered that the hologram records the whole of the light falling onto it. This light may be a focussed image together with unfocussed images before and behind it. Reconstruction with coherent light will allow the images before and after the hologram to be seen on looking through it, but when white light is used only the image in focus in the hologram plane is seen. A similar technique has been used in holographic microscopy to study the out of focus parts of the specimen as well as those parts situated in the focal plane. The technique has also been described by Welford (1966), Butters and

Denby (conference on Photography in Engineering 1969) and also by many other workers.

(iv) When it is not possible to use either a pulsed laser or an isolated worktable, the vibrational stability requirements of the system may be reduced by a 'scanned reference beam' holographic system described by Palais and Wise (Optical Society of America Spring Meeting 1970). The reference beam is increased in intensity, reduced to spot size and used to scan the hologram during the exposure. Extreme stability must be maintained only for the time needed for the reference beam to illuminate an area of hologram equal to its own spot size. The stability-time reduction is equal to the ratio of the area of the hologram to the area of the reference beam spot. Unreferenced light from the object will serve to increase the 'DC' level of the exposure as described above page ( 25 ) and the reduction of contrast caused by this may be troublesome.

(v) By polarising the reference beam at $90^{o}$ with respect to the original object beam, specualr reflection may be removed from the reconstruction as only diffusely reflected light will be recorded by the hologram. This technique (Rudder 1967) may be useful, for instance, for removing highlights on shiny white objects, or for allowing detail that would otherwise be swamped to be seen on almost perfectly reflecting objects. Rose et al (1970) have pointed out that the reconstruction brightness itself depends on the polarisation of the fields incident on the hologram - both in recording and in reconstruction.

(vi) Finally as described by Urbach and Meier (1969) the choice of the reference beam strength is very important as has been verified in these experiments. Amplitude transmission curves are a non-linear function of the exposure for all holographic recording media see fig ( 4 ) Non-linearities produce higher order images on reconstruction, but these

are not greatly important if they do not everlap the first order images. This may be ensured, in general by a suitable optical layout. However, additional disturbance terms which propagate along the first order image direction cause first order image blurring. As in any other analogue data handling system (such as tape recording for instance) an arbitrary permissible distortion figure must be decided upon. In this case the distortion depends on the deviation from linearity of the part of the amplitude transmission curve used to carry the fringe information. This, in turn, is determined by the ratio between the object beam and the reference beam intensities. If, say, a 5 per cent deviation from linearity is decided upon, the amplitude swing of the fringes will have to be greatly restricted by increasing the reference beam strength and reducing the exposure accordingly. This reduced modulation drastically reduces the diffraction efficiency of the hologram (The percentage of light incident on the processed emulsion diffracted into the image or images see 1.3 below).

For ins tance allowing only a 5 percent deviation reduces the diffraction efficiency (D.E.) from the theoretical maximum of 33.9 percent for thin phase holograms to a mere 9 percent. Goodman and Knight (1968) have computed the amount of image blur for two different reference to object beam ratios (fig 5 ). Some fringe modulations and corresponding diffraction efficiencies and reference to object beam ratios for a silver halide emulsion are shown in the following table.

| Ref./Object beam ratio | 2.5:1 | 1.25:1 | 13:1 |
|---|---|---|---|
| Fringe Modulation | .903 | .996 | .5 |
| Diffraction Effieiency | 5.64 | 6.24 | 1.5 percent |

Ratios of around 5:1 are generally used, though for precision work when exact fringe locations relative to object features are desired, ratios of up to 13:1 are sometimes used.

## 1.3) Holographic Recording Media

Most workers use silver halide emulsions for recording holograms, bleached or unbleached, but there an increasing number of other substances that may be used - and one of these may be more suitable for a particular application. Most of them are less sensitive but may have other advantages, like the 100 percent theoretical diffraction efficiency of dichromated gelatin for instance or the reusability of thermoplastics. A selection of these substances are described below.

i Urbach and Meier (1969) have presented the theory of the various types of recording media, and give the following information about their relative diffraction efficiencies.

For 'amplitude' holograms whose fringes allow a spatially varying amplitude of light to pass through them (eg unbleached silver halide emulsion holograms), the amplitude of either reconstructed wave is equal to $CM^2$ where C is a constant and M is the fringe modulation - the percentage of the maximum transmission variation (from opaque th transparent) used to carry the fringe variations. The central more linear, region of the exposure transmission curve (dark grey to light grey) is nearly always used fig ( 4 ).

The maximum value that C can have is 0.0625, so for a fringe modulation of 100 percent the maximum D.E. is a mere 6.25 percent. Results for the other types of recording media are given in the following table.

| | Amplitude | | | Phase | | |
|---|---|---|---|---|---|---|
| | thin | thick | | thin | thick | |
| | refl.& tran. | refl. | tran. | refl.& tran. sin. | refl. & tran. blazed* | |
| Theoretical | | | | | | |
| Max D.E. percent | 6.25 | 7.2 | 3.7 | 33.9 | 100 | 100 |
| Measured D.E. .. | 4.0 | 3.8 | 3.0 | 33.0 | 73 | 95 |
| Materials | ab | ab | ab | cde | c | cf |

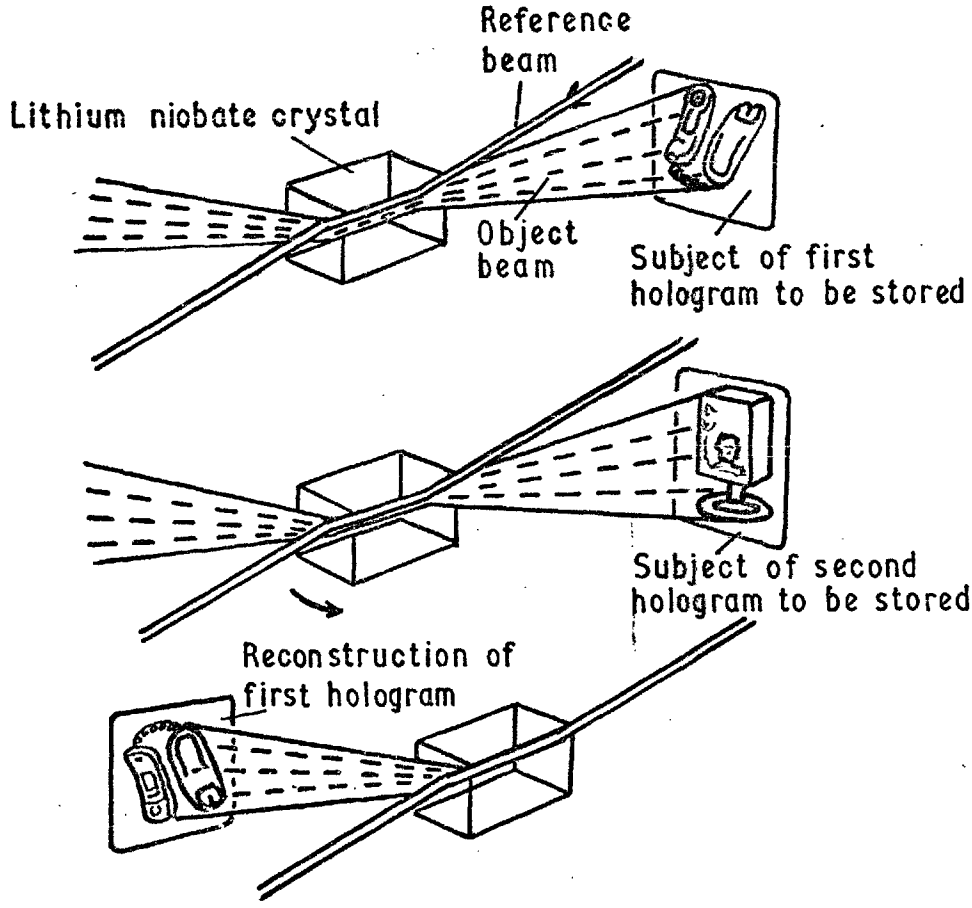



Figure 6 Use of Lithium Niobate to store up to 1000 Holograms

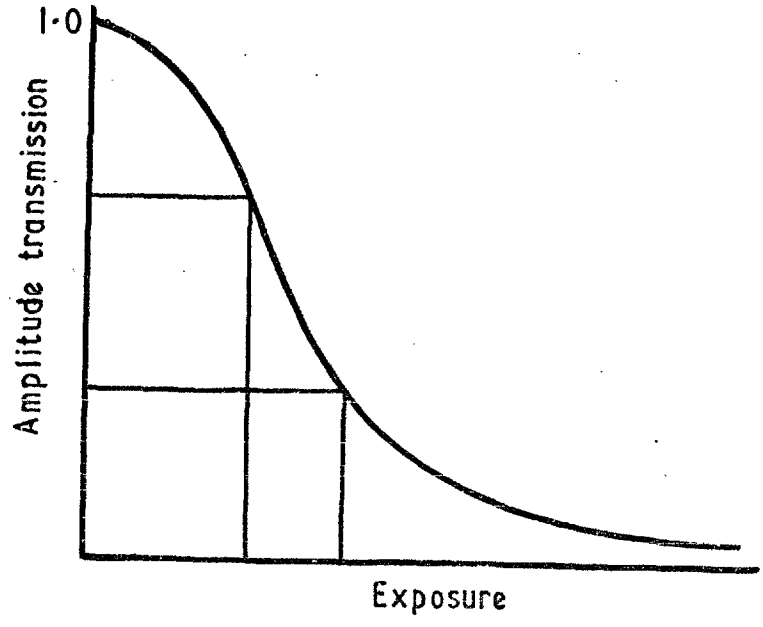



Figure 4 Transmittance exposure curve

(a) Silver halide conventional development

(b) Photochromics

(d) Thermoplastics (c) Bleached silver halides

(f) Photopolymers (e) Photoresists

* A technique whereby a 'stepped' surface is formed that directs most of the incident light into the desired order (image),Sheridon (1968).

(ii) Dichromated gelatin has a sensitivity and definition similar to Kodak 649F film but has the great advantage of a diffraction efficiency of up to 95 percent. Dichromated gelatin froms thick phase holograms which transmit effectively all the incident light, but whose fringes spatially vary the phase of the transmitted wavefront. Shankoff (1969) has suggested that variations in the thickness alter the phase in thin phase holograms. With thick phase holograms this variation also occurs but the gelatin also splits up into layers at the places where the maximum exposure occurs, and the resulting air-gelatin interfaces reflect light strongly.

Brandes, Shankoff and Francis (1969) have described the formation and development of dichromated gelatin films. A coating of an aqueous solution of gelatin of high 'bloom strength' is formed on a glass plate and is sensitised with ammonium dichromate. It is then dried and must be used within 12 hours. If it is then exposed to light the illuminated parts become hard and the parts that received insufficient exposure may be dissolved away with water or another suitable chemical solvent. This solvent is then removed with another chemical which does not affect the gelatin such as isopropanol. Shankoff et al suggest that the combination of water and isopropanol used on gelatin hardened with ammonium dichromate results in the best photographic speeds with the best signal to noise ratios, which may, in fact, be up to five times greater then 649F emulsion. Though the use of dichromated gelatin proved very attractive, ordinary silver emulsion plates were used in these experiments as they were readily available and, in fact,

easier to use.

(iii) Thermoplastics also have a sensitivity comparable to 649F plates, with the additional advantage of the possibility of erasure and re-use. A thermoplastic layer covers a photoconductor on top of a layer of transparent conductor which is in turn backed by glass. The thermoplastic is charged to a uniform potential and then exposed to the interference pattern to be recorded. Charges migrate to the exposed parts and the surface potential then varies as the interference pattern The thermoplastic is then recharged - increasing the charge in the exposed areas, and on heating by passing current through the conducting layer the plastic thickness increases in these areas (where there is a higher electric field). The thermoplastic layer, on cooling, acts as a thin phase grating which may have a D.E. as high as 33 percent. Erasure is accomplished by completely melting the thermoplastic.

(iv) Though they are relatively insensitive, lithium niobate crystals may be used to store large numbers of holograms, and up to 1000 have been stored in one crystal (Anon 1969). The crystal used is in the form of a'sugar lump' and the object and reference beams are projected onto it in the usual manner. Being a very 'thick film'it is extremely sensitive to the direction of the reference and signal beams and typically a new hologram is capable of separate storage when the crystal is rotated by a fraction of a degree. This has possible applications in high speed holography where a moving hologram of the event may be taken using a powerful pulsed laser and rotating the crystal a fraction of a degree between exposures.

(v) Ferroelectric - Photoconductor devices may also be used for recording phase holograms. (Keneman et al 1970). These devices consist of a layer of $Bi_4Ti_3O_{12}$ polished to 50$\mu$ thickness a 2$\mu$ layer of ZnSe photoconductor is evaporated onto one surface and semitransparent gold

electrodes evaporated onto both external surfaces. The fringes pattern falls onto the device and spatially modulates the conductivity of the Photoconductor. A voltage applied to the electrodes then switches the $Bi_4Ti_3O_{12}$ polarisation depending on the particular light-dark pattern incident. Sensitivity depends on the gain of the Photoconducting layer and have been measured at 10 J $mm^{-2}$, and a'phase readout'technique allows a reconstruction diffraction efficiency of .01 percent to be achieved with a resolution of 1000 lines per millimeter. There are, however, problems to be solved before this material becomes a really practical proposition for holography where its application will probably be in the field of computer memories.

(vi) Holograms may also be recorded on silicon 'n' type crystal wafers by using several different photo-electrochemical processes (Dalisa et al 1970). A surface relief pattern of up to 2,500 lines/mm can be produced, and high diffraction efficiencies of up to 25 percent can be achieved, though the sensitivity is likely to be low at present.

(vii) Magnetic recording has been used by R.C.A. (1969). This has the advantages of re-usability, high resolution (2000 lines per mm) and 10 nanosecond writing time (exposure time). A two micro-inch single crystal layer of manganese bismuth on a base of mica is used and at the point where the reference and object beams interfere additively the material is heated above the Curie point. The material, previously polarised (north poles upwards) by a strong magnetic field, has its polarity reversed in the heated regions only. The resulting magnetic fringe pattern may be used to reconstruct an image by transmitting a laser beam and using the Faraday effect or by reflecting the beam and using the Kerr effect. Erasure is accomplished by re-exposing the material to the polarising magnetic field. Sensitivity is not stated but the indications are that it is less sensitive than photographic plates.

(viii) Photopolymers may be used when rapid dry processing using ultra-violet light is desired, but their disadvantages of low sensitivity low singal to noise ratio and poor linearity, limit their usefulness (Close et al 1969). Photoresists (Sheridon 1968), Photochromics (Krik 1966) and liquid crystals (Kiemle and Wolff 1970) have all been used to record holograms but their disadvantages render them unsuitable for practical use at the present time.

1.4) Techniques For Maximum Light Utilisation

It is highly desirable in vibration analysis holography for the exposure time(s) to be as short as possible and the reconstructions to be as bright as possible. Short exposure times minimise the dimensional and vibrational stability requirements, but the techniques described below may also be used to allow much larger areas to be holographically recorded with the laser available. 'Q' switched ruby lasers (Hall, Gates and Ross 1970) giving two pulses per cycle greatly minimise the stability requirements but these may not be available on grounds of cost or limited coherence length, and in any case these techniques may be used with pulsed lasers as well as continuous wave lasers with the same advantages.

(i) The choice of photographic material is important in the maximum utilisation of available light. There is little point in having plates whose definition exceeds the experimental requirements - especially when this definition comes at the expense of sensitivity. The number of lines per millimeter needed is $1580 \sin\theta$ for helium neon lasers (Rogers 1966) where $\theta$ is the maximum angle between the object rays and the r eference beam. For a maximum angle of $45^{\circ}$ for instance, a definition of 1000 lines per millimeter is required. Agfa 10 E 70 and Ilford helium neon laser plates are satisfactory for this requirement and have a sensitivity well over an order of magnitude higher then Kodak 649F plates which have a definition of about 5000 lines per millimeter.

The definition capabilities of a few films are given below (Upatneiks 1969)

| Emulsion | Sensitivity (ergs $cm^{-2}$) | Resolution (Lines $mm^{-1}$) |
|---|---|---|
| Pan X | .1 | 150 |
| 10 E 70 | 50.0 | 2,800 |
| 649 F | 1000.0 | 5,000 |

It must be remembered when using fast films (which necessitate low object-reference beam angles) that larger film grains will diffract light and cause a bright glow around the reference beam direction. This glow may extend to the reconstruction and swamp parts of it (Lehman 1968 Urbach and Meier 1969).

The effective speed of some emulsions may be increased by hypersensitisation (Lin and Lobianco 1967) using Triethanolamine, ammonium hydroxide or water. The following table shows the increases in sensitivity that were obtained for 649F emulsions at different wavelengths, with no apparent decrease in resolution.

| Wavelength- Agent / | 6328Å | 5461Å | 4880Å | Hypersensitisation lasts for: |
|---|---|---|---|---|
| Triethanolamine | 4.2 x | 2.2 x | 2.1 x | one month |
| Ammonium Hydroxide | 2.6 x | 1.0 x | 1.0 x | one hour |
| Water | 2.0 x | - | - | - |

The best photographic contrast can usually be obtained with a final neutral density of about 1.0. If it requires T seconds to obtain unit density, holograms with almost the same final contrast may be made by exposing the photographic plate in the normal holographic manner for t seconds, then re-exposing the plate to coherent or incoherent light sufficiently to achieve the optimum density. This extra <u>pre</u> or <u>post</u> exposure thus acts as a kind of 'DC' bias bringing the AC fringe information to the central regions of the transmittance exposure curve fig (4) Though this technique effectively reduces the fringe modulation, Hallock

(1968) has described reductions in the final contrast of as little as two percent for t = T/15, i.e. an effective increase of 15 times in the film speed.

Finally it is desirable that the diffraction efficiency of the hologram should be as high as possible - especially in 'live fringe' work where it is not possible to direct the whole laser beam onto the hologram for reconstruction.

As has been described above, the diffraction efficiency of phase gratings is higher then simple amplitude (black and white) gratings, and an amplitude grating may be turned into a phase grating by bleaching it (latta 1968), this increases the diffraction efficiency from about 6 percent to about 30 percent. Unfortunately, bleaching increases the light scattered by the emulsion which may cancel out the advantage of increased image brightness (Wall 1969). This 'flare' light may be reduced by decreasing the low frequency response of the bleaching process (Lamberts and Kurtz 1970). Bleaching solutions which give increased brightness over ordinary bleaches, such as potassium dichromate, are tabulated below. Bleach (1), being a 'surface' bleach will not cope with high spatial frequency variations and should therefore only be used on holograms taken with small reference to object beam angles.

(1) One part of solution A + 1/10 part of B + 10 of water by volume

A = 500 ml distilled water + 20 g ammonium bichromate + 14 ml concentrated sulphuric acid + distilled water to make 1 Litre

B = 45 g sodium chloride + distilled water to make 1 litre.

(2) Equal parts of A and B where

A = 10 g $CuBr_2$ per litre

B = 3 percent hydrogen peroxide.

Bleach (1) is due to Russo and Sottini (1968) and Bleach (2) is due to Leonard and Smirl (1969).

Blazed gratings, dichromated gelatin and dielectric holograms give the maximum diffraction efficiencies but are usually less light sensitive than silver emulsions.

(ii) An equally important method of ensuring efficient light utilisation lies in the treatment given to the object. For the formation of a hologram most suitable for holographic interferometry light should fall on each part of the hologram from each part of the object with equal intensity, i.e. the object when seen from the hologram should appear to be equally bright all over.

Most workers use matt white paint so forming an approximation to the perfectly diffusing object, hence if the hologram is at a reasonable distance from the object most of the reflected light is not collected by the hologram. If all this reflected light could be directed to the hologram, this, using a simple comparison of areas arguement, would result in a fractional light saving of $2R^2/r^2$ - where R is the distance from the object to the hologram, and r is the radius of a circular hologram. For example with a hologram of radius 2 cm at a distance of one meter there is a 5000 fold saving.

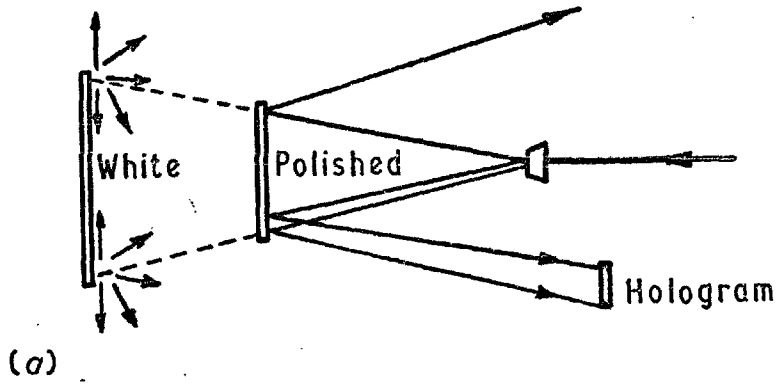
One way of treating the object is to coat it with 'Scotchlite' a reflecting preparation with many tiny glass balls in its surface and it has the property of reflecting back most of the incident light, in a narrow cone around the incident direction. Welford and Withrington (1968) have used this preparation to coat bubble chanmers and thus provide a bright background for the holography of bubble tracks. Jacobson (1969) has described the use of Scotchlite to enable a cylinder to be photographed, and a 35 fold saving in light was obtained. A half-silvered beam splitter is placed at $45^\circ$ in the object illumination beam path - therefore 50 percent of the light is wasted on illumination and collection, but there is still a considerable saving over a white painted object.

As mentioned above the object should not be painted white, nor should it be specularly reflecting. If it were, on reconstruction only a small spot of light would be seen whose location would depend on the position of the observers eye. This difficulty may be overcome by placing a diffusing screen in the object beam illumination path (after Stroke) but once again this wastes most of the incident light.

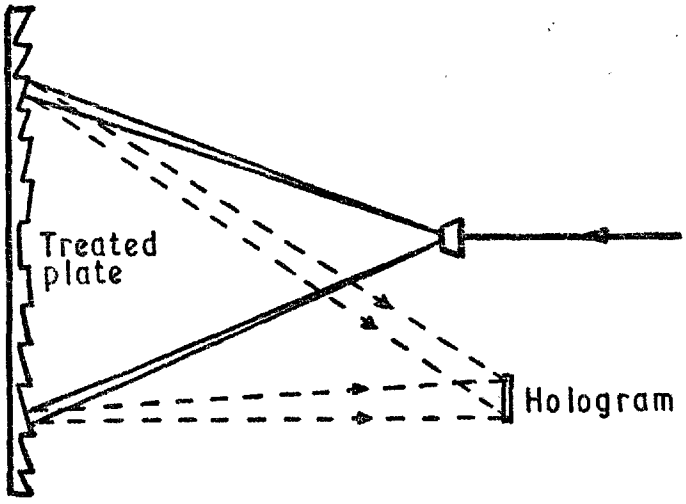
By simply roughening the object with a coarse grade of sand-paper some improvement is obtained, but the result is neither perfectly diffusing or perfectly reflecting and the image falls off in brightness towards the extremities - although there is a considerable overall improvement. The specular part may be removed by using a reference beam polarised at $90^{o}$ to the object beam but this again is light-wasting. The gaussian shape of the fundamental laser mode also reduces the brightness of the outer regions of the object and this effect is a disadvantage when using Scotchlite.

When the object is as simple as a flat plate a kind of'Fresnel mirror' i.e. a system of concentric grooves with a saw tooth profile may be formed on the plate (Fryer 1970) the rising floor of each groove may specularly reflect incident light onto the whole hologram (fig 7 ). Groove density and floor angle may be arranged to compensate for the various edge darkening and angle effects mentioned above.

A little more light may be saved by removing the beam splitter from the system. Reflection from the plane surface of the object beam expanding lens may be used to form the reference beam and this has proved to be of ample intensity for all eventualities in the present experiments. The intensity of the reference beam may be altered with a simple zoom lens system or more simply still by altering the position of the reference beam expanding lens, rather than with filters, and is therefore continuously variable.




(a)




(b)

Figure 7 (a) The difference in light reflection of a Perfectly Diffusing and a Perfectly Reflecting Object.

(b) Plate treatment can direct most of the incident light to the photographic plate.

Using only a poor approximation to the ideal Fresnel mirror and this last reference beam technique, an exposure time of 1/10 of a second has been achieved in the present experiments for a 30 cm diameter plate illuminated with a 15 mw laser. This may be considerably reduced by using all the techniques described above.

Loudspeaker cones which must not have a massive coating such as 'Scotchlite' applied have been successfully treated with a shiny silver paint. This, when sparingly applied with a spray, gives a discontinuous coating of tiny blobs which have a tendancy to reflect light back in the incident direction. This treatement increases the cone mass by as little as 5 percent (not counting the mass of the surround and coil). Sandwich speakers having an aluminium skin may merely be scratched with a fine grade of sandpaper to give vastly improved results.

## 2) The Stroboscopic Method

As mentioned in the general introduction, holography can offer many advantages over other methods of vibrational analysis. Stroboscopic illumination has the further advantages that the resulting fringes are of equal contrast out to regions of large object movement, and when moving from nodal regions each fringe encountered simply indicates that the vibration amplitude has increased by one half wavelength of the laser light used ( when illuminated and viewed normally). Further advantages are described in 2.3 below.

The basic experimental system is the same as for normal holography (figs 3 ) with the addition of some method of interrupting the laser light in synchronism with the object vibrations. If a 'strobe-disc' is used, further precautions must be taken to isolate vibrations and air currents caused by the addition of this device. The theory of

doubly exposed holography, which is the technique effectively used in stroboscopic holography is described below. Techniques for the interruption of the light and the utilisation of the stroboscopic method are disscussed and finally the advantages and disadvantages of the method are listed at the end of this sub-section.

## 2.1) Theory

Re-writing (1-4), the intensity at the holographic plate due to the combination of object and reference beams is given by:

$$I_p = I_r + I_o + or^* + ro^* \qquad (2\text{-}1)$$

On illuminating the developed plate with the reference beam the transmitted ~~intensity~~ AMPLITUDE is, as before:

$$T = rI_r + rI_o + rro^* + I_r o \qquad (2.2)$$

'$I_r o$' is the reference intensity modulated by the object amplitude.

If now two holograms of the same, but slightly displaced, object are recorded sequentially on the same photographic plate using the same reference beam, and if '$o_1$' and '$o_2$' represent the light amplitudes corresponding to the two object positions, then the hologram effectively superposes the two intensities as follows:

$$I_1 = I_r + I_{o1} + o_1 r^* + o_1^* r \qquad (2.3)$$

$$I_2 = I_r + I_{o2} + o_2 r^* + o_2^* r \qquad (2.4)$$

On summation:

$$I_{tot} = 2I_r + I_{o1} + I_{o2} + r^*(o_1 + o_2) + r(o_1^* + o_2^*) \qquad (2.\ )$$

After developing the plate and reconstructing with the reference beam of amplitude 'r' the term corresponding to '$I_r o$' in equation (2.2) is now:

$$I_r(o_1 + o_2) \qquad (2.6)$$

Neglecting the reference intensity onto which this is modulated the intensity of this image is:

$$I_{image} = (o_1 + o_2)(o_1^* + o_2^*) \qquad (2.7)$$

If the displacements of the object are small compared with its distance from the hologram, then $|o_1|$ may be regarded as approximately equal to $|o_2|$ thus:

$$o_1 = |o| e^{i\phi_1} \qquad o_2 = |o| e^{i\phi_2} \tag{2.8}$$

Therefore the image intensity may be written as

$$I_{image} = 2|o|^2(1 + \cos(\phi_1 + \phi_2) \tag{2.9}$$

The term $(\phi_1 - \phi_2)$ is a direct measure of the object displacement, i.e. if the hologram is illuminated and viewed normally and the object displacement is 'd' at the point in question, the corresponding path difference $\Delta$ is 2d and the phase change $(\phi_2 - \phi_1)$ is:

$$(\phi_2 - \phi_1) = (2\pi/\lambda)\Delta = (2\pi/\lambda)2d \tag{2.10}$$

Every time the phase changes by $2\pi$ a dark fringe appears and the object reconstruction. This equation therefore represents the contour map obtained w ith double exposure techniques where the second position of the object is formed by static displacement or by the stroboscopic freezing of a regularly occurring displacement.

The interferograms obtained are identical to those that would be obtained had classical two-beam interferometry been used, though this would have necessitated a specularly reflecting object. The fringes have the characteristic intensity variation of two-beam interferometry. Multiple beam fringes may also be formed utilising emulsion non-linearities as described on page ( 56 ).

## 2.2) The Basic Stroboscopic Method and Its Uses

The most straightforward utilisation of the strobe technique either flashes the laser at source, or 'chops' the laser light before it reaches the first component of the optical system. Thus both the object and the reference beams are chopped together.

Many workers arrange for one flash per object cycle and have an on-off ratio (duty cycle) of between 1:10 to 1:20. It is highly

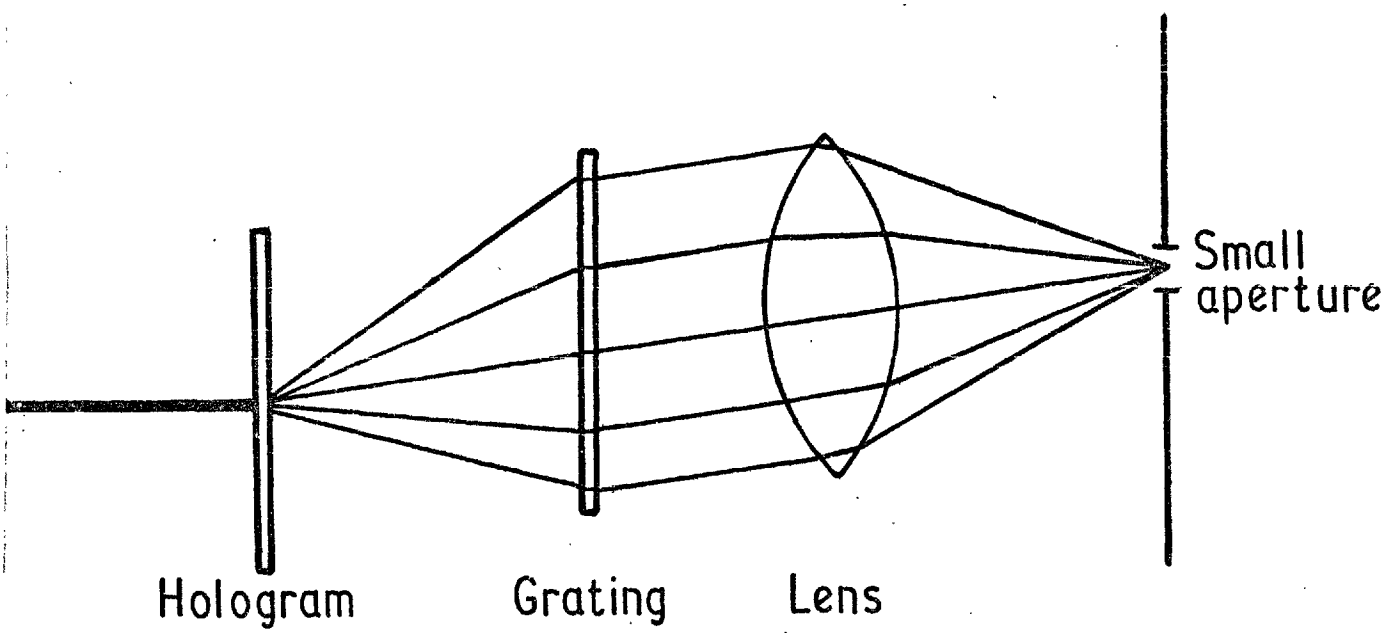
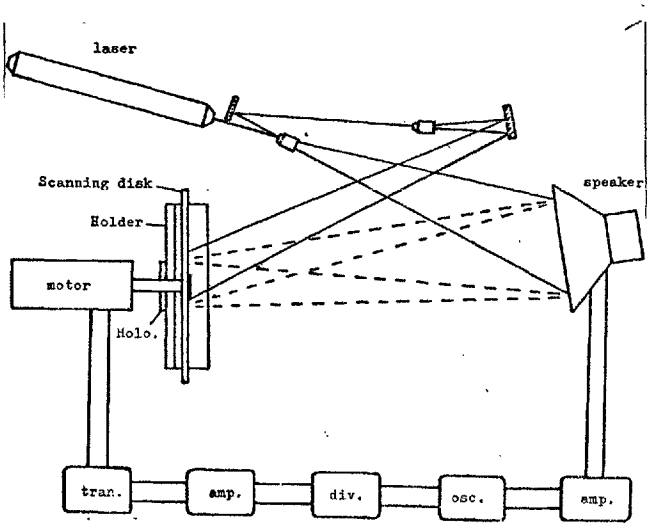



Figure 8 Optical system for multiple beam interferometry from a hologram

Figure 9 (a)
General Scanning
System



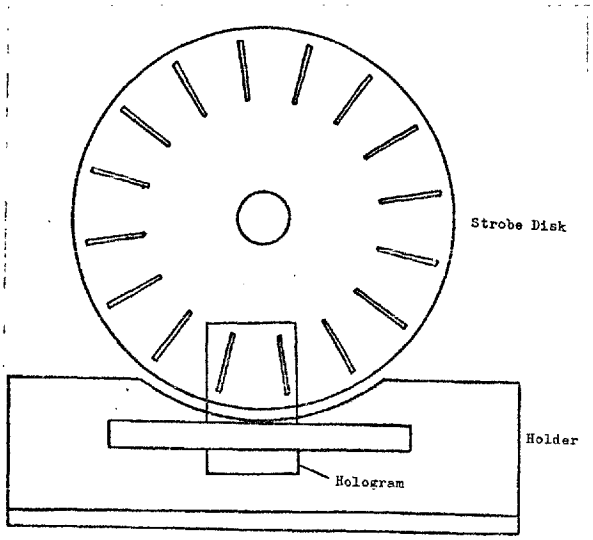
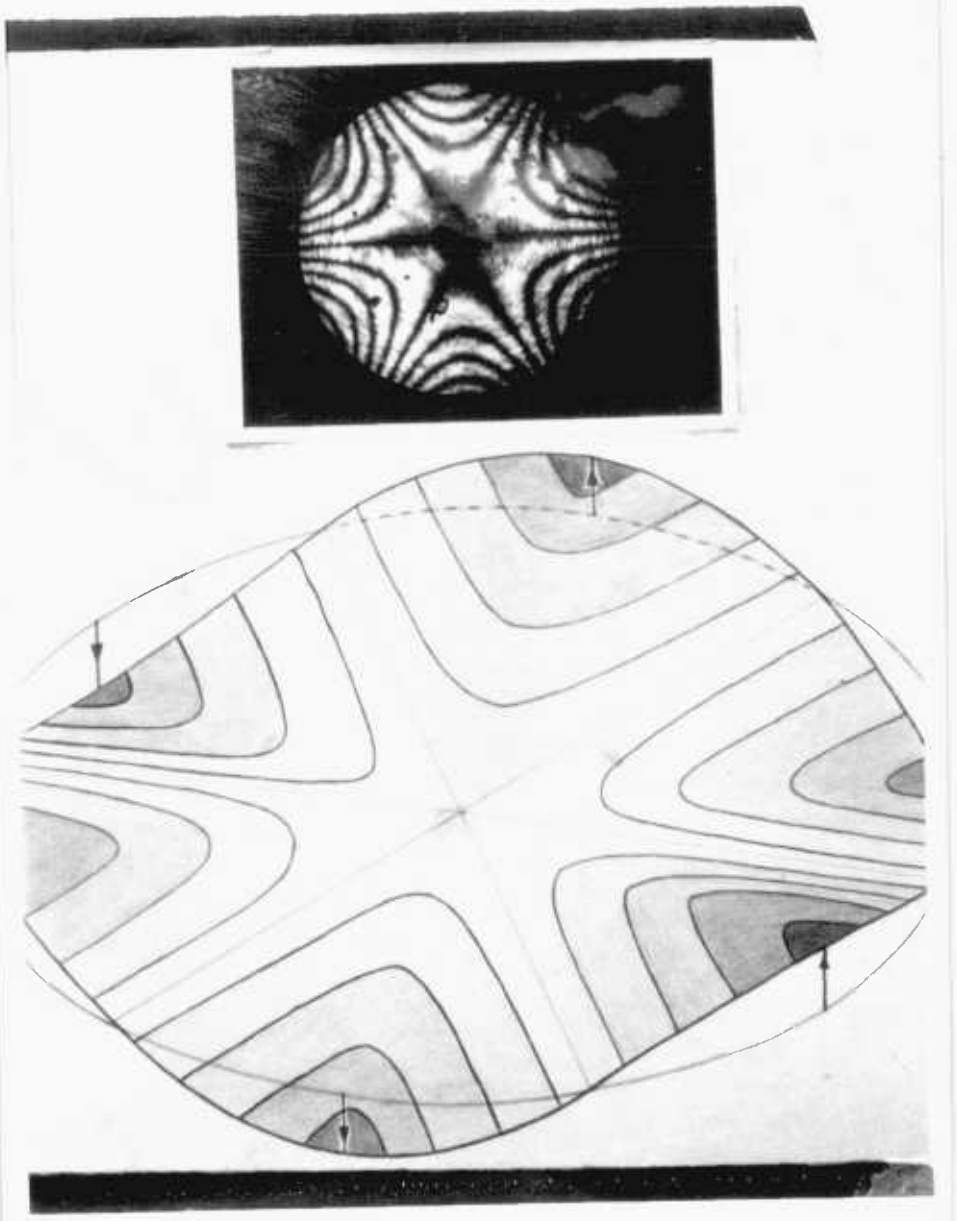




Figure 9 (b)
Strobe-Scan disc
and Plate Holder

Plate Number 3 (a)



Wall Chart with Photograph and Sketch of a Disc Vibrating at 1200 Hz. The Sketch Depicts three Antinodes as Hills and three as Valleys

desirable that the duty cycle should be as low as possible, so that the object does not move appreciably during each illuminating flash. If the light is <u>on</u> for too large a fraction of the object cycle time - only that part of the cycle during which the object moves least (i.e. near the maximum displacement for sinusoidal oscillations) can be effectively frozen. Other parts of the object cycle will produce an indistinct 'limited time average' system of fringes which correspond to the average of object positions during the 'on' period. A theoretical expression for this can be found on page (32). When the duty cycle is as high as 1:2.5 for instance , even the maximum displacement of a sinusoidal oscillation gives indistinct fringes, which are neither truly time-averaged or stroboscopic and are of limited use for measurement purposes.

Moffatt and Watrasiewicz (1971) have developed the theory of long exposure stroboscopic holography and by exposing for a fraction $\alpha$ of the object vibration period T obtain the following result:

$$o = 1/T \int_{o}^{\alpha T} e^{iK\sin\theta} dt \qquad \text{where } \theta = wt \qquad (2.11)$$

i.e.

$$o = \alpha J_o(K) + 1/\pi \sum_{n=1}^{\infty} 1/2n \; J_{2n}(K)\sin 4n\pi\alpha$$
$$-i \; 1/\pi \sum_{n=0}^{\infty} 1/2(n+1) \; J_{2n+1}(K)(\cos(2n+1)2\pi\alpha - 1) \qquad (2.12)$$

When $\alpha = 1$ this yields the normal time averaged result.

When integrating over time T symmetrically about zero object phase then:

$$o = 2\alpha J_o(K) + 1/\pi \sum_{n=1}^{\infty} J_{2n}(K) \; 1/n \; \sin(4n\alpha\pi) \qquad (2.13)$$

For example when integrating about zero by $\pm$ T, with $\alpha = 1/10$, the first bright fringe is reported as being three times further from the node than with normal time averaged holography - a result which should be compared with the temporaly modulated holography results of Aleksoff to be found later in this section.

A hologram of a stationary object is taken, develpped and accurately replaced in its original position. This is known as a 'live

fringe' hologram and will be dealt with more fully in (2.3) below. Part of the reference beam is then diffracted to form a virtual image located on the object. The reconstructed object beam then interferes with the real object beam and fringes are seen on the object corresponding to any movement between the object and its virtual image.

If the stroboscopically frozen vibrating object is viewed through this live fringe hologram, fringes are seen which are contour lines corresponding (when illuminated and viewed normally) to half wavelength increments of object movement - the first fringe out from a node however, corresponds to a quarter of a wavelength of movement. The phase of the strobe may then be set so that the desired part of the cycle is frozen and then a fresh photographic plate may be exposed to the vibrating object. The developed plate reconstructs both object states simultaneously and interference between the two reconstructions results in fringes which are known as 'frozen fringes'.

There are several variations on this theme. For instance Markova et al (1969) and many workers such as Wastrasiewicz, Shajenko Ostrovsky and Zaidel use two flashes per cycle and therefore only one effective exposure need be taken. The fringes that are seen with this method correspond to the difference in object amplitude at the two instances of illumination, these may be at the two peak amplitudes - doubling the number of fringes seen for a given object movement. When integer harmonics are present in the object vibration, assuming that they are in phase with the fundamental, an exposure between $0^{o}$ and $90^{o}$ in the fundamental removes the contribution due to even integer harmonics It is better to have one or more flashes per cycle rather than one flash every few cycles as this latter method increases the exposure time and puts demands on the mechanical and electrical stability of the system.

Using a 'Q' switched ruby laser, only two flashes are necessary and individual cycles or impulsive events may be studied - provided the flash timing can be accuratley adjusted. With this single or double shot illumination there are fewer problems with the stability of the system as a whole, and if the two fringes of the laser are within one cycle only, stability problems are non-existant. Transients may also be studied using ruby lasers (Hall et al 1970) and scatter plate holography suitably adapted to record a sequence of holograms on a single plate at repetition frequencies up to 12.5 KHz. A different area of scatter plate and hologram being selected for each exposure pulse from the laser by a disc with a number of holes pierced at the desired radius driven by a synchronous motor. Jacobson has also used high speed cine photography to investigate transients.

Using a technique recently described by the author (1970b 1972), a whole vibration cycle may be recorded on one hologram and the need for a live hologram and the setting of the strobe phase is obviated.

A strobe disc with an appropriate number of radial slits is attached to a synchronous motor and situated just in front of the holographic plate (fig 9 ). A given slit may be arranged to scan the plate while the object traces through any given fraction of a cycle, or indeed any number of cycles. The two exposures may then be taken in the normal way. The observer, on reconstruction will see the number of fringes on the reconstructed object increase from zero to the number corresponding to the maximum amplitude of object movement as he moves his eye along the path taken by the slit across the hologram. Tapered slits give differing on-off ratios and the most suitable one used for measurements.

The technique described by Hallock (1968) may be automatically incorporated in this apparatus by causing only the reference beam to scan the photographic plate. The unreferenced part of exposure to the object

Scanning Optical Layout

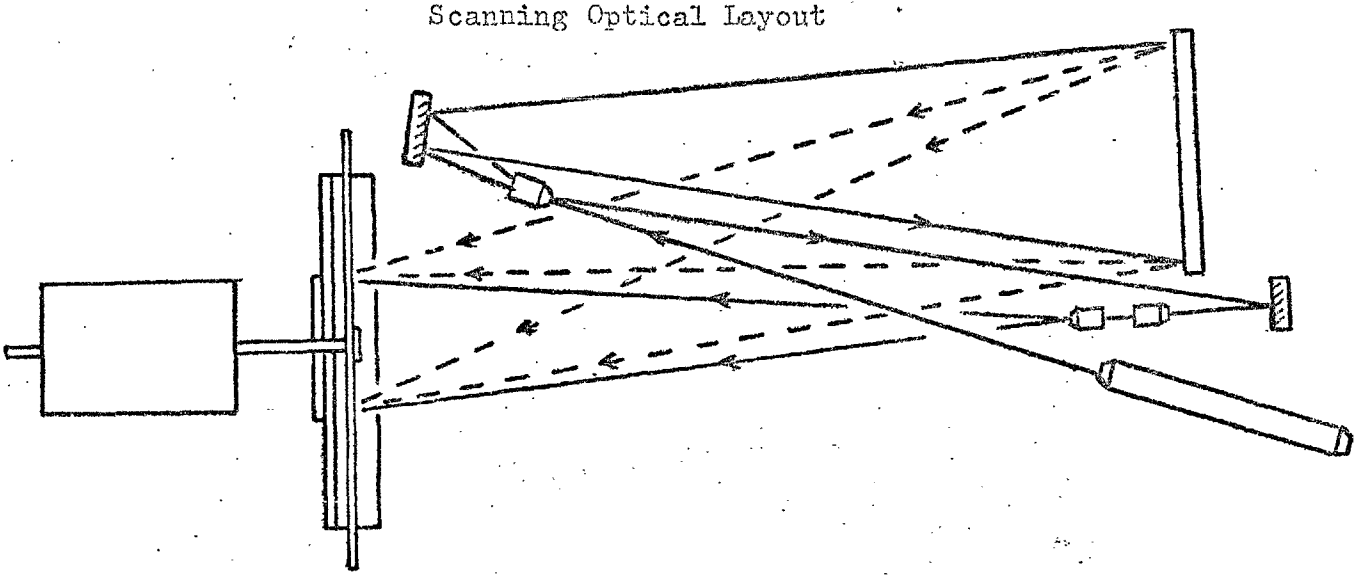
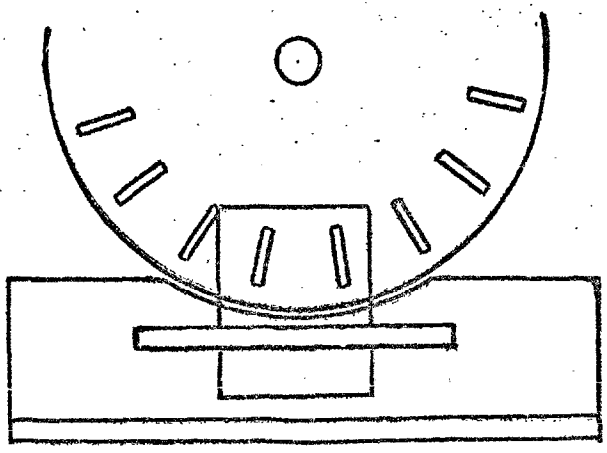


Figure 9 (c)



Ordinary Scanning Disc

beam - and it will be unreferenced for at least 9/10 of the time - increases the 'DC' level of the exposure and effectively decreases the total exposure time. A similar effect mey be achieved by increasing the distance between the scanning slits and the photographic plate - the two beams will then fall slightly out of register thus effectively decreasing the slit width while leaving the exposure unchanged.

Raster scanning or the use of spiraling slits may alow a cycle to be recorded in greater detail .Since the formation and dying away of fringes may be observed by moving the eye, the location of a node is made easier by the absence of any fringe movement through it. Further variations on the basic scanned technique together with the theory are described in Sections III and IV.

## 2.3) Live and Frozen Fringe Techniques

If the object is set into vibration and observed through a 'live fringe' hologram,defined above, weak fringes are seen. These are related to those (time averaged) fringes seen on the reconstruction of a hologram taken of a steady vibration, but are weaker as a consequence of the integrating time of the eye. Powell and Stetson (1965 a and b, 1966) and Brown Grant and Stroke(1969) have described the theory of these fringes - with time averaged holography (see section below) the intensity of the reconstruction is:

$$I(\text{image}) = I_o \, (J_o(K))^2 \qquad (2.14)$$

With real time viewing the intensity of the fringes is

$$I(\text{image}) = 2I_o(1 + J_o(K)) \qquad (2.15)$$

where $K = (2\pi/\lambda)2d_o$ and $d_o$ = max.vibration amplitude

This reduction in intensity renders live time-averaged fringes practically useless for all but setting the frequency for a proper time averaged exposure.

Live fringe arrangements come into their own when used in

conjunction with stroboscopic illumination. In this case the fringes seen on looking through a live fringe hologram at the stroboscopically frozen vibrating object are as sharp and clear as those seen on static deformation of the object - assuming of course that the stroboscopic flashes are of sufficiently short duration that the object does not move appreciably during the flash.

The main advantage of the method is that the phase of the strobe may be altered while viewing the fringes and whole vibration cycles may be observed. Also motion pictures may be taken as the phase or frequency are altered and photographs may be taken from the film at the desired points in a cycle or frequency scan and studied at leasure, this technique has been used at the N.P.L. For measurements to be taken from live fringe holograms there should be no fringe present on relocation of the hologram after development, and no subsequent drifts of either position or frequency during the experiments. Therefore dimensional stability, differential expansions emulsion shrinkage, and other similar effects tend to limit the usefulness of the live fringe technique.

Where accuracy is desired frozen fringes are almost invariably used. Because only one or perhaps two closely time related exposures are taken on the same plate, distorting effects are minimised and there is no problem over the relocation of the photographic plate. Also, in processing, whatever happens to one image will also happen to the other so accuracy is assured. The scanning method described above also allows whole cycles to be frozen and studied at leasure.

When live fringes are to be utilised, perhaps the most difficult aspect of the technique is the accurate re-location of the developed photographic plate - followed closely by the avoidance of differential expansions etc. Many ingenious plate holders have been designed to both hold the plate and, should it not be returned to within

1/8th of a wavelength of its original position, allow it to be moved in any direction or rotated in its own plane. Parallel fringes appear as a result of movement in the plane of the hologram, movement towards or away from the object results in circular fringes appearing (Vienot 1968) centered on the line passing through the object parallel to the direction of movement. Usually the initial support is a 'six point' contact system which completley locates the photographic plate with no redundant supports.

One way of eliminating some of these problems is to hold the plate in a fluid gate (Deelen and Nielsen 1969). The plate is processed in situ and consequently there are no problems of relocation. If the plate is not allowed to dry afterwards there are no problems of emulsion shrinkage either. The hologram is exposed while surrounded with water, this is then drained out and replaced with developer, then stopper, fixer rinses and finally water again - all at the same temperature. Biederman and Molin (1970) combine hypersensitisation with in situ processing and describe how compensation for emulsion swelling effects is also carried out in the fluid gate. A variation of this technique has been suggested by Castler and Pruet (1967), they soak the hologram in developer first and during the exposure they occasionally block off the object beam and observe the reconstruction. The exposure is finally terminated when the reconstruction is good enough. With the rapid exposure techniques that have been described above however this latter method may be of limited value.

Neuman and Rose (1967) describe a neat way of eliminating the gradual shift of live fringes due to system creep or warm air currents in which they stabilise the fringes by a feedback process. A motor driven optical wedge is inserted into the reference or object beam to alter the path length. The intensity of the fringes is observed with a photomulti-

plier and constancy is maintained by moving the wedge via a servo system. A closely related method has been described by Rose and Pruet (1968) where the length of the laser cavity is adjusted by servo, thereby s lightly altering the laser output frequency which causes a fringe shift due to unequal object and reference path lengths. Both of these techniques will only guard against effective changes in path length or las er output frequency and will not correct for translations or rotations in the plane of the hologram.

## 2.4) Strobing Techniques

The essential feature of all stroboscopic methods is that they interrupt the light falling on the vibrat ing object allowing (say) only one brief flash per cycle. If the flash lasts for a sufficiently small fraction of a cycle and recurs at the same point in succeeding cycles it seems to the observer that the object so illuminated is stationary.

Many ways have been used for interrupting the laser light and they fall into two main groups (a) causing the laser itself to flash and (b) chopping the light from a continuous wave laser.

### (a) Causing The Laser To Emit Pulses

### (i) 'Q' Switched Laser

For 'stroboscopically recording large objects ruby and neodymium-glass are the most suitable laser media at present (Bradley 1970, Gates and Hall 1968) how ever it should be noted that these lasers do not usually pulse continuously and may only be used as described in (2.2) above. Neodymium-glass lasers emit at 1060 nm which must be converted to second harmonic at 530 nm for use in optical holography, the loss of energy in the conversion process being more than made up for by the increased sensitivity of photographic emulsions at this wavelength. The coherence

lengths and power outputs of these lasers are being steadily increased coherence lengths of 1 m are common and peak powers of $10^9$ W for ruby lasers and $10^{13}$ W for neodymium-glass lasers have been achieved by 1969. Sufficient power and coherence length was available as early as 1967 for the first hologram of a living person to be taken (Siebert 1967) using a high coherence pulsed ruby laser, amply demonstrating the reduced stability requirements of pulsed laser holographic systems.

Ruby lasers are typically pumped with a photographic flash lamp, and at the correct instant of maximum storage the Kerr cell shutter between the high reflectivity mirror and the ruby rod is opened by shorting the high voltage plates to earth, producing a pulse lasting for tens of nanoseconds and with hundreds of kilowatts peak power. Rotating mirrors, Pockel cells and saturable dyes are also used as 'Q' switches and these are less easily damaged than Kerr cells, however Kerr and Pockel cells are often used because electro-optic initiation may be precisely timed. Pulse duration - normally about 20 transit times between mirrors - may be made shorter by various techniques such as 'mode-locking' (Bradley 1970), but when it becomes so short that the spatial length of the wave train given out is, for instance, less than the coherence length necessitated by the size of the object, a lower limit has been reached. For example, a pulse duration of 3ns corresponds to a coherence length of 1 m. Similarly stroboscopic freezing of moving objects reaches a limit when the shortness of the pulse, which has to be used to arrest the motion results in an insufficient coherence length or does not allow the object and reference beams to 'overlap' at the hologram.

(ii) Altering the C.W. Excitor

Some gas laser excitors have a built in facility for modulating the output of the laser within limits, this may only be used to give a rather poor strobing effect however, because the laser may not be switched off

Alternatively it is possible to alter the excitor of a C.W. laser and cause it to give out pulses which have a greater peak amplitude then the normal steady output of the laser. It is, however probably easier to use one of the methods of light interruption described below. When Gallium Arsenide diode laser have been developed to give sufficient output power, direct modulation will be a more practical alternative which will solve many problems.

(b) Interrupting the Laser Light

(i) One of the most sophisticated methods of interrupting the laser light uses a Pockels cell (fig II ) shows the experimental arrangement. A sine wave generator is used to drive the object plate and to synchronise a pulse generator which produces a pulse variable in phase and duration. This pulse is amplified and drives a Pockles cell with a D.C. half wave voltage of 1300 V. Without any voltage on the cell and polariser (Glan Thompson polarising prizm) is rotated until minimum transmission is achieved. This is less than 0.5 percent of the laser output of 70 mw. With the pulse voltage applied, 90 percent of the incident light is transmitted. Pockles cells have a rapid response time and therefore pulses of short duration may be used, allowing those parts of a vibration cycle where the object is moving rapidly to be studied. Von Winkle used two exposures per cycle aloowing peak to peak double exposures or comparison between any samll part of a cycle or any other part. For analysis of high amplitudes the exposure pulses may be moved so that the complete amplitude is covered in small increments.

(ii) Another interesting form of shutter is that described by Brandt (1970) which utilises a Bragg cell to do the switching. The ultrasonic acousto-optic Bragg cell consists of a 30 MHz quartz transducers feeding into water and is similar to that used by Korpel (page 185). In water

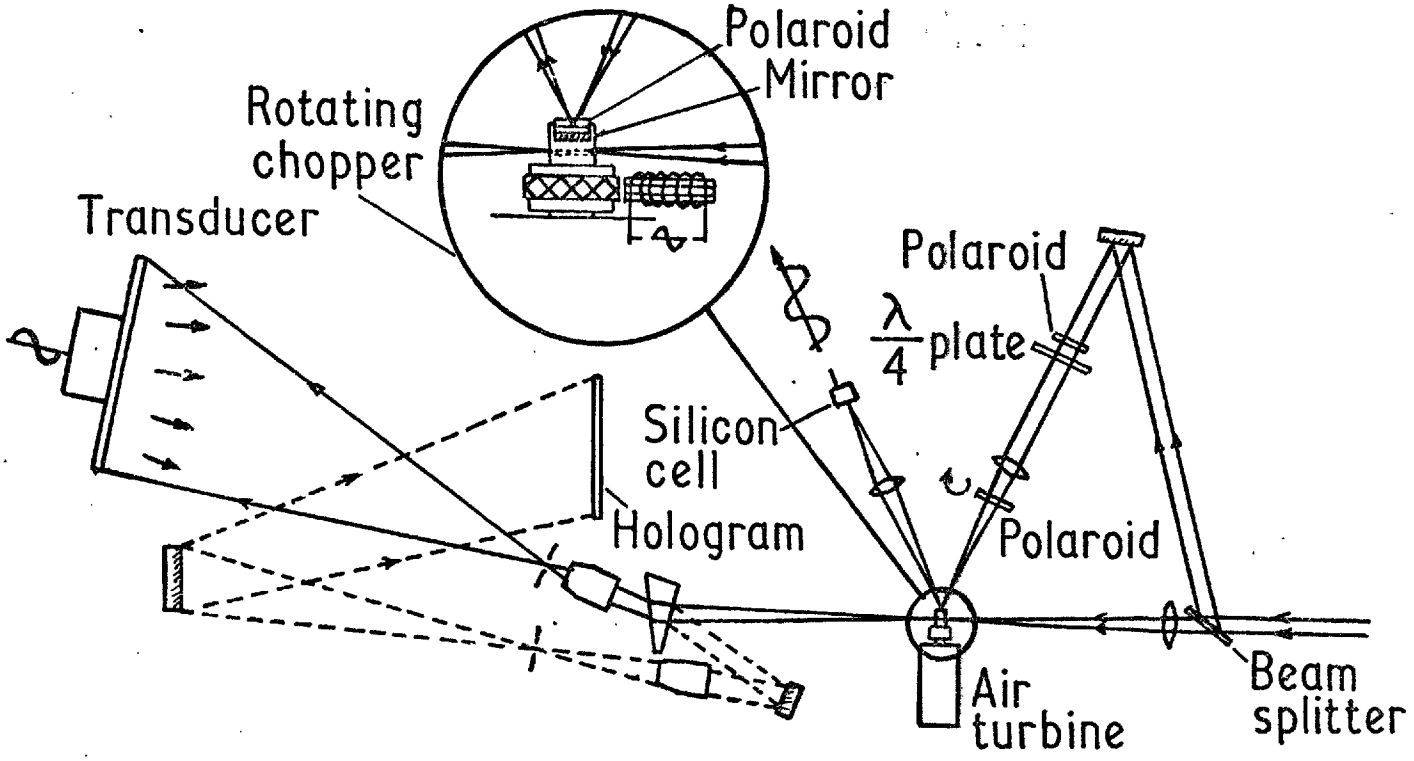



Figure 10 Strobing system in use at the National Physical Laboratcry

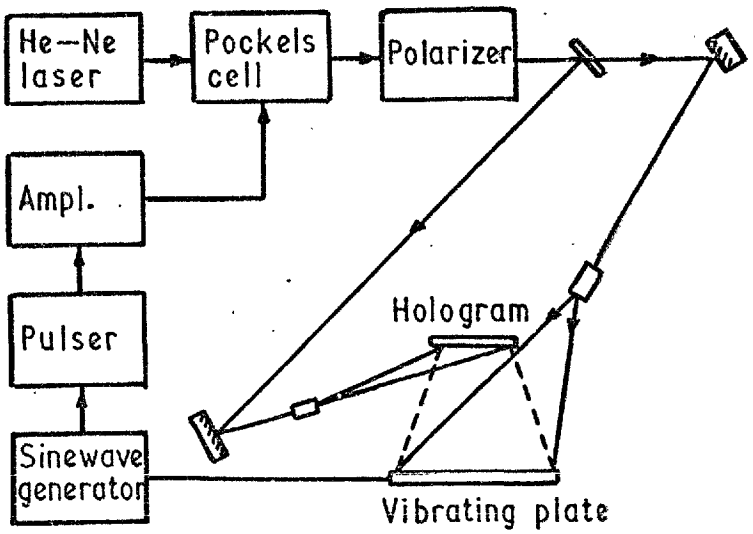



Figure 11 Schematic diagram for stroboscopic holography using a Pockel cell - after U.S. Navy Sound Laboratory

about 10 watts of energy diffracts about 90 percent of the incident light into higher orders. Thus the 90 watt transmitter supplying the crystal is on most of the time and is keyed off, when a pulse is desired, by a suitable pulse generator. Thus a complete range of frequencies and duty cycles may be obtained. This method suffers from the fact that even when 'off' 10 percent of the original light still falls on the holographic plate, though by placing Bragg cells in series a better on-off ratio may be obtained.

(iii) There are many methods that utilise a disc or plate to interrupt the light from a C.W. laser. A particularly elegant one has been used at the N.P.L. (Archbold and Ennos 1968). The laser beam is focussed through a small hole drilled diametrically across a steel spindle attached to a high speed air turbine of the type used to drive dentists drills. The electrical signal used to drive the object is derived by splitting off part of the laser beam and circularly polarising it by passing it through a filter and quarter wave plate. The beam is then passed through a second polaroid and the direction of the resulting plane of polarisation may be altered by rotating this polaroid - without altering the amplitude of the light. This light then falls on a polarising mirror fixed to the end of a rotating spindle. The reflected light, which varies in synchronism with the transmitted flashes, falls onto a silicon cell whose output is amplified and used to drive the object. The relative phase between the illuminating pulses and the electrical signal may be altered by rotating the second polaroid thereby allowing any part of the vibration cycle to be studied.

When this system is used to examine objects having sharp resonances (0.5Hz bandwidth), small variations in turbine frequency have to be overcome by building a small magnet into the spindle and placing a solenoid close to it. The turbine locks on when the solenoid is supplied with the object excitation frequency.

(iv) A less complicated system has been used by several authors (Wastrasiewicz et al 1968, Markova et al 1969 and Fryer 1970 and 1972). This utilises a strobe disc attached to a synchronous motor supplied with the frequency used to excite the object. These systems in their basically simple form are limited to frequencies of around 2 KHz by the tendency of the strobe disc to fly apart under rotational forces. If the laser is focussed down, the size of the holes and hence the strobe disc may be reduced for a given on-off ratio, and the upper frequency limit increased accordingly.

The author has used an integrated circuit frequency divider to supply the strobe motor - this preserves synchronism and allows the motor to run at a lower frequency than the object. By chopping only the reference beam at its focus a smaller disc may be used and the method of Halock (1968) may be automatically incorporated.

This part is completed with a list of the advantages and disadvantages of the stroboscopic method.

2.5) Advantages of the Stroboscopic Method

1) The greatest single advantage is the ease of fringe interpretation If the object is illuminated and viewed normally each fringe corresponds to an object movement of one half-wavelength of laser light.
2) The sensitivity may be changed slightly by exposing either peak to peak or peak to zero amplitudes.
3) Fringes are of equal contrast up to regions of high object amplitude.
4) Motions that are not sinusoidal i.e. have a large harmonic content, may be studied either by a scanning method or by taking many exposures at different phases and building up a picture of the amplitude variation during a cycle.
5) By allowing two flashes per cycle some harmonics may be automatically

removed and/or two separate exposures may no longer be necessary.

6) When using pulsed lasers stability requirements are very greatly reduced as only one cycle need be investigated.

7) Live fringes may be easily seen, facilitating the setting up of the experiment and aloowing cine films of the live fringes to be taken.

8) Using the techniques of Varner and Hovanesian, (detailed below), the phases of different parts of the object may be determined from the moire fringes produced.

9) Progressive waves due to a combination of two close frequencies may be seen with the 'live'system.

2.6) Disadvantages of the Stroboscopic Method

1) The apparatus is more complicated.

2) The position of nodes and antinodes may not be apparent and may have to be deduced. The scanning method allows this to be done more easily however.

3) Phase information may not be evident, but it can be deduced.

4) Longer exposure times are necessary with C.W. lasers though the method of Halock may be incorporated ny strobing the reference beam only, and this minimises the increase in the exposure time. With pulsed lasers this disadvantage does not apply.

5) There may be the need, when using some variations of the method, for two separate exposures which increases the long term stability requirements of the system.

3) The Time Averaged Method

The experimental arrangement for the basic method is the same as for the holographic recording of a stationary object, though perhaps some extra precautions may be necessary to ensure that the object vibrations

do not communicate themselves to the optical components. The photographic plate is simply exposed to the light from the vibrating object and also to a reference beam. Theexposure time is the same as that used for stationary objects though some modifications to the technique may require different exposures. The theory of time averaged fringes is described below and some of the many modifications to the basic technique, evolved mainly to overcome its disadvantages, will be discussed.

## 3.1 Theory

When two holograms are taken successively on one emulsion we have seen that the result is the superposition of the two reconstructed images, so that they appear to occur simultaneously (Part 2). If the emulsion is exposed to a vibrating object the resulting hologram is the superposition of a large number of separate holograms corresponding to each instantaneous position of the object. The hologram will simultaneously reconstruct the superposition of all these object positions weighted by the relative exposure time occupied by each of them (Powell and Stetson 1965).

Let $\bar{o}(rt)$ represent the amplitude of a light field from the object at position 'r' and time 't'. If a position '$r_1$' lasts for a fraction $\Delta t/T$ of the total exposure time when the image amplitude resulting from this is:

$$\bar{I}(r_1) = \bar{o}(r_1 t)\Delta t/T \qquad (3.1)$$

and there fore the total amplitude of the image is the sum of these individual contributions i.e. the time average, in the limit:

$$\bar{I}(r) = 1/T \int_0^T \bar{o}(rt)dt \qquad (3.2)$$

Now when the object displacement is small compared with its distance from the hologram:

$$\bar{o}(rt) = |o|e^{i\phi(rt)} \qquad (3.3)$$

Where $\phi(rt)$ is the'phase difference'due to object movement 'd'

Therefore substituting (3.3) an (3.2):

$$\bar{I}(r) = |o|1/T\int_o^T e^{i\phi(rt)}dt \qquad (3.4)$$

and the corresponding virtual image intensity on reconstruction is

$$\bar{\bar{I}}(r) = |o|^2|(1/T\int_o^T e^{i\phi(rt)}dt|^2 \qquad (3.5)$$

Expressions may be derived for the way in which the phase difference $\phi$ varies when the object movement 'd' is known, and the corresponding fringe systems may therefore be interpreted. For instance, if the object is illuminated and viewed normally, and is vibrating sinusoidally, than the object distortion 'd' at any point (corresponding to coordinates (r,t)) is:

$$d = d_o\sin wt = d_o\sin\theta \qquad (3.6)$$

where w ia the circular frequency of the object vibration and $\theta = wt$. The corresponding phase variation is:

$$\phi(rt) = (2\pi/\lambda)2d = (2\pi/\lambda)2d_o\sin\theta \qquad (3.7)$$

On substituting (3.7) in (3.5) and writing $K = (2\pi/\lambda)2d_o$ :

$$\bar{\bar{I}}(r) = |o|^2|(1/T\int_o^T e^{iK\sin\theta}dt)|^2 \qquad (3.8)$$

(In the more general case K will be a more complicated expression carrying information about different angles of illumination and viewing) Then

$$I(r) = |o|^2|1/T\int_o^T e^{iK\sin\theta}dt|^2 \qquad (3.8)$$

Now it is known that:

$$e^{iK\sin\theta} = J_o(K) + \sum_{n=1}^{\infty} J_{2n}(K)\cos 2n\theta + \sum_{n=o}^{\infty} J_{2n+1}(K)\sin(2n+1)\theta$$

When T is much larger than any individual cycle time, as is usually the case in time averaged work, T may be regarded as tending to infinity. All the Bessel functions under the integral then tend to zero except the zero order. Therefore in the limit:

$$\bar{\bar{I}}(r) = |o|^2|(1/T\int_o^T e^{i(K)\sin\theta}dt)|^2$$

$$= |o|^2|J_o(K)|^2 \text{ as } T\to\infty \qquad (3.9)$$

i.e.

$$= |o|^2|J_o(2\pi/\lambda)2d_o|^2 \qquad (3.10)$$

$(2\pi/\lambda)$ is usually refered to as the wave number.

The object reconstruction will be covered with fringes whose intensity follows a (zero order Bessel function)$^2$ law - see fig (12). The amplitude '$d_0$' is a function of position on the surface of the vibrating object and for instance, when the term $(2\pi)/\lambda\ 2d_0$ has the values 2.4, 5.52, 8.63 etc. the intensity of the object reconstruction will be zero - i.e. there is a dark fringe on the reconstruction. A more complete table of these zeros and the corresponding object movements is to be found in Brown Grant and Stroke (1969).

Similar expressions may be derived for the fringes corresponding to other simple object movements but the presence of harmonics makes the analysis more difficult (see below).

The advantages and disadvantages of the time averaged method will be listed first as most of the techniques described in this section are methods of countering the disadvantages.

## 3.2) Advantages and Disadvantages of the Time-Averaged Method

### (i) Advantages

1) The experimental arrangements are as simple a those for the basic holographic system.
2) Exposure times necessary are, in general, shorter than for stroboscopic holography.
3) The positions of the nodes, being brighter than the rest of the reconstruction, are easily found.
4) The basic technique may be modified in a growing number of ways - eliminating some of the disadvantages and making the technique more versatile.

### (ii) Disadvantages

1) The technique necessitates averaging over several cycles, and

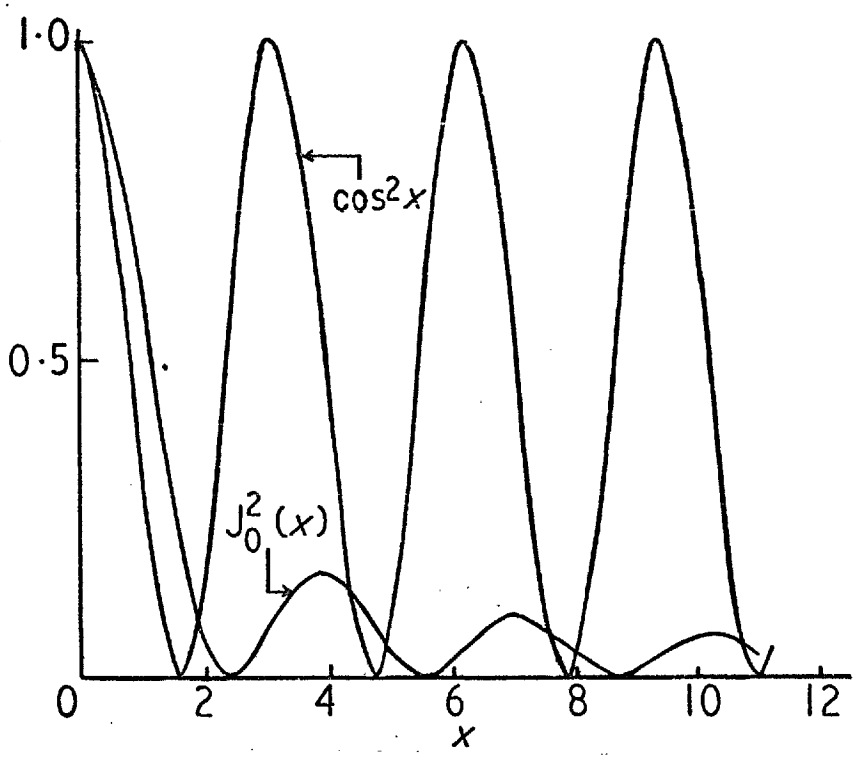



Figure 12 Comparison of (Bessel function)$^2$ fringes and $\cos^2$ fringes

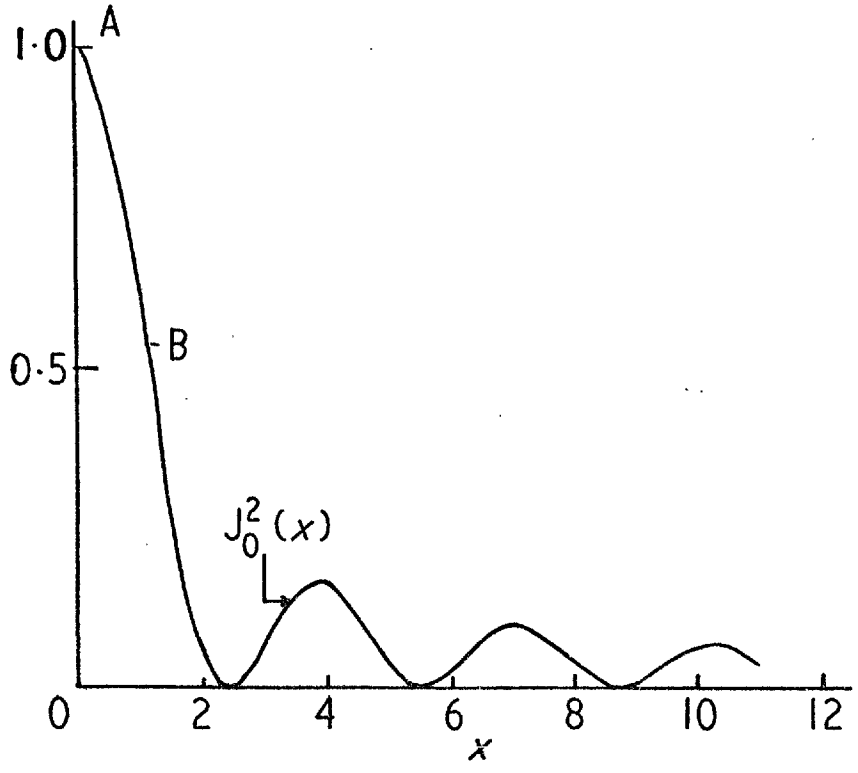



Figure 14 (Bessel function)$^2$ fringes showing regions of small intensity change for small object movement at A and large intensity change at B

therefore demands more mechanical and electrical stability than 'pulsed laser' strohoscopy - though less stability than 'interrupted laser' stroboscopy.

2) The vibration amplitude cannot be simply obtained - even for sinusoidal vibrations.

4) If the oscillations contain harmonics the analysis becomes more difficult (Wilson 1969 and 1970) and the intensity of succeeding fringes falls off very rapidly (see also Stetson et al 1969).

4) Asymmetric vibrations may not be studied at present.

5) The intensity of succeeding fringes for sinusoidal oscillations falls off as a (zero order Bessel function)$^2$, making high amplitude oscillations difficult to study.

6) Phase information is ordinarily lost.

7) No information about the frequency of the oscillations is recorded (Powell 1968) and oscillations involving several frequencies give fringes difficult to interpret.

8) Live fringe viewing is difficult.

9) A linear motion superimposed on the vibration completely erases the fringe pattern.

## 3.3) Modifications

(i) One of the disadvantages of the time-averaged method is that phase information is ordinarily lost. However Aleksoff (1969) has described a method whereby some phase information may be retained. With his procedure the reference beam is phase modulated with the function $b\cos(\omega t+\beta)$ so that a point on the object will reconstruct with a brightness proportional to $J_o^2(c)$, where $c^2 = a^2 + b^2 - 2ab\cos(\alpha-\beta)$. this means that fringes are not formed around the zero vibrational

amplitude, but about a vibrational amplitude determined by the modulation depth and phase of the reference beam.

The reference beam may be modulated by sending it through or reflecting it from any part of the object. Indeed the reference beam may be formed by imaging the object or part of the object onto the photographic plate. Any desired reference phase and amplitude may be obtained by reconstructing from the appropriate part of the hologram.

For example, by modulating the reference beam with the amplitude and phase of the maximum amplitude of the object vibration, this amplitude then becomes the most brightly reconstructed part of the object and adjacent lobes that are 180° out of phase are less brightly rec onstructed. Aleksoff has also described the techniques of temporally modulated holography in a later paper (1971). This excellent paper will be referred to again in more detail below as it can be used to both increase and decrease the sensitivity of time averaged holography. It also has the ability to increase the visibility of high order fringes and can be used in one of its variants to give information about the relative phases of the object vibrations. Information about the phase of the object vibrations may be obtained by sinusoidally phase modulating both the reference and the object illumination beams. This results in the relative phases of the object vibrations being encoded into the fringe system in a manner very similar to the above.

(ii) The effect on time averaged fringes of the simultaneous pres ents of several sinusoidal object vibrations having arbitrary amplitudes frequencies and relative phases has been dealt with by Wilson (1970) and also Wilson and Strope (1970). Combination modes have been dealt with by Molin and Stetson (1969). Molin and Stetson have shown that the joint characteristic function of an object vibrating with two irrationally related frequencies (i.e. not related by integer

ratio) is the product of the two individual fringe functions. The fringe function is the mathematical expression governing the brightness of the reconstructed image. This function:

$$I_r = J_0(I_1(r))J_0(I_2(r)) \qquad (3.11)$$

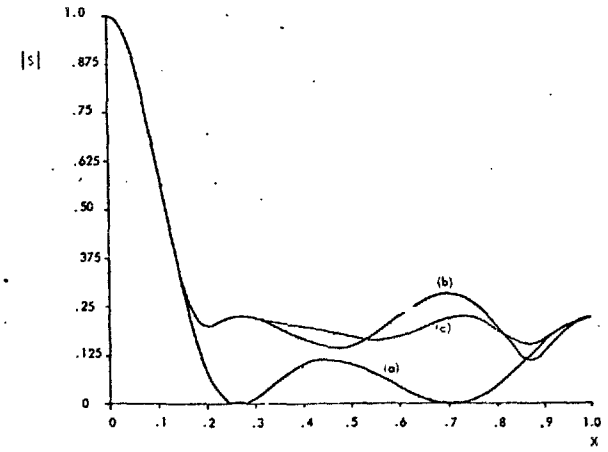
has nodes only at the intersection point of the components nodes and black fringes where either component has a black fringe. Wilson generalised this for the product of the fringe functions of N component vibrations.

Molin and Stetson (1969) have also cons idered the combination mode patterns at one frequency with two excitation points physically $90^\circ$ apart and differing phases of applied excitation. In this case the arguementsof the fringe function is the vectorial sum of the component arguments. If they are $180^\circ$ out of phase they will add algebraically and if there is an arbitrary phase difference then they may be resolved into in phase and quadrature components giving:

$$I_r = J_0(|\Phi_1(r) + \Phi_2(r)|) \qquad (3.12)$$

Where $\Phi_1$ and $\Phi_2$ are the phasor functions of the object vibrations for the latter case. This equation shows that the Bessel functions can be zero only when both phasor amplitudes are zero. All that remains of the component nodal lines are their points of intersection and if there is sufficient amplitude these points are circled with elliptical fringes which may be used to compute the phase difference between the two component vibrations.

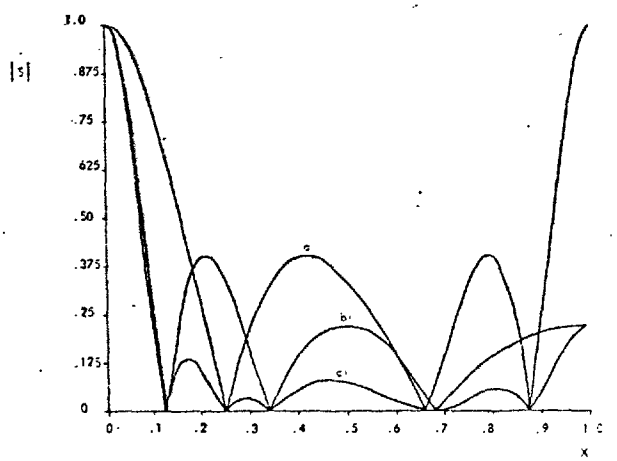
The situation is more complicated when the object is vibrating with several rationally related frequencies simultaneously, for example harmonics are a particular case. Wilson has shown that the fringe system resulting is dependent not only on the amplitudes of the respective modes but also on their relative phases (fig 13 ).




Magnitude of characteristic function of one half of a string vibrating simultaneously with amplitudes of one-half and one-quarter wavelength in fundamental modes, respectively. (a) $J_0$ product only, (b) next two Bessel-function products, and (c) five and greater-number Bessel-function products.

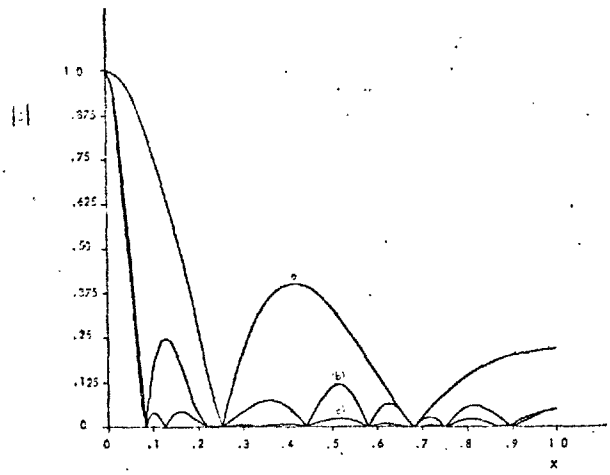
Figure 13 (a)

after A.D.Wilson




$J_0$ product of characteristic function for one half of a string, viewed and illuminated from the direction transverse to its axis and in the plane of vibration. One-half-wavelength amplitude of vibration of (a) fundamental and (b) second-harmonic mode, and (c), (a) and (b) simultaneously.

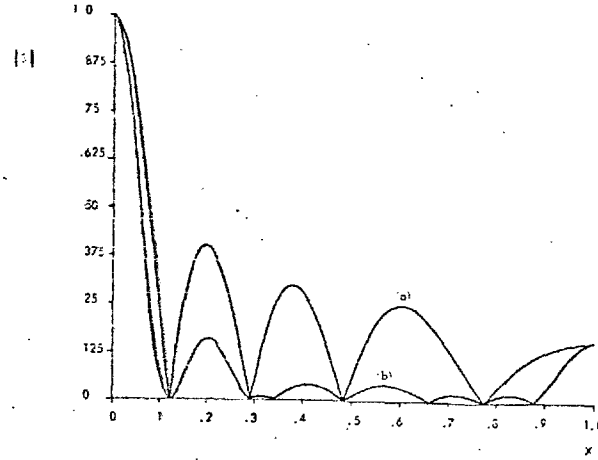
Figure 13 (b)




$J_0$ product of characteristic function for one-half wavelength of vibration in (a) fundamental mode, (b) fundamental and third harmonic simultaneously, and (c) fundamental, second, and third-harmonic modes simultaneously.

Figure 13 (c)

Figure 13 (d)




$J_0$ product of characteristic function for a vibration amplitude of (a) one-wavelength fundamental mode and (b) one-wavelength fundamental mode and one-half wavelength second-harmonic mode simultaneously.

The result is very complex, being the sum of a whole set of products of Bessel functions and exponential phase factors, the number of terms in each product is equal to the number of independent vibrations present. Stetson (1971) gives an even more general expression covering the case when the component vibrations are not sinusoidal. Wilson has worked out the fringe functions in a number of simple cases relating to a vibrating string and in every case the fringe visibility is drastically reduced when harmonics are present.

For each case described above, but particularly in the latter case, the fringe visibility is severely reduced and it is very difficult if not impossible to extract information about the different constituent vibrations from the fringes resulting in the presence of harmonics and other frequencies. It is therefore a serious disadvantage but it has a possible solution in the method described by Aleksoff (1971). Fringes due to individual simultaneous vibrations may be separated out by the method of multiple frequency phase modulation of the object wave - for small object vibration amplitudes. For example consider an object vibrating with just two frequencies given by:

$$\phi(t) = d_1\sin(w_1t + \theta) + d_2\sin(w_2t) \qquad (3.13)$$

now when the two object frequencies are rationally related (i.e. $f_1 = kf_2$ where k is an integer) then the 'beat' frequency $f = (pk-q)f_1 = nf_2$ w here p and q are integers. The Image Brightness Density or fringe function is proportional to:

$$J_p(d_1)J_{-pk+n}(d_2)e^{ip\phi} \quad 2$$

If the two frequencies were not rationally related then $f = pf_1 - qf_2$ and the IBD would be proportional to $J_p^2(d_1)J_{-q}(d_2)$

Now for small amplitude vibrations $J_o(d_n) \simeq 1$ and $J_n(d_n) = 0$ for $n > 2$ then at a frequency $f = f_1$ (say) the IBD is proportional to $J_1^2(d_1) = \frac{d_1^2}{4}$

Thus it is possible to filter out the component due to $d_1$ - removing that due to $d_2$ - by selecting that component of the optical frequency spectrum due to the frequency f. In general any order Bessel function may be picked out by frequency translating the reference wave (by $\Delta f$) to that order sideband of the optical frequency spectrum which is formed by the phase modulation of the carrier by the object vibration frequencies. This modulation, of course, produces a whole set of side bands corresponding to the different order Bessel functions. The frequency shifted reference beam hologram acts as a narrow band pass filter. The desired frequency shifts may be produced by a variety of effects, either for instance the doppler shifting of a Bragg cell - such as that used in the heterodyne detection systems described in appendix ( I ) - or by optical serrodyning whereby a sawtooth phase modulation is imposed on the beams, and the frequency shift can be made equal to the fundamental sawtooth frequency.

(iii) The sub-fringe technique of Metherell described in the next part may allow some phase information to be obtained as follows (this method has similarities with that of Aleksoff above). Vibrations whose amplitudes are less than half a wavelength of light are made visible by using an oscillating reference mirror, and information about the phase of the object vibrations may be obtained by noting the changes in the fringe pattern seen on inverting the phase of the reference mirror with respect to the object vibrations.

(iv) Another disadvantage of the time-averaged method is that the intensity of the fringes falls off with increasing amplitude of move - ment and soon becomes difficult to record on film and use for measure- ments. For example, the fringe intensity varies from 1 at zero amplitude position to .006 at fringe number 30 i.e. a ratio greater than 100:1. However from fringe number 10 to fringe number 40 the ratio

is only 5:1 (i.e.0.0225 to 0.0040). If the zero amplitude fringe could somehow be shifted to correspond to the 10 order fringe, much higher relative vibration amplitudes could be recorded and more easily studied. This effect would be achieved if the object were given piston motion or effective piston motion of the appropriate amplitude and phase (Fein and Green 1968). This piston motion may actually be imparted to the object, but the author suggests that the equivalent difference in phase may be applied anywhere in the object or reference beam paths by using a vibrating mirror as in Metherell's sub-fringe technique (1969), but with greater vibrational amplitude imparted to the vibrating mirror. Then a correspondingly larger number of fringes should be capable of reproduction. A similar result has also been achieved by the temporal modulation technique of Aleksoff (1971) described above, by making use of the fact that the primary maximum of the nth order Bessel function occurs for larger and larger values of the argument (i.e. the phase imparted to the object beam by the object's vibration) as n is increased Thus the brightest area of the reconstruction occurrs for larger and larger vibration amplitudes and also the brightness of succeeding fringes is more uniform. This nth order function can be selected by frequency shifting the reference beam by the appropriate amount. The theory of Wastrasiewicz et al (1971) on page ( 31 ) for long illumination duty cycle stroboscopy also gives a desensitisation result.

(v) Collins has shown (1968) that by altering the relative phase between the object and the reference beam by 180° between the two exposures necessary for a frozen fringe hologram, those parts of the object which remained undistorted or stationary will vanish on reconstruction. This phase shifting may be accomplished by varying the pressure in an air cell (Wilson and Strope 1970), and by utilising this device wide variations in phase may be produced if necessary. The theory is as follows:

Let the amplitude of the first reference beam be:

$$r = |r| e^{i\phi_r} \tag{3.15}$$

and that of the second be:

$$r_1 = |r| e^{i(\phi_r + \beta)} \tag{3.16}$$

Then the two image intensities are:

$$I_2 = I_{r_1} + I_{(o+\Delta)} + (o+\Delta)r_1^* + (o+\Delta)^* r_1 \tag{3.17}$$

$$I_1 = I_r + I_o + or^* + o^* r \tag{3.18}$$

Where 'o' is the amplitude of the light from the unchanged object and '$(o + \Delta)$' is the amplitude of the light from the distorted object, on summation therefore:

$$I_{tot} = I_r + I_{r_1} + I_o + I_{(o+\Delta)} + r^*(o+(o+\Delta)e^{i\beta}) + r(o^*+(o^*+\Delta^*)e^{i\beta}) \tag{3.19}$$

On developing the plate and reconstructing with the reference beam of amplitude 'r', from equation (2.6) and (3.19) the new image amplitude is:

$$I_r(o + oe^{i\beta} + e^{i\beta})$$

and its intensity is, neglecting the reference beam intensity:

$$I_{image} = |o(1 + e^{i\beta}) + e^{i\beta}|^2 \tag{3.20}$$

Now let the phase of the reference beam change by $180^\circ$ between exposures i.e. $\beta = \pi$, the resulting image exposure is then $|\Delta|^2$, being the change in the amplitude of the object light between exposures.

## 4) Alterations in Sensitivity

This part covers one or two techniques for altering the number of fringes, seen on the reconstruction, for any given magnitude of object movement. For precision work and for very low amplitude studies, such as the measurement of loudspeakers at high frequencies, more fringes may be desirable per unit displacement. For engineering inspection work and for large amplitude vibration studies, such as loudspeakers at low frequencies, far fewer fringes per unit displacement are necessary. Holographic

interferometry as such may give more information than is necessary for some applications and perhaps one of the related methods described in Appendix ( I ) could give the answer more rapidly and with less calculation, In the present experiments the 'straight' holographic method was used as most of the work described covered vibrations whose ranges of amplitude variation were approximately correct for the sensitivity of normal holography.

4.1) Methods for Increasing Sensitivity

(i) The technique of subfringe holography has recently been described by Metherell et al (1969). This technique may be applied to both time-average and stroboscopic methods and can increase the sensitivity to allow movements of as little as 3 Å to be recorded. This technique is related to that of Aleksoff described below.

With the time averaged technique the image intensity (fig 14 ) follows the well known (Bessel function)$^2$ relation. If the object vibrations are less than a wavelength of light in amplitude, the brightness of the reconstruction at points of object movement is only slightly less than the brightness at points of no object movement - point A in t he figure. As may be seen, the steepness of the 'image brightness intensity - object movement' curve in the neighbourhood of A is slight and very little change in image brightness will occur for movements of up to 1/10 of a wavelength. What is needed is some way of pushing the zero movement datum down the slope to the approximately linear region of the central peak at B. This is accomplished by placing a mirror in the object or reference beam paths and vibrating it with the required amplitude and phase. The amplitude in this case is less than a wavelength. In (3·3,iv) above a similar technique is described involving a vibrating mirror whose amplitude of vibration isseveral wavelengths in magnitude.

By changing the phase of the oscillating mirror certain parts of the object become dark and other parts become light and so information about the relative phases of various regions of the object may be extracted. With very small movements the contrast of the fringes may be improved by coherent optical filtering using a D.C. stop in the Fourier transform plane of a lens imaging the fringes. The overall grey background is then removed and the spatially varying parts of the image (the fringes) are more clearly seen.

(ii) A method of temporally modulated holography (Aleksoff 1971) whereby the sensitivity of time averaged holography may be greatly increased - indeed by the same order of magnitude as the (similar) subfringe technique described above - allowing vibrations as small as $\lambda/100$ i.e. about 60 Å to be recorded. The sensitivity may be increased still further when better techniques are available to maintain a dark background and if optical filtering techniques are used to remove some of the D.C. 'fogging' illumination.

This method which is analogous to the heterodyne detection systems described by Avsec et al (1969) and Korpel (1969), has the frequency shift carried out with an electro-optic modulator rather than a vibrating reference mirror or Bragg cell. For small values of the argument $\phi$ (where $\phi = (2\pi/\lambda)\ 2d$) and d is the amplitude of the vibrations, the zero order Bessel function $J_0$, which is normally used in time averaged holography, is essentially equal to unity, but the first order Bessel function $J_1$ is directly proportional to $\phi/2$. At these low amplitudes therefore, when the first order Bessel function is filtered out by the method of reference beam frequency shift to select the appropriate optical frequency sideband, changes in image brightness are directly proportional to changes in object vibration amplitude.

(iii) A method described by Wuerker Heflinger and Briones effectively doubles the sensitivity of the stroboscopic technique by recording holograms in ultra-violet light.

Red light from a 'Q' switched ruby laser is passed through a crystal of KDP. This crystal generates second harmonic ultra-violet light of wavelength (3471 Å). Two holograms are then simultaneously recorded using one 50 ns pulse on an ordinary 649F plate, and then the resulting two virtual images are reconstructed with a helium-neon laser giving wavelength (6943 Å). The two images may easily be spatially separated because the 'ultra-violet' hologram diffracts light at twice the angle of that diffracted by the'red' hologram, whose fringes may be used as a check.

The intensities of the red and ultra-violte illuminating beams were ballanced by inserting glass windows to absorb sufficient of the ultra-violte light. For good quality ultra-violet holograms special lenses should be used where necessary.

(iv) A method which does not actually increase the fringe sensitivity but which may make two beam (i.e. stroboscopic) fringes more easily seen operates by converting them to multiple beam fringes by utilising photographic non-linearities and a diffraction grating. This method has been described by Matsumoto (1969). See also the laser scanning methods of Korpel et al in Appendix ( I ) which are more sensitive than any straightforward holographic technique.

4.2) <u>Methods for Reducing the Sensitivity</u>

(i) The most powerful technique for desensitising time-averaged holography has been described once again by Aleksoff (1971) using one of the variations of temporally modulated holography. This technique when

properly used can also give information about the absolute motion of a vibrating surface as well as the relative motion between its parts. This absolute piston motion on which the relative (fringe) motion is superimposed results in there being no observable stationary point from which to count fringes unless the experimenter is lucky and either part of the surface itself is stationary or, in the case of Loudspeakers the surround may be seen clearly and fringes counted from the stationary chassis - this is in fact the case for the time averaged studies described in Section (IV).

The technique relies on the fact that the primary maximum of the nth order Bessel function (which is the brightest area in the reconstruction) occurs for larger and larger values of the argument $\emptyset$, and $\emptyset$ is proportional to displacement, as n increases. Thus practically any desired sensitivity and vibrational amplitude for the appearence of the initial brightest fringe can be chosen by utilising the appropriate order Bessel function. This function may be picked out of the many side-bands, which correspond to high order Bessel functions, produced by the phase modulation of the object vibrations onto the optical carrier. The desired order may be picked out,as described above, by frequency shifting the reference beam by the correct amount. This effectively converts the hologram into a band pass filter allowing the desired sideband of the object spectrum to be filtered out. Aleksoff calls these holograms Single Sideband Supressed Carrier n order holograms from the analogy communication using radio waves.

(ii) The second method relies on the use of oblique illumination and viewing. The most famous example of this technique has been described by Archbold and Ennos (1968) where it has been used for the inspection of cylinder bores where the main aim was to allow similar cylinders to be directly compared, the reduction in sensitivity being in fact less

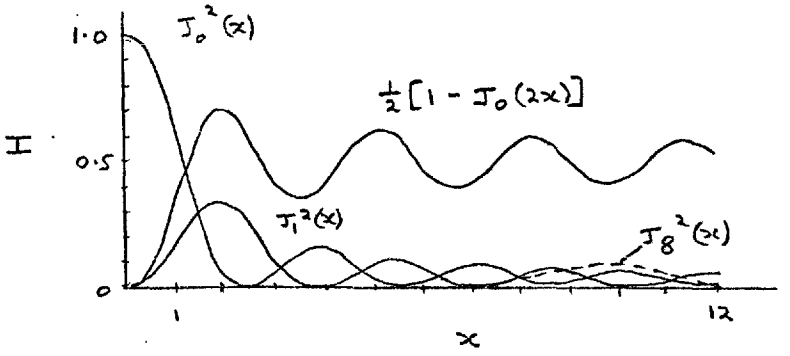



Figure 14a Some Bessel function plots(after Aleksoff)

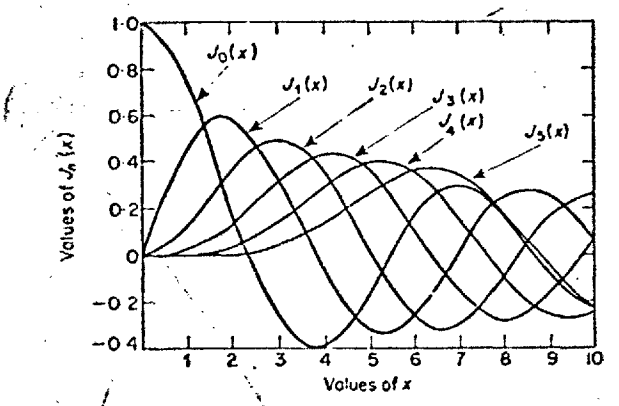



Figure 13. Plot of Bessel functions.

Figure 14 b Further Bessel function plots

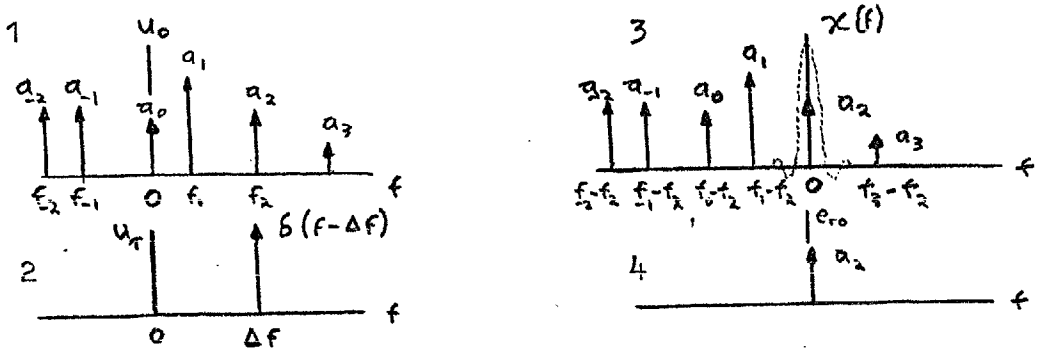



Figure 14 c (1) The object wave spectrum (2) The reference wave spectrum (3) The beat spectrum between object and reference (4) The resultant = desired sideband

important. With their technique (fig 15) an expanded laser beam passes through an annular conical lens which redirects it as a conical collimated beam onto the cylinder walls at an angle of $6^{\circ}$ off grazing incidence. The reference beam is derived from the central part of the beam which is expanded by a spherical concave lens. Contour spacings of half a micron have been demonstrated with this method. By inverting the illuminating annulus (fig 15) the fall in illuminating intensity with increasing initial beam radius may be compensated for by the reduced area that the beam has to fill after inversion.

(iii) A method which has a considerably lower sensitivity is the method of 'non-holography' (Redman et al 1969). This technique is limited to small objects or objects whose extremities or gross motions are of interest. The object moves by such a large amount duing the exposure, that no hologram of it is reconstructed. However, if the bright background is sufficiently stationary the moving object leaves a three dimensional holographic shadow against the stationary background. This shadow trajectory may be studied as if it were an actual hologram. Surface features and movements of the object surface will be lost but the gross movements and movements of extremities will be preserved, allowing low frequency oscillations of the whole object to be followed as the object moves along its trajectory.

Moire Techniques

The remaining desensitisation techniques rely on the formation of moire fringes between a set of lines connected in some way with the undistorted object and a corresponding set connected with the distorted object. The techniques differ in the ways in which the grilles are formed on, or related to, the object.

(iv) Hovanesian and Varner (1968) use the moire fringes formed

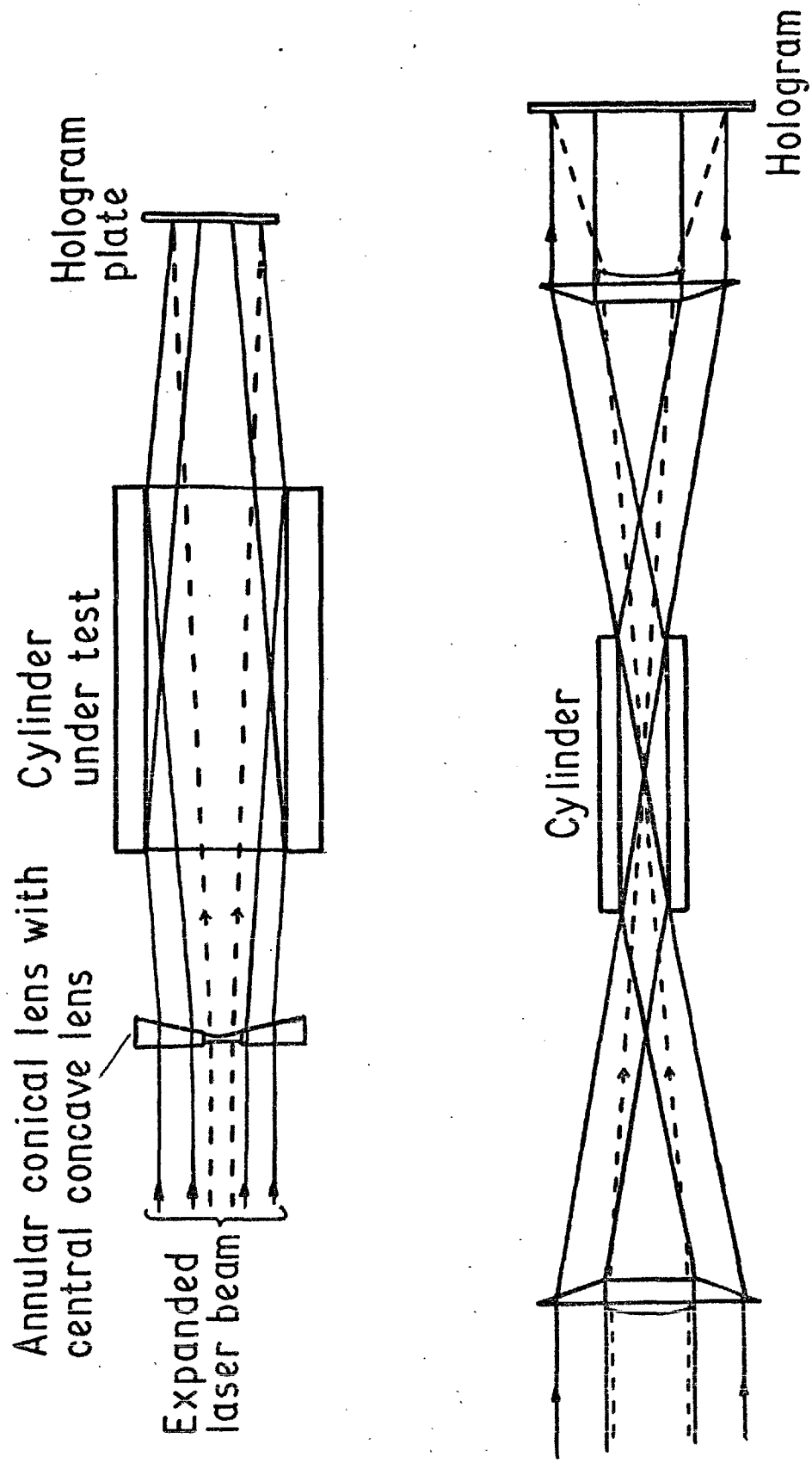



Figure 15 Two systems for making holograms of cylinder bores - also giving desensitisation

between two sets of 'contour fringes' formed on the object. The object is first holographically recorded using light of wavelength . The photographically processed plate is returned exactly to its former position and the reference beam mirror is rotated to position $M_2$. The object and hologram are then illuminated with light of wavelength and real time contour fringes are seen on the object when looking through the hologram. Each fringe occurs at a constant distance from the hologram and the distance between fringes depends on the wavelength difference and, of course , the shape of the object. A photograph is taken of the object plus fringes, the object is distorted and the whole procedure is repeated. Finally the two photographs are superposed and the object strain ( or frozen vibrational amplitude) is computed from moire fringe theory (Theocaris 1968). Alternatively quadruple exposures will result in frozen fringes being seen. The sensitivity depends on the contour pitch and therefore the wavelength difference.

Another method of forming the contours necessary for this method has been described by Tsuruta and Shiotake (1967). In this case fringes are formed firstly by exposing the photographic plate to the object immersed in one gas and then re-exposing with the object immersed in a gas of different refractive index. For instance, if air and $SF_6$ are used the 1 percent difference in their refractive indices produces beats (fringes) between their wavelengths separated by about .58mm. Practically any contour spacing may be achieved within a given range by using different gases or mixtures of gases.

Varner (1969) and (1970) has shown that by using two liquids or a liquid and a gas, wide variations in contour spacing may be achieved i.e. from $.75\lambda$ to $300\lambda$, these allow a correspondingly large variation in sensitivity. The moire fringe function resulting with this method

is given by $\cos(\Delta k \Delta z)$, where $\Delta z$ is the object movement and $\Delta k$ is the difference in the wavenumbers in the two fluids. The expression has a basic period ( fringe spacing) of $\lambda^2/\Delta\lambda$ .

The advantage of the two wavelength technique is that it allows the object to be 'contoured' in their own environment. The contour spacings, however, are limited to the laser lines available - the liquid-gas techniques allow almost any desired contour spacing to be achieved. Multiple exposure moire techniques rely on the interference between terms being independant of the fine surface structure of the object. If the object is sufficiently distorted that no correlation exists for a given resolution cell between the distorted and the undistorted state, then this method is of arguable application.

(v) Brooks and Heflinger utilise the moire technique in a different way (1969). 'Light sheets' formed by the interference between two coherent beams of light are projected onto the object. A laser beam is directed into a twyman green interferometer and then passed through a beam expansion system which projects the resulting sheets onto the object. The object is then viewed by a combination of telecentric lens and camera, the telecentric lens maintaining the apparent direction of view constant over the whole object. A master negative is taken of the whole object covered with its light sheets, and then returned to its original position When the object is viewed through this master negative it appears to be uniformly dark. Only positions of object movement are seen as the projected light sheets move out of register with the master negative. If the distance between the light sheets is 'd' and $\phi$ is the angle between the normal to the light sheets and viewing axis, then the contour spacing is $\delta = d/\cos\phi$. For example with d = .33mm and $\phi = 40^{\circ}$a shift of one fringe means an object movement of .43mm in the direction of view

(vi) Another technique involving a grid projected onto the object has been described by Hovanesian and Yung (1971). This has the advantages of continuously variable sensitivity, interferometric stability is not required and real time viewing of time averaged fringes is achieved without stroboscopy! Incoherently formed light sheets are projected by a transparency projector at a large distance from the object (to ensure minimal variation normal to the object).The resulting grid falling on the object is viewed at an angle from the illuminating wave normal. Moire fringes may now be formed between a photograph of the original and the new or distorted object. However, for the fringes to be visible, the original grid must also be visible and this limits the sensitivity when linear recording is used. This limitation is overcome by an intensity multiplication provess which also allows real time view ing. It may also be overcome by simultaneously superposing two object distorted gratings by means of a beam splitter and also by projecting two identical grids at equal angles of incidence to the viewing normal. This latter method doubles the sensitivity. When used for vibration analysis time averagedd fringes exactly analogous to Powell and Stetson fringes may be photographed, or if the grid is resolvable by eye, seen in real time - a major advantage. By using a transmission filter in the camera and viewing through this the fringes may be seen even when the grid is not resolved by eye.

(vii) Burch (1968) has been working on a technique involving the formation of a grill on the object utilising photoresist. This substance, when exposed to light becomes resistant to chemical attack. However, practical problems involved with this method have until the present time proved difficult to resolve.

(viii) Several variations on the straightforward double exposure holographic technique involving moire fringes have been suggested by

Hovanesian and Varner (1968), In their first technique a grille is formed on the object by rotating it between two holographic exposures. The photographic plate is exposed to the object which is then rotated through a small angle about an axis in its surface ( say). The photographic plate is then re-exposed. On reconstruction the object image has a linear fringe system superimposed in or near its surface, the spacing of these fringes (grille lines) is determined by the angle of rotation but may not be made arbitrarily large. A photograph can be taken of this master grille on high contrast film. A second photographic plate is then re-exposed to the distorted object rotated through the same angle as before (the hologram itself may be rotated about an axis in its plane with the same result), a photograph is taken of the new fringes produced. When the two photographs are superposed moire fringes are seen from which the distortion may be computed.There is a resolution cell correlation limit to the amount of rotation which may be used however.

A triple exposure technique using two reference beams allows frozen moire fringes to be produced. The first exposure is taken with two reference beams, the object is rotated and the second exposure is taken with the other reference beam. Reconstruction with both referenne beams gives the frozen moire fringes. The third exposure may, of course, be of the stroboscopically frozen vibrating object.

By studying their local curvature, moire fringes may be used to find positive and negative displacements of the object surface, i.e. the relative phases between various parts of the object.

Some of the methods detailed above have been applied to the study of vibrating discs and Loudspeaker cones. The particular techniques used are found described in more detail in Sections III and IV below.

# SECTION THREE

# EXPERIMENTS ON CIRCULAR PLATES

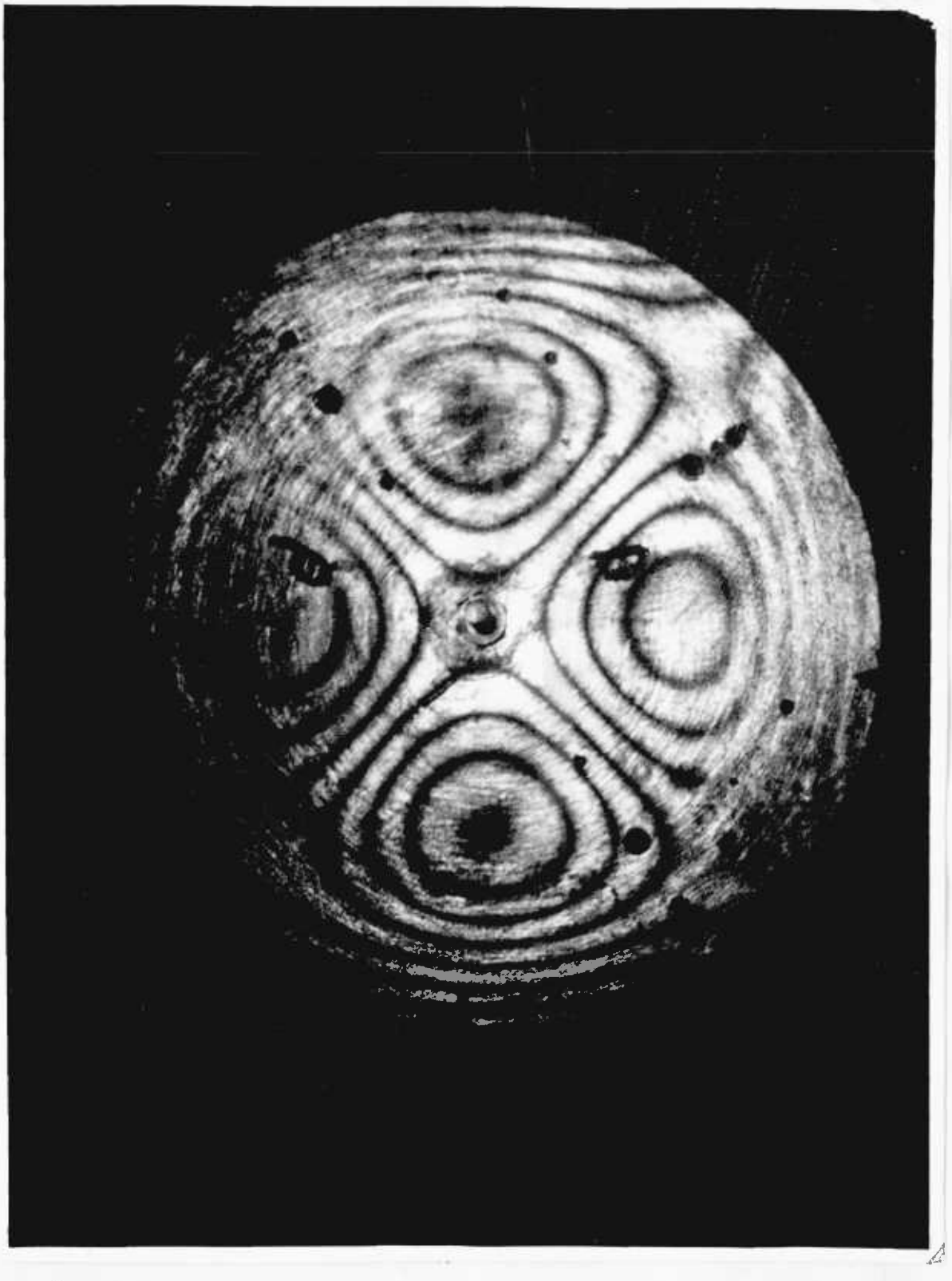
Contents - Section 3 - Experiments on Circular Plates


| | | |
|---|---|---|
| Introduction | | 64 |
| 3.1) | Development of a Plate Exciter | 65 |
| (i) | Introduction | 65 |
| (ii) | Impulsive Excitor | 66 |
| | (a) Design Requirements | 66 |
| | (b) Design Adopted | 67 |
| | (c) Rise and Contact Time Measurements | 69 |
| | (d) Energy Fed into the Plate | 69 |
| | (e) Sound Output | 71 |
| | (f) Shape of the Pulse Waveform | 72 |
| (iii) | Continuous Wave Excitor | 73 |
| 3.2) | The Reverberation Room | 74 |
| (i) | Discussion | 74 |
| (ii) | Reverberation Room Criteria | 75 |
| | (a) Diffusiveness | 75 |
| | (b) The Reverberation Time | 77 |
| | (c) The Size of the Room | 79 |
| | (d) Source Position | 80 |
| (iii) | Reverberation Room Construction | 80 |
| (iv) | Measurements | 82 |
| | (a) Reverberation Time | 82 |
| | (b) Average Sound Pressure Level | 84 |
| 3.3) | Apparatus Used | 87 |
| (i) | Overall Layout | 87 |
| (ii) | Details of the Apparatus | 88 |
| | (a) Holographic Table | 88 |
| | (b) The Laser(s) | 89 |
| | (c) The Optical System | 90 |
| | (d) The Shutter Mechanism | 90 |
| | (e) The Object Plate | 90 |
| | (f) & (g) Excitation and Microphone | 91 |
| | (h) Photographic Plate Holders | 91 |
| | (i) Scanning Discs and Motors | 93 |
| | (j) Motor Stand | 96 |
| | (m) Amplifiers | 97 |
| | (o) Spectrum Analyser | 98 |
| | (q) Frequency Divider | 98 |

| | | |
|---|---|---|
| 3.4) | Experimental Method | 99 |
| (i) | The Stroboscopic Method | 99 |
| (ii) | Simple Scanning System | 102 |
| (iii) | Stroboscopic Law | 103 |
| (iv) | Upper Frequency Limit of Disc Stroboscopy | 104 |
| (v) | The Time Averaged Method | 105 |
| (vi) | Plate Modes Studied | 106 |
| 3.5) | Results and Calculations | 107 |
| (i) | Power Level Calculations | 107 |
| | (a) Example Calculation | 108 |
| | (b) Variation in Calculated Power Levels | 109 |
| (ii-v) | Results Tables | 110 |
| (v) | Notes on the Results Tables | 112 |
| (vi) | Average Radiated Acoustic Power per Mode | 113 |
| 3.6) | Conclusions | 115 |
| | Suggestions for Further Work | 116 |


Total Number of Pages: 76

Plate Number 4



Frozen Fringe Hologram - Disc Vibrating at 3380Hz

## EXPERIMENTS ON CIRCULAR PLATES

### Introduction

This section covers the holographic investigation of modes of a circular plate, and associated measurements of the sound power output of each of the modal frequencies. The first part of the section describes the development of an impulsive excitor with the object of simulating many of the impulsive forces present in gear action, and also the development of a continuous excitor . The continuous excitor proved to be the most useful in practice but a few experiments carried out with the impulsive excitor, in which the frequency spectrum of the excitation is derived and the liklihood of plate mode excitation by such a spectrum is briefly discussed. (see also Appendix II). Holograms taken with the impulsive excitor showed that the fundamental was the main modal contributor to the actual object vibration amplitude, but response curves indicated that there was indeed a tendency for plate modes to be excited if they coincided with harmonics of the impulsive excitation. The conditions of excitation and support favoured the sole excitation of axially symmetrical modes.

The second part of this section describes some of the factors which must be considered in the design and use of reverberation chambers and these factors are then applied to the actual reverberation room which was unfortunately rather small due to spatial and financial restrictions. Never-the-less definite trends in the relative output of the plate modes could be derived from the holographic and sound pressure level measurements taken. The third part describes in detail the rest of the apparatus used , both holographic (with particular reference to Section II) and acoustical. Part 4 describes the experimental methods used for live,scanned, and stroboscopic holography and the actual method used for taking the sound pressure level measurements

The theory of scanned holography is described in more detail in Section IV. Finally in this section the results are presented and a few brief conclusions drawn. The results are considered more fully in Appendix II .

## 3.1) Development of a Plate Excitor

### (i) Introduction

Two types of plate excitor are required for these experiments, one to simulate the impulsive part of gear excitation, and the other to excite single plate modes purely and without interference with the vibrations themselves. The second continuous excitation system, which was in fact more used than the first, was developed using most of the parts of the impulsive excitor and therefore the impulsive one will be described first.

The methods commonly used in plate research for object excitation are musical instruement bows and the solid carbon dioxide method of Waller (1962). These methods have the advantage of not having natural frequencies of their own, and thus plate modes are excited depending only on the place of excitation and the conditions and places of support. However, these methods are not at all impulsive, neither are they convenient or sufficiently stable for controlled laboratory use as continuous excitors - especially when needed for holographic investigations, where the amplitude of the vibrations must be controlled during the exposure time, so these methods were dismissed.

Transducers such as piezo-electric crystals have a limited frequency response for the reproduction of suitable pulses and when plate resonances occur have difficulty in handling the large amplitudes of movement which occur, in fact in ultra-sonic work they are usually usedd at their own resonant frequencies. Large crystals, possibly having adequate power handling, would load the plates unduly. 'Prodders and

bangers' pushed by cams would prove unstable and would chatter. Gear action itself would be suitable were it not for the rotations involved which make mode visualisation difficult (though a method has been devised recently by which holography may be carried out on rotating objects - Tsuruta and Itoh 1970) and there are too many factors involved in the excitation mechanism for it to be used in a controlled experiment at this stage.

There are many methods of dropping or forcing a ball repeatedly onto a plate in a controlled manner and indeed the dropping ball has been used to calibrate transducers (Shweppe 1958). The bouncing ball has the desired characteristics for an impulsive excitor and so after several experiments with alternative systems this was the method which was chosen and developed as described below. This device enables repeatable and controllable short pulses to be applied to the test plate, and can be considered to be an approximation to the pitch line shock and tooth contact excitation frequencies which are an important factor in the excitation of gear wheels. The input power, the frequency, and the point and direction of application can be easily varied and the contact pulse is sharply defined. The bouncer is an extension of the bouncing ball electric pulse generator described in Electronics Letters (1966)

(ii) <u>The Impulsive Excitor</u>

The electrostatic repulsion used in the original design was replaced by electromagnetic attraction, the restoring force being supplied by spring loading, magnetic attraction and also by gravity when the device was used vertically.

(a) <u>Design Requirements</u>

1) The ball must strike the plate at a regularly maintained frequency
2) The velocity of impact must be variable
3) The frequency of bouncing must be variable.

4) The whole device must be simple and easily adaptable to continuous excitation.

5) The pulses produced must be sharp and of known shape.

6) Subsequent pulses must be of the same hight, be applied at the same point on the plate at regular constant intervals - this is necessary for holographic applications.

(b) Design Adopted

A relay coil of 15 ohms impedance (specially wound) is suspended above the ball bearing which is attached to a divided light rigid arm made of tubular aluminium (fig 16 ). The arm passes through the main framework where it is attached to another tubular arm at right angles to it. This is fixed at each end by ball races and is therefore free to rotate thus allowing the ball to move along a short vertical arc of a circle. The ball races are attached to a block through which pass the three main members of the device. The block may be attached to either the moveable central members, or to the two fixed outer members. The central member is supported by a spring at its lower end, and is held against this by a micrometer head at its upper end. Thus the central member may be accurately moved up and down relative to the two outer members which are rigidly attached to the base plate. The relay is attached to a block above that by which the arm and bearings are supported. Other blocks allow magnets, springs, etc. to be similarly held and accurately moved relative to each other. The whole device is very massive and thereby allows little motion to be imparted to the ball other than that desired. The overall bouncer device has supports to enable it to be mounted either horizontally or vertically.

The relay coil was wound to match the output impedance of the audio amplifier used and was fed with a sine wave. The amplifier, having

Ball Bouncer Final Design

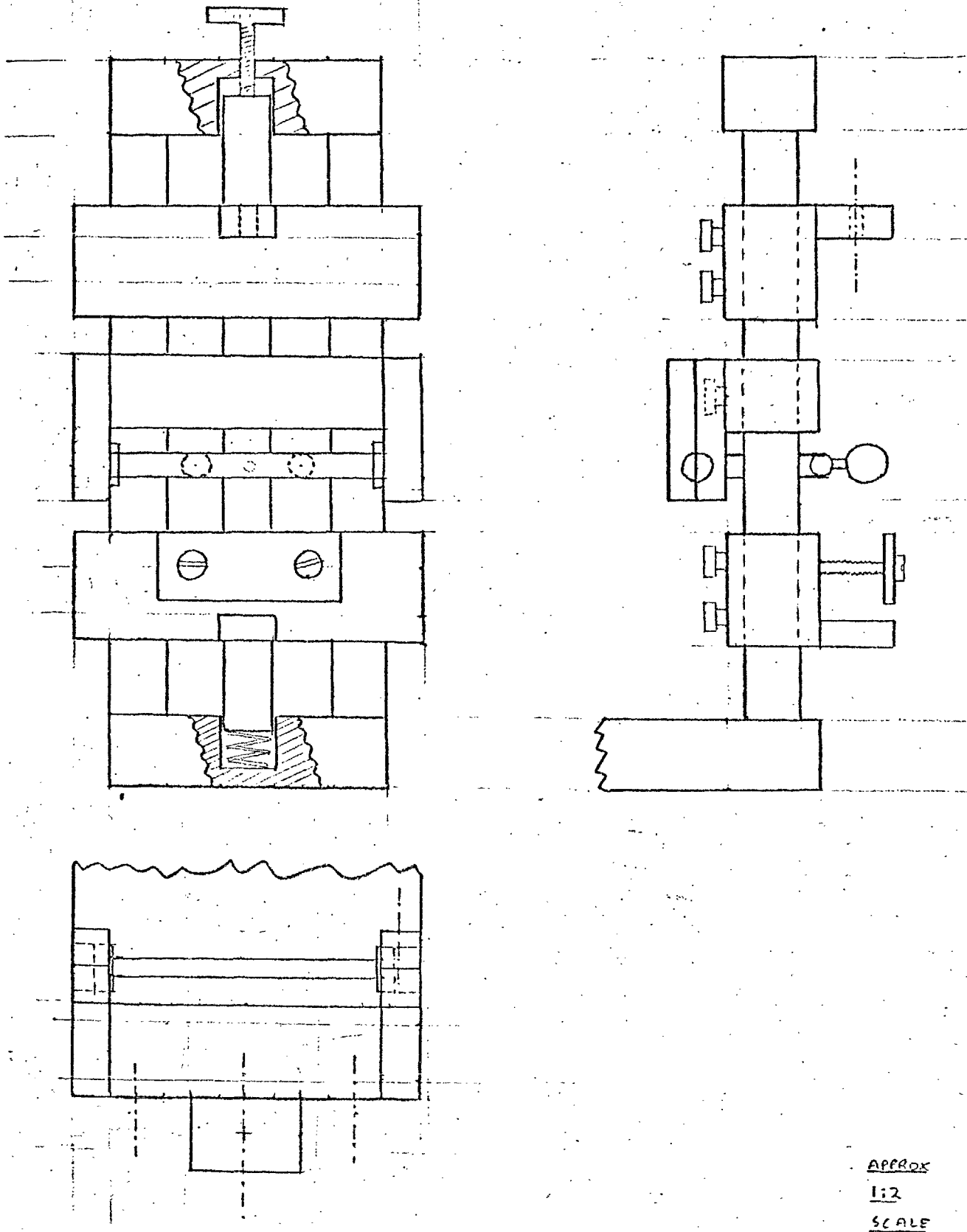



Figure 16 Impulsive Plate Excitor

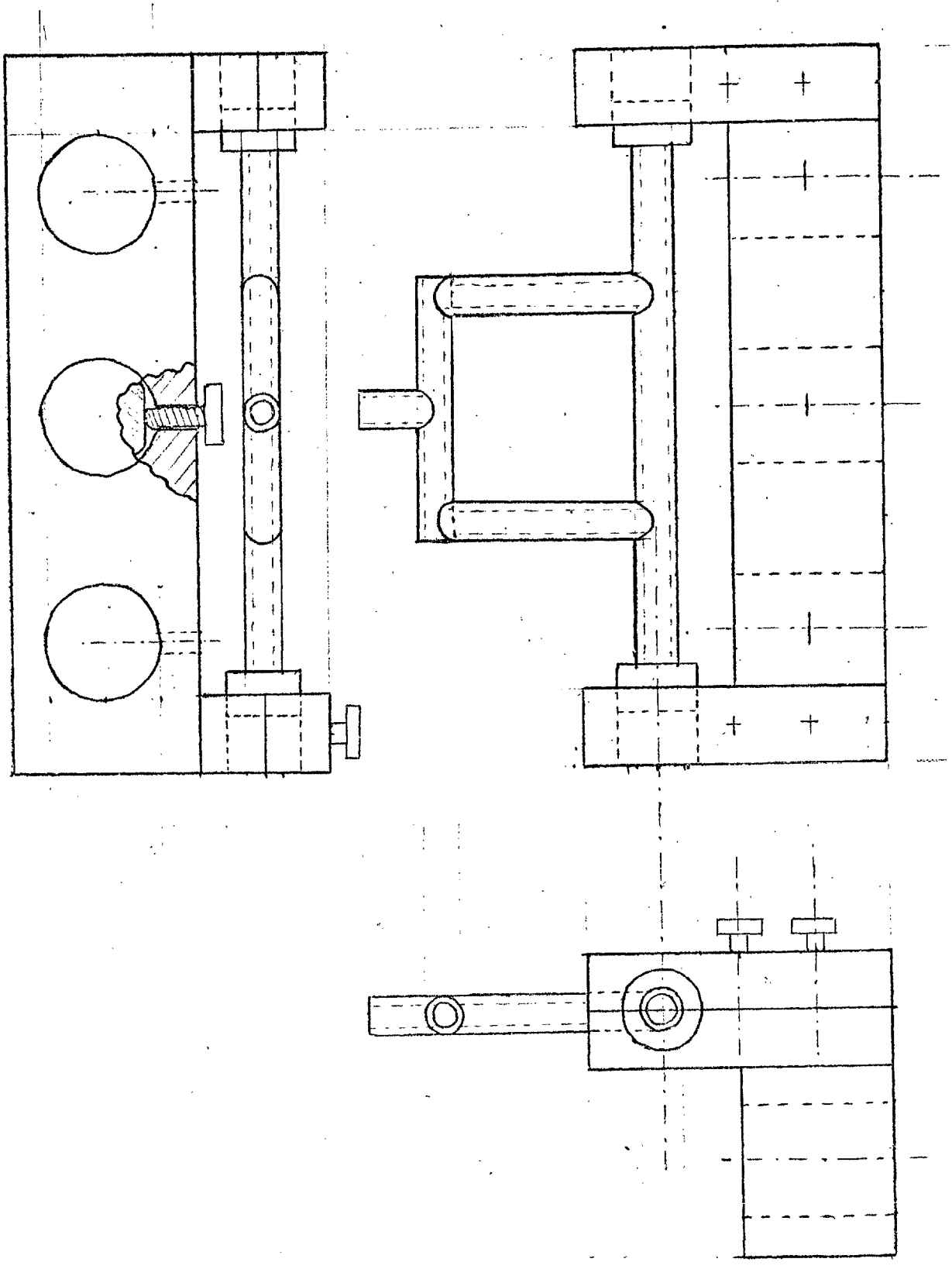
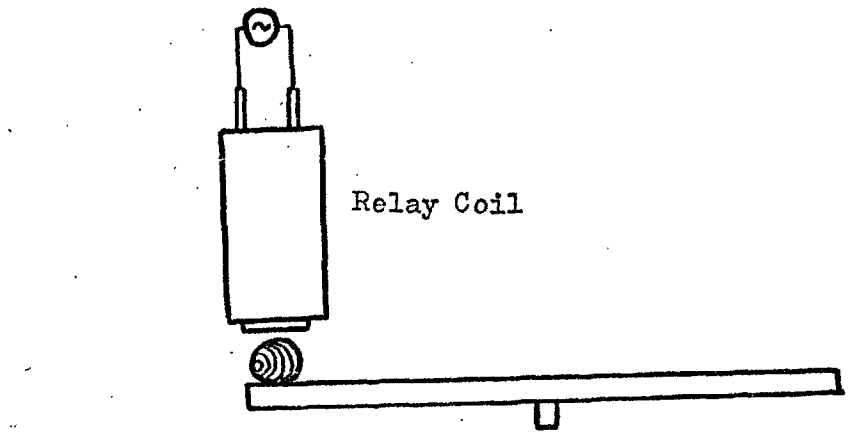


Figure 16 (b) Details of 'bouncer' axle

an output power of 100 watts was specially built and incorporates fixed bias in the output stages for maximum power output. Experiments with different wave shapes and with triggering mechanisms showed that a simple sine wave gave the best results. The sine waveform alone produced a 'cusp train' force waveform at twice the excitation frequency as shown in fig (17). Experiments with DC fed coils, permanent magnets and spring loading the lever arm, together with various combinations of all three resulted in the final combination shown in fig (18). The relay coil is polarised by a permanent magnet fixed above it and this renders the force waveform sinusoidal. Experiments with a stroboscope allowed the various parameters to be adjusted for the best ball bouncing action, i.e. the ball should not spend its time either stuck to or near to either end of its traverse.

The natural frequency of a ball bouncing under effective gravitational attraction 'g' to a height 'h' on a plate with a coefficient of restitution of unity is proportional to $1/\sqrt{R}$ that is: $h \propto g/f^2$. This means that as the frequency increases the height from which the ball bounces rapidly decreases and therefore the maximum gap between the pole piece and the plate will have to be reduced accordingly. The gap can of course be less than the maximum, when the ball will spend more time at either of the two ends. However if the gap is increased beyond the maximum the ball will merely rest at either end. If the ball is bouncing on a plate with a high 'Q' such that the fundamental or a harmonic of the pulse train produced by the bouncing action is near to a plate resonant frequency, then the ball will either oscillate sporadically, or the ball will be caused to oscillate at the same frequency. A wide maximum possible gap is therefore required so that the gap may be made less than this ensuring that the bouncing frequency is less dependent on the gap size. A wider gap also allows the velocity of the ball and hence the



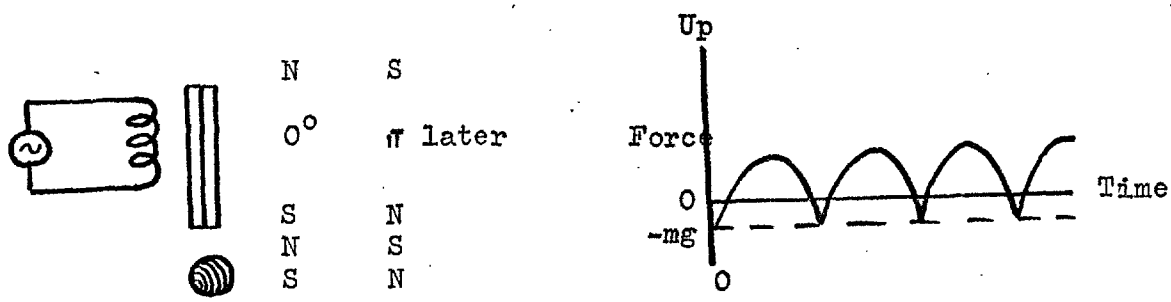




Figure 17 (a) Cusp train force history when only relay coil used

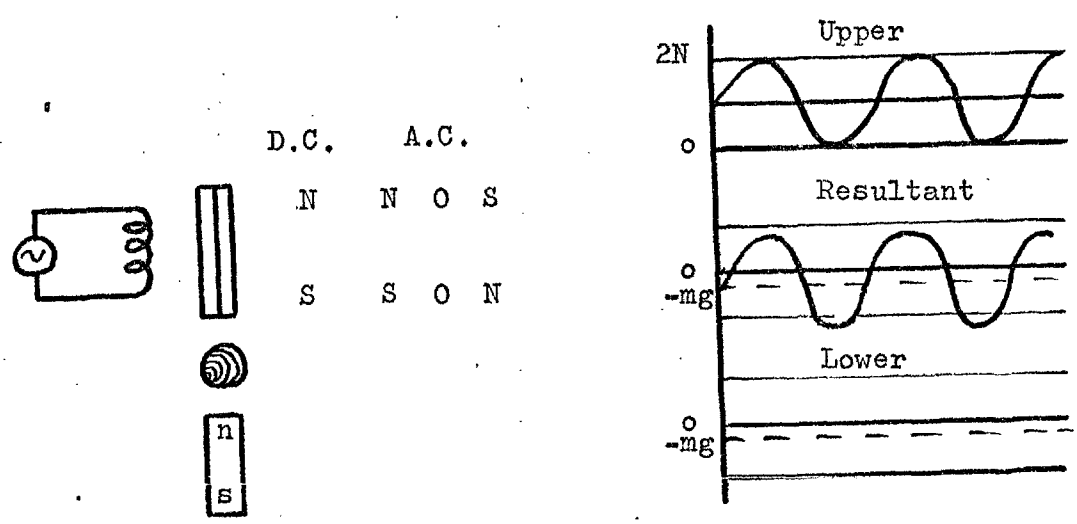



Figure 17 (b) An arrangement to render the force history sinusoidal ('mg' effectively increased by springs in Figure 18)

power fed into the plate at each impact to be increased.

The only way to increase the gap is to increase the effective acceleration due to gravity. This may be accomplished by pulling the ball downwards with a spring attached to the lever arm. Placing a permanent magnet below the plate also allows a larger gap for a given frequency, although the downward pull due to this magnet acting on the ball will to some extent be ccancelled by the upward pull induced in the relay coil by the top permanent magnet.

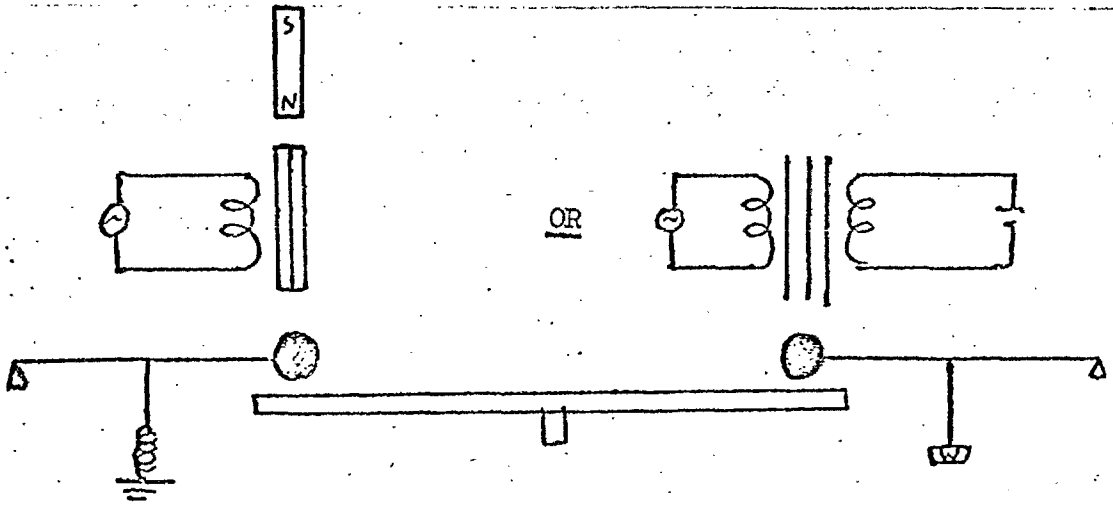
(c) Rise_and_Contact_Time Measurements

The circuit shown in fig (19) was set up. This enabled the contact time to be measured and it was found to be of the order of 100 microseconds with an aluminium plate whose coefficient of restitution was .2 . The voltage rise time was extremely sharp and could not be measured with the equipment available. The voltage decay time was longer however. The shape of the pulse derived from the apparatus is shown in fig (20).It is to be expected that the contact time will be much less with materials like glass which has a much higher coefficient of restitution (of the order of .8 with an impacting steel ball). The relation between these factors is described below.

(d) Energy_Fed_into the Plate

The energy fed into the plate by the bouncing ball may be calculated (if required) from measurements of the contact time which is itself related as follows to the velocity of impact by the Hertz theory. The contact time 't' is proportional to (impact velocity 'v')$^{1/5}$ or more exactly:

$$t = 2.943 \left[ 2.5\pi\rho \frac{(1-\nu^2)}{E} \right]^{2/5} Rv^{-1/5} \qquad (3.1)$$



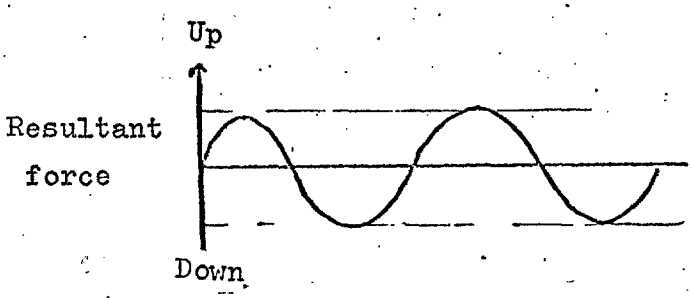




Figure 18 An arrangement of magnets and springs to give a sinusoidal force waveform.

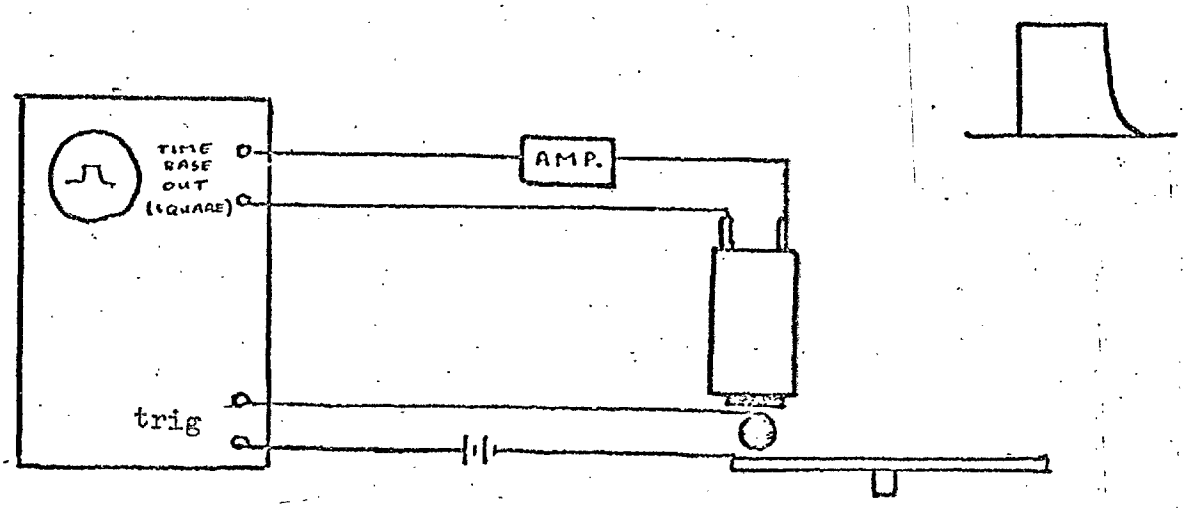



Figure 19 Block diagram for rise and contact time measurements

Where R is the radius of the ball. This is correct, according to Lifshitz and Kolsky (1964), for up to eight times the velocity corresponding to elastic yield at the point of impact. They also showed that the coefficient of restitution is dependent to a very great extent on the surface finish, much energy being expended in flattening surface asperities.

Zener (1941) gives a theoretical expression for the coefficient of restitution 'e' which almost agree with the practical results of Tillett (1954) for the variation of e with plate thickness:

$$e = \frac{1-R}{1+R} \quad \text{where} \quad R = 2\chi \frac{\int v^3 dt}{(\int a^{3/2} dt)^2} \tag{3.2}$$

$$\text{and where } \chi = \frac{\pi^{3/5}}{3^{1/2}} \left(\frac{r}{2R}\right)^2 \left(\frac{v_0}{v}\right)^{1/5} \left(\frac{\rho_1}{\rho_2}\right)^{3/5} \left(\frac{E_1'}{E_1' + E_2'}\right)^{2/5} \tag{3.3}$$

$$\text{where} \quad E_1' = \frac{E_1}{1-\nu_1^2} \qquad 1 \text{ for ball, } \quad 2 \text{ for plate.} \tag{3.4}$$

For small $\chi$ R tends to .42 as $\chi$ tends to 0 and therefore:

$$e \longrightarrow \frac{1-.84\chi}{1+.84\chi}$$

which is close to the value given by Raman (1920)

Contact time and coefficient of restitution measurements are described by Lifshitz and Kolsky (1964) and Tillett (1954) and an ingenious method of measuring the impact velocity (which is related of course to the height h from which the ball has been dropped under gravity) has been described in a recent Ph.d thesis (reference unfortunately mislaid). A grating is attached to the impacting sphere and a beam of light focussed onto it, this light passes through the grating, whose plane is perpendicular to ball surface, and falls onto a photocell. The frequency of the cell output being directly proportional to the impact velocity.

Sinclair (1964) quotes workers who have derived expressions for the energy fed into a plate by an impacting sphere and gives expressions for the displacements of the waves produced by the impact. Tillett

(1954) has shown that 70 to 80 percent of the injected energy is dissipated as shear waves at an 'equivalent frequency' approximately equal to 1/2t, where t is the contact time, at which the energy loss per cycle W is:

$$W = -A^2\pi\left(\frac{\eta w}{1-\left(\frac{\eta w}{E}\right)^2}\right) \qquad (3.5)$$

where E and  are the elastic modulus and shear viscosity associated with a Maxwell element (of a Maxwellian solid) and the displacement $x = Ae^{iwt}$. Therefore:

$$W \propto 2\pi\int_0^\infty \frac{\omega t}{1-\omega^2 t^2}\,\phi(t)\,dt \qquad (3.6)$$

where $\phi(t)$ is a function defining the relaxation time spectrum. Sinclair quotes Hunter's result (1957) for the energy absorbed by the vibrations at frequency w. The expression is very complicated but may be greatly simplified by taking particular force time histories, for example the expression becomes:

$$W = \frac{\rho(1+\nu)}{\rho c_0^2}\left\{\frac{1-\nu^2}{1-2\nu}\right\}^{\frac{1}{2}} M_0^2 \cos\omega_0 \qquad (3.7)$$

where $f(t) = M_0\cos(w_0 t)$ for $t \leq \pi/2\omega_0$

$= 0$ for $t \geq \pi/2\omega_0$

This expression may then be used to calculate the power W fed into the plate at the equivalent frequency w approximately equal to 1/2t, where t is the contact time which in turn depends on the velocity of impact and the coefficient of restitution e.

(e) The Sound Output from the Plate

The acoustical output of the circular brass plate diameter 30cms, supported at the center and excited at the edge was measured. It was struck at right angles to the plane of the disc (discussed in appendix II ) and the output was measured with a Bruel and Kjaer condenser microphone and frequency analyser. The experiment was repeated for a number of microphone positions

and 'bouncing frequencies'. It was found that there was a large peak in the response curve at the excitation frequency and also at some multiples of this frequency. A number of plate modes were excited quite strongly (eg fig 21 ) in the mid frequency region where they coincided with harmonics of the basic repetition frequency,some of these were excited more strongly than others however. The overall output of the bouncer plus plate over the range 20Hz to 20KHz was in the region of 105 db, and this is essentially limited by the size of the ball used and the power available from the amplifier. The excitation of plate modes by the bouncing ball and the likely excitation expected from gear action, which amoungst other things includes an impulsive excitation which moves round the rim of the gear is discussed in Appendix II.

(f) The Shape of the Waveform

The shape of the force waveform was investigated by firstly bouncing the ball onto a crystal which would not shatter and would give a suitable output - a disc of PZT5 was chosen. The shape of the waveform as seen on the oscilloscope at several frequencies is shown in fig ( 22 ). The PZT5 was then clamped below a small plate and the shape of the new waveform seen on the oscilloscope is shown in fig ( 23 ). The output from the crystal was fed into a Bruel and Kjaer spectrum analyser and the result is shown in fig ( 24 ). On plotting a series of equal amplitude harmonics using the theoretical band pass of the analyser (45db down per octave) a similar curve is obtained. Finally if the shape of the pulse is taken to be half a sine wave and the pulse length and repitition frequency are taken to be those actually measured and the resulting pulse train is then Fourier analysed the result is shown in fig ( 26 ). It can be seen that the spectrum is a series of equal amplitude harmonics up until the 25th when the amplitudes begin to fall off - finally reaching zero at about the 100th (for a pulse length equal to 1/100 of the repetition frequency).

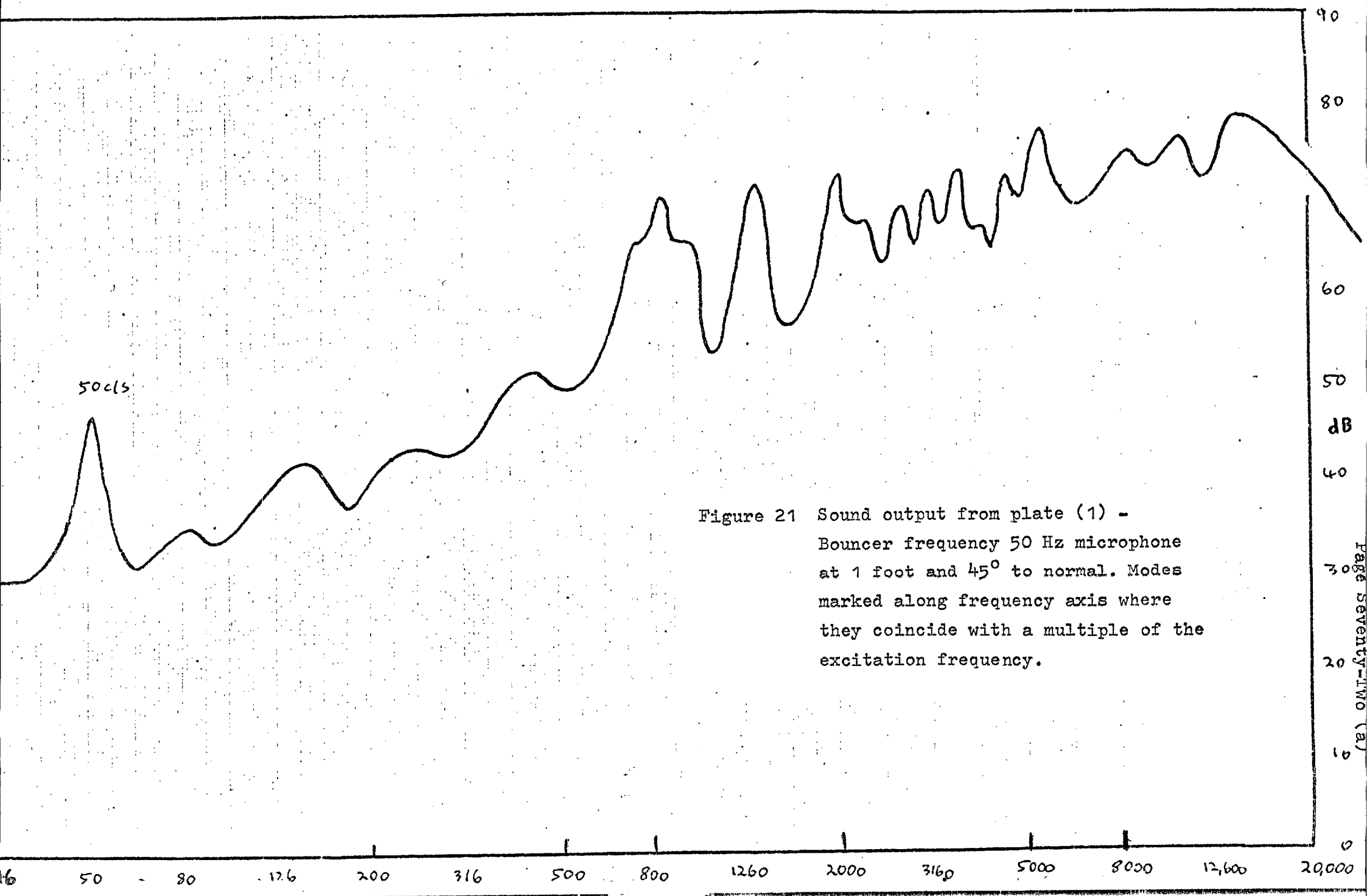
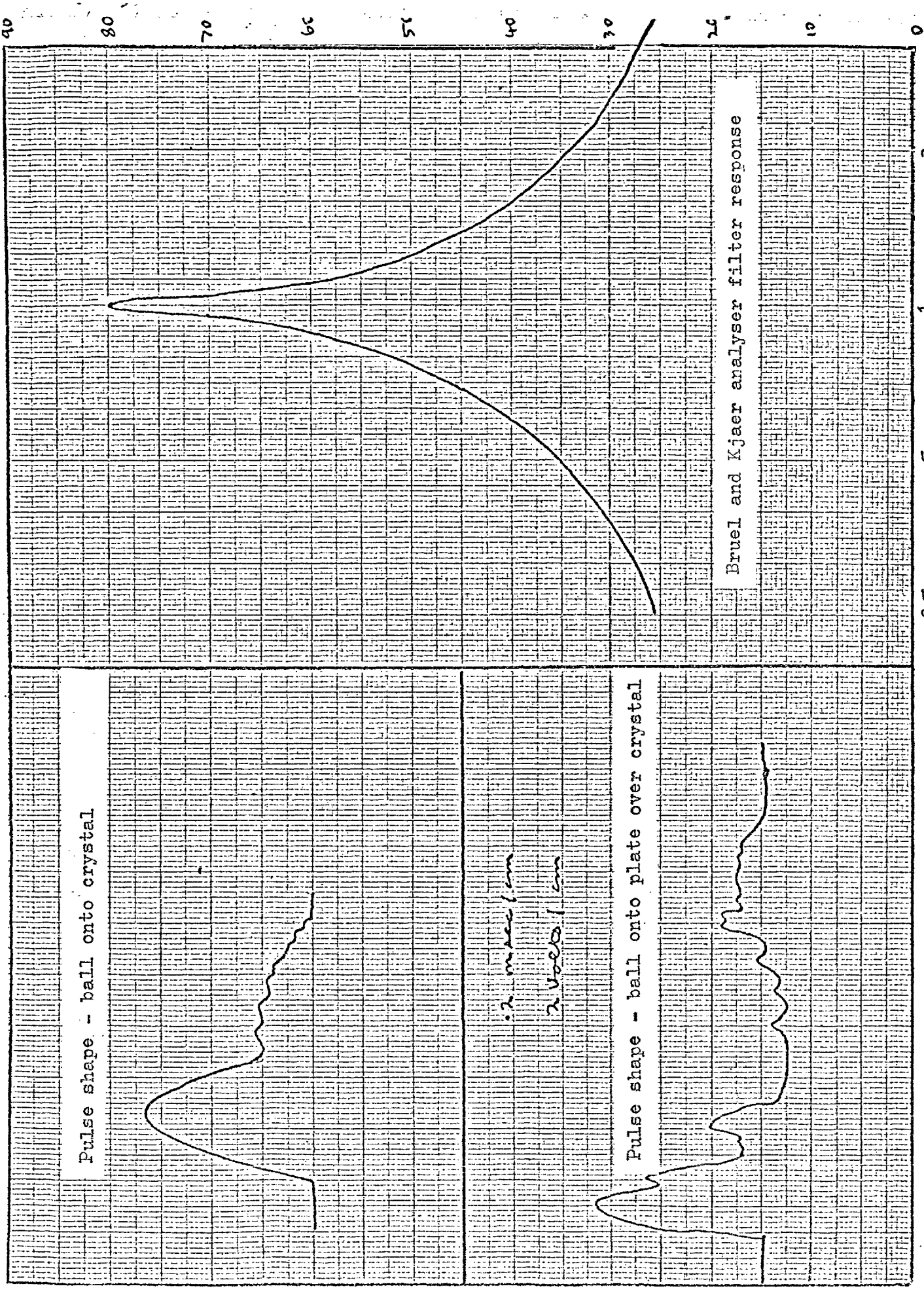



Figure 21 Sound output from plate (1) - Bouncer frequency 50 Hz microphone at 1 foot and 45° to normal. Modes marked along frequency axis where they coincide with a multiple of the excitation frequency.




Figures 22,23,24, Pulse shape on crystal, on plate over crystal, and B&K filter response

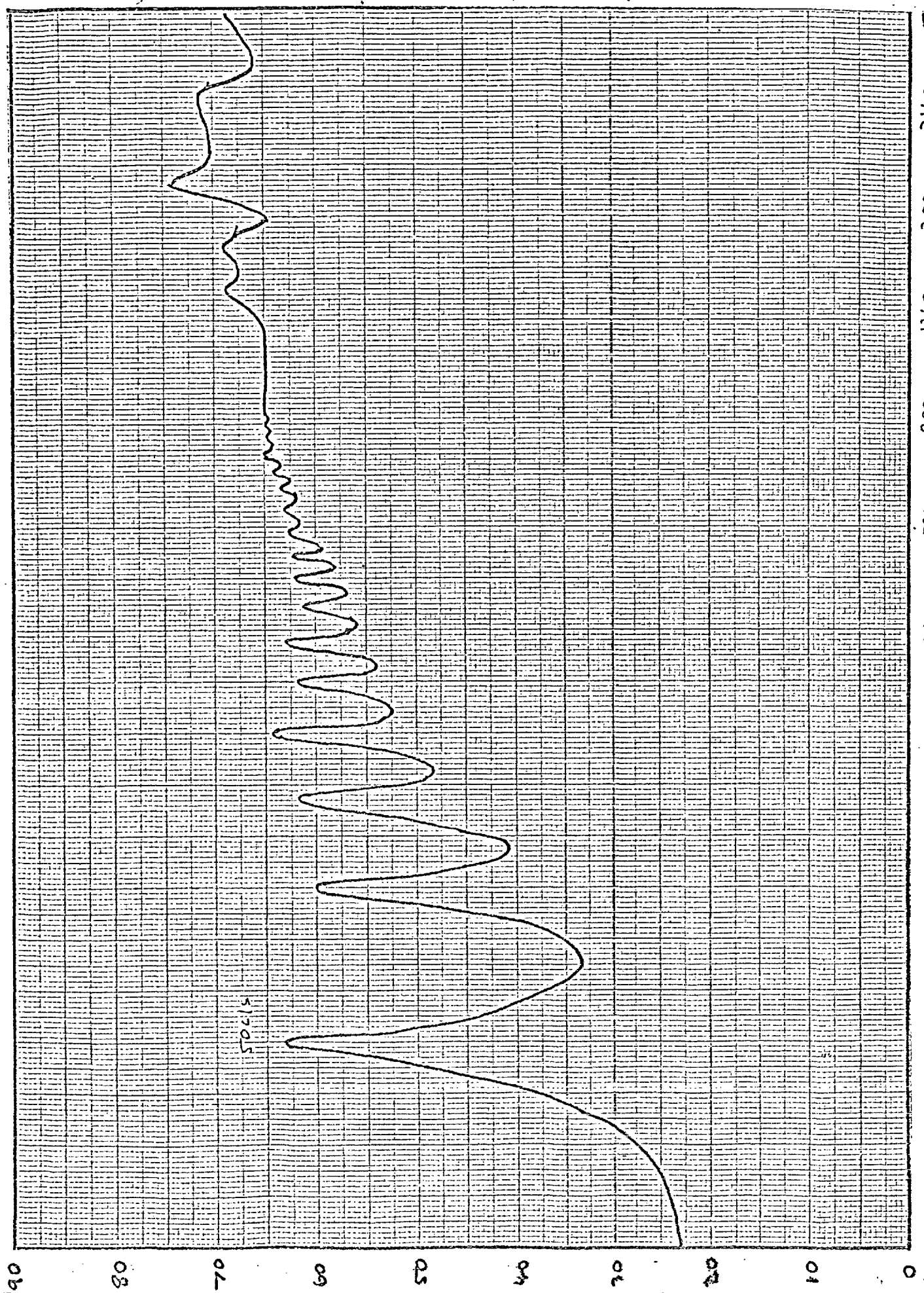


Figure 25 Spectrum analysis of the output of
a crystal under a plate, 50 Hz excitation, Bruel and Kjaer Filters

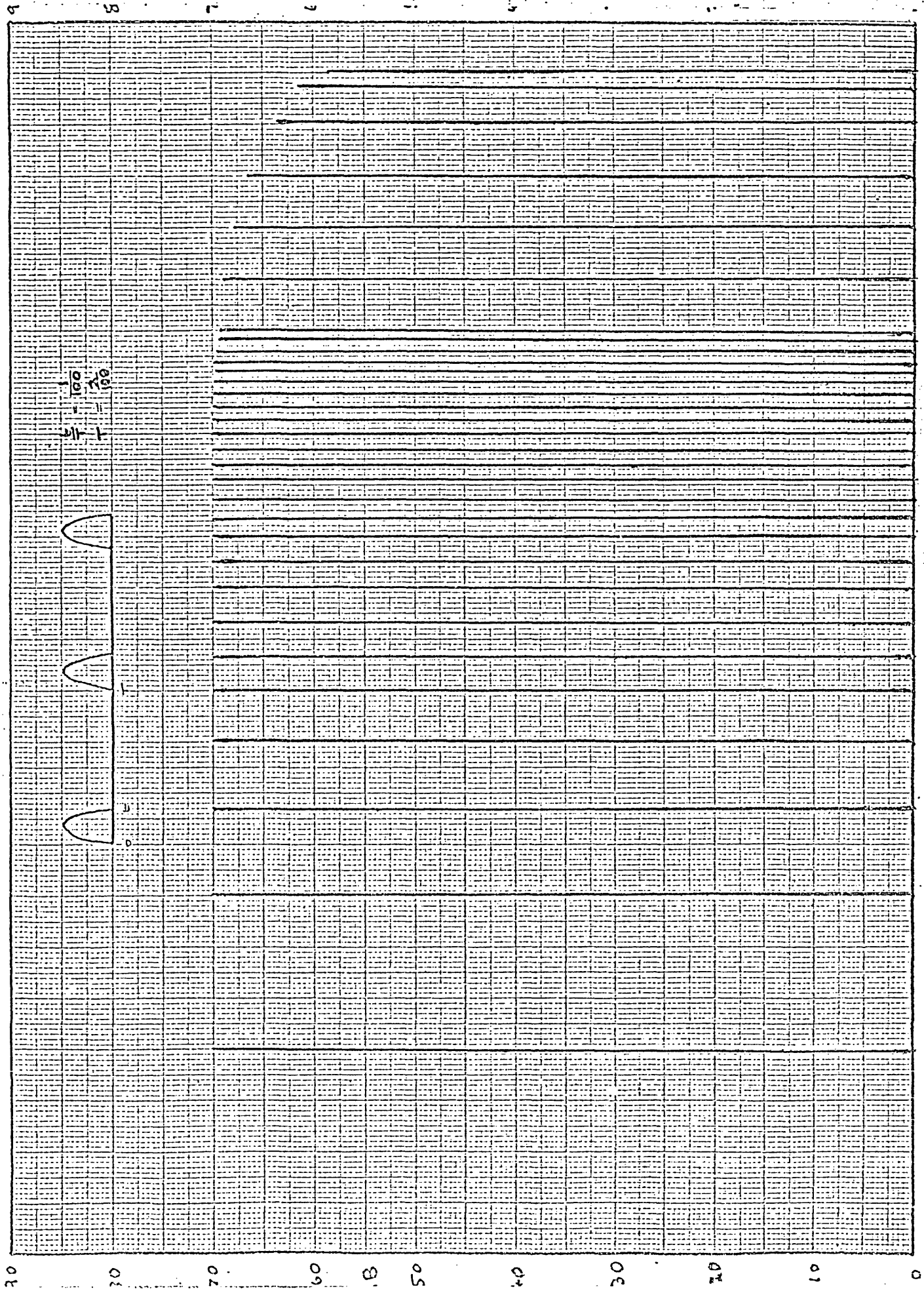



Figure 26 Fourier Analysis of a half sinewave pulse at 50 Hz with repetition rate = 1/50 sec and pulse duration of 1/5000 sec

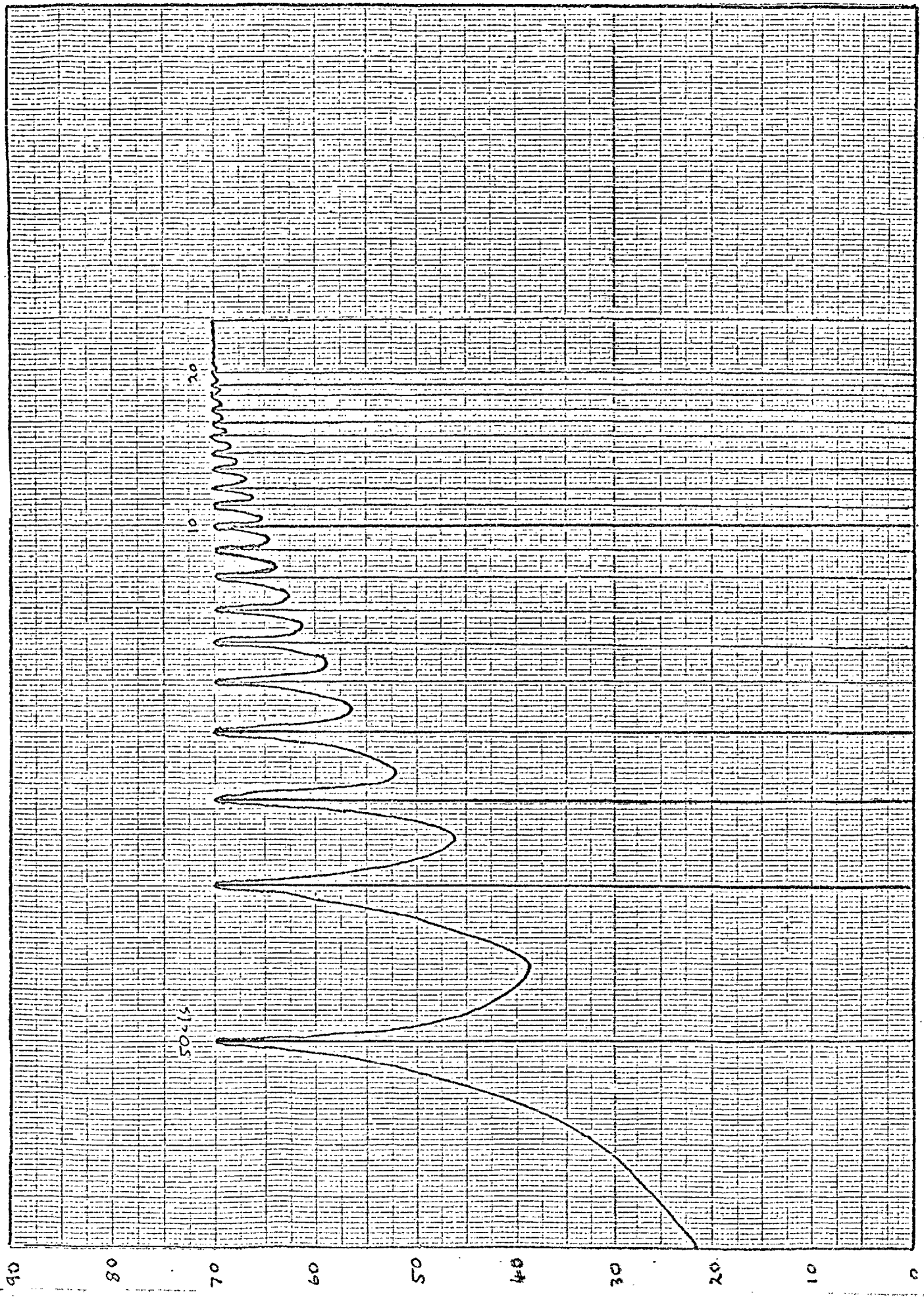



Figure 27 Spectrum analysis of equal amplitude

If the ratio between the pulse length and the repetition frequency is increased the amplitude of the harmonics is maintained up to higher numbers. If this ratio is increased by lowering the repetition frequency the upper limit is not altered. If the pulse length is decreased say by us ing a material of greater coefficient of restitution, the upper frequency limit is extended. For example: For a repetition time of 1/20 seeond, pulse time 1/10,000 second, the upper frequency limit is the 5000th harmonic = 10,000 Hz. For a repetition time of 1/200 second, pulse time 1/10,000 second, upper frequency limit is the 50 th harmonic = 10KHz. If the pulse time is reduced to 1/20,000 of a second, the upper frequency limit is correspondingly 20,000 Hz. With a very short pulse length and a long repetition time the ball effectively produces white noise over the whole audio spectrum, but in fact a series of equal amplitude harmonics spaced at the repetition frequency is produced. To reiterate: the longer the contact time the lower the top frequency to which the harmonics extend and this limit is unaffected by the repetition rate which only determines the spacing and number of the harmonics.

(ii) Design of a Continuous Wave Excitor for Single Mode Excitation

The basic ball bouncing device may be easily adapted for use as a continuous wave excitor. The ball with its arm(s) and supporting block was removed. This left the relay coil,with a sharpened center piece,and the blocks supporting the springs and permanent magnets attached to a device which could alter their relative positions with great accuracy. The principle of magnetic attraction was therefore used to excite the plates. If the plate was made of steel the relay coil was simply adjusted so that it was just clear of the back of the plate. On being fed with AC, and of course being biassed with permanent magnets to the correct degree, the plate experienced a sinusoidaly varying attractive force. Therefore the excitation

frequency could be accurately tuned onto a resonance frequency of the plate whose subsequent amplitude depended only on the amount of power fed into the relay coil and the proximity of the pole piece to the plate. Modes consisting only of nodal radii were relatively easily excited by this means and modes involving one or more nodal circles required more input power for the same vibrational amplitude but were still fairly easy to excite. The plates were supported at the center throughout these experiments. When the plate was made of brass a very small steel screw was threaded into the side of it and this was used to excite the plate. These arrangements proved to be entirely satisfactory and had minimal effect on the modes being excited (apart from determining the antinodal positions) while allowing the desired mode to be easily excited at the desired amplitude. Should precision electrical input power measurements have been desired, the distance of the pole piece from the plate would have had to be fixed by means of shims, and both the voltage and current fed into the coil accurately measured. In fact the pole piece was adjusted to be as close as possible without contact occuring on excitation, and only the voltage across the coil was measured to give a rough indication of the excitation level. The inductance of the relay coil, of course, would complicate matters at high frequencies and for exceptional power input requirements it would be necessary to tune out its inductance at the frequency of operation.

## 3.2) The Reverberation Room

### (i) Discussion

In order to measure the total energy output of the test plates it is necessary to use one of two alternative methods (there are many variations of the two basic methods of course - for instance the use of an acoustic waveguide as collector and conveyor of the sound to the microphone falls

under the 'reverberant' room' category). The two methods are:(a) to enclose the test plates in an anechoic chamber and measure the Sound Pressure Level at many points (at least 20) on the surface of a sphere enclosing the plate, and then find the average sound power radiated utilising the inverse square law. Or (b) to use an easier and more convenient method similar to that used at most acoustic energy measurement facilities. This method places the sound emitter in a reverberant room where the sound field is 'sufficiently diffuse'. In this enclosure the sound radiated in every direction, even from a directional source, is soon averaged out by the many reflections from the acoustically hard walls (and preferably moving diffusers) of the room. Using a suitable microphone technique and source position, the sound power output of the source may be calculated from measurements of the reverberation time and the S.P.L. averaged throughout the room. Finding the average S.P.L. and measuring the reverberation time are the chief experimental difficulties with this method.

(ii) Reverberation Room Criteria

There are several criteria which a reverberation room must satisfy for use in sound power measurement facilities and these are as follows:

(a) The Sound Field must be Diffuse

Definitions of diffusion are given by Schults (1971a): (i) In a diffuse field there is uniform total energy density at all points in the room and each volume element radiates equally in all directions;(ii)There is equal probability of energy flow in all directions and wavefronts fall on the boundaries of the room with random angles of incidence,and finally (iii) All directions of propagation are equally probable and phase relationships between the large numbers of propagating plane waves present are random at any given point. It is to be noted that the pressure is not necessarily

uniform throughout the room, and in fact even in 'diffuse'rooms the S.P.L. can vary with position by as much as $\pm$ 5.5 db with pure tone excitation.

A diffuse field is needed in sound power measurement studies for two main reasons: (a) To aid the steady state measurements of the space average pressure throughout the room by ensuring that the source feeds energy into as many room modes as possible. If only one or two were to be excited, large maxima and minima would occur throughout the room, and also failure to sample even one of these few modes would lead to significant innacuracy. And (b) it is also needed to ensure that the definitions of 'mean free path' used to determine the formulae for reverberation time are reasonably accurate. 'Frequency irregularity', which is the sum of all the peak db values minus the sum of all the valley values in a small frequency range, used to be used as a measure of diffusiveness. However, theory and experiment have shown that this parameter is dependent only on the reverberation time (Schroeder 1954, Kuttruff and Thiele 1954) and does not depend on the diffusiveness.

The required diffusion may be achieved in a number of ways. For a given size of room the diffusion is increased by making the room of irregular shape - avoiding square or oblong shapes and possibly having staggered walls. These minimise flutter echo and, while not increasing the actual mode number, do increase randomness of angle of incidence. The use of static diffusing panels is generally held to be of little value except in cases where one wall of the room is particularly more absorbing or reflecting than the others or where they may help to split up modal frequency degeneracies (hanging panels are only slightly more effective). In practice objects in the room comparable with the wavelength of sound used tend to render the natural frequency distribution random in any case (Dodd and Doak 1971).

Moving diffusers, however, are regarded as being highly effective provided they are large enough and move fast enough and indeed are massive enough to reflect the sound and shift the modal frequencies at the lowest frequencies used during the measuring time. Moving diffusers in effect convert a pure tone into a multitone spectrum (Lubman 1971) and so are similar in effect to the use of a warbletone rather than a single frequency - though moving diffusers act of course on all frequencies present. Increasing the size of the room (limited by air absorbtion) gives more modes in a given bandwidth and therefore this increases the diffusiveness.

(b) The Reverberation Time

The reverberation time is the time taken for the sound pressure level in a room (or single mode in that room)to decay - when the excitation is removed - from the steady state level to a level 60 db below this. It has long been thought that the reverberation time should be as high as possible in a reverberation room. A long reverberation time certainly ensures that, for all but the regions closest to the radiating body which receives mainly direct sound, the sound field is made up of reflections from the walls, however this is not the whole story. There is a direct relationship between the 'Q' of room modes in a diffuse reverberation chamber and the reverberation time. Lubman (1971) states that the bandwidth of a resonance is 2.2/T where T is the reverberation time. Thus, for a reverberation time of 1 second each mode will be approximately 2.2 Hz in width. For the field to be diffuse the energy from the source must be fed into as many room modes as possible - this means that for a given size of room it may be better, certainly at low frequencies where there are fewer room modes, to have a lower reverberation time. This will allow

more of the existing modes to be excited, and will result in less sharp maxima and minima in the spatial and frequency sound pressure level plots. There will however be a lower limit for the reduction of the reverberation time (R.T.) set, not only by the ratio of the direct to the reverberant sound, but also by the applicability of the formulae used to relate the S.P.L. to the R.T. and the room absorbtion.

The number of modes excited also affects the envelope of the decay curve. If the room is small and a pure tone is used to find the reverberation time, it is very likely that a multislope logarithmic decay curve will be obtained (Beranek 1954). This will be caused by several modes having been excited and each of these may have different reverberation times of their own. Since these modes will, in general, be at different frequencies, they will be excited to a different extent by the pure tone - but those with longer reverberation times will become apparent when the others have died away. With a larger room more modes will be excited by the pure tone, and the contributions to the decay curve tend to be averaged out giving a 'ragged' straight line curve similar to that for a single mode. The straight line decay curves allow the R.T. to be easily determined whereas multislope ones create difficulties in deciding which slope is the more important. This then is another reason to both excite and pick up all modes possible and this may be achieved both by an appropriate choice of reverberation time and appropriate receiver and transducer positioning (dealt with below).

There are two formulae relating the reverberation time to room absorbtion and sound pressure level in general use: those of Sabine and Eyring. The Sabine formula is more applicable for high reverberation times (low absorbtion) and the Eyring for low reverberation times (high absorbtion). They are both, more or less, applicable in the region around a 1 second R.T. When the room is very small or the frequency is very low, the

room may no longer be regarded as a whole and each individual mode must be treated separately. In fact in a small room a single frequency source may excite one or two modes only and there are several formulae for deciding if a room is sufficiently large for random statisitics to apply or whether each mode should be considered independantly (see Beranek 1954).

Schroeder's criterion (1962) states that modes should be spaced by their 1/3 power bandwidth, and this will occur above a critical frequency $f_C = 2{,}000\ (T/V)^{1/2}$ where V is the room volume in $m^3$, and T is the reverberation time.( $f_c = 1.2 \times 10^4 (T/V)^{1/2}$ with V in $ft^3$). Another criterion is due to Doak (1959) where the critical frequency $f_c$ is: $f_c = 24 \times 10^3 (T/V)$ and above this frequency the spacing between the modes is'small' compared with the half power width of the modes.

The number of modes in a given bandwidth is dependent only on the volume, the frequency, and the bandwidth itself, but increasing the size of the room will be frustrated by room air absorbtion. There will be at least 20 modes in a third octave band if the room size is at least four times the cube of the wavelength, and this may be taken as another criterion (Shultz 1971). Morse has yet another formula to decide when a room is large (1948): $f_c = (c^3/4\pi(f + 4/t))$ which becomes $10^4/(4V)^{1/2}$ for single frequency excitation. Above this frequency the S.P.L. in a room will supposedly be 'uniform', however spatial variations in S.P.L. near to these critical frequencies are of the order of 6db.

(c) <u>The Size of the Room</u>

In general the room should be as large as possible to allow as many modes as possible in a given bandwidth, however there is an upper limit set not only by the space and money available but also by the air absorbtion. It must be emphasised that if only a small room is available and/or low frequencies must be used, then more modes will be excited if the R.T. is

made a little lower as mantioned above. The few modes available will then cover the frequency range uniformly as possible.

(d) Source Position

Though not strictly a reverberation room criterion the position of the source in the room must also be chosen carefully if the source is to radiate a similar power to that which it would radiate if it were in free space. Waterhouse (1955,1958a,1958b,1967,1969) has dealt with the alterations in the radiation resistance which a source experiences in differing locations, and it is advisable that the source should be at least 1/4 of a wavelength away from any surfaces. It should also not be placed near to corners and edges where increases of 9 and 6 db are to be expected in the sound radiated. If the room is large compared with the wavelength there will be many modes at a given frequency, so that the effects of individual modes will cancel out and the source will radiate in a similar manner to a source experiencing free space conditions (Maling and Nordby 1967, Malling 1967). Rotating diffusers help to simulate this condition at low frequencies or in small rooms (Ebbing 1971). Free space simulation may also be helped by increasing the room absorbtion slightly but this practice must not destroy the diffusiveness of the room (Shultz 1971b). In real conditions the sound output may be 2-3 db more in the reverberation room than in free space.

(iii) Construction of Reverberation Room Used

The ideal reverberant room would be physically large and constructed of dense concrete with fixed and moving diffusers randomly situated and the reverberation time should be about 10 seconds. Unfortunately it was not possible to build such a large enclosure or to build it out of concrete, because neither the funds nor the space were available. A semi-reverberant

room was therefore constructed which was used to give rough estimates of the sound power output of the test plates. Most of the criteria described above however made the reverberant room a 'large' room at and above the lowest frequency used which was about 500 Hz.

The enclosure was constructed of 1 inch block board with a layer of black formica stuck to its inner surface. It was basically rectangular in shape, with dimensions being approximately 4:5:6. One wall was set at an angle in an attempt to improve the random incidence aspect of diffusion (ii a above). The door was very tight fitting and made of the same materials and using the same construction as the rest of the room. The floor was coated with hard araldite and the wooden worktable inside the room (this was the only item of furniture in the room) was covered with the same formica used in the room construction. This wooden worktable also served to increase the diffusion. The whole of the inner surface of the enclosure was painted with the acoustically hardest polyurethane paint known at the time. The actual dimensions of the room were as follows: Height 2.32 m ; Depth 1.485 m at one end, Depth 1.755 m at the other end; Width 2.00 m. The volume of the room less the volume of the table was 7.1334 cu metres and the average reverberation time was 0.7 seconds at 500 Hz reducing to 0.4 seconds at 10 KHz.

The cut-off frequencies above which the room may be regarded as 'large' are as follows:

Morse $f_c = 10^4(T/V4)^{1/2} = \frac{10^4(.7)^{1/2}}{(4\ 7.1\ 35.3)^{1/2}} =$ 250 Hz

Schroeder $f_c = 1.2\ 10^4(T/V)^{1/2} =$ 660 Hz

Doak $f_c = 24\ 10^3(T/V) =$ 460 Hz

It may be seen that the room can be regarded as large above about 500 Hz and then the spatial variation of S.P.L. will be about 6 db. The first natural frequency of the object plates used was about 550 Hz so it was

not necessary to treat each room mode separately when measuring the S.P.L. and determining the power output.

(iv) Measurements

(a) The Reverberation Time

An average reverberation time may be found by exciting the room with a warbletone. This is a single frequency tone which is swept repeatedly over a given bandwidth in a given time. It is in fact frequency modulation of a carrier - the actual 'tone'- with a waveform of the experimenters choice. If the modulating signal is a pure sine wave, Fourier analysis shows that this gives rise to a spectrum consisting of a band of single frequency sidebands of unequal amplitude centered on the original unswept frequency. If the modulating waveform is a triangular or sawtooth wave (Broch 1962), the amplitudes of the sideband frequencies become more nearly equal and therefore this is the more satisfactory form of modulation for R.T. measurements. The warbletone will therefore excite more room modes than a pure tone and will therefore give a more representative measurement of the average reverberation time over the bandwidth covered by the sidebands. If the tones making up the warble spectrum are separated by more than 2.2/T (the modal separation), the variance is then at least proportional to $1/\sqrt{N}$ where N is the number of higher amplitude tones in the band.

Perhaps the best method of all for the measurement of the R.T. averaged over a narrow band is to take the warble tone to its logical conclusion and excite the room with filtered white noise - or if the whole audio range must be averaged, a pistol shot may be used. The amplitude of the components of a warble tone spectrum are nearly constant, whereas those making up the continuous spectrum of a filtered white noise band vary randomly with time. This is only likely to be important, however, if there are any amplitude dependent effects present in the room eg helmholtz

absorbers with narrow 'necks'. These methods give a good general indication of the reverberation time over a narrow band, but if a single frequency of excitation must be used - as in the present experiments - the reverberation time at that frequency should preferably be found. This is because the R.T. may vary rapidly with frequency and with the position of the source in the room(which determines how many modes are excited).

The reverberation time was therefore measured at frequencies in narrow bands around each of the natural frequencies of the object plates used, and wherever possible measurements were also taken exactly at these natural frequencies. Other measurements were taken at room maxima and minima within the bands mentioned above. An average R.T. for the two corner microphone positions (see below), which according to Waterhouse (loc sit) will average the energy in all the modes excited by the speaker, was then calculated for each disc frequency, and also an overall averaged R.T. was obtained for the narrow frequency band around each disc mode taking into account room maxima and minima. The value of the R.T. obtained from this average will be comparable to that resulting from a warbletone of narrow bandwidth, but in this case each 'sideband' frequency is given equal weight.

A Bruel and Kjaer microphone amplifier and filterset, together with a Bruel and Kjaer pen recorder set to its fastest speed (100 mm $sec^{-1}$) were used for the R.T. measurements. A speaker with a baffle approximately the same size as the plates used was placed in the room exactly in the same position as that occupied by the test plates. The speaker was excited with pure tones, and time taken to ensure that steady state had been reached. The speaker was then disconnected with the ren recorder running, and the time taken for the level to fall 60 db was taken as being the R.T at the frequency of excitation. A Bruel and Kjaer 1/2 inch condenser microphone was placed in each of three positions in the room for each

frequency of measurement. Position (a) was as close as possible to the right angles corner of the room, position (b) was as close to the oblique angled corner as possible - a hole was drilled through the wall and the microphone diaphragm was placed flush with the surface for position (b) and about 1/10 inch from the corner for position (a). The final position, which was merely for comparison purposes, was randomly situated in a wall.

(b) Average Sound Pressure Level

Having measured the reverberation time the average sound pressure level in the room must be measured as accurately as desired. Waterhouse (1955) has shown that a microphone placed at a corner of the room will measure a S.P.L. 9 db higher than the average - 6 db for an edge position, and 3 db for a position in the middle of a wall. Simply measuring the S.P.L. at a corner and subtracting 9 db may give a rough figure for the average S.P.L. since in a rectangular room all the excited modes will be sampled. However this is not usually the case in practice, and a possible explanation is that it is very difficult to place the microphone within the 1/10 of a wavelength of the actual corner needed for this to be correct. This is because of the physical size of the microphone diaphragm available, so even at moderate frequencies this is an unreliable method - in fact a distance of 1/4 inch gives a maximum frequency of 4.8 KHz.

A method which is used in many facilities is the use of a random sample of N microphone positions (the standard deviation is reduced by $\sqrt{N}$), in fact 20 microphone positions are needed for a $\pm$ 2 db accuracy in the measured S.P.L. in a room containing 10 to 20 spatial maxima (Dodd and Doak 1971). Lubman (1971) gives a formula for the number of samples N that is needed for a given accuracy: $N > (1.96V/e)^2$, where V is the 'normalised spatial variance' which is unity for a pure tone excitation,

e is the desired sampling error and 1,96 is the value of a constant 'C' which allows 95 percent certainty that the sample means will differ from the true mean by less than e. There is a calculation using this formula below. Lubman (1971) has also given a nomogram involving the R.T. the bandwidth and the sample size allowing the third variable to be found from any two. He also pointed out that that any sample point the microphone meter averaging time must be at least three times the reverberation time, and that spatial averaging introduces a bias if the quantity averaged is anything other than the instantaneous squared value of the sound pressure. If the S.P.L. is averaged the bias to be added may be as high as 2.5 db when a pure tone is used, however if the root mean squared pressure is averaged only 1 db should be added.

The method of rapid microphone traverse is rapidly gaining favour and this was the method used in the present experiments. With this method the microphone traverses an arc (or a complete circle,Malling and Nordby 1967) and encounters pressure fluctuations at such a rapid rate that together with a'slow'meter setting or a level recorder with a slow writing speed, a very good approximation to the true spatial average S.P.L. is obtained because the meter or recorder effectively integrates the variations (Shultz 1971). The traverse should be as large as possible and Baad (1971) has given a formula for the equivalent number of samples in a given length of path: $N = (1 + 2X/\lambda)$ where X is the length of the path. Obviously a $10\lambda$ path corresponds to about 20 samples which give a 1 db confidence limit. Ebbing and Ingalls (1969) demonstrated that each extra dimension included in a given length of traverse gives about 1 db less in the spread of the results. The best traverse will then be along a room diagonal.

A small proportion of the measurements on object plate No.(1) were taken with the microphone situated in positions 1(a) and (b) as

defined in (iv a) above and the average S.P.L. in the room will be approximately 9 db less then these results. However most of the measurements were taken with a swinging microphone as this was regarded as the best technique of all. The microphone was suspended from the ceiling of the room by a length of its own cable. Just after each hologram was taken ( and occasionally just before as well to ensure that the S.P.L. did not vary in the experimental time) the microphone was set swinging very rapidly in a circle and, having shut the door to the reverberation room, the average S.P.L. was measured with a Bruel and Kjaer microphone meter set in the 'slow' mode of operation.

Variations on the meter were seen to be ± 1 db when the microphone was swinging rapidly (about 24 feet per second) increasing to ± 2 db as it slowed down and these variations were averaged out by eye. The path length was approximately 6 feet and this corresponds to a sample number N of $1 + 2(6)/2 = 7$ different samples at 500 Hz and 14 different samples at 1000 Hz with correspondingly more samples at higher frequencies. The path length could not be increased further as the microphone would pass too closely to the walls during its traverse if it were increased. Assuming therefore that the meter reading accuracy is ± 1/2 db, then the average sound pressure level is measured to a 90 percent confidence limit as follows : to ± 2 db at 500 Hz, to ± 1½ db at 1000 Hz and ± 1 db above 2000 Hz. These figures are derived from the previously quoted formula $N \geq (CV/e)^2$, where C = 1.96 if the sample averages are not to differ from the true mean by less then error 'e' with a 95 percent certainty, C = 1.65 gives a 90 percent confidence limit and C = .65 gives a 50 percent limit. Therefore taking a 90 percent confidence limit, 7 measurements and a pure tone (V = 1) then $e = 1.65/(7)^{1/2} = 66$ percent or about 2 db (Lubman 1971).

## 3.3) Apparatus Used

### (i) Overall Layout

The reverberant room was built inside a small dark room in the main acoustics laboratory. It was built in approximately 2/3 of the space and the rest was used to house the amplifiers and other equipment which had to be situated outside the reverberant room for reasons of heat output and experimental convenience. The smaller part of the enclosure was therefore used as a control room and alternative dark room (fig 28). The dark room was built of a dexion framework with hardboard panels, the whole being made light tight with self adhesive plastic tape.

The following apparatus was situated inside the reverberant room:

(a) The Holographic Table.

(b) The Laser(s).

(c) The Optical System - comprising optical benches and lenses.

(d) The Shutter Mechanism for controlling the exposure time.

(e) The Test Plate - supported by a 3 legged retort stand in turn fixed to a concrete block.

(f) The Plate Excitation Mechanism.

(g) A Microphone.

(h) The Photographic Plate Holder.

(i) The Scanning Disc and Synchronous Motor.

(j) The Synchronous Motor Stand.

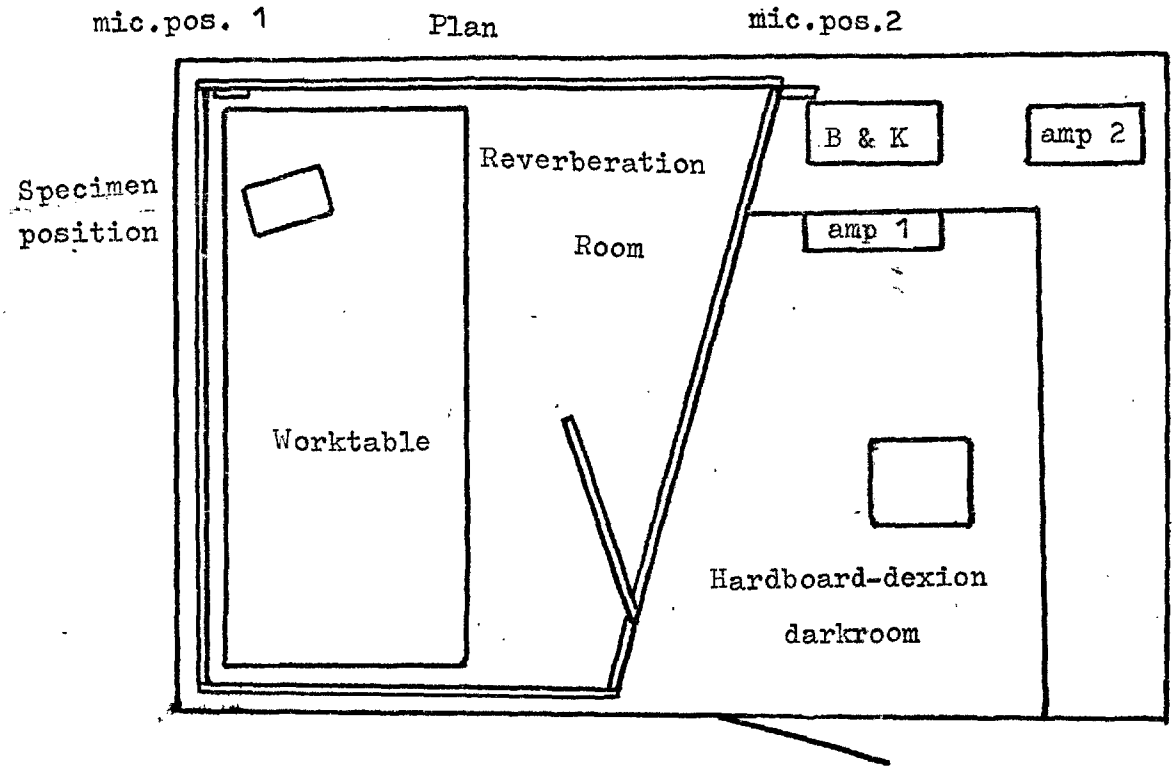
(k) Two Switchable Mains Plugs and various connecting sockets.

(l) A Thermometer and a Source of Illumination.

The following apparatus was situated in the 'control room':

(m) A 120 Watt Goodmans Vibrator Amplifier.

(n) A 100 Watt Amplifier (specially constructed).




Side Elevation

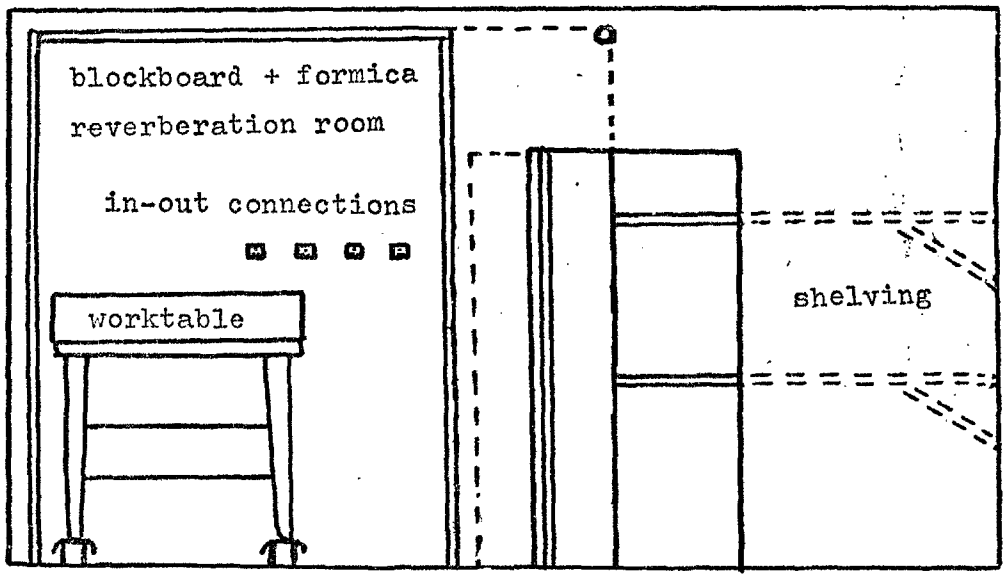



Figure 28 Double Dark Room Layout

(o) A Bruel and Kjaer spectrum analyser (filter set).

(p) A Stable Oscillator with fine adjustment.

(q) Frequency Divider with Power Supply.

(r) Switches for the Plugs inside the Reverberation Room.

The interior of the room was viewed with the aid of a fish_eye lens.

(ii) Details of the Apparatus

(a) The Holographic Table

The requirements for a holographic work bench have been dealt with in Section (II). The worktable used was a specially strengthened wooden table onto which had been cast a concrete raft reinforced with dexion. This raft was about 4 inches thick and provided the necessary stiffness and mass, also its coefficient of expansion was less than that of an equivalent steel table. The concrete raft therefore had the advantages of cheapness, convenience, stiffness, low expansion coefficient, reasonable damping, and high mass. The worktable was isolated from floor borne vibrations with appropriate 'Barrymounts' ( which are rubber annuli working in shear) resting in boxes of dry sand. The vertical resonance frequency with four mounts for the half-ton table was about 10 Hz and the horizontal frequency was about 5 Hz. The volume of the table was .3996 $m^3$ and the whole of the surface of the table was covered with formica, the concrete itself being also painted with polyurethane paint. A similar concrete raft was used in the experiments on Loudspeakers (Section IV) where the isolation was provided by special 'pimpled' rubber mats and the rubber was again in shear.

(b) The Laser

Two lasers were available for use in the experiments on plates and they were shared with another experiments - resulting in only one laser being available at any one time. They were a 1 mw and a 15 mw Spectra Physics

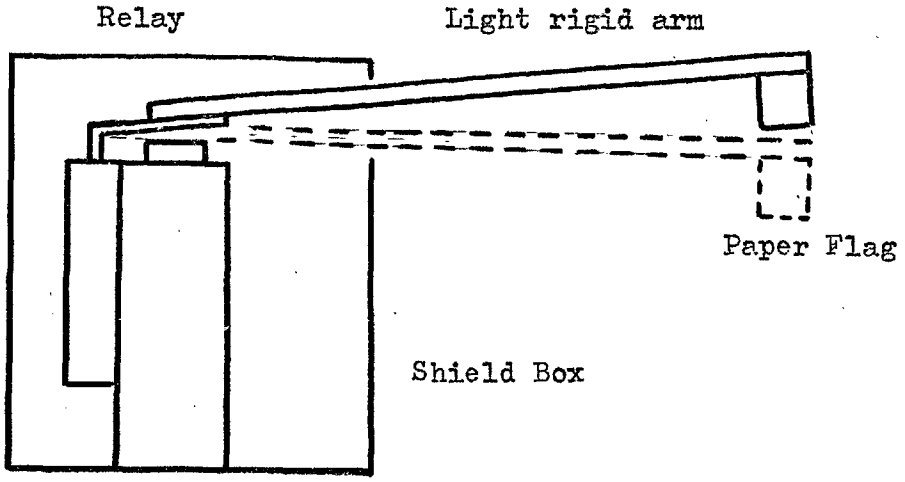



Figure 29 Shutter Mechanism

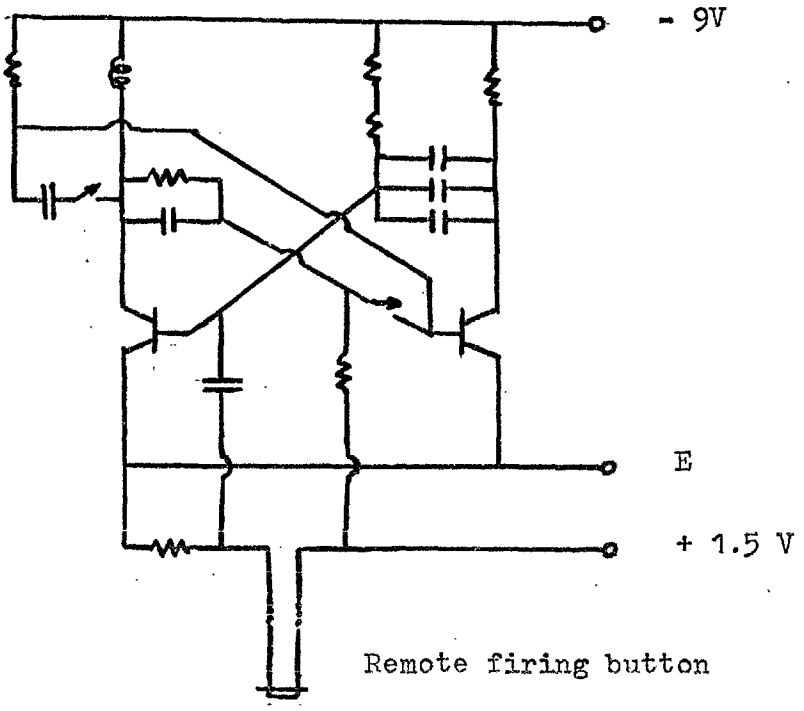



Figure 30 Circuit of Shutter (convertable into 1 sec.timer)

Laser. Using the former holography of a 30 cm diameter plate was difficult but possible when utilising some of the light saving techniques described in section (II). Using the more powerful laser holography was greatly facilitated, and much larger plates could be treated - a 46cm diameter plates being the largest actually hologrammed.

(c) The Optical System

Light from the laser, after passing through the shutter mechanism (fig 19), was passed through a metallurgical microscope objective chosen to diverge the beam sufficiently to cover the whole of the object plate which was placed at a convenient distance (bearing in mind the 1/8 wavelength stability requirement) from the lens and the hologram. The light reflected from the plane front surface of the lens, which would normally be wasted was diverted with a front silvered mirror. It was then passed through either a simple zoom lens system or another microscope objective, and then directed with a further mirror to fall onto the photographic plate held in the plate holder. This light formed the reference beam and was found to be sufficiently intense for all applications. The actual intensity of this beam was made continuously variable by the use of the zoom lens system or more simply by altering the position of the second microscope objective.

The various lenses and mirror were attached to the optical benches by means of ordinary 'riders'. However these riders had their posts and fixings removed leaving only the actual sliding part. The optical components were then fixed directly to these by means of cubically shaped pieces of plasticine. This material coupled the components well to the optical benches (and thence to the worktable) at low frequencies, and it would not permit the components to oscillate at high frequencies. By using cube shaped pieces of plasticine creep was eliminated. The plasticine also permitted easy adjustemnt of the optical components . In fact holograms

were taken at first with the posts and fixings of the 'riders' in place - when the holograms appeared to be slightly blurred. It was likely that the particular conditions present in the laboratory caused the components on top of these posts to oscillate at high frequency.

(d) The Shutter Mechanism

This was adapted from a simple multivibrator circuit and the final circuit used is shown in fig (30). The shutter itself is a small black paper flag on the end of a 6 inch arm of very light and rigid construction. This arm is attached to the armature of a relay whose coil has a 2 Kohm impedance. Exposure times as short as 1/20 second have been used and the extinction ratio is 100 percent with this arrangement. The unpowered position of this device is 'open' allowing setting-up operations. When switched 'on' the flag drops and subsequently opens for the desired exposure time on pressing the remote firing button. The exposures, available in three continuously variable ranges, are from 1/20 second to 10 seconds. The device is simply converted, with the aid of a switch, to a one second metronome which may be used for timing development etc. Lin and Beauchamp (1970) have described a similar device which has the added facility of automatic exposure time setting - this is accomplished with the aid of a photoconducting cell. No automatic device was considered when the present shutter was designed as in practice one or two test exposures gave the correct exposure for any change in layout or beam intensity.

(e) The Object Plate

The treatment given to the test object plate has been fully described in Section (II) where it is shown that a system of concentric grooves reflects far more of the incident light towards the hologram than almost any other method - save only the use of a half silvered mirror and 'Scotch-lite' tape. The plate was not painted white nor was it specularly polished

but an approximation to the ideal Fresnel mirror which would reflect all the incident light to the hologram plate was obtained by careful 'scoring' with a hand scourer. The plate itself was attached to a three legged laboratory stand base with a piece of studding at the centre. The sstand base was, in turn, rigidly glued to a very massive concrete block which rested on the worktable, thus the centre of the test plate was rigidly coupled to the workbench. This was shown to be a satisfactory method of coupling the test plate to the worktable as no fringes were ever observed to pass through thecentre of the plate when holograms of the double exposed and time average type were taken.

(f & g) The Plate Excitation Mechanism and The Microphone Used

The positions and working of the 1/2 inch Bruel and Kjaer condenser microphone used have been fully described in (3.2 (iv b)) above. And the plate excitation mechanism is fully covered in (3.1) above.

(h) The Plate Holders

Two photographic plate holders were necessary, one for live fringe work and the other for scanned holographic work. The first holder had to ensure that the developed plate could be relocated very accurately, but nevertheless an extremely simple construction was adopted (fig 31 ). The holder was basically a thick piece of aluminium with one corner removed making it 'L' shaped. Three screws were fixed as shown and large sleeved were passed over them before tightening them up. This arrangement allowed the photographic plate to be easily fixed into the holder in the dark and the three screws completely defined the position of the plate in its own plane, with the aluminium surface defining it in the direction normal to its plane. Though a three point location would have been more desirable it was found that the aluminium surface was entirely satisfactory provided it was regularly cleaned with acetone to remove grease and dust. Spring -

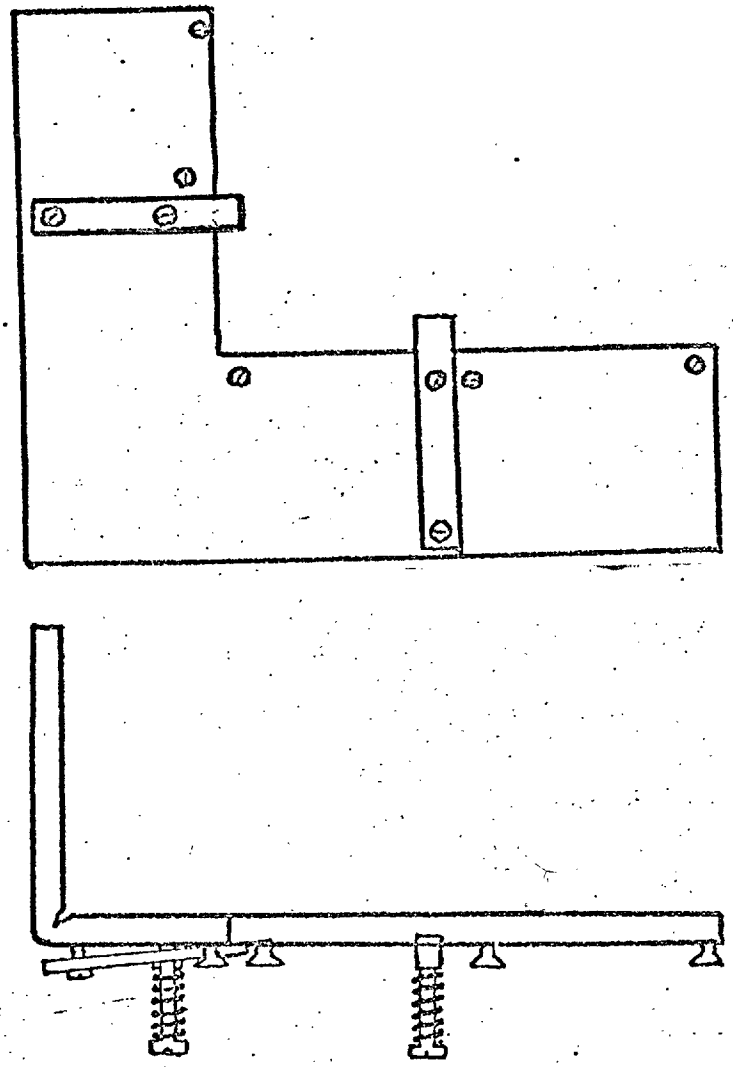


Figure 31 'Live Fringe' Plate holder

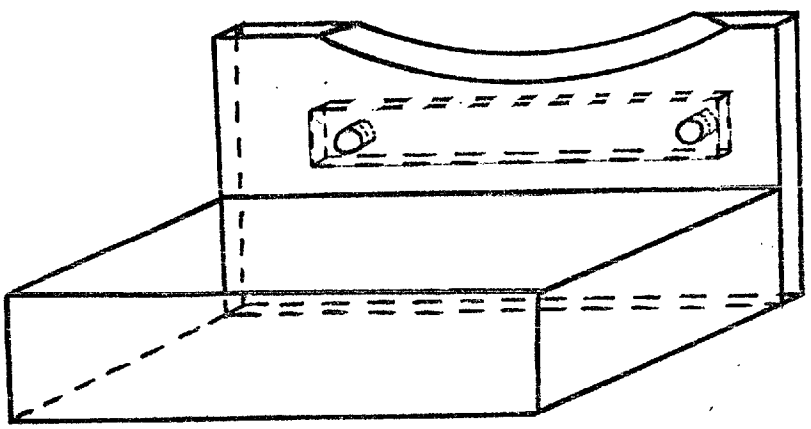


Figure 32 Scanned Holography Plate Holder (Dia 1)

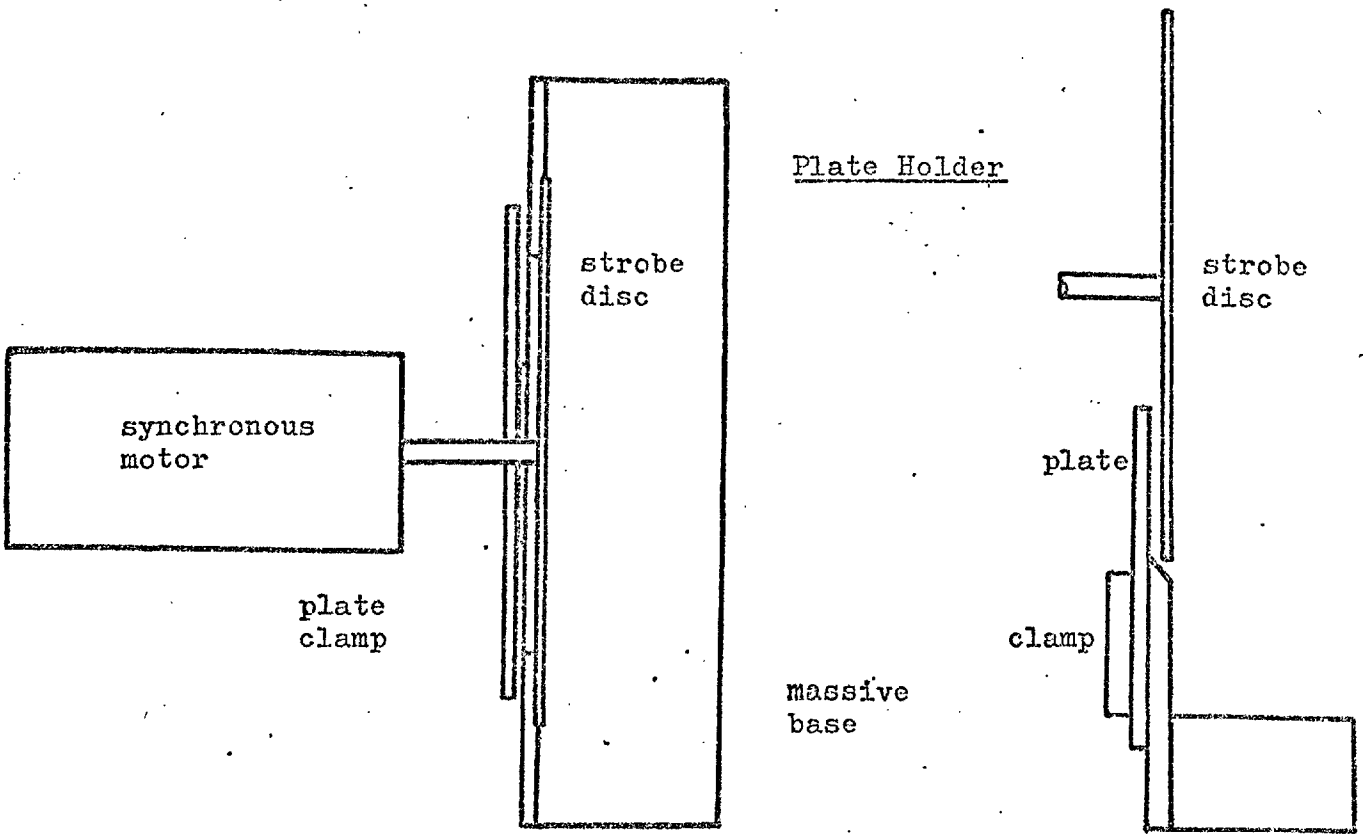
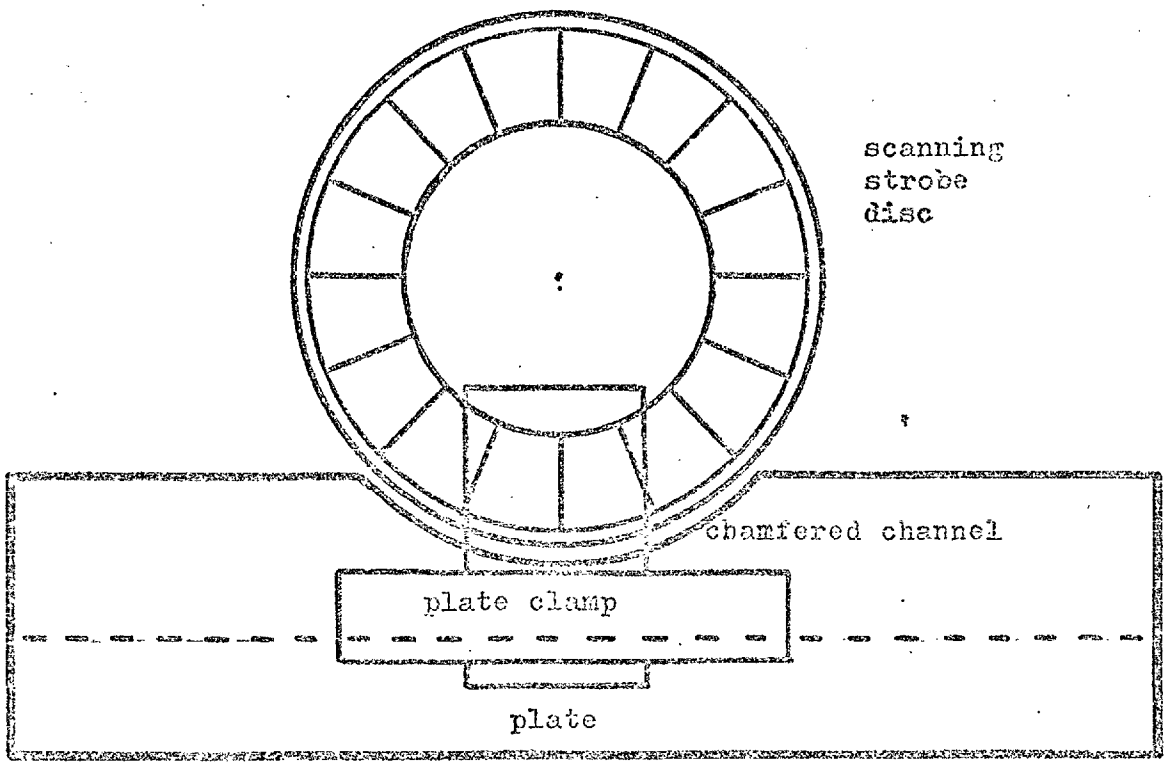



Figure 33 (a) (b) and (c) Scanned Plate Holder (Dias 2,3 and 4)



loaded levers with their operating points just over the aluminium edge ensured that the plate was (not too firmly) held in place. These levers extended beyond the edge of the aluminium which also helped the fixing of plates in the dark. The whole holder was strongly glued to a stone block which rested on three legs on the worktable when in use. The original design had screw thread facilities to move the photographic plate in any direction in its own plane after development and return to the holder. However it was found that on relocation a maximum of three parallel fringes was observed and no curved fringes were seen at all. This meant that the plate was located to within about 1/8 of a wavelength in the direction normal to its surface and only slightly out in rotation and/or in the plane of its surface. This misalignment was corrected very easily with a steady hand and so the screw adjustments were therefore removed. This holder was designed for 'live fringe' work, but of course could also be used for time averaged work and double exposure holograms. In this case the spring loaded arms maintained the position of the photographic plate ensuring that no movement occurred during or between exposures.

The second hologram holder had to fulfil quite different requirements. There was no need for accurate realignment, but the plate had to be held exactly in place against strong vibrational air movement forces created by the scanning disc which was in close proximity to the photographic plate. Once again this was accomplished very simply with the plate holder shown ( fig 32). The holder was made of a single piece of aluminium fixed to a heavy glass block. An arc of a circle of the same radius as the scanning disc was cut out of its top surface and the edge of this arc nearest to the scanning disc was chamfered away at a steep angle. This important feature of the holder guided the air from the spinning disc away from the photographic plate. When the photographic plate is in position, half of it projects above the aluminium and is subsequently

exposed. The lower half is held very firmly against the aluminium holder by means of rubber springs and a flexible back plate. The photographic plate has vertical locating screws and horizontal 'position limiting' screws, since exact positioning accuracy is not at all important. The back plate also has travel stops preventing it closing completely against the aluminium and this allows the plates to be easily fixed in the dark. Three metal feet complete the simple design of this effective plate holder which allows two exposures per plate and may also be used for time average and double exposures. It was found in practice that the spinning disc, which may have been expected to shake the photographic plate by more than 1/8 of a wavelength, as a consequence of its high rotational speed and close proximity, did not affect the holographic process even at the highest speed of rotation. The photographic plates originally 9 x 12 cms were cut into 4, thus each ordinary plate gave eight holograms - two per 4.5 x 6 cm piece.

(i) The Scanning Disc(s) and the Synchronous Motor

The configurations and numbers of the slits and holes used in the scanning discs will be described in the experimental method below. The discs themselves were made of aluminium alloy. The central regions were about 1/16 inch thick but the outer regions, which contributed most of the moment of intetia, were turned town to about 1/2 mm. This thinning of the outer regions not only reduced the moment of inertia (and to a smaller extent the air drag) but greatly reduced the 'siren effect' whereby the passage of the holes in the spinning discs gave rise white noise with peaks at the passage frequency and its harmonics. This effect was minimised with the discs used and was not troublesome. (Object plate sound output measurements were, of course, not taken with the discs spinning). The thinning down was limited by the ability of the outer regions of the discs to resist bending during normal handling and , lacking the correct taper to ensure uniform stress, to counteract centrifugal forces when rotating at high rotational

speeds.

Having thinned the discs down they had to be balanced as accurately as possible to avoid the generation of vibrationary forces which could be transmitted to the worktable. This was accomplished by placing the discs onto a wheel of large radius - the center hole of the disc resting on the edge of the wheel. The disc was then made to balance in two directions at right angles with the aid of this wheel and small pieces of masking tape fixed in the appropriate places. The balance of the disc was checked by taking it up to speed attached to the motor spindle. Thus out-of-balance forces were reduced until they were no longer troublesome.

It was important that the discs were maintained flat, because they had to be placed very close to the holographic plate to avoid excessive misregistration of the reference and object beams as these subtended about $30^{\circ}$ at the photographic plates when some optical layouts were used. To reduce the effect of any misregistration the photographic plates were always exposed with the emulsion side next to the scanning disc. The effect could be almost completely removed by causing the reference beam to come from above or below the object when misregistration is limited to the width of the object, but in practice this arrangement gave experimental difficulties (though it was used in some experiments on loudspeakers) and the holograms produced were in fact not of such good contrast as those obtained with the side-by-side arrangement.

Since the object and reference beams did subtend about $30^{\circ}$ at the photographic plate, the distance of the scanning disc from the plate could be used to control the duty cycle of the stroboscopic action (fig 34). For example, if the basic duty cycle were 1/10 this could be increased to 1/20 by arranging the scanning disc so that only half the reference and object beams were correctly registered. The unreferenced parts of the beams merely act as pre and post-exposures and reduce the contrast slightly.

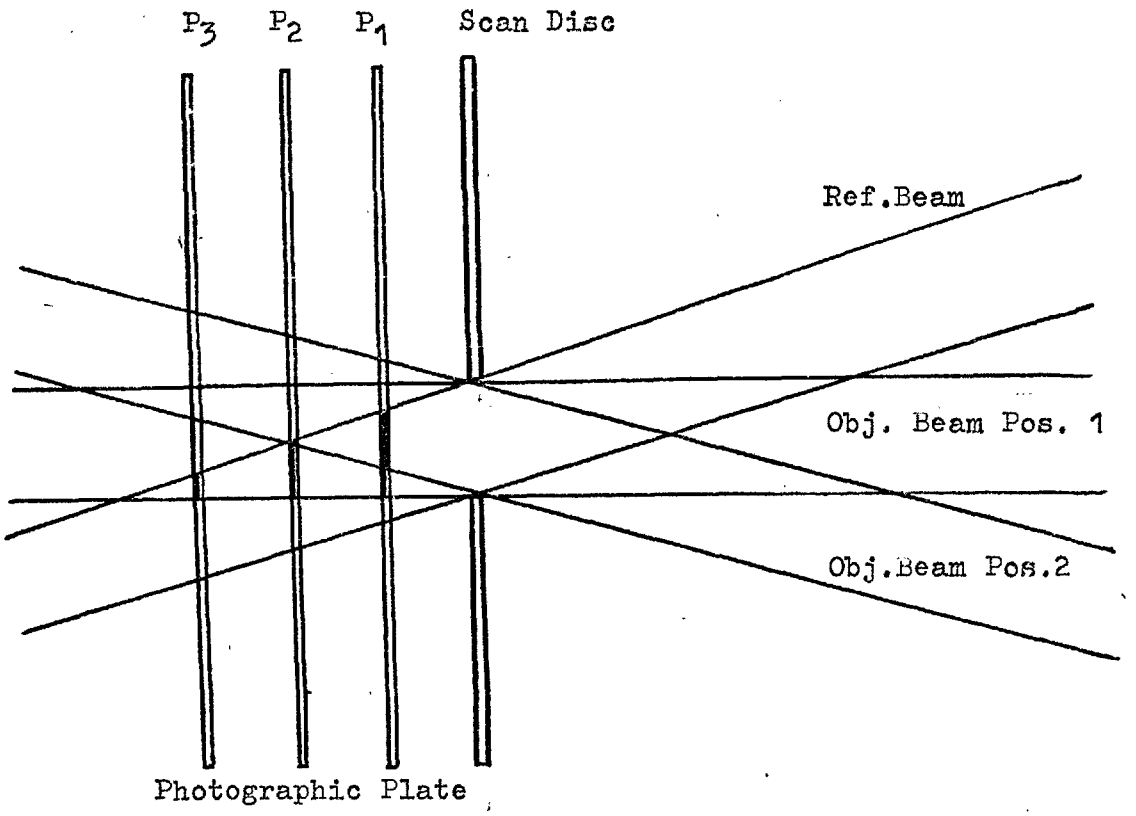



Figure 34 (a) Variation of duty cycle with plate-disc distance for 'side' reference beam

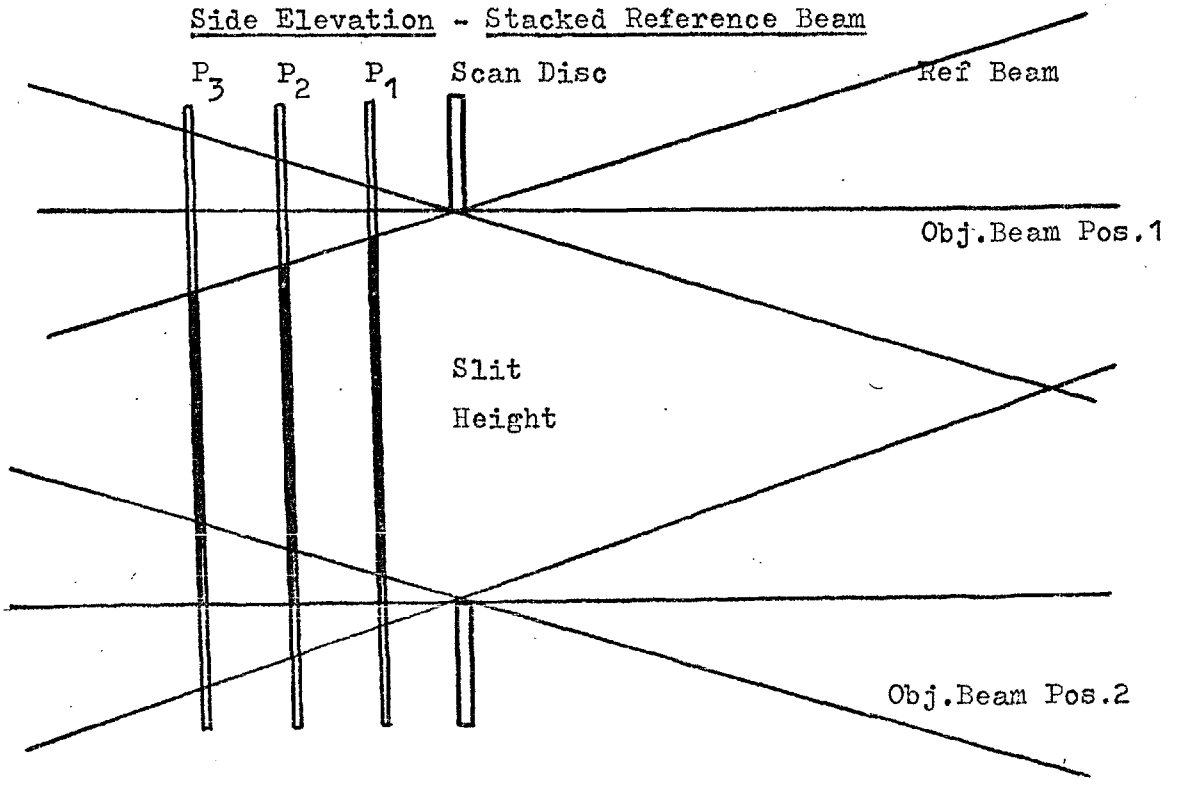



Figure 34 (b) Variation of height of plate in registration with reference beam with 'stacked' reference beam

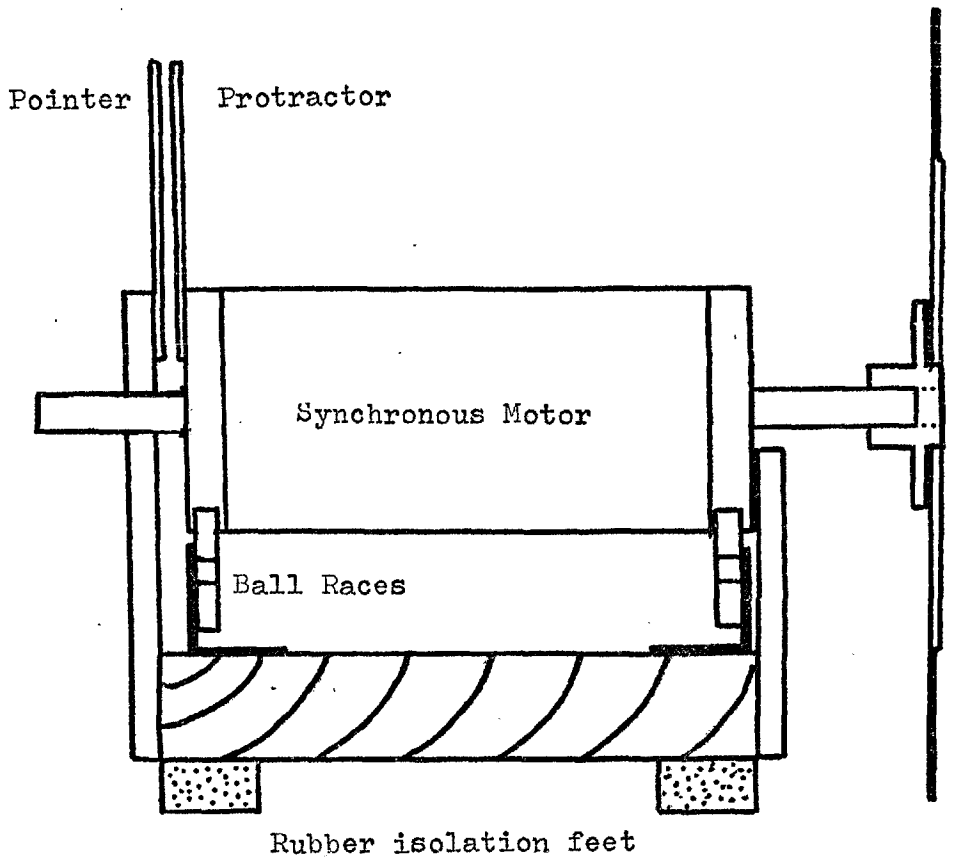
The disc used for normal stroboscopic holography was, of course, not placed next to the photographic plate but next to the laser, chopping the light before it entered the holographic system. When the reference beam only is to be scanned (giving more pre and post-exposure and less 'working' exposure) the scanning disc may be placed anywhere after the final reference beam expanding lens. The disc used for this purpose may be much smaller than that used for ordinary scanned holography and this is one way in which the upper frequency limit of the process may be increased. The upper frequency limit will also be discussed in the experimental method below.

The synchronous motor used had 70 watts power handling and was the most powerful 'Dunkermotor' available. Being a four pole motor it gave 1/2 a revolution per cycle. It was designed for 50 Hz mains frequency work however the excellent ccoupling between the fields of the rotor and the stator, the precision of the bearings used , and the quality of the balancing carried out on the rotor enabled this motor to be driven at frequencies far in excess of the design frequency. For every doubling of the excitation frequency, the value of the phasing capacitor should be reduced by 1/4 and the voltage applied should be increased by four - this latter requirement limits the maximum frequency which may be used because of the possibility of insulation breakdown. Also more and more power is needed to bring the scanning disc up to speed at high frequencies so power dissipation and power availability also limit the highest frequencies which may be applied. In practice 600 Hz applied frequency was about the safe limit corresponding to 300 Hz rotational frequency. Therefore wwith a f/32 frequency division an experimental frequency of 9600 Hz was attainable. By accepting lower effective duty cycles, however, (i.e. one stroboscopic flash every other cycle or every four cycles etc.) higher experimental frequencies may be reached (see experimental method below).

This particular motor had a very useful characteristic which enabled the experimenter to know when it was running with synchronous speed. When running up to speed the voltage across the motor was read from the meter and at the instant of attaining synchronism the voltage across the motor jumped by about 1/3. The starting torque of this motor was virtually the same as the running torque, but this increase of motor impedance at synchronism enabled the drive voltage and power to be greatly reduced after synchronism had been attained. At the highest frequencies used the motor gained speed faster if it was excited with a frequency higher than that to be used (and that which the motor ever reach). The final frequency was then switched in after which the motor fell down into synchronism, or the oscillator frequency reduced faster than the motor could loose speed until the desired frequency had been reached when it once more fell down into synchronism.

(j) The Synchronous Motor Stand

For ordinary stroboscopic work the phase of the strobing action had to be easily and accurately adjustable, also the motor vibrations had to be isolated, if possible, from the worktable. These two requirements were achieved with the design shown in fig (35 ). The motor body was entirely tubular and so this body was supported on four ball-races, two at each end, with plastic end stops to keep the motor in position. Thus the whole motor body could be rotated about its spindle axis, and this rotation effectively altered the phase of the strobing action of the disc attached to the spindle. A transparent plas tic lever was screwed to the motor body at one end and this registered with a protractor attached to the body of the holder, therefore the number of degrees by which the motor was rotated could be accurately determined (this rotation was, of course, related by the frequency division ratio,between the object and motor signals, to the phase change in the stroboscopic action). This lever arm



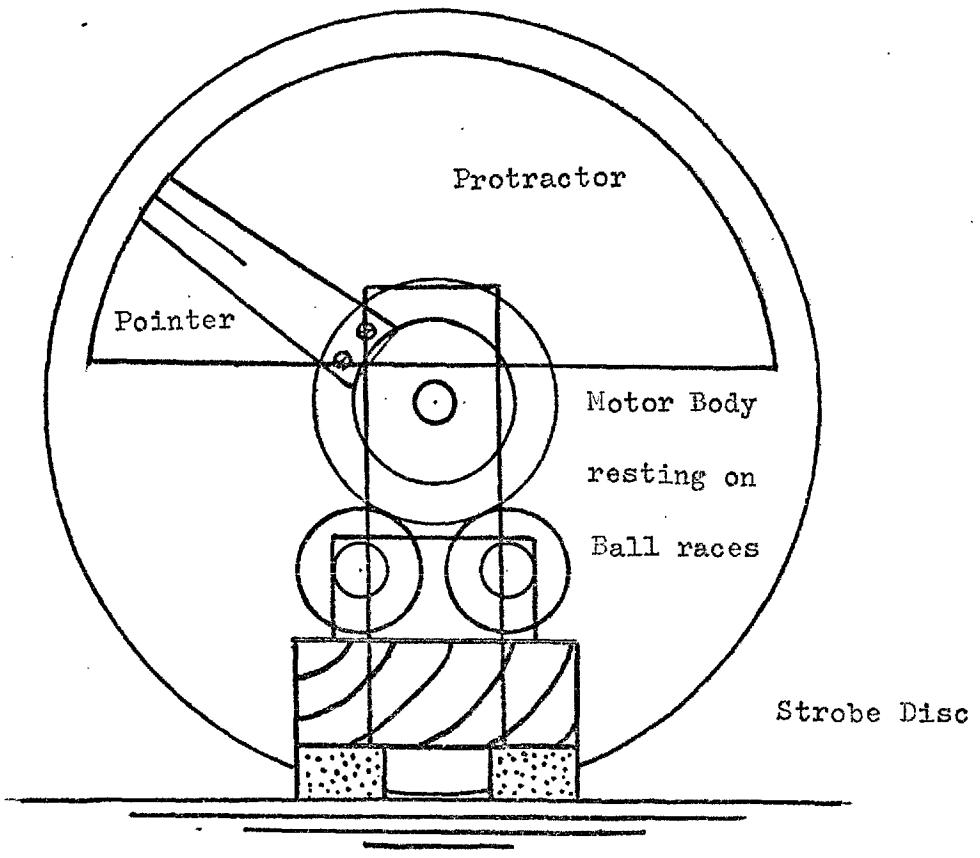




Figure 35 (a) and (b) Synchronous Motor Stand

could also be used to lock the motor body to its holder with a simple clamp, and this was the arrangement used for scanned holography. The position along the hologram at which the peak to peak fringes could be seen was, of course, adjustable by rotating the whole motor by the desired number of degrees. Lead weights were placed on the stand under the motor and foam rubber feet completed the isolation system which minimised the transmission of vibration of the motor to the worktable. In the experiments on Loudspeakers it was possible to mount the motor off the holographic table altogether thus permitting extra isolation to be gained from the table suspension itself.

(m) The Goodman Amplifier

This 120 watt amplifier with integral oscillator had 8 KT88 valves in the output stage. It was used to drive the synchronous motor so the full output power was only used on running up to speed. However the HT current was roughly the same wether the load was applied or not and the resulting heat (roughly equivalent to a 2 Kw electric fire) had to be channeled outside the laboratory with a system of ducting. The original circuit was modified so that one of the two valves of the oscillator section could be used as a straight amplifier when a jack plug was inserted into its socket. This facility was used as described in the final paragraph of (j) above. The integral output current meter being a hot wire device was easily burned out and so a simple voltmeter was used to monitor the output intead.

(n) The Second Amplifier

This specially designed and constructed amplifier giving 100 watts was used to drive the plate exciter. The circuit was a hybrid of several commercial circuits with the first stages being due to Radford and the final fixed bias stage being a modified Lowther circuit. The two KT88

valves and fixed bias allowed 100 watts to be achieved with only a fraction of the heat output of the Goodman amplifier. The fixed bias voltage had to be supplied from a low impedance source and had to be very well smoothed and regulated as there was a pronounced tendency for one or other of the output valves to glow red-hot without these precautions.

(o & p) The Spectrum Analyser and Stable Oscillator

A new Bruel and Kjaer filter set was used for all the measurements involving sound pressure level. When pure tones were used the noise level was effectively reduced by using the filters set to the narrowest pass band. The reverberation times were measured with a Bruel and Kjaer chart recorder tracing on white wax paper. The oscillator available was sufficiently stable to ensure that it did not drift from the high 'Q' resonance frequencies of the test plates but it had insufficient fine tuning to enable these resonances to be easily excited to their peak values. It was capacity tuned, so a small trimmer was wired in parallel allowing the frequency to be finely tuned over a range of 10 Hz and this was sufficient to allow the plate resonances to be accurately tuned. The actual frequencies of the resonances were read off the Bruel and Kjaer filter set and should even greater accuracy have been desired a digital frequency meter was available from another experiment.

(q) The Frequency Divider

This was an integrated circuit which, when fed with a 9 volt input of frequency F, gave 9 volt square wave outputs at F/2, F/4 ..... F/128. A simple limiting amplifier was used to provide the required sensitivity of 1/2 volt. A stabilised power supply was built to provide the necessary 27 and 11 volt supplies. The outputs were isolated with capacitors and the circuit covers most needs for frequency division. The motor will work satisfactorily when fed with square waves, but they were fed in through a low pass filter to avoid high frequency high voltage transients.

## 3.4) The Experimental Method

### (i) The Normal Stroboscopic Method

In order to find the correct phase for the stroboscopic disc, a 'live' hologram had to be taken first. The relative strengths of the object and reference beams were arranged at about one to five respectively and the unexposed photographic plate was then carefully slid into place in the appropriate holder. It was pushed gently against the three position stops and then was left for about two minutes for the heat of the observers hand to dissipate. The plate was then exposed to the light from the stationary object for thepreviously determined correct exposure time. It was developed in Ilford D19B (later plates were developed in caustic hydroquinone) for three minutes, fixed in Hypam + hardener for one minute, washed and dried as quickly as possible and then returned to the holder where it was pushed gently against the end stops. On looking through it at the object, with the exposure shutter raised, the holographic reconstruction and the object itself could be seen in registration. Interference between the light from these two 'images' often caused up to three fringes of translation to be observed. The plate was then delicately adjusted until, at most, only one fringe covered the whole object. This live fringe hologram could be used for several days, provided the room temperature was maintained constant (it was always approximately $24^{o}$).The small shifts which did occur,due to shrinkage and other effects, could be corrected by moving the hologram. Eventually the accumulation of these movements necessitated the taking of a new live hologram.

Next the resonance of interest was selected and the oscillator tuned to its peak with the aid of the microphone meter. To collect energy from all the room modes excited by the object the microphone should be in a corner position. However, plate modes had a higher 'Q' than room modes

so there was little error in tuning onto a plate peak (rather then a room peak) with the microphone in the more convenient position from which it would subsequently be set swinging for measuring the average S.P.L. (p 84). Next the strobe disc, with 16 holes of such diameter that the duty cycle was 1/10, was placed in the path of the laser beam - before it passed into the optical circuit. The motor was then brought up to speed (p 96) and the object again observed through the live hologram. Fringes were then probably seen on the object - the phase of the strobe being entirely random in relation to the object vibrations. The motor was then rotated until the maximum number of fringes were seen on the object or the desired phase of strobing was achieved.

The following steps were then taken:

(1) The live fringe hologram was quickly removed and the shutter mechanism switched on.

(2) An unexposed photographic plate was inserted and the first of the two exposures needed for a 'frozen fringe' hologram was taken.

(3) The excitation to the object was cut-off by pulling out the input plug.

(4) After the plate vibrations had died down, the second, rest position exposure was taken with the same exposure time and with the strobe disc still rotating. This ensured that each exposure was exactly the same and, assuming a 1/10 duty cycle, each exposure needed would be 5 times that for a live hologram.

(5) The exposed frozen fringe hologram was then placed in a light tight box prior to development.

In order to measure the sound pressure level in the enclosure only a short time after the hologram was taken the following procedure was adopted:

(1) The excitation to the strobe disc was switched off and the excitation to the object plate was restored to its former level by reinserting the

input plug.

(2) The microphone was set swinging rapidly in a large circle, but avoiding close proximity to any of the room walls.

(3) The average S.P.L. was then read from the microphone meter, set to 'slow' and noted.

This sound pressure level was measured at a time slightly after the hologram was taken. To ensure that it corresponded with that at the time the holograms was taken a S.P.L. reading was sometimes taken before the hologram was exposed for checking purposes. This showed that in the small time needed to carry out the above procedure, the equipment and room conditions and indeed plate resonsnce frequencies were all completely stable. Thus readings taken immediately after the hologram was exposed correspond exactly to the S.P.L. at the time the hologram was taken.

The photographic plate was developed and fixed, and viewed with the exposure flag in the raised position with the object beam blanked off. A set of fringes corresponding to the maximum object displacement were then seen allowing the mode shape to be observed and the number of fringes giving the vibration amplitude corresponding to the measured S.P.L. in the reverberant room to be noted. The number of fringes could be measured by eye to within 1/3 of a fringe by looking at the reconstruction. A photograph of the reconstruction would be needed for a more accurate measurement. For even greater accuracy the photograph would have to be studied with a microdensitometer which can read accurately to about 1/100 fringe, though there is little point in reading to such accuracy when the S.P.L can only be read to ± 2 db according to theory and possibly only ± 3 db in practice. Measurements by eye were therefore used to compile the results table. Photographs were taken, however, for example purposes and the detailed procedure followed for this operation is described in Section (IV) where the actual positioning of the fringes and the mode shape described by them is more important than with discs which have very regular modal patterns.

(ii) The Simple Scanning Method

This method was developed to remove many of the disadvantages of the ordinary stroboscopic method while retaining its advantages which have been fully described in Section (II) - the main ones being high fringe visibility and ease of fringe interpretation. In addition this new technique has several advantages of its own and developments from the basic technique are even easier to use and may give additional information - these are described in Section (IV) together with their theory.

Basically the strobe disc is removed from the input to the optical system and placed immediately in front of the hologram. Its holes are extended to radial slits which allow virtually the whole of the top half of the photographic plate to be exposed through the spinning disc. The object and reference beams pass through the disc from different directions and so the disc must be sufficiently close to the photographic plate for the desired fraction of each beam to be in registration (p 94). This misregistration may be used to increase the off-on ratio without changing the exposure time and with a small sacrifice in image contrast (hallock 1968) see also page 95. The loss in image quality resulting from scanning the reference beam only, with only a slight possible gain in top operating frequency, meant that this variation of the technique was not used in the main experiments.

The procedure detailed in (i) above was then carried out with the following additions: The body of the synchronous motor was locked into place and the disc mode and correct frequency division selected. The photographic plate was inserted and the first exposure (to the vibrating object) taken with the disc spinning just in front of the plate. N.B. no preliminary live fringe hologram is necessary. The second exposure was then taken with the object excitation removed. On development and viewing

with the reference beam a second advantage of the method is seen: On moving the eye along the hologram, fringe systems are seen in sequence on the object corresponding to practically all phases of the object motion. Only those regions of maximum velocity being too blurred to see with a practical off-on ratio, which in practice is no serious disadvantage. Asymmetrical vibrations may be studied since each peak to zero fringe pattern may be seen by moving the eye to the appropriate part of the hologram, and nodes may be'picked out' since fringes are stationary there. All the fringes seen on the object are due to the excited vibration and not due to any translation or mis-location of a live hologram which is needed to obtain cine pictures of a whole vibration cycle - this being previously the only other way to study whole vibration cycles at leasure.

(iii) The Stroboscopic Law

According to the book 'Stroboscopes' by J. Rutowski there is a strobe law defined as follows:

$$f_a = f_r - M/N\, f_o$$

Where $f_a$ is the frequency at which the object appears to vibrate if the strobing frequency differs from the object frequency.

$f_r$ is the strobing frequency

$f_o$ is the object frequency

M is the image 'multiplicitance'

N is the image'repetitance'.

For a stationary image to be seen $f_a = 0$ i.e.

$$f_r = M/N\, f_o$$

A single image is seen when M = 1, a double when M = 2 etc. There will be a motionless single image when M = 1 and N = 1,2,3,4 .... etc. Therefore obviously the strobing frequency may be any integer submultiple of the object frequency for a stationary image to be observed. However, if the

strobing frequency is say 1/2 of the vibration frequency of the object this is then sampled once in every two cycles and therefore the duty cycle is reduced by the same amount since a correspondingly larger portion of each cycle is sampled. There is therefore a limit to the extent to which N may be increased. In the present experiments the maximum N used was 4 giving a resultant duty cycle of 1:5 taking into account the improvement in the effective duty cycle obtainable for object reference beam misregistration. The methods of Single Scan I and II described in Section (IV) make use of image multiplicity in that the strobing frequency is twice the object frequency for SSI and four times the object frequency for SSII. When Single Scan III is used there is only one flash per object cycle but no stationary exposure both N and M are then unity.

(iv) The Upper Frequency Limit of Disc Strobing Systems

The maximum frequency attainable with a disc strobing system, either normal strobe of any of the scanning systems, is limited initially by two factors (1) The speed at which the disc will 'fly apart' and (2) The speed to which the motor may be driven - limited in this case by the high voltages necessary for supplying sufficient power. The latter is the more serious limitation limiting the rotation speed to 300 revs/sec. Since the motor has four poles the spindle rotates once for every two cycles applied, therefore a disc with two holes in it will allow an experimental frequency of 600 Hz for one flash per cycle. The maximum on-off ratio is limited initially by the diameter of the laser beam for normal stroboscopy and by the proximity to the photographic plate necessary for beam registration when using a narrow slit in scanned holography. (with vertically stacked object and reference beams the limit is much finer and corresponds to the angular width of the object). This minimum hole and slit size allows very large on-off ratios up to 1:80 for frequencies below 600 Hz with a 15 cm diameter scanning disc, though any smaller

ratio may of course be obtained with larger holes. To reach higher frequencies, the frequency applied to the motor is divided by multiples of two and the number of holes is increased in the same ratio. The limit to this process is reached when there are 32 holes in the 15 cm disc circumference, each one being the same diameter as the laser beam (with scanned holography 32 slits of laser beam width also represents a practical limit). The corresponding object frequency will then be 9.6 KHz. To reach higher object frequencies the on-off ratio may be reduced, from the 1:10 obtained with 32 holes/slits, to 1:5 by allowing one flash every other cycle . This results in an upper frequency limit of 19.2 KHz which is entirely satisfactory.

Should it have proved necessary to increase the on-off ratio still further in ordinary stroboscopy, smaller holes would have had to be used and the laser beam focussed down in order to pass through them - this would incidentally also have allowed a smaller disc to be used but would have resulted in much light being wasted. Strobing only the reference beam at the focus of the zoom lens system would also have allowed smaller holes to be used though, as described above, the image contrast would suffer from the build-up of bias due to the unreferenced parts of the object wave. The upper freque ncy limits of SS I and SS II may only be extended by increasing the number of slits and relying on beam misregistration to maintain a satisfactory on-off ratio, alternatively very narrow slits may be used in conjunction with a stacked reference beam. With 32 slits giving an on-off ratio of 1:10 the upper frequency limit is SS I is 4.8 KHz that of SS II is 2.4 KHz and that of SS III is 9.6 KHz.

(v) <u>The Time Averaged Method</u>

The unmodified time average method was used on occasions, due to circumstances beyond the author's control in the case of experiments on plates*

*due to time taken to replace faulty motor

and out of choice for ssome of the experiments on Loudspeakers. At high frequencies the disc scanning method is not as sensitive or convenient as the unmodified time averaged method which had the requisite sensitivity.

The required resonance was selected as detailed above and an unexposed photographic plate inserted into the scanned holography holder. The plate was exposed to light from the vibrating object for an exposure time similar to that required for live holography. On viewing the reconstruction approximately twice as many finges are seen for a given object movement as with the normal stroboscopic method. Using tables of Bessel function zeros, these results were corrected to correspond to ordinary or scanned strobe results and noted. The S.P.L. was taken with the swinging microphone set in motion when the observer left the reverberation room in order to take the hologram.

(vi) Plate Modes Studied

Holograms and S.P.L. measurements were taken at each of the object plate modes that were capable of excitation with the 'edge' transducer. This was in fact every single mode, including the umbrella, which are possible with a center supported system (Waller 1962) (see also fig 36 ). Holograms were taken at many different vibration magnitudes at several of the modal frequencies. Finally it was attempted to take holograms when the object was excited with the impulsive 'banger' at several frequencies, and in fact poor contrast holograms were produced showing a blurred fundamental mode. This was to be expected since most of the vibrational amplitude is due to the fundamental under impulsive excitation conditions whereas the actual acoustic radiation is modified by increasing radiation resistance at higher frequencies (approximately as $f^2$), and complicated by cancellation from the rear of the object plate, and also the coincidence critical frequency. A suitable topic for further work would be a detailed study of all phases of the vibration under impulsive excitation however the amplitudes of the various harmonics present may be more easily found from the -

- response curve

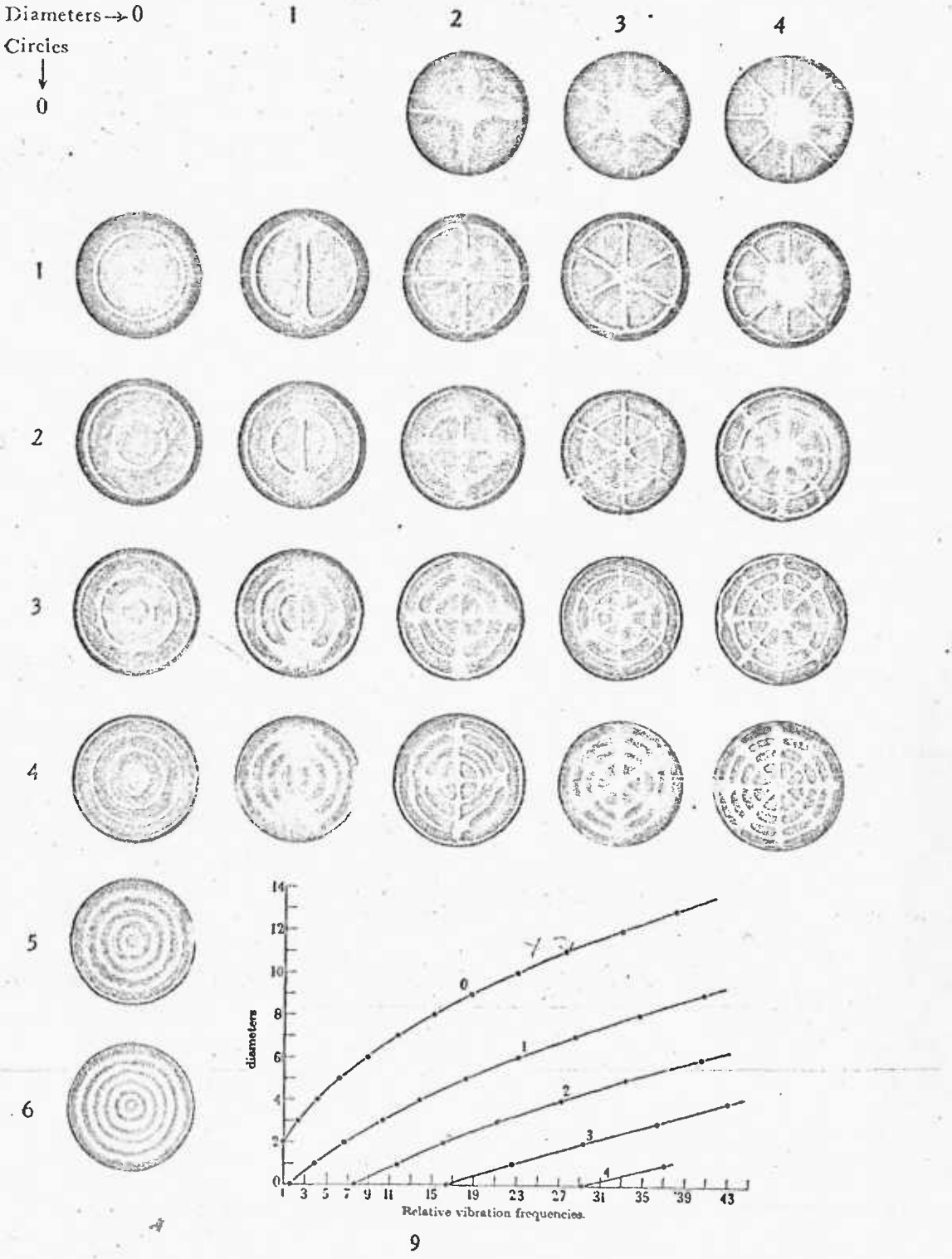
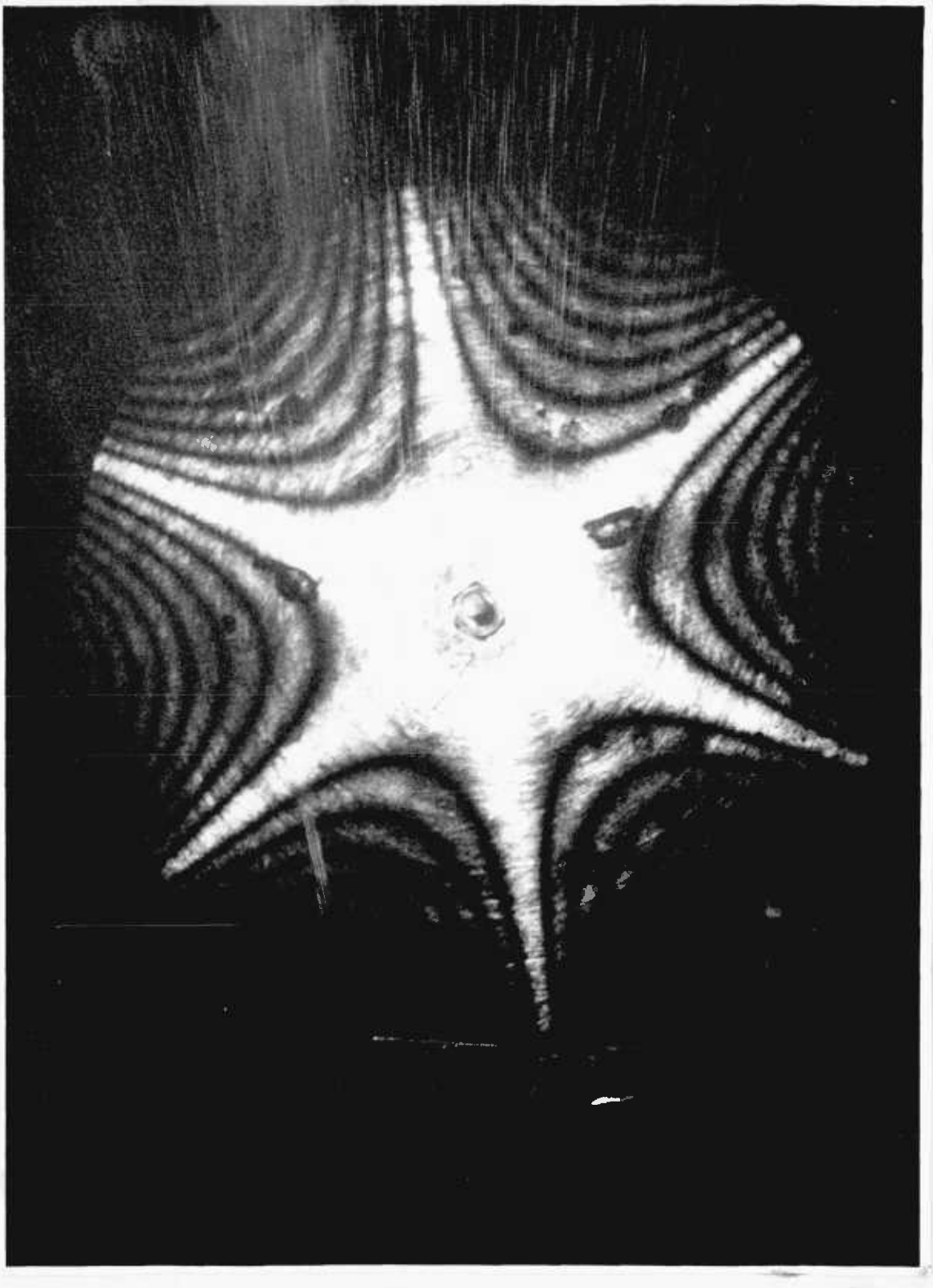



Figure 36 Modes of a Free Disc (After Waller)

N.B. Column 1 not found with center supported disc. and I nodal dia is possible with finite clamping radius at center

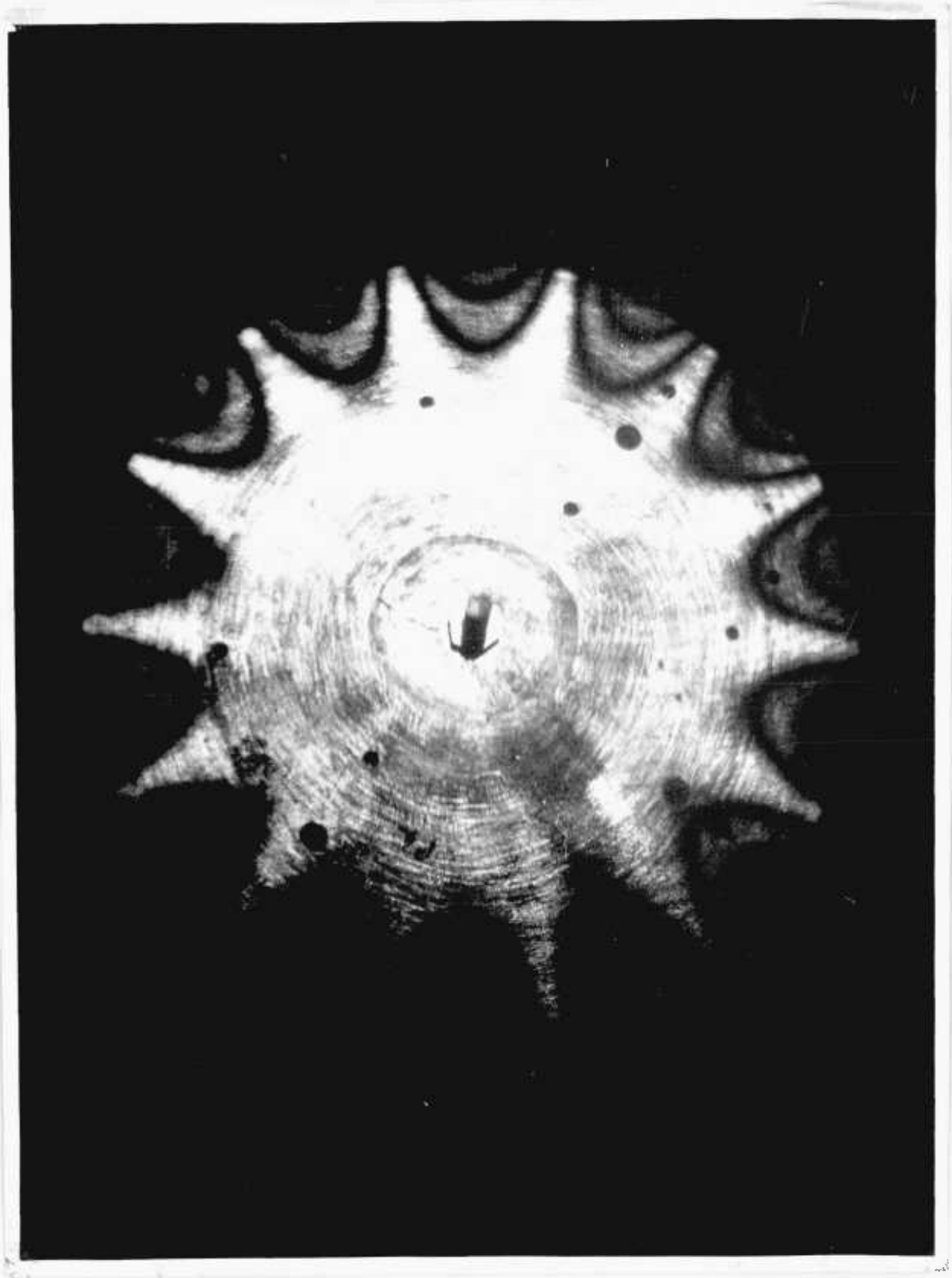
Plate Number 5



Time Averaged Hologram - Disc Vibrating at 1200Hz

(same amplitude as disc in Plate 1)

Plate Number 6



Time Averaged Hologram - Disc Vibrating at 5700Hz

Plate Number 7



Frozen Fringe Hologram - Disc Vibrating at 2050Hz

(photograph of plate 7 in thesis copy number 1)

## 3.5) Results and Calculations

### (i) Power Level Calculations

The formula used to calculate the sound power given out by tthe object plates was taken from 'Acoustics' by L.L.Beranek (1954). The following formulae were also used:

Sabine reverberation time $T_s = \frac{55.26\ V}{S\alpha c} = \frac{.049\ V}{S\alpha}$ (3.11)

Eyring reverberation time $T_e = \frac{55.26\ V}{Sc\log_e(1-\alpha)} = \frac{.049\ V}{S\log_e(1-\alpha)}$ (3.12)

in metric units: $T_s = \frac{.161\ V}{S\alpha}$ $T_e = \frac{.161\ V}{S\log_e(1-\alpha)}$ (3.13)

(N.B. in a sabine room the direct sound equals the reverberant sound at a distance $r = (S\alpha/2\pi)^{1/2}$ )

With the volume of the reverberation room used the Sabine R.T. becomes:

$$T_s = 1.146/T \quad (3.14)$$

Now $P_{rms} = \left[\rho_o cW\left(\frac{1}{4\pi r^2} + \frac{4(1-\alpha)}{S\alpha}\right)\right]^{1/2}$ (3.15)

and so S.P.L. = P.W.L. + $10\log_{10} c - 36 + 10\log_{10}\left(\frac{1}{4\pi r^2} + \frac{4(1-\alpha)}{S\alpha}\right)$ (3.16

now P.W.L. = $10\log_{10}\frac{W}{10^{-13}} = 10\log_{10}W + 130$ db (3.17)

and so S.P.L. = $10\log_{10}W + 130 + 26.1 - 36 + 10\log_{10}\left(\frac{1}{4\pi r^2} + \frac{4(1-\alpha)}{S\alpha}\right)$ (3.18)

Where S.P.L. = Sound Pressure Level in db re .0002 microbar

r = distance from the source in metres.

W = power emitted by the source in watts.

$\rho_o c$ = characteristic impedance of air = 407 at 22°C and 751 mm

$10\text{Log}_{10}\rho_o c$ = 26.1 db M.K.S. units.

V = room volume in cubic metres.

S = room surface area in meters$^2$ $S\alpha$ = total absorbtion

$P_{rms}$ = foot mean square averaged sound pressure in the room

$\alpha$ = average absorbtion coefficient.

Therefore the power radiated in watts W is:

$$W = \text{antilog}\left(\frac{S.P.L}{10} - 12.01 - \log_{10}\left(\frac{1}{4\pi r^2} + \frac{4(1-\ )}{S}\right)\right) \qquad (3.19)$$

Taking the Sabine R.T. from equation (3.13) with V = 7.1334 cu. metres

$$W = \text{antilog}\left(\frac{S.P.L.}{10} - 12.01 - \log_{10}\left(\frac{1}{4\pi r^2} + \frac{4(1-\ )T}{1.146}\right)\right) \qquad (3.20)$$

Taking r = 1.5 m and the lowest R.T. = .5 seconds with S = 2.292 $m^2$

The first term in the log bracket = 1/(4π2.25) = 0.04452

and the second term = 2/1.146 = 1.745

Since therefore the first term is only 2.5 percent of the second even in the worst case, it may be neglected - bearing in mind that the S.P.L. may only be read theoretically to ± 2 db. Therefore using the Sabine R.T.

$$W = \text{antilog}\left(\frac{S.P.L}{10} - 12.01 - \log_{10}\left(\frac{4T}{1.146}\right)\right) \qquad (3.21)$$

$$W = \text{antilog}\left(\frac{S.P.L}{10} - 12.55 - \log_{10}(T)\right) \qquad (3.22)$$

---

(b) Example Calculation

Object plate number (2) Steel Gear Wheel 30 cm diameter.

Mode: Two Nodal Diameters, 7.5 fringes , 540 Hz , R.T. = .75 secs

$$\log_{10}W = 66.5/10 - 12.55 - \log_{10}.75$$

$$= 6.65 - 12.55 + .1249$$

$$= -5.778$$

$$= \bar{6}.222$$

$$W = 10^{-6} \times 1.67 \text{ acoustic watts.}$$

| No. | Log. |
|---|---|
| .75 | $\bar{1}.8751$ |
| i.e | - .1249 |

Where the S.P.L. is measured to ± 2 db , the R.T. to ± .1 seconds and the volume and surface area are measured to at least an order of magnitude more accurately.

(c) Variations in the Calculated Power Levels

(1) If the S.P.L. of the example had been + 2 db (and for 10 percent of the time it will be outside even this limit) and the R.T. had been .1 second less then:

$$\log_{10}W = 6.85 - 12.55 - \log_{10}.65 \qquad .65 \;\; \bar{1}.8129$$
$$= 6.85 - 12.55 + .1871 \qquad \text{i.e.} \;\; -.1871$$
$$= -5.516$$
$$= \bar{6}.484$$
$$W = 10^{-7} \times 30.48 \text{ acoustic watts}$$

(2) If the S.P.L. of the example had been - 2 db and the R.T. had been .1 second more then:

$$\log_{10}W = 6.45 - 12.55 - \log_{10}.85 \qquad .85 \;\; \bar{1}.9294$$
$$= 6.45 - 12.55 + .0306 \qquad \text{i.e.} \;\; -.0306$$
$$= -6.072$$
$$= \bar{7}.928$$
$$W = 10^{-7} \times 8.47 \text{ acoustic watts}$$

Therefore it can be seen that in this example the output calculated may vary from $30 \times 10^{-7}$ to $8.5 \times 10^{-7}$ acoustic watts. This is a threefold variation for 90 percent of the time and an even greater variation for the other 10 percent. Therefore only differences of an order of magnitude or more in the results table can be taken as showing any definite trends.

The uncertainty in the measurement of the number of holographic fringes is about ± 1/3 fringe in about 8 fringes or at most 5 percent with a maximum error of 33 percent when only one fringe is present. At higher frequencies the ± 1 db variation theoretically calculated still results in the major error being due to the S.P.L. measurements and not to the counting of holographic fringes.

(ii) Results Object (2) Steel Gear Wheel (.64 cm Thick)

| Frq. Hz | modes | holo | fringes | S.P.L. meter | S.P.L. corr. | Frq. R.T. | band R.T. | Acoustic Watts total. | per ampl. $\lambda/4$ |
|---|---|---|---|---|---|---|---|---|---|
| 540 | 2 d | 56 A | 8 | 52 | 66.5 | .78 | .72 | $1.67\times10^{-6}$ | $.11\times10^{-6}$ |
| 5440 | | 56 B | 7.5 | 52 | 66.5 | .78 | .72 | $1.67\times10^{-6}$ | $.12\times10^{-6}$ |
| 540 | | 55 | 7 | 51 | 65.5 | .78 | .72 | $1.32\times10^{-6}$ | $.10\times10^{-6}$ |
| 910 | umb | 52 | 6 | 69 | 83.5 | .72 | .66 | $8.95\times10^{-5}$ | $8.1\times10^{-6}$ |
| 1260 | 3 d | 57 | 11.5 | 59 | 73.5 | | .69 | $8.73\times10^{-5}$ | $4\times10^{-6}$ |
| 2150 | 1d1c | 90 | 1.5 | 70 | 84.5 | .66 | .61 | $7.89\times10^{-5}$ | $39.4\times10^{-6}$ |
| 2200 | | 77 | $1\frac{2}{3}$ | 69 | 83.5 | .61 | .61 | $1.03\times10^{-4}$ | $51\times10^{-6}$ |
| 2050 | 4 d | 74 | 17 | 75 | 89.5 | .60 | .61 | $4.15\times10^{-4}$ | $12\times10^{-6}$ |
| 2050 | | 75 | 7.5 | 73 | 87.5 | .60 | .61 | $2.62\times10^{-4}$ | $19\times10^{-6}$ |
| 2100 | | 85 | 4 | 63 | 77.5 | .53 | .61 | $2.97\times10^{-5}$ | $4.2\times10^{-6}$ |
| 2100 | | 86 | 7 | 72 | 86.5 | .53 | .61 | $2.36\times10^{-4}$ | $18\times10^{-6}$ |
| 2100 | | 89 A | 3 | 61.5 | 76.0 | .53 | .61 | $2.1\times10^{-5}$ | $4\times10^{-6}$ |
| 2100 | | 87 | 3 | 62 | 76.5 | .53 | .61 | $2.36\times10^{-5}$ | $6\times10^{-6}$ |
| 2100 | | 89 B | 11.5 | 75 | 90.5 | .53 | .61 | $4.7\times10^{-4}$ | $21\times10^{-6}$ |
| 2130 | | 58 | $2\frac{2}{3}$ | 64 | 78.5 | .6 | .61 | $3.3\times10^{-5}$ | $8\times10^{-6}$ |
| 2150 | | 88 B | .5 | 55 | 69.5 | .66 | .61 | $3.77\times10^{-6}$ | $6.5\times10^{-6}$ |
| 2150 | | 91 | 1 | 62 | 76.5 | .66 | .61 | $1.89\times10^{-5}$ | $19\times10^{-6}$ |
| 2200 | | 104 | 1 | 63 | 77.5 | .61 | .61 | $2.58\times10^{-5}$ | $26\times10^{-6}$ |
| 3180 | 5 d | 59 A | 11.5 | 88 | 102.5 | .55 | .5 | $8.97\times10^{-3}$ | $407\times10^{-6}$ |
| 3180 | | 59 B | 7.0 | 84 | 98.5 | .55 | .5 | $3.57\times10^{-3}$ | $300\times10^{-6}$ |
| 3380 | 2d1c | 60 A | .5 | 71 | 85.5 | .56 | .5 | $1.77\times10^{-5}$ | $34\times10^{-6}$ |
| 3380 | | 60 B | 4 | 86 | 100.5 | .56 | .5 | $5.6\times10^{-4}$ | $80\times10^{-6}$ |
| 3380 | | 88 A | 2 | 77.5 | 92.0 | .56 | .5 | $7.9\times10^{-5}$ | $36\times10^{-6}$ |
| 4400 | 6 d | 61 | $1\frac{1}{3}$ | 72 | 86.5 | .52 | .53 | $2.4\times10^{-4}$ | $150\times10^{-6}$ |
| 4400 | | 61 B | 1.5 | 72 | 86.5 | .52 | .53 | $2.4\times10^{-4}$ | $120\times10^{-6}$ |
| 4400 | | 66 | $1\frac{2}{3}$ | 69 | 83.5 | .52 | .53 | $1.2\times10^{-4}$ | $60\times10^{-6}$ |
| 4600 | | 67 | $\frac{1}{3}$ | 66 | 80.5 | .64 | .53 | $4.9\times10^{-5}$ | $196\times10^{-6}$ |
| 5000 | 3d1c | 63 | 1 | 79 | 83.5 | .53 | .54 | $1.18\times10^{-3}$ | $1180\times10^{-6}$ |
| 5100 | | 66 | $1\frac{1}{2}$ | 82 | 96.5 | .53 | .54 | $2.36\times10^{-3}$ | $1180\times10^{-6}$ |
| 5800 | 7 d | 67 | 2 | 79 | 93.5 | .45 | .50 | $1.39\times10^{-3}$ | $460\times10^{-6}$ |
| 5700 | | 64 | .5 | 68 | 82.5 | .55 | .50 | $9.05\times10^{-5}$ | $180\times10^{-6}$ |
| 5700 | | 64 | 1 | 78 | 92.5 | .55 | .50 | $9.05\times10^{-4}$ | $905\times10^{-6}$ |
| 5900 | | 71 | $2\frac{2}{3}$ | 81 | 95.5 | .51 | .50 | $1.95\times10^{-3}$ | $490\times10^{-6}$ |

| Frq. Hz | modes | holo | fringes | S.P.L. meter | S.P.L. corr. | Frq. R.T. | Band R.T. | Acoustic total | Watts per $\lambda/4$ ampl. |
|---|---|---|---|---|---|---|---|---|---|
| 6900 | 4d1c | 69 | 1 | 72 | 86.5 | .56 | .54 | $2.28\times10^{-4}$ | 228 x $10^{-6}$ |
| 7500 | 8 d | 68 | 1⅓ | 73 | 87.5 | .55 | .43 | $2.86\times10^{-4}$ | 180 x $10^{-6}$ |

(iii) Results Object (2a) Steel Gear Wheel (1.9 cm Thick)

| | | | | | | | | | |
|---|---|---|---|---|---|---|---|---|---|
| 1290 | 2 d | 47A | 9.5 | 76.5 | 82.0 | | .69 | $8.10\times10^{-5}$ | 50 x $10^{-6}$ |
| 1280 | | 46 | 1 | 70 | 75.5 | | .69 | $1.44\times10^{-5}$ | 144 x $10^{-6}$ |
| 2900 | 3 d | 47 | 5 | 91 | 96.5 | .5 | .5 | $2.50\times10^{-3}$ | 260 x $10^{-6}$ |
| 2875 | | 48 | 2 | 68 | 73.5 | | .5 | $3.53\times10^{-4}$ | 118 x $10^{-6}$ |

(iv) Results Object (1) Brass Plate (1.27 cm Thick)

| | | | | | | | | | |
|---|---|---|---|---|---|---|---|---|---|
| 540 | 2 d | 8 | 7.5 | 68.5 | 73.0 | .78 | .72 | $7.16\times10^{-6}$ | .51 x $10^{-6}$ |
| 520 | | 12 | 5 | 67 | 72.5 | .71 | .72 | $6.25\times10^{-6}$ | .7 x $10^{-6}$ |
| 525 | | 27 | 10 | 68 | 73.5 | .72 | .72 | $8.04\times10^{-6}$ | .42 x $10^{-6}$ |
| 1200 | 3 d | 33 | 7⅔ | 68 | 73.5 | .74 | .7 | $8.95\times10^{-6}$ | .6 x $10^{-6}$ |
| 1200 | | 35 | 2 | 60 | 65.5 | .74 | .7 | $1.4\times10^{-6}$ | .36 x $10^{-6}$ |
| 1200 | | 10 | 26 | 73 | 78.5 | .74 | .7 | $2.68\times10^{-6}$ | .52 x $10^{-6}$ |
| 2050 | 4 d | 28A | 3.5 | 85.5 | 91.0 | .6 | .61 | $5.87\times10^{-4}$ | 97 x $10^{-6}$ |
| 2070 | | 36A | 2 | 80 | 85.5 | .6 | .61 | $1.6\times10^{-4}$ | 53 x $10^{-6}$ |
| 2100 | | 26 | 4.5 | 85 | 90.5 | .53 | .61 | $6.0\times10^{-4}$ | 75 x $10^{-6}$ |
| 3100 | 5 d | 22 | 1⅓ | 71 | 76.5 | .41 | .5 | $4.8\times10^{-4}$ | 240 x $10^{-6}$ |
| 3100 | | 38 | 2.5 | 87 | 92.5 | .41 | .5 | $1.2\times10^{-3}$ | 300 x $10^{-6}$ |
| 3100 | | 28B | 1⅓ | 80 | 85.5 | .41 | .5 | $2.4\times10^{-4}$ | 120 x $10^{-6}$ |
| 3380 | 2d1c | 31 | 3.5 | 75 | 80.5 | .56 | .5 | $5.6\times10^{-5}$ | 9.3 x $10^{-6}$ |
| 3400 | | 38 | 4.5 | 84 | 89.5 | .43 | .5 | $4.9\times10^{-4}$ | 98 x $10^{-6}$ |
| 4250 | 6 d | 29A | 2 | 70 | 75.5 | .5 | .53 | $2.0\times10^{-5}$ | 6.3 x $10^{-6}$ |
| 5600 | 7 d | 39A | 2.5 | 88 | 93.5 | .54 | .54 | $1.16\times10^{-3}$ | 290 x $10^{-6}$ |
| 4950 | 3d1c | 39B | 1⅔ | 90 | 95.5 | .53 | .54 | $1.84\times10^{-3}$ | 740 x $10^{-6}$ |
| 4950 | | 29B | 1⅓ | 83.5 | 88.5 | .53 | .54 | $3.7\times10^{-4}$ | 350 x $10^{-6}$ |
| 6530 | 4d1c | 41 | ⅔ | 75 | 80.5 | .45 | .54 | $7.0\times10^{-5}$ | 100 x $10^{-6}$ |
| 6530 | | 40 | 1 | 80 | 85.5 | .45 | .54 | $2.21\times10^{-4}$ | 220 x $10^{-6}$ |
| 2070* | | 36B | ⅔ | 63 | 68.5 | .6 | .61 | $3.3\times10^{-6}$ | 5 x $10^{-6}$ |

(v) Notes on the Results Table

(1) Modes Column: 'd' refers to nodal diameters and 'c' refers to nodal nodal circles.

(2) The fringes column: Time averaged results have been converted to the equivalent stroboscopic values. When there is no 'A' or 'B' following the hologram number, the value given in the 'fringes' column is the average of two results - the two exposures on one plate - with the same excitation and the same S.P.L. resulting from this. The fringe counts differed by a maximum of 1 fringe in 10. Also, if the vibrations were asymmetrical the figure given is the average of the positive and negative excursions.

(3) The 'S.P.L. corr.' column: With Plate (1), where a corner microphone position was used, this is the S.P.L. meter reading plus the 14.5 db microphone correction minus the 9 db positional correction i.e. + 5.5 db. With Plate (2) , where the swinging microphone technique was used, this is the S.P.L. meter reading plus the 14.5 db microphone correction only.

(4) 'Frq R.T.' refers to the reverberation time at the modal frequency 'Band R.T.' is the average R.T. over a narrow band around the modal frequency.

(5) Acoustic Watts: 'Total' is the total power given out at the given frequency and 'per $\lambda/4$ ampl.' is the power given out per $\lambda/4$ movement of the object plate at the antinodal regions, where $\lambda$ = 6328 Å

(6) It is regretted that there are gaps in the results table, particularly with regard to Plate (1) which was used primarily to develop the apparatus. These gaps could not be filled because the author had to vacate the laboratory before having the oportunity to resume tests on Plate (1) or being able to run a series of tests on this plate with the superior swinging microphone technique.

(7) Object (2a). This was object (2) before it was turned down to match the resonance frequencies of plate (1). Experimental difficulties prevented further high frequency modes of this plate being studied prior to turning down. A series of experiments on similar plates of differing thickness is a suitable topic for further work which would point to the relevance of the coincidence critical frequency ($f_c$) in sound radiation from circular plates.

(vi) Average Radiated Acoustic Power Per Unit Displacement

| | | Plate (2) Steel | | | Plate (1) Brass | | |
|---|---|---|---|---|---|---|---|
| Frq.Hz | Mode | (W per $\lambda/4$)* | norm. | (*)/$f^2$ | (W per $\lambda/4$)* | norm | (*)/$f^2$ |
| 540 | 2 d | .1 | 1 | 1 | .5 | 1 | 1. |
| 1260 | 3 d | 4 | 40 | 7.5 | .5 | 1 | 0.34 |
| 2050 | 4 d | 13 | 130 | 9 | 75 | 150 | 10.4 |
| 3180 | 5 d | 350 | 3500 | 100 | 220 | 440 | 12.7 |
| 4400 | 6 d | 130 | 1300 | 20 | 63 | 126 | 2. |
| 5700 | 7 d | 550 | 5500 | 50 | 290 | 580 | 5.2 |
| 7500 | 8 d | 180 | 1800 | | - | - | - |
| 910 | umb | 8 | 80 | 28 | - | - | - |
| 2150 | 1d1c | 45 | 450 | 28.4 | - | - | - |
| 3380 | 2d1c | 50 | 500 | 13 | 50 | 100 | 2.6 |
| 5000 | 3d1c | 1180 | 11800 | 138 | 545 | 1090 | 12.8 |
| 6900 | 4d1c | 228 | 2280 | 14 | 100 | 200 | 1.2 |

From theoretical considerations it is to be expected that the object plates will radiate more efficiently above the coincidence critical frequency ($f_c$) than below it . Therefore the critical frequencies for Plate (1) brass and Plate (2) steel are calculated below:

The coincidence critical frequency is given by

$$f_c = \frac{(v_{air})^2}{1.8\,h}\sqrt{\frac{\rho}{E}} \qquad (3.23)$$

Where $h$ = Plate thickness

$E$ = Youngs modulus of elasticity

$\rho$ = Density of Plate material

(1) For the Steel object plate (no 2):

$h = .25$ inch $\qquad \rho = 8$ gm cm$^3$

$E = 21 \times 10^{11}$ dyne/cm$^2$ $\qquad v_{air} = 1132$ ft per sec 22°C

Therefore

$$f_c = \frac{1132\ 1132\ 30.48\ 12}{1.8\ \ .25} \sqrt{\frac{8}{21 \times 10^{11}}} \qquad (3.24)$$

$$= 2050 \quad \text{Hz}$$

(2) For the Brass object plate (no 1):

$h = .5$ inch $\qquad \rho = 8.5$ gm cm$^3$

$E = 10 \times 10^{11}$ dyne/cm$^2$

From these

$$f_c = 2870 \quad \text{Hz}$$

It may be seen from the above table that these coincidence critical do indeed coincide with the transition from poor radiation efficiency to good radiation efficiency.

It may also be seen that some modes radiate far more efficiently than others, in particular the 5 nodal diameter and the 3 diameter 1 circle modes have a large radiation resistance. Others, however, do not radiate efficiently, in particular the 6 nodal diameter and the 2 and 4 diameter 1 nodal circle modes. Some theoretical investigations into the reasons for this are reported in Appendix II.

The 'umbrella' mode radiates with average efficiency even though it is below the critical frequency. This is because it is a special case having no regions vibrating in antiphase giving rise to volume velocity for cancellation purposes.

In theoretical work there is a 'large' plate criterion. The plate is acoustically large if $k_{air}\, a > 1$ or $a > \lambda_{air}/2\pi$ where a is the radius. Therefore the present object plates are acoustically large above 350 Hz.

## 3.6) Conclusions ..... Section III (Circular Plates)

(1) It has been demonstrated, using an impulsive excitor to model many of the more impulsive components of gear action, that when a plate mode coincides in frequency with a harmonic of the excitation frequency, this mode is more likely to be excited.

(2) A new method of stroboscopic holographic interferometry - that of ' Scanned Holography' has been devised and put to good use in the study of plate vibrations. This technique has several advantages, some of which are: The live 'phase setting' hologram is no longer necessary; Asymmetrical vibrations may be studied, and whole vibration cycles are preserved on one hologram. (This technique will be further developed in Section IV where it has been adapted to show subharmonics only).

(3) A reverberation room, though relatively small, has been successfully used in conjunction with Scanned Holography to find the relative radiation efficiencies of the plate modes studied.

(4) It has been found that the coincidence critical frequency ($f_c$) does coincide with a transition from modes of low radiation efficiency to modes of higher radiation efficiency.

(5) It has also been found that some modes above $f_c$ have a markedly greater radiation efficiency than others (p 114), while others radiate less strongly than the average. Therefore the conditions of excitation and support, the deployment of damping materials and finally the fundamental frequencies of impulsive gear action should all be arranged to avoid the excitation of these high efficiency modes.

## Suggestions For Further Work

(1) A series of experiments on plates of (a) different materials and (b) different thicknesses should be carried out. This would verify the significance of the coincidence critical frequency in sound radiation theory and reveal how the modes of high radiation efficiency are deployed when parameters change.

(2) The results table should be extended by (a) taking more readings at varying levels of excitation - especially at those modal frequencies where only a few results are reported; (b) Plate (1) should be reinvestigated using the swinging microphone technique.

(3) A detailed study of object plates excited with an impulsive device may be carried out utilising the facility of Scanned Holography to preserve whole vibration cycles for study. Amplitude - phase curves would then result.

(4) A more quantitative study of the relative ease with which each plate mode can be excited, (a) supported in the center and excited at the edge perpendicular to the plane of the plate and (b) supported in the center and excited at the edge tangentially should be carried out.

(5) The method of Scanned Holography has been developed further in the next section. This new and versatile technique has further potential for development which should be explored.

# SECTION IV

# EXPERIMENTS ON LOUDSPEAKERS

CONTENTS - Section 4 - Experiments with Loudspeakers


| | | |
|---|---|---|
| Introduction | | 118 |
| 4.1) | Holographic Methods Applied to Loudspeakers | 120 |
| (i) | 'Live' and 'Frozen Fringe' Holography | 120 |
| (ii) | Basic Scanned Holography | 122 |
| (iii) | Single Scan I | 123 |
| (iv) | A Phenomenon Observed with Single Scan I | 123 |
| (v) | Single Scan II | 126 |
| (vi) | Single Scan III | 127 |
| 4.2) | Theory of Scanned Holography | 128 |
| (i) | Double Exposure Holograms | 128 |
| (ii) | Basic Scanned Holography | 129 |
| (iii) | Single Scan I | 131 |
| (iv) | Single Scan II | 131 |
| (v) | Single Scan III | 132 |
| (vi) | Possible Explanations for 'Blanking Fringes' | 133 |
| | (a) Linear Motion | 134 |
| | (b) Sinusoid plus Linear Motion | 135 |
| | (c) Single Scan I plus a General Harmonic | 136 |
| | (d) Single Scan I plus Even Harmonics | 137 |
| | (e) Single Scan I plus Odd Harmonics | 137 |
| | (f) Single Scan I plus the First Subharmonic | 137 |
| | (g) Collection of results | 140 |
| 4.3) | Experimental Points | 141 |
| (i) | Treatment Given to Loudspeakers | 141 |
| (ii) | Vibration Isolation Loudspeakers and Hum | 142 |
| (iii) | Experimental Layout | 144 |
| (iv) | Photography of Reconstructions | 144 |
| 4.4) | Experimental Method | 146 |
| 4.5) | Typical Features in the Holograms of Loudspeakers | 147 |
| (i) | Hypothetical Ideal | 147 |

(ii) Real Loudspeakers - Classification of Fringes 148

(a) 'Re-entrant' 149
(b) 'Hill and Dale' 149
(c) 'Edge Bending' 150
(d) 'Umbrella' 150
(e) 'Rocking' 151
(g) Chassis 152

4.6) Discussion of Results - Paper Cones 152

(i) to (vii) Individual Speakers 152

(viii) Conclusions 157

4.7) Sandwich Bass and Treble Units 157

(i) Introduction 157

(ii) Discussion of Results 159

(a) Bass Units 159
(b) Treble Units 162

(iii) Relation between Modal Patterns and Radiated Sound 163

4.8) Conclusions 166

(i) Mid Range Paper Units 166

(ii) Sandwich Units 166

(iii) General 167

4.9) Further Work 167

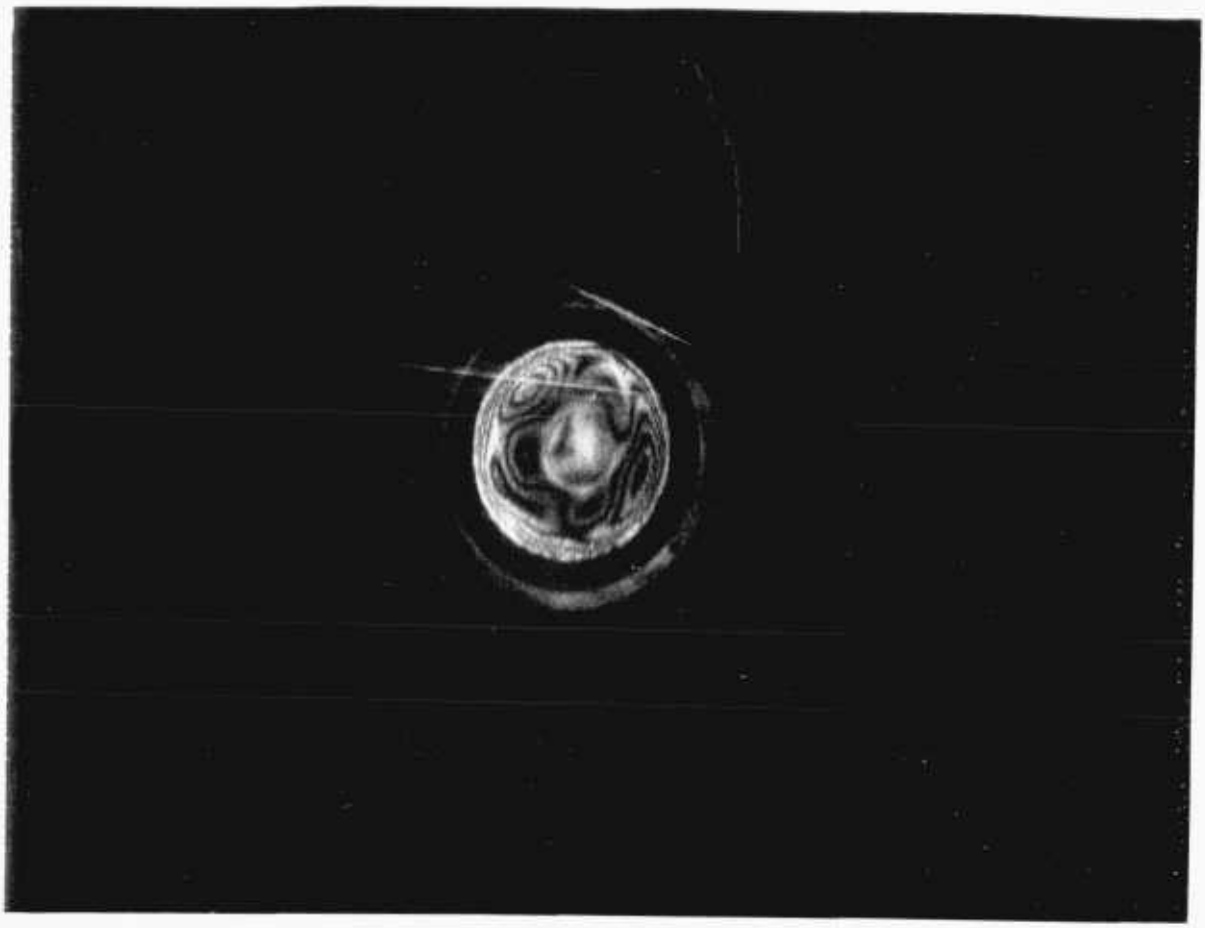
(i) Mid Range Units 167

(ii) Sandwich Units 168

(iii) General 168

Total Number of Pages: 102

Plate Number 8



Photograph taken from a Scanned Hologram with slit set for maximum amplitude. Speaker 1, 2.2K

## EXPERIMENTS ON LOUDSPEAKERS

### Introduction

The purpose of a Loudspeaker is to translate electrical signals from an amplifier into equivalent variations of sound pressure. When the signals are applied to the voice coil this in general moves in synchronism with the applied signal. The cone or diaphragm of the Loudspeaker, however, does not move uniformly as a piston, but tends to 'break-up' above certain frequencies (and amplitudes) - i.e. different parts of the cone move at different amplitudes and in different phases with respect to the signal in the voice coil. These 'break-up' patterns may in some cases resemble plate modes - being radial and/or circumferential in character - especially so in Loudspeakers utilising 'sandwich' construction. In most paper cones the 'break-up' patterns are more or less random in character and in some cases the sound output is apparently unaffected by the irregularities. This effect is more likely to occur if the 'break-up' is below the coincidence critical frequency when regions of a given phase give rise to volume velocity which cancels out with regions of opposite phase in the near field. In other cases large variations in power output with frequency can be measured with no exact explanation for their occurrence. Up to the present time the design of Loudspeaker systems has therefore been left in the hands of experts who have gathered their expertise from years of measurement of response curves and impulse test and aural assessment of hundreds of Loudspeakers and associated cabinets. Holographic interferometry can now be applied to the assessment of Loudspeakers and enables the non-expert and expert alike to be better able to asses the merits, or otherwise, of Loudspeaker cones, diaphragms suspension systems etc.

Loudspeaker designers have been aware of the phenomenon of cone 'break-up' for many years but have been unable to investigate it in detail

because of the very small physical movements involved. Even at the lower break-up frequencies a Loudspeaker moves only a few hundredths of a cm for a relatively intense acoustical output. At higher frequencies the movements are of the same order as the wavelength of light, therefore unmodified stroboscopic scanned and basic time averaged holography are directly applicable. Attempts have previously been made to see the break-up patterns by using lycopodium powder or by observing bass units under stroboscopic lighting at low frequencies. These experiments showed that severe break-up occurred but these methods were insufficiently precise and severely limited in sensitivity and frequency of applicability so they were not useful to any great extent in helping the designer to reduce break-up by any significant amount.

Largely as a result of the uncertainty surrounding the exact nature of the break-up patterns and the mechanisms by which they are produced, a series of empirical design philosophies have grown up in the Loudspeaker industry. The majority of designers curve the radius of the cone (creating a geodesic surface) to give it extra stiffness, but the amount of curvature varies greatly from one designers to another. Some designers favour particularly hard cone materials such as aluminium (as used in the G.E.C. metal cone Loudspeaker), or titanium (as used in Jordan's A & D system), while others use particularly floppy lmaterials such as plasticised p.v.c. to great effect (like the K.E.F. mid-range units). One successful design uses a 'sandwich' consisting of expanded polystyrene between two skins of thin aluminium (Barlow 1970). Yet another design relies on a peculiarly shaped asymmetrical expanded polystyrene bowl in a doubtful attempt to spread out the break-up resonances and reduce their effect at any given frequency (the Yamaha). All of these designs break-up at some frequency or another and much of the design thought goes into producing edge suspensions and center spiders to surpress or help to absorb as many unwanted resonances as possible.

The application of holographic interferometry enables us to see precisely what the Loudspeaker cone is doing at any frequency and any amplitude within wide limits. It also enables us to see what the suspension and chassis are doing at the same time. Different holographic techniques are more appropriate for different types of Loudspeaker and for different frequency ranges to obtain the best results. They are described fully in this Section. In particular, because of stability difficulties, the methods of Simple Scanned Holography and Single Scan (I) (SSI) lend themselves to the study of Loudspeakers (Fryer 1972). The methods and theory of SSI and Single Scan II (SSII) and Single Scan III (SSIII) and some of the results obtained with Loudspeakers are described in this Section. Other results have been withheld because of the possibility of their being of use to Rank Wharfedale (who sponsored this research) competitors.

## 4.1) Holographic Methods Applied to Loudspeakers

### (i) Stroboscopic Live and Frozen Fringe Holography

As described in Section II live fringe holography enables the observer to see a contour map of the loudspeaker vibrations as they actually happen (i.e. in real time). With this system therefore the speaker may be ' 'whistled' up its entire frequency range and any points of interest then observed in more detail. A complete vibration cycle may be studied by appropriately altering the phase of the strobing system and the effect of altering the amplitude, frequency, and/or phase of the Loudspeaker may be directly studied merely by observing the speaker through the live fringe hologram. Cine films may be taken of complete'runs' or of whole vibration cycles to observe asymmetry.

Unfortunately tests have shown that paper Loudspeaker cone materials are not very stable, and in the time taken to develop, fix and dry the photographic plate the cone shifts in a random manner. When the

live fringe hologram is replaced, a system of fringes resembling wood grain is seen over the surface of the cone. Further tests using a double exposure technique, thus completely removing the effects of misalignment of the live hologram, showed that in 20 seconds no cone movement occurred, but in four minutes about five fringes of movement had taken place. The chassis of the speaker is, however, completely stable showing no fringes at all over long periods - this shows that the fringes on the cone are due only to its own random movement and its shifting in and out on its compliant suspension in response to minute air currents. The use of a fluid gate (see Section II) would give only a slight gain in 'fringe free' time and possibly the only real solution would be the use of a temperature controlled,draft free,humidity controlled enclosure. This was unfortunately not possible. The possibility of the use of 'live fringe' holography for the study of units having stiffer suspensions and cones of materials other than paper is being investigated at present.

Ordinary frozen fringe holography using a simple strobe disc as described in Section III was also made very difficult but not impossible by this random speaker movement. This is obviously because the system requires a live fringe hologram to select the correct phase for the stroboscopically frozen part of the double exposure. The presence of up to five fringes of random movement necessitates considerable interpretation to be exercised by the observer in deciding when the correct phase has indeed been achieved for this exposure. Therefore this system was not used for studies on Loudspeaker cones. The frozen fringe system also suffers some uncertainties which are described in (ii) below and which are removed by the use of SSI.

(ii) Basic Scanned Holography

The scanning system has been described on pages (102 to 104) and ( 34 ). This system removes the need for a live hologram to set the phase since it

stores on one hologram fringe systems corresponding to all phases of the object movement. The fringes corresponding to the desired object phase can be seen by moving the eye along the hologram until they are seen. This system still requires two exposures however, and this gives rise to a doubt about the reliability of the second exposure in view of the random movement of the loudspeaker cones. Test holograms were taken to resolve this problem. Double exposed holograms were taken, the first exposure being of a stationary Loudspeaker and the second also being of the stationary loudspeaker, but in this case the speaker was excited for a variable period and with variable amplitude between exposures ( but it was not overloaded or driven 'hard',as the non constant magnetic field within and near the gap causes the cone of speakers to either jump out of the gap near to resonance or shift their 'rest' positions at other frequencies when overdriven). These tests showed that the speaker did return to the same rest positon provided the time between exposures was not too long when 'wood grain' fringes would appear as described above.

If the scanning disc is driven in phase with the vibrating speaker, a given slit reaches a given part of the photographic plate at the same phase in every object cycle - it is to be noted that the passage frequency need not be the same as the object frequency. If it is, say, half that of the object, a given slit will still reach a given part of the plate at the same point in an object cycle but the difference is that twice as many object cycles will be seen as the observer moves his eye along the developed plate. Also the effective on-off ratio is reduced by a factor of two as described on page (105). The upper frequency limit may be increased within limits by narrowing the slits and stacking the reference beam above the object speaker as described above. The simple theory of this method is described on page (129).

Though this simple scanning system lends itself to the study of Loudspeakers a modification of the system which removes the necessity for

two exposures was thought to be desirable and this was called the Single Scan I method.

(iii) Single Scan I (SSI)

This system is identical in every way with scanned holography described above except that the disc slit passage frequency must be exactly twice the object frequency. This results in a given slit tracing one interslit distance along the photographic plate while only 1/2 an object cycle takes place. The following slit scanns the same interslit distance while the other half of the object cycle takes place (see theory below). On reconstruction the fringes seen correspond to the difference in object vibration amplitude between different parts of the same object cycle. In fact, as the eye is moved along the hologram, fringe systems are seen which map amplitude differences between phases of an object cycle differing by a constant 180°. At one point along the hologram therefore there will be fringes on the reconstructed pbject corresponding to the difference between the two peaks of the object cycle. Thus there are effectively twice as many fringes produced with this method for a given amount of movement as with the former method. Also only one exposure is taken (which is twice as long as that of each exposure of the former method) removing uncertainties about random movement between exposures and also uncertainties about the cone returning to its rest position after excitation. The fact that the slit passage frequency has to be twice the object frequency results in an upper frequency limit of 4.8 KHz with the unmodified apparatus used. It may be increased, of course, merely by doubling the number of slits and halving their width, and possibly using a stacked reference beam, - but the length of the hologram path corresponding to one cycle of object movement is reduced correspondingly.

(iv) A Particular Phenomenon Discovered with SSI

The method of SSI works very well and has brought to light an interesting

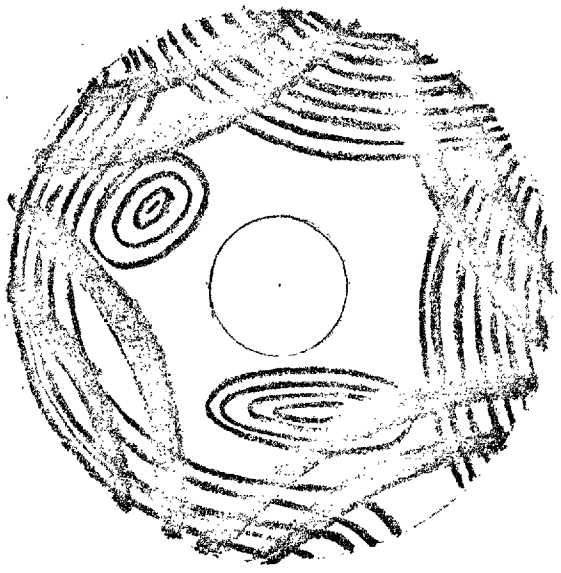
phenomenon (Fryer 1972) which occurs when this method is used to take holograms of speakers moving with medium or large amplitudes. At one point along the hologram the fringes scorresponding to the peak to peak object displacement are seen. At this point the fringes are very similar though twice as many, as those seen with ordinary scanned holography. If, however, we move along the hologram to positions corresponding to different object phases we see that every now and then, the speaker cone completely blanks out - almost as if it were moving with piston motion. Immediately the blanking phases region is left behind the more ordinary fringes are seen once again. If the excitation is increased the 'blanking fringes' assume the form of low amplitude ordinary fringe systems, though the ordinary fringe system may still be seen in the white parts of the reconstruction (see fig 37 ). Therefore the blanking fringe function multiplies the ordinary fringe function in the composite function which describes the total object intensity.

There are three possible explanations for this phenomenon and they are (1) Linear motion superimposed on the vibrations (2) Harmonics even or odd and (3) Subharmonics . All these motions have been shown to occur in loudspeakers and the three possibilities are dealt with theoretically below.

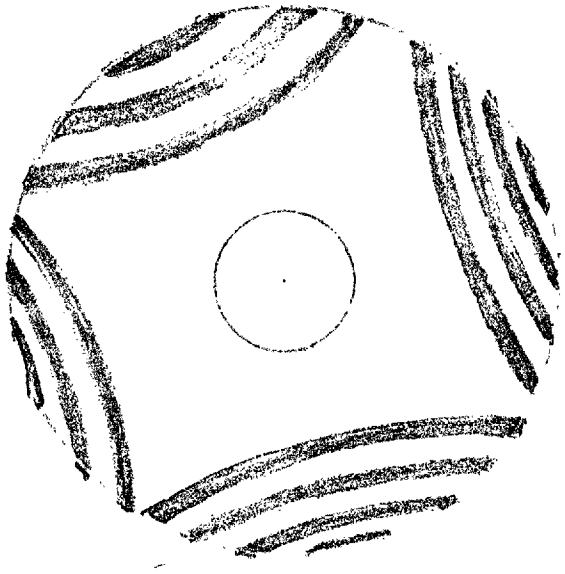
The first possibility was also tested practically. An exposure was taken using the system of SSI at low vibrational amplitude. During the exposure time a steady DC current was increased linearly to reach its maximum value at the end of the exposure, this caused the voice coil to move linearly during the exposure. This was tried with a variety of final DC levels and the expected result was found - the whole speaker was either reconstructed complete with its fringes or it was not reconstructed at all - corresponding to a zero on the $\text{sinc}^2$ curve for the linear movement.

On looking at a diagram (fig 38 ) of the fundamental plus harmonics, it may be easily seen that in fact the contribution from even

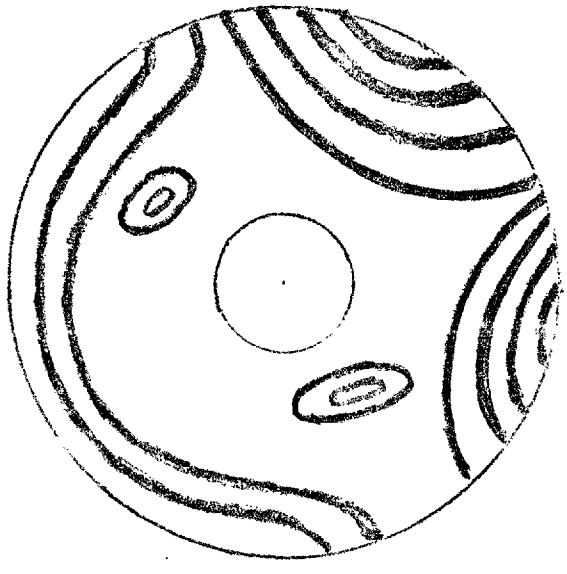
ILLUSTRATIONS OF THE FRINGE SYSTEMS SEEN



With Single Scan I fundamental + subharmonic. Fundamental at twice the sensitivity of ordinary scan



With Single Scan III Subharmonic only, at twice the sensitivity of Single Scan I

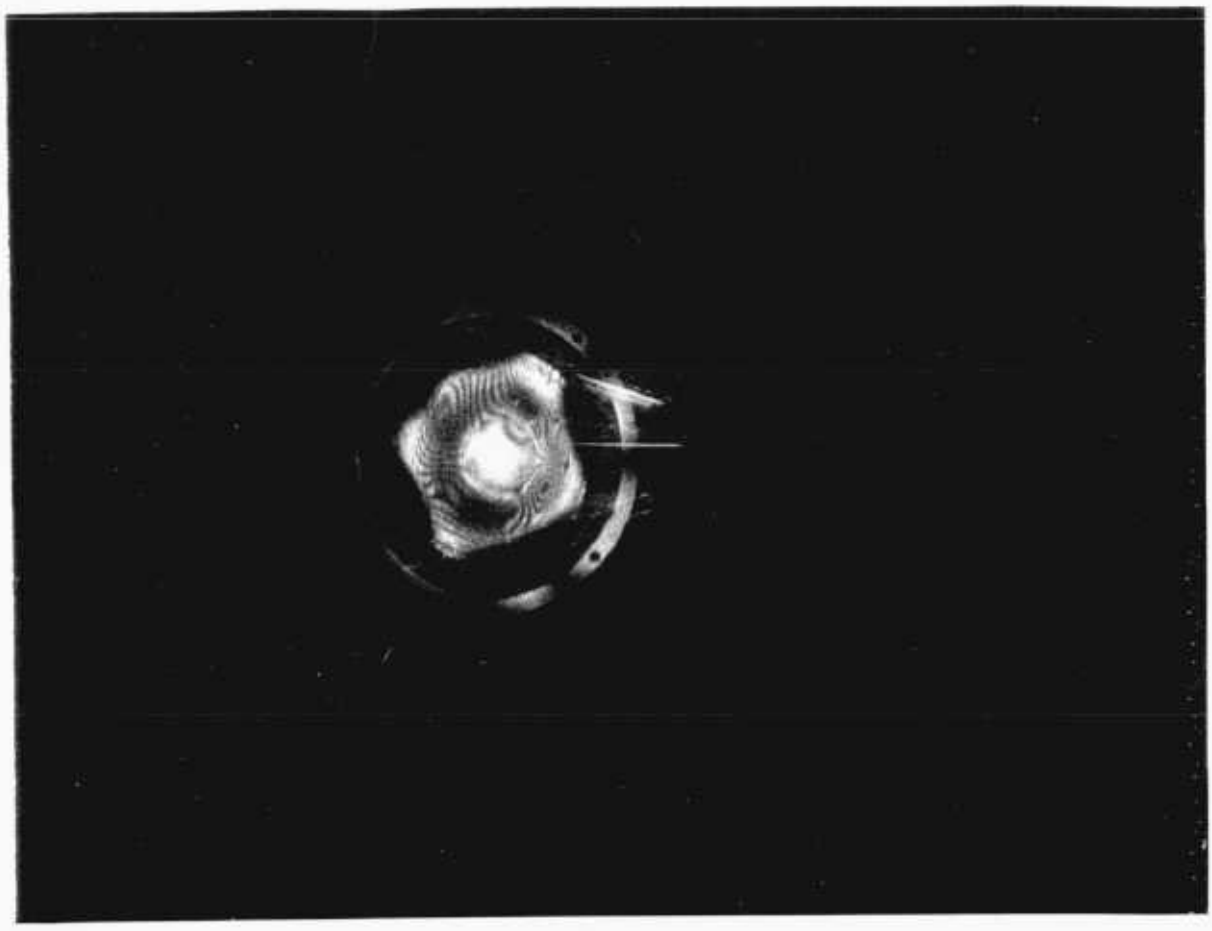


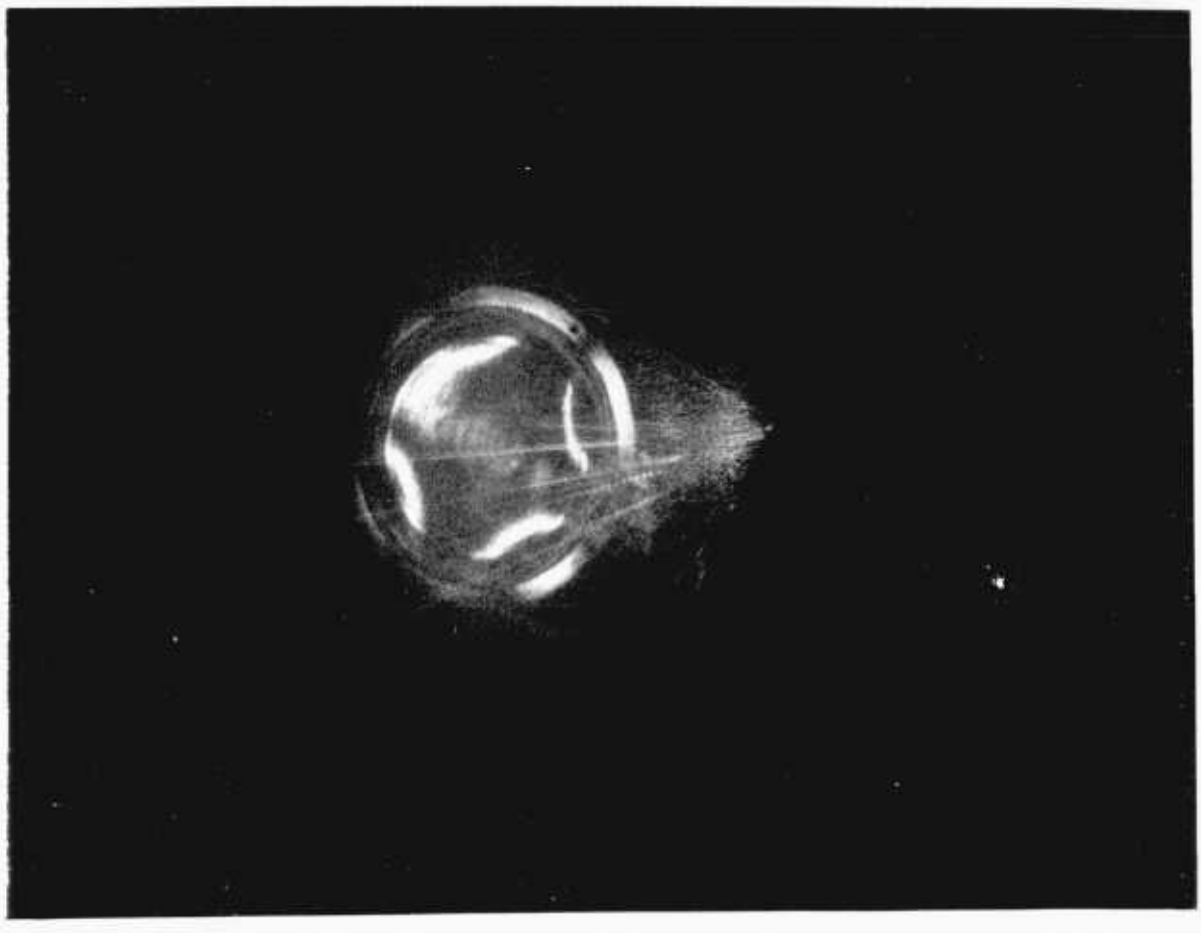
With Ordinary Scan fundamental only at half the sensitivity of single scan I

Figure 37 An illustration of the form of 'Blanking Fringes'

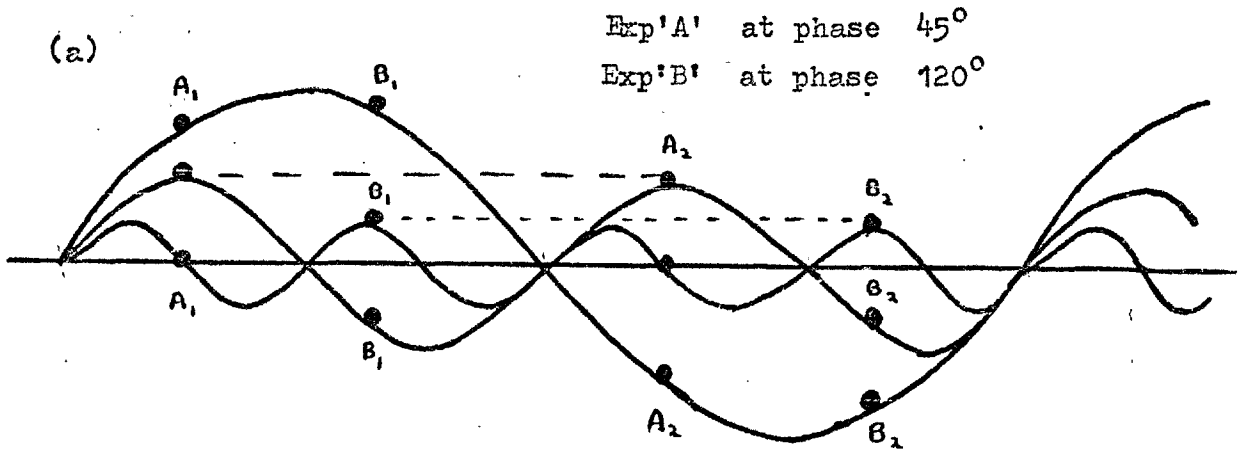
(see also plates on next page)

Plates 9 and 10

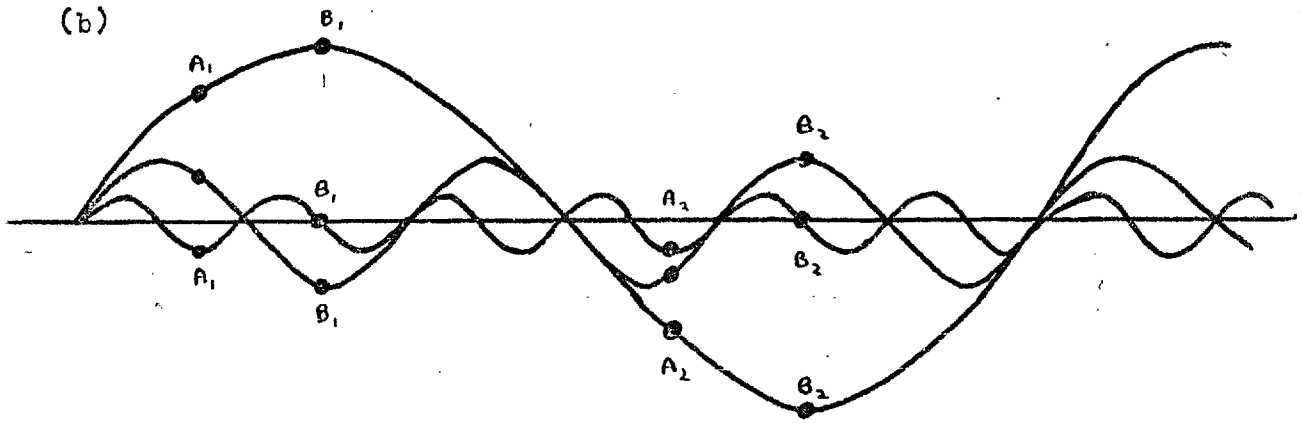




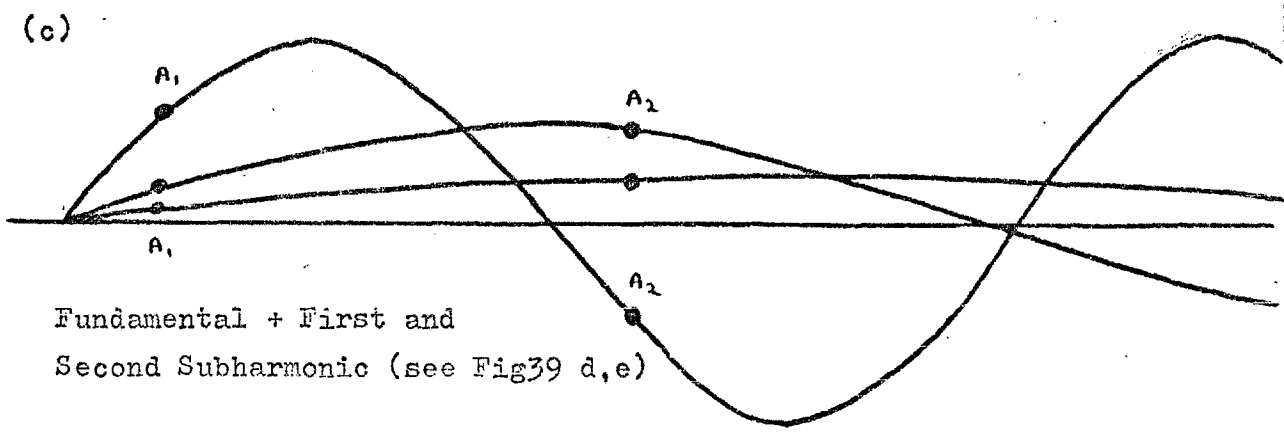
Two Phases of a Speaker Cycle Taken from Scanned Hologram clearly illustrating 'Blanking Fringes'




Fundamental + even harmonics. It can be seen that there is no amplitude difference due to the even harmonics with SS I




Fundamental + odd harmonics .The amplitude difference due to the odd harmonics adds to that due to the fundamental




Fundamental + First and
Second Subharmonic (see Fig39 d,e)

Figure 38 Amplitude differences due to Fundamental + Harmonics with Single Scan I (see also Fig.39 )

harmonics simply cancels out with SSI - since at the sampling points during a cycle the contributions are equal . It may also be seen that the contributions due to odd harmonics merely add to the fundamental. There is also another consideration to be borne in mind and that is the relative amplitudes to be expected of the various harmonics. For a given sound output the amplitude of Loudspeaker vibrations decreases fourfold for each doubling of the frequendy. This means that even if the first harmonic was causing the blanking fringes - which give at most one fringe for every ten 'ordinary' fringes - the sound output due to this harmonic would be 2/5ths of the fundamental for this amplitude of vibration - clearly this is not the case.

When we consider subharmonics however, even the first subharmonic is sampled four times in its cycle which extends over two cycles of fundamental, this indicates that the fringe function due to the subharmonic may be multiplicative (see theory below). Let us consider once again the harmonic amplitude to be expected: For a given sound output the amplitude of the Loudspeaker will increase fourfold for every halving of the input frequency. This means that for the observed maximum 1:10 ratio between blanking and ordinary fringes the amplitude of the sound output due to the first subharmonic need only be 1/40th of the fundamental, this is much more reasonable. It is also to be noted that if the 1/2 or 1/4 subharmonic is causing these fringes they will be more apparrent if the fundamental is twice or four times the frequency of a particular disc like mode of the Loudspeaker when the 'blanking' fringes will assume the shape of this mode. This has been checked experimentaly and found to be correct. From these arguements alone it seems that the blanking fringes are due to subharmonics. If this is the case the method of SSI will give the experimenter information both about the fundamental and the subharmonics of a vibration, and the fringe system is such that both pieces of information may be picked out separately. One way of using the system is to take a SSI hologram of a

vibration. The SSI hologram gives the fundamental amplitude simply but the subharmonic not so simply. Therefore the SSI hologram is best used to indicate the presence of a subharmonic - its amplitude then being found easily from a SSIII hologram which shows subharmonics only. The phenomenon of increasing amplitude with decreasing frequency has also lead to trouble with amplifier hum as described below .

(v) Single Scan II (SSII)

This method is a simple extension of SSI. The fringes and sensitivity resulting are similar to those of ordinary scanning and with the strobe disc illustrated it allows us to observe asymmetry once again.(The method of SSI effectively adds the positive and negative excursions of the vibration which prevents asymmetry from being observed). This method preserves the advantages of a single exposure, but the upper frequency limit is even more severely limited at present to around 2.4 KHz. The disc illustrated is driven so that a given slit traces one inter slit distance along the hologram while the object executes 1/4 of a cycle. The next slit traces the next 1/4 cycle and then there is a gap equivalent to two slits which means that the negative half of the object cycle is not scanned.

With the design shown the inner band of slits will scan those half cycles which are 180° out of phase with the half cycles scanned by the outer band of slits. Thus slits are made to scan the hologram at phases corresponding to 90° phase differences in the object cycle-but only every other half cycle. Points along the hologram where no fringes are seen will correspond to the interference between two identical amplitudes in each half cycle. These scanning systems remove one dimension of redundancy in the information carried by a hologram while the method of SSII also halves the other dimension of hologram redundancy. Since this method is severely limited in its upper frequency it has not been used to any great extent in the present experiments.

(vi) Single Scan III (SSIII)

Following the deliberations set out in (iv) above and the theoretical study of SSI below, the method of SSIII was derived. On looking at a diagram of the fundamental together with subharmonics (fig 39 ) it can be seen that if the fundamental were sampled only once per cycle all contributions due to the fundamental and (super)harmonics would cancel out - since each successive exposure finds them all at the same amplitude. However, the first subharmonic (the 1/2 subharmonic) is then sampled twice in its ccycle in a manner exactly analogous to the scanning method of SSI. The fringes seen with SSIII therefore are the ordinary SSI fringes corresponding to the subharmonic only. The scanning disc used is that of ordinary Scanned Holography and it is used in exactly the same way as for Scanned Holography except that the second, stationary object, exposure is not taken. The upper frequency limit is the same as for Scanned Holography (ii above) and may be extended by sampling once in any odd numbef of cycles of fundamental.

By sampling once in every two cycles of fundamental (or any even multiple of fundamental cycles) the fundamental and (super)harmonics together with the first subharmonic also are excluded,and what are then seen are the 'SSI' fringes due to any 1/4 subharmonic which may be present. The presence of a large component of 1/4 subharmonic when sampling once per cycle (i.e. scanning for the 1/2 subharmonic only) will result in blanking fringes being seen on top of the fringes due to the 1/2 subharmonic in the same way that the 1/2 subharmonic blanks out the fundamental. This phenomenon has not yet been observed by the author, however.

It is possible, of course, to take an SSI hologram and an SSIII hologram on the same photographic plate with an appropriate scanning disc (fig38a) .Other configurations of slits may be worked out to allow any combination of the various scanning methods to be taken on one hologram.

Complete System

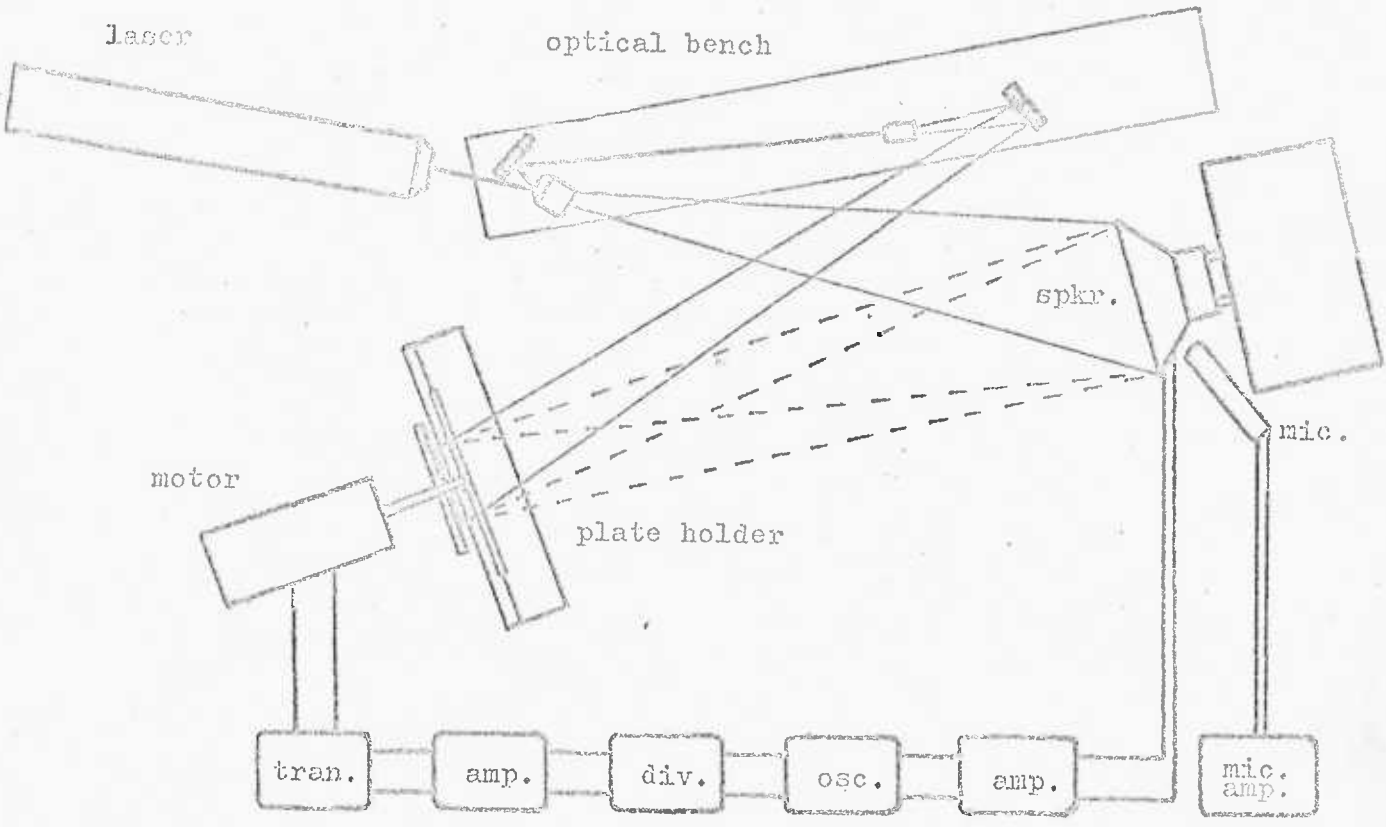
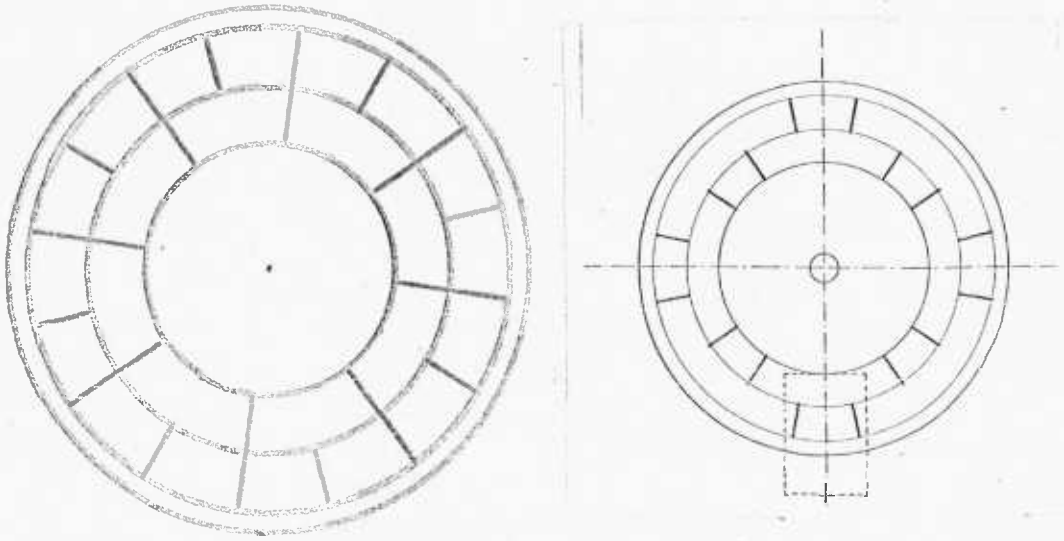
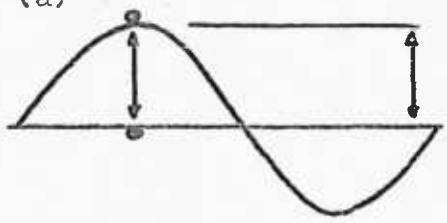



Figure 38 (a)- SSI and SSIII combined disc

Figure 38 (b) SSII disc



(a)

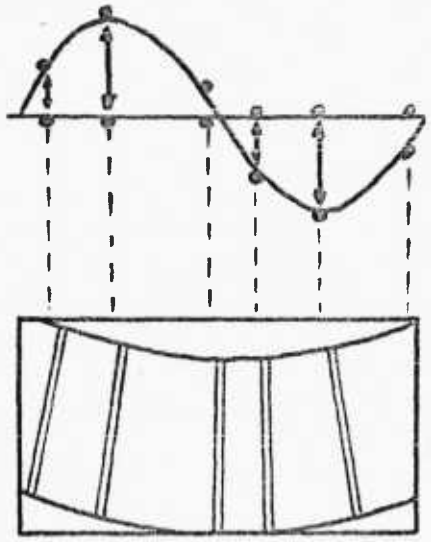


Ordinary Stroboscopy - two exposure points only

● points of exposure

↕ object amplitude difference between exposures

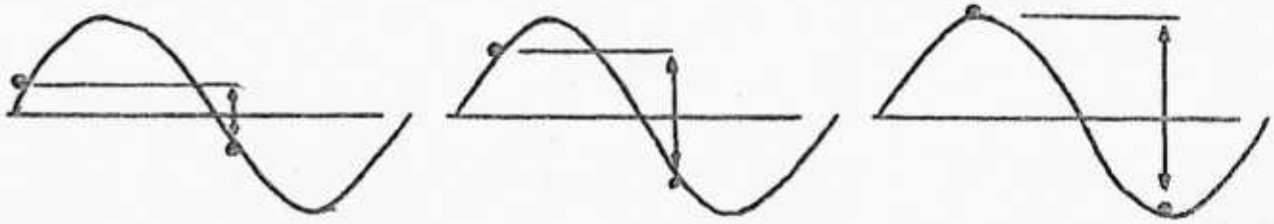
(b)



track on photo. plate

Scanned Holography - exposures at rest and a whole cycle also

(c) '20°' '45°' '90°'

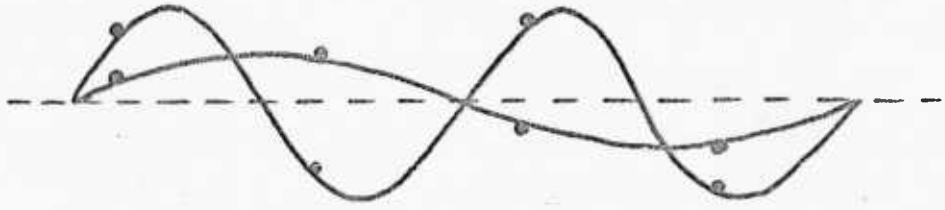


Single Scan I exposures at points 180° out of phase throughout a cycle



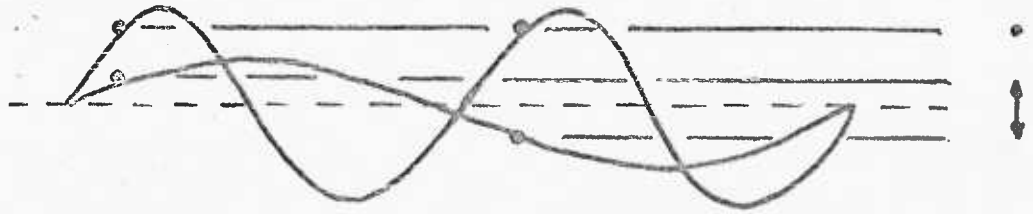
Position of slit along the hologram at above phases

(d)



Two cycles of fundamental + one of subharmonic Single Scan I

(e)



Shows no amplitude difference due to fundamental Single Scan 3
Subharmonic amplitude difference equivalent to Single Scan I

Figure 39 Exposure point diagrams for Scan and Single Scan and SS III

A series of holograms has been taken using, in turn, the methods of Scanned Holography, SSI and SSIII, the loudspeaker used was vibrating with the same amplitude for each exposure. The fundamental frequency was chosen to be twice that of a known modal resonance of the speaker. Scanned Holography showed only fringes due to the fundamental. SSI showed fringes due to the fundamental, but there were twice as many as in the previous hologram, the blanking fringes which were now present assumed the form of the known modal resonance. Finally SSIII showed fringes of the form of the known modal resonance only-there being almost twice as many fringes due to the subharmonic with SSIII as with SSII. The blanking fringe systems of SSI and the fringes of SSIII were checked against a hologram previously taken using Scanned Holography with the known modal resonance as the fundamental, and they were all found to represent the same mode.

## 4.2) Theory of Scanned Holography

The theory of basic holographic reconstruction appears on page (14) and that of doubly exposed holography appears on page (30). For the sake of clarity the latter is repeated here since the scanned holographic theory follows directly from it.

### (i) Double Exposure Holograms

If two holograms of the same but slightly displaced object are recorded sequentially on the same photographic plate using the same reference beam of amplitude 'r' the hologram will superpose the two intensities and give

$$I_{tot} = 2I_r + I_{o_1} + I_{o_2} + r^*(o_1 + o_2) + r(o_1^* + o_2^*) \qquad (4.1)$$

After development, the illuminating reference wavefront is modulated with the above 'frozen' intensity giving:

$$I_{tran} = 2rI_r + rI_{o_1} + rI_{o_2} + rr^*(o_1 + o_2) + rr(o_1^* + o_2^*) \qquad (4.2)$$

The term $I_r(o_1 + o_2)$ is the sum of the two sequentially recorded image amplitudes modulating the reference beam intensity. The intensity of this combined image is:

$$I_{image} = (o_1 + o_2)(o_1^* + o_2^*) \qquad (4.3)$$

Now if the object does not move appreciably between exposures (compared with its distance from the photographic plate) then only the phases of the two wavefronts may be considered to have changed, therefore:

$$o_1 = |o|\, e^{i\phi_1} \qquad o_2 = |o|\, e^{i\phi_2} \qquad (4.4)$$

Giving from (4.3)

$$I_{image} = |o|^2(e^{i\phi_1} + e^{i\phi_2})(e^{-i\phi_1} + e^{-i\phi_2}) \qquad (4.5)$$

$$= |o|^2(2 + 2\cos(\phi_1 - \phi_2)) \qquad (4.6)$$

The term $(\phi_1 - \phi_2)$ is the difference in phase between the two wavefronts at the two exposures and is related to the distance (d) moved by the object: $(\phi_1 - \phi_2) = (2\pi/\lambda)2d$ . Sine the path difference = 2d the phase difference $= (2\pi/\lambda)2d$. Each time the object moves to change the phase by $2n\pi$ , where n is an integer, a dark fringe will reappear on the object.

(ii) <u>Basic Scanned Stroboscopic Holography</u>

Wavefronts corresponding to object displacements at $0^\circ$ and $\theta^\circ$ in an object cycle are collected at a given point 'x' along the hologram and they are added on reconstruction. The object phase $\theta$ reconstructed is directly proportional to the position 'x' along the hologram. In fact $x = r\theta/n$ where r = radius of the scanning disc, n = the number of slits and there is one slit scanning the photographic plate per object cycle, see below for the case when the scanning frequency does not equal the object frequency The amplitude of the wave resulting on reconstruction is therefore:

$$o = |o|\, e^{i\phi_1} + |o|e^{i\phi_2} \qquad (4.7)$$

Now $\phi_1 = (2\pi/\lambda)\, 2d\sin\theta$ $\phi_2 = (2\pi/\lambda)\, 2d\sin 2n\pi$ (4.8)

Where $\theta$ is the phase of the object movement, $\phi$ is the phase of the light wavefront, and here d is the peak to zero amplitude at a given point on the object. Now, for notational convenience:

Let $K = (2\pi/\lambda)\, 2d$ (4.9)

Therefore from (4.7), (4.8) and (4.9)

$$o = |o|\, e^{iK\sin\theta} + |o|\, e^{iK2n\pi} \quad (4.10)$$

Since $I = oo^*$ Then

$$I_{sc.} = |o|^2(e^{iK\sin\theta} + e^{iK2n\pi})(e^{-iK\sin\theta} + e^{-iK2n\pi}) \quad (4.11)$$

$$= |o|^2(2 + 2\cos K(\sin\theta - \sin 2n\pi)) \quad (4.12)$$

$$= |o|^2(2 + 2\cos(K\sin\theta)) \quad (4.13)$$

OR $I_{sc.} = |o|^2(4\cos^2(K\sin\theta/2))$ (4.14)

Now a position 'x' along the photographic plate corresponds to object phase $\theta$ . When the scanning frequency is the same as the object frequency a whole cycle i.e. $2\pi$ radians is covered in arc distance 'X' corresponding to the stationary distance between two slits of the scanning disc. If the scanning frequency is 1/n th of the object frequency, $2\pi$ radians are covered in 1/n th of the distance between two slits, or alternatively $2n\pi$ object radians are covered in the whole distance between two slits 'X'.

Therefore finally:

$$I(\text{scan}) \text{ at } x = (X\theta)/(2n\pi) = |o|^2(2 + 2\cos(K\sin\theta) \quad (4.15)$$

Where $X = 2\pi r/z$ = one interslit distance

$r$ = radius of the scanning disc

$z$ = the number of slits

$n$ = the 'repetitance' (see page 103)

$K$ = defined in equation (4.9) above

$x$ = the distance along the hologram from $\theta = 0$ image

(iii) Single Scan I (SSI)

Wavefronts corresponding to object positions $\pi$ radians out of phase are recorded on the hologram at any given position 'x' along the hologram and are added on reconstruction. Therefore the amplitude of the resulting wave is:

$$o = |o|\, e^{i\phi} + |o|\, e^{i(\phi + \pi)} \qquad (4.16)$$

where $\phi = K \sin\theta$ (see equ. (4.9)

Therefore the resulting amplitude for SSI with the fundamental only present is:

$$o = |o|\, e^{iK\sin\theta} + |o|\, e^{-iK\sin\theta} \qquad (4.17)$$

And so

$$I_{SS_1} = |o|^2(e^{iK\sin\theta} + e^{-iK\sin\theta})(e^{-iK\sin\theta} + e^{iK\sin\theta}) \qquad (4.18)$$

$$= |o|^2(2e^{o} + e^{2iK\sin\theta} + e^{-2iK\sin\theta}) \qquad (4.19)$$

$$= |o|^2(2 + 2\cos(2K\sin\theta)) \qquad (4.20)$$

OR $$I_{SS_1} = |o|^2(4\cos^2(K\sin\theta)) \qquad (4.21)$$

Where $I_{SS}$ is the image intensity at the point 'x' along the hologram and $x = (X\theta)/2n\pi$ as shown in (ii) above.

It may be easily seen that this gives twice as many fringes as the ordinary scanning method and also when $\theta = \pi/2$ the peak to peak fringe system is seen and in this case "$\phi_1 - \phi_2$" $= 2(2\pi/\lambda)2d$ and so there are twice as many fringes as with the ordinary stroboscopic method from one peak to a zero amplitude.

(iv) Single Scan II (SSII)

A given slit traces the distance between two slits in 1/4 of an object cycle, the following slit traces the same path during the next 1/4 of a cycle - the next 1/2 cycle is not traced. Thus there are two exposures effectively $90^{o}$ apart which are added on reconstruction.

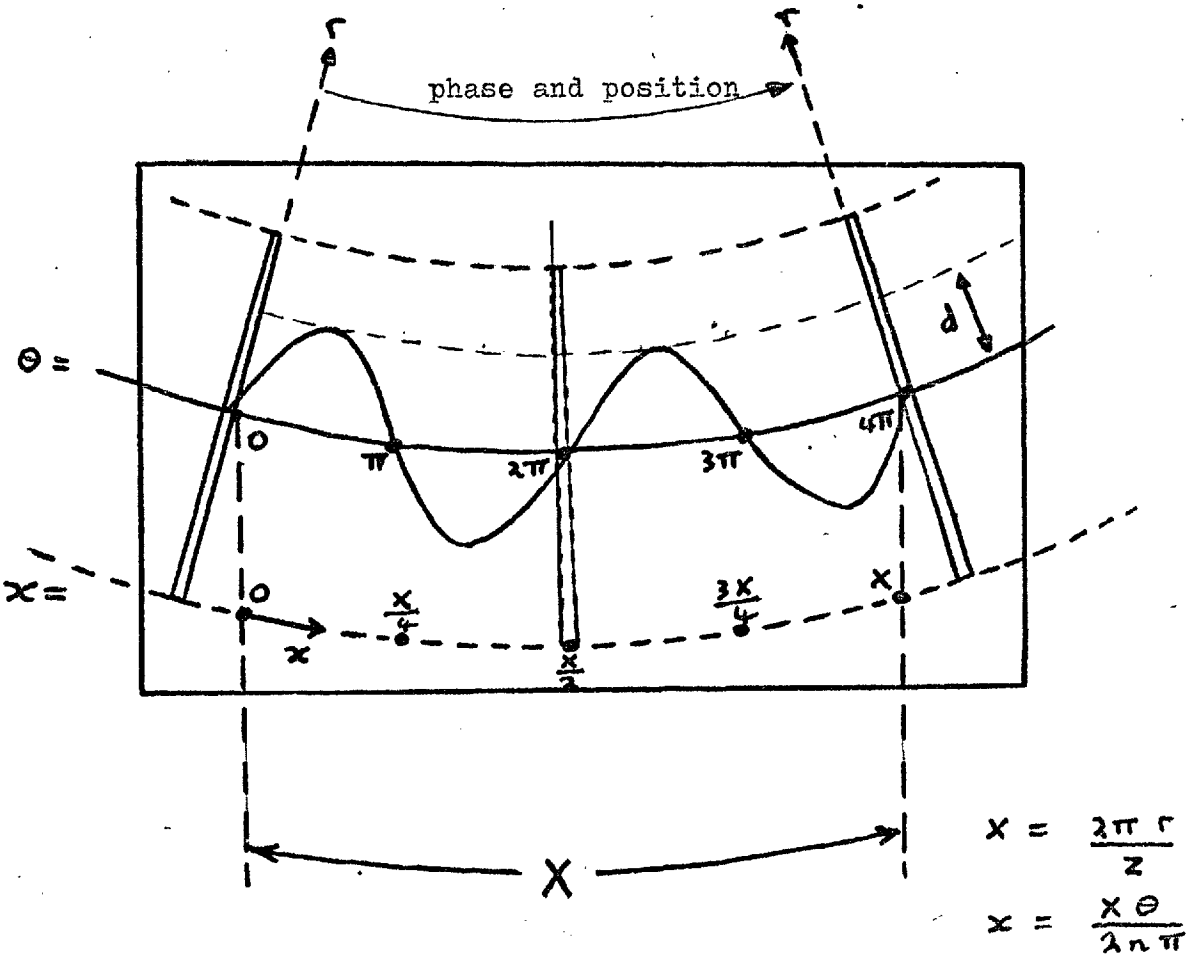



Figure 40 Scan Relationships. X is one interslit distance. x is the distance along the hologram. For this diagram the scanning frequency is 1/2 of the object frequency thus two complete cycles are covered in one interslit distance.

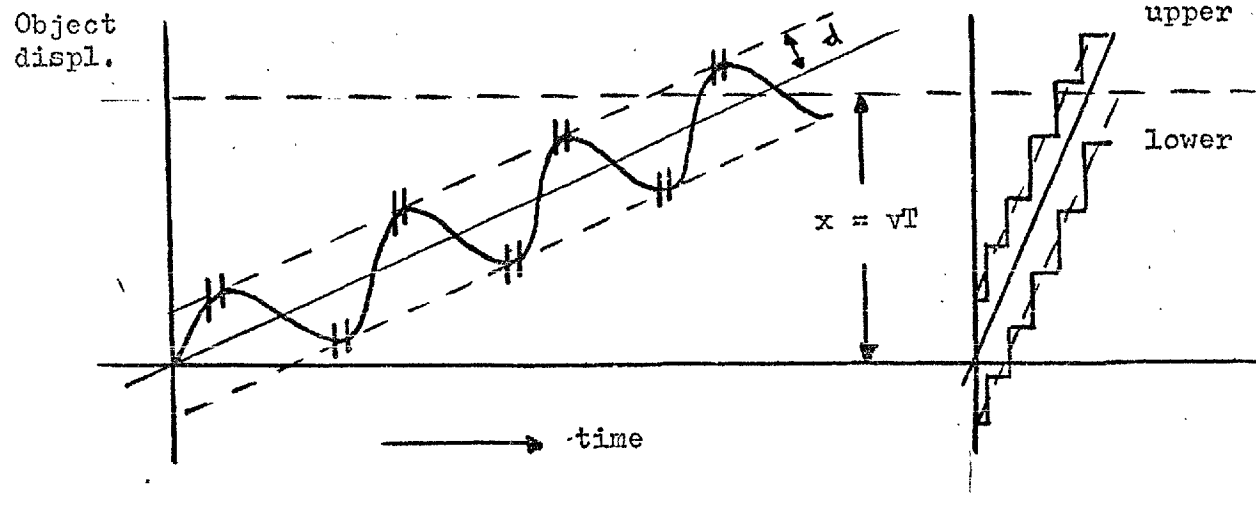



Figure 42 Single Scan I with sinusoid superimposed on linear motion may be regarded as two time averaged exposures of linear motion

giving $o = |o|\, e^{iK\sin\theta} + e^{iK\sin\theta + \frac{\pi}{2}} \qquad 0 \leq \theta < \pi$ (4.22)

Therefore

$$I_{ss} = |o|^2(e^{iK(\sin\theta)} + e^{iK(\cos\theta)})(e^{-iK(\sin\theta)} + e^{-iK(\cos\theta)}) \quad (4.23)$$

$$= |o|^2(2 + 2\cos K(\sin\theta - \cos\theta)) \quad (4.24)$$

OR $$I_{ss} = |o|^2\left(4\cos^2\left(\frac{\sin\theta - \cos\theta}{2}\right)\right) \quad (4.25)$$

For Example:

when $\theta = 0$ $I = |o|^2(4\cos^2(2\pi/\lambda)2d)$

when $\theta = \pi/4$ $I = |o|^2(4\cos^2(\ 0\ )\ ) = |o|^2$

when $\theta = \pi/2$ $I = |o|^2(4\cos^2(2\pi/\lambda)2d)$

i.e.when $\theta = 0$ or $\theta = \pi/2$ the result is the same as for ordinary stroboscopy.

(v) <u>Single Scan III (SSIII)</u>

A given slit traces one interslit distance 'X' in one object cycle and there is no stationary exposure. Therefore, when the object vibration fundamental only is present:

$$o = |o|\, e^{iK\sin\theta} \quad (4.26)$$

$$I = |o|^2(e^{iK\sin\theta})(e^{-iK\sin\theta}) = |o|^2 \quad (4.27)$$

As expected therefore there is no fringe information due to the fundamental. However when there is also a component of the first (f/2) present this will be sampled twice in its cycle giving two exposures to be added:

$$o_1 = |o|\, e^{i\phi_1} \qquad o_2 = |o|\, e^{i\phi_2} \quad (428)$$

Therefore:

$$I_{ss} = |o|^2(e^{i\phi_1} + e^{i\phi_2})(e^{-i\phi_1} + e^{-i\phi_2}) \quad (4.29)$$

$$= |o|^2(2e^{o} + e^{i(\phi_1 - \phi_2)} + e^{i(\phi_2 - \phi_1)}) \quad (4.30)$$

$$= |o|^2(2 + 2\cos(\phi_1 - \phi_2)) \quad (4.31)$$

$$\text{Now} \qquad \phi_1 = K\sin\theta + \frac{K}{p}\sin\frac{\theta}{2} \tag{4.31}$$

$$\phi_2 = K\sin(\theta+2\pi) + \frac{K}{p}\sin\left(\frac{\theta + 2\pi}{2}\right) \tag{4.32}$$

$$\text{Therefore } I = |o|^2\left(2 + 2\cos\left(\frac{2K}{p}\sin\frac{\theta}{2}\right)\right) \tag{4.33}$$

Which is the SSI result for the subharmonic only.

A similar result is gained for the 1/4 subharmonic if one interslit distance is traced during two object cycles. The author has not observed 1/4 subharmonics though they have been predicted by Aldoshina (1971) and are known to exist.

When both subharmonics are present simultaneously the result will be similar to that detailed in (vi g) below for the fundamental + 1/2 subharmonic when using SSI.

(vi) Possible Explanations For The 'Blanking' Fringes

(a) Having considered the basic theory of the four scanning methods we will now consider the various explanations for the blanking fringes observed with SSI . Taking first the linear motion idea we must consider again the basic theory of time average holography as follows:

If $o(r,t)$ represents the instantaneous amplitude of the object wavefront which now depends on position 'r' and time 't'. Then any position $r_1$ lasts for a fraction of the exposure time $t/T$ and the image amplitude resulting from this is:

$$i_{r_1} = o(r,t)\ t/T \tag{4.34}$$

Therefore the total amplitude of the image is the sum of all the individual contributions, becoming in the limit:

$$i(r) = 1/T \int_0^T o(r,t) \tag{4.35}$$

Once again when the object displacement is small compared with its distance from the hologram, we can write

$$o(r,t) = |o|\, e^{i\phi(r,t)} \qquad (4.36)$$

Now $\phi(r,t)$ describes how the phase of the object wavefront from the point 'r' on the object varies with time, it may be a sinusoidal variation or a linear drift or indeed may describe any motion. In sound radiation theory a similar term also describes the modes shape. (Appendix III)

(b) Linear Motion

If the object moves with velocity 'v' in time 't' it moves a distance 'x'

where $x = vt$

therefore $P.D. = 2vt$ (nb P.D. is the Path Difference)

hence the required phase difference is:

$$\phi(r,t) = (2\pi/\lambda)2vt \qquad (4.37)$$

Substituting (4.37) in (4.36) and in ((4.35).

$$i(r) = |o|\, 1/T \int_o^T e^{i(2\pi/\lambda)2vt}\, dt \qquad (4.38)$$

$$i(r) = |o|\, 1/T \left( \frac{e^{i(2\pi/\lambda)2vt}}{(i2\pi 2v)/\lambda} \right)_o^T \qquad (4.39)$$

$$= |o| \left( \frac{e^{i(2\pi/\lambda)2vt} - 1}{(i2\pi 2vt)/\lambda} \right) \qquad (4.40)$$

put $\phi(r,t) = (2\pi 2vt)/\lambda$ from (4.37)

then $i(r) = |o| \left( \frac{e^{i\phi} - 1}{i\phi} \right)$ (4.41)

Following from this the image intensity I ( = oo*) is:

$$I = |o|^2 \left( \frac{i - ie^{i\phi}}{\phi} \right) \left( \frac{-i + ie^{i\phi}}{\phi} \right) \qquad (4.42)$$

$$= |o|^2/\phi^2 ((i - i\cos\phi + \sin\phi)(-i + \sin\phi + i\cos\phi))$$

$$= |o|^2 \left\{ \frac{2 - 2\cos\phi}{\phi^2} \right\} \qquad (4.43)$$

Where $\phi$ is defined in (4.37) above. This is the $\mathrm{sinc}^2$ function represented in fig ( 4.1 ) which shows that whenever $\phi(r,t) = 2n\pi$ i.e. $vt = \lambda/2$ the resulting intensity is zero - a dark fringe.

(c) Sinusoid + Linear Motion = Sinusoid Stroboscopically Frozen

A stroboscopic double exposure, provided the strobe duty cycle is short enough and the object does not move appreciably during each flash, is exactly like an ordinary double exposure. Referring to fig ( 42 ) the sine wave with, say, the maximum exposure 'chopped out' for exposure purposes and having a linear motion superimposed may be regarded as two time averaged linear motion exposures superimposed. With the SSI method of stroboscopic holography the two exposures are each taken within every single cycle. If the number of cycles 'n' is sufficiently large each exposure increment is sufficiently small that the total exposure may be regarded as two superiposed time averaged linear motion holograms.
Now the time averaged exposure for the upper line is:

$$i_1(r) = |o|\, 1/T \int_o^T e^{i\frac{2\pi}{\lambda}(2vt+2d)}\,dt \qquad (4.44)$$

Where the distance of the line from the origin at time t = 0 is '0 + d' giving a phase difference of $(2\pi/\lambda)(2x0+2d)$.

$$i_1(r) = |o|\, 1/T \left(\frac{e^{i(2\pi/\lambda)2vt}}{(i2\pi 2v)/\lambda)}\right)(e^{i(2\pi 2d)/\lambda})_{\theta}^{T} \qquad (4.45)$$

$$i_1(r) = |o|\left(\frac{e^{i\bar{\phi}}-1}{i\bar{\phi}}\right)(e^{i\theta}) \qquad (4.46)$$

Where $\bar{\phi}$ now = $(2\pi 2vT)/\lambda$

and $\theta = (2\pi 2d)/\lambda$

and the distance of the line from the x axis at time t = T is 'vT + d' giving a phase difference of $(2\pi/\lambda)(2vT+2d)$.

Similarly:

$$i_2(r) = |o|\left(\frac{e^{i\bar{\phi}}-1}{i\bar{\phi}}\right)(e^{-i\theta}) \quad \text{-for the lower line} \qquad (4.47)$$

Now in a similar manner to that considered with double exposures above the intensity of the combined image will be given by:

$$I_{image} = (i_1 + i_2)(i_1^* + i_2^*)$$

Therefore:

$$I = \left\{\left[\frac{ie^{i\phi}-1}{-\phi}\right]\left[e^{-i\theta}\right] + \left[\frac{ie^{i\phi}-1}{-\phi}\right]\left[e^{i\theta}\right]\right\}\left\{\left[\frac{-ie^{-i\phi}+i}{-\phi}\right]\left[e^{i\theta}\right] + \left[\frac{-ie^{-i\phi}+i}{-\phi}\right]\left[e^{-i\theta}\right]\right\}$$

Giving:

$$I = |o|^2\left\{\frac{4 - 4\cos\phi}{\phi^2}\right\} + \left\{\frac{2 - 2\cos\phi}{\phi^2}\right\}\left(e^{2i\theta} + e^{-2i\theta}\right) \qquad (4.49)$$

Finally:

$$I = |o|^2 2\left\{\frac{2 - 2\cos\phi}{\phi^2}\right\}\left(2 + 2\cos 2\theta\right) \qquad (4.50)$$

= (linear motion result)(double exposure result)

Now this means that whenever the linear distance moved, OR the difference between two frozen stroboscopic amplitudes is usch as to give a dark fringe, the combined image has a dark fringe: each term may be zero independently and the resultant image intensity will then be zero. The linear motion fringe will not depend on the phase or the magnitude of the stroboscopic fringes. Therefore if there is sufficient linear motion to cause a dark fringe reconstruction, ( and the whole of the object will move as a piston for this linear motion) , the whole hologram will give a dark reconstruction - not just parts of it corresponding to various phases in the scanned object vibration.

(d) Single Scan I plus a general harmonic

In all cases considered the amplitude of the n th harmonic is'$d/p_n$'where the amplitude of the fundamental is 'd' . The path difference (P.D.) due to the harmonic alone is:

$$\text{P.D.} = (2\pi/\lambda)(2d/p_n)\sin n\theta$$

and so the phase difference $\phi$ due to the fundamental + the harmonic is

$$\phi = K(\sin\theta + (\sin n\theta)/p_n) \qquad (4.51)$$

Therefore with SSI the amplitude of the reconstructed object wave together with a (super)harmonic is:

$$o_{ss1} = |o|\, e^{iK(\sin\theta + (\sin n\theta)/p_n)} + |o|\, e^{iK(\sin(\theta + \pi) + \frac{\sin(n\theta + n\pi)}{p_n})}$$

$$= \text{'(first exposure)'} + \text{'(second exposure)'}$$

We will consider first even harmonics when 'sin(nθ + nπ) = + sin(nθ).

(e) Single Scan I plus Even Harmonics

The intensity due to the fundamental plus an even harmonic is:

$$I = |o|^2 \left\{e^{iK(\sin\theta + (\sin n\theta)/p_n)} + e^{iK(-\sin\theta + (\sin n\theta)/p_n)}\right\} x$$

$$\left\{\bar{e}^{iK(\sin\theta + (\sin n\theta)/p_n)} + e^{iK(+\sin\theta - (\sin n\theta)/p_n)}\right\}$$

$$= |o|^2 \left(2 + e^{iK(-2\sin\theta)} + e^{iK(+2\sin\theta)}\right) \qquad (4.54)$$

$$= |o|^2 \left(2 + 2\cos(2K\sin\theta)\right) \qquad (4.55)$$

This is, as expected, the result for the fundamental only.

(f) Single Scan I plus Odd Harmonics

The intensity due to the fundamental plus an odd harmonic is:

$$I = |o|^2 \left\{e^{iK(\sin\theta + (\sin n\theta)/p_n)} + e^{iK(-\sin\theta + (\sin n\theta)/p_n)}\right\} x$$

$$\left\{\bar{e}^{iK(\sin\theta + (\sin n\theta)/p_n)} + e^{iK(+\sin\theta + (\sin n\theta)/p_n)}\right\}$$

Which gives:

$$I = |o|^2 \left(2 + 2\cos 2K\left(\sin\theta + (\sin n\theta)/p_n\right)\right) \qquad (4.57)$$

The amplitude of the odd harmonic merely adds to that of the fundamental in the expression for the image brightness 'I'.

(g) Single Scan I plus The First Subharmonic

The first subharmonic case (n = 1/2) must be taken over two cycles of the fundamental since the sign of the subharmonic changes at the 2π phase of the fundamental. Therefore there are four contributions to the final image amplitude which are added on reconstruction, these give corresponding phase differences as follows:

Over the fundamental '$\theta$' region (cycle number one)

$$\phi_1 = K(\sin\theta) + K(\sin\tfrac{\theta}{2})/p_n$$

$$\phi_2 = K(-\sin\theta) + K(\cos\tfrac{\theta}{2})/p_n \qquad (\text{for } \theta + \pi)$$

Over the region '$\theta + 2\pi$' (fundamental cycle number two)

$$\phi_3 = K(\sin\theta) - K(\sin\tfrac{\theta}{2})/p_n \qquad (\text{for } \theta + 2\pi)$$

$$\phi_4 = K(-\sin\theta) - K(\cos\tfrac{\theta}{2})/p_n \qquad (\text{for } \theta + 3\pi) \qquad (4.58)$$

Therefore:

$$o_{tot} = |o|( e^{i\phi_1} + e^{i\phi_2} + e^{i\phi_3} + e^{i\phi_4}) \qquad \text{and so-} \qquad (4.59)$$

$$I = |o|^2( 4e^0 + 2\cos(\phi_3 - \phi_1) + 2\cos(\phi_3 - \phi_2) + 2\cos(\phi_3 - \phi_4) + 2\cos(\phi_2 - \phi_1) + 2\cos(\phi_2 - \phi_4) + 2\cos(\phi_4 - \phi_1)) \qquad (4.60)$$

On substituting (4.58) into (4.60), after manipulation we find:

$$\begin{aligned} I = |o|^2( 4 &+ 2\cos(\tfrac{2K}{p}\sin\tfrac{\theta}{2}) + 2\cos(\tfrac{2K}{p}\cos\tfrac{\theta}{2}) \\ &+ 2\cos(2K\sin\theta - \tfrac{K}{p}(\sin\tfrac{\theta}{2} + \cos\tfrac{\theta}{2})) \\ &+ 2\cos(-2K\sin\theta - \tfrac{K}{p}(\sin\tfrac{\theta}{2} + \cos\tfrac{\theta}{2})) \\ &+ 2\cos(2K\sin\theta - \tfrac{K}{p}(\sin\tfrac{\theta}{2} - \cos\tfrac{\theta}{2})) \\ &+ 2\cos(-2K\sin\theta - \tfrac{K}{p}(\sin\tfrac{\theta}{2} - \cos\tfrac{\theta}{2}))) \end{aligned} \qquad (4.61)$$

Giving finally:

$$\begin{aligned} I = |o|^2( &8\cos(2K\sin\theta)\cos(\tfrac{K}{p}\sin\tfrac{\theta}{2})\cos(\tfrac{K}{p}\cos\tfrac{\theta}{2}) \\ &+ 4\cos^2(\tfrac{K}{p}\cos\tfrac{\theta}{2}) + 4\cos^2(\tfrac{K}{p}\sin\tfrac{\theta}{2})) \end{aligned} \qquad (4.62)$$

This expression contains some multiplicative phase dependent subharmonic terms. Let us substitute the value $\theta = 0$ when there should be no contribution due to the fundamental:

$$I = |o|^2( 8\cos(\tfrac{K}{p}) + 4\cos^2(\tfrac{K}{p}) + 4 ) \qquad (4.63)$$

$$I = |o|^2\left(4\left(\cos\frac{K}{p}+1\right)^2\right) = 8|o|^2\cos^4\left(\frac{K}{2p}\right) \qquad (4.64)$$

This result is to be compared with that for SSIII at $\theta = \pi$ :-

$$I = |o|^2\left(2\left(\cos\frac{2K}{p}+1\right)\right) = 4|o|^2\cos^2\left(\frac{K}{p}\right) \qquad (5.65)$$

Now $\theta = 0$ for SSI and $\theta = \pi$ for SSIII both give the maximum sensitivity for the subharmonic. Thus it may be seen that with SSI we get half as many $\cos^4$ fringes of subharmonic as SSIII gives $\cos^2$ fringes. This agrees completely with the experiment described on page(128) where the increased sensitivity of SSIII over that of SSI to the subharmonic was demonstrated.

Let us now substitute the value $\theta = \frac{\pi}{2}$ in equation (4.62)

$$I = |o|^2\left(8\cos(2K)\cos^2\left(\frac{K}{\sqrt{2}p}\right) + 8\cos^2\left(\frac{K}{\sqrt{2}p}\right)\right) \qquad (4.66)$$

$$= |o|^2\left(16\cos^2(K)\cos^2\left(\frac{K}{\sqrt{2}p}\right)\right) \qquad (4.67)$$

This shows there is the maximum contribution due to the fundamental multiplied by a contribution due to the subharmonic.

It may be concluded therefore that the 'blanking fringes' of SSI are due to the subharmonic , and there are about 1/2 the number of 'blanking' fringes with SSI as there are subharmonic fringes with SSIII.

It is interesting to investigate why the subharmonic is not so evident in ordinary scanned or stroboscopic holography. The fringe function for ordinary scan plus the 1/2 subharmonic is:

$$I = |o|^2\left(4\sin^2\left(\frac{K}{p}\sin\frac{\theta}{2}\right) + 16\cos^2\left(\frac{K}{2}\sin\theta\right)\cos\left(\frac{K}{p}\sin\frac{\theta}{2}\right)\right) \qquad (4.68)$$

When $\theta = 0$ therefore:

$$I = |o|^2(16)$$

i.e. no fringes due to the subharmonic are seen in the region of $\theta = 0$ which is the region of greatest sensitivity to the subharmonic with SSI.

(h) Collection of Results

$$I_{scan} = |o|^2(2 + 2\cos(\tfrac{2\pi}{\lambda})2d\sin\theta)$$

$$I_{ss1} = |o|^2(2 + 2\cos 2(\tfrac{2\pi}{\lambda})2d\sin\theta)$$

$$I_{ss2} = |o|^2(2 + 2\cos(\tfrac{2\pi}{\lambda})2d(\sin\theta - \cos\theta))$$

$$I_{lin.} = |o|^2\left(\frac{2 - 2\cos(2\pi/\lambda)2vt}{((2\pi/\lambda)2vt)}\right)$$

$$I_{\substack{ssi \\ +lin.}} = |o|^2(2 + 2\cos(\tfrac{2\pi}{\lambda})2d\sin\theta)\left(\frac{2 - 2\cos(2\pi/\lambda)2vt}{((2\pi/\lambda)2vt)}\right)$$

$$I_{\substack{ss1 \\ +even}} = |o|^2(2 + 2\cos(\tfrac{2\pi}{\lambda})2d\sin\theta)$$

$$I_{\substack{ss1 \\ +odd}} = |o|^2(2 + 2\cos(\tfrac{2\pi}{\lambda})2d(\sin\theta + \frac{\sin(n\theta)}{p_n}))$$

$$I_{\substack{ss1 \\ +sub}} = |o|^2((8\cos 2K\sin\theta)(\cos\tfrac{K}{p}\cos\tfrac{\theta}{2})(\cos\tfrac{K}{p}\sin\tfrac{\theta}{2}) + 4\cos^2(\tfrac{K}{p}\cos\tfrac{\theta}{2}) * 4\cos^{2}\tfrac{2K}{2}\sin\tfrac{\theta}{2}$$

$$I_{ss3} = |o|^2(2 + 2\cos(\tfrac{2K}{p})\sin\tfrac{\theta}{2})$$

Where $K = (\frac{2\pi}{\lambda})2d$ $\theta$ = object motion phase

$d$ = zero to peak object movement

$vt$ = linear distance moved in time t.

The results for conventional stroboscopy may be found by substituting $\theta = \frac{\pi}{2}$ in $I_{scan}$ and $I_{ss2}$ and also in $I_{ss1}$ divided by 2.

Similar results may, of course, be calculated for SSI plus the 1/4 subharmonic and for SSII plus harmonics but these are not reported here. It is also possible that in response to future needs other scanning regimes will be developed and potential certainly remains for further development of the technique of scanned holography.

## 4.3) Experimental Points

### (i) Treatment Given To Loudspeakers

Most paper cone Loudspeakers are black and it is not practical (though highly desirable optically) to have them moulded out of white paper, some treatment is therefore necessary. It is not possible to coat them with Scotchlite as is too massive and would affect the speaker cone resonances. Painting them white is suitable but it is not the best treatment which may be applied (see Section II). The treatment which was selected was to give them a very thin coat of shiny silver spray paint. This coating was so thin that individual drops of the paint spray did not link-up, and so the stiffness of the paper was unaffected while most of the incident light. The mass of the spray coating in the worst case (i.e. thickest coat on thinnest diaphragm tested) was 10 percent of the mass of the actual paper - this was not taking into account the mass of the voice coil, the spider and the surround. More often the mass of the paint was less than 5 percent of that of the cone. Response curves taken before and after the spray treatment showed that while the paint was drying out it damped out the resonance dips in the response curve. When the paint was completely dry there was no detectable difference in the curves before and after treatment.

Aluminium sandwich cone Loudspeakers were practically specularly reflecting. This surface was also not suitable for holography in an untreated state and so it was lightly scored with a very fine grade of glass paper. This allowed a great deal of the incident light to be reflected back to the hologram and did not affect the response of the speaker. Loudspeakers were not used fixed into their cabinets when scanned holography was employed. This was because chipboard cabinets were found to sag rapidly and to do so over long periods of time. They were fixed instead onto massive brick or stone blocks which coupled their chassis

well to the vibration table. When time averaged holography, with its much shorter exposure times, was used then speakers in cabinets or merely resting on the vibration table gave a satisfactory hologram.

(ii) Vibration Isolation, Loudspeakers and Hum

The fringes resembling wood grain which are seen with live fringe holograms have already been described (page 121). The grosser movements of the speaker cone in response to extraneous vibrations and hum will be considered here.

Most of the mid-range speakers (i.e. covering the range 500 Hz to 5 KHz) studied in these experiments had very stiff suspensions. This meant that they did not move much in response to structure borne vibrations or air currents, and satisfactory holograms were taken of these and also of treble units without special precautions being necessary. However, when bass units were studied ( and mid-range units with very complient suspensions) it was found immediately that a satisfactory hologram could not be taken, though results obtained were better when the exposure times were as short as possible. It was realised that the fundamental resonances of these units fell very close indeed to the fundamental resonance of the isolation table on its suspension - both being of the order of 14 to 20 Hz. This meant that no isolation was being achieved from floor borne vibrations at around these frequencies and the transmitted vibrations were exciting the bass resonances of the Loudspeakers. In fact there may even have been some amplification floor borne vibrations which would then cause the experimental oscillations to be swamped. One way to remedy this situation was to decrease the resonance frequency of the isolation table. Unfortuanately this was not practical as it was already as low as the static deflections easily obtainable would allow. The next best thing was tried, and this was to lower the resonance frequencies of the speakers themselves while hopefully leaving their cone resonances unaffected .. Increasing their

resonance frequencies by stiffening up their suspensions was not practicable as methods of doing this would undoubtedly affect the resonances of the units. The resonance frequencies were lowered by fixing weights of up to four times the cone mass to the central'bung' , this lowered the resonance frequencies by a factor of two and, as was verified later (see below) did not affect the cone 'break-up' resonances. It did, however, result in decreasing the vibrational amplitudes at high frequencies and this was compensated for by increasing the electrical input. This treatment gave satisfactory results when used in conjunction with time averaged holography.

Further thought revealed the main cause of the trouble. It has been mentioned elsewhere that for a given electrical input (sound output) the amplitude of the speakers vibrations increases fourfold for every halving of the input frequency. Now the amplifiers used, while being very good by most standards, still gave sufficient hum to move the speakers appreciably during the holographic exposures. These vibrations,of course, would not be in phase with any stroboscopic method and, since they cause the cone to move as a piston at these low frequencies, would drastically lower the visibility of time averaged and stroboscopic fringes alike. For example a hum voltage only 40 db below a 3.2 KHz signal would give the same amplitude of vibration! and of course the hum voltages present must give a vibration amplitude much smaller than that due to the signal. In fact the mass treatment detailed above would tend to reduce the effect of hum a little since it lowers the broad fundamemental resonance further away from the hum frequencies .

It was fortunate that the speakers were already isolated to DC originating in the transistorised amplifier used to drive them, by two medium valued non-electrolytic capacitors. These capacitors acted as high pass filters, and did cut down some of the amplifier hum. The small DC currents in the amplifier output can vary with the AC level and would affect holography by superposing linear motion contributions, so they had

to be isolated from the speaker. To greatly improve the holographic results therefore all that was necessary was to place a properly designed high-pass filter with a cut-off frequency of about 400Hz between the amplifier and Loudspeaker, the low valued inductor across the output of this filter also helped to damp the bass resonance of the speaker.

(iii) Experimental Layout for Loudspeaker Studies

This was identical with the systems used for the studies of plates, except that it was situated in a different laboratory wwith some different though very similar apparatus. The laser used was a Ferranti 30 mw laser, the amplifiers were of different design but similar power to those used previously and the rest of the optical apparatus was exactly the same. The isolating table was of similar construction to the one previously used, though its mass was doubled and it was isolated by rubber mats having dimples in their surfaces causing the rubber to be used in shear. These rubber mats rested in a solid concrete plinth. The amplifiers, laser, etc were supported away from the isolated table in.The synchronous motor with its stand was also situated free from the isolating table which gave further isolation from the vibrations set up by the out of ballance masses remaining in the attached discs. It was unfortunately not possible to build another reverberation room at the new experimental location, so power output measurements on loudspeakers were not taken.

(iv) The Photography of Holographic Reconstructions

When taking photographs of ordinary double exposed or time averaged holograms there is no problem. The whole of the laser light is diverged and directed onto the hologram, which has been cleaned of dust and grease. The camera is opened up to full aperture and placed behind the hologram so that the diffracted light may enter the camera, but screens are placed to block the entry of the zero order (direct beam). The wide aperture

reduces the size of the speckles seen on the photograph of the reconstruction. The reconstruction is preferably located with a reflex lens system and a series of test exposures is taken to determine the exposure time required (though there is often enough light to work an exposure meter) after which photographs may be taken of the reconstructed image.

When taking photographs of scanned holograms the situation is a little different, because large areas of the hologram may not, obviously, be used for reconstruction purposes. The desired phase of the object vibration must be selected using a mask with a slit of similar width to that used to take the hologram. The mask (which may of course be the original scanning disc with other slits blanked off) is then fixed to the hologram on the side of the incident light. The camera, once again with full aperture, is placed behind the hologram and the direct light is blanked off by a stop on the camera side of the hologram. Thus the whole height of the scanned part of the photographic plate is used in the photography which serves to minimise the increase in the speckle size on the resulting photograph. The photographs resulting were of entirely acceptable quality.

Some photographs taken of Brass Plate reconstructions are presented here. These were taken with a 'reflex' camera of high quality with the most suitable lens fitted. It is regretted that some photographs of Loudspeaker reconstructions, also presneted here, had to be taken with a simple non-reflex polaroid camera with only one lens available. This resulted in an image size which varies with the size of the object and which may not be exactly in focus. However sketches made from the actual reconstructions are also presented. Indeed in many cases more information about the fringe systems may be gained from these 'observer sharpened' sketches. Both sketches and photographs are presented of sample reconstructions to serve as a check.

## 4.4) Experimental Method for Investigating Loudspeakers

A series of qualitative experiments was carried out firstly on a number of similar mid-range units with stiff felt suspensions. These were modified in a number of ways to see how the fringe patterns were affected. The main feature of interest in these experiments is the actual shape and configuration of the interference fringe patterns produced. The relative outputs of each mode being obtained from response ucurves in the usual manner. The level of excitation fed to each speaker was roughly the same in a given frequency range and was measured by noting the voltage across the speaker and later by noting also the voltage output of a microphone amplifier at each of the resonance 'peaks' and 'dips' surveyed. When similar speakers are quantitatively compared in later experiments the voltage across the speakers was adjusted to be the same and the actual fringe number then gained in significance.

The methods of Scanned Holography, SSI and time averaged holography were used where appropriate: SSI at lower frequencies, Scan at mid-frequencies and when using speakers with stiff suspensions and time averaged holography at high frequencies. Also, because of the smaller exposure times required, time averaged holography was used for speakers with complient suspensions and surrounds. These methods have been fully described above, but some additional points are detailed below.

(a) A response curve was taken using the microphone later used to set up each holographic exposure. The peaks and dips were each assigned an identification letter and from the shapes of the response curves fpr each of the similar speakers, equivalent resonances were identified and lettered. It is important that holograms should be taken at equivalent features in the response curves and not just at the same frequencies because the resonance frequencies themselves sometimes move quite considerably with changes of temperature and humidity.

(b) Holograms were then taken at each of the peaks and dips in the speaker response curves. The vibration amplitude was usually chosen to give from three to ten break-up fringes on reconstruction. At frequencies of around 500 Hz this corresponds to about .3 volts, 1.5 KHz 1 volt and 2.5 KHz 4 volts from the microphone preamplifier. Since the technique allows a separate hologram to be taken for each half of the photographic plate - the same resonance was taken for each half, but with a different speaker vibration amplitude. The frequency range covered with mid-range units was 500 Hz to 4 KHz, for sandwich bass units 1 KHz to 6 KHz and treble units were investigated over the range 1KHz to 17 KHz.

4.5) Typical Features Found In The Holograms Of Loudspeakers

(i) Hypothetical Ideal Loudspeaker

A holographic reconstruction of a hypothetical Loudspeaker vibrating in an ideal manner should have the following features (see fig 43 ):

(a) The cone area should be of uniform shading i.e. showing no fringes and being totally reconstructed as black, grey or white. With the scanning methods the cone area will change from black through grey to white several times as the eye is moved across the hologram.

(b) The surround should show circular fringes concentric with the centerr of the loudspeaker. With time averaged holography the outermost bright fringe will be the greatest intensity while with scanned holography the fringes should move in and out as the observers eye is moved across the hologram.

(c) The chassis should be reconstructed bright only: any dark areas or lines show that the chassis is moving while the cone is vibrating.

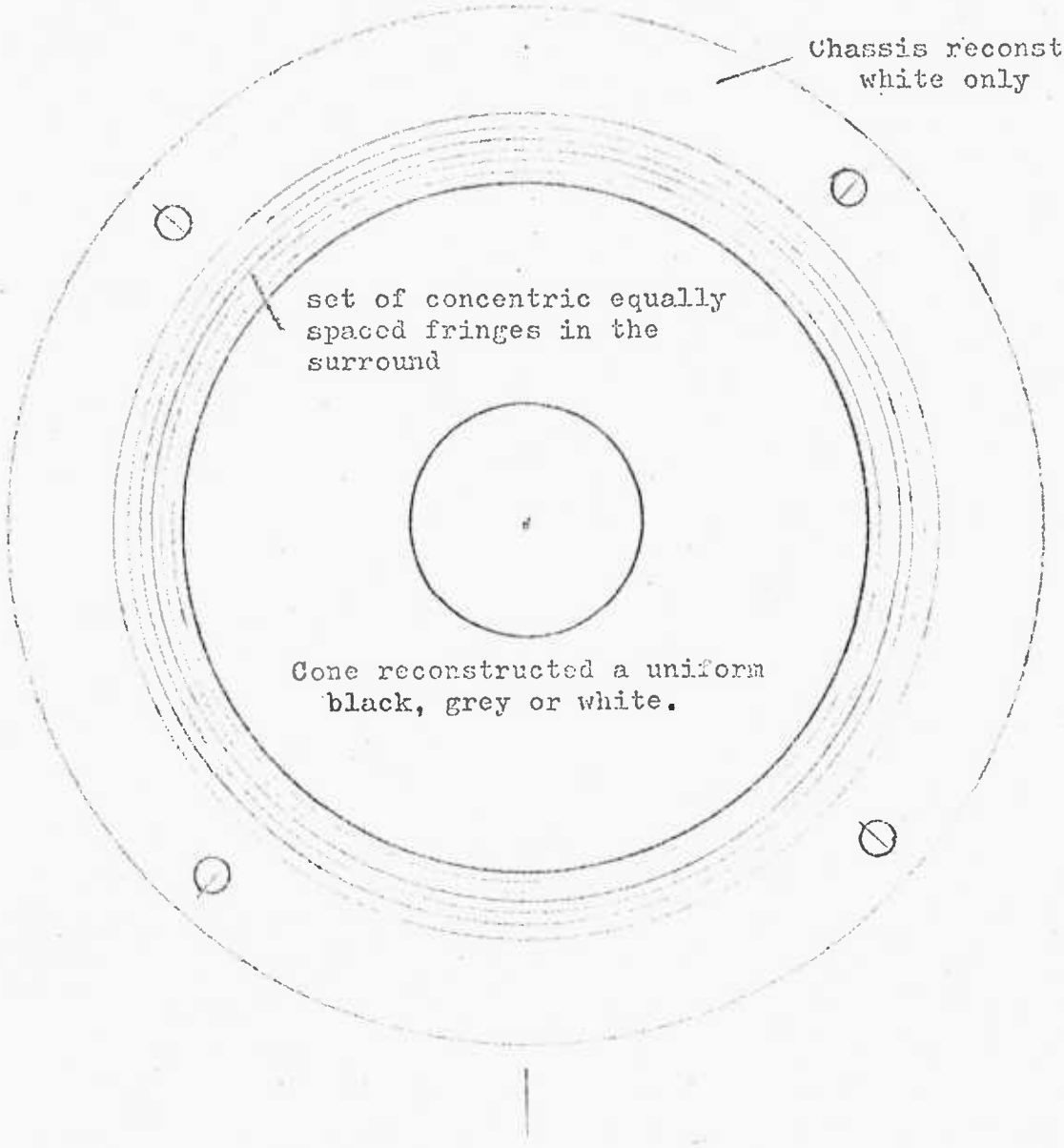



Fig (43) Reconstruction of Loudspeaker vibrating perfectly

(theoretical only)

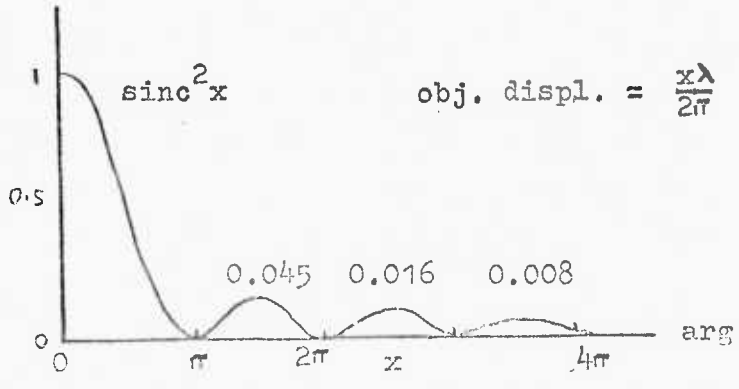
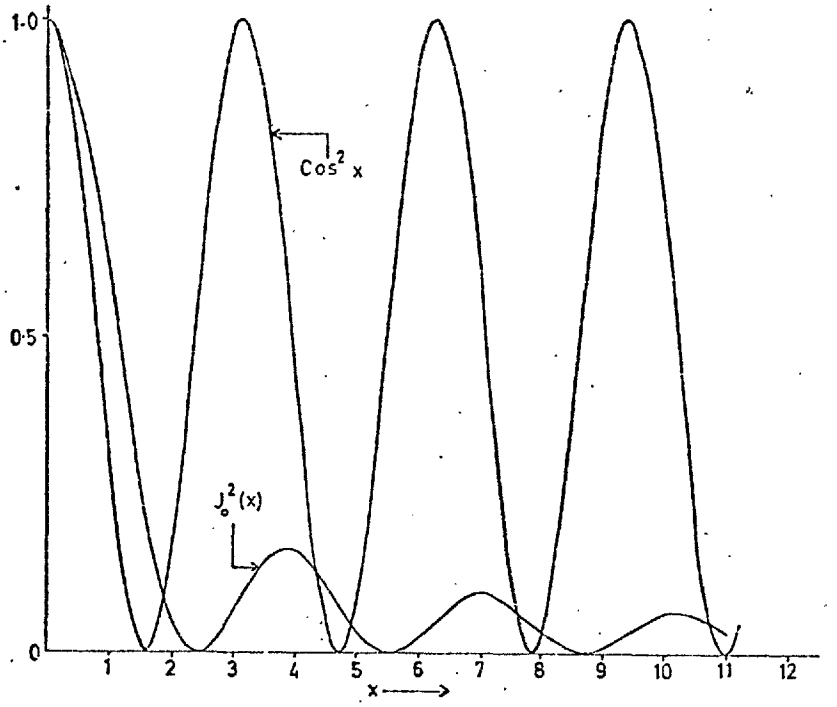
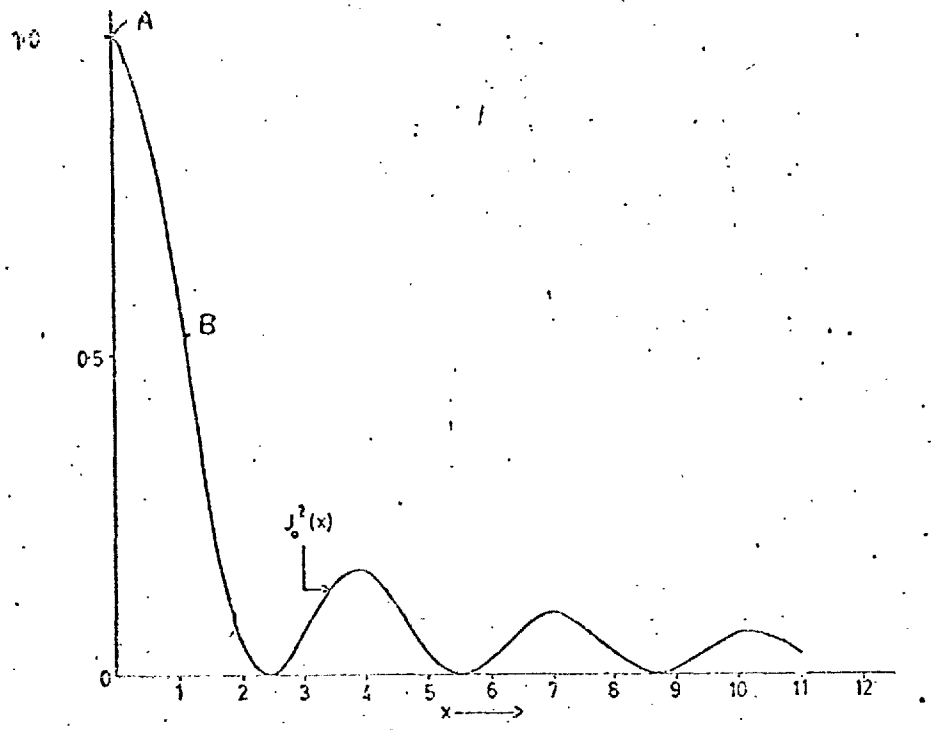



Fig 41 The $\text{sinc}^2$ function for linear motion




Figures 12 and repeated for convenience

(ii) Real Loudspeakers

The cone is usually covered with a system of fringes mapping the difference in amplitude between neighbouring regions. These fringes often fall into definite configurations resembling those found om objects behaving like the discs discussed in Section (III). This disc-like behaviour is more likely to happen in the case of speakers of sandwich construction. Each disccmode has associated with it a definite number of nodal diameters and nodal circles as shown in (fig 36 ) and Mary Wallers sand patterns. Holographic fringes, of course, do not pass through nodes (unless there are other motions present) but, step by step map out increases in vibration amplitude up to an antinode. Stroboscopic methods allow these break-up patterns to be easily seen even when they are superimposed on top of large amounts of piston type motion. The basic time averaged methods gives a greatly reduced fringe visibility if the break-up patterns are superimposed on piston motion of any great amplitude. This is because the nodal regions do not then correspond to the central peak in the Bessel function (fig 12 ) but are carried out to a region of lower intensity by the piston motion. One of the modifications of the time averaged method - particularly one of those due to Aleksoff - will find certain applicability for the study of Loudspeakers in future since they overcome this disadvantage.

For the purposes of this study the various types of fringe system found in Loudspeakers have been given descriptive names. For instance when there are two nodal diameters and no nodal circles the fringes occur as shown in fig ( 44 ) and they are called 're-entrant fringes'. When there is a nodal circle present as well, fringes which resemble hill contours on a map occur between the nodal diameters and the nodal circle - these are called 'hill and dale fringes'. These re-entrant and hill and dale systems when found on Loudspeakers often occur in seemingly random arrangements unrelated to standard 'nodal circle nodal diameter' resonance patterns . It is therefore convenient to group the fringe systems found

Fig ( )

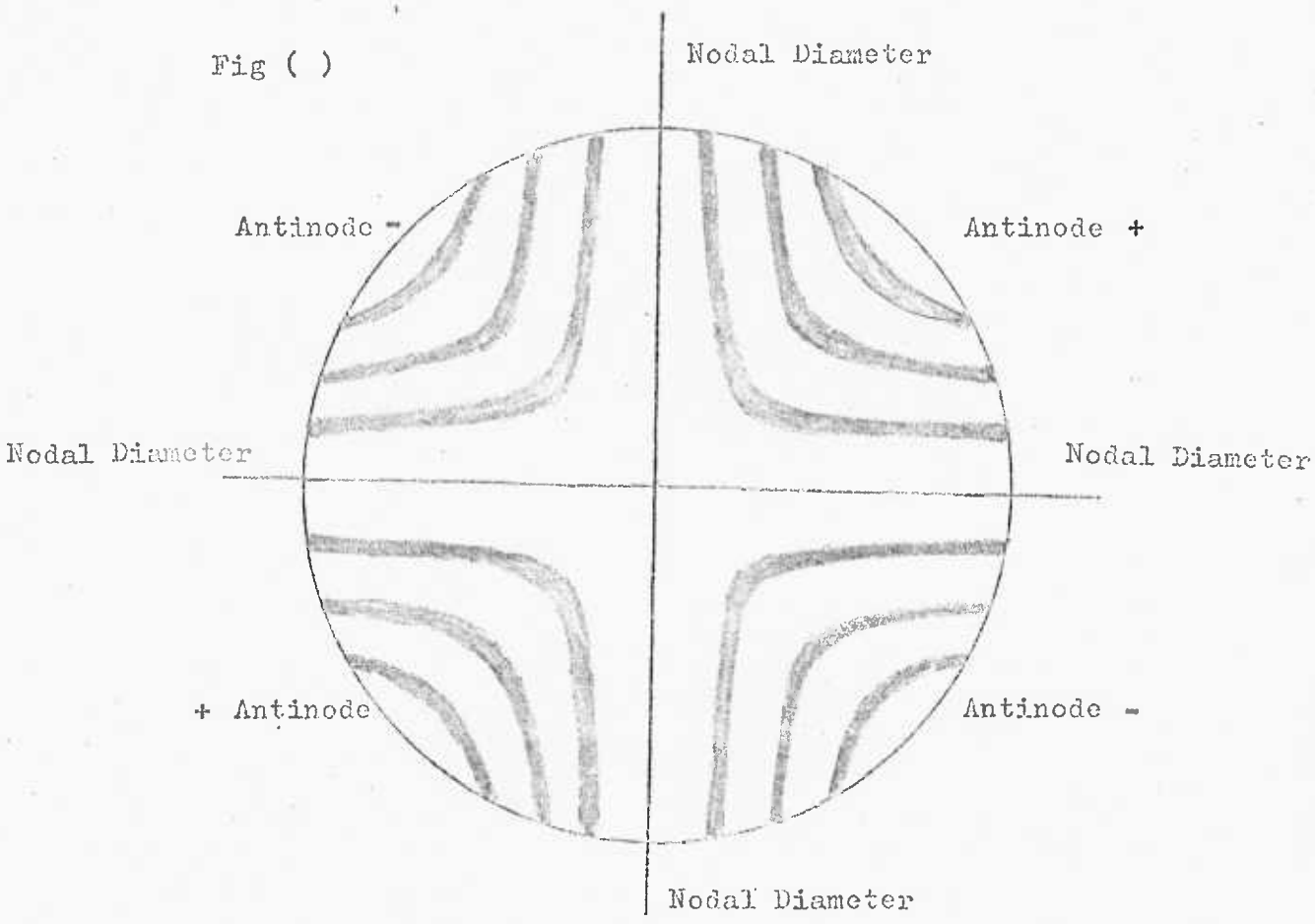
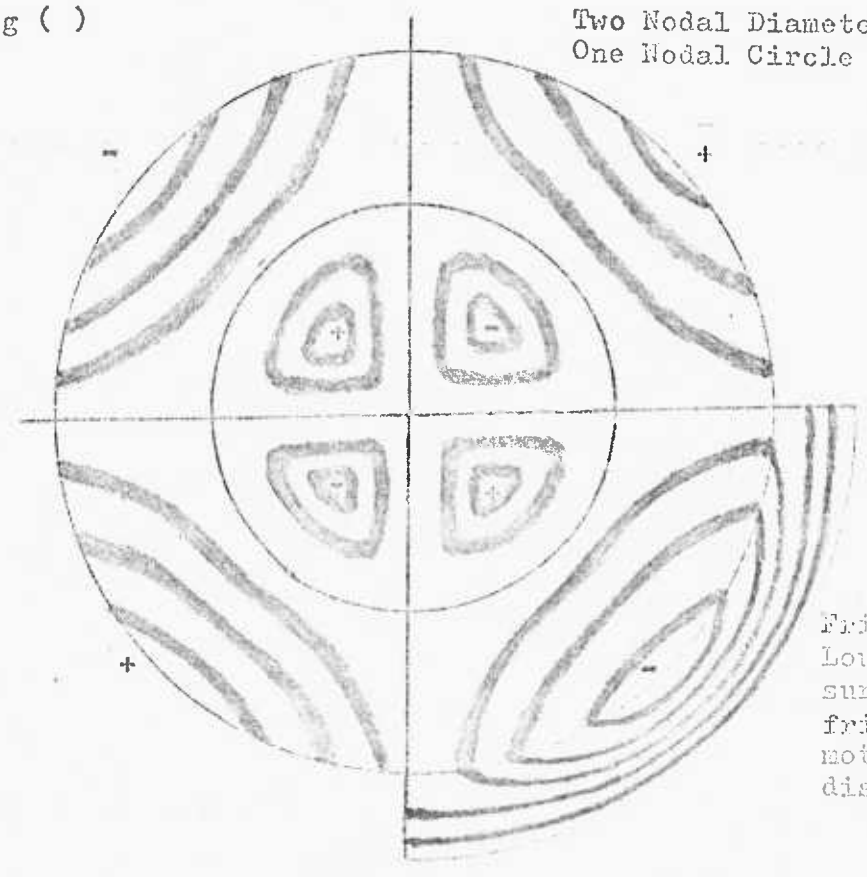



Fig ( )

Two Nodal Diameters
One Nodal Circle




Fringes seen in a Loudspeaker surround with two fringes of 'piston' motion and three of disc mode break-up.

Figure 44 Fringes seen on a Loudspeaker cone with 'Disc-like' modes

on Loudspeakers into four main categories:

(a) Re-entrant

The first kind of fringe formation is found at the edges of the cone and they are the re-entrant fringes described above. Re-entrant fringes on opposite sides of the cone may be vibrating in antiphase like the equivalent disc mode. When the Loudspeaker cones are made of paper the coincidence critical frequency ($f_c$) is supersonic and so there will be some cancellation of the sound radiated by these modes which lessens their effect on the response curve (Maidanik (1962) described in Appendix (II)). With sandwich treble units these re-entrant fringes more strongly resemble disc modes but in this case the frequencies at which they occur fall above the coincidence critical frequency, and will therefore radiate independently giving rise to stronger peaks in the response curve. With the sandwich bass unit re-entrant fringes have not been found at all under normal excitation conditions as discussed below. When the frequencies at which these fringes occur fall above $f_c$ they will radiate wavefronts differing in phase which may well have a deleterious effect on stereophony. With paper cones they fall below $f_c$ but the fringes are often not symmetrical and so complete cancellation of the radiated sound seldom occurs. Also discontinuities exist in paper cones caused by changes in Young's Modulus of up to 100 percent and scattering of waves occurs at these locations which contribute to the output power even below coincidence (Maidanik 1962).

(b) Hill and Dale

The second kind of fringe system may be found all over the cone but is more likely to be found approximately half-way between the center and the edge fig (44). These regions look like hills and dales on a contour map and their effect on the response curve is likely to be complex. These regions will be vibrating more(or less) than neighbouring regions of the cone and they may be leading or lagging in phase ( as distinct from the

re-entrant kind which will be either plus or minus $\pi$ radians out of phase). Therefore phasing troubles encountered with these may be more disturbing and listening tests do show that the hill and dale kind of break-up is more irritating that the re-entrant variety. These hill and dale fringes are very often found in the vicinity of the lead-in wires, which are often both passed through the cone at the same point about 1/3 of the way out. the mass and stiffness of the lead-in wires often drastically affects neighbouring regions of the cone as may be seen especially from the drawing on page (156d), and can cause severe rocking especially in sandwich treble units.

(c) Edge Bending

The third type of fringe system is often encountered with paper cones and these fringes are called edge-bending fringes. These fringes are found in the outer regions of the cone and are exactly like the fringes found in an ideal surround. Indeed they show that the speaker cone is doing part of the work of the surround in that its outer regions are flexing. This means that a smaller region of the cone behaves as a piston and the sound output will therefore be lower. At certain frequencies there will be resonances associated with this phenomenon similar to those found in imperfect surrounds see pages (163def). Often the resonances in the surround are of high amplktude but the smaller radiating area associated with them may reduce their effect on the sound field radiated.

(d) Umbrella

The fourth kind of fringe formation is caused by the umbrella mode. This is the lowest frequency mode possible in a center supported disc - the one nodal diameter mode which is possible in the case of an annular disc has a lower frequency and may be mistaken for (e) below. The fringes of the umbrella mode are circular and concentric, and like the edge bending fringes show that the whole cone is flexing and 'flaring' in and out like

an umbrella. They are unlike the edge bending fringes however because there is a node at the outer edge of the cone and it is the rest of the cone - not the edge regions - which is flexing. This is particularly well demonstrated with the bass sandwich unit. This resonance affects a very large area of the cone but there are no regions in antiphase to allow cancellation ( the frequency of this mode is always below $f_c$) and it does not have a very high 'Q' therefore the increase in vibration amplitude experienced in the central regions nearly compensates for the loss of radiating cone area and the effect on the overall response curve is minimal.

(e) Rocking

The fifth and final group of fringes 'rocking fringes' are usually found near to the center of the cone and especially with sandwich treble units. They are a set of 'parallel' lines usually distributed equally on each side of the center of the cone. They indicate that the voice coil is rocking as it moves in and out of the gap and this behaviour is usually caused by the mass and stiffness of the 'lead-in' wires particularly in the case of the sandwich treble units. It is possible also that at low frequencies this is the one nodal diameter mode mentioned above and in Appendix ( II ). The effect of cone rocking on the response curve is certainly minimal below coincidence since there is likely to be complete cancellation and even above coincidence its effect will be small since it extends over a very wide frequency range, changing amplitude only gradually in the range.

The felt surrounds of the mid range speakers are usually too darkly reconstructed to show any fringes, but occasionally fringes may be seen in this region. They then show up continuations of the re-entrant type of fringe system, in fact joining them up, and are seldom like the ideal circular fringes concentric with the cone center which are desired for the surround. 'Rubber Roll' surrounds approximate more closely to the ideal however. The surround of the sandwich treble unit breaks-up spect-

acularly at many frequencies often at high amplitude and with a number of nodal circles of its own.

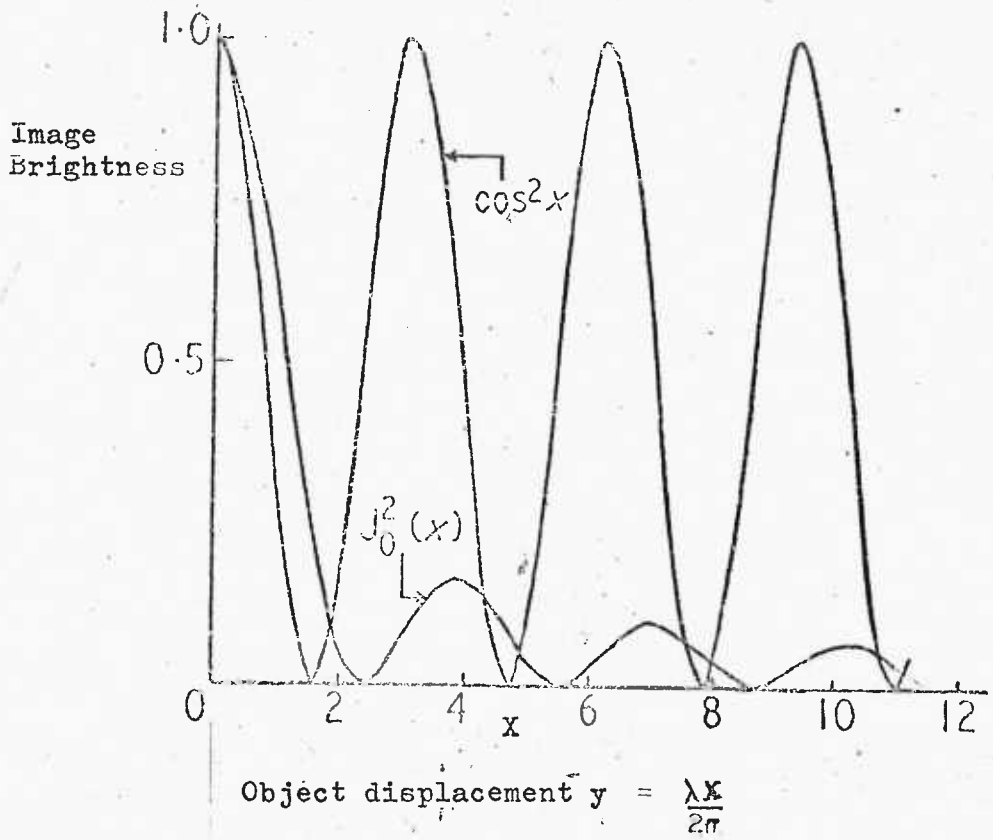
(g) Finally the chassis in most high amplitude holograms shows signs of bending and sometimes this is severe. When the speakers are fixed into cabinets it is expected that this effect will be less severe. It is interesting to note that the 'blanking fringes' noticed with SSI continue into the chassis in many cases.

It is worthwhile to note again here that the form of the fringes themselves also varies according to the holographic system used. Stroboscopic fringes have a $(\cos)^2$ profile and constant visibility whatever the vibration amplitude. This makes them easy to see but, in the absence of a scanning technique the nodes may be difficult to locate. However when basic Time Averaged holography is used, the dark line positions correspond to the zeros of a Bessel function (fig 12 ) and the brightness in between the zeros also follows the Bessel function curve. This means that the reconstruction becomes darker as regions of high vibrational amplitude are approached. Fringe visibility is consequently poorer but the nodal regions stand out - being the most brightly reconstructed parts. If there are no true nodes on the cone itself the 'break-up nodes' are not so easy to pick out with the basic time averaged method, because the difference in intensity between these regions and neighbouring white fringes will not be so pronounced since they have been carried further out along the Bessel function curve by the piston motion present.

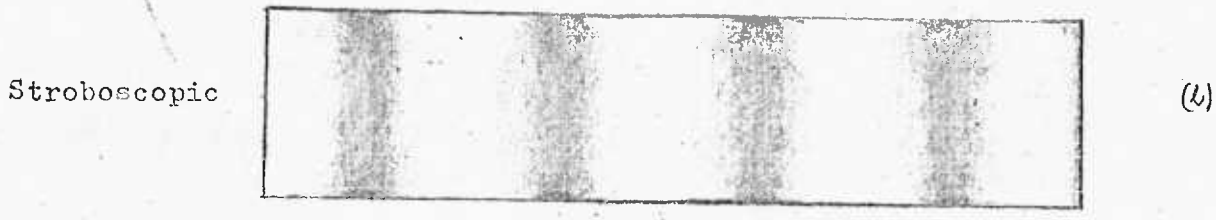
## 4.6) Discussion of Results on Paper Cone Mid-Range Units

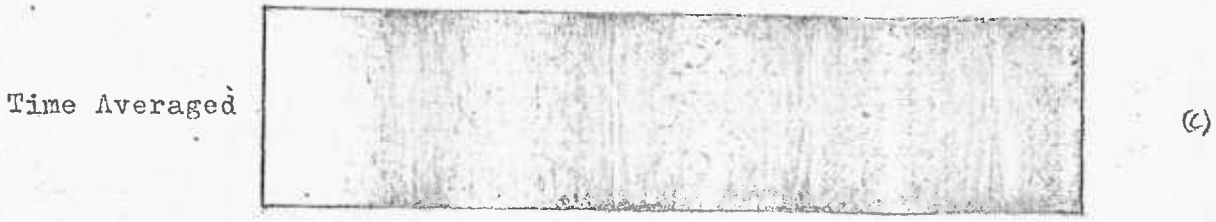
(i) Number (1) A mid-range unit with a felt surround - taken as the standard. The holograms taken of this unit indicate the following points:

(a) Central regions of the cone are reproduced grey over the range covered (1 to 4 KHz) showing that this part of the cone behaves as a piston over this frequency band.




Object displacement $y = \frac{\lambda x}{2\pi}$



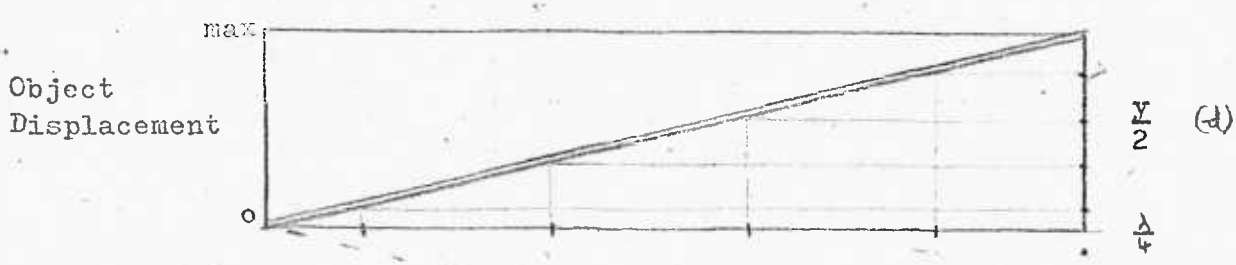




Figure 12 (a)

(b) Outer regions often showed 'edge bending' fringes suggesting that the suspension was too stiff.

(c) 'Re-entrant fringes' in nodal diameter configuration were sometimes seen indicating that outer regions of the cone were not stiff enough - the cone was practically flat in these regions.

(d) The lead-in wires (over certain frequency ranges) retard the motion of the cone in their vicinity.

(e) Occasionaly, with high amplitudes of excitation, the chassis shows signs of movement.

(f) Cone behaviour is best between 1 KHz and 2KHz where the fringe formations resemble disc-like modes. Above this range cone imperfections begin to show up as circular 'hill and dale' systems.

When observing Loudspeaker fringe systems it must be remembered that they are usually superimposed onto a greater total movement of the cone/coil assembly. Sometimes this movement, which may be as high as twenty fringes, can be seen in the surround when the fringes are circular and closely spaced.

The features above suggest the following modifications, the first to show up features of cone movement more clearly and the other four which may help to produce better loudspeakers:

(a) Removal of the surround. This may allow the modal structure to show up more definitely and therefore indicate the effect that the surround has on the cone vibrations.

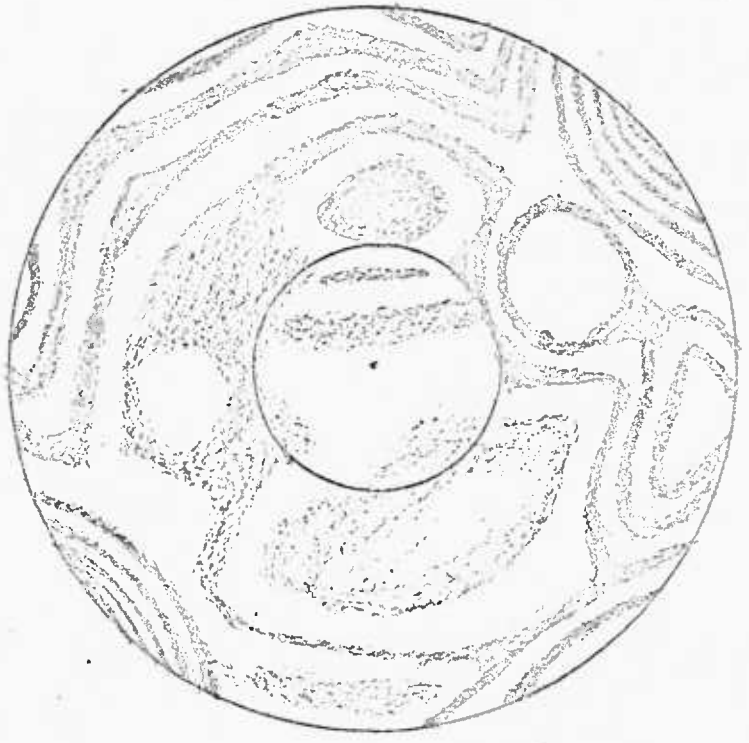
(b) Taking the lead-in wires directly to the chassis without passing through the cone, this may show how significant is the distortion produced by the wires on paper mid-range units.

(c) A speaker with a less stiff more linear suspension coupled with a profile which is less 'flat' in its outer regions to try and avoid the bending of these regions.

| | |
|---|---|
| SPEAKER | NO 1 |
| HOLOGRAM | NO 40 |
| RESONANCE | A Dip |
| FREQUENCY | 500 Hz |
| DETAILS | Low audio output |
| COMMENTS | Shows the effect of the lead in wires even at this low amplitude |



| | |
|---|---|
| SPEAKER | NO 1 |
| HOLOGRAM | 111 |
| RESONANCE | A |
| FREQUENCY | 535 Hz |
| DETAILS | Medium audio output |
| COMMENTS | Shows rocking of the voice coil |



Results Figure 1 Speaker Number 1

SPEAKER NO 1

HOLOGRAM 108

RESONANCE B Peak

FREQUENCY 610 Hz

DETAILS

COMMENTS Shows the effect of the lead-in wires



Results Figure 2 Speaker Number 1

SPEAKER NO 1

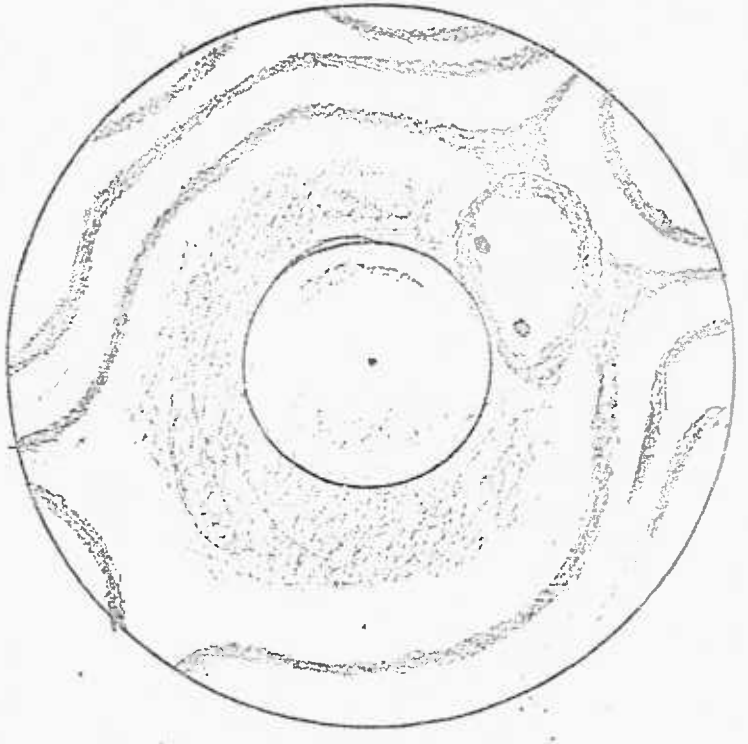
HOLOGRAM 105

RESONANCE C Peak

FREQUENCY 755 Hz

DETAILS

COMMENTS Evidence of one nodal diameter



| | | |
|---|---|---|
| SPEAKER | NO | 1 |
| HOLOGRAM | 100 | |
| RESONANCE | E | Peak |
| FREQUENCY | 950 | Hz |
| DETAILS | | |
| COMMENTS | Evidence of two nodal diameters<br>Fringes seen in the felt surround | |



Results Figure 3 Speaker Number 1

| | | |
|---|---|---|
| SPEAKER | NO | 1 |
| HOLOGRAM | 104 | |
| RESONANCE | C | |
| FREQUENCY | 1130 | Hz |
| DETAILS | | |
| COMMENTS | Evidence for 3 nodal diameters | |



SPEAKER NO 1

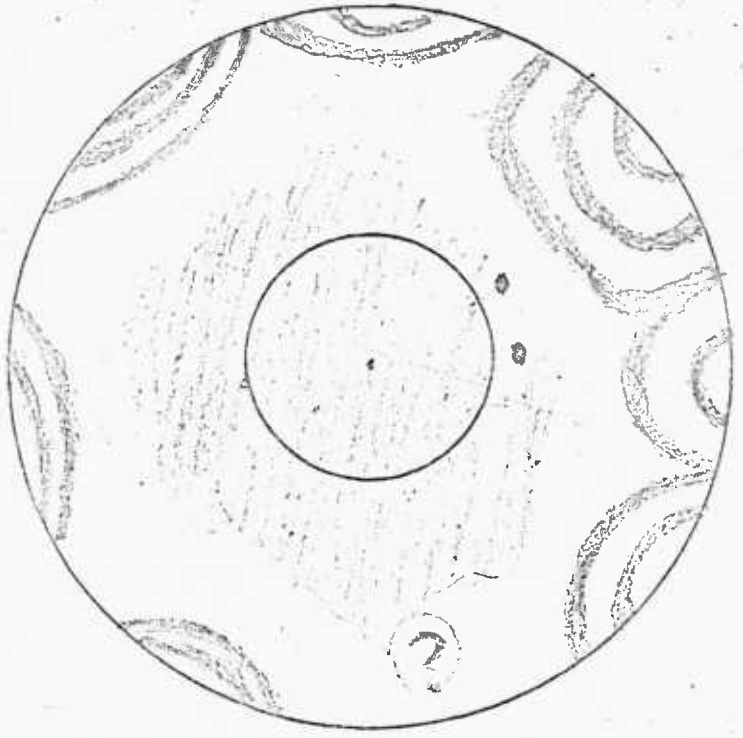
HOLOGRAM 101

RESONANCE I

FREQUENCY 1240 Hz

DETAILS

COMMENTS Evidence for 4 nodal diameters



Results Figure 4 Speaker Number 1

SPEAKER NO 1

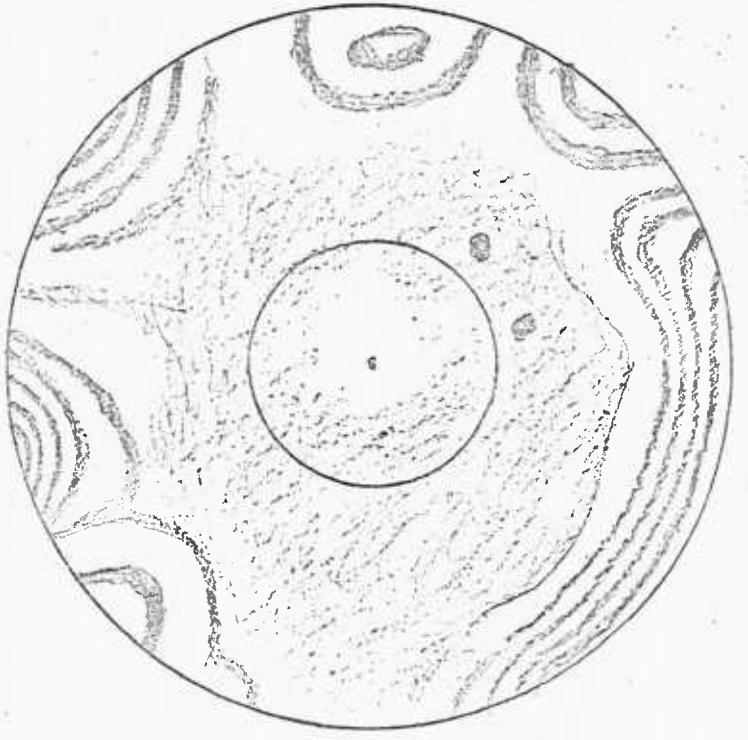
HOLOGRAM 98

RESONANCE J

FREQUENCY 1320 Hz

DETAILS

COMMENTS



SPEAKER NO 1

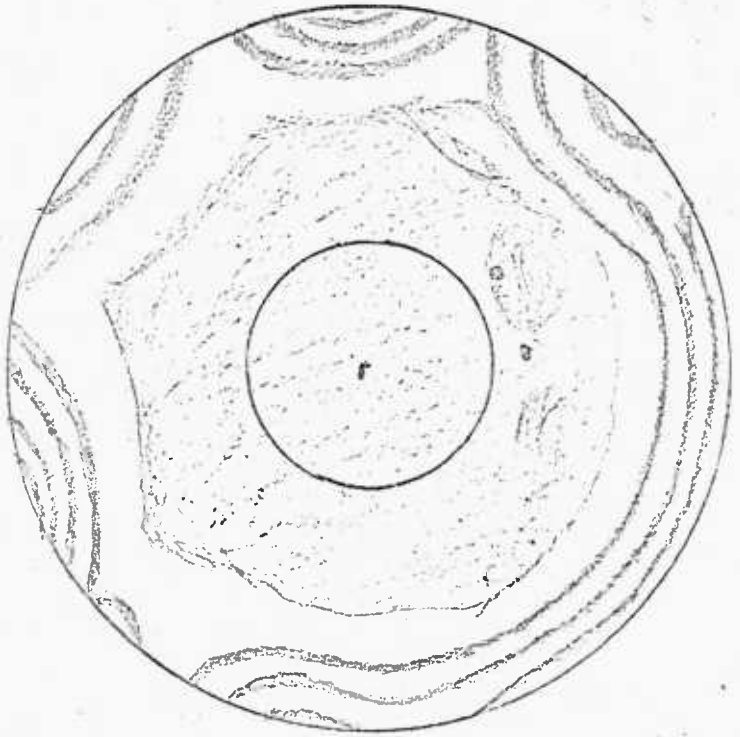
HOLOGRAM 99

RESONANCE K

FREQUENCY 1550 Hz

DETAILS

COMMENTS



Results Figure 5 Speaker Number 1

SPEAKER NO 1

Hologram 107 A

RESONANCE 0

FREQUENCY 2100 Hz

DETAILS Phase $\pi_2$

COMMENTS Surround moves very asymmetricall;



SPEAKER NO 1

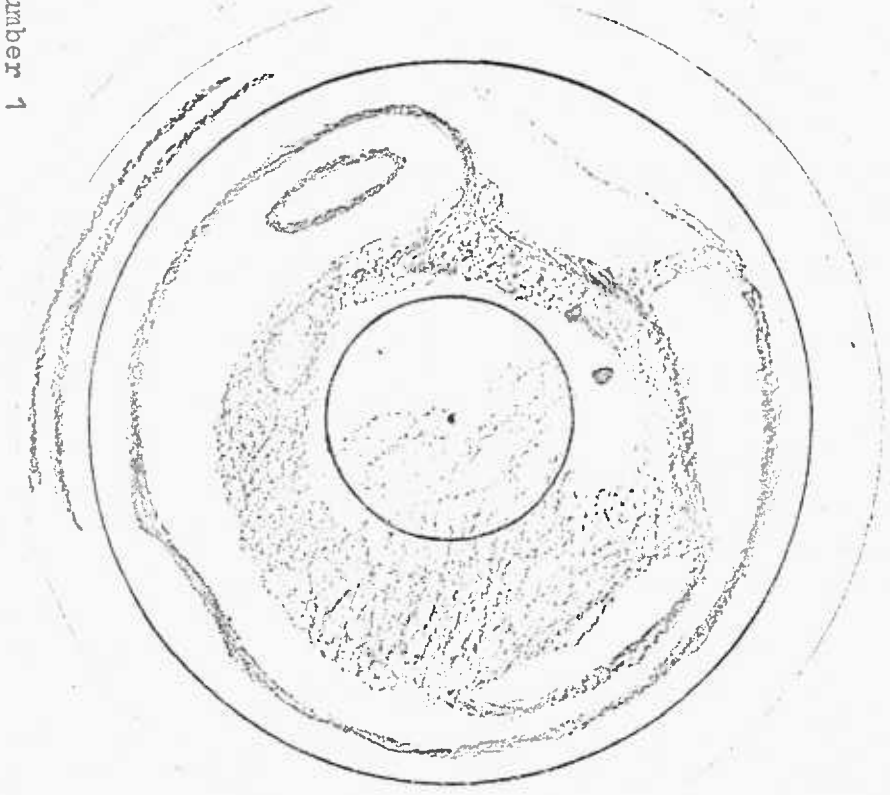
Hologram 107 B

RESONANCE 0

FREQUENCY 2100 Hz

DETAILS Phase 3π/2

COMMENTS



Results Figure 6 Speaker Number 1

SPEAKER NO 1

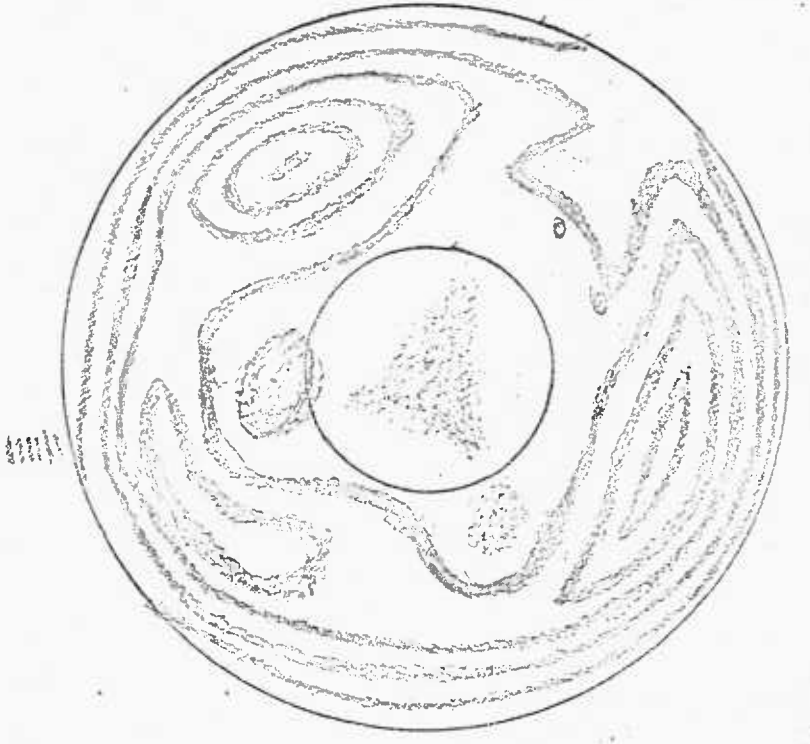
HOLOGRAM 21

RESONANCE 0

FREQUENCY 2.2 KHz

DETAILS High audio output

COMMENTS



SPEAKER NO 1

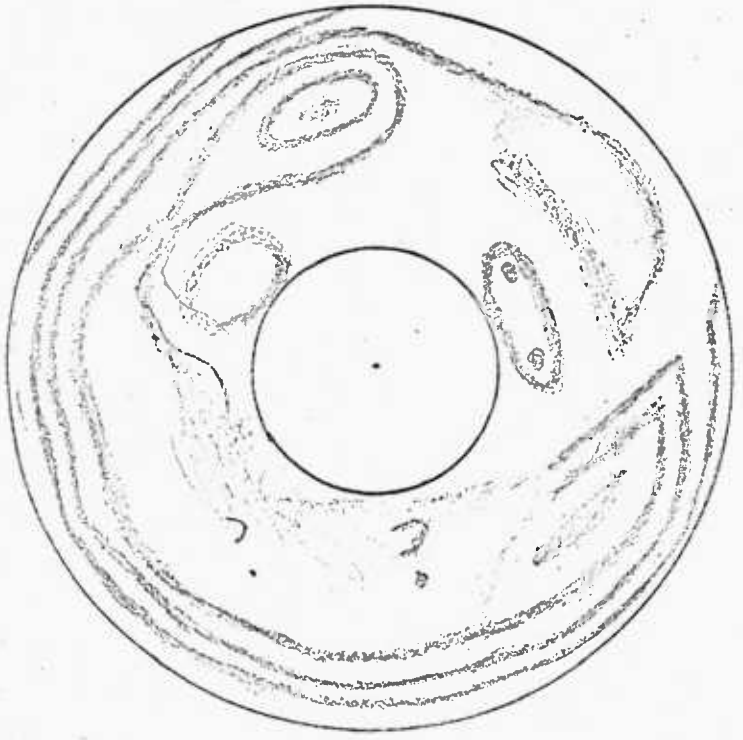
HOLOGRAM 109

RESONANCE Q

FREQUENCY 2720 Hz

DETAILS

COMMENTS



Results Figure 7 Speaker Number 1

SPEAKER NO 4

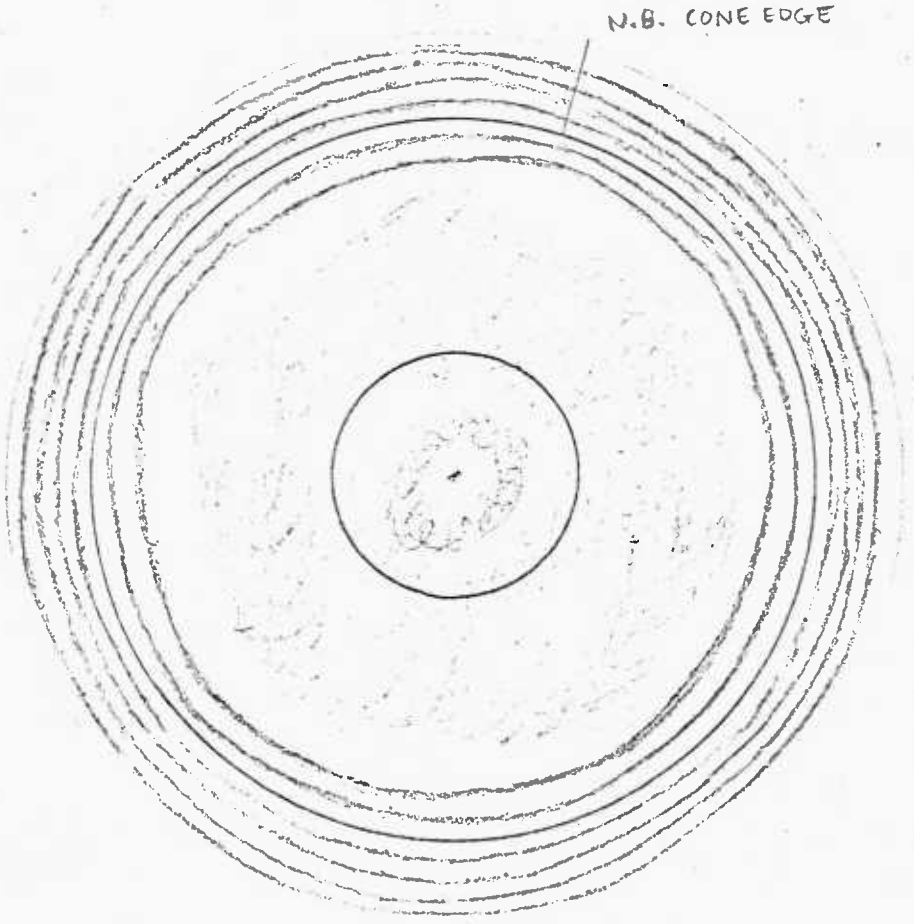
HOLOGRAM 124

RESONANCE

FREQUENCY 2100 Hz

DETAILS

COMMENTS Almost perfect piston motion at this frequency



(d) A cone with a sharper cone angle but with the same radius or 'sagitta' for its profile.

(e) A cone with the same profile as the standard but with the outer regions removed and a new surround fitted - thus removing the regions which suffer most from 'bending' and 're-entrant' fringes while leaving other regions untouched.

It was fortunately possible to investigate some of these modifications and also to investigate speakers of totally different construction and these investigations are described below:

(ii) Number (4) A mid-range unit with a 'doped' plastic diaphragm and a large rubber roll surround.

Before the investigations of modified Loudspeakers were carried out this unit of entirely different construction was studied. Over the range 850Hz to 3400Hz it showed almost perfect piston motion (page $153_g$). The maximum departure observed was about 1 fringe of movement at low frequencies. Loudspeaker Engineers have pointed out that this result agrees with listening tests and the unit is regarded as being good when tested by more conventional means. They suggested however, that it was not so good above 4.5 KHz. These frequencies have been investigated and break-up patterns do occur at higher frequencies.

Unit (4) differs from unit (1) as follows -

(a) It has a large rubber roll surround.(1) has stiff inhomogeneous felt.
(b) The spider of no (4), though made of similar material to that of no(1) is very large with deep corrugations. This together with the rubber surround permits large cone excurtions and therefore small movements may be more linear. (1) has a small spider with small corrugations.
(c) No (4) has a sharp cone angle with a slight radius. No (1) has a shallow cone with nearly flat edges but a similar radius or sagitta.

(d) The plastic cone of (4) is heavily coated with damping material on both sides, while the paper cone of (1) is not so heavily damped and is consequently lighter.

(e) No (4) has a very powerful magnet, in part needed to drive the heavier cone.

(f) The lead-in wires of (4) are taken out from opposite side of the voice coil through eyelets fairly close to it. No (1) passes them toget her sometimes as much as halfway up the cone.

(g) Finally No (4) has a smaller diameter with a greater linear movement capability.

Which of these factors is the most significant may be determined from the investigations of the modified standard speakers below.

(iii) Number (5) Modification (a) - no surround

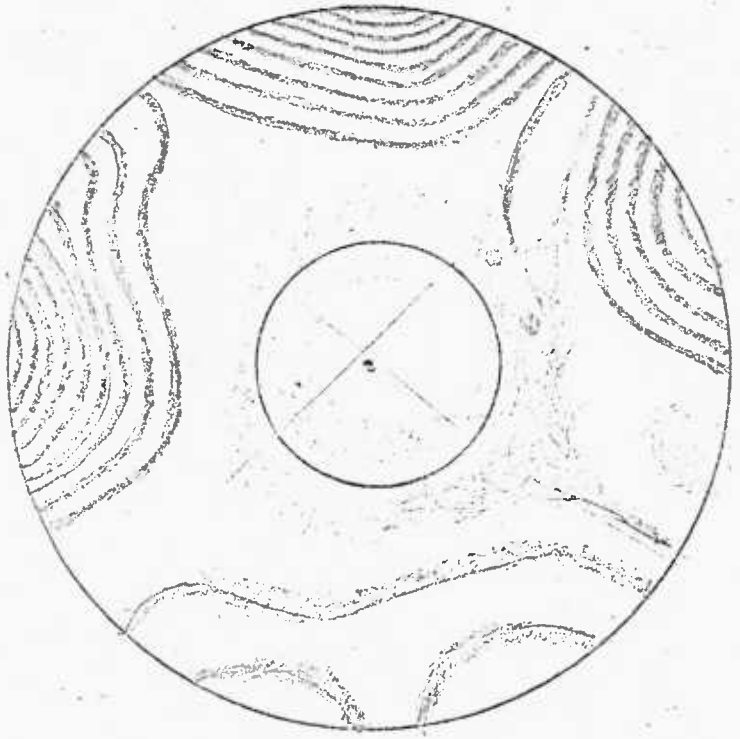
Disc like modes are more apparent with this speaker and the effect is more pronounced when the fringes are actually seen moving in and out. Reducing the size of the cone by 1/4 inch may partially eliminate this. There are no traces of nodal circles, even when amplitudes are very high, but the number of fringes observed are far greater than the number seen with (1) for the smae acoustic output.

(iv) Number (6) Modification (b) - no lead-in wires through the cone.

The results of this investigation were not conclusive any improvements due to the removal of the lead-in wires were masked by the poor hill and dale type behaviour of the cone itself.

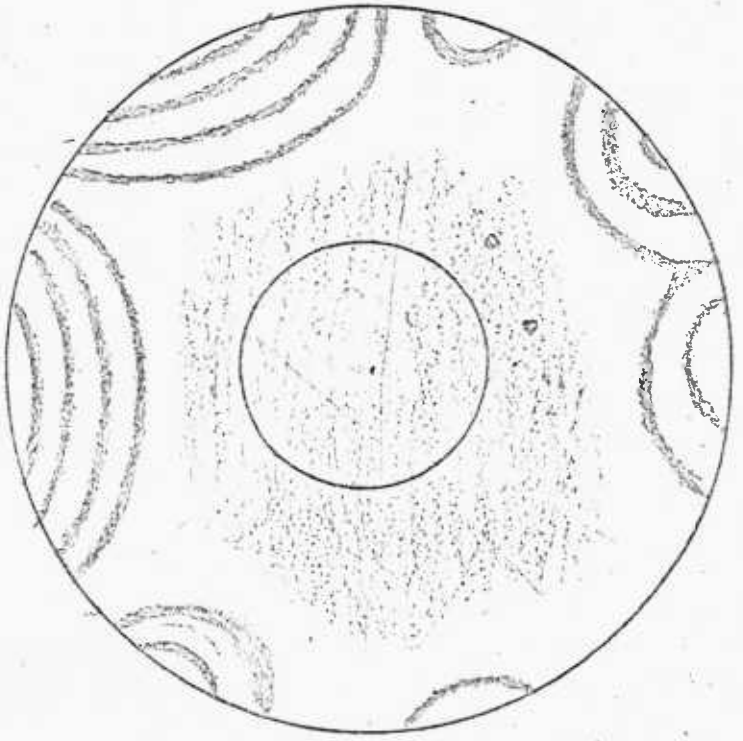
There was some evidence with this speaker that the nodal structure was one nodal circle and 'n' nodal diameters in the region 1 to 2 KHz (hologram 149). The regions below 1 KHz will then correspond to 'n' nodal diameters only. Indeed the frequency relationships between similar patterns above and below 1 KHz fit Wallers results for discs (19-62) see Appendix( II ).

| | |
|---|---|
| SPEAKER | NO 5 no surround |
| HOLOGRAM | 160 |
| RESONANCE | B |
| FREQUENCY | 955 Hz |
| DETAILS | High audio output |
| COMMENTS | Evidence for two nodal dias. |



Results Figure 8 Speaker Number 5 - No Surround

| | |
|---|---|
| SPEAKER | NO 5 no surround |
| HOLOGRAM | 136 |
| RESONANCE | B |
| FREQUENCY | 975 Hz |
| DETAILS | Mid audio output |
| COMMENTS | equivalent to 600 Hz two nodal diameters |



HOLOGRAM 137

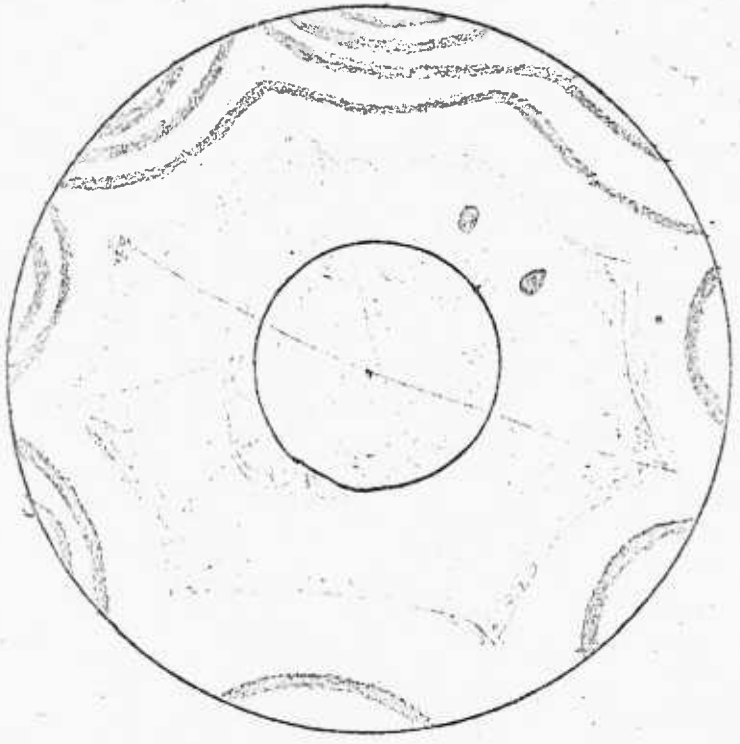
SPEAKER NO 5 no surround

RESONANCE G

FREQUENCY 1900

DETAILS

COMMENTS Evidence for 4 nodal diameters



Results Figure 9 Speaker Number 5 - No Surround

SPEAKER NO 7 separated surround

HOLOGRAM 154

RESONANCE K ?

FREQUENCY 2000 Hz

DETAILS 3volts from microphone amplifier

COMMENTS



Speaker Number 7 - Surround Separated from Chassis

SPEAKER NO 6 no lead wires

HOLOGRAM 142

RESONANCE C

FREQUENCY 720 Hz

DETAILS

COMMENTS Shows the movement of the surround well



SPEAKER NO 6 'no lead in wires'

HOLOGRAM 148

RESONANCE A dip

FREQUENCY 460 Hz

DETAILS

COMMENTS



Results Figure Number 10 Speaker Number 6

Lead in wires passed directly to chassis without passing through the cone

SPEAKER NO 6 'no lead-in wires'

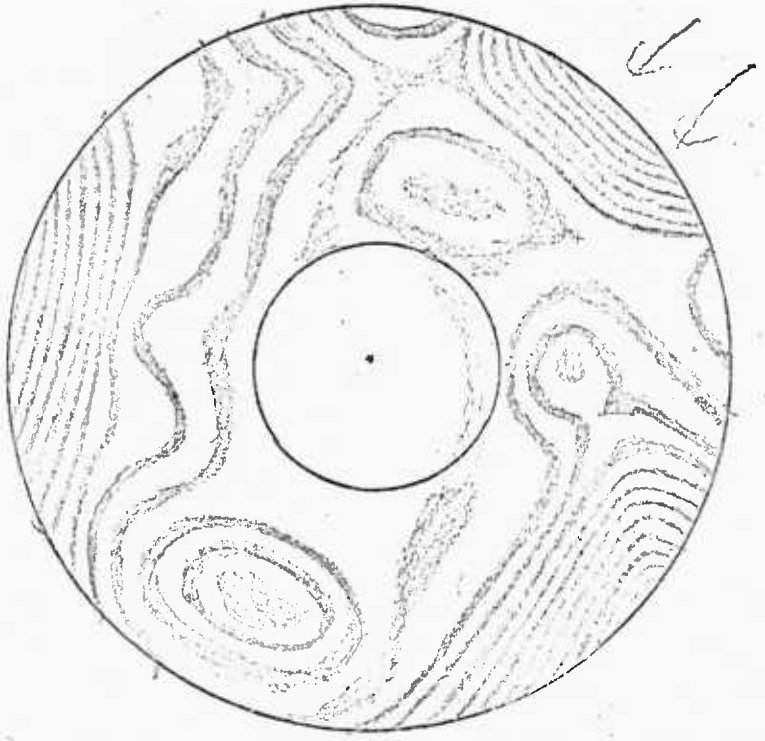
HOLOGRAM 159

RESONANCE E

FREQUENCY 850 Hz

DETAILS

COMMENTS



Results Figure Number 11 Speaker Number 6 Lead in wires directly to the chassis

SPEAKER NO 6 'no lead in wires'

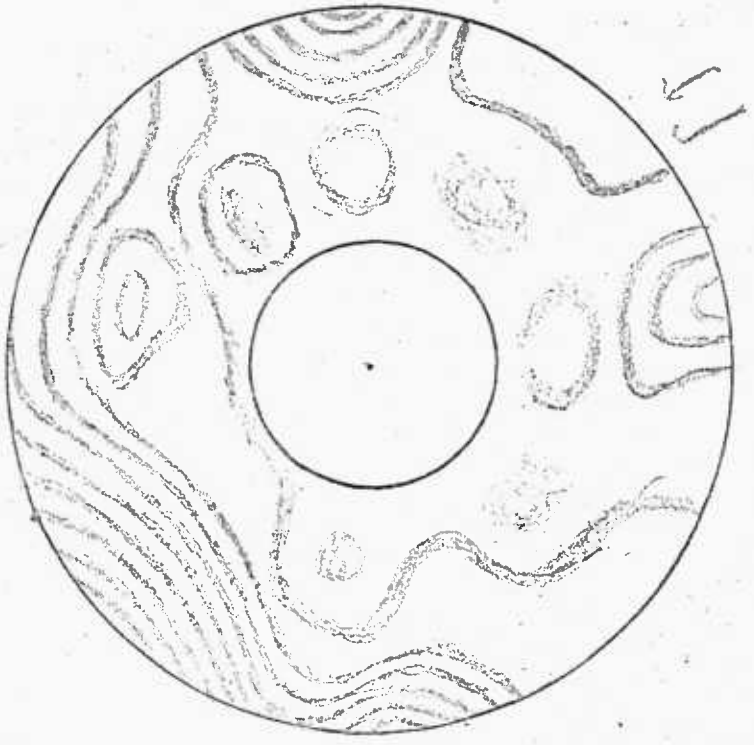
HOLOGRAM 149

RESONANCE I

FREQUENCY 1340 Hz

DETAILS

COMMENTS Evidence of one nodal circle



SPEAKER NO 6 'No lead in wires'

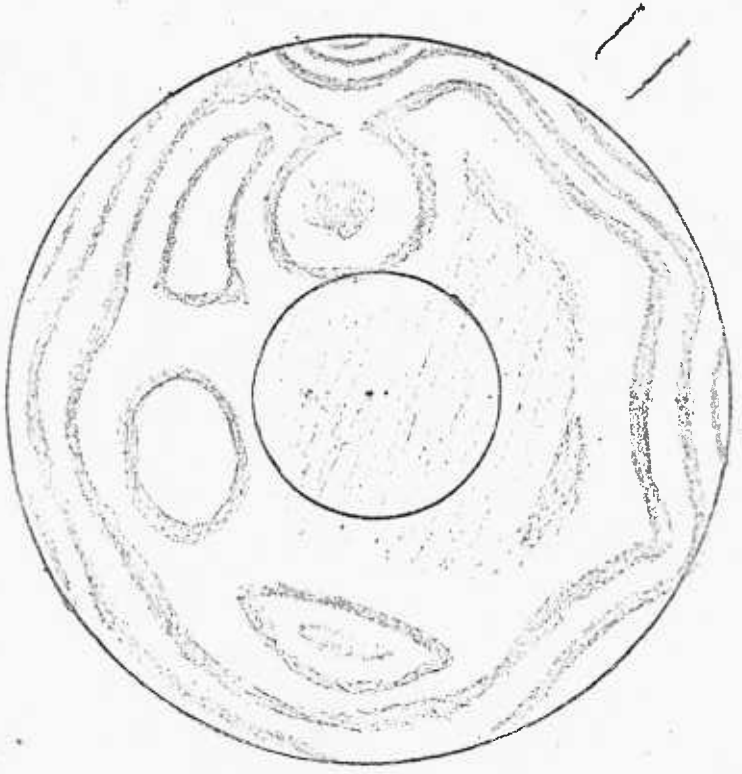
HOLOGRAM 146

RESONANCE K

FREQUENCY 1650

DETAILS

COMMENTS



Results Figure Number 12 Speaker Number 6 Lead-in wires directly to the chassis

SPEAKER NO 6 'no lead-in wires'

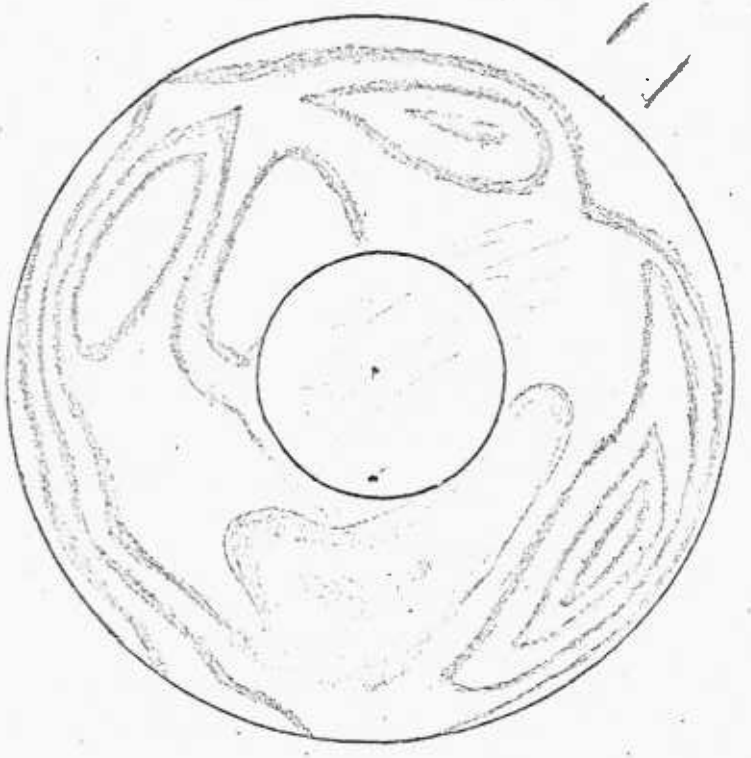
HOLOGRAM 147

RESONANCE 0

FREQUENCY 2570 Hz

COMMENTS

DETAILS



Experiments with speaker number (5) at high amplitude may have been clouded by the effect of its lead-in wires. However Loudspeaker No (10) (straight sided cone) which is a great deal less stiff than the standard (No 1) gives further pointers to the nodal circle idea. Further work is necessary to clarify this point completely.

(v) Number (9) Modification (c) rubber roll surround - but same profile.

The investigations of Nos (1) and (4) suggest that a rubber roll surround may well give the required linear motional freedom (to stop 'edge bending') and circular rigidity (to help prevent nodal diameter modes). A reasonably soft rubber roll having 1/3 of the diameter and opposite sense to that of No (4) (whose roll projects outwards) was fitted to a standard cone. The resulting speaker behaved worst at low, and best at high frequencies. Below 1200 Hz its behaviour was similar to No (1) (holograms 177 and 175). At 1250 Hz there were fewer re-entrant fringes, more of the edge bend type and three sharply defined hill and dale regions (holograms 168 and 170). At higher frequencies there were fewer edge bend and hill and dale until at 2100 Hz (hologram 177) the speaker was behaving very well indeed at quite a high audio output. These results suggest:

(a) A different roll giving more movement capability at low frequencies

(b) Once again, the removal of the outer 1/4 inch of the standard cone or a sharper cone angle to give greater effective stiffness.

(vi) Number (10) Straight Sided Cone

It is expected that this cone will be less stiff to diametral forces than the standard cone. Listening tests show that this type of cone sounds unpleasant and the fringe patterns observed are mainly of the hill and dale variety symmetrically distributed around the cone in a disc-like manner, with 'one nodal circle - 'n' nodal diameters'. The nodal circle being possibly at the outer edge of the cone. The regions through which

SPEAKER NO 9 Rubber Roll Surround

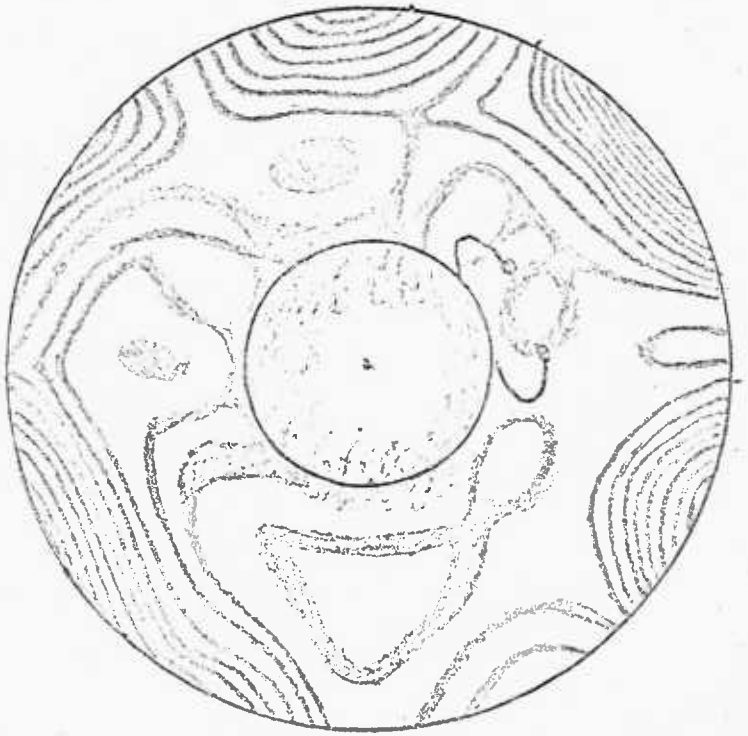
HOLOGRAM 177 A (Knicked end)

RESONANCE

FREQUENCY 900 Hz

DETAILS .3 volts from Microphone preamplifier

COMMENTS



SPEAKER NO 9 Rubber Roll Surround

HOLOGRAM 175 B (Knicked end)

RESONANCE

FREQUENCY 1250 Hz

DETAILS .7 V

COMMENTS



Results Figure Number 13 Speaker Number 9 Rubber Roll Surround same cone profile

SPEAKER NO 9 Rubber Roll Surround

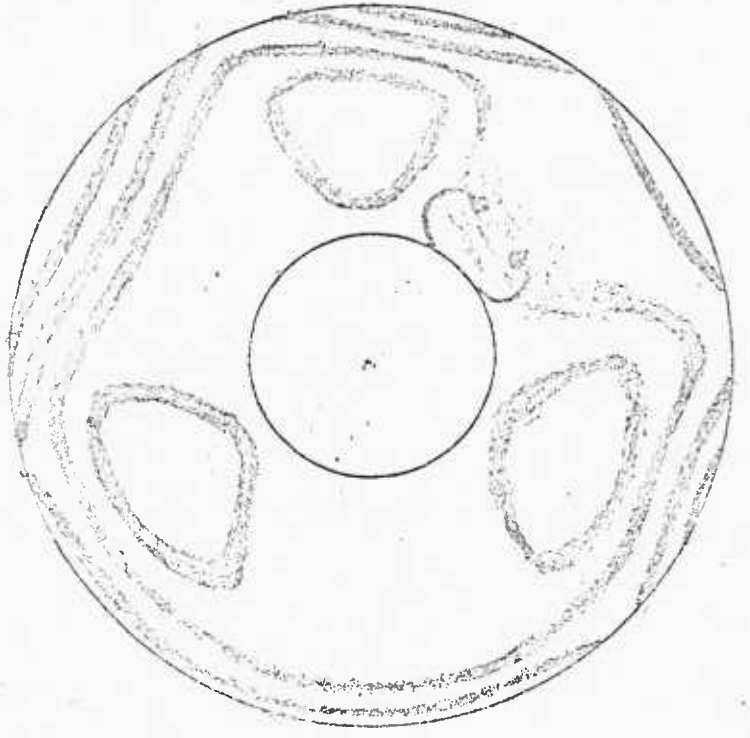
HOLOGRAM 168 B

RESONANCE

FREQUENCY 1400 Hz

DETAILS

COMMENTS Excellent hologram quality
Fewer 're-entrant' fringes



Results Figure Number 14 Speaker Number 9 Rubber Roll Surround
same cone profile

SPEAKER NO 9 Rubber Roll surround

HOLOGRAM 170

RESONANCE

FREQUENCY 1620 Hz

DETAILS 3 volts from microphone preamplifier

COMMENTS



SPEAKER NO 9 Rubber Roll Surround

HOLOGRAM 177 B (knicked end)

RESONANCE

FREQUENCY 2100 Hz

DETAILS 3 Volts from microphone preamplifier

COMMENTS Close to piston motion at this frequency



Results Figure Number 15 Speaker Number 9 Straight Sided Cone
Speaker Number 10 Rubber Roll Surround

SPEAKER NO 10 Straight sided cone

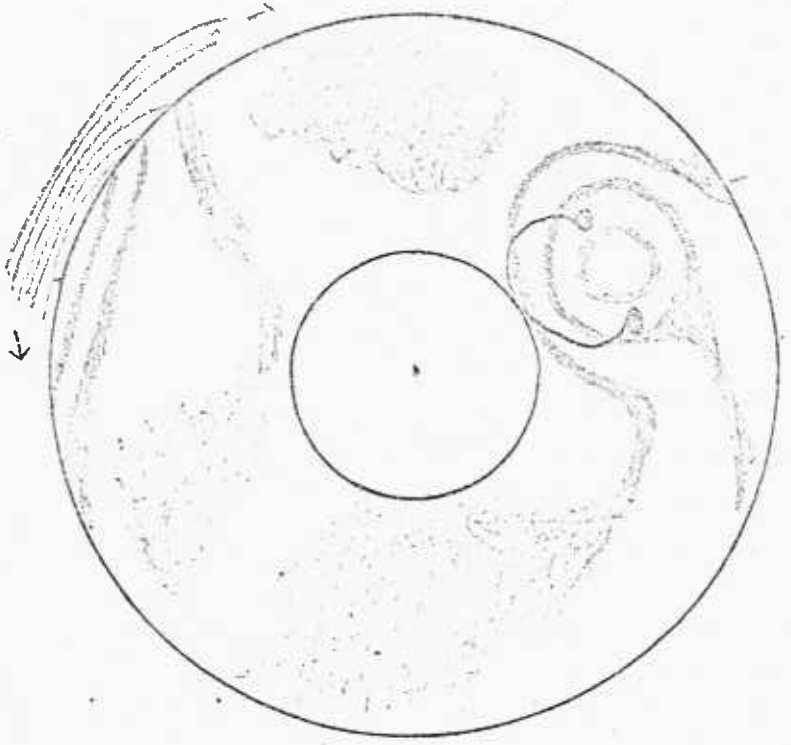
HOLOGRAM 182

RESONANCE

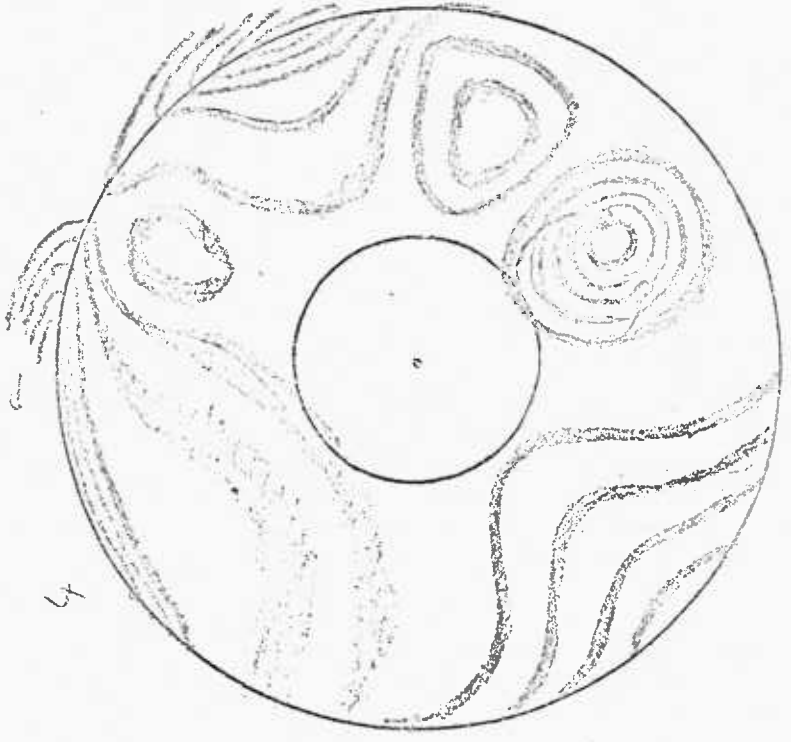
DETAILS

FREQUENCY 800 Hz

COMMENTS This cone is good below 1KHz
Good fringes in surround



| | |
|---|---|
| SPEAKER NO | 10 straight sided cone |
| HOLOGRAM | 180 |
| RESONANCE | 1050 Hz |
| DETAILS | |
| COMMENTS | Clear fringes in surround evidence for nodal circle becomeing evident |



Results Figure Number 16 Speaker Number 10
Straight Sided Cone

| | |
|---|---|
| SPEAKER NO | 10 Straight sided cone |
| HOLOGRAM | 179 |
| RESONANCE | |
| FREQUENCY | 1400 Hz |
| DETAILS | |
| COMMENTS | Strong suggestion of nodal circle near cone edge |



the lead-in wires pass are greatly affected by them - the region of influence extending up to 1/8 of the cone area.

This Loudspeaker is best at low frequencies becoming progressively worse as the frequency is increased (holograms 182,180 and 179). This behaviour and that of No (9) suggests that a good Loudspeaker may be one with a slight radius and a large rubber roll surround which may combine the advantages of both speakers.

(vii) Numbers 8 and 11 Standard with no damping and Plastic with no damping

These cones were the worst tested. At modest input levels they break-up into many hill and dale regions and only a representative sketch of (11) could be completed (hologram 184)

(viii) Conclusions

The conclusions reached after studying the results of this mid-range unit investigation will be found at the end of this section in '4.8 a' on Page ( 166 ).

4.7) Sandwich Bass and Treble Units

(i) Introductory Discussion

The sandwich principle, whereby a very stiff light composite material is made up of a light rigid foam with two skins having low elastic extension per unit force bonded onto its surface, has long been used in the air - craft industry and other applications requiring a high stiffness to weight ratio. In 1958 D.Barlow (1970) first applied the principle to the manufacture of Loudspeaker cones, where high stiffness and low mass are required to ensure that the edges of the cone follow the movements of the voice

SPEAKER NO 8 No dope on cone or surround

HOLOGRAM 167

RESONANCE G

FREQUENCY 1300

DETAILS

COMMENTS Break-up very severe



Results Figure 17 Speaker Number 11 Plastic cone - no dope

Speaker Number 8 Paper core - no dope

SPEAKER NO 11 Plastic Cone

HOLOGRAM 184

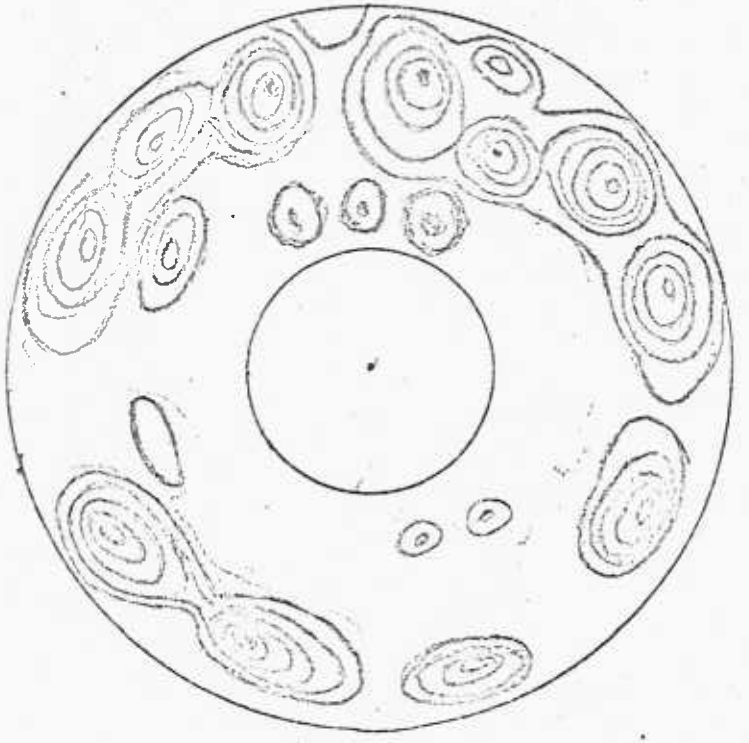
RESONANCE

FREQUENCY 1600 Hz

DETAILS

COMMENTS Very large numbers of 'hill' type patterns

REPRESENTATIVE ONLY



coil attached to its center. This application of an 'aluminium-expanded-polystyrene-aluminium' sandwich resulted in perfect piston motion over a wider frequency range than had been achieved with more conventional materials. However, when the sandwich material does begin to 'flex' or 'break-up the resulting modes have a higher 'Q' than more conventional cones resulting in higher peaks in the response curve. These modes also fall above the coincidence critical frequency for the cone material and so mode segments will radiate independently - again increasing the size of the peaks in the response curve. This means that the cross-over frequencies have to be set well into the piston action region to ensure that the input to the voice coil is well down at these resonance frequencies and so some of the piston bandwidth is wasted.

This problem may be tackled in at least six ways:

(a) Move the resonance frequencies even higher by stiffening the cone by increasing the foam thickness or

(b) By giving the cone a slight radius. This approach though greatly increasing the diametral stiffness has manufacturing difficulties, for instance sections of skins would have to be laid individually onto the polystyrene or complete skins would have to be 'explosion' formed out of aluminium sheet.

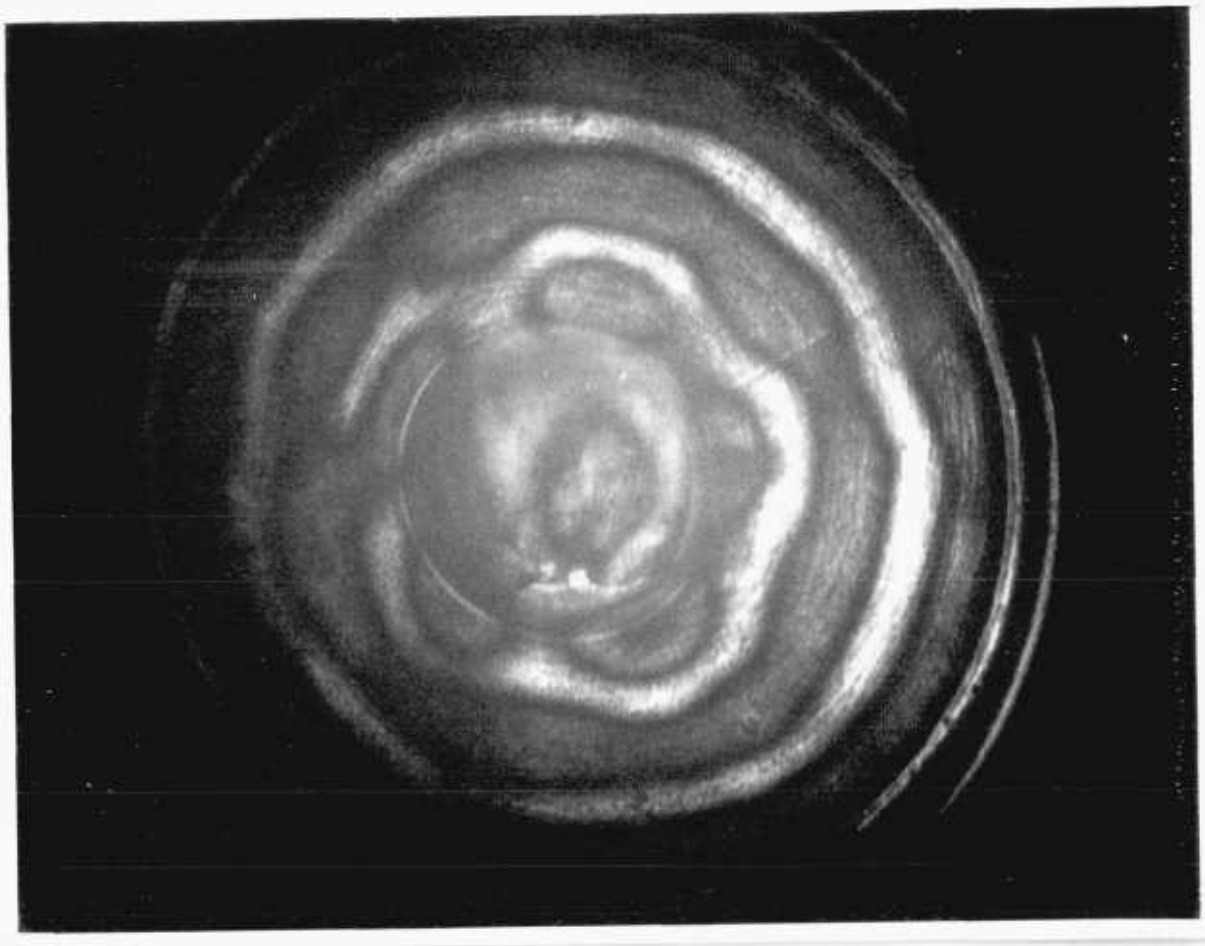
(c) Stiffners may be placed onto the cone either radially (utilising bending stiffness) or circumferentially (utilising torsional stiffness (Leisa 1967).

(d) Alter the cone angle until the optimum is found. The present angle is arbitrary.

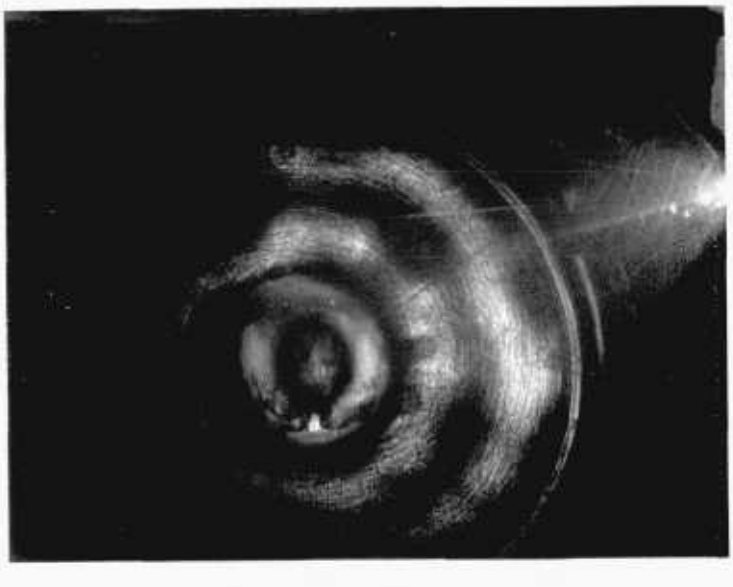
(e) Damp out the resonances by using a lossy glue or a more lossy foam sandwich filling or, as has been suggested by these investigations, by using an appropriately placed 'lumped damper' and finally

(f) If the coincidence effect is the major reason that the modes cause high peaks in the response curve it may be advantageous to reduce the

Plates 11 and 12 (See sketches page 159 d)

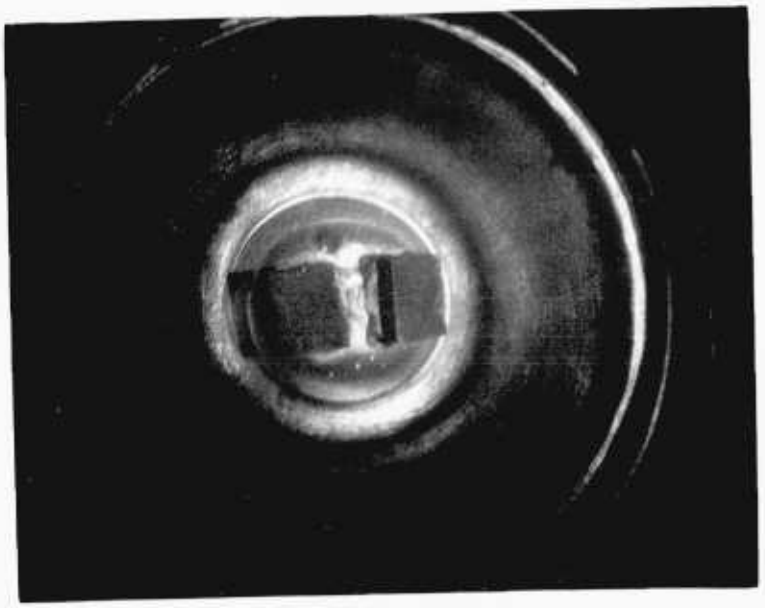


Sandwich Bass.T.A. 5.4 KHz;see sketch;+ ribbs



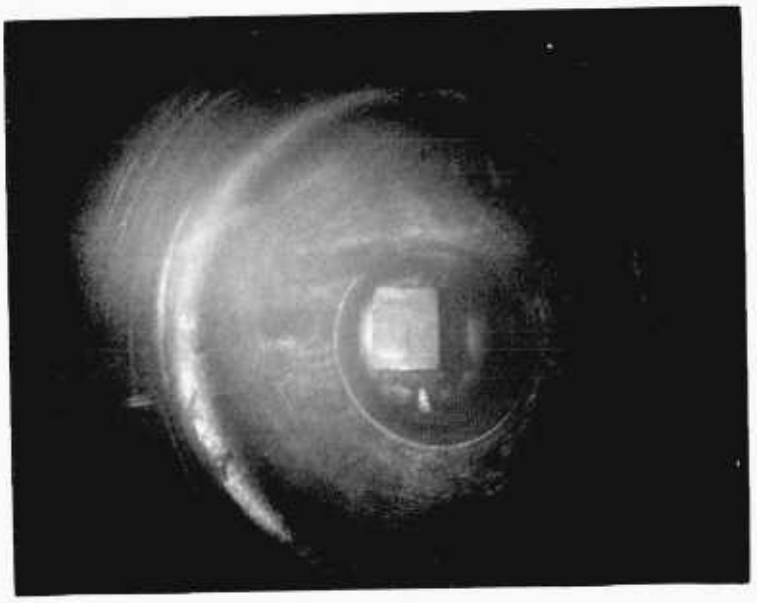
Sandwich Bass.T.A. 5 KHz, sketch also given

Plate 13 (see also sketch page 159 b)



Sandwich Bass, T.A. 3 KHz 1 nodal circle

Plate 14 (see also sketch page 159 a)



Sandwich Bass, T.A. 1.3 KHz Sketch also given

stiffness slightly. The coincidence critical frequency will rise above the working region and more modes will fall into the working region. These modes, however, may well radiate less strongly since the volume velocities of neighbouring mode segments will now tend to cancel out. This hypothesis has yet to be tested by experiment, but some of the other points were tested in the experiments detailed below.

A holographic investigation was carried out on a sandwich bass unit. After the experimental difficulties detailed above were overcome good results were obtained which strongly suggest that a sharper cone angle and/or a thicker filling would give improved results. Experiments with the treble unit showed that the main fault with this unit is 'cone-rocking' largely caused by the mass and stiffness of the lead-in wires. The surround of this speaker showed severe vibration modes of its own - in many cases having higher amplitude than the cone vibrations.

(ii) Discussion of Results

(a) Bass Unit

Time averaged holograms were taken at each of the main resonances up to 6 KHz and at the 'dips' in between them. The patterns observed were unlike any previously seen in that they consisted only of circular fringes concentric with the voice coil. Checks on all these frequencies verified that there was not a trace of the 'nodal diameter' type of fringe system and only nodal circles were present. The position and number of the nodal circles varied, of course, with the frequency of excitation.

The first mode encountered is the umbrella at 1.3 KHz, where the outer edge of the speaker is stationary, with the central regions vibrating in the normal manner but with slightly higher amplitude. This was in fact a peak in the response curve, though not as pronounced as that due to the next resonance, which was situated at 2.5 KHz with a node roughly at the edge of the central bung. This resonance gives the highest

SPEAKER Sandwich Bass Unit with 5 Sandwich Stiffners

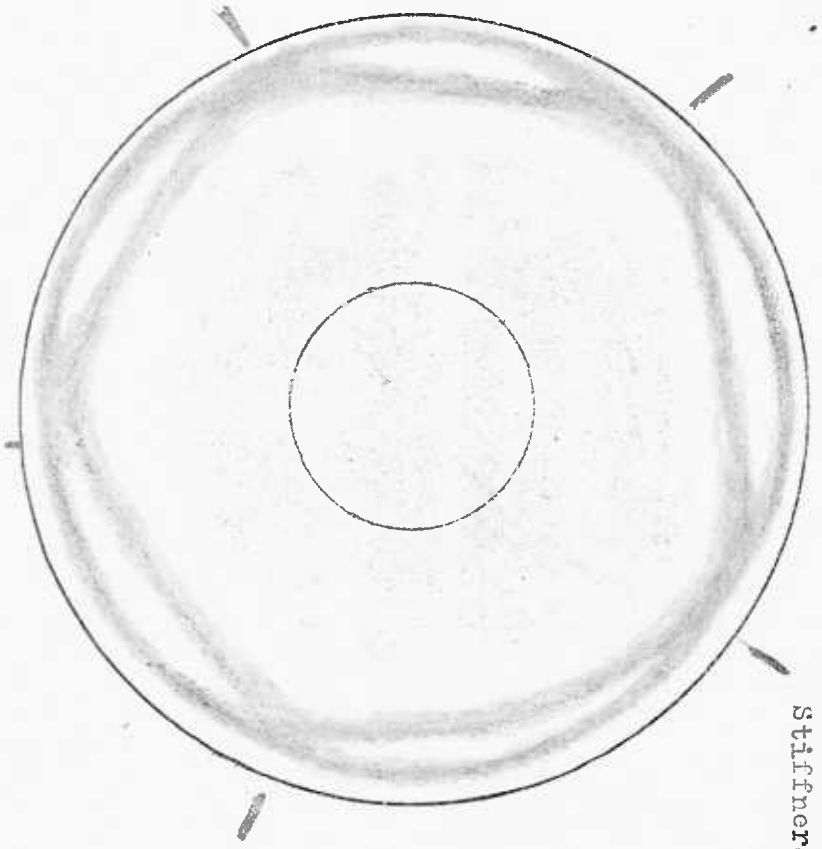
HOLOGRAM 345

RESONANCE umbrella - node at outer edge

FREQUENCY 1.2 KHz

DETAILS Time averaged

COMMENTS Stiffners have the desired effect at this frequency - they push the fringes outwards but only immediately under themselves




Results Figure 18 Sandwich Bass Unit

SPEAKER Sandwich Bass Speaker

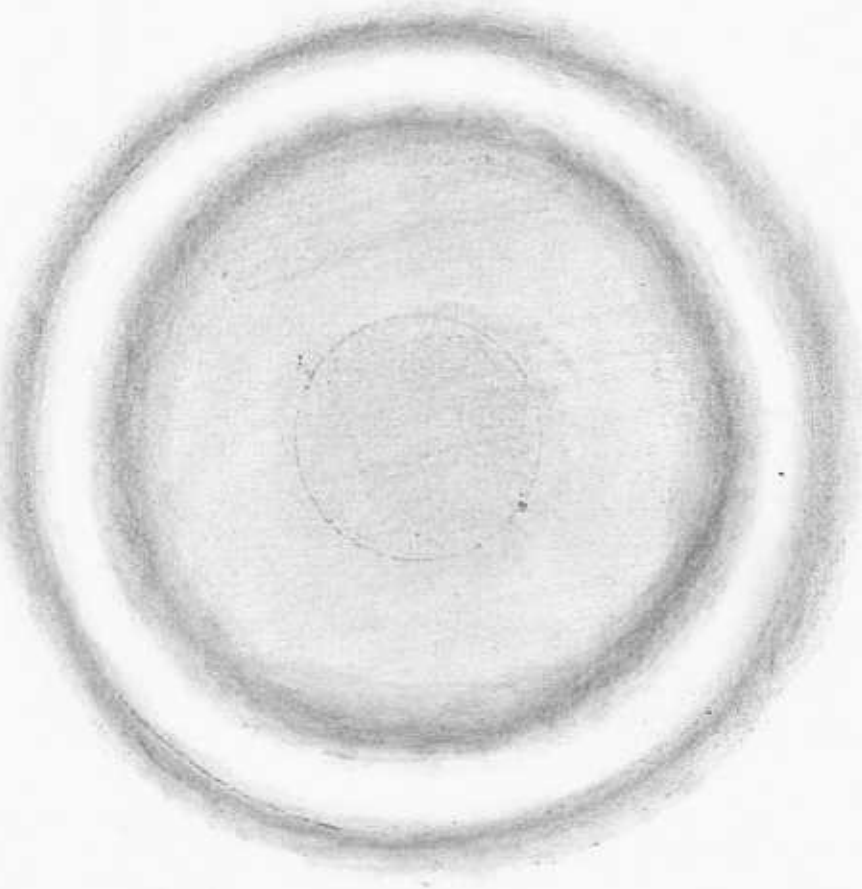
HOLOGRAM 333

FREQUENCY 1.3 KHz

RESONANCE Umbrella

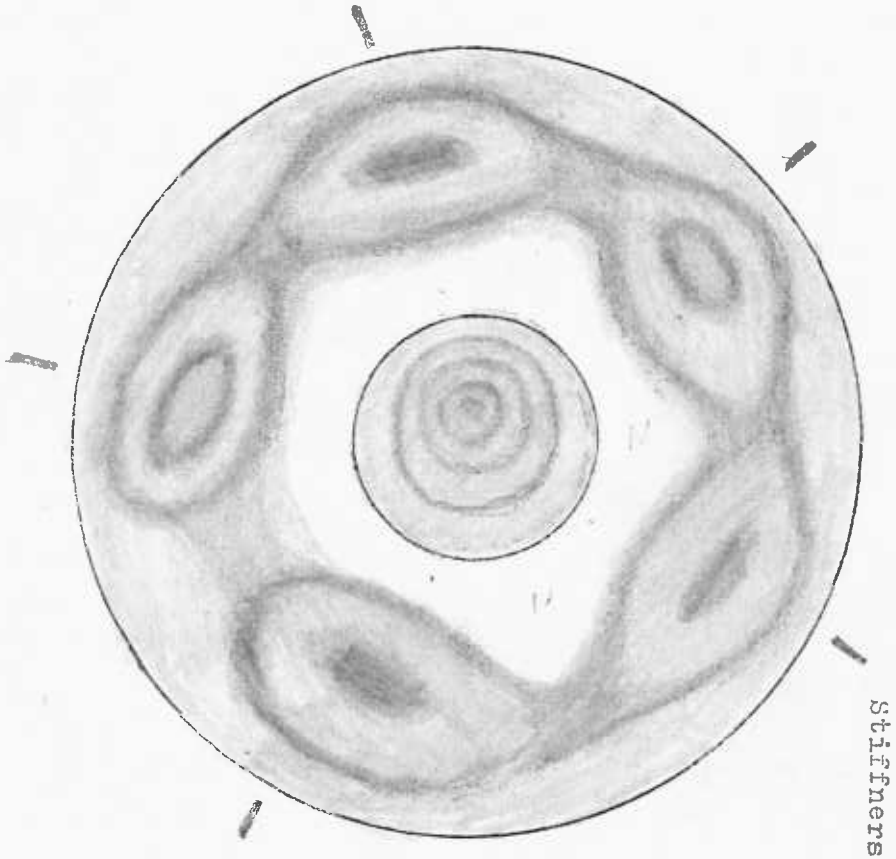
DETAILS Time Averaged Holography used

COMMENTS



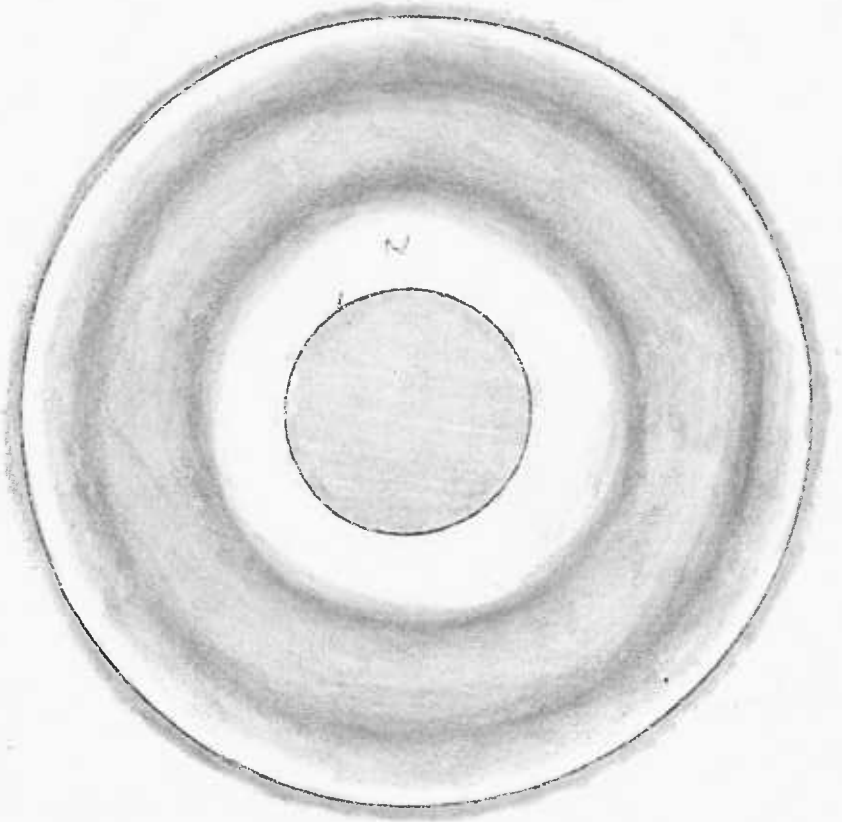
One Hundred and Fifty-Nine (a)

SPEAKER Sandwich Bass Unit with 5 Sandwich Stiffners
HOLOGRAM 343
RESONANCE
FREQUENCY 2.7 KHz
DETAILS Time averaged
COMMENTS The effect of the stiffners at this frequency is the opposite of that desired.

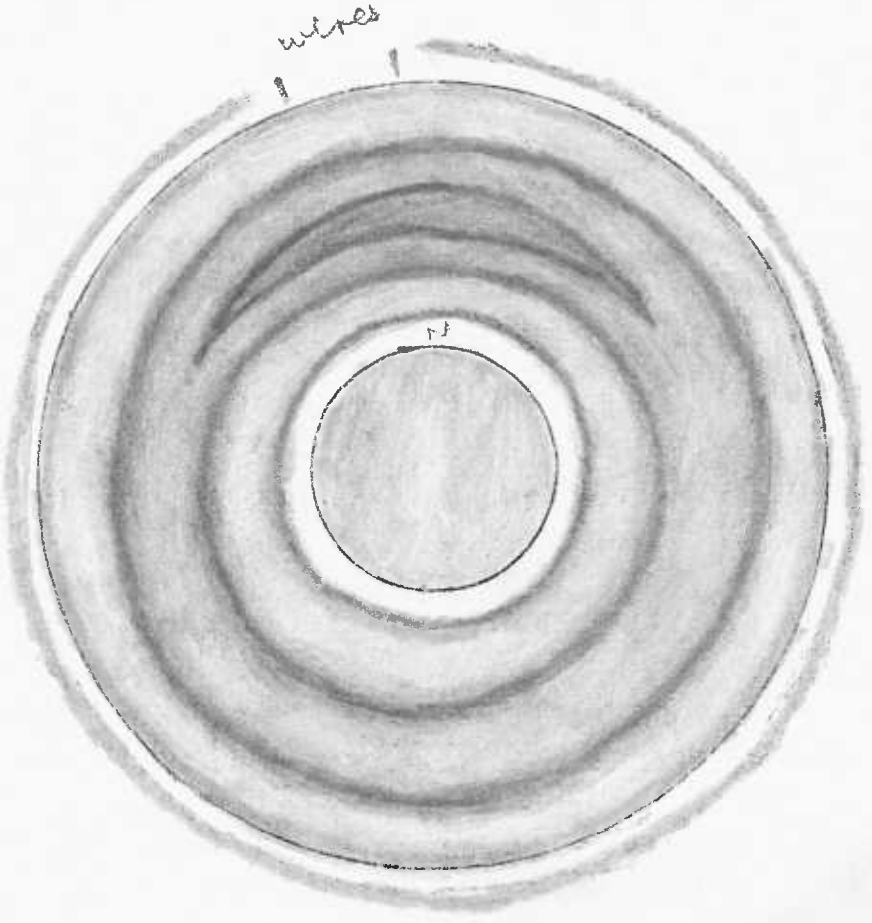



Results Figure 19 Sandwich Bass Unit

SPEAKER Sandwich Bass Speaker
HOLOGRAM 263, 266.
RESONANCE
FREQUENCY 3 KHz
DETAILS Time averaged
COMMENTS

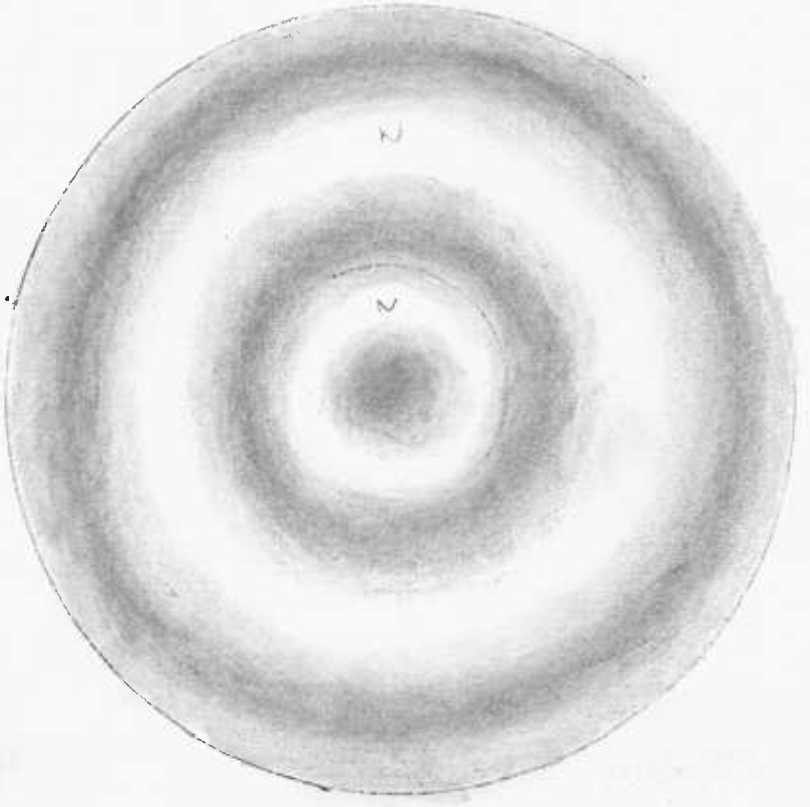


SPEAKER Sandwich Bass Speaker
HOLOGRAM 334 , 261 and 262 similar
FREQUENCY 2.5KHz
RESONANCE Nodal circle at center 'bung radius'
Details Time averaged hologram
Comments

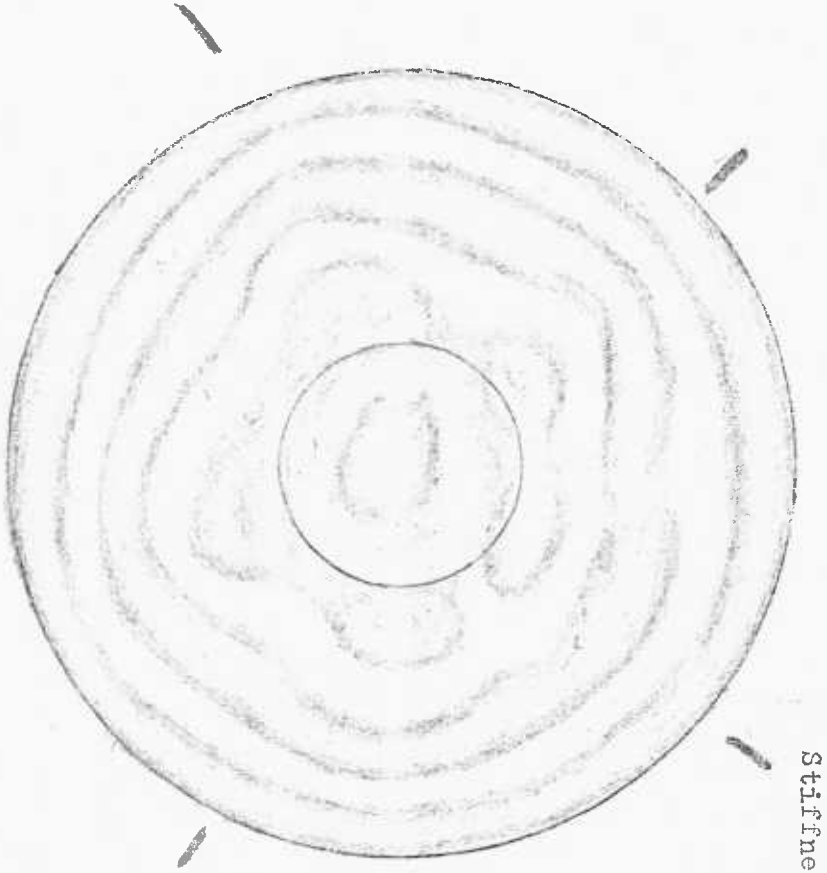



Results Figure 20 Sandwich Bass Unit

SPEAKER Sandwich Bass Speaker
HOLOGRAM 337
RESONANCE 2 nodal circles
FREQUENCY 4 KHz
DETAILS Time averaged
COMMENTS



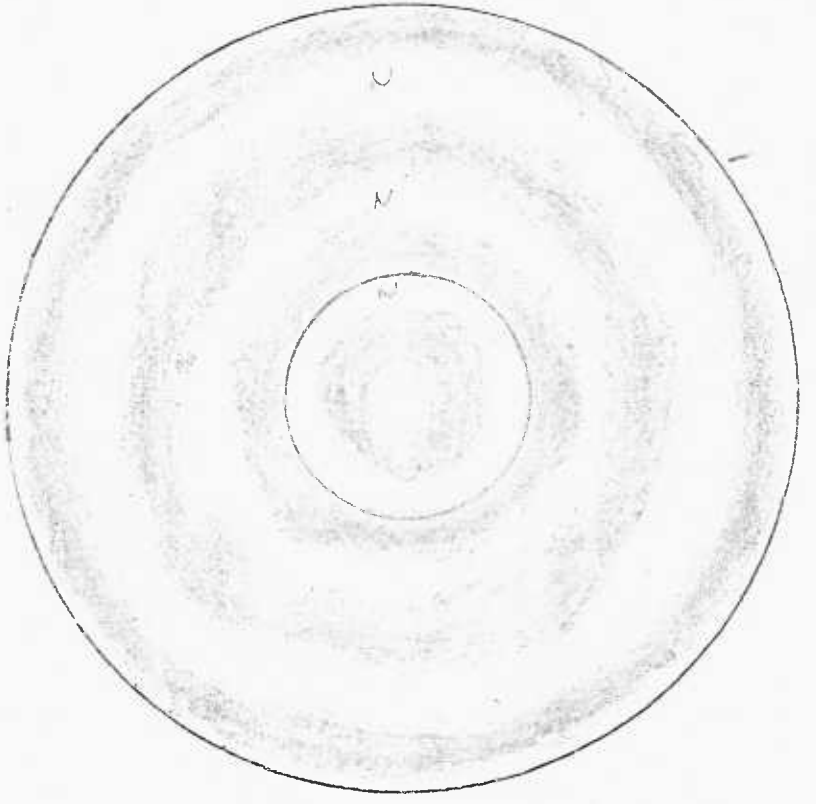
| | |
|---|---|
| Speaker | Sandwich Bass with 5 sandwich stiffners |
| Hologram | 350 |
| Resonance | 3 nodal circles |
| Frequency | 5.4 KHz |
| Details | time averaged |
| Comments | stiffners have relatively little effect at this frequency |



Stiffners

Results Figure 21 Sandwich Bass Unit

| | |
|---|---|
| SPEAKER | Sandwich Bass Speaker |
| HOLOGRAM | 341 and 338 |
| RESONANCE | 3 nodal circles |
| FREQUENCY | 5 KHz |
| DETAILS | time averaged |
| COMMENTS | |



peak in the response curve and can be up to 12 db above tthe mean level. The two nodal circles resonance occurs at 4 KHz and the three nodal circles resonance at 5 KHz (Fig 45 ).Holograms taken at the dips in the response curve showed nothing conclusive though the fringes were still arranged in concentric circle, though nodeless, configurations intermediate to those found at the resonances themselves.

This form of break-up suggests that the cone is stiffest when being compressed along a diameter but less stiff when being compressed in an axial direction. It is to be expected that the perfectly suspended and completely homogeneous loudspeaker would not show fringes of the 'nodal diameter' type, as all the excitation forces are tending to produce the 'nodal circle' type of break-up. Only when suspension restoring forces are not uniform around the circumference, or when the cone is not of uniform mass or stiffness will there be energy and forces available for the excitation of 'nodal diameter' type modes. In fact it has been found that the Younge's Modulus of different parts of a single paper cone can vary by 100 percent though the thickness and density vary by less then 5 percent and 10 percent respectively. The density, thickness and stiffness of a sandwich cone are much more uniform which may help to explain the lack of the 'nodal diameter' break-up. The lead-in wires with sandwich cones are taken directly to the chassis without passing through the cone - so further reducing the 'out of ballance' forces.

Investigations previously carried out at the National Physical Laboratory showed good pictures of 'nodal diameter' type modes in a sandwich bass unit. To obtain these pictures, however, the speakers were excited at a point near to their circumference with the excitation forces directed radially. This, as was to be expected, resulted in the 2,3 and 4 nodal diameter modes (at 446,980 and 1544 Hz respectively) being strongly excited. When the speakers are excited axially at their centers via a voice coil - i.e. normal speaker excitation - these modes are not excited.

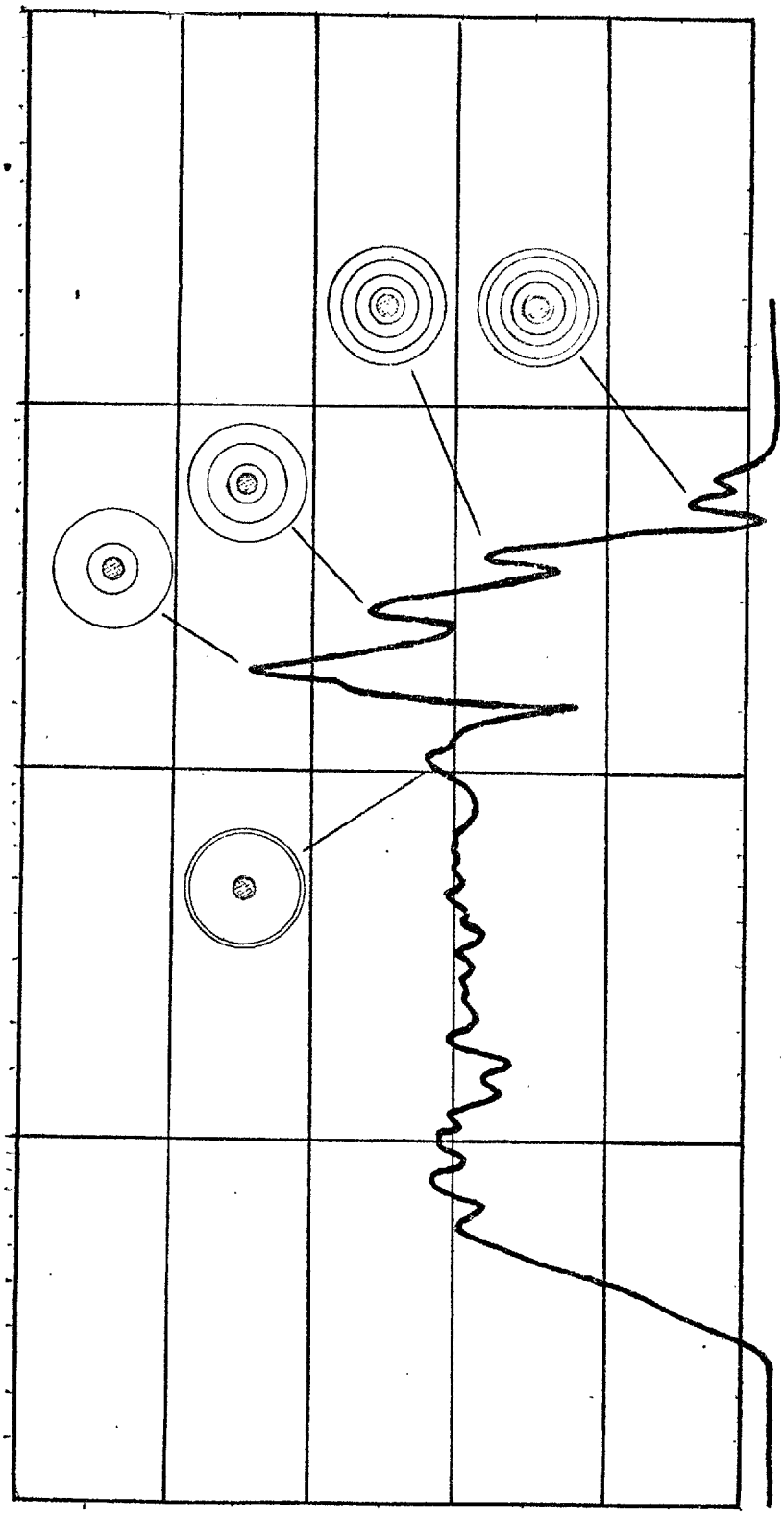


Figure 45 Response curve of Bass Sandwich Unit - resonances corresponding to each peak marked

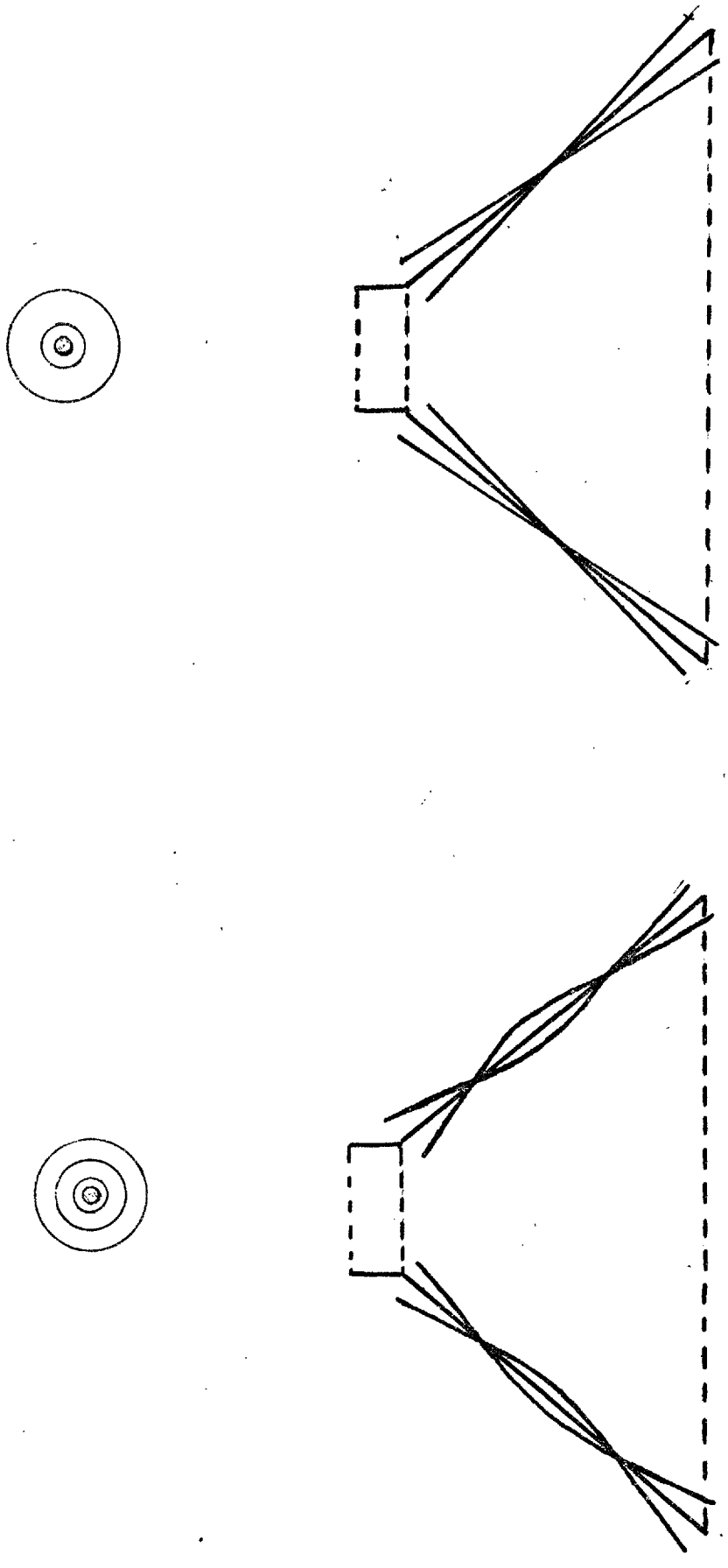


Figure 46 Side View of the One and Two Nodal Circle Modes

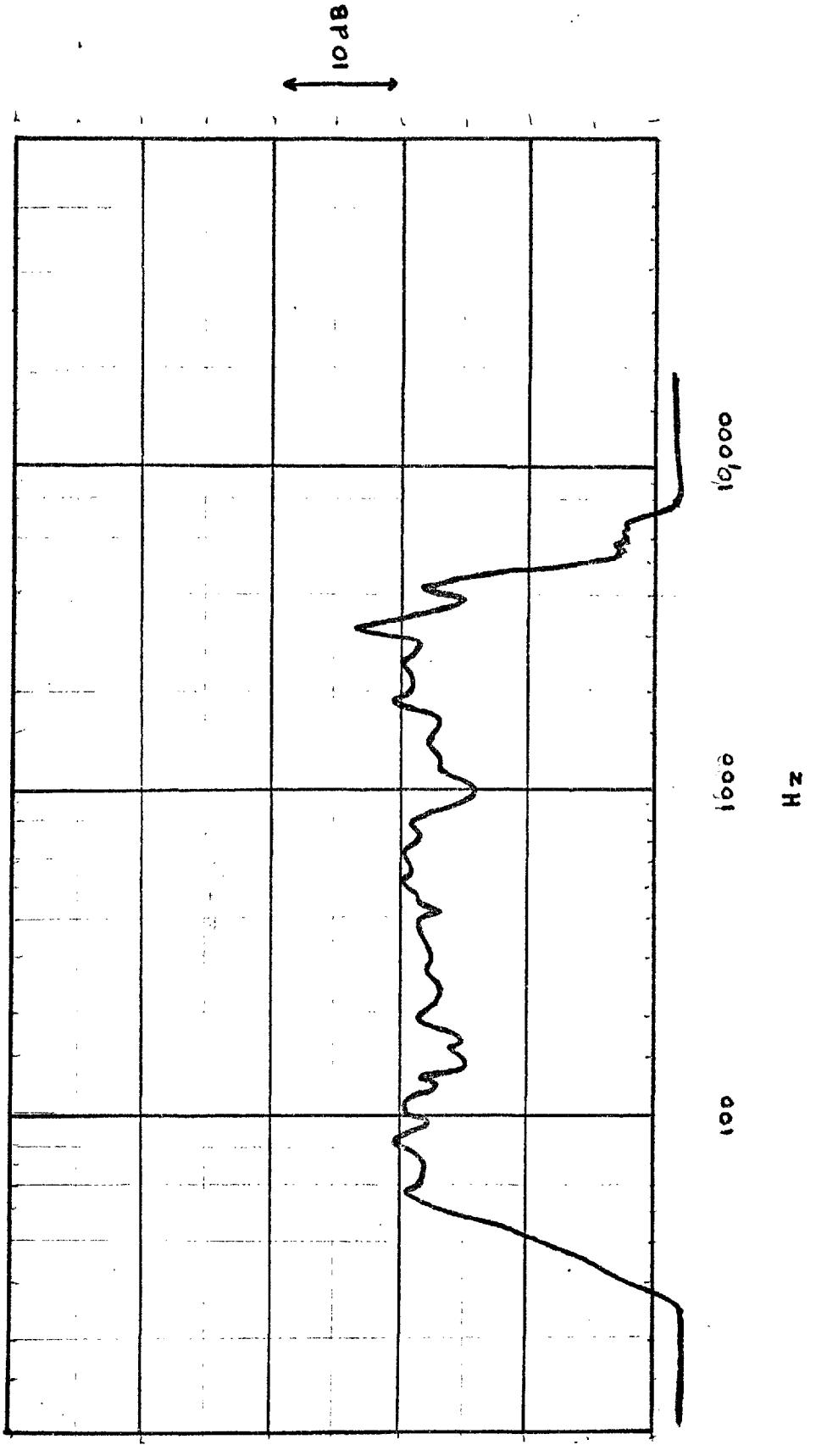
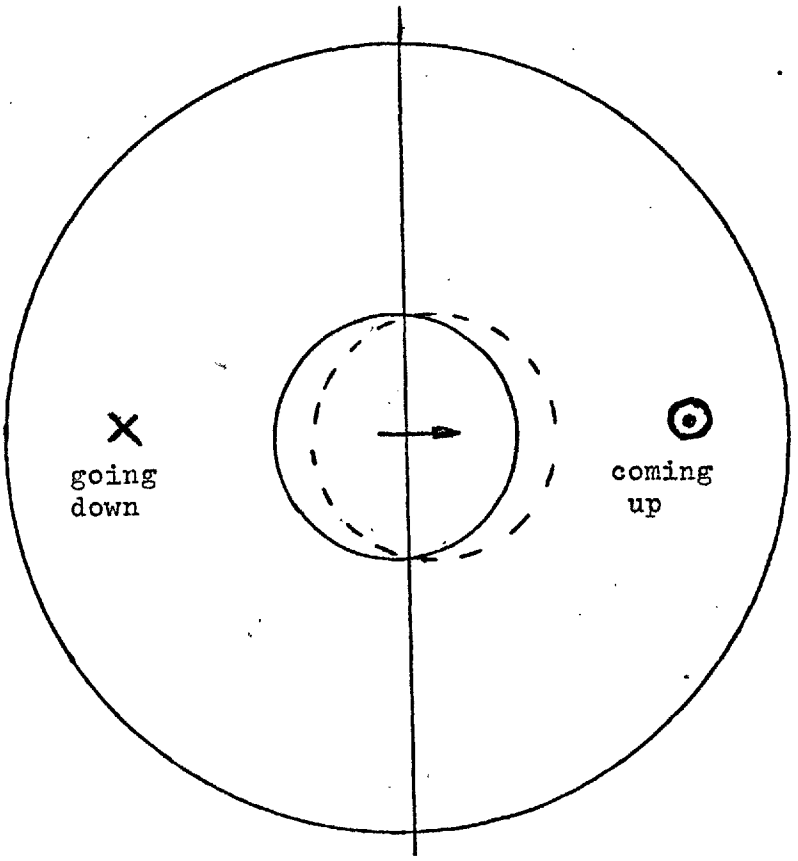



Figure 47 Same Sandwich Bass Unit with a 20 gm 'Lossy Bung' (cone mass 40 gm) see also Fig. 49

In fact holographic investigations with a normally excited speaker showed piston motion up to at least 700 Hz and then a few circular fringes leading up to the umbrella mode at 1300 Hz. This is supported by toneburst tests which show excellent performance below 1 KHz.

Non-axial movement of the voice coil is observed with all Loudspeakers and it may be expected that this will tend to excite 'nodal diameter' modes. This motion effectively produces a component of movement at right angles to its axis, the tilt in the voice coil merely gives a static deflection constant at all phases of the vibration. The 'right-angles' component tends to stretch the cone at one end of a given diameter and compress it at the other, with regions along a perpendicular diameter experiencing shear forces. Considering sections of the cone including the surround, an extension force will tend to make the cone go downwards and a compression force will tend to make it go upwards. As shown in Fig ( 47 ) the arrow symbols indicate that movements of opposite sides of the cone caused by non-axial voice coil movement are <u>out</u> of phase. Now on considering the 'nodal diameter' or non-axisymmetric modes of a disc,we see that opposite lobes of modes having an even number of nodal diameters are <u>in</u> phase. Thus there is little tendency for non-axial voice coil movement to excite even cone modes. With an odd number of nodal diameters opposite lobes are <u>out</u> of phase but neighbouring lobes cancel out any tendency for the disc to be 'up' or'down' on either side of a diameter. Thus there may be a slightly greater tendency for 'odd number' nodal diameter modes to be excited but this is still small.

A similar argument may be applied to resonances of the voice coil itself. Considering the fundamental voice coil resonance (Fig 47 ), this will cause movements of the cone which exactly correspond to the two nodal diameter natural cone mode. However it is very unlikely that the mode in the coil and cone will coincide both in frequency and nodal pattern. It is possible that voice coil modes will fall near to other nodal diameter




(a)

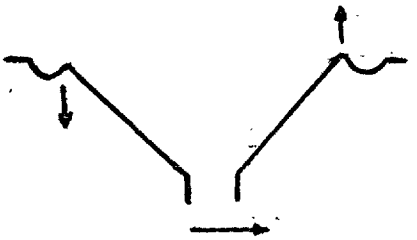
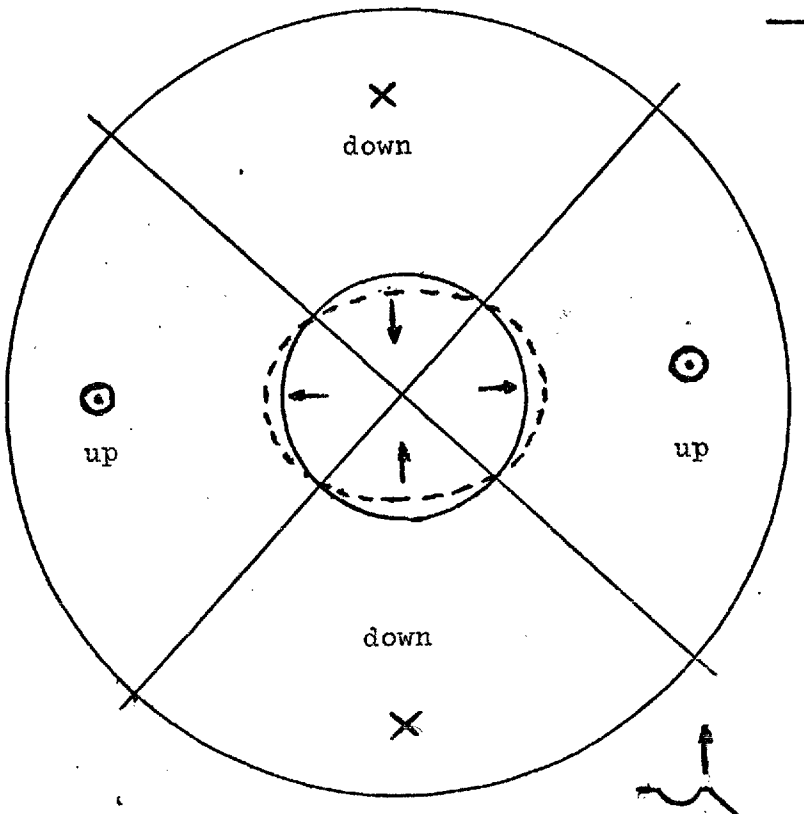
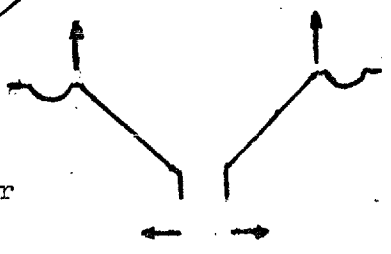


Figure 48 Effect of coil resonances on cone movement




(b)



this is also the correct phasing for the two nodal diameter disc mode

cone modes having different numbers of nodal diameters and then there will be a tendency for these to be excited; the amount of energy available for excitation in this way will, however, be comparatively small with sandwich cones. With paper cones where the mass of the voice coil is comparable with that of the cone the coil vibrations will have a greater effect on those of the cone.

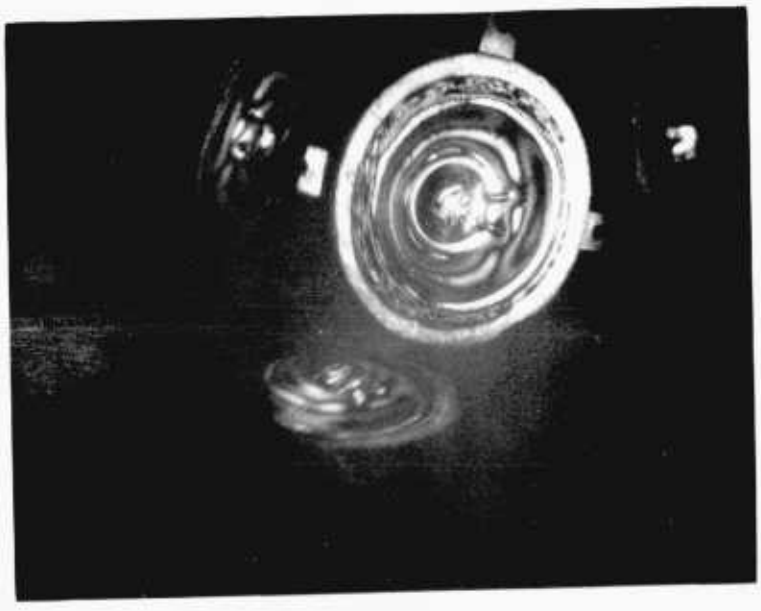
The results that follow for the sandwich treble units show that nodal diameter type fringes do occur with this unit, but in this case the lead-in wires form a very large inhomogeneity indeed and the suspension is not close to the ideal.

A simple experiment to try and increase the stiffness of the bass unit cone in the axial direction was carried out. Five stiffeners cut from a sandwich cone were glued to the back of a cone with araldite. An odd number was chosen to try and minimise the possible tendency for 'nodal diameter' modes to be excited by the inhomogeneities produced. In general the stiffeners have the opposite to the desired effect though the following trend may be seen: Below 1 KHz to 2 KHz the stiffeners do slightly reduce the number of fringes seen but only immediately underneath them - the majority of the cone is unaffected. Near the powerful resonance at 2.5 KHz the fringe pattern is considerably distorted - especially underneath the stiffeners and it seems that at these frequencies the stiffener mass is the more important factor. At 5 KHz the stiffeners have a smaller though a deleterious effect and finally at 6 KHz practically all the vibration occurs near the stiffeners - an inferior result. A circular reinforcing ring working in torsion has yet to be tried.

(b) Sandwich Treble Units of Old and New Construction

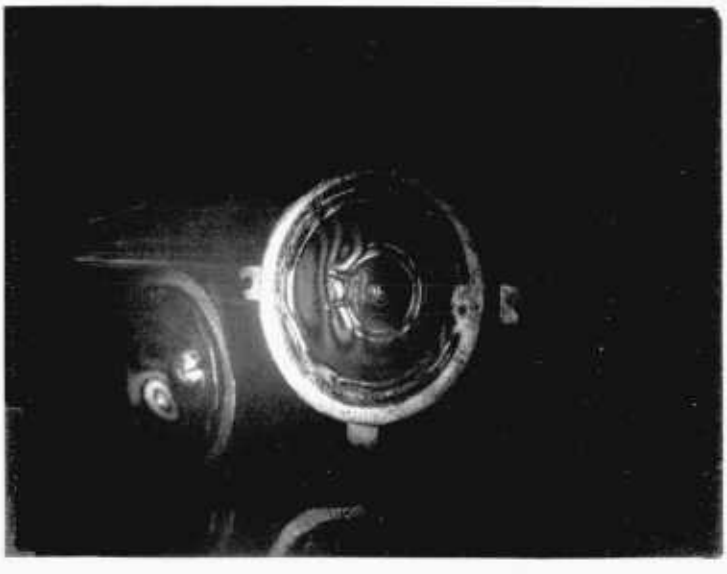
Four specimens of this unit were investigated, two of old construction and two of recent manufacture which were significantly better. From 1 KHz to about 2.5 KHz the scanning method showed that all specimens gave practically

Plate Number 15



Sandwich Treble Unit, Time Averaged, 15 KHz

Plate Number 16 (see also sketch page 163 e)



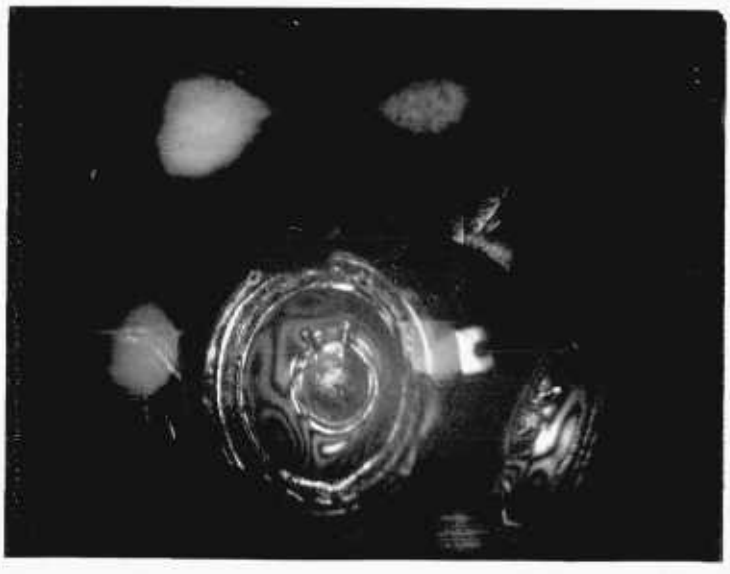
Sandwich Treble, 10 KHz, T.A. Sketch also given

Plate Number 17



Sandwich Treble Unit KHz Time Averaged

Plate Number 18 (see also sketch page 163 g)



Sandwich Treble, T.A. 12.5 KHz Sketch also given

perfect piston motion. The time average and scanning methods showed the surround behaving in a proper manner but there was just a slight trace of dust cap flexure.

From 3 KHz to 8 KHz - leaving out the fundamental cone resonance at 5 KHz - an increasing amount of cone rocking occurs otherwise the cone behaves reasonably well. The surround,however, shows resonances of its own which can have amplitudes many times greater than the amplitude of the cone. The rocking motion, which will aggravate spurious surround movements, occurs about an axis passing through the lead-in wires. These effects have a slightly smaller magnitude with the newer units.

From 9 KHz to 10 KHz with the new units and to 12 KHz with the old units, the cone breaks-up in a drastic and irregular manner. There is a greater rocking component with the newer units. Throughout this region the dust cap performs high amplitude gyrations and the surround has broken up into two distinct vibrating regions with a node between them - verifying the results of the investigations at the N.P.L.

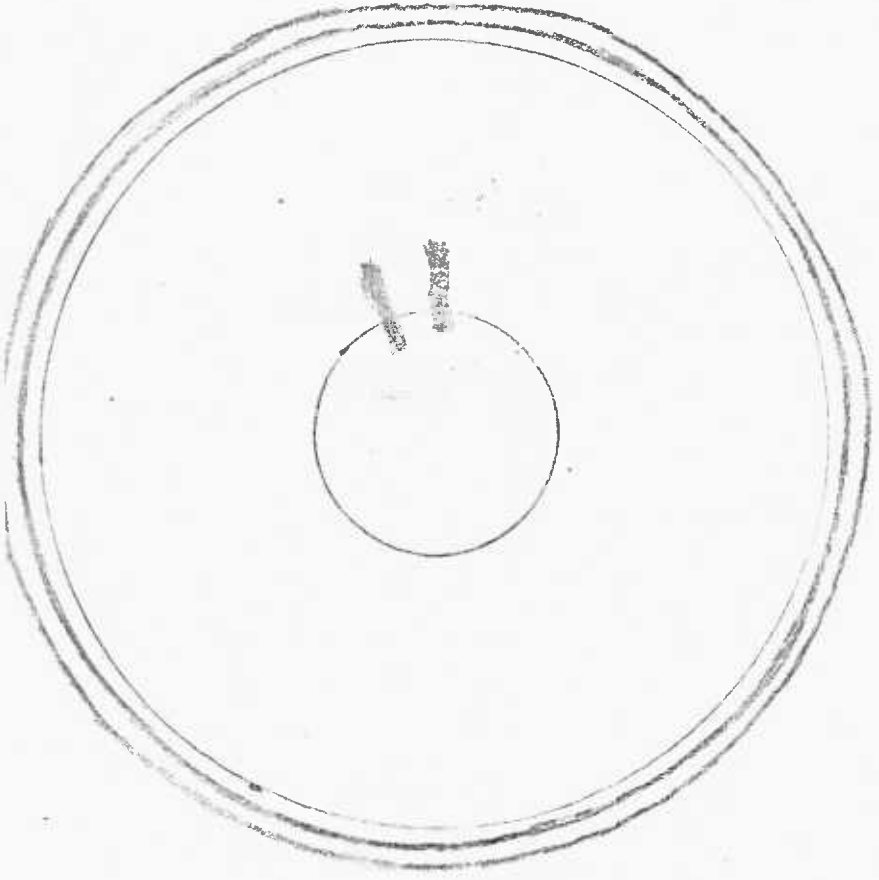
From 15 to 17 KHz both speakers display more disc-like behaviour, exhibiting a tendency towards a nodal circle nodal diameters system. To summarise the speaker behaves as a piston up to 2.5KHz where it begins to rock. At around 10 KHz both cone and surround behave irregularly but when 15 KHz the behaviour is more disc-like in character.

These results suggest a different arrangement of the lead-in wires i.e. passed out diametrically opposite to each other or taken directly to the chassis. Recent experiments show that the former arrangement largely prevents the rocking motions and the fundamental at 5 KHz is no longer excited.

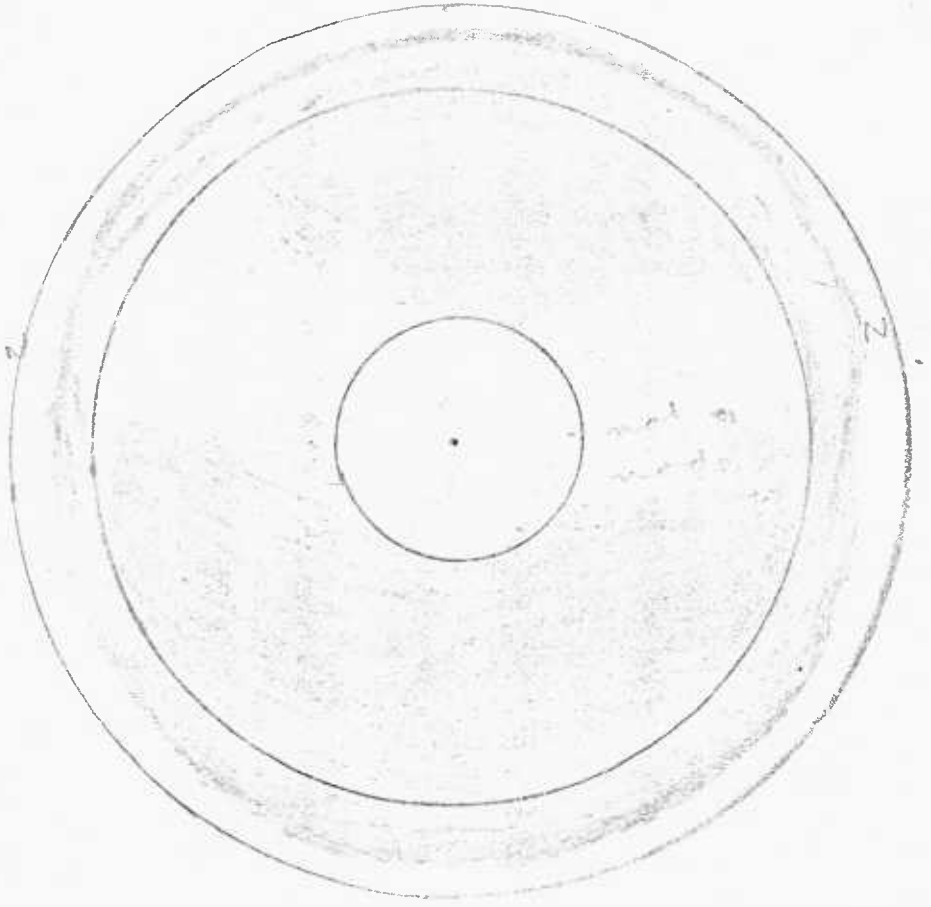
(iii) Relation between Modal Patterns and the Sound Energy Radiated

(See also Appendix II ). There is a phenomenon in acoustics known as the 'Coincidence Effect'. Above a certain frequency it is possible for the

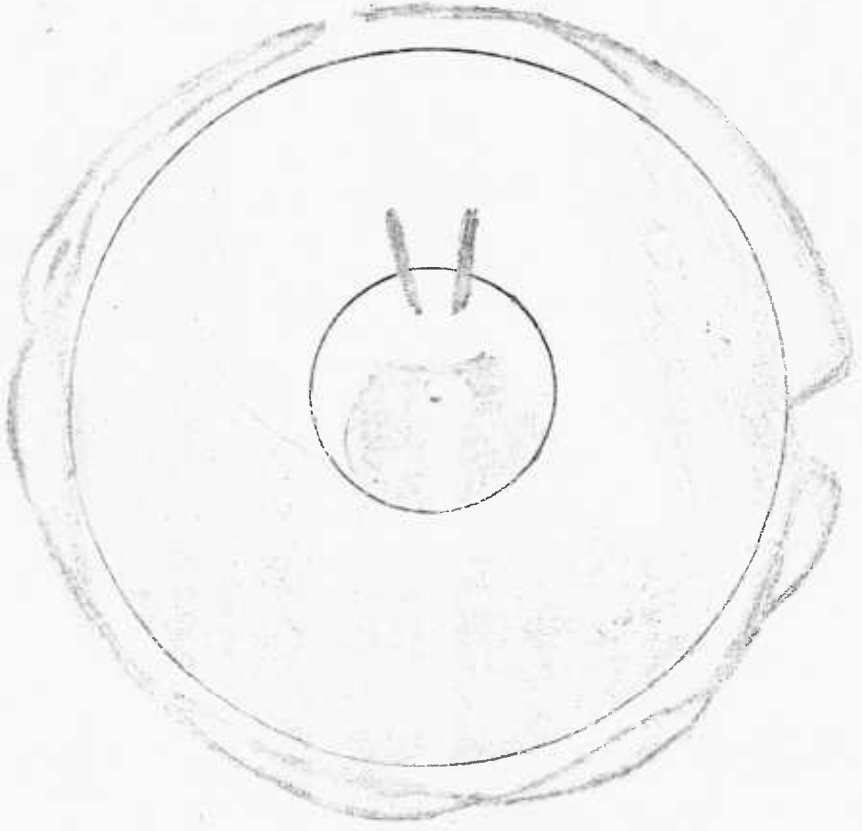
SPEAKER Sandwich Treble Unit (old) specimen no 1
HOLOGRAM 279 Also 326 (New) Specimen 3
RESONANCE None whatsoever
FREQUENCY 2 Khz (also at 2.5 KHz)
DETAILS Scanning method used
COMMENTS Perfect piston motion, surround behaves well also at this frequency and below it



SPEAKER Sandwich Treble Unit (old) specimen no 1
HOLOGRAM 284
RESONANCE
FREQUENCY 3.5 KHz
DETAILS Time averaged
COMMENTS First evidence of cone rocking otherwise good motion band across the middle is not a node.

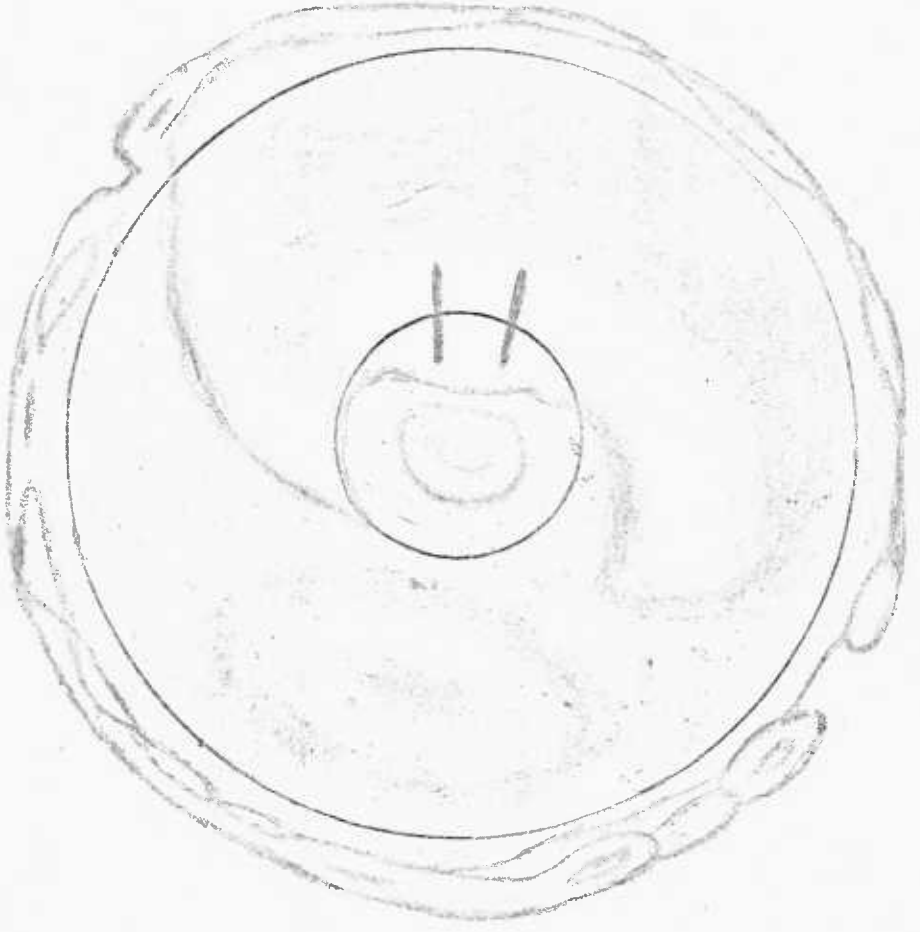


SPEAKER Sandwich Treble Unit (New) Specimen 2
HOLOGRAM 315
RESONANCE
FREQUENCY 7.5 KHz
DETAILS Time averaged
COMMENTS Rocking less pronounced



Results Figure 23 Sandwich Treble Unit

SPEAKER Sandwich Treble Unit (New) Specimen 2
HOLOGRAM 306
RESONANCE
FREQUENCY 8 KHz
DETAILS Time averaged
COMMENTS Rocking strongly present
Behaviour of surround better than Old Leak Treble unit.



SPEAKER Sandwich Treble Unit (Old) Specimen 1

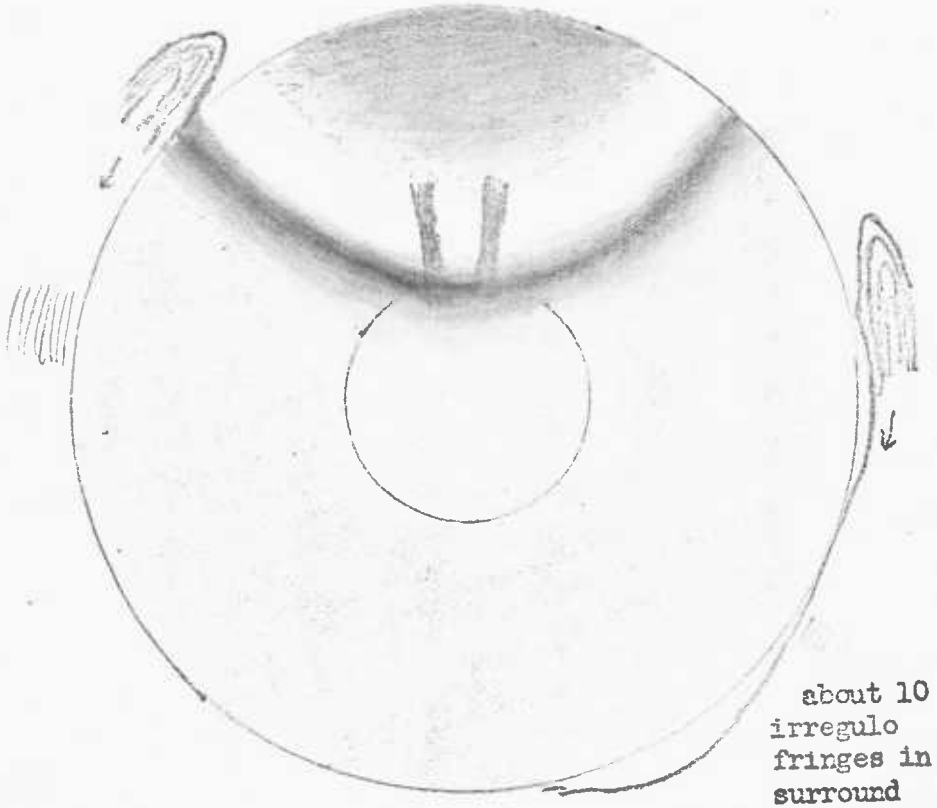
HOLOGRAM 286

RESONANCE

FREQUENCY 6 KHz

DETAILS Time averaged

COMMENTS Cone rocking clearly shown surround has peaks higher than cone movement.



about 10 irregulo fringes in surround

SPEAKER Sandwich Treble Unit (Old) Specimen 1

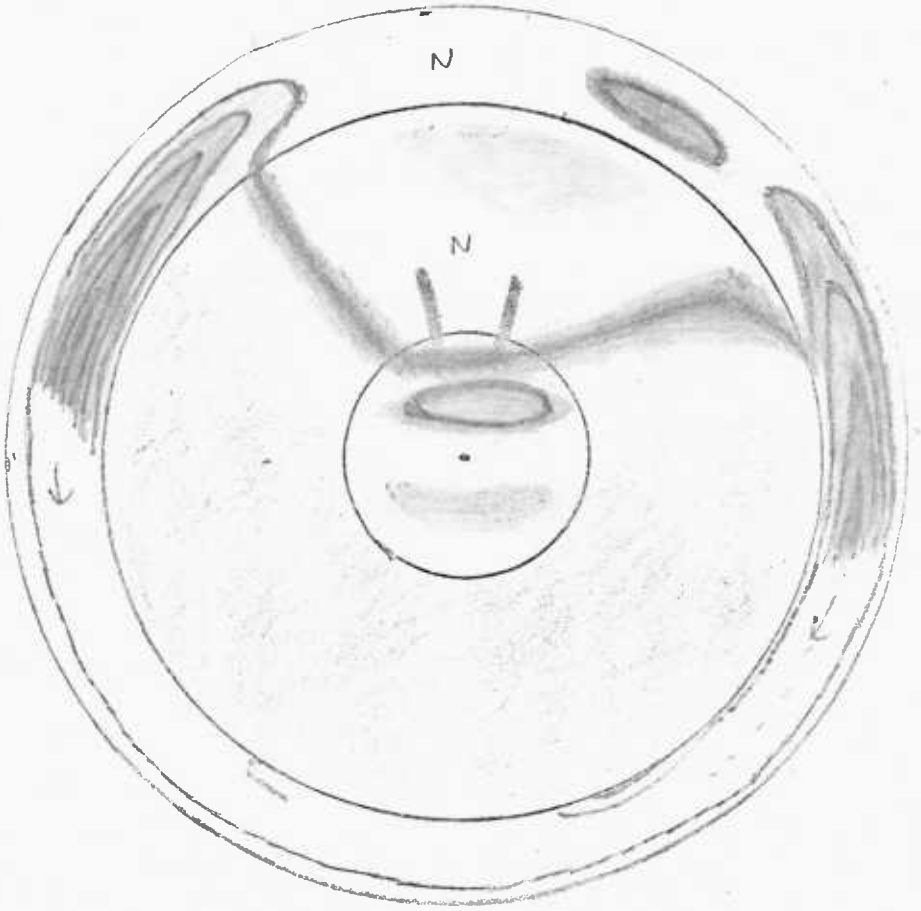
HOLOGRAM 296

RESONANCE

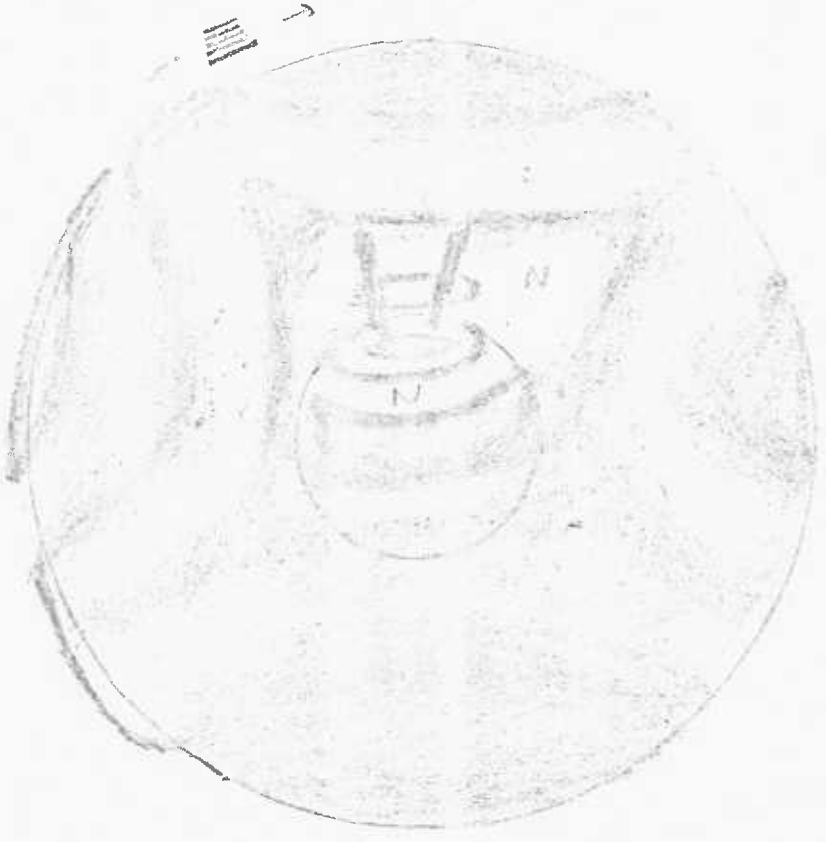
FREQUENCY 6.4 KHz

DETAILS Time averaged

COMMENTS Cone rocking shown clearly(larger effect at higher frequencies) Surround has its own peaks higher in amplitude than the cone movement.

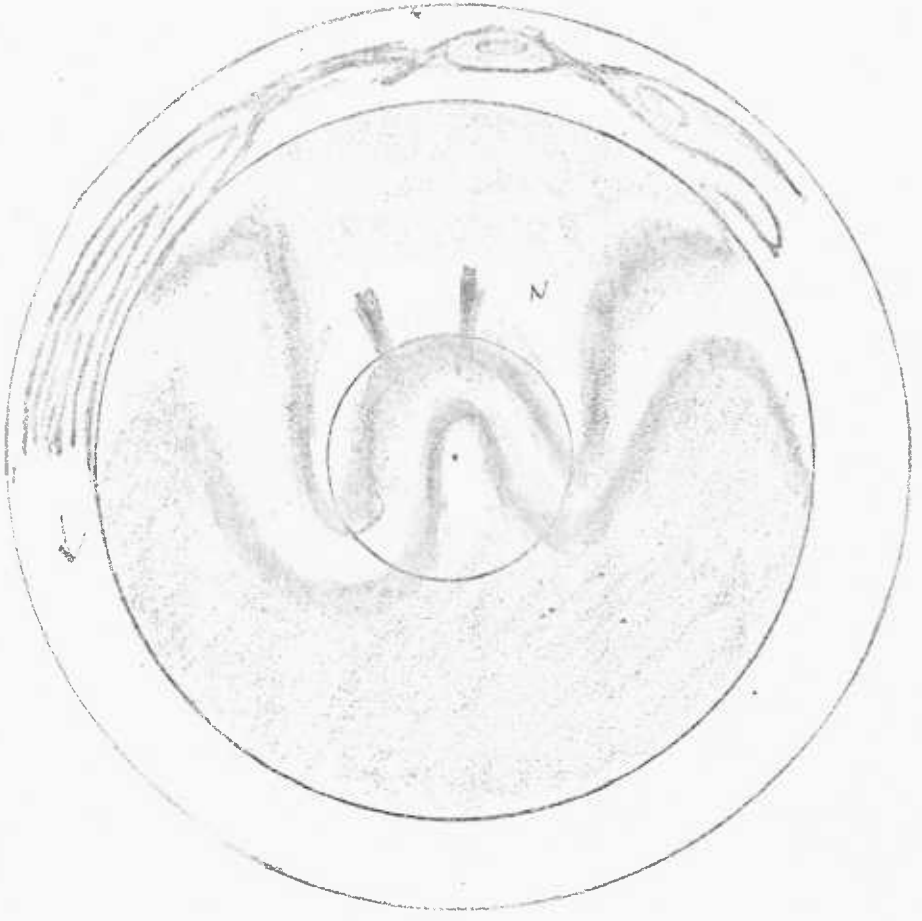


| | |
|---|---|
| SPEAKER | Sandwich Treble Unit (Old) Specimen 1 |
| HOLOGRAM | 293 |
| RESONANCE | Two nodal diameters - fundamental |
| FREQUENCY | 5 KHz |
| DETAILS | Time averaged |
| COMMENTS | Two clearly defined nodal diameters<br>Surround shows 5 fringes of piston motion and 2 of surround flap |

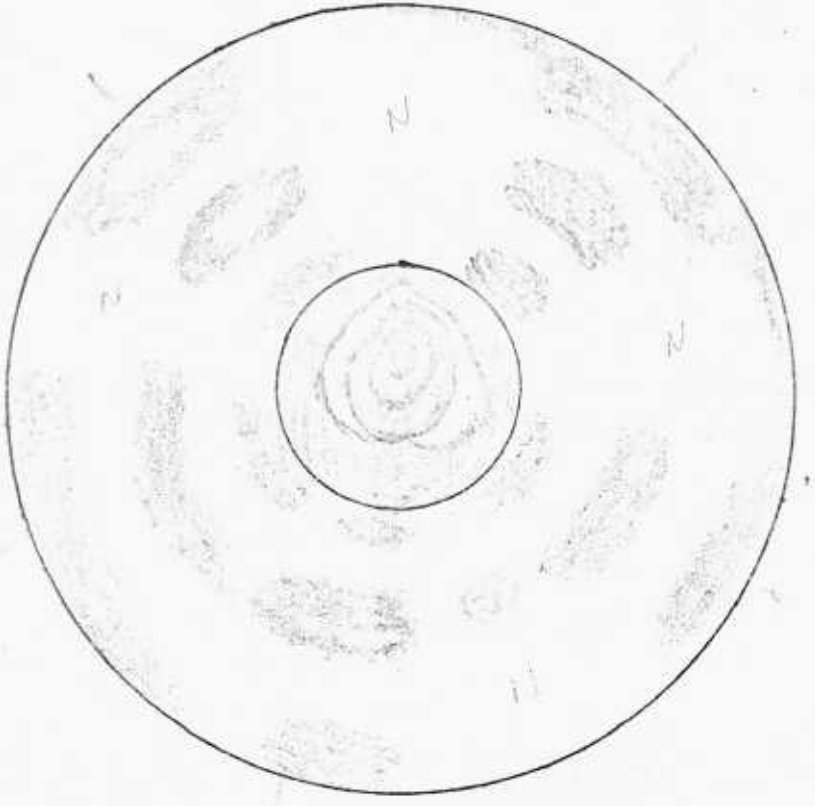


Results Figure 24 Sandwich Treble Unit

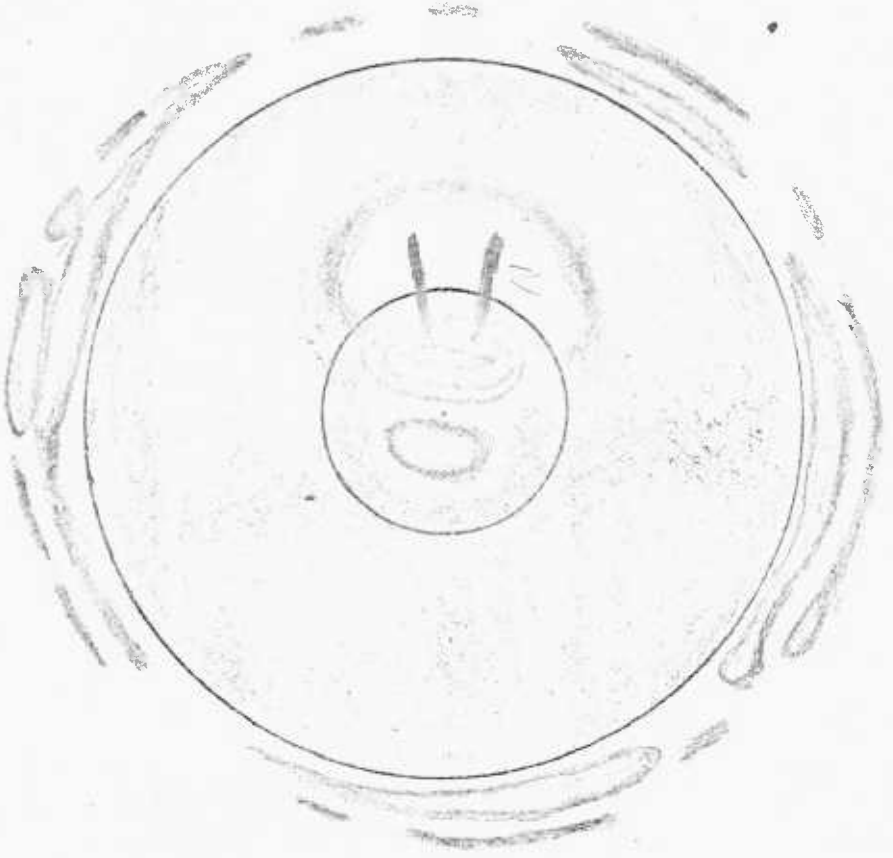
| | |
|---|---|
| SPEAKER | Sandwich Treble Unit (Old) Specimen 1 |
| HOLOGRAM | 300 |
| RESONANCE | |
| FREQUENCY | 8.1KHz dip |
| DETAILS | Time averaged |
| COMMENTS | Cone shows considerable rocking-effect of lead in wires is extreme .<br>Surround shows peaks in its own movement which are considerably higher than the piston motion of the cone. |



SPEAKER Sandwich Bass Unit with 5 Sandwich Stiffners
HOLOGRAM 349
RESONANCE
FREQUENCY 6.2 K Hz
DETAILS Time averaged
Comments The stiffners have an unusual effect in that most of the cone movement occurs underneath them at this frequency. Other parts of the cone are stationary



SPEAKER Sandwich Treble Unit (New) Specimen 2
HOLOGRAM 308
RESONANCE
FREQUENCY 12.4 KHz
DETAILS Time averaged
COMMENTS Behaviour of this unit is very much better than the old unit at this frequency



SPEAKER Sandwich Treble Unit (New) Specimen 2

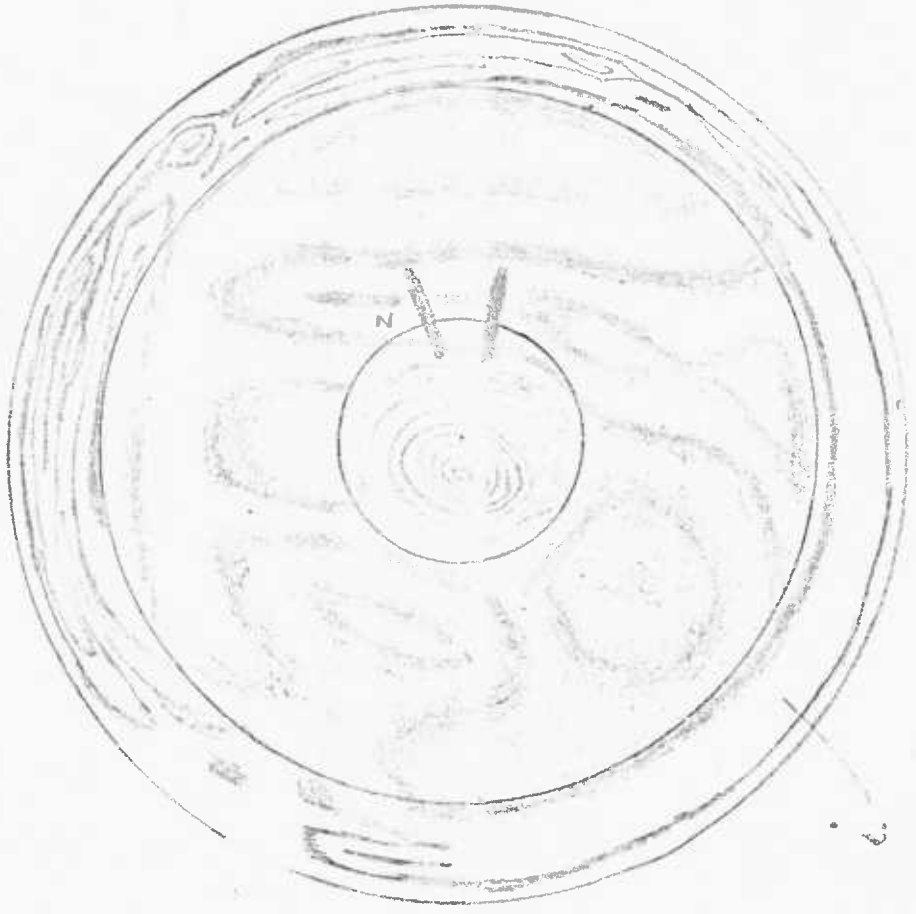
HOLOGRAM 313 and 314

RESONANCE

FREQUENCY 10.7K and 10.0 KHz

DETAILS Time averaged

COMMENTS Rocking is evident no definite modal pattern. (Photograph available of this reconstruction)



SPEAKER Sandwich Treble Unit (New) Specimen 2

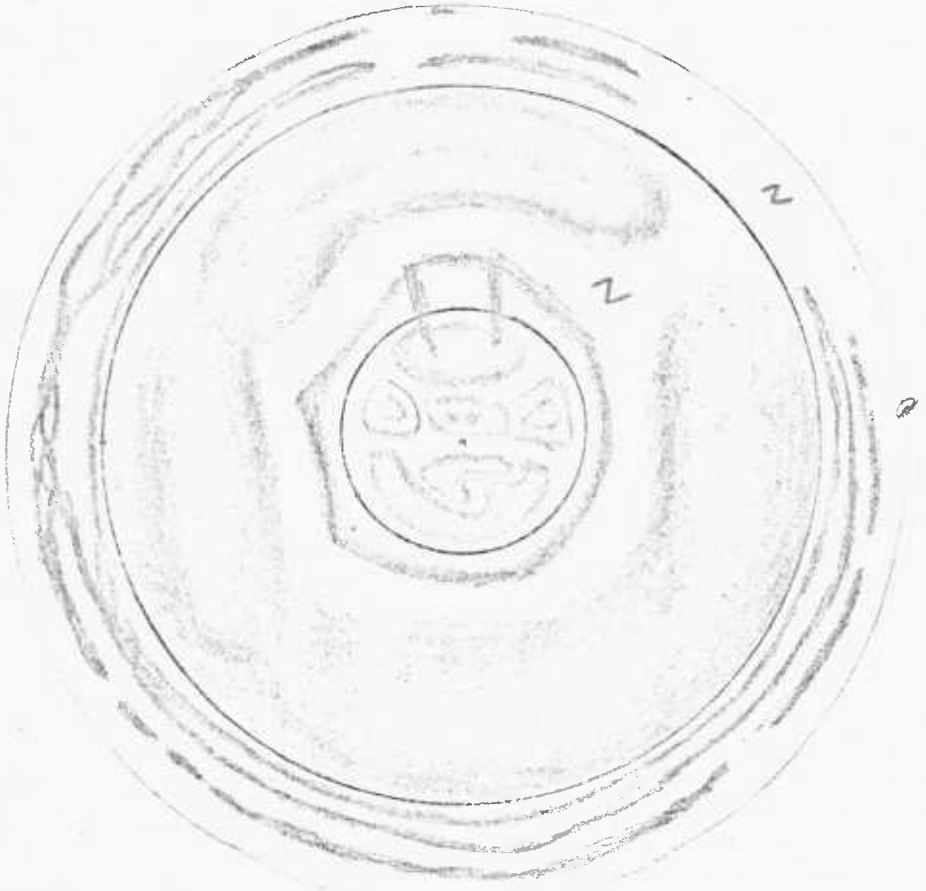
HOLOGRAM 310

RESONANCE one nodal circle

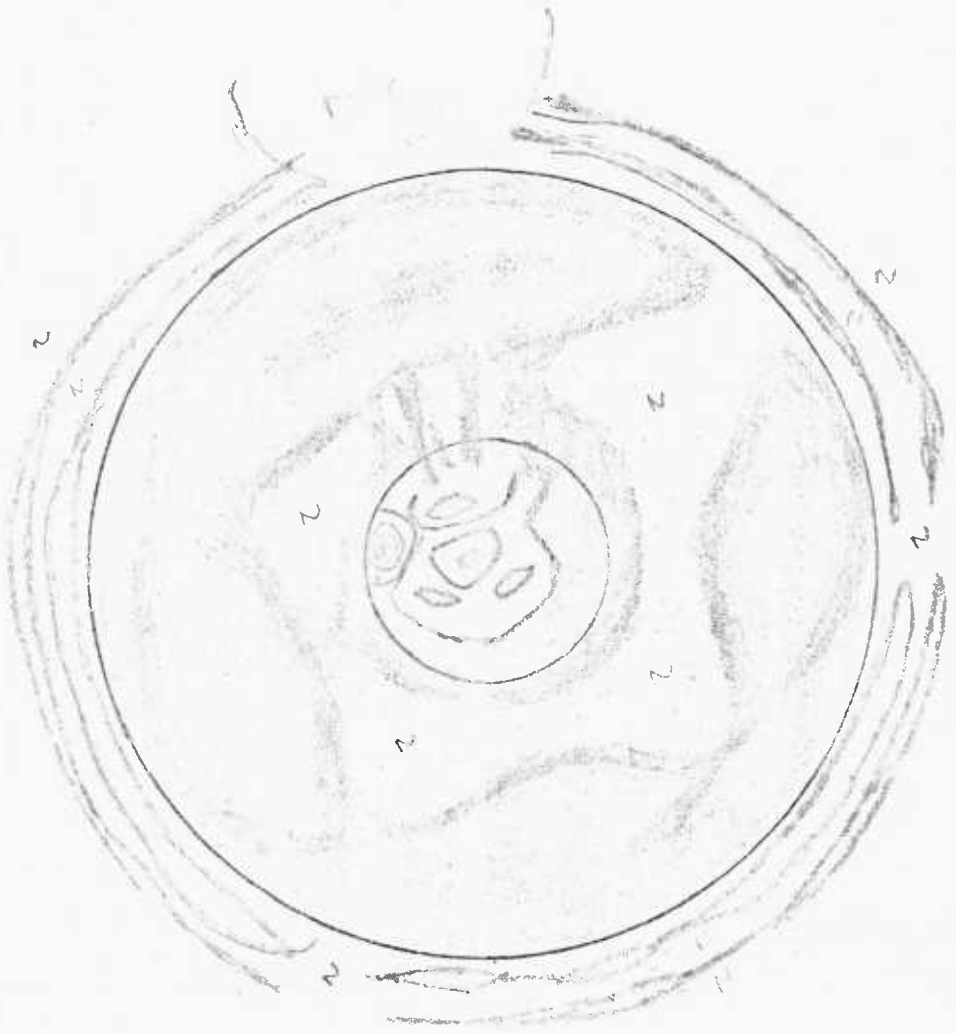
FREQUENCY 15.5 KHz

DETAILS Time averaged

COMMENTS The behaviour of the new unit is better defined than the old unit (holo 328 etc) less evidence of nodal diameters .



SPEAKER Sandwich Treble Unit (Old) Specimens 1 and 4
HOLOGRAM 328 ( Spec 4) 291 (Spec 1) 299 (Spec 1).
RESONANCE
FREQUENCY 15 Khz
DETAILS Time averaged
COMMENTS Surround has two nodes in it running completely round the speaker as well as a number of stationary areas



Results Figure 27 Sandwich Treble Unit

SPEAKER Sandwich Treble Unit (Old) Specimen 1
HOLOGRAM 297
Resonance
FREQUENCY 17 KHz
DETAILS Time averaged
COMMENTS Similar to behaviour at 15 K one extra nodal region has appeared in the cone



SPEAKER Sandwich Treble Unit (Old) Specimen 4
HOLOGRAM 327
RESONANCE
FREQUENCY 9.1 KHz
DETAILS Time averaged
COMMENTS All specimens of this unit show erratic behaviour from 9 Khz to 11 KHz though the new vertion is always noticeably better



Results Figure 28 Sandwich Treble Unit

SPEAKER Sandwich Treble Unit (Old) Specimen 1
HOLOGRAM 290
RESONANCE
FREQUENCY 12.5 K (10KHz very similar)
DETAILS Time averaged
COMMENTS Representative drawing only
Surround shows many fringes having a nodal pattern of its own.
No regular modal pattern shown here



bending wave in a panel to coincide both in wavelength and frequency with the projected wavelength of an incident sound wave, provided its angle of incidence is correct. There is a lower limit to this effect known as the coincidence critical frequency ($f_c$) which corresponds to grazing incidence for the air wave. Above $f_c$ each mode segment, which is made up of two standing bending waves, is able to radiate independently since its component bending waves can couple well to the air at certain angles of radiation. Below $f_c$ , however, they cannot couple well in this way, and in fact neighbouring mode segments, which are out of phase with each other, can cancel out in the near field - therefore below $f_c$ a given panel will radiate much less energy for a given amplitude of vibration. Indeed according to Beranek (1959), below $f_c$ the radiated sound may be 20 db less than that above it for the same amplitude of movement when considering a flat plate. Theoretical expressions for the sound radiated by a rectangular plate above and below $f_c$ have been given by M.J.Croker (see appendix III ) Below $f_c$ only uncancelled volume velocities at the edges of panels or those caused by stiffeners or by mode segments with unequal amplitudes give rise to sound radiation. Above $f_c$ each mode radiates as a whole and will therefore cause a large peak in the response curve.

Putting it another way: below $f_c$ the bending wavelength corresponding to the modes in the plate (which are a standing bending wave phenomenon) is greater than any possible wavelength in air and so the radiation cancels out in the near field (with the possible exception of the umbrella mode which has no regions with which to cancel. Above $f_c$ the wavelength of the bending waves which go to make up a given mode is equal to a projected wavelength of sound in air , so that the mode will radiate as a whole with perhaps preferred directions of radiation - a suggestion which should be investigated in future.

It is interesting to work out some of the coincidence critical frequencies for plates made of materials currently used to make Loudspeaker cones. These come out as follows:

Paper Cones - approximately 200 KHz i.e. ultrasonic

Sandwich Treble - 4.5 KHz

Sandwich Bass - 1.6 KHz

This means that the break-up modes of the ideal loudspeaker with a paper cone would cancel themselves out - but only if the paper cone were entirely homogeneous with no regions stiffer than the others and if it were terminated with an ideal surround also. In fact they are far from ideal and both radiation and conversion between various types of wave travelling in the cone occurs at the regions of greater stiffness.

When we consider sandwich speakers, however, the situation is more interesting not only because the cones are more homogeneous but also because the critical frequency falls inside the working band. For instance the bass cone critical frequency occurs just above the umbrella mode and just below the first serious break-up mode which has a very large effect on the response curve. This serious effect may not be due entirely to a possible high 'Q' but more probably to the fact that the whole cone mode will radiate without cancellation. As listed in (4.7 i) above this suggests that by reducing the stiffness slightly a better Loudspeaker may be produced. The increased number of resonances then lying in the working frequency band would be less effective radiators since they would be below $f_c$ hence giving a smoother response curve.

Another approach suggested by the 'well behaved' nodal circle modes found in sandwich speakers is to place damping material at an antinode. There are two antinodes common to all the nodal circle modes - the circumpherence and the voice coil. Placing a plasticine 'lumped damper' at the voice coil in the form of a 'bung' and suitably shaping it to avoid diffraction and wavelength cancellation effects completely removed the high 'Q' 12 db peak at 2.5 KHz and greatly decreased the effect of the other nodal circle resonances (Fig 49 ).A weighting ring placed at the same radius merely lowers the frequency of this first peak and overall

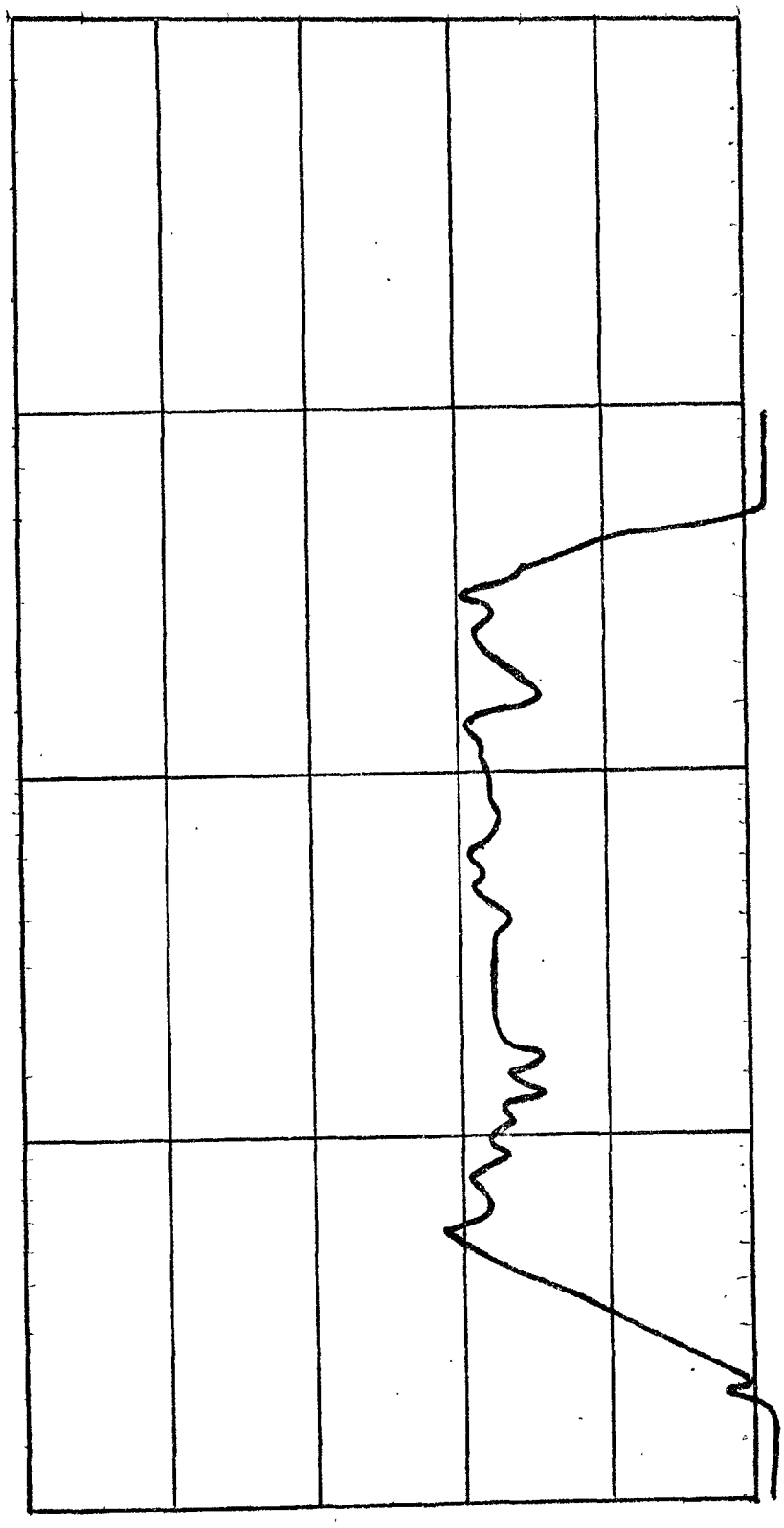


Figure 49 Sandwich Bass unit with 40 gm 'lossy bung' effect of resonances on response curve almost completely removed. Cone mass 40 gm

damping of the cone is in fact very difficult because of its great flexural stiffness. Layers of commercial damping materials placed at the voice coil also give greatly improved results. This is a very clear example of how holography has given information about the vibrations of a loudspeaker cone which in turn has lead to an effective treatment resulting in a better Loudspeaker.

4.8) Conclusions

(i) On Mid-Range Paper Cone Loudspeakers

The holographic investigations detailed in (4.6) above have brought to light the following points:

(a) Mid-range units should have included cone angles of around 90° and should have a slight radius - there is probably an optimum for both

(b) Cones should be highly 'doped' - a compromise must be reached between magnet size and the amount of dope used.

(c) The lead-in wires should either pass through the cone on opposite sides of the cone, or go directly to terminals on the chassis without passing through the cone.

(d) Rubber surrounds are better than felt between 1 KHz and 3 KHz.

(e) Larger amplitudes of movement and smaller cone sizes seem to give the best results.

(ii) On Sandwich Bass and Treble Loudspeakers

(a) Bass units break-up only in nodal circle modes.

(b) The effect of these modes on the response curve may be minimised by the use of a lumped damper situated at the antinode common to all axisymmetric modes - the voice coil.

(c) The coincidence critical frequency ($f_c$) may well be a factor of importance in the understanding of sandwich speaker response curves.

(d) Lead-in wires have a large effect on Treble units which may be minimised by their redeployment.

(e) Improved Treble units can give almost perfect piston motion up to about 8 KHz - however piston motion is not the only criterion of excellence which must be satisfied by a good speaker.

(iii) General Conclusions Section IV

(a) Holography is a very useful and effective tool which can help in the design of improved loudspeakers.

(b) Loudspeaker break-up fringe systems can be classified into distinct categories - some of which indicate more serious defects than others

(c) Several new scanning systems have been specially developed and may be used to advantage for the study of Loudspeaker cone break-up phenomena.

(d) Subharmonics may now be studied holographically-both in conjunction with and separate from the fundamental vibration.

(e) The interpretation of break-up fringe systems must be carried out bearing in mind that below the coincidence critical frequency ($f_c$) the radiation from many of the mode segments mapped by the fringes will cancel out in the near field - a situation which always applies with paper cones but applies to only half of the working region of sandwich cones.

4.9) Suggestions for Further Work

(i) On Mid-Range Paper Cones

Virtually every speaker tested has given pointers to further work. The best and worst speakers should be tested at higher and lower frequencies. This may shed further holographic light on the nodal structure operating

in the standard and similar cones and thence indicate treatments to more effectively damp these modes. Different kinds and combinations of cone and surround must be tried, notably the rubber surround with a smaller size of cone. There is obviously a great deal of holographic work remaining in the study of the many different kinds of Loudspeaker (both in free space and in their cabinets) on the commercial market, and in the correlation of fringe systems with subjectively 'good' loudspeakers.

(ii) On Sandwich Units

A series of experiments to determine the optimum cone angle should be undertaken - perhaps in conjunction with an investigation into the influence of the coincidence critical frequency on the radiation efficiency of cone modes. Other arrangements of the lead-in wires should be tried with the treble units which should also be holographically investigated fitted with surrounds of differing construction.

(iii) On General Topics

(a) The method of SSII should be investigated more fully both experimentally and mathematically when it is possible that effects similar to the 'blanking fringes' of SSI may be discovered.

(b) Other scanning regimes must be considered and thought given to the development of a scanning system to show (super)harmonics only.

(c) The method of SSIII may be used to gain knowledge of the factors affecting the generation of subharmonics in vibrating structures.

(d) Structures related to loudspeakers i.e. cabinets voice coils etc. should be holographically investigated.

N.B. Experiments on Gear-Like Plates

Conclusions relating to the experiments on gear-like plates can be found on page (115).

# APPENDIX (I)

## OTHER METHODS OF MODE VISUALISATION

CONTENTS - Appendix 1 - Other Methods of Mode Visualisation


| | | |
|---|---|---|
| Introduction | | 170 |
| A I.1) | General Methods | 170 |
| | (a) Strain Gauges | 170 |
| | (b) Fibre Optics | 171 |
| | (c) Schlieren | 172 |
| | (d) Multiple Beam Interferometry | 172 |
| | (e) Lycopodium Powder | 173 |
| | (f) Photoelastic Coatings | 173 |
| | (g) Stroboscopically | 174 |
| | (h) Moire Fringes | 175 |
| A I.2) | Methods Utilising a Laser | 177 |
| (i) | Speckle Patterns | 178 |
| (ii) | Laser Scanning | 183 |


Total Number of Pages: 24

## OTHER METHODS OF MODE VISUALISATION

### Introduction

This appendix briefly describes some of the methods of mode visualisation considered before the method of holographic interferometry was finally chosen for use in the experiments described above. Their advantages and disadvantages are compared and it is pointed out that some techniques, eg speckle correlation interferometry and laser scanning may have advantages over holographic interferometry for some applications.
The methods considered were:

(a) The use of Strain gauges.

(b) Optical methods using fibre optic devices.

(c) The Schlieren method.

(d) Multiple beam interferometry.

(e) The use of lycopodium and other light powders.

(f) The utilisation of photoelastic coatings.

(g) Direct stroboscopic illumination - both unaided using a discharge lamp such as the 'strobokin' but also combined with other techniques.

(h) The moire fringe method in one of its many forms.

(i) The use of laser speckle patterns.

(j) Laser scanning mehtods.

These methods are now described in more detail.

### (a) Strain Gauges

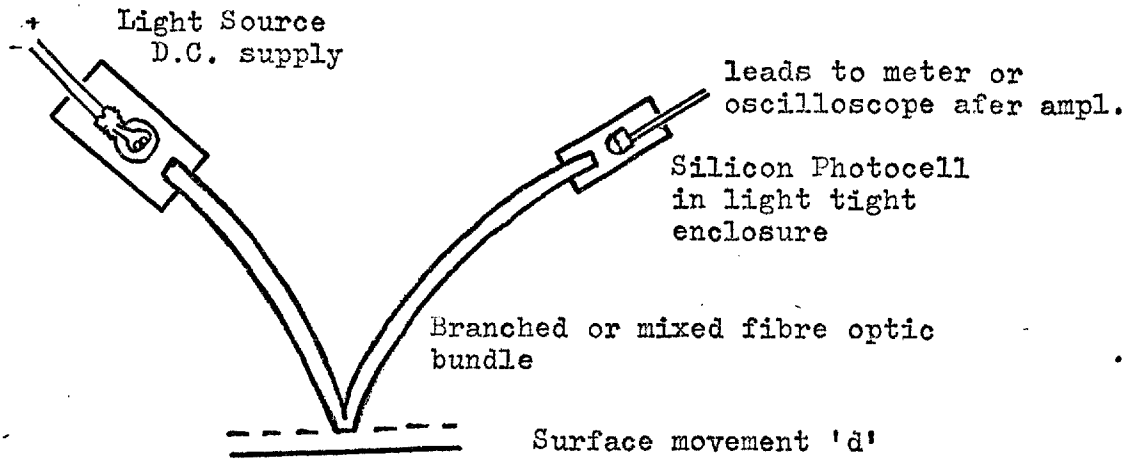
Strain gauges placed at suitable intervals over the surface of the object could yield information about the varying stresses over its surface. This method is , however, cumbersome, highly localised , not very sensitive and in the case of light objects like loudspeaker cones would unduely affect the vibrations themselves and so this method was not used.

(b) Optical Methods Using Fibre Optics and Optical Scanning Methods

A non-coherent optical scanning method has been described by Yorke (1961) This self correcting scanning device has been used to study vibrations of the whole cone when break-up resonances were detected at around 250 Hz with a paper cone. This device with all its correcting servo-systems is extremely complicated and has frequency and sensitivity limitations which preclude its use in these experiments.

The advent of fibre-optics has allowed the development of a similar kind of non-coherent movement sensor which may be much more easily scanned across the Loudspeaker cone but which shares some of the complications of Yorke's method. The relative lack of sensitivity - maximum about 1 micron - may be an advantage in some applications, for instance when dealing with bass speaker vibrations, but the necessity to maintain the sensing head at a precise distance from the cone while the scanning is carried out prevents the use of this method also.

In one scheme for fibre optical distance measurement two randomly interlaced bundles of optical fibres are used, one bundle conducts a high intensity light beam onto the necessarily reflecting object surface, tthe other bundle directs reflected light onto a photocell. A micrometer head may be used to produce the callibration curve shown (Fig 50 ), the shallow part of the curve may be used for high amplitude vibrations and the steep parts for vibrations of small amplitude. Sensitivity may be increased and fibre-object spacing decreased by reducing the diameters of the fibres. In another arrangement (Tourret 1971) the light is directed down a central bundle and picked up by an outer annulus of fibres. In this case the sensitivity is reduced but large measuring ranges may be achieved (30 microns to several millimeters. Variations in the reflectivity of the surface also alters the output of the devices but a second transducer working as a reflectometer may be used to obviate this effect.



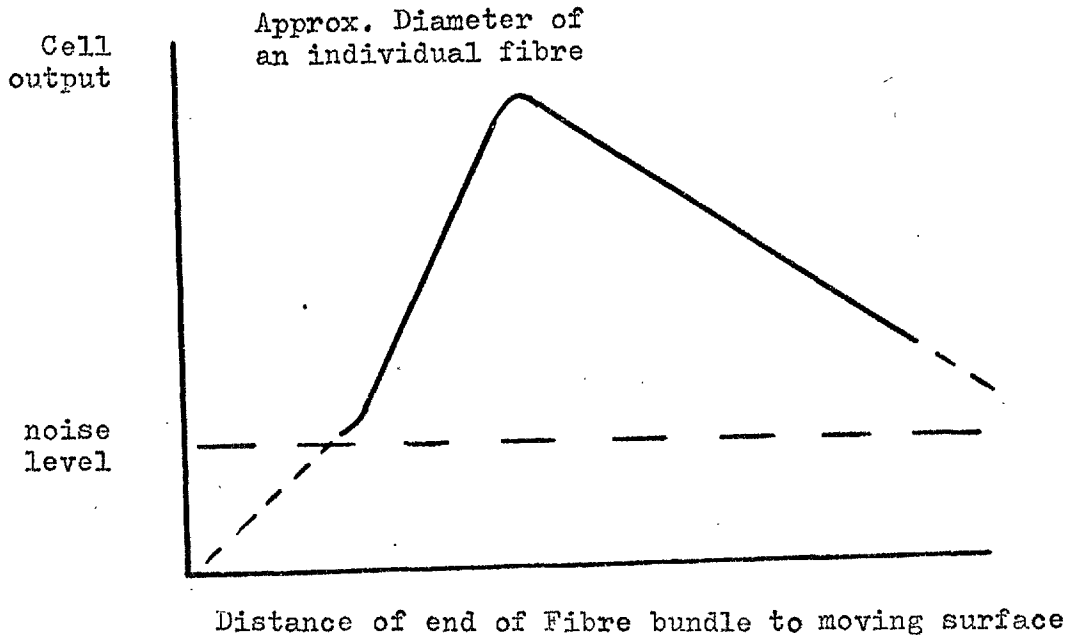



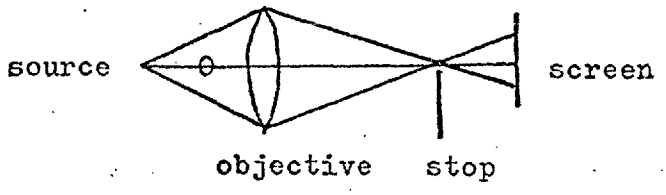

Figure 50 Use of Fibre Optics in vibration measurement

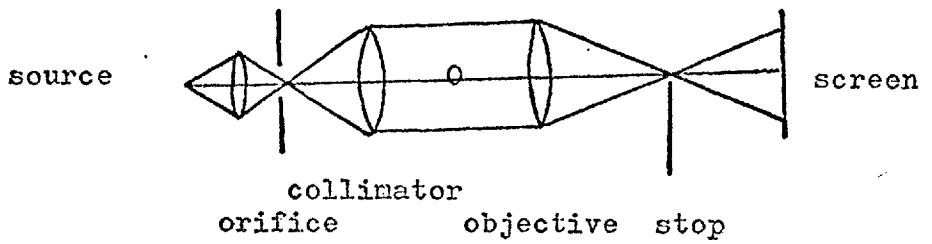
(c) The Schlieren Method

This method can only be used with transparent plates and shows up variations in density caused by the passage of stress waves. There are several different experimental layouts in use, but basically the system is as follows: Light from a point source illuminates the medium under study (Fig 51 ) the light is brought to a focus at the stop by an objective lens, the function of this stop is to block the transmission of light to the viewing screen. If the light strikes an inhomogeneity in the medium 'D' the ray is refracted by an angle that depends on the gradient of the refractive index along the path of the ray and it is not then focussed in its normal position in the plane of the stop. If the ray is refracted upwards the knife edge does not cut it off, however if it is refracted downwards it is completely cut off. In practice the edge is adjusted to eliminate most of the light and the resulting sparsely illuminated area displays variations of light intensity that reproduce the pattern of the inhomogeneities in the medium.

(d) Multiple Beam Interferometry - Flatness Interferometry

This technique can be utilised to observe the vibrations on the surface of a plate and also the system can be set up to observe effects within a plate. The vibrating surface is matched against an optical flat and the resulting fizeau fringes, vibrating with the plate reveal the positions of the surface nodes. The system is described in detail by Tolansky and Wood (1958). With the two optical surfaces slightly inclined and illuminated with monochromatic light, sharp straight parallel multiple beam Fizeau fringes are produced. If the lower surface is vibrating, where the top surface is at rest the fringes remain sharp and narrow, but where the surface undergoes a normal displacement, the fringes broaden. The resulting modal pattern can then be photographed. When the interference takes place between light beams reflected from the two coated surfaces of the test




O = material under investigation

Figure 51 The Schlieren Method

plate the changes in the fringes caused by vibration are due to combined changes in the thickness of the plate and in the refractive index (assuming a transparent plate). The Optical Metrology Division of the N.P.L. has improved the use of the Fizeau Interferometer for measuring the flatness of plates, and a photoelectric method has been developed to measure up to 1/100th of a fringe, equivalnet to $10^{-7}$inches (Drew 1964,1966).

(e) Lycopodium or Other Powders

This method has been used by many workers in the field - notably Chladni himself and also by Mary Waller (1961) who used 'bomb dust'. Some powders have a tendency to collect at the nodal regions of a vibrating plate and thus show up the modal pattern, others have been known to collect in the antinodal regions. The method of powder collection is not the most sensitive of methods however since it gives no information about local amplitude variations and may only be used if the objects are in a horizontal position, so this method was not chosen for the present experiments.

(f) Photoelastic Coatings

Many transparent materials are not naturally doubly refracting in an unstressed state, but become so under the influence of stress. This phenomenon is called stress birefringence. The magnitude of the optical effect produced by the stress is usually a direct linear function of the stress magnitude. The method was developed into a practical technique by Coker and Filon of University College,London . When polarised light passes through a transparent substance that exhibits sstress birefringence, it is split into two orthogonally polarised components, each parallel to a direction of principal stress. These components propagate through the material at different velocities. For monochromatic light the velocities are proportional to the magnitude of the principal stress lying in the plane of the vibration. Thus on emergence the two components will have

suffered a relative change of phase proportional to the difference in in velocities multiplied by the thickness. If the emergent light is viewed through a polariser crossed with the original polariser only one component of the two rays is seen. When the relative retardation is such that the two components are vibrating in phase, a dark fringe is seen for every point in the photoelastic structure which has a similar value of principal stress difference.

Other conditions enable the directions of the principal stresses at every point on the structure to be determined. Coloured fringes can also be produced giving information which enables the magnitudes of the principal stresses to be determined as well. High speed variations may be followed and shock waves studied with the aid of high speed cameras, but the method is relatively insensitive, models have to be made or coatings applied which will affect the object vibrations, and the method is complicated to set up and interpret so it was not chosen.

(g) Stroboscopically

This method is not usually applicable unaided but may well be a useful addition to many of the other methods described above and below and of course it has been used in the present experiments in conjunction with holography. By using light flashes of as short a duration as possible at a repition rate set to be the same or a submultiple of the object or phenomenon to be studied, motion can be frozen, at that frequency, at any stage during a cycle (Rutkowski 1960). If a plate were moving with a very large amplitude and the strobe frequency were set to be very slightly different to that of the object then it would be seen to trace cycles of the oscillation slowly and information about its movement may be gained. This method is especially applicable to the study of the low frequency motion of bass Loudspeakers where the motions involved are relatively large. The stroboscopic technique may also be sometimes used to pick out

motions at a particular frequency from a composite motion of several frequencies. The passage of a stress wave through a bar of photoelastic material may be seen by 'strobing' it at a suitable frequency and by using a high speed camera synchronised with the strobe flashes. Sometimes the method of high speed photography (Reid 1967) may also be applied unaided and whole cycles of a continuous vibration or alternatively an impulsive non-repetitive even may be studied directly with the aid of high speed photography (Dally and Thau 1967). However when the size of the vibrations or photoelastic distortions are very small, these events may still not be capable of study in this way, though a microscope may sometimes help. When used in the ways described above or more often in conjunction with other methods, the strobe technique allows information to be obtained which may not be easily obtained of continuous light were used.

(h) The Moire Fringe Method

There are many different ways to use the phenomenon of moire fringes (named after the patterns seen in moire silk) to enable us to visualise vibrations or static distortions. In its simplest form, used for detecting the flatness of an object surface, a grating is simply layed on the surface and illuminated with a parallel beam of light. The grating throws a shadow onto the surface and moire fringes are seen between the grating and the reflection of the shadow of its rulings which indicate the points on the surface departing from the flat. By giving the underside a deliberate tilt moire fringes at right angles to the grating rulings may be formed which could be used to detect vibration in much the same way as that described under multiple beam interferometry above.

The simplest really practical way to observe moire fringes is that described by Ligtenberg (1955) which compares two reflections of a single diffraction grating in the polished flat surface of the object (this is immediately seen to be a disadvantage of the system). The reflection is

first photographed with the object stationary and then again (or doubly exposed) with the object moving. Moire fringes can be obtained between the two exposed prints and the motion deduced from these fringes, which are broadened in the antinodal regions (Oster et al 1964, Nickola 1966, Theocaris 1967,1969).

A more complicated system which is more versatile has been described by Theocaris. Fig ( 53 ) shows a section of the plate P, reference grating $g_1$ and the second grating $g_2$. A parallel beam of monochromatic light obliquely incident at an angle $\theta$ to the surface of the plate is reflected on the polished surface of the plate and passes through the lens $L_2$ which forms an image of $g_1$ on the screen S at unit magnification. Also placed at the screen S is the second grating $g_2$ where moire fringes are produced by interference between the image of $g_1$ and $g_2$ itself. If the plate is undistorted and the second grating is in its correct position no fringes are produced , or more accurately - the initial moire pattern shows the irregularities of the plate.

If $g_2$ is displaced from its original position, a number of equidistant fringes parallel to the lines of the grating will appear, these facilitate the determination of the nodal and antinodal regions of the test plate. With the plate flexed a ray parallel to the axis of the system will be deviated through an angle $2\phi$ where $\phi$ is the angle of rotation at the point where the ray strikes the plate. The deviated rays of the reflected beam interfere with $g_2$ and produce the moire pattern which shows up the partial slope contours of the plate.

The pitch p of the two gratings as well as the distance'a' and the angle $\theta$ all influence the sensitivity of the method. If $\Delta u$ is the local shift of the image of $g_1$ due to the vibrating plate which is deformed at the point P where the ray being considered strikes it, and is deflected through an angle $\Delta\phi$ then this shift is given by:

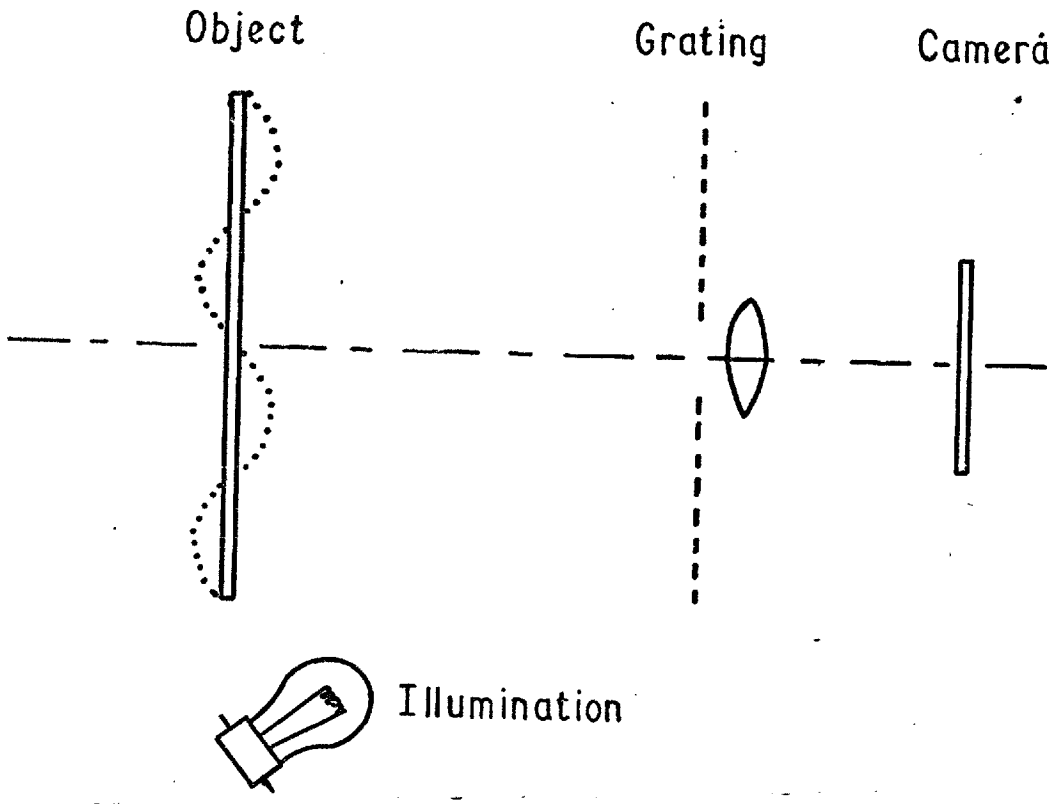



Figure 52 Moire Fringe Technique of Ligtenberg

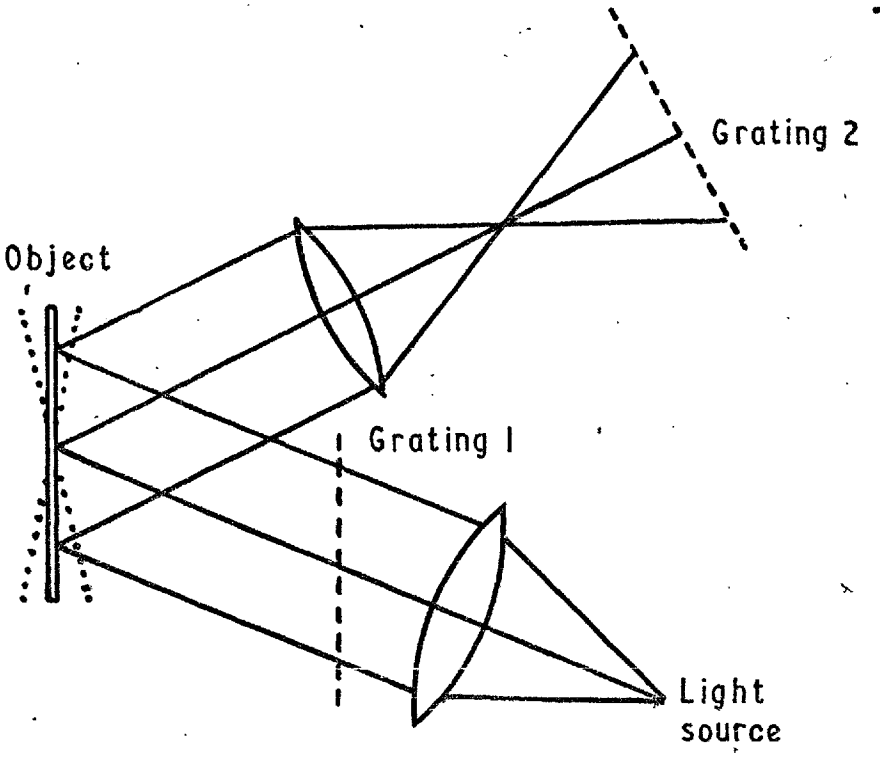



Figure 53 Moire Fringe Technique of Theocaris

$$\Delta u = \frac{2a\,\Delta\phi}{\cos^2\theta}$$

For example with a grating of 8 lines per millimeter $\theta = 10^{\circ}$ and $a = 160$cms and assuming that fringes can be located to within 1/15 of a fringe this gives a sensitivity of $2.5 \times 10^{-5}$ rad. per fringe.

Using continuous light clear pictures of the vibrating nodes of the plate may be obtained, but these pictures give no information about the amplitudes of the localised vibrations on the surface of the plate. By strobing the plate it is possible to see the moire fringes corresponding to, say the maximum amplitude of vibration.

Though this method can be made very sens itive with the use of fine gratings large spacings etc. it has many attendant experimental difficulties,and the interpretation of the results obtained is difficult because fringes only give information about changes in the slope of the object surface. Therefore though it was tried initially it was abandoned in favour of Holographic Interferometry.

Methods Utilising a Laser (excluding holography)

The following methods do not directly rely on holography (which was chosen for the present experiments) but all use a laser and some property of coherent light to render movement and vibration visible and measurable. Some were considered because they give less confusing information about a particular experimental situation and therefore may possibly allow results to be achieved more quickly; others because they allow in-plane movements to be studied and finally others, though more complicated to set up experimentally, may be used to provide increased sensitivity should this become necessary. The sensitivity of the basic holographic methods described in Section II were however of the correct order of magnitude for the present experiments except where very high or very low frequencies were to be studied with their respective low and high amplitudes of movement.

(i) The Use of Speckle Patterns

A surface illuminated with coherent light and viewed through a limited aperture such as the eye pupil, exhibits a mottled or speckled appearence and the reason for this has been described by Leendertz (1970)(amoungts others). When a non-speckular surface is illuminated with coherent light the phases of the contributions to the total amplitude reflected from neighbouring scattering centers are not independent. Light from each center can be received over a wide viewing angle and over this angle contributions arrive having phases from 0 to $2\pi$. When the summation is confined to that light emitted within a small solid angle such as that subtended by the eye pupil or camera aperture, discrete maxima and minima arise. The speckle size increases as the viewing angle is reduced and fewer random phase contributions are added to the total amplitude.

Any speckle pattern contains information about the incident light wavefront; the position of the scatterer relative to the source and the observer, and the scattering properties of the illuminated surface. A wide variation in any of these three properties causes the speckle pattern to change and this change may be measured by comparison with a pattern recorded earlier, or utilising persistence of vision when directly observing the vibrating objects.

If an object vibrating with an amplitude of more than a few wavelengths of light is illuminated by dispersed laser light, the laser speckle pattern will be blurred at the antinodes and it may be seen only at the nodal regions (Eliasson and Mottier 1970), the patterns are thus analogous to the chladni sand patterns of Waller (1961). The sensitivity of the method may be altered within limits by changing the geometrical parameters of the experimental system (see the method of Groh below). If the vibration amplitude is lower than that required to blurr the speckle pattern Fernelius and Tome have suggested (1971) that an object having a moderately rough surface produces a pattern in the antinodal regions which

has more dark areas interspersed with brighter light areas than the pattern seen in the nodal regions. This pattern is thus complimentary to most Chladni patterns (most powders collect at nodes though a few powders will collect at the antinodes). Butters and Leendertz (1971) describe how variations in the number of speckles per unit area can be converted to intensity variations using spatial frequency filtering in the Fourier plane They also extend the technique, adapting it for use with video processing, when speckle pattern combinations and filterings may be carried out electronically. The intensities of the resulting fringes are similar to those of time averaged holography but they have the considerable advantages of stroboscopic real time viewing.

Normally, in fact, if the illuminated surface moves towards or away from the observer relatively little change in the appearence of the speckle patterns will occur unless a component of tilt is also present (massey 1968) when 'laser streak patterns' are observed. Detection of surface motion can be made more sensitive by adding a coherent reference beam, at the viewing aperture, which has a similar intensity to the speckle pattern (Archbold et al 1969). Interference between the two beams causes the speckles to undergo cyclic brightness variations, twinkles, every time the object displacement in the line of sigth changes by one quarter wavelength. Faster motion blurrs the speckles at all but the nodal regions, as described above.

Archbold et al used a telescope with an iris diaphragm at the entrance pupil to observe the speckles. If the effective eye pupil is reduced to 0.5 mm the resulting speckle size of about 5' of arc allows the antinodal blurring to be easily seen but necessitates the use of as powerful a laser as possible. The reference beam is obtained by splitting off a small fraction of the illuminating laser light and focussing it onto the telescope aperture. The speckle and reference intensities are balanced with polarising filters. The twinkle effect due to slow movements - which

would completely obliterate holographic fringes - aids the observation of nodal regions. Indeed if there is not sufficient natural twinkle it can be introdcued by varying the pressure in a gas cell placed in one of the beams. This speckle technique provides a quick method of assessing the nature of the vibrations and indicates whether the conditions are sufficiently stable for the recording of a hologram.

Displacements in the plane of the object may be determined by using the 'speckle correlation interferometer' of Archbold, Burch and Ennos (1970). This is a development of the method described by Leendertz (1970) which uses two symmetrical illumination beams and is not sensitive to movements normal to the object (see also Butters and Denby 1969). The method of Groh described below has the disadvantage of sensitivity to motion in several planes. With Leendetz' method whenever displacement occurs, the speckles are shifted bodily sideways and eventually the resultant fringe contrast in a doubly exposed photograph (with one exposure being taken at each object position) is reduced to zero. The fringe visibility falls to 1/3 of its original value when the image motion $\Delta x$ is equal to one speckle diameter. The image speckle size is $\sigma = 1.2F$ and the number of fringes observable is:

$$N = (2m\sigma \sin\theta)/\lambda$$

Therefore

$$N = 2.4mF\sin\theta$$

Where F is the 'f' number of the lens, m is the demagnification i.e. $m\sigma$ is the speckle size on the object, and $\theta$ is the angle which both laser beams make with the object surface normal. Archbold et al describe the criteria for the best signal to noise ratio (fringe to speckle size ratio) and fringe visibility and show that the lens aperture F and the demagnification m should be chosen to suit both the maximum movement to be observed and the characteristics of the film used - this should in general be an emulsion with a high resolving limit.

This technique has been extended by Archbold et al to allow greater displacements to be measured with only one illumination beam and with the use of two beams to allow surface deformations to be measured independently of the whole body translation. This is accomplished by viewing the negative in a different manner to that used by Leenderz. When only one beam is used for illumination and the displacement is greater than one speckle diamter, no fringes are seen when viewing in the normal manner. However, the double exposure generates a diffraction spectrum, consisting of a set of parallel straigth fringes, which may only be seen if their angular spread is inside the original diffraction halo generated by a single speckle pattern exposure and this occurs when the displacement itself is greater than one speckle width The spacing of these fringes (which are considered as being the original halo distribution multiplied by a Youngs two pinhole fringe pattern) is $\alpha = \lambda/\Delta x$ where $\Delta x$ is the displacement.

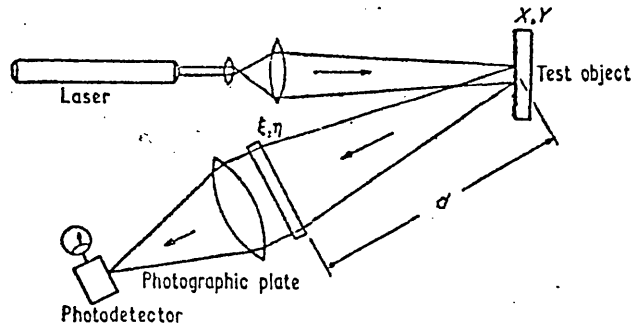
With this system the fringe contrast is degraded if deformation has taken place in the area which is selected for observation of the fringes, or if some movement normal to the object plane has caused defocussing. When two beams are used and some deformation has occurred as well as translation , fringes corresponding to the deformation only may be seen by illuminating the resulting negative with a collimated beam of light and viewing from the direction corresponding to a maximum in the original Young pattern for one illumination beam. They may also be seen with better contrast if viewed from a Young pattern minimum direction but the overall brightness is about 1/3 of the above.

This ability to measure small amounts of distortion in the presence of translation in several planes is the strongest feature of this technique. It may conceivably be used to measure vibrations by using a stroboscopic technique when it will have the advantage of low sensitivity which is desirable when large movements are to be observed. In these experiments however, displacements normal to the plane of the object are studied.

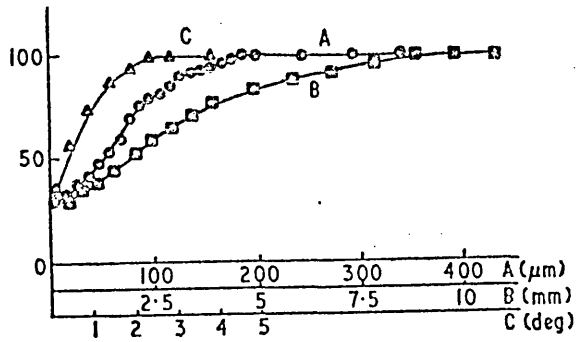
Another technique utilising speckle patterns has been described by Groh (1968) who uses the experimental system shown in fig ( 54 ). The laser beam may be made convergent divergent or parallel before illuminating the test object. The scattered light falls onto a photographic plate which may be returned to its original position after processing. Since it is a photographic negative the plate will blot out the bright parts of the speckle pattern and the transmitted intensity will be at a minimum. The object may be either viewed through the negative, with the aid of a diffuser placed behind it, or the light passing through may be focussed onto a photodetector.

If the object is slightly displaced a moire pattern is observed between the recorded and the actual speckle patterns. A rotational disturbance causes the outer regions of the negative to brightan up, and the greater is the rotation the greater the encroachment of brightness towards the dark central regions. If the object is laterally displaced as well the position of the dark area moves in the direction of the displacement. Fig ( 54 ) shows the total intensity passing through the plate as a function of the lateral and rotational displacements. With collimated illumination the displacement sensitivity is relatively low. But when the object is illuminated with a converging beam the sensitivity is increased. The measuring range is increased if the size of the illuminated area is reduced, the following table gives a few examples; .6mm displacements and ,3mm displacements are measurable with a 1.5 mm and a 3.8 mm diameter illuminated area respectively. Maxium transmission is achieved for an object movement of:

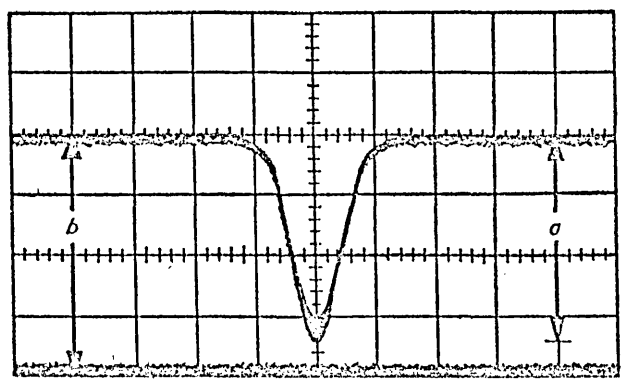
| Illumination (2 mm dia.) | Lateral displ. | Depth displ. | Rotation (1) | Rotation (2) |
|---|---|---|---|---|
| parallel beam | .2 mm | 8 mm | $2.5^{\circ}$ | $5^{\circ}$ |
| converging to 50 mm behind | .02 mm | .3 mm | - | $1^{\circ}$ |
| converging to 5 mm behind | .01 mm | .06 mm | - | - |



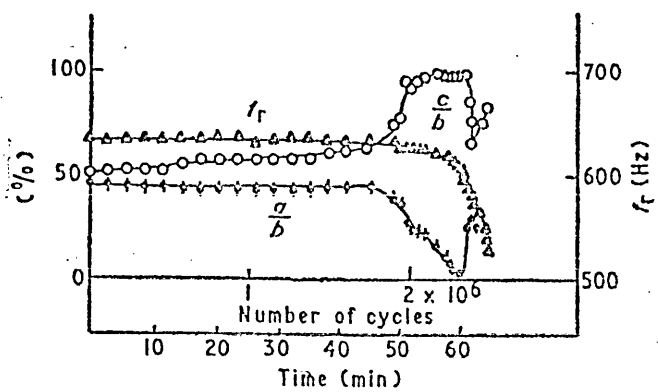

. Apparatus for photographic laser speckle patterns (after Groh 1970).




. Intensity of light passing through the negative of the speckle pattern as a function of (A) lateral, (B) longitudinal and (C) rotational displacements. The rotation is about an axis normal to the surface of the object.




. Photodetector signal when the test object is vibrating.




. Ratios of *a/b*, *c/b* and the resonance frequency of a steel plate spring as a function of time during a fatigue test.

Figure 54 (a to d) Some Speckle Pattern Results (after Groh)

Rotation (1): about an axis normal to the surface.
Rotation (2): about an axis in the scattering surface.

When the object is vibrating, the transmitted intensity variations may be displayed on an oscilloscope screen as shown in Fig ( 54 ). The minimum corresponds to the rest position. The minimum to maximum transmission is denoted as 'a', maximum to zero as 'b' and minimum to zero as 'c'. If the ratios of a/b and c/b are plotted against the number of cycles undergone by the object, they show in a highly sensitive manner when fatigue has altered the surface characteristics as shown in Fig ( 54 ) The changes in these curves occur well before either changes in the resonance frequency or microscopic surface changes become visible.

(j) Laser Scanning Methods

Korpel et al have described several techniques for rendering visible and for measuring the amplitude of surface waves. They all use a probing coherent light beam and differ in the size of the beam and the way in which the vibrational information is 'decoded' from the reflected beam.

The first of these methods (Korpel et al 1968) has been later called the knife edge technique (Korpel et al 1969), and the experimental arrangement is as follows: Light from a laser is passed through a scanner and lens ($L_1$) and comes to a focus at the specimen - which must be flat and specularly reflecting (Fig 55a ). The spot of laser light then traverses the surface when the scanner angle is changed, and the reflected light passes through lens ($L_2$) to subsequently fall on the knife edge and photodetector. Since the object lies in the fourier transform plane of the scanner, and the detector in the Fourier transform plane of the object, the detector is therefore in the image plane of the scanner. Because of this, the light beam always strikes the knife edge and detector in the same place whatever the scan angle and position of the spot on the object surface.

In one particular system the light beam scans across the surface at 240 m/sec which is about 8 percent of the velocity of the type of surface wave being studied. This corresponds to a doppler shift of ± 640 KHz on an 8 MHz signal and the photodetector has an output of 8 MHz together with the two doppler shifted frequencies. The doppler shift may have any intermediate value depending on the angle of the surface wave propagation with respect to the scanning beam. The photodetector output may then be fed into a television system where the spot on the screen is scaned in synchronism with the laser scanning mechanism. A picture would be seen on the screen whose brightness was proportional to the local surface amplitude - which since this is rapidly varying, would not be visible. To make the surface waves visible they can be strobed by heterodyning one or other or both of the doppler shifted signals with the original from the signal generator. By using only one doppler signal, surface waves travelling in one direction may be preferentially selected.

This may be interpreted as a synchronous detection process where the acoustic phase at each point is compared with the reference phase. Depending on the acoustic phase at any given point, the detector gives an output which is either black grey or white on the screen. Before doppler frequency is selected some signal is split off and used to give an ordinary television background of surface features against which to observe the vibrations. The weakest signals observable with this technique correspond to about 0.1 Å of object movement, making this just about the most sensitive method available.

The second technique is an optical heterodyning method having a similar sensitivity to the knife edge technique. It differs from the above system in that the light reflected from the surface (and acoustically perturbed at a frequency $f_m$) is heterodyned with a reference beam at a frequency $f_o + f_s$ where $f_s \neq f_m$. The additional frequency $f_s$ is added

by passing the light through a Bragg cell filled with water and excited at the appropriate frequency. The frequencies $f_s \pm f_m$ are produced by this process and their amplitudes are proportional to the amplitude of the surface waves. These signals may be ultimately used to modulate either the amplitude of an oscillescope trace in a one dimensional scanning system, or the brightness of the oscilloscope spot as in the previous method. Two different ways of achieving the superposition of the reference and probing beams have been described by Korpel et al (1969).

Their final method is called the amplitude grating method. Again the sensitivity is similar to the above techniques but uses a probing beam which is several acoustic wavelengths wide. The surface waves impress a moving phase ripple onto the reflected light beam which may be regarded as a zero order beam together with two first order beams having an apparent phase velocity. Whenever the zero order differs in phase by multiples of $90^\circ$ with respect to the other beams, the phase ripple becomes an 'amplitude ripple'. If a grating of the correct spatial frequency is placed at an optimum position, a time-varying light power will pass through it. This can be detected by a photodetector and used as in the above two methods.

The above three methods have a similar sensitivity but do have differences which may make one or toher more applicable for a given application. For instance, the knife edge technique is more readily adapted to three dimensional display and the superheterodyne technique is the best one for measuring long surface wavelengths, and also has no directional sensitivity. The three techniques require more sophisticated equipment ta than the most complicated holographic system but they are more sensitive than even the subfringe technique of Metherell or the temporal holographic systems of Aleksoff (1969 and 1971 resp.)

Finally, another related superheterodyne system has been described by Avsec, Botcherby and Davis (1969). The frequency off-set

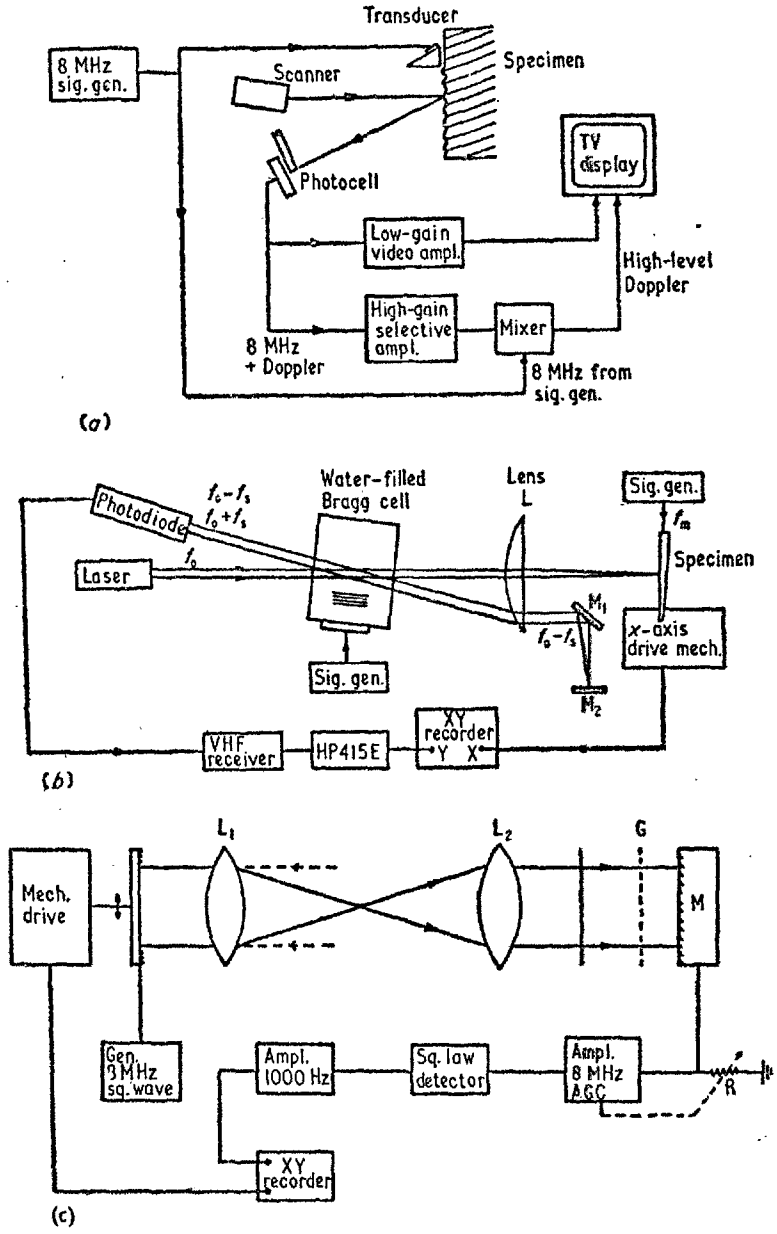



Figure 55. (*a*) Schematic diagram of laser spot scanning system for surface wave visualization; (*b*) heterodyne; (*c*) amplitude grating technique. (After Korpel and Whitman 1969).

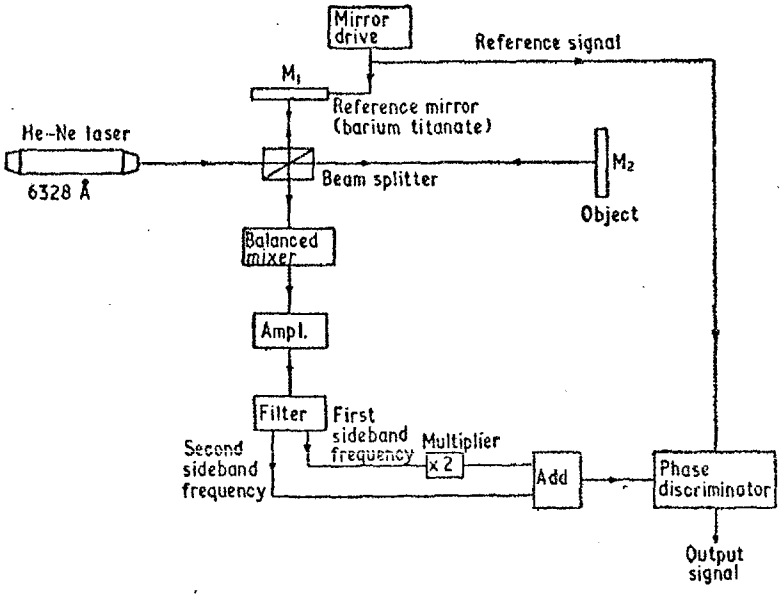



Figure 56 Vibration measurement using an optical superheterodyne system (after Avsec *et al.* C.L.E.A. conference 1969).

between the two beams is achieved by vibrating a reference mirror Fig( 56 ) $M_1$ sinusoidally with a much greater amplitude than that of the object $M_2$. The output signal of the photodetector has a series of Bessel function related sidebands (since this is a carrier wave, frequency modulated by both the reference mirror and the object). The first sideband may be frequency doubled and combined with the second sideband which is in quadrature with the first. The phase modulated wave produced has a deviation proportional to movement of the object and the amplitude related to the light intensity falling on the photodetector. This method has the advantage of relative simplicity when compared with the other similar methods.

All the methods described above were dismissed in favour of the holographic technique and its derivatives as described in Sections II III and IV.

# APPENDIX (II)

## MODES AND RADIATION

CONTENTS - Appendix 2 - Modes and Radiation


Introduction 188

A II.1) Modal Frequencies 188

(i) to (v) Thin Discs 188

(v)) Stiffening Ring 191

(vii) Thick Discs 191

(viii) Experimental (Waller) 192

(ix) Comparison of Calculation and Experiment 192

(x) Relation of 'gear' to'Ideal' plates 193

(xi) Relation of Loudspeaker to 'Ideal' plates 194

A II.2) Excitation of Plate Modes and Their Surface Displacement

(i) Discussion 195

(ii) Surface Displacement 198

(a) to (c) Thin Discs 198
(d) Thick Plates 200
(e) High Amplitudes 200

A II.3) Radiation from a Modal Piston 202

(i) Discussion of Radiation Theory 202

(ii) Treatment of Objects to Reduce Sound Radiation 204

(iii) Theory Applied to Rectangular Plates 209

(1) Large Panel 212
(2) Small Panel 213

(iv) Theory Applied to Circular Plates 214

(a) Calculation of Sound Pressure 214

(1) Below fc small panel 216
(2) Above $f_c$ small panel 217
(3) Above $f_c$ large panel 218
(4) Below $f_c$ large panel 219
(5) Comparisons 219

(b) Calculation of Radiation Restance 221

(1) Below $f_c$ small panel 223
(2) Above $f_c$ small panel 225

(v) Some Standard Results for Comparison 229


Total Number of Pages: 51

## APPENDIX (II)

## Modes and Radiation

### Introduction

This appendix covers some expressions for the frequencies of the modes of circular plates. Also listed are some of the expressions given in the Literature for the actual deflection of the disc surface at its various modal frequencies. Radiation theory is discussed and expressions given for the radiation resistance of a modal rectangular plate both above and below the coincidence critical frequency. Finally there is an attempt to deduce similar expressions for the circular disc.

### AII.1) Modal Frequencies

(i) According to Timoshenko (1954) the natural frequencies of a circular plate with a fixed center are given by the formula:

$$f = \frac{\alpha_m}{a^2}\sqrt{\frac{gD}{\gamma h}}$$

$$f = \frac{\alpha_m h}{a^2}\sqrt{\frac{E}{12(1-\sigma^2)\rho}}$$

Where h = plate thickness , a = plate radius $\alpha_m$ = a constant for each mode E = Young's Modulus $\rho$ = density $\sigma$ = Poissons ratio which for metals is approximately 1/3 D = $(Eh^3)/(12(1-\sigma^2))$ D is the flexural rigidity and $(\gamma h)/g = h\rho$ mass per unit area. Values of $\alpha_m$ for different 'n' the number of nodal circles and 's' the number of nodal diameters is given below (page 189 ).

Table from Timoshenko (1954):-

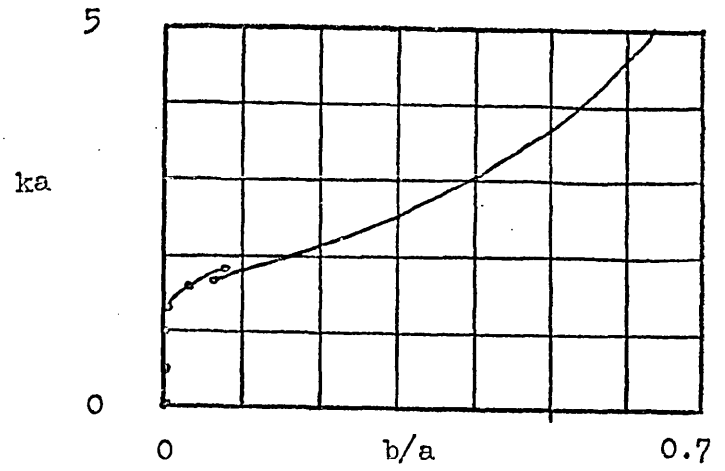
| Diameters 's' | Clamped at Center | | | | Free |
|---|---|---|---|---|---|
| Circles 'n' | s=0 | s=1 | s=2 | s=3 | s=0 |
| n = 0 | 3.75 | 0 | 5.251 | 12.23 | - |
| n = 1 | 20.91 | 20.52 | 35.24 | 52.91 | 9.076 |
| n = 2 | 60.28 | 59.86 | - | - | 38.52 |
| n = 3 | 119.7 | - | - | - | - |

(ii) Southwell (1922) derives a similar formula from the differential equation describing the motion of the plate (see below). He derives the natural frequencies for a clamped plate with a varying clamping radius. Southwell states that the natural frequencies for a plate clamped at zero radius at the center of the disc are the same as those of a free disc (treated by Kirchoff) (Rayleigh 1945). when there <u>are</u> any nodal diameters present. When there are <u>no</u> nodal diameters present the natural frequencies of a disc clamped at a center of zero radius are completely different. Southwell also shows that the effects of clamping on the natural frequencies is very small for small radius of clamping 'b' radius except for s = 1 (one nodal diameter) when the resonant frequency increases very rapidly from 0 Hz as the clamping radius is increased only slightly from zero (see table). The general shape of the frequency curve as the clamping radius is increased is shown in Fig ( 56 ). Southwell gives the following formula and table:

$$2\pi f = \frac{\sqrt{\mu}h}{a^2}\sqrt{\frac{E}{\rho}}$$

| Diameters 's' | s = 0 | | free or clamped s= | | | s = 0 |
|---|---|---|---|---|---|---|
| Circles 'n' | free | clamped $\frac{1}{\infty}$ | 1 | 2 | 3 | $\frac{h}{a}$ clamped = |
| n = 0 | 0 | 5.16 | 0* | 10.61 | 56.87 | 1.937 |
| n = 1 | 29.67 | 160.2 | 154.3 | 443.9 | 1040 | 4.573 |
| n = 2 | 577 | 1349 | 1222 | 2624 | 4285 | 7.79 |
| n = 3 | 2983 | 5250 | 5266 | 8574 | 13287 | 10.94 |

Table for $\mu$




a = plate radius
b = clamping radius

after Southwell

1 nodal diameter

(a) Showing very rapid rise in frequency as clamping circle radius – increases from zero when there is 1 nodal diameter

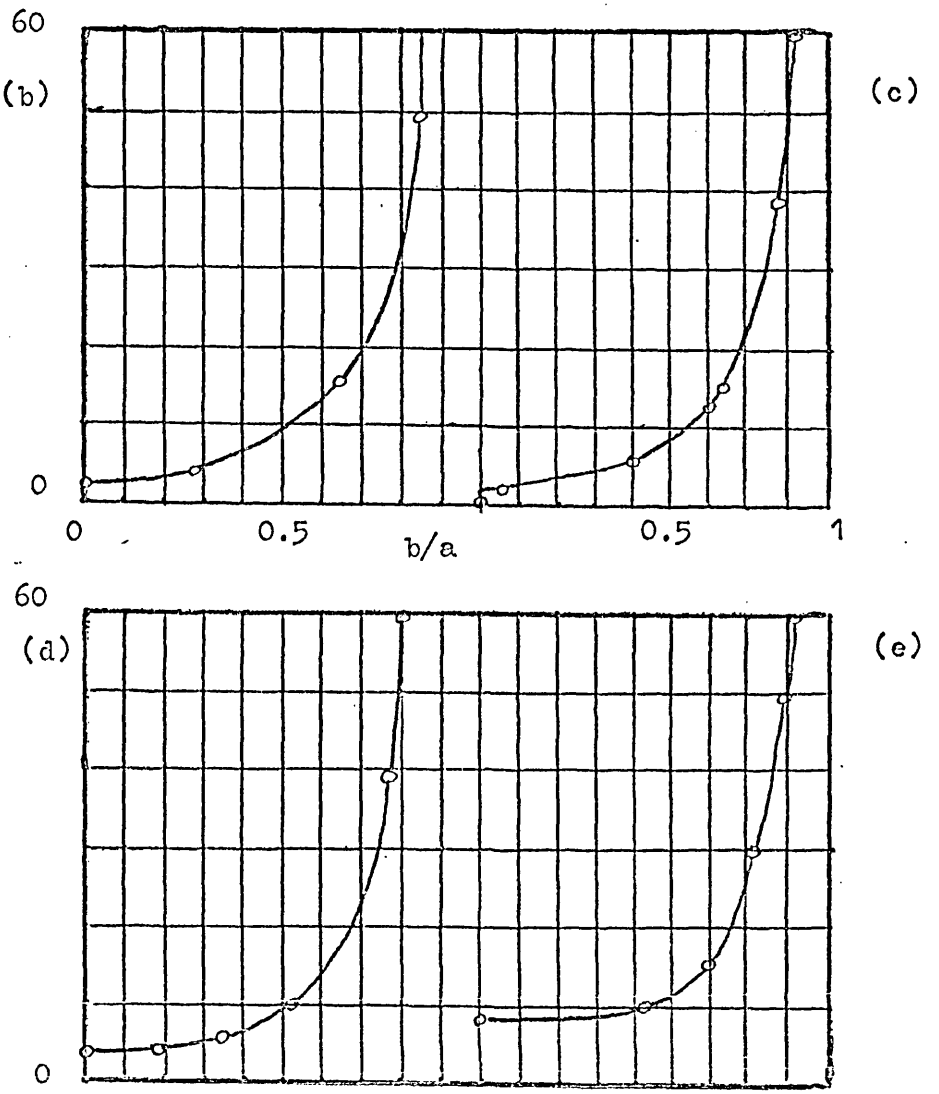



Figure 56 (a) as caption above . (b) - (e) connect " $p\sqrt{\frac{\rho a^4}{Eh^2}}$ " with the ratio b/a where p is the frequency (b) s = 0 no nodal diameters (c) s = 1 as in (a) one nodal dia. (d) s = 2 and finally (e) s = 3

*When clamping radius is finite but very small 1.05 may be placed here.

The one diameter no circle mode is directly applicable to loudspeakers where the 'clamping' radius may be taken as the voice coil radius and the mode manifests itself as a rocking action excited by the out of ballance masses of the lead-in wires. However rocking occurs over a wide frequency band and the actual frequency of 'resonance' is difficult to find.

(iii) Southwell has also given the following table of 'Ka' against 's' number which may be used when the clamping radius 'b' is not infinitely small and this applies to the no nodal circles - nodal radii only case.

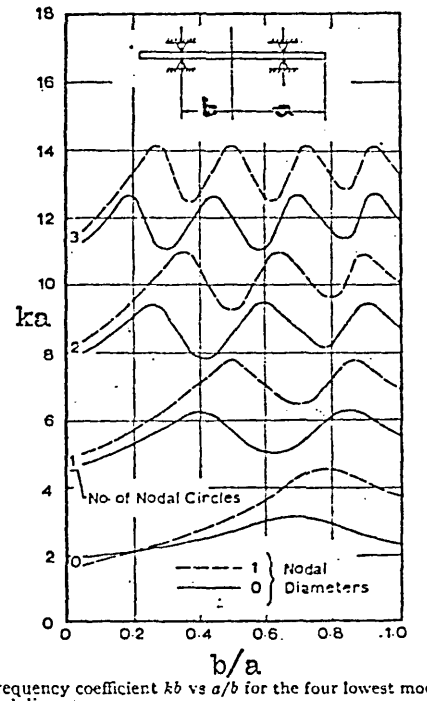
$$k^4 = \frac{3(1-\sigma^2)f^2\rho}{E\,h^2}$$

$$\text{therefore } f = \frac{(ka)^2 h}{a^2}\sqrt{\frac{E}{3(1-\sigma^2)\rho}}$$

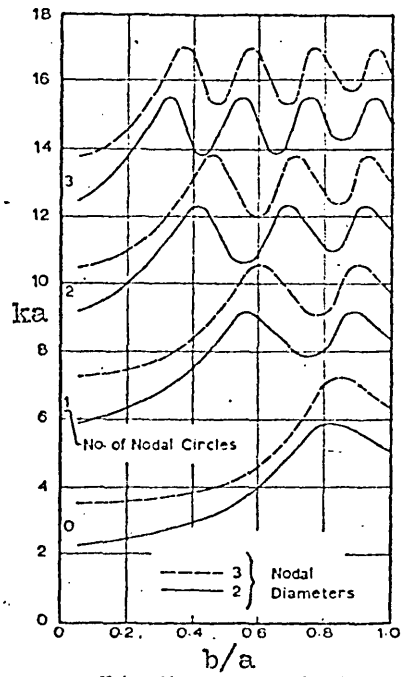
| s = 0 | | s = 1 | | s = 2 | | s = 3 | |
|---|---|---|---|---|---|---|---|
| b/a | ka | b/a | ka | b/a | ka | b/a | ka |
| 0.276 | 2.50 | .060 | 1.68 | .186 | 2.50 | 0.43 | 4.0 |
| 0.642 | 5.00 | .377 | 3.00 | .349 | 3.00 | 0.59 | 5.0 |
| 0.840 | 9.00 | .603 | 4.60 | .522 | 4.00 | 0.71 | 7.0 |
| | | .634 | 5.00 | .769 | 8.00 | 0.82 | 10.0 |
| | | .771 | 8.00 | .81 | 10.0 | | |
| | | .827 | 11.0 | | | | |

(iv) There are many tables given in the literature allowing modal frequencies to be found for different conditions of support. In particular Bodine (1966) (Fig 57 ) gives a complete set of frequency curves for a plate simply supported at a ring of arbitrary radius. When the ring shrinks to an infinitessimal point his results are the same as those of Southwell. Graphs of ka against a/b for different number of nodal circles and diameters are reproduced here. The frequency is given in this case by

$$w = \frac{h(ka)^2}{a^2}\sqrt{\frac{E}{12(1-\sigma^2)}} \qquad \text{where } w = 2\pi f$$




Frequency coefficient $kb$ vs $a/b$ for the four lowest modes having 0 and 1 nodal diameters.



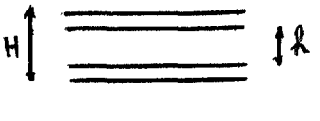

Frequency coefficient $kb$ vs $a/b$ for the four lowest modes having 2 and 3 nodal diameters.

Figure 57 Values of ka for conditions indicated-to substitute

in: $\omega = (ka)^2(D/mha^4)^{\frac{1}{2}}$ $D = Eh^3/12(1-\nu^2)$

(v) Sheldon and Sewards (1970) have given very complete graphs of ka/2 against b/a ffor many different conditions of edge and center support, viz: free, clamped, pinned or sliding inner and/or outer edges. The appropriate value of ka is read off the graphs and substituted in their formula which has the advantage of applicability to sandwich materials.

$$f = \frac{k^2}{2\pi}\sqrt{\frac{EI}{(1-\sigma^2)\rho H}}$$



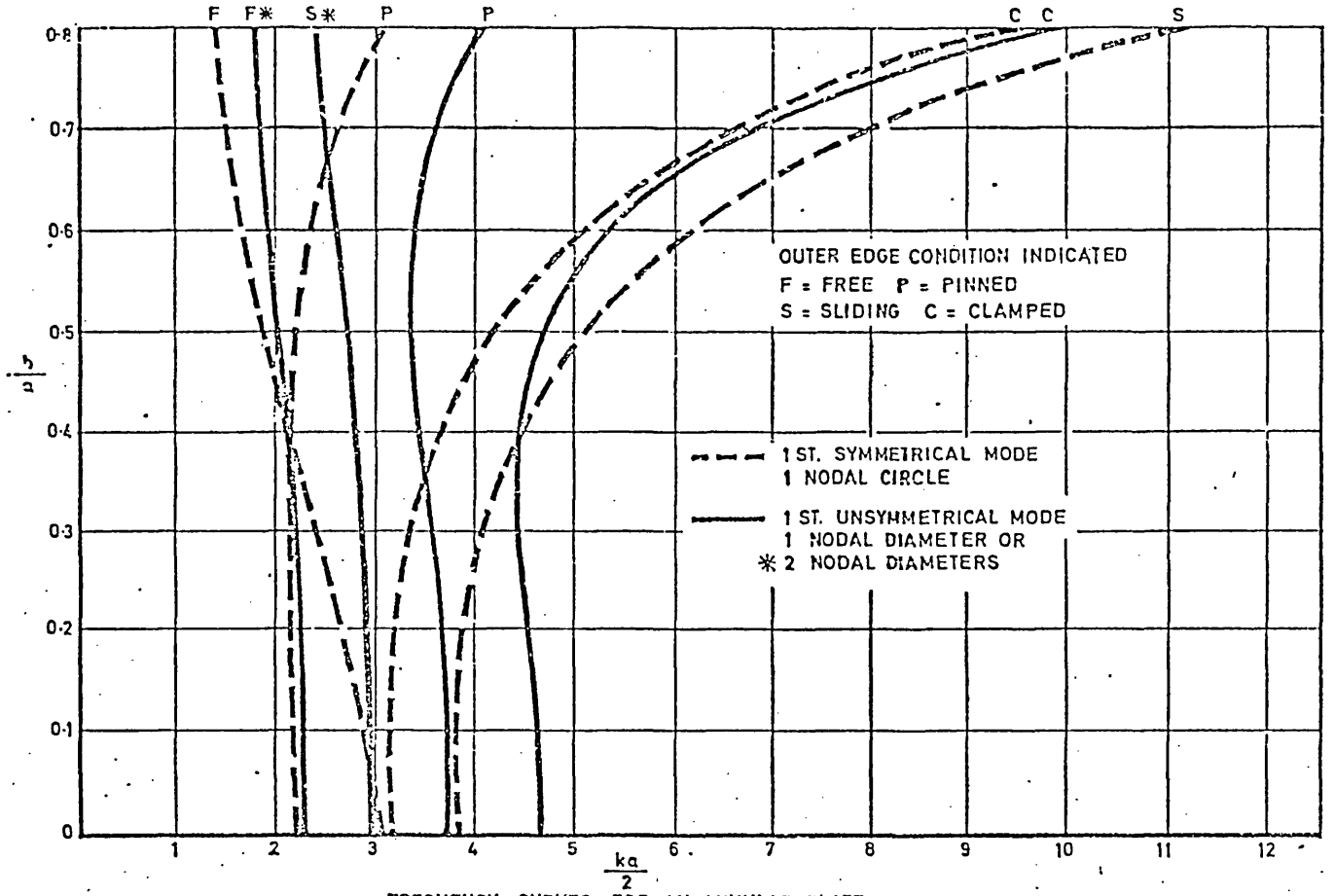

Where I is the second moment of area which = $1/(12)(H^3 - h^3)$

i.e. $I = 1/(12)\ H^3$ for a solid 'non-sandwich' material when $h = 0$

This equation may therefore be used to work out the natural frequencies of discs made of the same composite material used to make comercial aluminium-polystyrene-aluminium sandwich speakers. Their graphs are reproduced as Figures (58abcd).

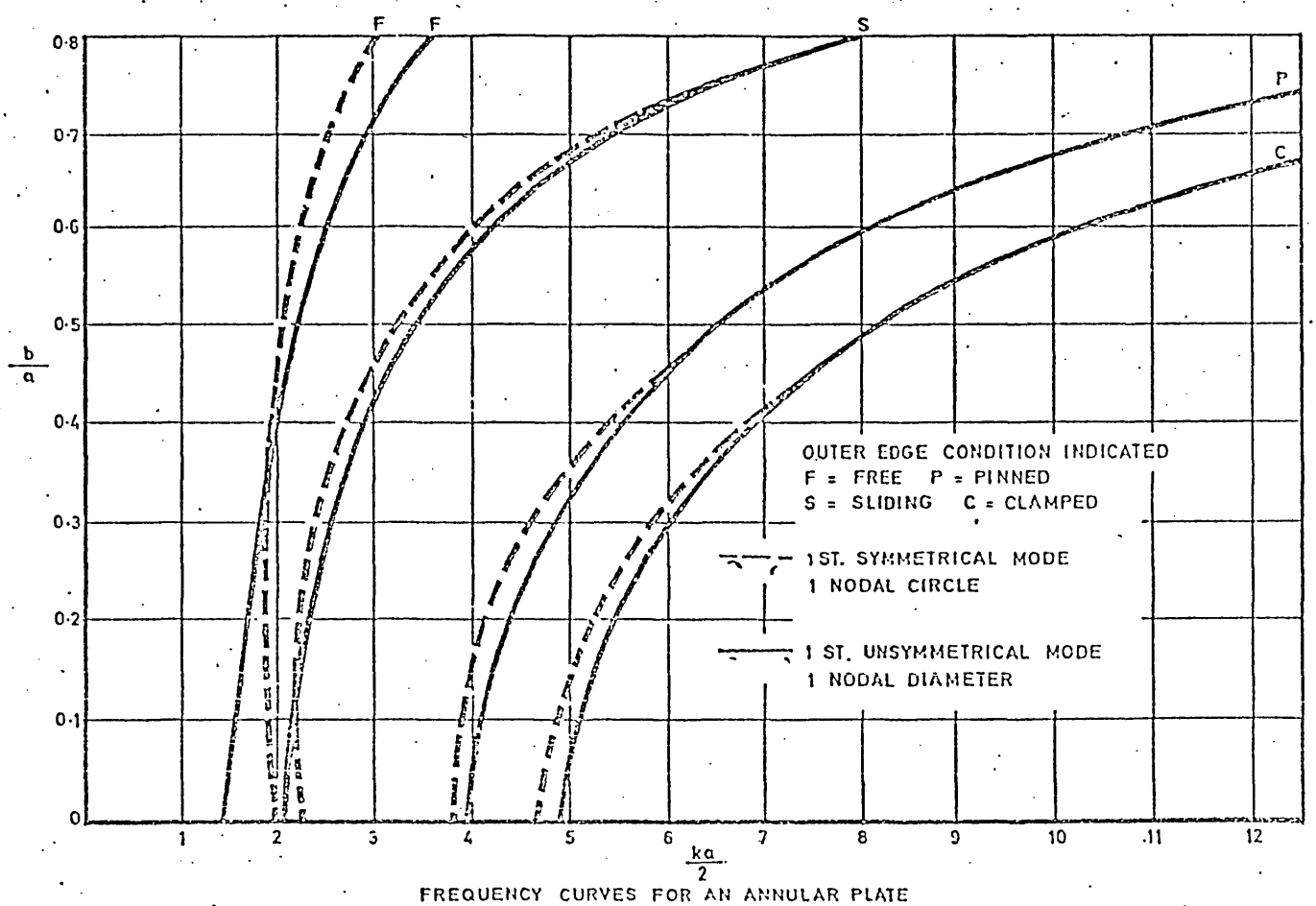
(vi) The frequencies of plates stiffened by a ring of variable cross-section mass and stiffness with the plate clamped at the edge have been given by Kirk and Leissa (1967) for the axisymmetric case (i.e. no nodal diameters). Their results are given in the form of graphs of the ratio of the "natural frequencies of stiffened to unstiffened plates" against the radius of the stiffeneing ring. Each curve corresponds to a different value of the other parameters i.e. mass, stiffness, and cross section of the stiffening ring. They found that the frequency is increased or decreased depending on the radius at which the stiffening ring is fixed and that increases of up to 1.6 times in the natural frequency are possible. This has particular relevance to sandwich bass loudspeakers as rings may be used to increase the natural frequencies of these speakers because they vibrate only in axisymmetric modes.

(vii) Very Thick Discs - have been treated by Onoe and Yano (1968). They give graphs of normalised frequency $\Omega = wh\sqrt{\mu/\rho}$ against the diameter thickness ratio for modes up to $s = n = 3$ and these are applicable to the completely free disc.



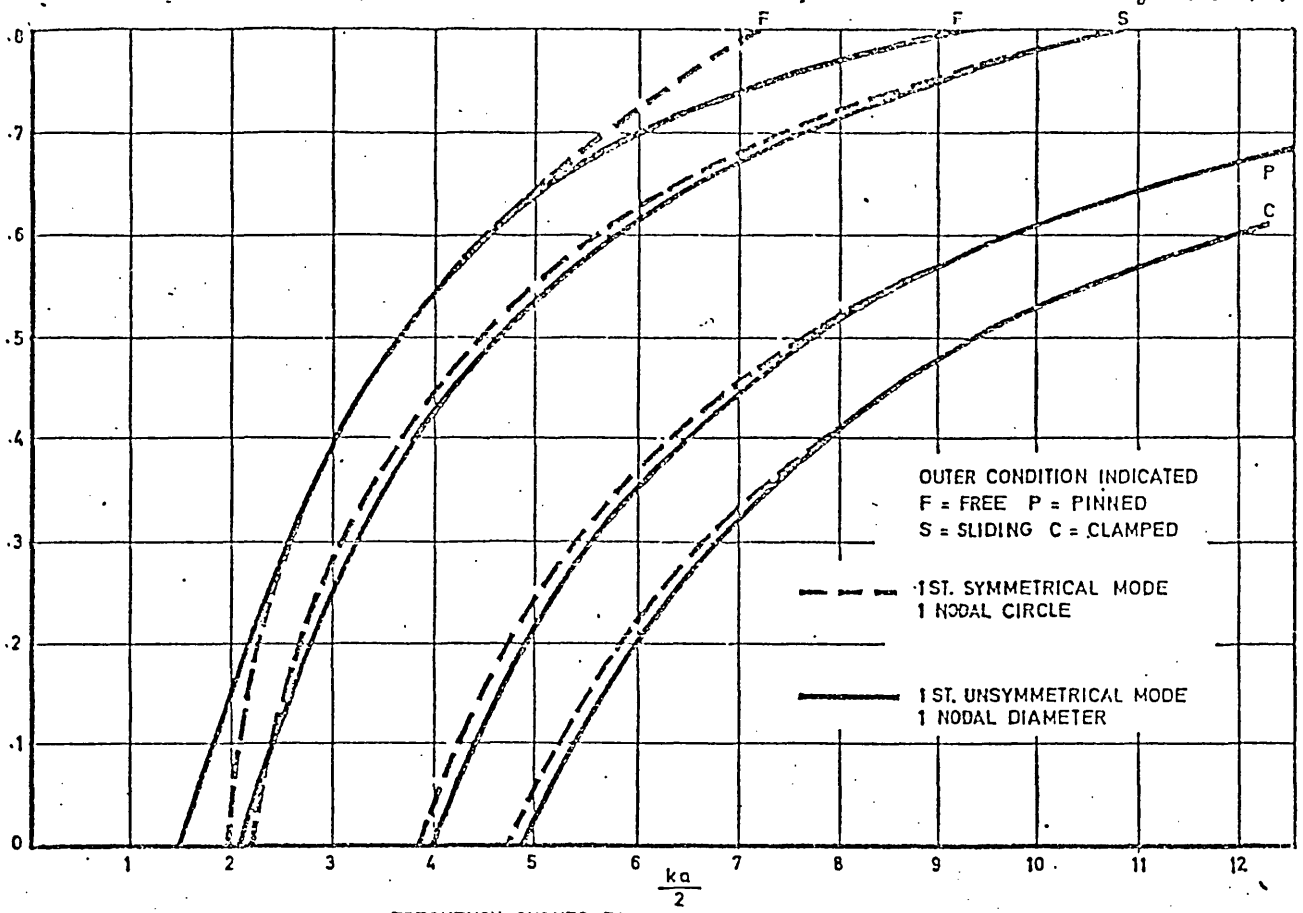

FREQUENCY CURVES FOR AN ANNULAR PLATE.

FIG. 58a FREE INNER EDGE



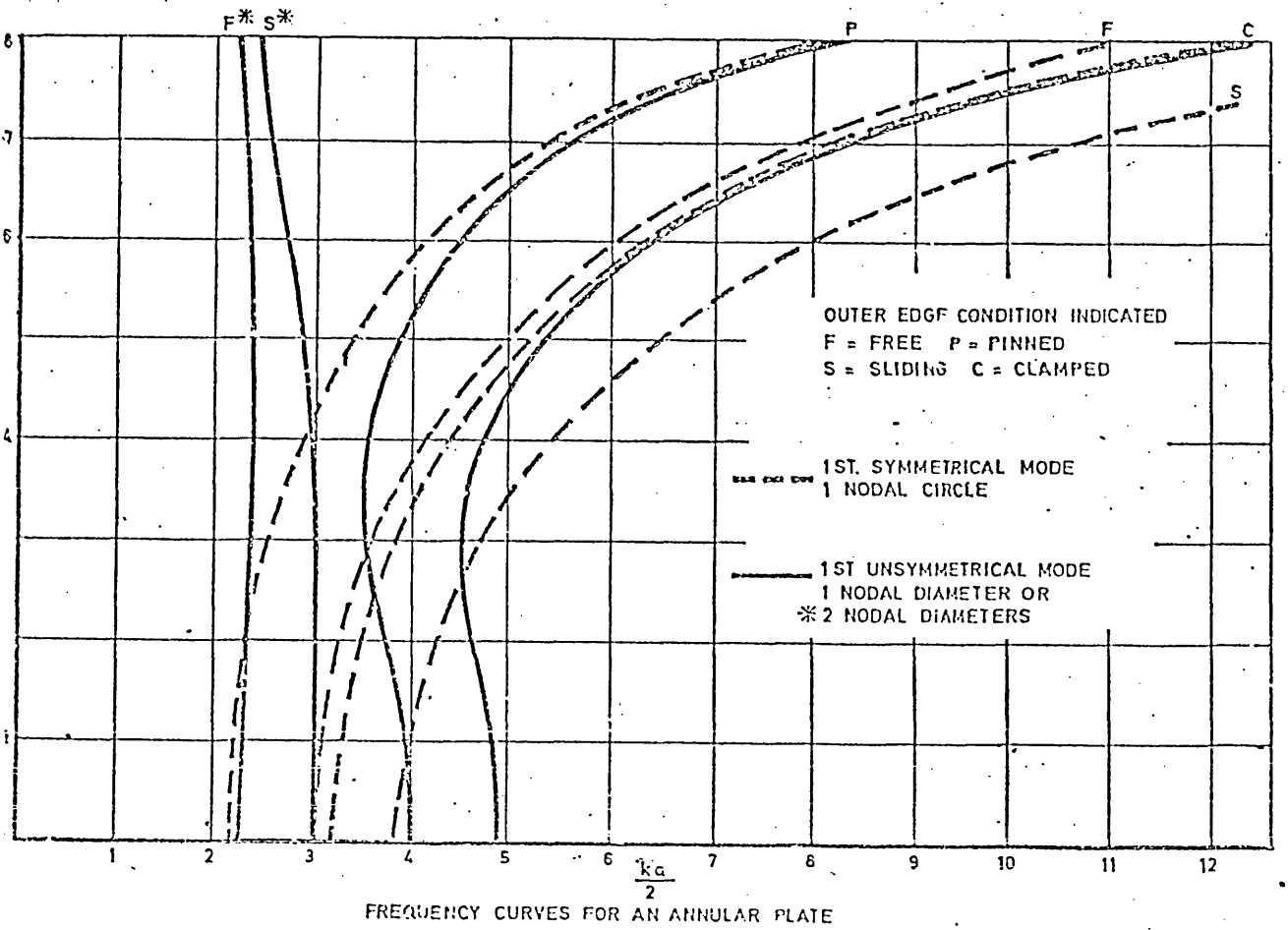

FREQUENCY CURVES FOR AN ANNULAR PLATE

FIG. 58b PINNED INNER EDGE




FREQUENCY CURVES FOR AN ANNULAR PLATE

FIG.58c CLAMPED INNER EDGE




FREQUENCY CURVES FOR AN ANNULAR PLATE

FIG.58d SLIDING INNER EDGE

(viii) Finally Mary Waller (1961) has given tables of experimental frequencies in the form of ratios to the fundamental for thin brass discs together with a table of nodal circle radii relative to that of the disc and these are presented below:

Relative Disc Vibration Frequencies (experimental)

| s = | 0 | 1 | 2 | 3 | 4 | 5 | 6 | 7 | 8 | 9 | 10 | 11 | 12 |
|---|---|---|---|---|---|---|---|---|---|---|---|---|---|
| n = 0 | | | 1 | 2.29 | 4.10 | 6.19 | 8.80 | 11.7 | 15.1 | 18.8 | 23.0 | 27.6 | 33.0 |
| 1 | 1.70 | 3.99 | 6.79 | 10.3 | 13.8 | 18.1 | 23.1 | 28.6 | 34.7 | 40.8 | 47.5 | 54.7 | 63.0 |
| 2 | 7.51 | 11.7 | 16.1 | 21.2 | 27.1 | 33.4 | 40.5 | 47.7 | 56.0 | 65 | 75 | 86 | 100 |
| 3 | 16.4 | 22.7 | 29.4 | 36.3 | 43.0 | 50.5 | 59 | 69 | 80 | 90 | 104 | 118 | 135 |
| 4 | 29.1 | 37.0 | 43.2 | 53.1 | 63.0 | 74 | 86 | 99 | 120 | 145 | | | |
| 5 | 47.0 | 56.0 | 66 | 77 | 92 | 110 | 135 | | | | | | |
| 6 | 72.7 | 83 | 100 | 127 | 147 | | | | | | | | |
| 7 | 110 | 132 | 160 | | | | | | | | | | |

Abridged Table of Nodal Circles relative to disc radius taken as 1000

| s = | 0 | 1 | 2 | 3 | 4 | 5 | 6 | 7 | 8 | 9 | 10 | 11 |
|---|---|---|---|---|---|---|---|---|---|---|---|---|
| n = 1 | 680 | 781 | 823 | 843 | 859 | 871 | 880 | 889 | 897 | 903 | 909 | 912 |
| n = 2 | 391 | 497 | 562 | 604 | 635 | 662 | 681 | 702 | 715 | | | |
| | 843 | 867 | 887 | 898 | 906 | 915 | 922 | 927 | 932 | | | |
| n = 3 | 257 | 349 | 415 | 461 | 505 | 531 | | | | | | |
| | 591 | 643 | 681 | 706 | 728 | 745 | | | | | | |
| | 895 | 902 | 913 | 919 | 925 | 933 | | | | | | |
| n = 4 | 190 | 269 | 328 | 374 | 411 | 443 | | | | | | |
| | 441 | 495 | 540 | 571 | 596 | 623 | | | | | | |
| | 692 | 726 | 748 | 764 | 779 | 794 | | | | | | |
| | 918 | 928 | 934 | 938 | 941 | 944 | | | | | | |

(ix) Comparison of Calculated and Experimental Frequencies of Plates

The natural frequencies of the plates used in the present experiments together with the frequencies extrapolated from Wallers tables and calculated from the graphs of Sheldon and Sewards are tabulated below:

| Circles n = | Diameters s = | Observed Freq. Plate (1) | (2) | Waller ratio | freq. | Southwell Calculated |
|---|---|---|---|---|---|---|
| Umbrella | | 910 Hz | - | 1.7 | 920 | 820 |
| 0 | 1 | - | - | - | - | 150 |
| 0 | 2 | 540 | 525 | 1.0 | 540 | 500 |
| 0 | 3 | 1260 | 1200 | 2.3 | 1235 | 1150 |
| 0 | 4 | 2050 | 2100 | 4.1 | 2210 | - |
| 0 | 5 | 3180 | 3100 | 8.8 | 4770 | - |
| 0 | 6 | 4400 | 4250 | 11.7 | 6300 | - |
| 0 | 7 | 5800 | 5600 | 15.1 | 8150 | - |
| 0 | 8 | 9350 | - | 18.8 | 10300 | - |
| 1 | 0 | - | - | - | - | - |
| 1 | 1 | 2150 | 2200 | 4.0 | 2160 | 1850 |
| 1 | 2 | 3380 | 3400 | 6.8 | 3670 | 3130 |
| 1 | 3 | 5100 | 4950 | 10.3 | 5500 | 4840 |
| 1 | 4 | 6900 | 6530 | 13.8 | 7050 | - |
| 1 | 5 | 9000 | - | 18.1 | 9750 | - |
| 2 | 0 | 4680 | 4100 | 7.5 | 4050 | 5500 |
| 2 | 1 | - | - | 11.7 | 6400 | 5225 |
| 2 | 2 | 8000 | 8000 | 16.1 | 8700 | 7700 |
| 2 | 3 | 10500 | 10500 | 21.2 | 10500 | 9800 |
| 3 | 0 | 8150 | - | 16.4 | 8850 | 11000 |

(x) Relation of 'Gear' to 'Ideal' Plates

The Vibrating Discs of Section (III) may be approximated to discs of medium thickness clamped at zero radius in the center . The actual gear-like plate would be clamped at the center and 'slidingly' or simply supported at one (variable) point on the circumference, the appropriate boundary conditions for this may be substituted into the assumed solution of one of the equations of motion given for plates of medium thickness.

Thence the constants in the equation and the natural frequencies of the plate modes may be determined. The'real-gear' situation is however, further complicated by the fact that the excitation occurs at the outer support, with many of the excitation forces tending to excite radial rather than the lower frequency 'in plane' plate vibrations, and so it is not proposed to carry out these manipulations here (this would be a suitable topic for further work). However, mode excitation is discussed more fully in (AII.2 i) and it is thought possible that only those modes with nodal diameters present would tend to be excited in such a system - with a node passing through the edge support.

(xi) Relation of the'Loudspeaker'to the'Ideal'Plate

The Loudspeaker with its cone of ellipsoidal, hyperbolic or exponential section presents more problems. The simple conical Loudspeaker cone has been treated by Zimmerman (1969 in French) and subharmonics have been predicted by Aldoshina (1971). Zimmerman has shown that the resonance frequencies of conical shells do not depend to any great extent on wether the edge is clamped or free but in both cases they are different from the resonace frequencies of a circular plate, he does not however give a table of resonance frequencies. In general, however, the natural frequencies or the equations of motion of conical s urfaces have not been extensively treated in the literature. It is likely that conical surfaces may be treated in a similar manner to flat discs by assuming that the conical shapes have a greater flexural rigidity. This will effectively increase the natural frequencies over those of a disc made with the same materials. The conditions of support also present problems in that they are a combination of free and simple support at the edge and, in the absence of connections to the amplifier, relatively free at the center. (the dynamic stiffness of the spider and the surround are less important than the mass of the cone above the fundamental resonance). However when the voice coil is connected to an amplifier with a low internal resistance there is

considerable damping experienced by the (effectively shorted) voice coil in its strong magnetic field. The center of the speaker may be likened therefore to a poor simple support or possibly to a sliding support. When When the radius of the voice coil is large the cone may no longer be approximated to a disc but must be approximated to an annulus whose inner edge may be regarded as simply or slidingly supported. The terms $Y(x)$ and $K(x)$ must then be included in the solutions of the equations of motion. In this way plate theory may be innaccurately applied to give a rough indication of the behaviour of Loudspeaker cones.

## AII.2) Excitation of Plate Modes and their Surface Displacements

### (i) Discussion

It is expected that with an infinitely small center support and excitation at the edge all possible plate modes are capable of excitation except the one nodal diameter-no nodal circle mode whose frequency will be zero. With even a small but finite radius of clamping this mode becomes capable of excitation having a low but definite frequency. For the completely free plate, of course , the no nodal circles-no nodal diameter mode will not be capable of excitation and neither will the no nodal diameter-one nodal circle mode. With a continuous excitor those modes will be excited which fall exactly on the frequency of excitation and also those whose frequencies are relatively close, so allowing the excitation frequency to fall on the skirts of its resonance curve. With plates most of the modes in the audio range are well spaced in frequency, so that in general only one mode will be stromgly excited by the continuous excitor when placed at the edge of the disc. The exceptions are the four diameter mode and the one diameter-one circle mode whose frequencies are very nearly coincident.

With an impulsive excitor those modes will be excited which fall onto the fundamental or one of its harmonics particularly if the point of excitation is at the edge which is always an antinode. Waller

used different conditions of support and places of excitation to ensure that her excitation device (solid carbon dioxide),which has no natural frequency of its own, excited only that mode which she desired. It is obvious that a mode will not be excited if it is supported at an antinode and 'excited' at a node. Theoretically therefore, only nodal circle type modes should be excited by loudspeaker voice coils and this does indeed happen with sandwich loudspeakers (which are very homogeneous) as described in Section IV.With paper cones , inhomogeneities in both mass and stiffness allow some energy to be diverted into the excitation of nodal diameter modes.

When a constant load or an oscillating load is moved around a fixed position in a circular orbit then another modes become capable of excitation (Raske and Schlack 1966). This will be the condition in the case of gear excitation where tooth contact gives repetition frequencies and their harmonics and the point of excitation is moving around the circumference of the disc at the same time. Raske and Schlack have shown that for circularly orbiting point forces and oscillating forces about a general point on the object,very many combinations of oscillation frequency and 'intrinsic' frequency of the force will excite plate modes. In the case of a square plate with the oscillating (variable)force or the circularly orbiting (constant) force both moving about the center of the plate the following become the resonance conditions:

$$\bar{\lambda} = \bar{w} \qquad \bar{\lambda} + \bar{w} = 2i\bar{\beta} \qquad |\bar{\lambda} - \bar{w}| = 2i\bar{\beta}$$

- for the oscillating force, and for the circularly orbiting force:

$$\bar{\lambda} = 2i\beta \qquad \bar{\lambda} = 2j\bar{\beta} \qquad \bar{\lambda} = 2(i+j)\bar{\beta} \qquad \bar{\lambda} = 2|i-j|\bar{\beta}$$

Where w is the transverse frequency of the load $\beta$ is the frequency of the longitudinal oscillation of the load and $\lambda$ is a parameter depending on the natural frequencies of the plate as follows:

$$\bar{\lambda}^2 = (m^2 + (\alpha_1 n)^2)^2 + \alpha_2 m^2 + \alpha_3(\alpha_1 n)^2 + \alpha_4$$

When the circularly orbiting force is also variable the conditions of (1) above are joined by the following;

$$\bar{\lambda} + \bar{w} = (2i + 1)\bar{\beta} \qquad |\bar{\lambda} - \bar{w}| = (2i + 1)\bar{\beta}$$

Crocker (1967) has aanalytically determined the response of a simply supported panel to a sinusoidally oscillating schock wave. He found that not only do modal resonances occur when the rotation frequency is equal to a resonance frequency w but also to an infinity of subharmonics w/3, w/4 etc. It is possible that a component of gear action running round the gear circumference may similarly excite subharmonics. It may be seen therefore, that very many natural frequencies (in bending) are capable of excitation by the impulsive and rotational nature of the gear excitationa mechinism.

Naturally, with real gear action all types of plate wave wwill be set up and their corresponding modes or standing wave patterns will occur. The surface waves and pulse shapes produced by Hertzian impact on an infinite half solid have been theoretically described by Tsai (1966) where the Hertz impact theory is again verified. According to Sinclair (1963) quoting Lamb (1917) the flexural wave motion set up in a thin plate is of two types asymmetrical and symmetrical and in fact mostly of the slow moving 'asymmetrical' type with velocity c,where $0 < c < c_r$ where $c_r$ is the velocity of Rayleigh waves, though the wave predominating depends on the duration of impact. The main alternative modes set up by gear action will be torsional and radial and they have been dealt with by Kleesattel (1968). Waves other than bending have not been considered here however, because the frequencies of these other modes are much higher than those of bending waves, and also bending waves couple far more effectively into the air. Even though gear action itself will tend to predominantly excite torsional and radial waves it is assumed that there is sufficient convertion between the various wave types for beding waves to cause the majority of the radiation from gear wheels. The

propagation of stress waves in solids has been dealt with by Kolsky (1953) and those due to impact reviewed by Sinclair (1964), those in plates and tubes have been covered by Redwood (1960). The speckle correlation interferometer of Archbold et at is an ideal tool for studying in-plane motions which correspond to the torsional and radial modes in real gears. To simulate the excitation action giving rise to radial and torsional waves the ball bouncer could be set to strike a tooth like appendage fixed to the circumference of the plate and this is another suitable project for further work.

(ii) <u>The Displacement of the Disc Surface</u>

(a) There are many expressions given for the displacement of the disc surface for the different conditions of support and different thickness to radius ratios. Lord Rayleigh gives Kirchoffs analysis for a rigid disc (1945). The differential equation used by Rayleigh for the motion of the disc is:

$$(\nabla^2 - k^2)(\nabla^2 + k^2)\eta = 0 \qquad (3)$$

Where $$\nabla^2 = \frac{d^2}{dr^2} + \frac{1}{r}\frac{d}{dr} + \frac{1}{r^2}\frac{d^2}{d\theta^2} \qquad (4)$$

and the assumed solution is, neglecting the time varying term, of the form

$$\eta(r,\theta) = (A(J_n(k_p r) + \lambda J_n(k_p r))\cos(n\theta + \alpha) \qquad (5)$$

The term $\cos(n\theta + \alpha)$ gives rise to nodal diameters and the term $J_n(k_p r) + J_n(ik_p r)$ gives rise to nodal circles. $(J_n(ik_p r) = i^n I(k_p r))$

(b) This is not the most general solution however, which was given by Southwell (1922) as the solution of the equation:

$$\rho\frac{\partial^2 w}{\partial t^2} + \frac{Eh^2}{3(1-\sigma^2)}\left[\frac{\partial^2}{\partial r^2} + \frac{1}{r}\frac{\partial}{\partial r} + \frac{1}{r^2}\frac{\partial^2}{\partial\theta^2}\right]^2\eta = 0 \qquad (6)$$

The solution is of the form:

$$\eta = W\sin(s(\theta - \theta_0))\sin(f(t - t_0)) \qquad (7)$$

Where s = number of nodal diameters and f is the modal frequency.

on substitution of (7) in (6) we get:

$$\left( \frac{d}{dr^2} + \frac{1}{r}\frac{d}{dr} - \frac{s^2}{r^2} \right)^2 W - k^4 W = 0 \qquad (8)$$

Where $$k^4 = \frac{3(1-\nu^2)\rho f^2}{Eh^2}$$

and so the complete expression for 'W' is found as the sum of the solutions of the following two equations:

$$\left[ \frac{d^2}{dr^2} + \frac{1}{r}\frac{d}{dr} - \frac{s^2}{r^2} + k^2 \right] W = 0 \qquad (9)$$

$$\left[ \frac{d^2}{dr^2} + \frac{1}{r}\frac{d}{dr} - \frac{s^2}{r^2} - k^2 \right] W = 0 \qquad (10)$$

Thus the complete general solution (given also by Bodine 1967) is:

$$(r,\theta) = ( a_1 J_n(k_p r) + a_2 Y_n(k_p r) + a_3 I_n(k_p r) + a_4 K_n(k_p r)) \sin(n\theta + \theta_o)$$

Where $J_n$ and $Y_n$ are Bessel functions of the first and second kinds and $I_n$ and $K_n$ are modified Bessel functions of the first and second kinds. This expression was also used by Kirk and Leissa (1967) to calculate the effects of a circular reinfircing ring using appropriate boundary conditions at the ring; and by Amon and Widera (1970) for the effects of the ring at radius r = a simply supported.

(c) Stavsky and Loewry (1971) have also given a yet more general equation for axisymmetric vibrations of a composite disc including the effects of rotary inertia following the work of Mindlin (1951), Deresiewicz and Mindlin (1955) and Deresiewicz (1956) which includes extra terms in $J_o(kr)$

$$W_{n=0}(r) = -( G_1(J_o \mu_1 r)/\mu_1 + G_2(J_o \mu_2 r)/\mu_2 - G_3(I_o m_3 r)/m_3 + H_1(Y_o \mu_1 r)/\mu_1 + H_2(Y_o \mu_2 r)/\mu_2 + H_3(K_o m_3 r)/m_3 ) \qquad (12)$$

Equation (12) applies to an anhular plate when $H_i$ and $G_i$ are found with the aid of the extra boundary conditions applicable. It is fortunate however, that the three constants $H_i$ vanish for a complete disc - i.e.

a disc that is <u>not</u> annular in form.

(d) In general different differential equations are solved by workers dealing with thick plates. For example, Ono and Yano (1968) obtain the following general solution for a thick disc, which includes terms allowing for the distance of the top and bottom surfaces of the disc from the central plane i.e. $z = \pm h$ is the surface.

$$\eta(r,\theta,z) = (\alpha B\cos(\alpha z) - \frac{k}{r} D\cos(\gamma z))J_n(kr)\sin(n\theta) \qquad (13)$$

Where $\frac{D}{B} = \frac{((1-\tau)q^2+p^2)\sin p}{(\tau q^2 - 2p^2)\sin q} = \frac{(2-\tau)pq\cos p}{((1-\tau)q^2 + p^2)\cos q}$

and $\tau = \frac{2\mu}{\lambda+2\mu} = \frac{1-2\sigma}{1-\sigma}$ $\lambda$ and $\mu$ are Lame constants

$p = \alpha h$ $q = \gamma h$ $\rho$ is the plate density

$k^2 = \frac{\rho w^2}{\lambda+2\mu} - \alpha^2 = \frac{\rho w^2}{\mu} - \gamma^2$ is the radial wave number

Potter and Leedham (1971) obtain a very similar expression for a thick disc for axisymmetric vibrations which has, however, more terms involving 'cos(const.z) and sin(const.z)' included.

(e) There are also expressions given for many other contingencies, for example non-linear high amplitude vibrations (Tobias 1957 and Nestov 1965) which we will not consider here. Since we are dealing with the analysis of plat plates of medium thickness clamped at the center or at small radius and without stiffening rings the analysis of Southwell will be used below.

When the center is clamped at a very small radius the terms $Y_n(k_p r)$ and $K_n(k_p r)$ vanish (Rayleigh, Kirk and Leissa, Amon and Zimmerman and Widera) since when $r \to 0$ these Bessel functions tend to infinity. Thus the general solution reduces to:

$$\eta(r,\theta) = A(J_n(k_p r) + I_n(k_p r))\sin(n\theta)$$

Where we continue to neglect the time varying term. N.B. for a membrane even $I_n(k_p r)$ may be removed but for annuli and large clamping radii all the terms must be included.

When $n = 0$ , at the disc center therefore:

$$0 = A( J_0(0) + \lambda I_0(0) ) \quad \text{therefore} \quad \lambda = -1$$

Lett the maximum amplitude of movement be '$d_o$' which in the case of the umbrella mode occurs at $r = a$ therefore:

$$d_o = A( J_0(k_{oo}a) - I_0(k_{oo}a) )$$

where $k_{oo}a$ is the value of $K_p a$ when $s = n = 0$ . From Southwell $k_{oo}a \doteq 1.6$ in this case therefore

$$A = \frac{d_o}{J_0(1.6) - I_0(1.6)} = - \frac{d_o}{}$$

and so for each mode the motion of the disc surface is now completely defined. We will use equation (14) in the sound radiation derivations below.

## AII.3) Radiation From A Modal Piston

### (i) Discussion of Radiation Theory

The most important single factor in radiation theory can be regarded as the coincidence critical frequency ($f_c$). This is the lowest frequency at which the projected wavelength of sound in air is equal to the bending wavelength in the plate. The bending wavelength in a plate is given by:

$$\lambda_p = \left( \frac{1.8\,h}{f} \left( \frac{E}{\rho(1-\sigma^2)} \right)^{\frac{1}{2}} \right)^{\frac{1}{2}}$$

and therefore the coincidence critical frequency is given by :

$$f_c = \frac{(c_{air})^2}{1.8\,h} \left( \frac{\rho_p}{E} \right)^{\frac{1}{2}} \qquad (15)$$

where h is the plate thickness in cms f is the frequency $\rho$ is the plate density and E is Young's modulus, $c_{air}$ is the velocity of sound in air.

The coincidence effect was first described by Cremer (1942). In the case of an infinite plate there would be no radiation at frequencies below $f_c$, but in the case of finite plates radiation occurs where the bending waves interact with edge discontinuities or inhomogeneities in the panle giving rise to uncancelled volume velocities. Below coincidence the panel, vibrating in a given modes shape, may be thought of as being split up into phase cells whose boundaries are nodal lines. The volume velocity of each cell cancels out that due to each neighbouring cell until the boundaries (or inhomogeneities causing differences in the amplitudes of the effective average volume velocities of each cell) are reached. There will be uncancelled terms of volume velocity remaining at the boundaries and these will radiate. If the panel size is larger than the acoustic wavelength, these uncancelled volume velocities at the edges and or conners and/or inhomogeneities of the panel can be treated as independent radiators. If the panel size is smaller than the acoustic wavelength

at the modal frequency then these simple radiators will interact with each other. The most significant contributions to this theory are due to Maidanik (1962) and Lyon (1964). Their theory has been extended by Davies (1971), from the panel sizes either greater or smaller than the acoustic wavelength, to the case when the acoustic wavelength is comparable with the dimensions of the panel, and also extended by Nikiforov (1963) who dealt with different boundary conditions. It has also been treated in simplified form by Crocker in a series of papers, in particular (1968) and a Ph.d thesis (1969) where one of Maidanik's formulae is corrected. Their analysis is discussed more fully below and their results, which are for a rectangular panel, presented prior to the calculation of similar expressions for a circular modal panel.

At and above the critical frequency the panel radiates sound wave in which the particle displacement is nearly equal to the surface displacement of the panel itself (Beranek 1959), the air wave will then be radiated at the coincidence angle. Westphal (1957) and Gosele (1956) have shown that below $f_c$ the radiated sound may be 20 db less than that radiated above it for the same amplitude of bending wave (Fig 59 ). The graphs indicate the effect of damping above and below $f_c$ for an infinite and a finite panel, and the amplitude of the bending waves after damping is restored to its former value by increasing the excitation. In practice of course, the amplitude and hence the radiation would be reduced for a given excitation (see also Heckl (1967) where it is shown that there is a limit to the amount of damping which may be effectively applied (page 204).

In general the power radiated from a simply supported panel is proportional to the 'perimeter' of the panel (if stiffners are present they contribute twice their length to the perimeter for vibrations below $f_c$ , and to the area of the panel above the critical frequency (Crocker 1968 and Maestrello 1967). When the boundaries are clamped the radiation

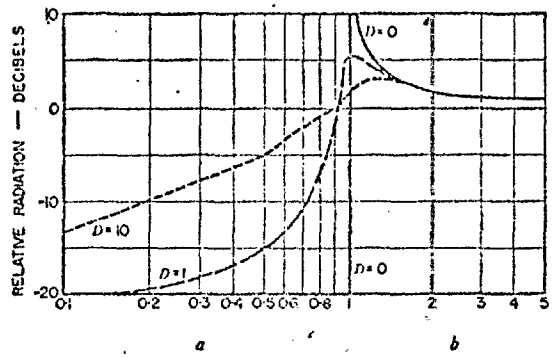



*Fig 59a Relative Radiation of a Free-travelling Plane Bending Wave from an Infinitely Large Plate*

The parameter D is the damping of the bending wave (in dB/wavelength). (After Westphal (28).)

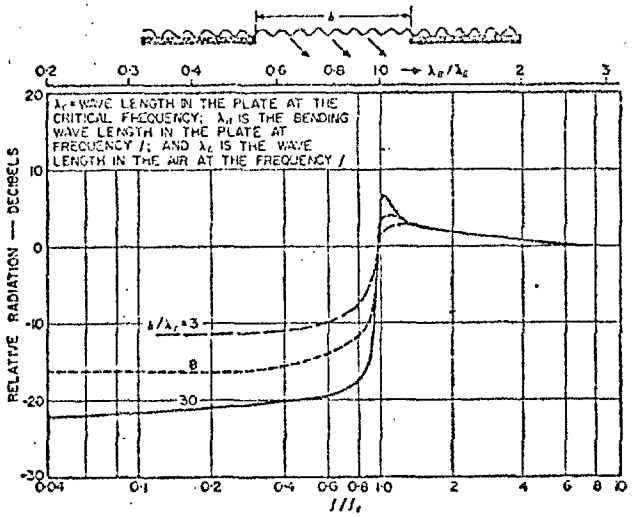



*Fig. 59b Effect of Finite Plate Size (Width b) on the Radiation Efficiency of Plates*

Note both the upper and lower ordinates. *D* (Fig. 16) is equal to about 0·01. (After Goesele (31).)

from the panel will be twice that of the simply supported case below $f_c$ - since at low frequencies there will be a contribution from the near field which is then produced at the edges and which is not produced in the simply supported case. However, above $f_c$ the radiation resistance is approximately the same as that for the simply supported case (Maidanik 1962, Heckl 1960).

(ii) Treatment of Objects to Reduce Sound Radiation

The first and most obvious treatment is the addition of one or more damping layers. If the properties of the layer are suitably chosen a reduction of the mean square vibrational velocity of the object will result for a given exciting force and there will be consequently less radiation. Heckl (1967) states that damping treatments are most effective when the sound is radiated by one resonant mode and in this case the damping produces a reduction in the mean square velocity which is proportional to $1/\eta^2$ where $\eta$ is the loss factor which = $W''/2\pi W'$ where $W''$ is the energy lost per cycle and $W'$, the stored energy of bending waves, is proportional to the bending stiffness. If many modes of the structure are responsible for the radiation the total radiated power can be expressed as:

$$P_r = \frac{S}{2} \sum v_n^2 \sigma_n$$

where $v_n$ is the modal velocity and $\sigma_n$ is the radiation coefficient which is a complicated function but is approximately equal to unity for low frequency modes and very small for high frequency modes. It may be possible that the application of a damping treatment reduces the mean square velocity but has little effect on the radiated power. Below the coincidence critical frequency, the radiated power from a point driven thin plate is given by: (Heckl 1967)

$$P_r = \frac{F^2 \rho_o}{4\pi c_o m^2} \left( 1 \quad \frac{U}{2 S k_p \eta} \right)$$

Where F is the exciting force, $\rho_o$ is the density of the air, $c_o$ the sound velocity in air , S the area of the plate of circumference U, m the mass per unit area and $k_p$ the wavenumber ($2\pi/\lambda$) for bending waves. It may be seen that increasing the damping beyond a certain value $\eta_{limit} = U/2Sk_p$ has no further effect on the radiated sound.

Various observers including Fryer et al (1967) have demonstrated the effect of damping on the sound transmission curve, it may be seen (appendix III) that the effect of panel resonances in increasing the transmission above that given by the mass law may be completely removed by damping. The acoustic transmissivity has been related to the radiation from the plate by Shenderov (1967) where they are shown to be directly proportional to one another. Thus transmission loss curves give an indication of the way in which the radiation from a panel will vary with frequency under constant excitation. According to Shenderov:

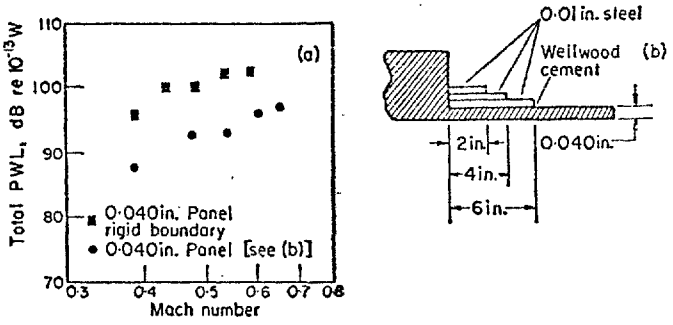
$$B = \frac{c\rho}{S\cos\theta}\int_S v_o(r)\, e^{ik\,r}\, dS \qquad P = \frac{-iw\, e^{ik\,R_o}}{4\pi R_o}\int_S v_o(r) f(r) dS$$

Where P is the acoustic pressure generated by the plate at distance $R_o$ along the axis, f(r) is the plate forcing function, $v_o(r)$ is the velocity function of the plate (i.e. the mode shape function) $\rho$ is the air density, $B = P_d / P_d^o$ is the acoustic transmissivity and $P_d$ is the acoustic pressure at point 'd' due to source at 'q' behind the plate with the plate in position, and $P_d^o$ is the pressure at the same point without the plate. It may be seen that both the above expressions depend on the mode shape $v_o(r)$.

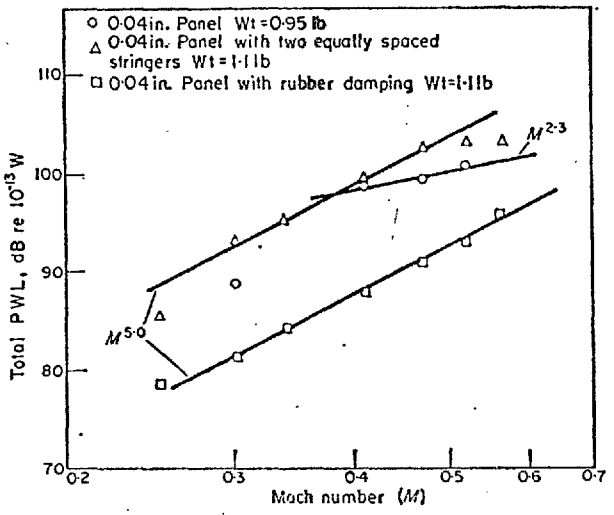
The effective application of damping material is greatly aided by a knowledge of the way in which the objects are vibrating. In the above papers the damping was applied over the whole area of the plates concerned. The present experiments have confirmed that damping may be applied more effectively at antinodal regions or regions of high stress depending on the type of damping applied. When brass plates were being investigated

a piece of plasticine was placed at the observed antinode of the 4 nodal diameters mode and the amplitude of the vibration was reduced, for the same excitation, from about 20 fringes to one fringe and the sound pressure and the resulting sound pressure was reduced from 115 db to 97 db. The experiments on sandwich cone Loudspeakers have demonstrated this effect even more clearly. The one nodal circle mode for the sandwich bass Loudspeaker is responsible for a very sharp peak in the response curve which is over 12 db in height. The application of damping material (either plasticine or bitumenised felt) to an antinode of this resonance completely removed its effect on the response curve. The application of a simple massive'weighting ring' (which is normally used to provide a mechanical 'cross-over' action by rolling off the treble frequencies) to the same area - the voice coil - merely altered the frequency of this mode and only slightly reduced its amplitude. In both the above examples the damping material probably acts as a combination of seismic mass with a lossy coupling and further experiments are called for along these lines. Incidentally all the modes of the sandwich Loudspeaker are of the nodal circle type and so they all have antinodes at the voice coil allowing the above treatment to either completly eliminate them or greatly reduce their effect on the response curve - a clear example of how a knowledge of the behaviour of the vibrating object can lead us to more effective ways of eliminating unwanted resonances.

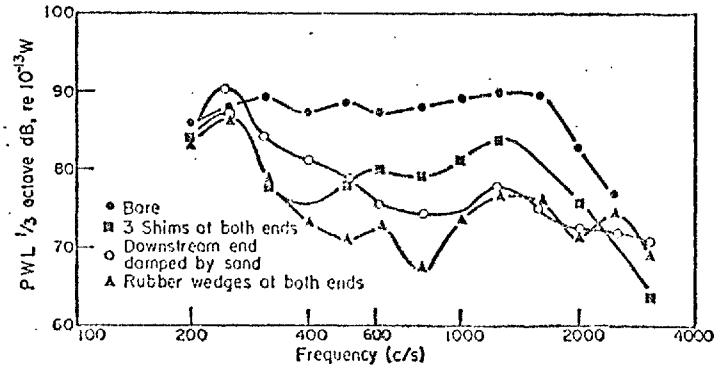
Below $f_c$ the major source of sound radiation arises from the interaction of plate bending waves with boundaries and/or inhomogeneities. Maestrello (1967) states that for rectangular panels where the distance between the uncancelled volume velocities remaining at the discontinuities is more than a wavelength then for odd-odd modes the radiation is equivalent to monopole radiation, for even-odd modes to dipole radiation, and for even-even modes to quadrupole radiation. Maestrello claims an average reduction of as much as 10 db in the sound radiation below coincidence




Total acoustic power (36 in. × 6·5 in. panel).




Total acoustic power (36 in. × 6·5 in. panel).




Sound power level for 36 in. × 6·5 in. × 0·04 in. panel at $M = 0·47$.

Figure 59 (c) Maestrello's curves showing the effect of different terminations at panel ends

with the addition of 15 percent extra weight to modify the panel boundaries, and so reduce the uncancelled volume velocities. Rubber wedges gave the best results, damping the ends with sand the next best, and stiffening up the ends with a progressively thickening layer of shims of steel gave the least reduction-which was still of the order of 5 db on average. Nikiforov has given the following table comparing expressions for the power radiated from a plate and the reflection coefficient for bending waves for several different boundary conditions below $f_c$. It may be seen that the edges radiate most effectively when clamped and weakly when there is minimal impedance to bending waves at the edge. Nikiforov also shows that when the plate is small in comparisom with the air wavelength the radiation is twice that radiated when the plate is large ($k_a a >> 1$ )

| Boundary Conditions, below $f_c$ for a 'large' panel | $\alpha$ | $\beta$ | $W = \frac{4\rho_o w r v_o^2}{k_b^2}$ mult. by: |
|---|---|---|---|
| Edges free; $z_f = z_m = 0$ | 0 | 0 | 0 |
| -supported; $z_f = \infty$ $z_m = 0$ | $\infty$ | 0 | 4 |
| -clamped $z_f = z_m = \infty$ | $\infty$ | $\infty$ | 8 |
| $z_f = 0$ $z_m = \infty$ | 0 | $\infty$ | $2k_a^2/k_b^2$ |

Nikiforov also gave values for intermediate edge conditions.

$z_f$ and $z_m$ are the impedances to transverse force and bending moment resp. $k_b$ is the flexural wave number, $\alpha = z_f/z_{of}$, $\beta = z_m/z_{om}$ $z_{of} = mc_b$ $z_{om} = mc_b/k_b^2$ $c_b$ = bending wave velocity. m = plate mass per unit area The values of W given in the above table were derived from the following formula:

$$W = \frac{4\rho_o w v_o^2}{k_b} \left( 2|\phi|^2 + \frac{k_o^2}{k_b} |\psi|^2 \right) \text{ for } k_a a << 1$$

and W is halved when $k_a a >> 1$

Where $\phi = -j + jR - R'$ and $\psi = -1 - R + R'$

where R and R' are the reflection coefficients of travelling and inhomogeneous bending waves given by:

$$R = \frac{1 - j - 2\alpha + 2j\beta + \alpha\beta(1-j)}{1 + j + 2\alpha + 2j\beta + \alpha\beta(1+j)}$$

$$R' = \frac{2(1 - \alpha\beta)}{1 + j + 2\alpha + 2j\beta + \alpha\beta(1+j)}$$

Using the above expressions we can calculate the energy radiated by the plate for any boundary conditions at the edges, for instance when $z_f = z_{of}$ and $z_m = z_{om}$ then $\alpha = \beta = 1$ and $W = \frac{4\rho_o w v_o^2}{k_b^2}\left(1 + \frac{2k_a^2}{k_b^2}\right)$

Sound radiation may therefore be reduced by altering the conditions of the edge support when the frequency is below the coincidence critical frequency

The fact that sound radiation coefficients are much lower below $f_c$ gives rise to another line of approach in reducing the sound radiation from a body. The material out of which the gear, panel or speaker cone is made or the thickness of the material may be chosen so that $f_c$ is well above the working region. Resonant frequencies are brought down in the same ratio that $f_c$ is raised - thus more modes occur below $f_c$ after 'treatment' but their radiation coefficients will be greatly reduced. This technique, as mentioned above (Section IV), may be particularly applicable to sandwich bass Loudspeakers (though the use of a 'lossy' bung is very satisfactory) since the critical frequency occurs inside the working range - a halving in the stiffness will give worthwhile results.

The calculation of the sound pressures and radiation resistances of acoustically large and small panels above and below $f_c$ are found below. Crocker and Maidaniks results give an indication of the relative radiation resistances for rectangular plates - which may be loosly applied to circular ones. McLachlan early results for a circular modal piston only apply to one or two of these cases (i.e. above & below $f_c$ , or acoustically large or small) and it is hoped that the further analysis

attempted here will give results equivalent to those of Crocker but for the case of a circular modal plate.

(iii) Theory Applied to Rectangular Plates

From Crocker (1968), drawing from the work of Maidanik (1962): Assuming that there are many point acoustic sources distributed on an infinite plane then the pressure at a point distance R from the plane is:

$$P_R = \frac{iw\rho_a v_o e^{-ikR}}{4\pi R}\left(-2\int_{\text{area of panel}} \psi_m(\bar{r}) e^{-i\bar{k}_a\cdot\bar{r}}\, dr\right) \qquad (22)$$

where $k_a = (2\pi f)/c_{air} = 2\pi/\lambda_{air}$ and $\psi_m(\bar{r})$ is the function describing the distribution of the velocity sources on the plane - the mode shape function. The directivity function $\Gamma$ may be defined as follows:

$$\Gamma(\bar{k}_a) = -2\int_{\text{area}} \psi_m(\bar{r}) e^{i\bar{k}_a\cdot\bar{r}}\, dr \qquad (23)$$

where $\rho_a$ = air density, $c_a$ = air velocity, $v_o$ = velocity of panel. Now the sound intensity is given by:

$$I = \frac{\langle p^2\rangle_t}{\rho_a c_a} = \frac{|p|^2}{2\rho_a c_a} = \frac{w^2\rho_a^2 v_o^2}{2\rho_a c_a 16\pi^2 R^2}\left|\Gamma(\bar{k}_a)\right|^2 \qquad (24)$$

and so the power radiated into an element of area dS at distance R, where $dS = Rd\theta Rd\psi$ and the element of solid angle $d\Omega = d\theta d\psi$ is:

$$dW = IdS = \frac{1}{2c_a}\frac{w^2\rho_a v_o^2}{16\pi^2 R^2}\left|\Gamma(\bar{k}_a)\right|^2 d\Omega \qquad (25)$$

Therefore the total power radiated is found by integrating this expression over the halfspace above the plane of the baffle in which the panel is situated, giving finally:

$$W_{tot} = \left(\frac{1}{2}v_o^2\frac{k_a^2\rho_a c_a}{8\pi}\right)\left(\frac{1}{2\pi}\int_{\frac{1}{2}\Omega}|\Gamma|^2\, d\Omega\right) \qquad (26)$$

$$W_{tot} = \frac{1}{2} v_o^2 \left( \frac{k_a^2 \rho_a c_a}{8\pi} \right) \langle |\Gamma|^2 \rangle_{\frac{1}{2}\Omega} \qquad (27)$$

$$= v_{rms}^2 \left( \frac{k_a^2 \rho_a c_a}{8\pi} \right) \langle |\Gamma|^2 \rangle_{\frac{1}{2}\Omega}$$

also

$$P_{tot} = v_{rms}^2 \; R_{rad} \qquad \text{where } R_{rad} \text{ is the radiation resistance}$$

and therefore:

$$R_{rad} = \frac{k_a^2 \rho_a c_a}{8\pi} \langle |\Gamma|^2 \rangle$$

$$= \left( \frac{k_a^2 \rho_a c_a}{8\pi} \right) \left( \frac{1}{2\pi} \int_{\psi=0}^{\psi=2\pi} d\psi \int_{\theta=0}^{\theta=\frac{\pi}{2}} d\theta |\Gamma|^2 \right) \qquad (28)$$

$\frac{1}{2}$ space

The term $i \exp(-i\bar{k}_a.\bar{r})$ gives a measure of the interaction between individual radiators and is similar in effect to Maidaniks "$R_{ij}$" and his acoustic field cross correlation $\phi(x_1x_2) = \sin(k_a r)/r$ where r is the distance between $x_1$ and $x_2$ (see below). This interaction term is also taken care of in Bouwkamp's contribution to the theory of the radiation from a modal membrane (1946) used in the analysis below. The expression for the radiation resistance given by Lyon and Maidanik (1962) is:

$$R_{rad}(w) = \left(\frac{16}{\pi^4}\right) \rho_a c_a k_a^2 \iint_{-\infty}^{+\infty} dx_1 dx_2 \, \psi(x_1x_2) \phi(x_1x_2) \qquad (29)$$

where the term within the integral sign is zero outside the panel boundaries. This expression was derived using statistical modal analysis and considering the power flow between coupled oscillators (an important result from this technique is that power flows until all loosly coupled oscillators have the same energy). $\psi(x_1x_2)$ is the vibration field cross correlation which included the mode shape function, and $\phi(x_1x_2)$ is the acoustic field cross correlation which gives a measure of the acoustic interaction between neighbouring regions of the plate. A similar expression is derived by Maidanik when considering the panel as an assemblage of monopoles having the amplitude and phases given by their position in the appropriate mode shape function of the panel. In this case the power

radiated by an assemblage of monopoles is:

$$W_{tot} = \langle v_p \rangle^2 R_{rad} = \frac{1}{2} \sum_{ij} R_{ij} U_i U_j^* \qquad (30)$$

where $U_i$ is the amplitude of the volume velocity of the ith monopole which is equal to $dx_i dy_i v_{xy}$ where $v_{xy}$ is the amplitude of the velocity of the i th monopole determined by the mode shape function. $R_{ii}$ is the radiation impedance of the i th monopole in the absence of all the other monopoles and $R_{ij}$ $(i \neq j)$ is the measure of the coupling between the i th and the j th monopoles i.e. the mutual radiation impedance of the i th and j th monopoles.

$$R_{ij} = \frac{1}{2\pi} \rho_a c_a \frac{\sin k_a r_{ij}}{k_a r_{ij}} = \rho_a c_a f \frac{\sin k_a r_{ij}}{r_{ij}} \qquad (31)$$

where $r_{ij}$ is the distance between the i th and the j th monopole. The '1/2' is included in the expression for $W_{tot}$ to allow for the fact that the i th monopole influences the j th in the same way that the j th influences the i th i.e. each term appears twice. Replacing the summations with integrals over the area of the panel we obtain an expression similar to that of Crocker and Bouwkamp. The coupling term is automatically taken care of in the derivation of the pressure at a distance R from a simple piston below used as a basis for the calculation of the pressure from a modal piston.

The mode shape function for a rectangular panel is:

$$\Psi_m(x,y) = 2 \sin(k_{px}x)\sin(k_{py}y) \qquad (32)$$

where

$$k_{px} = \frac{2\pi}{\lambda x} = \frac{m_x \pi}{l_x}, \quad k_{py} = \frac{m_y \pi}{l_y} \quad \text{i.e. } k_p = \frac{2\pi}{\lambda_{\text{bending in panel}}}$$

where $l_x$ and $l_y$ are the half lengths of the panels in the 'x' and 'y' directions respectively and $m_x$ and $m_y$ are the numbers of elastic half waves in the x and y directions for each mode.

Crocker used the above mode shape and the expression given in equation (28) above to derive the formulae below for the radiation resistance of a rectangular panel at above and below $f_c$ for both an acoustically large and small panel. Maidanik includes a few more cases in his results (1962) which are extended by Davies (1971) to when the size of the panel is equivalent to the acoustic wavelength in air, the formulae are:

(1) Large Panel $2\pi l_x/\lambda_a > 1$ and $2\pi l_y/\lambda_a > 1$

(a) Above $f_c$ $k_p/k_a < 1$ i.e. $k_a > k_{px}$ and $k_a > k_{py}$

In Crocker's terminology both directions 'x' and 'y' are acoustically fast and the whole panel radiates giving:

$$R_{rad} = \rho_a c_a A_p (1 - f_c/f)^{-1/2} \qquad (33)$$

where $A_p$ = area of the panel.

(b) Above $f_c$ with $k_a > k_{px}$ but $k_a < k_{py}$ i.e. one direction acoustically fast, the other direction acoustically slow. In this case only the uncancelled volume velocities at the edges parallel to the x direction will radiate giving:

$$R^x_{rad} = \frac{2 k_a \rho_a c_a l_x}{k^2_{py}} \quad \text{similarly } R^y_{rad} \qquad (34)$$

(c) Below $f_c$ with both $k_a < k_{px}$ and $k_a < k_{py}$ i.e. both directions acoustically slow. In this case only uncancelled volume velocities at the corners of the panel will radiate and these will radiate independently provided the air wavenumber $k_a$ is larger then both $l_x$ and $l_y$ giving:

$$R_{rad} = \frac{8 k^2 \rho_c a^2}{m^2_x m^2_y \pi^4} \qquad (35)$$

(2) Small Panel $2\pi l_x/\lambda_a < 1$ and $2\pi l_y/\lambda_a < 1$

(a) Above $f_c$

$$R_{rad} = 2\rho_a c_a A_p (1 - f_c/f)^{-1/2} \quad (36)$$

which is twice the result for a large panel

(b) At $f_c$

$$R_{rad} = 2\rho_a c_a A_p \left( \left(\frac{l_x}{c}\right)^{1/2} + \left(\frac{l_y}{c}\right)^{1/2} \right) \quad (37)$$

(c) Below $f_c$

$$R_{rad} = 2\rho_a c_a A_p \left( \frac{\lambda_c \rho_a}{A_p} 2\left(\frac{f}{f_c}\right) g_1\left(\frac{f}{f_c}\right) + (P\lambda_c/A_p) g_2\left(\frac{f}{f_c}\right) \right) \quad (38)$$

where $\lambda_c$ = wavelength of bending waves in the panel at $f_c$

and

$$g_1\left(\frac{f}{f_c}\right) = \left(\frac{4}{\pi^4}\right)\left( 1 - 2\left(\frac{f}{f_c}\right) \Big/ \left(\frac{f}{f_c}\right)^{1/2} \left(1 - \left(\frac{f}{f_c}\right)\right)^{1/2} \right) \quad \text{for } f < \tfrac{1}{2} f_c$$

$$= 0 \quad \text{for } f > \tfrac{1}{2} f_c$$

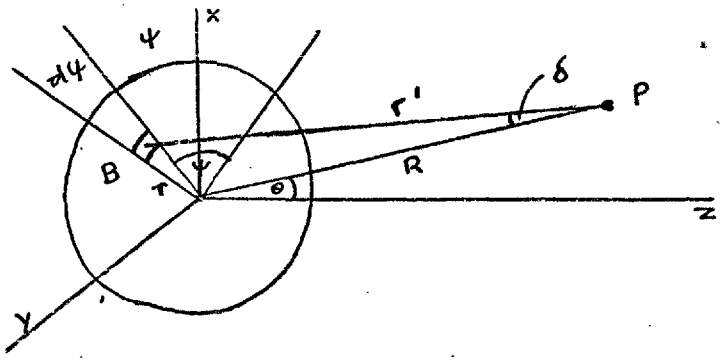
and

$$g_2\left(\frac{f}{f_c}\right) = \left(\frac{1}{4\pi^2}\right)\left( (1 - \frac{f}{f_c}) \log_e \left( (1 + \left(\frac{f}{f_c}\right)^{\frac{1}{2}} \Big/ (1 - \left(\frac{f}{f_c}\right)^{\frac{1}{2}}) + 2\left(\frac{f}{f_c}\right)^{\frac{1}{2}} \right) \right) \Big/ (1 - \frac{f}{f_c})^{3/2}$$

Maidanik (1962) also gives expressions for the radiation resistance of odd and even numbers of equivalent monopoles representing the mode segments in both the 'x' and 'y' directions.

(iv) Theory Applied to Circular Plates

(a) Calculation of The Sound Pressure From a Modal Piston




$\Psi_o$ on object (for modes)

$\Psi$ in space

Starting with basic piston theory (D.I.C. notes). Each element of area B is small enough to be considered a simple source. Therefore the pressure at point 'P' due to the element of area 'B' is:

$$dp = j\omega \rho_a \dot{d}\, e^{j\omega t}\, \frac{e^{-jk_a r'}}{2\pi r'}\, dA \qquad (39)$$

where dA is the element of area at point 'B' = $r dr d\Psi_o$, $\dot{d}_o = i\omega d_o$

and $d_o$ is the maximum movement of the disc surface. 'd' the movement of an arbitrary element of area is a function of both r and $\Psi_o$ ie $\dot{d} = \dot{d}_o F(r, \Psi_o)$

Now from notes if $R >> r$ it can be shown that:

$$dp = \frac{j\omega \rho_a}{2\pi R}\, \dot{d}_o F(r, \psi_o)\, e^{j(\omega t - k_a[R - r\cos(\psi - \psi_o)\sin\theta)}\, r\, dr\, d\psi_o \qquad (40)$$

utilising the fact that:

$$(r')^2 = R^2 + r^2 - 2rl\cos\delta$$

$$\cos\delta = \sin\theta\cos(\psi - \psi_o) . \qquad (41)$$

Therefore the total pressure at point 'P' due to the whole modal piston is:

$$p = \frac{\rho_a \omega^2 d_o}{2\pi R}\, e^{j(\omega t - k_a R)} \left[ \int_{r=0}^{r=a} r\, dr \int_{\psi_o=0}^{\psi_o=2\pi} F(r, \psi_o) e^{-jk_a r \sin\theta \cos(\psi - \psi_o)}\, d\psi_o \right] \qquad (42)$$

The term in the square brackets is equivalent to " $K(\theta\psi)$" of Bouwkamp(1946)

Now Let:

$$'Q' = \left\{ \frac{\rho_a \omega^2 d_o\, e^{j(\omega t - k_a R)}}{2\pi R} \right\} \qquad (43)$$

and so:

$$p(R, \theta, \psi, t) = Q \int_{r=0}^{r=a} r\, dr \int_{\psi_o=0}^{\psi_o=2\pi} F(r, \psi_o)\, e^{-jk_a r \sin\theta \cos(\psi - \psi_o)}\, d\psi_o \qquad (44)$$

Now for a vibrating disc or annulus, from Southwell (1922)

$$F(r,\psi_o) = (AJ_s(k_p r) + BY_s(k_p r) + CI_s(k_p r) + DK_s(k_p r))\cos(s\psi_o)e^{jwt} \quad (45)$$

where s is the number of nodal diameters present.

we will have a separate integral for each Bessel function $A_i Z_i(k_p r)$

$$p(r,\theta,\psi,t) = Q\sum_{i=1}^{4}\int_0^a r\,dr\int_{\psi_o=0}^{2\pi}\left[A_i Z_i(k_p r)\right]\cos s\psi_o\, e^{-ik_a r\sin\theta\cos(\psi-\psi_o)}\,d\psi_o \quad (46)$$

Now from Bouwkamp (1946) mathematical appendix:

$$\frac{1}{2\pi}\int_0^{2\pi} e^{-iz\cos(\psi-\psi_o)}\cos s\psi_o\,d\psi_o = \cos s\psi\; e^{-\frac{s\pi i}{2}} J_s(z) \quad (47)$$

that is:

$$\int_0^{2\pi} e^{-ik_a r\sin\theta\cos(\psi-\psi_o)}\cos s\psi_o\,d\psi_o = 2\pi i^{-s}\cos(s\psi)J_s(k_a r\sin\theta)$$

Therefore:

$$p(r,\theta,\psi,t) = \frac{Q\cos(s\psi)2\pi}{i^s}\sum_1^4\int_0^a r\,J_s(k_a r\sin\theta)\left[A_i Z_i(k_p r)\right]dr \quad (49)$$

Now, when the plate is clamped at the center terms $Y_s(k_p r)$ and $K_s(k_p r)$ go to infinity there, and so they must be left out of a real solution. For $s \geq 1$ the modal frequencies and mode shapes are the same as a completely free disc (Southwell 1922) but only if the clamping radius is small for $s > 1$ and actually equal to zero for $s = 1$. The case $s = 0$ must be treated separately, and this case has been treated approximately by McLachlan (1932) see below. Therefore for a complete disc clamped at the center:

$$F(r\,\psi_o) = \cos(s\psi_o)\left[A\,J_s(k_p r) + B\,I_s(k_p r)\right] \quad (50)$$

giving the following two integrals:

$$p(r,\theta,\psi,t) = \frac{Q\cos(s\psi)2\pi}{i^s}\left[A\int_0^a r J_s(k_a r\sin\theta)\,J_s(k_p r) + B\int_0^a r J_s(k_a r\sin\theta)I_s(k_p r)\right]$$

Now there are standard forms for these two integrals giving:

$$p(r,\theta,\psi,t) = \frac{Q\cos(s\psi)2\pi A}{i^s}\left[\frac{k_p a J_s(k_a a\sin\theta)J_{s+1}(k_p a) - k_a a\sin\theta\, J_{s+1}(k_a a\sin\theta)J_s(k_p a)}{-k_a^2\sin^2\theta + k_p^2}\right]$$

$$+ \frac{Q\cos(s\psi)2\pi B}{i^s}\left[\frac{k_p a J_s(k_a a\sin\theta)I_{s+1}(k_p a) + k_a a\sin\theta\, J_{s+1}(k_a a\sin\theta)I_s(k_p a)}{k_a^2\sin^2\theta + k_p^2}\right] \quad (51)$$

These results may be evaluated in several regions of 'k' space'as follows:

$k_p \gg k_a$ i.e. $\lambda_p \ll \lambda_{air}$ i.e. $f \ll f_c$ below coincidence ($f_c$)

$k_p = k_a$ i.e. $\lambda_p \simeq \lambda_{air}$ i.e. $f = f_c$ at coincidence crit.frq.

$k_p \ll k_a$ i.e. $\lambda_p \gg \lambda_{air}$ i.e. $f \gg f_c$ above coincidence.

and these three conditions may be combined with either a large or small or intermediate plate cf the air wavelength:

$k_a a \ll 1$ i.e. $3a \ll \lambda_a$ small panel wrt.air wavelength.

$k_a a = 1$ i.e. $3a \doteq \lambda_a$ panel approx. equal to air wavelength.

$k_a a \gg 1$ i.e. $3a \gg \lambda_a$ large panel wrt.air wavelength.

We will take these conditions in turn as follows.

(1) Below The Coincidence Critical Frequency . Small Panel

$k_p \gg k_a$ i.e. $k_p/k_a \gg 1$ and $k_a/k_p \ll 1$

also $k_a a \ll 1$ in this case the following approximation may be used:

$$J_s(k_a a \sin\theta) \doteq \frac{(k_a a \sin\theta)^s}{2^s\ s!} \quad \text{and} \quad J_o(k_a a \sin\theta) \doteq 1 \qquad (52)$$

The expression for 'p' given in equation (51) may be split into four terms and so substituting (52) into (51) we have:

Term (1) becomes -

$$\frac{A(k_p a)(k_a a)^s(\sin\theta)^s J_{s+1}(k_p a)}{2^s\, s!\left[-\left(\frac{k_a}{k_p}\right)^2\sin^2\theta + 1\right](k_p)^2} = + \left(\frac{k_a}{k_p}\right)\frac{A\,(a)^{s+1}(\sin\theta)^s J_{s+1}(k_p a)(k_a)^{s-1}}{2^s\, s!}$$

Term (2) similarly -

$$- \frac{A(k_a a \sin\theta)(k_a a)^{s+1}(\sin\theta)^{s+1} J_s(k_p a)}{2^{s+1}(s+1)!\left[-\left(\frac{k_a}{k_p}\right)^2\sin^2\theta + 1\right](k_p)^2} = - \left(\frac{k_a}{k_p}\right)^2 \frac{A\,(a)^{s+2}(\sin\theta)^{s+2} J_s(k_p a)(k_a)^s}{2^{s+1}(s+1)!}$$

(53) & (54)

Term (3) -

$$\frac{B\,(k_p a)(k_a a)^s(\sin\theta)^s\, I_{s+1}(k_p a)}{2^s\, s!\left[\left(\frac{k_a}{k_p}\right)^2\sin^2\theta + 1\right](k_p)^2} = + \left(\frac{k_a}{k_p}\right)\frac{B\,(a)^{s+1}(\sin\theta)^s I_{s+1}(k_p a)(k_a)^{s-1}}{2^s\, s!}$$

Term (4) -

$$\frac{B\,(k_a a\sin\theta)(k_a a)^{s+1}(\sin\theta)^{s+1} I_s(k_p a)}{2^{s+1}(s+1)!\left[\left(\frac{k_a}{k_p}\right)^2\sin^2\theta + 1\right](k_p)^2} = + \left(\frac{k_a}{k_p}\right)^2\frac{B\,(a)^s(\sin\theta)^{s+2} I_s(k_p a)(k_a)^s}{2^{s+1}\,(s+1)!}$$

Giving finally

$$p(R,\theta,t,\varphi) = \cos(s\varphi)\left[\frac{\rho_a \omega^2 d_o e^{j(\omega t - k_a R)}}{R\, i^s}\right]\left[\frac{a^{s+1}(k_a\sin\theta)^s}{k_p^2\, 2^s\, s!}\right]\times$$

$$\left[\frac{a(\sin\theta)^2 k_a^2\{-A J_s(k_p a) + B I_s(k_p a)\}}{2(s+1)} + \frac{k_p\{+A J_{s+1}(k_p a) + B I_{s+1}(k_p a)\}}{}\right] \quad (57)$$

(2) Above The Coincidence Critical Frequency . Small Panel

$k_p \ll k_a$ i.e. $k_p/k_a \ll 1$ and $k_a/k_p \gg 1$

the approximations applying for a small panel are given in equation (52)

In this case the denominator of the above expressions is as follows:

$$\left[\pm\sin^2\theta \quad \left(\frac{k_p}{k_a}\right)^2\right](k_a)^2 = \pm(k_a)^2\sin^2\theta, \qquad \underline{\theta > 0}$$

and so similarly to (1) above

$$p(R,\theta,t,\varphi) = \cos(s\varphi)\left[\frac{\rho_a \omega^2 d_o e^{j(\omega t - k_a R)}}{R\, i^s}\right]\left[\frac{a^{s+1}(k_a\sin\theta)^{s-2}}{2^s\, s!}\right]\times$$

$$\left[\frac{a(\sin\theta)^2 k_a^2\{A J_s(k_p a) + B I_s(k_p a)\}}{2(s+1)} + \frac{k_p\{-A J_{s+1}(k_p a) + B I_{s+1}(k_p a)\}}{}\right] \quad (58)$$

for the same amplitude of panel movement.

values of $k_p a$ are taken from tables giving a value for each disc mode

(3) Above the Coincidence Critical Frequency . Large Panel

All the Brass Discs and all the Loudspeakers used in the present experiments are acoustically large above about 500 Hz i.e. $k_a a > \lambda_a$

When $J_n(x)$ is very large a crude approximation to its behaviour is:

$$J_n(x) = \left(\frac{2}{\pi x}\right)^{1/2} \cos\left(x - \frac{n\pi}{2} - \frac{\pi}{2}\right) \qquad (59)$$

above coincidence:

$$\left[-\sin^2\theta + \left(\frac{k_p}{k_a}\right)^2\right](k_a)^2 = -k_a^2 \sin^2\theta \qquad \theta > 0$$

term (1) now becomes:

$$-\frac{A(k_p a)\, J_{s+1}(k_p a)}{k_a^2 \sin^2\theta}\left(\frac{2}{\pi k_a a \sin\theta}\right)^{\frac{1}{2}} \cos\left(k_a a \sin\theta - \frac{s\pi}{2} - \frac{\pi}{4}\right) \qquad (60)$$
$$\theta > 0$$

term (2) similarly:

$$+\frac{A(k_a a)\sin\theta\; J_s(k_p a)}{k_a^2 \sin^2\theta}\left(\frac{2}{\pi k_a a \sin\theta}\right)^{\frac{1}{2}} \cos\left(k_a a \sin\theta - \frac{(s+1)\pi}{2} - \frac{\pi}{4}\right) \qquad (61)$$

and so finally:

$$p(R,\theta,t,\varphi) = \cos(s\varphi)\left[\frac{\rho_a \omega^2 d_o e^{j(\omega t - k_a R)}}{R\, i^s}\right]\left[\frac{2}{\pi k_a a \sin\theta}\right]^{\frac{1}{2}}\left[\frac{1}{k_a^2 \sin^2\theta}\right]$$

$$\left\{\left[k_p a \cos\left(k_a a \sin\theta - \frac{s\pi}{2} - \frac{\pi}{4}\right)\left\{-A J_{s+1}(k_p a) + B I_{s+1}(k_p a)\right\}\right] +\right.$$

$$\left.\left[k_a a \sin\theta \sin\left(k_a a \sin\theta - \frac{s\pi}{2} - \frac{\pi}{4}\right)\left\{A J_s(k_p a) + B I_s(k_p a)\right\}\right]\right. \qquad (62)$$

(4) Below the Coincidence Critical Frequency . Large Panel

Below $f_c$ the denominator approximates to $+ k_p^2$ and the approximation for $k_a a \sin\theta$ large ( $\theta > 0$ ) is given in equation (59). Therefore in a similar manner to the above cases:

$$p(R,\theta,t,\psi) = \cos(s\psi)\left[\frac{\rho_a \omega^2 d_o e^{j(\omega t - k_a R)}}{R i^s}\right]\left[\frac{2}{\pi k_a a \sin\theta}\right]^{\frac{1}{2}}\left[\frac{1}{k_p^2}\right]$$

$$\left\{\left[k_p a \cos\left(k_a a \sin\theta - \frac{s\pi}{2} - \frac{\pi}{4}\right)\left\{A J_{s+1}(k_p a) + B I_s(k_p a)\right\} + \right.\right.$$

$$\left.\left.\left[k_a a \sin\left(k_a a \sin\theta - \frac{s\pi}{2} - \frac{\pi}{4}\right)\left\{-A J_s(k_p a) + B I_s(k_p a)\right\}\right]\right\}$$

(5) Comparisons

Small Plate:

$$\frac{p_{above}}{p_{below}} = \frac{a(\sin\theta)^2 k_a^2\left\{A J_s(k_p a) + B I_s(k_p a)\right\} + 2k_p(s+1)\left\{-A J_{s+1}(k_p a) + B I_{s+1}(k_p a)\right\}}{a(\sin\theta)^2 k_a^2\left\{-A J_s(k_p a) + B I_s(k_p a)\right\} + 2k_p(s+1)\left\{+A J_{s+1}(k_p a) + B I_{s+1}(k_p a)\right\}}$$

$$\times \frac{k_p^2}{(k_a \sin\theta)^2}$$

Large Plate:

$$\frac{p_{above}'}{p_{below}} = \frac{k_a a \sin\theta \sin\left(k_a a \sin\theta - \frac{s\pi}{2} - \frac{\pi}{4}\right)\left\{A J_s(k_p a) + B I_s(k_p a)\right\} + k_p a \cos\left(k_a a \sin\theta - \frac{s\pi}{2} - \frac{\pi}{4}\right)\left\{-A J_{s+1}(k_p a) + B I_{s+1}(k_p a)\right\}}{k_a a \sin\theta \sin\left(k_a a \sin\theta - \frac{s\pi}{2} - \frac{\pi}{4}\right)\left\{-A J_s(k_p a) + B I_s(k_p a)\right\} + k_p a \cos\left(k_a a \sin\theta - \frac{s\pi}{2} - \frac{\pi}{4}\right)\left\{A J_{s+1}(k_p a) + B I_{s+1}(k_p a)\right\}}$$

$$\times \frac{k_p^2}{(k_a \sin\theta)^2}$$

Similar comparisons may be made above and below coincidence for a large compared with a small plate.

From equation (51) when $\theta = 0$ we have an expression for the sound pressure on the normal running through the center of the disc which is as follows:

$$p = \frac{Q \cos(s\tfrac{\pi}{4})\, 2\pi A}{i^s}\left[\frac{k_\rho a\, J_s(0)\, J_{s+1}(k_\rho a)}{k_\rho^2}\right] + \frac{Q \cos(s\tfrac{\pi}{4})\, 2\pi B}{i^s}\left[\frac{k_\rho a\, J_s(0)\, I_{s+1}(k_\rho a)}{\quad}\right] \qquad (66)$$

Now $J_s(0) = 0$ when $s > 0$

and $J_0(0) = 1$

Therefore the sound pressure on the axis of a disc is zero when there are nodal diameters present. When there are no nodal diameters present the sound pressure is :

$$p = \frac{Q\, 2\pi\, A}{i\, k_\rho}\left[a\, J_1(k_\rho a)\right] + \frac{Q\, 2\pi\, B}{i\, k_\rho}\left[a\, I_1(k_\rho a)\right] \qquad (67)$$

McLachlan (1934) obtained an expression for the on axis sound pressure from a circular membrane which contained only the first term of (67)-as would be expected. His expression for the sound pressure from a membrane is

$$p = \frac{\rho_o \ddot{d}_o}{R}\left(\frac{a}{k_\rho^2 - k_a^2 \sin^2\theta}\right)\left[k_\rho J_0(k_a a \sin\theta)\, J_1(k_\rho a) - k_a \sin\theta\, J_0(k_\rho a)\, J_1(k_a a \sin\theta)\right]$$

From McLachlan; at a vibration mode $J_0(k_p a) = 0$ and so this reduces to:

$$p = \frac{\rho_o \ddot{d}_o}{R}\left(\frac{k_\rho a}{k_\rho^2 - k_a^2 \sin^2\theta}\right) J_0(k_a a \sin\theta)\, J_1(k_\rho a) \qquad (69)$$

furthermore when $k_p^2 \gg k_a^2 \sin^2\theta$ (which we now define as being below the coincidence critical frequency) this becomes:

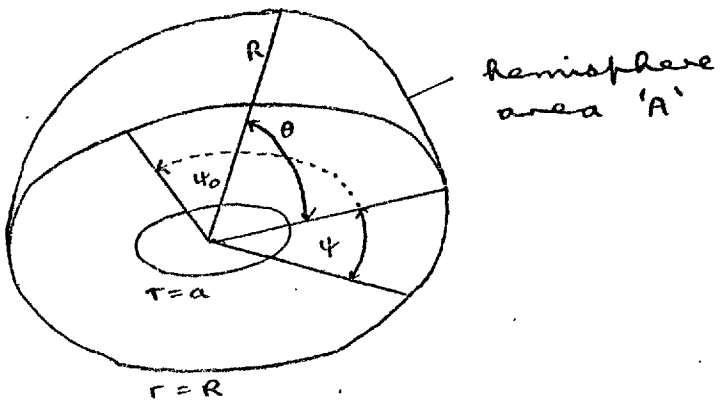
$$p = \frac{\rho_o \ddot{d}_o\, a^2}{R}\left(\frac{J_1(k_\rho a)}{k_\rho a}\right) J_0\, k_\rho a \sin\theta \qquad (70)$$

By taking $d = d_0 \left(\frac{r}{a}\right)^s \sin s\psi_0$ as the mode shape function McLachlan obtained the following expression for the sound pressure from a free edge disc with s nodal diameters

$$p = \frac{\rho_0 \ddot{d}_0 a^2}{R} \sin s\psi \; \frac{J_{n+1}(k_a a \sin\theta)}{k_a a \sin\theta} \qquad (71)$$

he points out that the pressure on the axis is zero if there are any number of nodal diameters present, and gives a comprehensive table of results both for the sound pressure form various vibrating objects and their radiation characteristic also , though he takes simplified mode shape functions for his analysis.

(b) Calculation of the Radiation Resistance of a Modal Piston




From Bouwkamp (1946)

$$R_{rad} = c_a \rho_a k_a^2 \int_{\psi=0}^{\psi=2\pi} d\psi \int_{\theta=0}^{\theta=\frac{\pi}{2}} |K(\theta,\psi)|^2 \sin\theta \, d\theta \qquad (72)$$

Now the 'K' of Bouwkamp is the '$\Gamma$' of Crocker (1968)

And:

$$K(\theta,\psi) = \frac{1}{2\pi} \int_A F(r,\psi_0) \, e^{-i k_a r \sin\theta (\cos\psi - \psi_0)} \, dA \qquad (73)$$

Let us take as in the sound pressure level calculations above:

$$F(r,\psi_0) = [A J_s(k_\rho r) + B I_s(k_\rho r)] \cos(s\psi_0)$$

giving:

$$K(\theta,\psi) = \cos(s\psi)\, e^{-\frac{s\pi i}{2}} \int_0^a J_s(k_a r \sin\theta)[A J_s(k_\rho r) + B(k_\rho r)]\, r\, dr \qquad (74)$$

and therefore:

$$R_{rad} = c_a \rho_a k_a^2 \int_{\psi=0}^{\psi=2\pi} \frac{\cos^2(s\psi)\, d\psi}{(i^s)^2} \int_{\theta=0}^{\theta=\frac{\pi}{2}} \left[\int_0^a r J_s(k_a r \sin\theta)\{A J_s(k_\rho r) + B(k_\rho r)\}\, dr\right]^2 \sin\theta\, d\theta \qquad (75)$$

Now -

$$\int_0^{2\pi} \cos^2(s\psi)\, d\psi = \frac{2\pi}{\varepsilon_s} \quad \text{where} \quad \begin{array}{l} \varepsilon_s = 1 \text{ when } s=0 \\ \varepsilon_s = 2 \text{ when } s>0 \end{array} \qquad (76)$$

The term in the square brackets has already been integrated giving the four terms of equation (51). When this is squared it will give rise to the following terms inside the $\int_{\theta=0}^{\theta=\frac{\pi}{2}}$ sign. WHERE $X = (k_a a \sin\theta)$, $Y = (k_\rho a)$.

$$I_1 = A^2 \left[\frac{(k_\rho a)^2 \sin\theta\ J_s^2(X)\ J_{s+1}^2(Y)}{(-k_a^2 \sin^2\theta + k_\rho^2)^2}\right] \qquad \text{III}$$

$$I_2 = A^2 \left[\frac{(k_a a)^2 \sin^3\theta\ J_{s+1}^2(X)\ J_s^2(Y)}{(-k_a^2 \sin^2\theta + k_\rho^2)^2}\right] \qquad \text{II}$$

$$I_3 = B^2 \left[\frac{(k_\rho a)^2 \sin\theta\ J_s^2(X)\ I_{s+1}^2(Y)}{(k_a^2 \sin^2\theta + k_\rho^2)^2}\right] \qquad \text{III A}$$

$$I_4 = B^2 \left[\frac{(k_a a)^2 \sin^3\theta\ J_{s+1}^2(X)\ I_s^2(Y)}{(k_a^2 \sin^2\theta + k_\rho^2)^2}\right] \qquad \text{II A}$$

$$I_5 = 2A^2 \left[\frac{k_\rho k_a a^2 \sin^2\theta\ J_s(X)\ J_{s+1}(X)}{(-k_a^2 \sin^2\theta + k_\rho^2)^2}\right]\left[J_{s+1}(Y)\, J_s(Y)\right] \qquad \text{I}$$

$$I_6 = 2B^2 \left[\frac{k_\rho k_a a^2 \sin^2\theta\ J_s(X)\ J_{s+1}(X)}{(k_a^2 \sin^2\theta + k_\rho^2)^2}\right]\left[I_{s+1}(Y)\, I_s(Y)\right] \qquad \text{I A}$$

$$I_7 = 2AB \left[\frac{(k_\rho a)^2 \sin\theta\ J_s^2(X)}{(k_a^2 \sin^2\theta + k_\rho^2)(-k_a^2 \sin^2\theta + k_\rho^2)}\right]\left[J_{s+1}(Y)\, I_{s+1}(Y)\right] \qquad \text{III B}$$

$$I_8 = 2AB \left[\frac{k_\rho k_a a^2 \sin^2\theta\ J_s(X)\ J_{s+1}(X)}{(k_a^2 \sin^2\theta + k_\rho^2)(-k_a^2 \sin^2\theta + k_\rho^2)}\right]\left[J_{s+1}(Y)\, I_s(Y)\right] \qquad \text{I B}$$

$$I_9 = -2AB\left[\frac{k_a k_p a^2 \sin^2\theta\ J_{s+1}(x)\ J_s(x)}{(k_a^2\sin^2\theta + k_p^2)(-k_a^2\sin^2\theta + k_p^2)}\right]\left[J_s(y)\ I_{s+1}(y)\right] \quad \text{I B}$$

$$I_{10} = -2AB\left[\frac{(k_a a)^2 \sin^3\theta\ J_{s+1}^2(x)}{(k_a^2\sin^2\theta + k_p^2)(-k_a^2\sin^2\theta + k_p^2)}\right]\left[J_s(y)\ I_s(y)\right] \quad \text{II B} \qquad (77)$$

These give just three basic integral types as marked and these are listed below where 'K' is a different constant for each of the above 10 integrals

$$(I) = K\int_0^{\frac{\pi}{2}} \frac{k_p k_a a^2 \sin^2\theta\ J_s(k_a a\sin\theta)\, J_{s+1}(k_a a\sin\theta)}{(-k_a^2\sin^2\theta + k_p^2)^2}\, d\theta$$

$$(II) = K\int_0^{\frac{\pi}{2}} \frac{(k_a a)^2 \sin^3\theta\ J_{s+1}^2(k_a a\sin\theta)}{(-k_a^2\sin^2\theta + k_p^2)^2}\, d\theta$$

$$(III) = K\int_0^{\frac{\pi}{2}} \frac{(k_p a)^2 \sin\theta\ J_s^2(k_a a\sin\theta)}{(-k_a^2\sin^2\theta + k_p^2)^2}\, d\theta \qquad (78)$$

Where the denominators are different for cases 'A' and 'B'

The basic integral within the square brackets itself has proved intractable and therefore these three integral types must be evaluated above and below the coincidence critical frequency and also for large and small plates

(1) Below the Coincidence Critical Frequency . Small Plate

$k_p \gg k_a$ and therefore $(\pm k_a^2\sin^2\theta + k_p^2)^2 \simeq k_p^4$

$(-k_a^4\sin^4\theta + k_p^4) \simeq k_p^4$

$k_a a \ll 1$ and therefore $J_s(k_a a\sin\theta) \simeq \frac{(k_a a\sin\theta)^s}{2^s\, s!}$

$$(I) = K\int_0^{\frac{\pi}{2}} \frac{k_p k_a a^2 \sin^2\theta\ (k_a a\sin\theta)^s (k_a a\sin\theta)^{s+1}}{k_p^4\ 2^s\, s!\ 2^{s+1}(s+1)!}\, d\theta$$

$$(I) = K\int_0^{\frac{\pi}{2}} \frac{(k_a)^{2s+2}\,(a)^{2s+3}\,(\sin\theta)^{2s+3}}{(k_p)^3\;\; 2^{2s+1}\;\; s!\;\; (s+1)!}\cdot d\theta$$

$$(II) = K\int_0^{\frac{\pi}{2}} \frac{(k_a)^{2s+4}\,(a)^{2s+4}\,(\sin\theta)^{2s+5}}{(k_p)^4\;\; 2^{2s+2}\;\; (s+1)!\;\; (s+1)!}\, d\theta$$

$$(III) = K\int_0^{\frac{\pi}{2}} \frac{(k_a)^{2s}\;\; (a)^{2s+2}\;\; (\sin\theta)^{2s+1}}{(k_p)^2\;\; 2^{2s}\;\;\; s!\;\; s!}\, d\theta \qquad (79)$$

Now:

$$\int_0^{\frac{\pi}{2}} \sin^{2p-1}x\, dx = \frac{\sqrt{\pi}\;\Gamma(p)}{2\,\Gamma(p+\frac{1}{2})} \qquad (80)$$

$$\Gamma\,(p+\tfrac{1}{2}) = \frac{\sqrt{\pi}\;\Gamma(2p+1)}{2^{2p}\;\Gamma(\,p+1)}$$

and so:

$$\int_0^{\frac{\pi}{2}} \sin^{2s-1}\theta\, d\theta = \frac{\sqrt{\pi}\;\Gamma(s)\,2^{2s}\,\Gamma(s+1)}{2\sqrt{\pi}\;\Gamma(2s+1)} = \frac{\Gamma(s)\,2^{2s-1}\,\Gamma(s+1)}{\Gamma\,(2s+1)} = \frac{(s-1)!\;2^{2s-1}\;s!}{(2s)!}$$

$$\int_0^{\frac{\pi}{2}} \sin^{2s+1}\theta\, d\theta = \frac{s!\;\; 2^{2s+1}\,(s+1)!}{(2s+2)!}$$

$$\int_0^{\frac{\pi}{2}} \sin^{2s+3}\theta\, d\theta = \frac{(s+1)!\;\; 2^{2s+3}\,(s+2)!}{(2s+4)!}$$

$$\int_0^{\frac{\pi}{2}} \sin^{2s+5}\theta\, d\theta = \frac{(s+2)!\;\; 2^{2s+5}\,(s+3)!}{(2s+6)!} \qquad (81)$$

Therefore:

$$(I) = K\;\frac{k_a^{2s+2}\;\; a^{2s+3}\;\; (s+1)!\;\; 2^{2s+3}\;\; (s+2)!}{(k_p)^3\;\; 2^{2s+1}\;\; s!\;\; (s+1)!\;\; (2s+4)!}$$

$$= K\;\frac{k_a^{2s+2}\;\; a^{2s+3}}{(k_p)^3}\;\;\frac{1}{(2s+3)(2s+1)(2s!)}$$

$$(II) = K \frac{k_a^{2s+4} a^{2s+4} (s+2)! \; 2^{2s+5} (s+3)!}{(k_p)^4 \; 2^{2s+2} (s+1)! (s+1)! (2s+6)!}$$

$$= K \frac{k_a^{2s+4} a^{2s+4}}{(k_p)^4} \frac{2(s+2)}{(2s+5)(2s+3)(2s+2)(2s+1)(2s!)}$$

$$(III) = K \frac{k_a^{2s} a^{2s+2} s! \; 2^{2s+1} (s+1)!}{(k_p)^2 \; 2^{2s} s! s! (2s+2)!}$$

$$= K \frac{k_a^{2s} a^{2s+2}}{(k_p)^2} \frac{1}{(2s+1)(2s!)} \qquad (82)$$

Giving finally:

$$R_{Rad} = \left[\frac{c_a \rho_a k_a^2 2\pi}{\varepsilon_s}\right]\left[\frac{k_a^{2s} a^{2s+2}}{(2s+1)(2s!) k_p^2}\right] \times \left[\text{terms below}\right]$$

$$\left\{\left[A^2 J_{s+1}^2(Y) + B^2 I_{s+1}^2(Y) + 2AB J_{s+1}(Y) I_{s+1}(Y)\right] + \right.$$

$$\frac{k_a^2 a}{k_p (2s+3)}\left[2A^2 J_{s+1}(Y) J_s(Y) + 2B^2 I_{s+1}(Y) I_s(Y) + 2AB\left(J_{s+1}(Y) I_s(Y) - I_{s+1}(Y) J_s(Y)\right)\right] +$$

$$\left.\frac{k_a^4 a^2 2(s+2)}{k_p^2 (2s+5)(2s+3)(2s+2)}\left[A^2 J_s^2(Y) + B^2 I_s^2(Y) - 2AB J_s(Y) I_s(Y)\right]\right\}$$

(83)

(2) Above the Coincidence Critical Frequency . Small Plate

$k_p \ll k_a$ and therefore $\left(\pm k_a^2 \sin^2\theta + k_p^2\right)^2 \simeq k_a^4 \sin^4\theta$

$\left(-k_a^4 \sin^4\theta + k_p^4\right) \simeq -k_a^4 \sin^4\theta$

$k_a a \ll 1$ and therefore $J_s(k_a a \sin\theta) \simeq \frac{(k_a a \sin\theta)^s}{2^s s!}$

N.B. when the numerator contains a minus sign there is a possibility that as $\sin\theta \rightarrow (k_p^2/k_a^2)$ the integral will become indeterminate, and the author has yet to verify mathematically that this does not in fact happen. However, as $\sin\theta$ tends to ( $k_p^2/k_a^2 \simeq 0$) the contribution to the integral must be very small as this is the region when $p \rightarrow 0$ when $s \neq 0$. When s is equal to zero however the position is different and this case must be considered separately. Maidanik in his appendix (A) (1962) shows that the main contribution from a similar integral is from the region where $\theta \rightarrow \pi/2$.

In this case therefore:

$$(I) = K\int_0^{\frac{\pi}{2}} \frac{k_p k_a a^2 \sin^2\theta (k_a a \sin\theta)^s (k_a a \sin\theta)^{s+1}}{k_a^4 \sin^4\theta \; 2^s s! \; 2^{s+1}(s+1)!}\, d\theta$$

$$= K\int_0^{\frac{\pi}{2}} \frac{k_p (k_a)^{2s-2} (\sin\theta)^{2s-1} a^{2s+3}}{2^{2s+1} s! \; (s+1)!}\, d\theta$$

$$= K\left[\frac{a^{2s+3} k_p (k_a)^{2s-2} (s-1)! \; 2^{2s-1} s!}{2^{2s+1} s! \; (s+1)! \; (2s)!}\right]$$

$$= K\left[\frac{k_p (k_a)^{2s-2} (a)^{2s+3}}{4 (s)(s+1)(2s)!}\right]$$

$$(II) = K\int_0^{\frac{\pi}{2}} \frac{(k_a a)^2 \sin^3\theta (k_a a \sin\theta)^{2s+2}}{k_a^4 \sin^4\theta \; 2^{2s+2} (s+1)! (s+1)!}\, d\theta$$

$$= K\left[\frac{(k_a)^{2s} (a)^{2s+4} \; s! \; 2^{2s+1} (s+1)!}{2^{2s+2} (s+1)! (s+1)! \; (2s+2)!}\right]$$

$$= K\left[\frac{(k_a)^{2s} (a)^{2s+4}}{2 \; (s+1)(2s+2)!}\right]$$

$$(III) = K\int_0^{\frac{\pi}{2}} \frac{(k_p a)^2 \sin\theta (k_a a \sin\theta)^{2s}}{k_a^4 \sin^4\theta \; 2^{2s} (s!)(s!)}\, d\theta$$

$$= K\left[\frac{(k_p)^2 (k_a)^{2s-4} (a)^{2s+2} (s-2)! \; (s-1)! \; 2^{2s-3}}{2^{2s} (s!)(s!) \; (2s-2)!}\right]$$

$$= K\left[\frac{(k_p)^2 (k_a)^{2s-4} (a)^{2s+2}}{8 \; s^2 (s-1) (2s-2)!}\right]$$

$$R_{rad} = \left[\frac{c_a \rho_a k_a^2 2\pi}{\varepsilon_s}\right]\left[\frac{k_a^{2s-4} a^{2s+2}}{(2s!)\ 2}\right]$$

$$\left\{\left[\frac{k_\rho k_a^2 a}{2s(s+1)(2s!)}\right]\left[A^2 J_{s+1}^2(\gamma) + B^2 I_{s+1}^2(\gamma) + 2AB\left(J_s(\gamma) I_{s+1}(\gamma) - J_{s+1}(\gamma) I_s(\gamma)\right)\right]\right.$$

$$+\left[\frac{k_a^4 a^2}{(s+1)(2s+2)(2s+1)}\right]\left[A^2 J_s^2(\gamma) + B^2 I_s^2(\gamma) + 2AB\, J_s(\gamma) I_s(\gamma)\right]$$

$$\left.+\left[\frac{k_\rho^2 (2s-1)}{2s(s-1)}\right]\left[A^2 J_{s+1}^2(\gamma) + B^2 I_{s+1}^2(\gamma) - 2AB\, J_{s+1}(\gamma) I_{s+1}(\gamma)\right]\right.$$

Cases (3) and (4) for a large plate have so far proved to be intractable because the approximation for $J_s(k_a a \sin\theta)$ only applies when $(k_a a \sin\theta)$ is very large-which is clearly not always the case. However, Nikiforov (1964) has shown that for rectangular plates the energy radiated by small plates below the coincidence critical frequency is twice that radiated by a large plate below coincidence and it is possible that the relationship holds for a circular plate also.

McLachlan (1934) gives expressions for the acoustic power given out by a circular membrane and a free edge disc as follows:

The acoustic power from a membrane at symmetrical modes of vibration (i.e. no nodal diameters is:

$$W = \frac{4 W_o}{k_a a}\left[\frac{J_1(k_\rho a)}{k_\rho a}\right]^2 \sum_{r=0}^{\infty} J_{2r+1}(2 k_a a)$$

$$W_o = \frac{\rho_o \pi a^4 \omega^4 d_o^2}{c} = \rho_o c A (k a)^2 \dot{d}_o^2$$

for an acoustically small plate below the coincidence critical frequency, where $W_o$ is the power radiated on both sides of a rigid disc in an infinite baffle and $R_{rad} = W/\dot{d}_o^2$.

McLachlan's result for a free edge disc with s nodal diameters using his result given in equation (71) above for the sound pressure from a similar disc is:

$$w = \frac{w_0}{(s+1)(k_a a)^2}\left[J_{2s+2}(2k_a a) + 2\sum_{r=0}^{\infty} J_{2s+2r+3}(2k_a a)\right]$$

and finally his result for a free edge disc with one nodal circle using $d = d_0(1 - 2r^2/a^2)$ as the mode shape function below $f_c$ is:

$$w = w_0\left\{\frac{1}{3(k_a a)^2} + \frac{J_3(2k_a a)}{(k_a a)^3}\left[1 - \frac{2}{(k_a a)^2}\right] - 6\frac{J_4(2k_a a)}{(k_a a)^4}\right\}$$

he demonstrates with this equation the 'acoustic short circuit' or cancellation of the volume velocities resulting from the inner and outer regions of the disc below $f_c$ .

It is clear that the rectangular plate has been well treated in the light of the 'coincidence' theory of radiation by Maidanik and others. But the circular plate has not been so well treated. Above may be found a brief attempt to c ver some cases applicable to the circular plate but there is clearly much further work to be done.

(v) Some Standard Results for Comparison

(a) Pulsating Sphere in Free Space

$$p = \frac{\rho_a c_a k_a [4\pi a^2 \dot{d}_0]}{4\pi r} e^{j(\omega t - k_a r)}$$

$$I = \frac{\rho_a c_a k_a^2 [4\pi a^2 \dot{d}_0]^2}{32\pi^2 r^2} \quad \left(\text{N.B. } I = \frac{|p|^2}{2\rho_a c_a}\right)$$

$$P_\omega = \frac{\rho_a c_a k_a^2 [4\pi a^2 \dot{d}_0]^2}{8\pi} \quad \left(k_a = \frac{\omega}{c_a}\right)$$

Where [ ] is known as the source strength and is the volume velocity of the small source.

(b) Hemisphere in Infinite Baffle (one side only)

The source strength is half the above therefore the intensity and power are 1/4 the above.

(c) Circular Piston in Infinite Baffle - far field (one side only)

$$p = \frac{\rho_a c_a k_a [\pi a^2 \dot{d}_0]}{2\pi r} \left[\frac{2 J_1(k_a a \sin\theta)}{k_a a \sin\theta}\right] e^{j(\omega t - k_a r)}$$

$$I = \frac{\rho_a c_a k_a^2 [\pi a^2 \dot{d}_0]^2}{8\pi^2 r^2} \left[\frac{2 J_1(k_a a \sin\theta)}{k_a a \sin\theta}\right]^2$$

(d) Circular Piston in Infinite Baffle - near field (One side only)

$$p = 2\rho_a c_a \dot{d}_0 e^{j\left(\omega t - \frac{k_a}{2}\left(\sqrt{r^2+a^2}+r\right)\right)} \sin\frac{k_a}{2}\left(\sqrt{r^2+a^2}-r\right)$$

$$I = 2\rho_a c_a \left[\dot{d}_0 \sin\frac{k_a}{2}\left(\sqrt{r^2+a^2}-r\right)\right]^2 \quad \text{ON AXIS}$$

(e) Dipole - far field

$$p = \frac{\rho_a \omega [4\pi a^2 \dot{d}_0] \ell k_a \cos\theta e^{\pm j(\omega t - k_a r)}}{4\pi r}$$

$$I = \frac{\rho_a \omega k_a^3 \ell^2 [4\pi a^2 \dot{d}_0]^2 \cos^2\theta}{32\pi^2 r^2} \quad \left(\int_0^{\frac{\pi}{2}} \cos^2\theta \, d\theta = \frac{\pi}{4}\right)$$

$$p = \frac{\rho_a w k_a^3 [4\pi a^2 \dot{d}_o] \rho^2}{12\pi}$$

(f) Quadrupole Sources

$$I \propto \frac{\beta^6 \sin^2 2\Theta}{r^2}$$ Lateral (square) quadrupole

$$I \propto \frac{\beta^6 \cos 4\Theta}{r^2}$$ Longitudinal (linear) quadrupole.

Where $\rho_a$ is the air density; $c_a$ is the velocity of sound in air; $k_a$ is the air wave number = $2\pi/\lambda_a$ ; a is the radius of the disc or hemisphere. r is the distance from the radiator (much greater than any of its dimensions for the far field cases). $d_o$ is the amplitude of the object movement and $\dot{d}_o$ is the velocity of the source ;p is the sound pressure and P is the sound power and I is the sound intensity. l is the distance between the two elements of the dipole.

More results can be found in McLauchlan (1934) 'Loudspeakers' Dover. and in Morse'Vibrations and Sound' (1948), Kinsler and Frey 'Fundamentals of Acoustics' (1962) and 'Acoustics' by L.L.Beranek (1954).

# APPENDICES (III) (IV) (V)

## (III) PRELIMINARY TRANSMISSION EXPERIMENTS WITH AN ACOUSTIC WAVEGUIDE

## (IV) FACTORS INFLUENCING GEAR NOISE

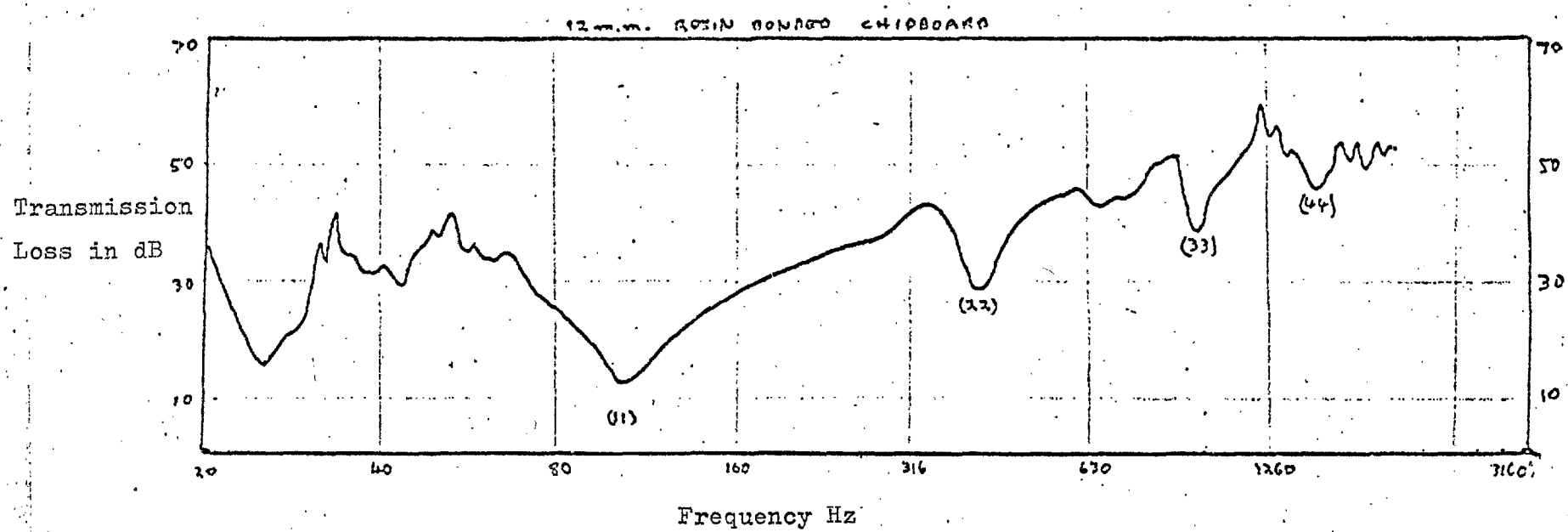
## (V) A FURTHER SCANNING PHENOMENON

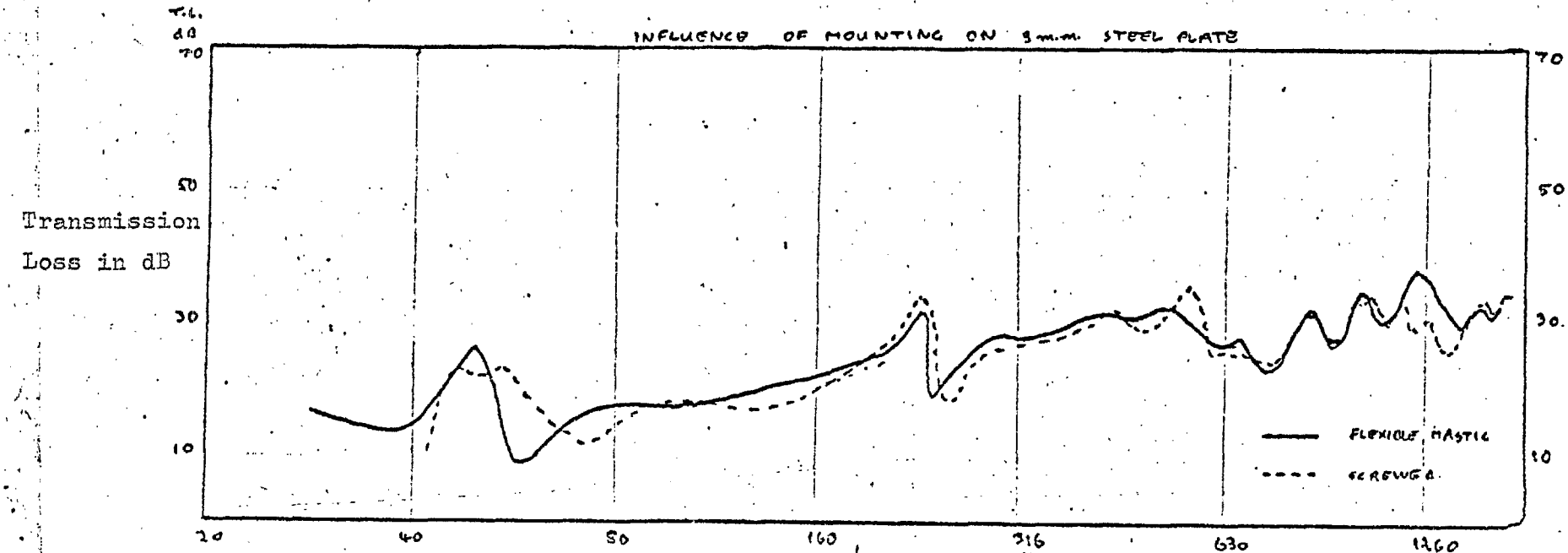
## APPENDIX (III)

### Preliminary Experiments With An Acoustic Waveguide

Some peripheral pointers were gained to modal structure, the coincidence effect and sound radiation and excitation from a series of preliminary experiments with an acoustic waveguide. A more detailed description of the apparatus and technique used can be found in Fryer (1966) which is reproduced at the end of this thesis.

The panels which were most useful in these studies were as follows: Eigth inch steel plate, damped and undamped. This panel demonstrated how the various panel modes can be damped, completely in some cases, with corresponding reductions in the radiation from the back of the panel (see Fig 60 ). It can be seen that the (1,1) and the (2,2) modes are completely damped out and that overall radiation from the back of the panel is free from large peaks of'preferred radiation' at any frequency in the experimental range. The effect of different types of fixing can be seen in Fig ( 61 ). It can be seen that the main resonance frequencies are slightly altered, as the 'screw fixed' panel is more stiffly fixed being no longer an approximation to a simple support this is to be expected. Effects such as these in square plates can also be applied to circular plates and used to alter the main resonance frequencie cies, possibly to regions where they may no longer be preferentially excited. Panels such as the half inch chipboard illustrated the ease with which the expected panel modes can be excited, and showed that modes which at first sight should not have been excited by the plane waves used for the experiment were in fact excited quite strongly (Fig 62 ). This panel also indicated that the effects of the edge conditions on small panels were significant. The resonances in the chipboard panel which would be considered to be heavily damped were much deeper than in the




Figures 60 and 61 Transmission Loss Curves for chipboard and Steel

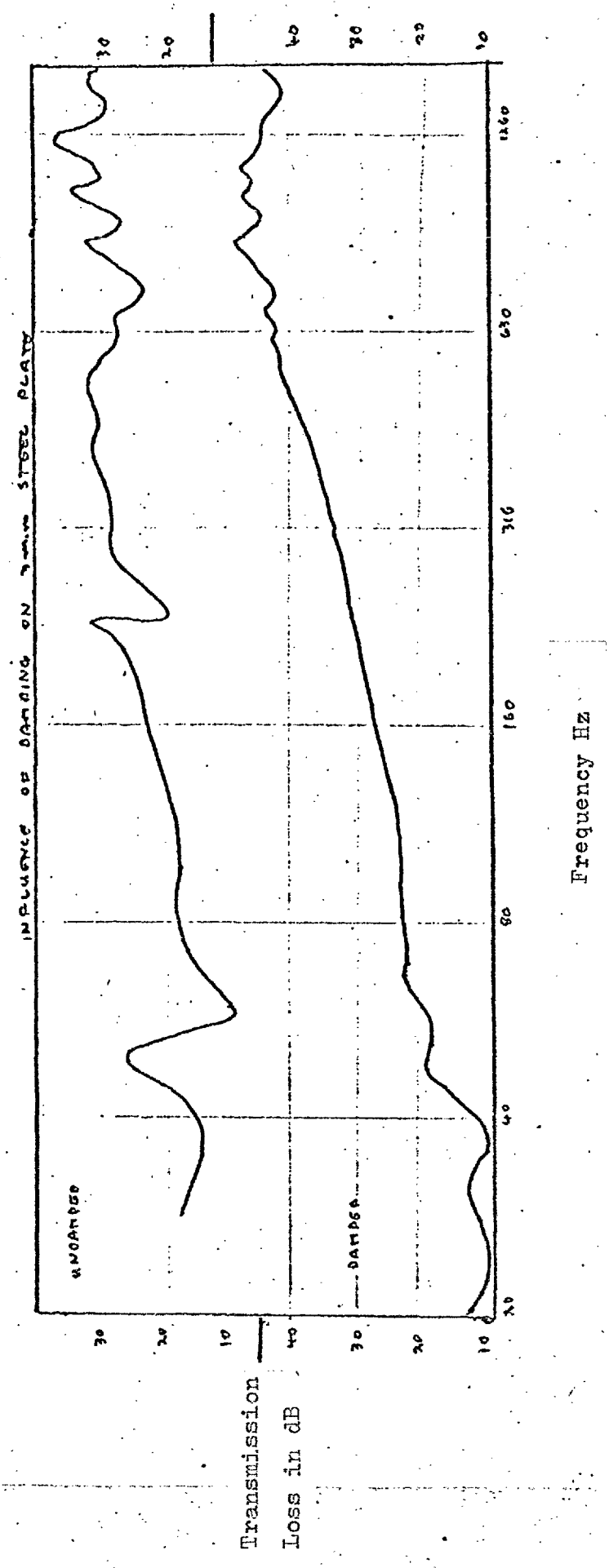



Figure 62 Influence of Damping on the Transmission Loss and hence the radiation of a 3 mm Steel Plate

glass panel. This can be loosly explained by supposing that the edge damping could'couple in' more effectively to the stiffer glass panel, while the less stiff chipboard vibrated and radiated relatively unaffected by the edge and fixing conditions.

Below the coincidence critical frequency($f_c$) the radiation from a quarter wavelength of a mode segment is cancelled out by the radiation from the adjacent segment which is out of phase with it. Just above $f_c$ however, this process is no longer in operation and each mode segment effectively radiates as a separate entity - the radiation efficiancy is thus increased. Far above $f_c$ the modal density is increasing but the strength of each mode is then relatively less so the significance of the radiation from a mode rather than the whole panel is less at high frequencies. The smaller the panel the higher the frequency at which edge effects and individual modes loose their importance. Above $f_c$ the radiation from a panel is directive, there being a peak in the polar diagram at the coincidence angle. It was hoped that the acoustic waveguide facility, which had the capability of exciting pure transmission waveguide modes could be used to demonstrate the coincidence effect. Each waveguide mode has a particular angle of incidence associated with it (Fryer 1969) which varies with the frequency being propagated - there being grazing incidence at the cut off frequency of the given mode. To demonstrate the coincidence effect in the waveguide however requires the further coincidences that the waveguide modal frequency is such that the angle of incidence of the waves impinging on the test panel is that required to excite the bending waves in the panel. These bending waves in turn, since the test panel is small, will only show up to any great extent if their wavelength is such that a standing wave just fits the waveguide i.e. when the standing waves form a mode of the test panel. There was one panel tested which satisfied all these conditions and its transmission curve is presented here (Fig 62)

In the case of a gear wheel excited by impulsive mechanisms having a wide spectrum, the coincidence effect of radiation may well

cause sound to be radiated in preferred directions over a particular band of frequencies. As mentioned in Appendix II there is a relation given by Shenderov (1967) between sound transmission and sound radiation .

## APPENDIX (IV)

### Factors Influencing Gear Noise

The main work of this thesis is to describe experiments carried out on the visualisation of modes in discs and Loudspeakers and also the power radiated from them . This course of action was decided upon after some work had been done on the elements of gear noise excitation and propagation It was seen that much work had already been carried out into the mechanisms of gear noise excitation and that there are many remedies already in existence to reduce this excitation and radiation. It was felt that the resources available to the author would not result in any great decrease in noise excitation if they were applied to the study of the actual excitation mechanisms of gear noise.Therefore only a brief summary of some of the elements of gear noise and excitation with one or two possible methods of overcoming them are presented here, as the main purpose of the thesis is the holographic investigations described above.

The gear noise chain can be listed as follows:

(i) Generation of the noise itself by the many factors involved in gear action, some of which are:-

(a) 'Stick-slip' friction (Sinclair 1964) during sliding rather than the desired rolling when teeth are meshing. The rolling itself, by deforming the teeth, also gives rise to:

(b) Deformation under stress leading to impact noise at the tooth contact frequency and its harmonics, this also leads to variation in tooth root stresses during the mating cycle which set up wave motions in the body of the gear wheel.

(c) Pitch-line shock. This is the impulsive change in direction of rolling as the teeth firstly mesh in and then change direction to mesh out. The involute profile minimises this though other profiles such as the 'Novikov' are sometimes favoured ( ).

(d) The lubricant film may be sheared by rough gear surfaces and may also be squirted from regions of contact, both of these effects giving rise to noise. Insufficient lubrication will also lead to more noise.

(e) Limitations in the accuracy of the gear profile, and in the surface finish are a very serious cause of gear noise. The inaccuracies in the tooth profile lead to repetition frequencies and those in the surface finish lead to more general 'white' noise - both may be improved if greater financial expenditure is allowable.

(f) Errors in alignment of two mating gears or individual gears on their own shafts give rise once again to repetition frequencies.

One of the major causes of innaccurate gear profiles is, of course an incorrectly aligned and insufficiently accurate hobbing machine, with axial float in its worm shaft together with periodic error in its worm thread or error in the actual worm thread profile itself. The axis of the worm wheel may be off-set from the wheel axis, and there may also be pitch error in the driving gear of the worm wheel. These faults and similar effects give rise to unbalance, excentricity, ovality, circular and axial pitch error and error in the helix angle. Cyclic errors may result from cutting table motion, wave errors from cyclic errors in hob feed, and progressive errors from temperature variations while cutting.

(ii)This gear action generated noise will excite gear wheel modes, and also modes in connected and related structures. The conditions of support, the effective point of excitation, which is at one of the 'supports' and also the fact that this point of excitation moves rapidly round the circumference of the gear will all have considerable bearing on which disc modes will be excited (Raske and Schlack 1967 se also Appendix II). The fact that the there is frictional contact between the two mating gears at the point of excitation (where the gear noise is generated) will tend to damp out vibrations which are produced, but never-the-less there may be a case for improved damping, for better location of damping materials or a change in the conditions of support to reduce modal excitation, particularly of those modes most effective in radiation. Statistical modal analysis (Lyon and Eichler 1964, Newland 1968) shows that in loosly coupled systems energy will flow until each mode has the same energy. Once again therefore, improvement may result by altering the effective coupling between the various parts of the whole equipment containing the gears i.e. gears, shafts, body,casing and enclosure.

(iii) Having excited modes in the gears and related structures and also having set up standing waves and travelling waves of all the possible varieties (eg Lamb, Love, Rayleigh etc.) these modes and waves will couple into the air. The present experiments show that some modes will radiate preferentially and suitable manipulation of the clincidence critical frequency as well as alteration of the conditions of support and damping to minimise these modes and/or their relative radiation coefficient will give and improvement (see appendix II).

The noise produced and radiated may therefore be reduced by applying some of the following remedies and suggestions in approximate order of importance. (refs: El Abdin 1963, Royal Society Conference 1967)

(a) Develop toothed belts thereby eliminating many of the causes of gear noise excitation.

(b) Where possible use damped materials for gear manufacture with good surface finish and low coefficients of friction, such as: Nylon, PTFE, and similar strong polymerised materials which are often self lubricating.

(c) Reduce the loading on any given tooth by:-

(1) Increasing the number of teeth. The number of teeth in contact on meshing increases as does the contact time for any given tooth. Changes in relative velocity are also reduced and the effect of errors in manufacture and alignment are minimised.

(2) Increasing the face width of the teeth. A three fold increase gives about a 10 db reduction in the noise radiated and also reduces the tooth deflection.

(3) Reducing the speed of revolution and hence the speed of tooth contact - halving the speed reduces the S.P.L. by 6 db.

(d) Reduce the many errors of manufacture, for instance by using better machines or by using split hobbing worm wheels which halve errors. Reducing the pitch error from 50 $\mu$ to 6 $\mu$ reduces the sound output by about 10 db.

(e) Increase the contact ratio by changing the gear profile-a change in the contact ratio from 1.75 to 4.73 results in a Sound reduction of about 10 db.

(f) Increase the accuracy of alignment both of the two mating gears and also of each gear on its own shaft.

(g) Use gears lubricated with a ir fed in under pressure.

(h) Reduce the coupling between the gears and the gear shafts and then to the rest of the apparatus. This may be accomplished by inserting annuli of suitable damping material - though tests have not in fact shown this to be greatly effective.

(i) Enclose the whole apparatus in a massive limp cylindrical housing made of lead or roofing felt and use transmission loss effects and absorbtion inside the housing to contain the radiated sound (Herman 1966).

(j) Prevent oil film shearing or squirting and use helical involute gear profiles wherever possible.

(k) Manipulate the coincidence critical frequency - pushing it above the range of interest - and also the conditions of excitation and support as mentioned above.

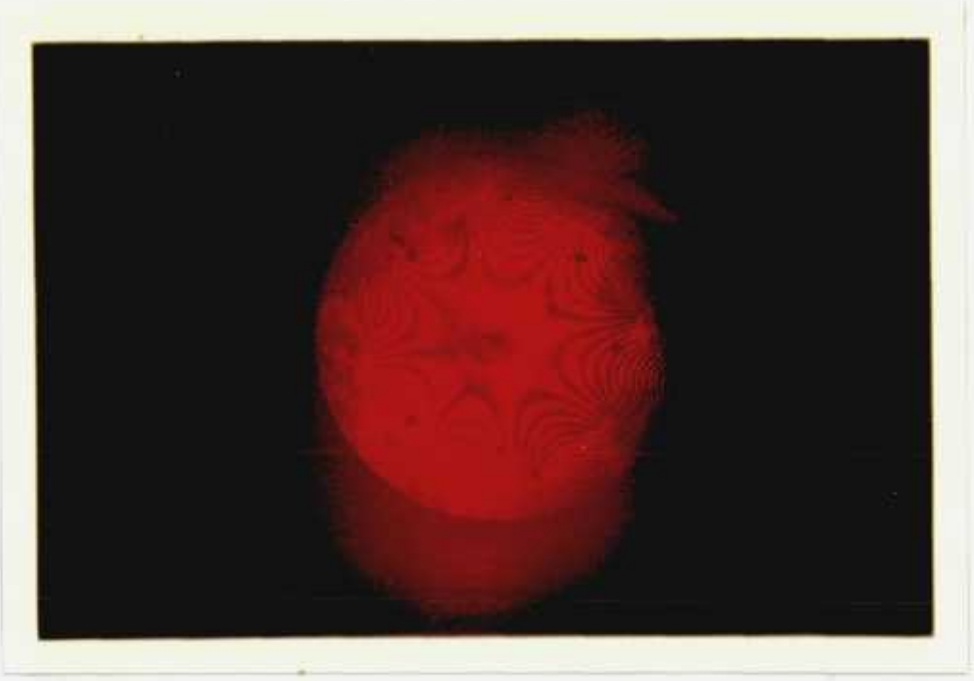
## APPENDIX (V)

### A Further Scanning Phenomenon

When the observer moves his eye along a scanned hologram he sees fringe systems corresponding to most phases of the object vibration 'wax and wane'. For instance if a 2 nodal diameter disc mode is observed, the fringes move out between the nodes from the disc center as we move from regions of the hologram representing the rest position to regions representing the maximum object amplitude. To observe this the observer must place his eye as close as possible to the hologram. If his eye is only a small distance from the hologram all parts of the object are not then seen at the same phase of the object cycle .The fringes then seem to 'roll around' the object as the observer moves his eye along the hologram. If he moves his eye still further away from the hologram he still sees a fringe system but it bears only little relation to that seen with his eye close up to the hologram. The author feels that more information about the object vibration is contained in this fringe system, which may be an 'average' of the systems neighbouring in phase, because its character changes from

object to object vibrating in an apparrently similar manner. This fringe system is also more different from the 'close up' system in the case of Loudspeakers than for brass and steel discs. There is clearly a need for a theoretical and practical investigation of this phenomenon.

Plate Number 19



Stroboscopic Frozen Fringe Hologram, 2050 Hz

Plate Number 20



Frozen Fringe Hologram at 2050 Hz - regretted print taken from slide is over exposed

# REFERENCES

REFERENCES

ABRAMSON N.,(1968), E.U.H.*

ALDOSHINA I.A.,(1971), Sov. Phys. Acoust. (17), no 1, 15-18.

ALEKSOFF C.C.,(1969), Appl. Phys. Lett. (14), no 1, 23.

ALEKSOFF C.C.,(1971), Appl. Opt. (10),no 6, 1329-1341.

AMON R. & WIDERA O.E.,(1970),J. Sound Vib. (12),no 4, 475-477.

ANON.,(1966),Electronics Letters (2), no 5.

ARCHBOLD E. & ENNOS A.E.,(1968), E.U.H.*

ARCHBOLD E. & ENNOS A.E.,(1968b), Laser Focus, October edn.

ARCHBOLD E., BURCH J. & ENNOS A.E.,(1970), Opt.Acta (17) no 12,883-893.

BAAD, P.K.,(1971), J. SOUND Vib. (16), no 1, 131-135.

BARLOW, D.,(1970), J. Audio Eng. Soc. (18) no 3 , 269.

BERANEK, L.L.,(1954), 'Acoustics' McGraw Hill.

BERANEK, L.L.,(1959), Proc. Inst. Mech. Eng. (173), 12-35.

BIEDERMAN, K. & MOLIN, N.E.,(1970), J. Sci. Instr. (3), 669-679.

BLAND, R.E. & PELICK T.J.,(19 ), Trans. A.S.M.E., 61-WA-47.

BODINE, R.Y.,(1967), J. Acoust, Soc. Amer. ( ), 1551.

BOUWKAMP, S.J.(1946), Phillips Res. Rept. (1), 251-277.

BRADLEY, D.J.,(1970), Phys.Bull. (21),116-122.

BRANDES, R.G., SHANKOFF, T.A. & FRANCOIS, EE.,(1969), Appl.Opt.(11),1166-1179.

BRANDT, .,(1970), Opt. Spectra. U.S.A. (4),no 9,26-31.

BROCH, J.T.,(1962), Bruel & Kjaer Tech. Rev. no 4, 3-17.

BROOKES, R.E.,& HEFLINGER, L.O.,(1969), Appl.Opt. (8), 935-9.

BROWN, G.M., GRANT, R.M. & STROKE, G.W.,(1969), J.Acoust.Soc.Amer.(45),1166-79

BURCH, J.M.L.,(1970), E.U.H.*

BUTTERS, J.N. & DENBY, D.,(1969), Proc.Conf.Phot.in Eng. - Inst.Mech.Eng.Lnd

BUTTERS, J.N. & LEENDERTZ, ,,(1971),Opt.& Laser Tech.Feb, 26.

CASTLER,D.H. & PRUET,H.D.,(1967),Appl.Phys.Lett.(10),341-2.

CLOSE,D. et al.,(1969), Appl.Phys. Lett.(14),159-160.

COLLINS,L.F.,(1968), Appl.Opt. (7),203-5.

CREMER,L.,(1942), Akust Zeit. (7),81.

CROCKER,M.J.,(1967), J.Sound Vib. (6), no 1,38-58.

CROCKER,M.J.,(1968), Acoust.Res. Council Rept. BS/A/68-2.

CROCKER,M.J.,(1969), Phd Thesis, Univ.of Liverpool.

CURTIS G.,(1966), D.I.C. Notes in Acoustics, Imperial College.

DALISA,A.L. et al,(1970), Paper Th.B16 Opt.Soc.Amer.meeting 30 Sept.

DALISA,A.L. et al,(1970b),J.Sci.Instr. (3),789.

DALLY,J.W.& THAU,S.A.,(1967), Int.J.Solids Structures,(3),293-308.

DAVIES,H.G.,(1971),J.Acoust.Soc.Amer. (49),no 3,part 2, 878-889.

DEELEN,W.Van & NIELSON,P.,(1969), Appl.Opt. (8),951-5.

DERESIEWICZ,H,(1956), J.Appl. Mech. (23),319.

DERESIEWICZ,H, & MINDLIN,R.D.,(1955),J.Appl.Mech.(22),86-88.

DEVELIS,J.B.& REYNOLDS,G.O.,(1967), Theory and Applications of Holography (London:Addison and Wesley).

DEW,G.D.,(1964), J.Sci.Instr. (41),160-162.

DEW,G.D.,(1966), J.SCi.Instr. (43),409-414.

DOAK,P.E.,(1959), Acustica, (9),1.

DODD, .,& DOAK,P.E.,(1971), J.SOUND Vib. (16), no 1, 89-98.

DWIGHT,H.B.,(1961), Tables of Integrals and Other Mathematical Data (New York: Mackmillan).

EBBING,C,E,(1971), J.Sound Vib.(16),no 1, 100.

EBBING,C.E, & INGALLS, D.J.,(1969),paper 7D4 Acoust.Soc.Amer.Autumn conf.

EL-ABDIN,H.Z.,(1963), M.Sc Thesis, University of London.

ELIASON,B. & MOTTIER,F.M.,(1970), Opt.Soc.Amer. Spring Meeting. Fe 18.

FEIN,M.O. & GREEN,E.L.,(1968), Appl.Opt. (7), 1864-5.

FERNELIUS,N. & TOME,C.,(1970), J.Opt.Soc.Amer.(80),739.

FERNELIUS,N. & TOME,C.,(1971), J.Opt.Soc.Amer.(81),no 5, 566-572.

FERRIER,W.G.,(1969), Contemp.Phys. (10), 413-36.

FRYER,P.A. et al.,(1967), Proc.Int.Symp.on the Damping of Plates by means of a Layer Leuven 15 Sept.

FRYER,P.A.,(1968), D.I.C. Thesis, University of London,Imperial College.

FRYER,P.A.,(1969) ,Opt. Tech. (2),36-39.

FRYER,P.A.,(1970b), Appl.Opt. (9), 1216.

FRYER,P.A.,(1971), Repts.Prog. Phys. (33),no 5, 489-531.

FRYER,P.A.,(1972), Appl.Opt.(11).7, 1642-1646.

GABOR,D.,(1948), Nature Lond.(161),777-8.

GABOR,D, ET AL, (1965), Phys. Lett.(18), 116-8.

GATES,J.W.C. & HALL, R.G.N.,(1970), E.U.H.*

GOODMAN,J.W. & KNIGHT,G.R.,(1968), J.Opt. Soc. Amer. (58), 1276-83.

GOSELE, .,(1956), Acustica,(6), 94.

GROH,G.,(1970), E.U.H.*

HALLOCK,J,N.,(1968), Amer.J.Phys.(36),762-3.

HALL,R.G.N.& GATES,J.W.C. & ROSS, .,(1970), J.Sci.Instr.(3),789.

HECKL,M.A.,(1960), B.B.N. Rept. no 773.

HECKL,M.A.,(1967), Proc.Int. Symp. on the Damping of Plates bya layer.

HERMAN,J.,(1966), Phd Thesis, Rhein Westphalia Technical High School,also Min.of Def. R.& D. dept. trans no 1647.

HERTZ,H.,(1881), J.Reine Angew Crelle (92) 115.aslo collected works (1882).

HOLLISTER,G.S.,(1962), Appl.Mat.Res. (1), 149-59.

HOVANESIAN, J. Der & VARNER,J.,(1970), E.U.H.*

HOVANESIAN, J. Der & YUNG,YY.,(1971), Appl. Opt. (10), no 12, 2734-38.

HUNTER,S.C.,(1957), J.Mech. Phys. Solids (5), 162.

JACOBSON,A.P.,(1969), J.Opt. Soc. Amer. (59),1529.

KENEMAN,et al.,(1970), Appl.Opt. (9),no 10, 2279.

KIEMLE, H. & WOLFE,U., (1970) Paper ThB15, Opt. Soc.Amer.Spring Meeting.

KIRK,J.P. (1966), Appl. Opt.(5),1684-5.

KIRK,J.P. & LEISSA,A.W.,(1967), J. Sound Vib. (5),no 2, 178-184.

KINSLER,L.E. & FREY,A.R.,(1950), Fundamentals of Acoustics.

KLEESATTEL,C.,(1968), Acustica,(20),no 1,1-13.

KOLSKY,H.,(1953), Stress Waves In Solids O.U.P.

KORPEL,A. & WHITMAN,R.L.,(1968),Appl.Opt(8),1567-76.

KORPEL,A. & WHITMAN,R.L.,(1968b), I.EEE. Trans.Sonics & Ultrasonics SU1557

KUTTRUFF & THIELE,R., (1954), Acustica (4), 614.

LAMB,H., (1917), Proc.Roy.Soc. (93A),114.

LAMBERTS,R.L. & KURTZ,C.N.,(1970), J.Opt.Soc.Amer. (60),724.

LATTA,J.N.(1968), Appl.Opt. (7), 2409-6.

LEENDERTZ, .,(1970), J. Sci.Instr. (3),no 2, 214-8.

LEHMAN,M.,(1970), E.U.H.*

LEITH,E.N. & UPATNEIKS,J.,(1962), J.Opt.Soc Amer. (52),1123-30.

LEONARD,C. & SMIRL,A.,(1969), J.Opt.Soc.Amer.(59), 1530.

LIFSHITZ,J.M. & KOLSKY,H.,(1964), J.Mech.Phys.Solids (12), 33-43.

LIN,L.H. & BEAUCHAMP,H.L.,(1967), Appl. Opt. (6), 1255-8.

LIN,L.H. & BEAUCHAMP,H.L.,(1969), J.Opt. Soc.Amer. (59),1529.

LIN,L.H. & BEAUCHAMP,H.L.,(1970), Rev. Sci. Instr. (41), no 10.

LUBMAN,D.,(1971), J.Sound Vib. (16),no 1, 43-58.

LYON,R.H. & EICHLER,E.,(1964), J. Acoust. Soc. Amer.(36),no 7, 1344-1354.

MAESTRELLO,I.,(1967), J.Sound Vib. (5),no 3, 407-448.

MALLING,G.C.,(1967), J.Acoust.Soc.Amer. (42),no 4, 859-865.

MALLING,G.C. & NORDBY, .,(1967), I.B.M. Res. Rept (11) 492.

MAIDANIK,G. (1962), J.Acoust. Soc. Amer. (34),no 6, 809-826.

MARKOVA,G.V. et al.,(1969), Sov. Phys. Tech.Phys. (13),1470-3.

MASSEY,G.A.,(1968), U.S. Dept of Commerce doc. no. N68-14070.

MATSUMOTO,K. (1969), J. Opt. Soc. Amer. (59), 777-8.

McLACHLAN,N.W.(1934), Loudspeakers, new Dover Edn (1960).

MELROY,D.O.,(1967), Appl. Opt. (6),2005.

METHERELL,A.F. et al,(1968), Appl. Phys. Lett. (12), 340-3.

METHERELL,A.F. ET al,(1969a), Appl. Opt. (8), 1533-6.

METHERELL,A.F. et al,(1969b), Sci. Amer. Oct, 36-44.

METHERELL,A.F. et al,(1969c), J. Opt. Soc. Amer. (59), 1534-5.

MOFFATT,C.T. & WATRASIEWICZ,B.M.(1971), Paper 6-2, Symp.Appl. Holography Besancon.

MOLIN,N.E. & STETSON,K.A.(1969), J.Sci.Instr. (2), 602-12.

MOTTIER,F.M. & ELIASSON,B.,(1970),J.Opt. Soc. Amer.(60), 739.

NESTOV,S.V.,(1965), Sov.Phys. Acoust. (11) no 1, 60.

NEUMAN,D.B. & ROSE,HHW.,(1967), Appl.Opt. (6),1097-104.

NEWLAND,D.E.,(1968), J.Acoust.Soc.Amer. (43),553 (also D.I.C. notes)

NICKOLA,W., (1966), Exp. Mechs. Dec edn, 593-602.

NIKIFOROV,A.S.,(1964), Sov.Phys.Acoust. (10),no 2, 178-182.

ONOE,M. & YANO.T.,(1968), IEEE. Trans. Sonics & Ultrasonics (15),no 3.

ORR,L.W. et al, (1968), Appl. Opt. (7),202-3.

OSTER,G.,WASSERMAN,M. & SWERLING,C.(1964),J.Opt.Soc.Amer(54),no 2,109-75.

PALAIS,J,C, & WISE,J.A.,(1970).J.Opt.Soc.Amer. (60),60-714.

POTTER, . & LEEDHAM, . .,(1971),

POWELL,R.L.,(1970),E.U.H.*

POWELL,R.L. & STETSON,K.A.,(1965a), J.Opt.Soc.Amer. (55),1593-8.

POWELL,RLL. & STETSON,K.A.,(1965b), J.Opt.Soc.Amer. (55),1694-6.

POWELL,R.L. & STETSON,K.A.,(1966) , J.Opt.Soc.Amer. (56),1161-7.

RASKE,T.F. & SCHLACK,AL.,(1967), J.Acoust. Soc.Amer. (42),no 3, 625-635.

RAYLEIGH Lord (J.W.STRUTT) (19 ) Theory of Sound, Dover.

R.C.A.,(1969), Wireless World, Sept. 402.

REDMAN,J.D. et al (1969), J.Opt.Soc.Amer. (59),1545.

REDWOOD,M.,(1960), Mechanical Waveguides,Pergammon.

RELTON,E.E.,(1946), Applied Bessel Functions,Blackie.

REID,C.D.,(1967),Inst.of Phys.Meeting:'Opt.Methods for dynamic stress analysis' 18 April.

ROSE, ., et al (1970),Appl.Opt. (9),no10, 2394.

ROYAL SOCIETY CONFERENCE (1967), 'Origin and Treatment of Noise in Industrial Environments' March.

RUTKOWSKI, .(19 ), 'Stroboscopes'.

RUDDER,C.L.,(1967),Appl.Phys.Lett. (10),270-2.

RUSSO,V.& SOTTINI,S.,(1968), Appl.Opt. (7),202.

SCHROEDER, .,(1954), Acustica, (4), 594.

SCHROEDER .,(1962), J.Acoust.Soc.Amer. (34), 1819.

SHELDON,D.F. & SEWARDS,G.B.,(1970),Eng.Mat. & Design, p 843.

SHERIDON,N.K.,(1968), Appl.Phys.Lett. (12), 316-18.

SHENDEROV,E.C.,(1967), Sov.Phys.Acoust. (12), 336-338.

SHULTZ,T.J. (1971a), J.Sound Vib. (16),no 1, 17-28.

SHULTZ,T.J.,(1971b), J.Sound Vib.(16),no 1, 119-129.

SHWEPPE,J.L.,(19 )

SIEBERT,L.D.,(1967), App.Phys.Lett. (11),326-8.

SINCLAIR,R.,(1964),M.Sc. Dissertation,Imperial College. Impacting Bodies.

SOUTHWELL,R.V.,(1922), Proc.Roy.Soc. (A101),133-153.

STAVSKY,Y. & LOEWY, .,(1971), J.Acoust.Soc.Amer. (49), no 5,pt 2,1542.

STETSON,K.A.,(1967), Appl.Phys.Lett. (11),225-6.

STETSON,K.A.,(1969), Optik, (29), 386-400.

STETSON,K.A.,(1971a), N.P.L. Reports (Privately Communicated).

STETSON,K.A.,(1971b), Private Communication.

STROKE,G.W.,& HALIOUA.,(1970), Phys.Lett.(33A),no 1, 3.

THEOCARIS,P.S.,(1969), Moire Fringes in Strain Analysis. Pergammon N.Y.

THEOCARIS,P.S.,(1964), Proc.Soc. Exp.Stress Anal. (21), 153-9.

THEOCARIS,P.S.,(1967), Brit. J. Appl. Phys.(18), 513-19.

THOMPSON,B.J.& PARRENT,G.B.,(1967), Science,J. (2),49-9.

TILLETT,J.P.A.,(1954), Proc.Phys.Soc. (B 67),677.

TIMOSHENKO, . .,(1954), Vibration Problems in Engineering.

TOBIAS,S.A.,(1957), Chartered Mech.Eng. March, 124.

TOKITA,Y.,(1961), J,Phys.Soc.Jap. (16),no 5, 1008-1019.

TOLANSKY,S. & WOOD,A.F.B.,(1958), Physica (24), 508-18.

TONNDORF,J.,(1970). J.Acoust.Soc.Amer. (47),pt 1, 60.

TOURRET,J.,(1971), Electro-Opt. Internat.March.session X paper 4 A.

TSAI,Y.M.,(1966), N.S.F.- GP-2010/5 Brown University U.S.A.

TSAI,Y.M.,(& KOLSKY,H.,(1967)., J.Mech.Phys.Solids,(15),263-278.

TSURUTA,T, & ITOH,Y.,(1970), Appl.Phys.Lett. (17),no 2, 85-86.

TSURUTA,T. & SHIOTAKE,J.,(1967), Jap.J.Appl.Phys. (6),1166.

UPATNIEKS,J.,(1969),J.Opt.Soc.Amer.(59), 1539.

UPATNIEKS,J. & LEONARD,C., (1970), J.Opt.Soc.Amer. (60),297-305.

URBACH,J.C. & MEIER,R.W.,(1969),Appl.Opt.(8), 2269-91.

VARNER,J.,(1970), Appl.Opt. (9),2098-2100.

VARNER,J. & ZELENKA,J.S.,(1969),Appl.Opt. (8),2269-91.

VIENOT,J.Ch. et al (1970), E.U.H.*

WALLER,M.D.,(1961),Chladni Figures. London, G.Bell.

WATERHOUSE,R.V.,(1955), J.Acoust.Soc.Amer. (27),no 3, 247-258.

WATERHOUSE,R.V.,(1958a),J.Acoust.Soc.Amer. (30),no 1, 4-13.

WATERHOUSE,R.V.,(1958b),J.Acoust.Soc.Amer. (35),no 8,1144-51.

WATERHOUSE,R.V.,(1968), J.Acoust.Soc.Amer. (43),no 6,1436-44.

WATERHOUSE,R.V.,(1970), J.Acoust.Soc.Amer. (47),no 4,pt 1, 961-7.

WATRASIEWICZ,B.M.,(et al),(1968a),Nature Lond. (217),1142-3.

WATRASIEWICZ,B.M.,(et al),(1968b), Optics Technol. (2), 20-3.

WELFORD,W.T.,(1966),Appl.Opt. (5), 872-3.

WESTPHAL, . .,(1957),Acustica (7),335.

WILSON,A.D.,(1970), J.Opt.Soc.Amer. (60),no 8, 1068-71.

WILSON,A.D.,(1970b),J.Opt.Soc.Amer.

WILSON,A.D., & STROPE,D.H.,(1970a),J.Opt.Soc.Amer.(60),no 9, 1162-65.

WILSON,A.D., & STROPE,D.H.,(1970b), Rev.Sci.Instr.(U.S.A.),881-2.

WITHRINGTON,R.J.,(1968)(1970), E.U.H.*

YORKE,R., (1961),Lecture to Brit.I.R.E. London Nov 29.

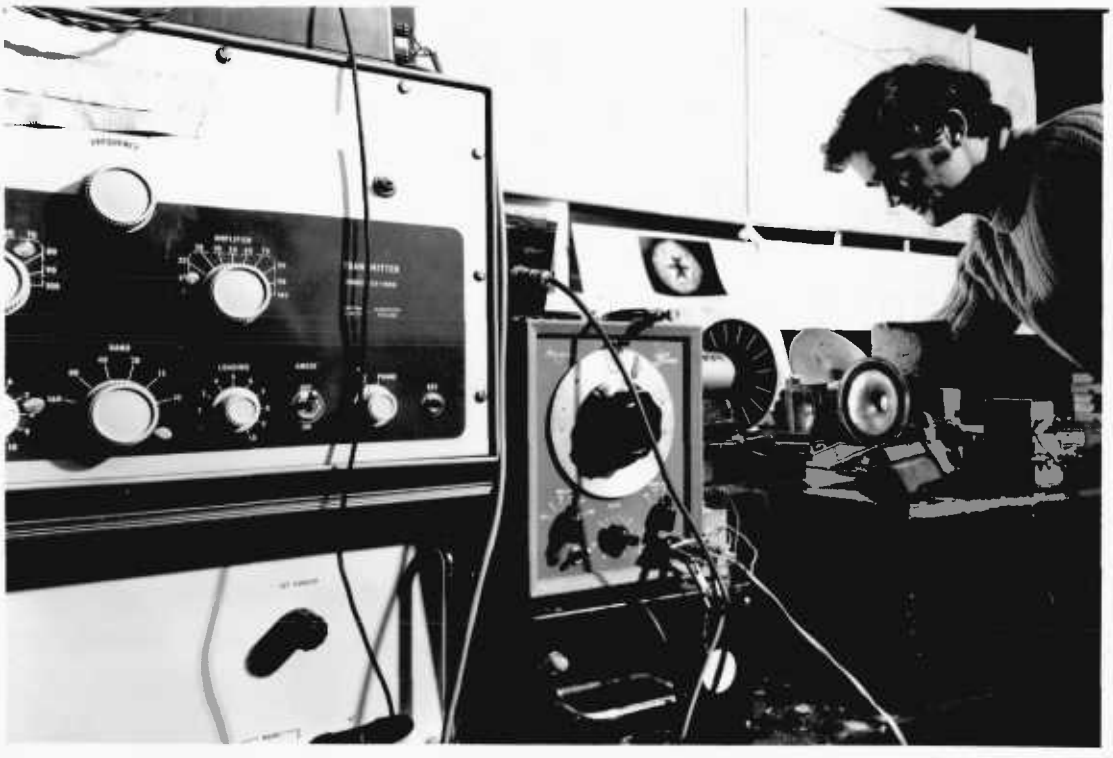
WUERKER,R.F., & HEFLINGER,L.O.,(1970), E.U.H.*

WUERKER,R.F., & HEFLINGER,L.O.,& BRIONES,R.A.,(1968),App.Phys.Lett (12) 302-3.

ZIMMERMAN,S.,(1969),Acustica, (21),no 2, 61-73.(In French).

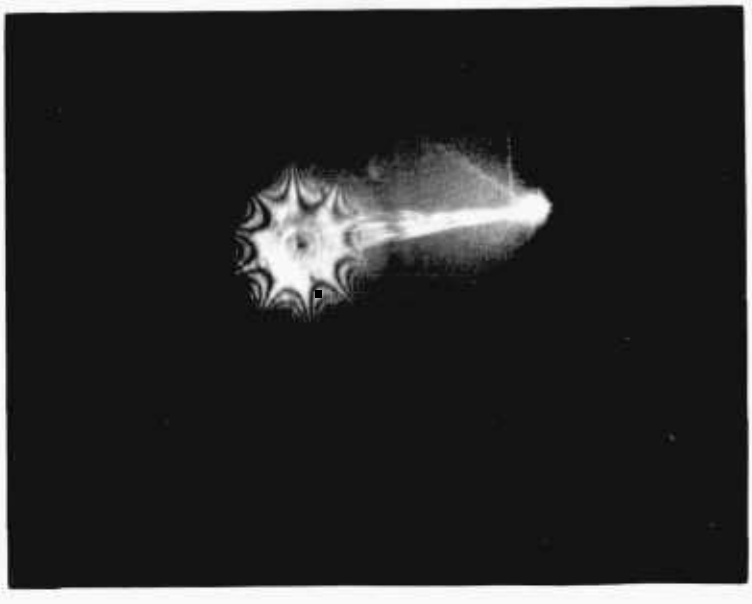
ZENER,C.,(1941),Phys.Rev. (59),669.

Plate Number 21



The Author scanning a plastic cone speaker

Plate Number 22



Photograph from 3180 Hz Scanned Hologram, Plate 1

## Principal Mathematical Symbols

| | |
|---|---|
| $a$ | Amplitude of Light Wave |
| $a$ | Radius of Plate |
| $A$ | Area of Plate |
| $b$ | Clamping Radius |
| $c_a$ | Velocity of Sound in Air |
| $d$ | Distance moved |
| $d_o$ | Maximum Object Displacement |
| $\dot{d}$ | Object Velocity |
| $\ddot{d}$ | Object Acceleration |
| $D$ | Flexural Rigidity |
| $e$ | Coefficient of Restitution |
| $E$ | Younge's Modulus |
| $F(r)$ | Mode Shape Function |
| $f$ | Frequency |
| $f_a$ | Difference Frequency |
| $f_c$ | Coincidence Critical Freq. |
| $f_o$ | Object Frequency |
| $h$ | Thickness (or 1/2 Thickness) where shown |
| $h$ | Sandwich Filler Thickness |
| $H$ | Sandwich Total Thickness |
| $I$ | Sound Intensity |
| $I$ | Light Intensity |
| $I$ | Second Moment of Area |
| $I_n$ | Bessel Function (mod 1st kind) order n |
| $I_{tot}$ | Total Light Intensity |
| $I_{sc}$ | Scanned Light Intensity |
| $I_p$ | Intensity at Photographic Plate |
| $I_{im}$ | Image Light Intnesity |
| $J_n$ | Bessel Function order n |
| $K_n$ | Mod. Bessel Function (type 2) |
| $k_o = k_a$ | Air Wave Number $= 2\pi/\lambda_a$ |
| $k = k_p$ | Plate Wave No. $= 2\pi/\lambda_b$ |
| $l$ | Dipole Separation |
| $l_{x\ y}$ | Half lengths of panel in x and y directions |
| $M$ | Image Multiplicitance |
| $m_{x\ y}$ | Nos of elastic half waves in the x and y directions |
| $N$ | No. of S.P.L. samples |
| $N$ | Image Repitance |
| $o$ | Object Beam Amplitude |
| $p$ | $2\pi f$ |
| $p$ | Sound Pressure |
| $P$ | Power Output |
| P.W.L. | Power Watt Level |
| P.D. | Path Difference $= 2\pi/\lambda\ 2d$ |
| $1/p_n$ | Fractional harmonic ampl. |
| $Q$ | The mode strength measure |
| $r$ | Amplitude of Reflected Light wave |
| $r$ | Radius of Scanning Disc |
| $r$ | Distance Coordinate |
| $R$ | Distance |
| $r^*$ | Cplx.Conj. of r |
| $R\ R'$ | Reflection Coefficients for Travelling and Inhomogeneous Bending Waves. |
| $R_{ii}$ | Rad. Resistance ith monopole |
| $R_{ij}$ | Measure of Interaction ith and jth monopole |
| $s$ | Number of Nodal Diameters |
| $S$ | Surface Area |
| $S$ | Total Absorbtion |
| S.P.L. | Sound Pressure Level dB ref .0002 microbar. |

$T$ Total Time
$t$ Instantaneous Time
$t$ Contact Time

$U$ Plate Circumpherence
$V$ Room Volume
$v$ Velocity = $\dot{d}$

$W$ Power Output in Watts
$W''$ Energy Lost per Cycle
$W'$ Energy Stored per Cycle

$x$ Distance along Hologram
$X$ Path Length of Microphone
$X$ Interslit Distance

$z$ Number of Slits
$\mathfrak{Z}_{f,m}$ Impedances to transverse and bending waves resp.

$\theta$ Object Phase
$\Theta$ Angle to Plate Normal

$\phi_{1\ 2}$ Phases of Light Wavefronts

$\Psi_o \Psi$ Angles in Plane of Plate
$\Psi_m(r)$ Mode Shape Function

$\lambda$ Wavelength
$\lambda_a$ Wavelength in air
$\lambda_b$ Bending Wavelength

$\Gamma$ Directivity Function

$\eta$ Distance = d
$\eta$ Loss Factor = $W''/2\pi W'$

$\mu = \alpha_m$ Constant depending on mode no.
$\omega =$ $2\pi f = p$

$\rho$ Density
$\rho_a$ Air Density
$\sigma = \gamma$ Poissons Ratio

Glossary (Some terms not fully explained in the text)

Acoustic Waveguide. Tube with walls of acoustic impedance greater or less than its contents causing sound waves to be guided by reflections.

Acoustically Fast or Slow. Bending wavelength in the Panel is greater or less than the longest possible projected air wavelength.

Base Unit. Loudspeaker handling the lower frequency range usually between 20 Hz and 1 KHz.

Bomb Dust. Fine dust from ruined houses. Found by Waller to be better than Lycopodium in making nodal lines visible.

Break-up. All parts of a Loudspeaker cone exhibiting Break-up do not follow the movements of the voice coil exactly.

Cavitation. Negative pressure on a liquid of sufficient magnitude causes 'holes' or vapour bubbles to form which can then collapse impulsively.

Coherence Length. Maximum distance along a ray path over which there is a definite phase relationship.

Coefficient of Restitution. The ratio of two heights: the height from which an object is dropped and the height to which it rebounds.

Chladni Sand Patterns. Chladni used sand to show up the nodal regions of vibrating plates.

Chassis. Frame onto which the Loudspeaker magnet, spider and surround are attached.

Diffraction Efficiency. Fraction of incident light intensity diffracted into useful images.

'Dips'in Response Curve. Narrow frequency bands in which the response falls below the average level, usually showing a definite minimum.

Fresnel Mirror. Mirror with a stepped profile having similar optical properties to a concave or convex mirror - analogous to Fresnel Lens.

Flutter Echoe. High 'Q' room mode usually between two hard parallel walls allowing a set of rapid,decaying echoes to be heard after impulsive input

Filter Set. (One of many Types made by Bruel and Kjaer of Denmark) In these experiments: Constant percentage selectable bandwidth tuneable notch pass filter. Heterodyne filter gives constant cycles bandwidth.

Gear-Like. Exhibiting some of the vibration properties of real gears.

Geodesic. Curving in two dimensions.eg saddle or globe shaped - imparts possible increase in stifness.

'Hum'. Unwanted presence of 50 Hz and/or 100Hz components in a signal usually picked up from mains or power supply.

Lumped Damper. All the damping properties of the material effectively or even actually applied at one point.

Live Fringe Hologram. Allows real time fringes to be observed showing the difference between original (exposure) and final object positions.

Light Sheets. Parallel planes in space exhibiting regularly alternating changes in light intensity.

Lycopodium. Fine pollen used to show up plate modal patterns.

Modal Piston. A Piston having bending resonances causing it to exhibit nodal circels (qv) and Nodal Diameters (qv).

Mid Range Speaker. Speaker capable of handling or only fed with frequencies within a band of about 300 Hz to 10KHz.

Nodal Diameters, Circles. Diameter connecting points of zero or minimum vibration amplitude, circle connecting points .....

Pitch-line schock. Impulsive change in gear meshing direction as teeth change from rolling in to rolling out of mesh.

'Peaks' in Response Curve. Narrow frequency bands in which the response rises above the average level, often showing the characteristics of a resonance curve with a definite maximum.

Rayleigh Waves. Surface waves on a solid where the particles execute ellipsoidal motion, the amplitude decays exponentially with depth.

Rubber Roll Surround. Loudspeaker surround (qv) being a half torroid of rubber, cross section usually a half circle.

Sagitta. Term describing departure from linearity: chord length/ distance from chord center to arc mid point.

Stick-Slip. Impulsive 'jerky' motion where one object moves over another in a series of approximately equal impulsive steps.

Sandwich. Composite materi al of high bending stifness to mass ratio, usually having thin stiff skins bonded to a light 'filling' with good resistance to crushing.

Surround. Part of a Loudspeaker connecting the outer edge of the cone to the chassis, often designed to help in surpressing break-up (qv) modes.

Solid $CO_2$ Method. (After Waller) Small sharp chip solid $CO_2$ heated by adjacent plate sublimes gas which forces plate away thence diminishing chip heating - plate returns and cycle repeats.

S.P.L. Sound Pressure Level = 20 $\text{Log}_{10}$(p/ref p) ref p = 0.0002 microbar ($2 \times 10^{-5}$ Newton/$m^2$)

Scotch Lite. A retroreflective preparation relying on many tinly glass spheres to reflect a large fraction of the incident light into a narrow cone around the incident direction.

Stacked Reference Beam. Reference beam directed to holographic plate from above or below the object (beam).

Spider. Device for centering the voice coil (qv) in the magnet gap.

(Super)Harmonic. Frequency being an integer multiple of the fundamental

Subharmonic. Frequency being an integer submultiple of the fundamental

Seismic Mass. Mass used to give an approximation to a 'stationary surface' - its main property is high inertia.

Treble Unit. Speaker handling frequencies above from 3 to 10 KHz.

Transmission Loss. Ratio of the sound pressure at a point P with to without the panel in position expressed in db.

Weighting Ring. Mass placed at the voice coil to lower the overall response curve and roll off the treble at a lower frequency.

Wood Grain Fringes. Fringes 'mapping' random movement in a Loudspeaker cone.

Voice Coil. Coil of wire attached to the apex of the Loudspeaker cone resting in a magnet gap. Signal current passed through it causes movement of the cone .

## Acknowledgements

The Author would like to thank the Admiralty for supporting the first part of this work and for providing the topic: "Gear Wheel Noise".

He would also like to thank Rank Wharfedale Ltd. for supporting the holographic work on Loudspeakers and for giving permission to use Loudspeaker material in talks, lectures and papers which material has been included here.

Finally he would like to thank Dr. R.W.B. Stephens for his advice and encouragment and Mr D.I.Pullen of'H.J.Leak and Co'and'Rank Wharfedale'for his advice and encouragement also. The author is grateful to his collegues in the Acoustics Laboratory of Imperial College Physics Dept. for helpfull discussions - in particular J. Scott (now PHd) and B.Ray (now PHd).

# PAPERS CITED IN SUPPORT OF THIS THESIS

# Inexpensive system for live stroboscopic holographic interferometry

P. A. FRYER

Acoustics Group, Physics Dept, Imperial College, London

A simple inexpensive system for live stroboscopic holographic interferometry is described. Particular attention is given to the light-saving techniques made necessary by the low-cost, and therefore weak, lasers available. Time averaged and stroboscopic methods are discussed and a simple stroboscopic system is described. Finally some techniques for altering the basic sensitivity of the method are briefly outlined.

THE AUTHOR'S INTEREST in holography stems from its use for vibration analysis in engineering. Most of the requirements for the system can be met very cheaply with no sacrifice in the quality of the holograms produced. The most expensive single item is the laser, but the expense can be kept to a minimum by using lasers of fairly low power. The system described below is in use in the analysis of plate vibrations at Imperial College.

## BASIC ELEMENTS OF THE SYSTEM

**The laser.** For the experimental system two relatively weak lasers were available giving 1mW and 15mW output. The more powerful of the two makes live fringe work easier, though the weaker one can be used with difficulty.

**Vibration isolation and dimensional stability.** For a good hologram, the various parts of the system must not move relative to each other by more than, at most, one eighth of a wavelength of light used. For these experiments a massive concrete raft was cast on top of a specially strengthened workbench. This was isolated from floor-borne vibrations by 'Barry Mounts' resting in dry sand. This arrangement results in live fringes which are completely stable and unaffected by vibrations from the floor. The rigid concrete raft also maintains the relative positions of the various optical components to within high tolerances and good holograms are produced.

**Constant temperature conditions.** To avoid relative expansions of the system and alterations in path lengths due to hot air currents, the whole system should be enclosed in a constant temperature enclosure. The small dark room used for this experiment satisfies this condition if the various power amplifiers necessary for the experiment are located outside it.

**Optical components and holders.** Many commercial components are available for holography but these were considered unnecessary. All that was used for these experiments were some metallurgy microscope objectives, small front silvered mirrors and plasticine. The plasticine, if used correctly, prevents creep or high frequency oscillations and also couples the components well to the massive table.

**The hologram holder.** A difficult aspect of live fringes work is the relocation of the exposed hologram to within a fraction of a wavelength of light used. This is simply accomplished with the plate holder shown in Fig 1.

Provision was made to delicately move the photographic plate if it didn't re-locate correctly (not shown in the figure), but it can be easily corrected with the fingers. Displacements or rotations of the object or the hologram in the plane of the hologram produce parallel fringes in live fringe work. Movement towards or away from the object produces circular fringes. In practice more than three fringes on relocation are rare and the fringes that do occur are easily removed.

If the apparatus is left for any length of time emulsion shrinkage and other effects cause more fringes of the parallel type to occur, but because this process takes several days it is not troublesome over a short period.

## LIGHT-SAVING TECHNIQUES

Because lasers available for this system are low power, several light saving techniques were developed

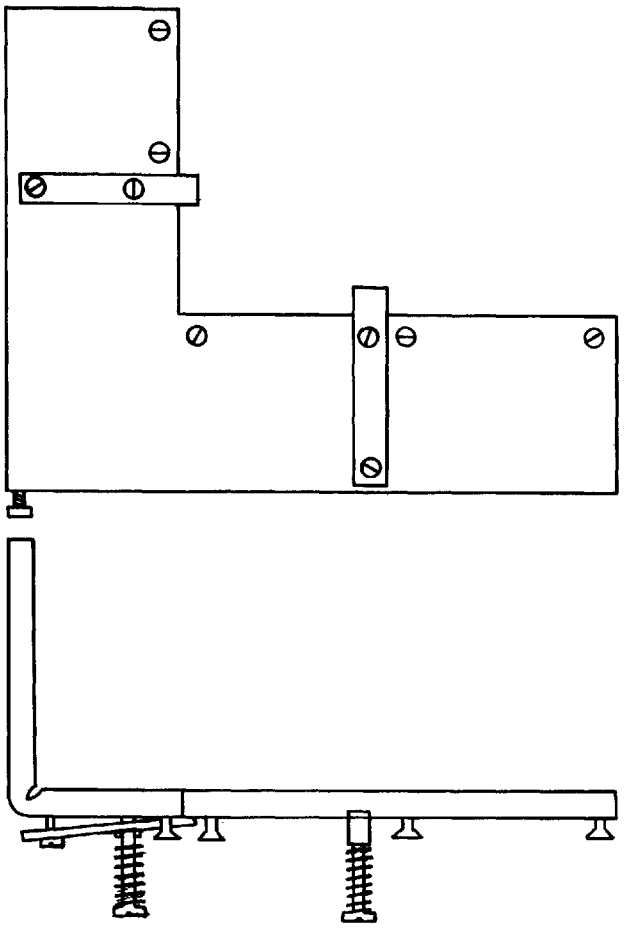


*Fig. 1 Simplified plate holder.*

to allow live fringes to be seen unaided by the eye. The problem is not so acute if frozen fringes are taken because long exposure times can make up for lower powers. Long exposure times put great demands on mechanical and electrical stability of the system however, and so they are not desirable. The most important way of saving light lies in the treatment of the object itself. Objects should not be painted white as most of the light falling on the plate is then wasted.

If all the light falling on the object could be directed back onto the hologram this would result in an intensity multiplication of at least $\pi r^2$, where r is the distance between the object and the hologram. The object must also not be specularly reflecting. If it were, on reconstruction a small spot of light would be seen to move about in space as the head of the observer was moved (Fig 2).

For the formation of a hologram useful for interferometry, light should fall on each part of the hologram from each part of the object with equal intensity. If the object is a flat plate, simply roughening its surface gives some improvement, but as the object is made larger the outer regions of the plate become less bright compared to the centre. This is not only because the laser beam is not equally bright over its cross section, but also because a simply scored plate is neither perfectly diffusing nor perfectly reflecting. Also with poorer quality lasers spatial and

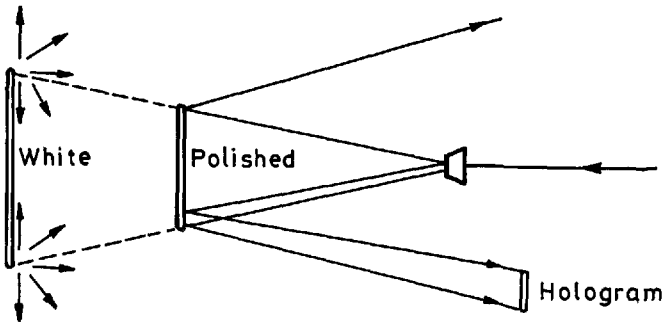



*Fig. 2 Shows the difference in light reflection between a white painted object and a polished object.*

temporal coherence may not be very good and this would also tend to give a reconstruction whose outer regions are less bright than the central regions.

So the object must form all the incident light into a beam which can then be directed onto the hologram. Also all parts of the object must equally illuminate all parts of the hologram.

The simplest way of doing this is to coat the object with Scotchlite. This is a type of paint used for country road signs. It consists of a reflecting paint onto which are sprayed many tiny glass balls. It reflects incident light back where it came from—or rather in a narrow cone around the incident direction. This narrow cone was too sharp for the present experiments however. Cinema screen beading should spread the light over a wider cone, but this means that less light will fall onto the area of the hologram.

Recently Jacobson has described a technique using a 50% transmission beam splitter set at 45° in the object beam illumination path. This enables Scotchlite to be used with a 35-fold improvement over the 'white' object (Paper FB14 Opt. Soc. Am. Conference, October 1969).

The method is a watered down version of the ideal reflection plate which is a kind of Fresnel mirror (Fig. 3). A system of concentric grooves with a saw

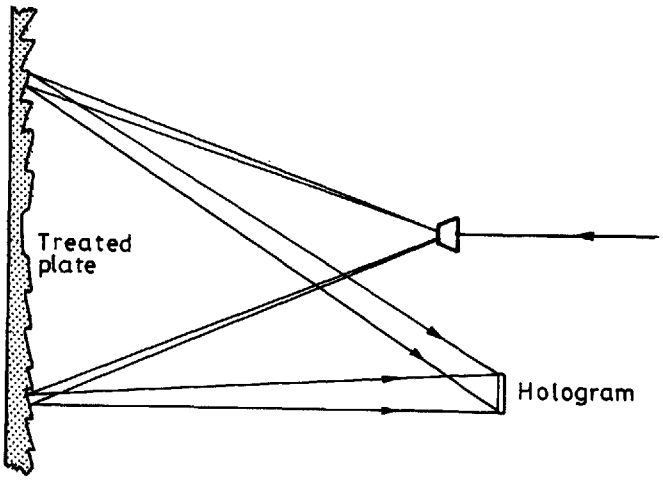



*Fig. 3 Plate treatment allows plates up to 46cm to be taken.*

tooth profile should be formed on the plate. The rising floor of each groove should specularly reflect incident light onto the whole hologram. Groove density, floor angle etc. can compensate for the various darkening and angle effects.

Workshop-turned and hand-gouged plates are a poor compromise but the hand gouged plate is the better. It is also better than Scotchlite and cinema screen beading and forms a beam which can be directed onto the hologram. Though some light is still wasted a saving of about 100-fold is achieved over the white painted object.

The next most important way of saving light stems from the fact that no beam splitter is used. Light reflected from the plate front surface of the object beam expanding lens is used as the reference beam, therefore light that would normally be wasted makes a beam splitter unnecessary. The intensity of the reference beam is varied by using a zoom lens system made from two microscope objectives (Fig 4).

A further way of saving light relies on a technique recently described by Hallock. Best contrast can usually be obtained with a final neutral density of about 1.0. If it requires say T seconds to do this, holograms of almost the same final contrast can be made by exposing the photographic plate in the normal manner for say t seconds, and then re-exposing the plate to coherent or incoherent light sufficiently to bring the final neutral density to about 1.0. This additional light places the final exposure in the centre of the linear portion of the amplitude transmittance curve where contrast is greatest, and it can be added before or after the hologram is taken. Reductions of 2% in contrast have been described with $t = T/15$.

The final way of saving light lies in the choice of photographic plate. There is little point in having plates whose definition exceeds the experimental requirements—especially when this definition comes at the expense of film sensitivity. The number of lines per millimeter needed is $1580\sin\theta$ for helium neon lasers, where $\theta$ is the maximum angle between the object rays and the reference beam. For a maximum $\theta$ of about 45° a definition of about 1000 lines/mm is required. Ilford helium neon laser plates have a capability of about 1500 lines/mm and are relatively sensitive, though Agfa 10 E 70 plates have comparable resolution and may be faster. These plates are developed, washed and fixed in the experimental darkroom under constant temperature conditions.

## TIME AVERAGING VERSUS STROBOSCOPIC HOLOGRAPHY

With time averaging the photographic plate is exposed to the vibrating object and the hologram produced is a kind of average of all the positions covered by the plate during the exposure. (Powell & Stetson, December 1965). For a sinusoidally vibrating plate the result is similar to the hologram that would be produced if the photographic plate were exposed only to the extreme ends of the movement. This is because the object spends most of its time at these two ends.

The time-averaged reconstructed image will be covered with fringes and the spacing between them corresponds to movements of approximately $\frac{1}{4}\lambda$.

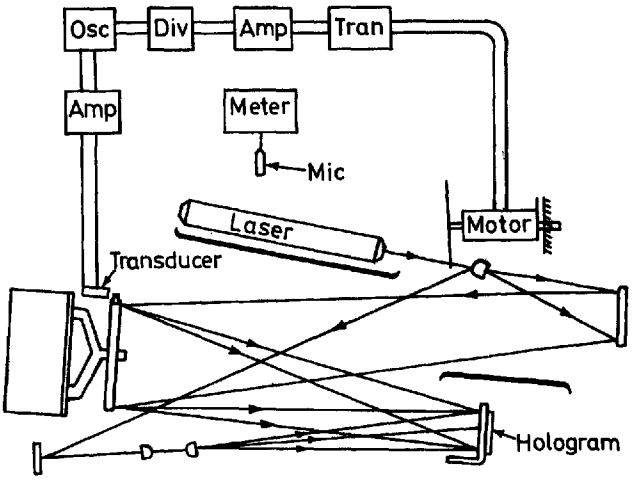



*Fig. 4 Schematic diagram of experimental system.*

The higher order fringes diminish rapidly in amplitude, but the brightly reconstructed nodal lines are easy to pick out.

The biggest advantages of time-averaged holography are its simplicity and the short exposure times needed. A disadvantage is the complexity of the interpretation needed to find the motion from the fringes.

With stroboscopic holographic interferometry, as generally applied, roughly half the number of fringes are produced for the same amplitude of movement. This is because the fringes produced are usually the result of interference between the stationary plate and one of the extremes of the motion. The fringes produced by the time-averaged method are, effectively, the interference between the two ends of the motion.

Two advantages of the stroboscopic method are firstly, that the fringes are of equal contrast right out to the edges of the test plate, and secondly, vibrations that are not sinusoidal can be studied by altering the phase of the strobe, and therefore finding the amplitude of the motion at any desired point in a cycle.

Possibly the best and most efficient way of arranging a stroboscopic holographic experiment is to cause the laser to flash once per cycle. This can be done by using a Q-switched ruby laser, or by altering the exciter of a continuous wave laser so that it flashes once per cycle, possibly with an increased output per flash. The phase of the flashes must be altered electronically with this method. By far the simplest way of strobing the light is to place a chopper disc between the laser and the experiment. This will unfortunately waste at least nine tenths of the light and means that for live work a 15mW laser is preferable. This method, however, has the advantages of simplicity and flexibility.

One way of chopping the light is to use a powerful synchronous motor, with a strobe wheel attached, fed from the same source as the object excitor. The motor, though it was designed for 50Hz work, is easily run up to much higher frequencies by altering its capacitor and allowing for the much higher voltages necessary. The phase of the strobe is simply altered by rotating the whole motor about its spindle axis.

With this simple system object vibrations up to 1000Hz may be studied. For higher object frequencies a separate amplifier must be used to drive the motor and this is then fed via a simple integrated circuit frequency divider. With this system the top frequency limit is greatly extended and the motor remains locked in phase with the object vibrations at all times.

Each time the strobe driving frequency is halved, the size of the holes in the strobe disc should also be halved and their number doubled. This is to maintain the chosen on-off ratio and to ensure one pulse per cycle. If the light is on for too large a fraction of a cycle, only that part of the cycle during which the object moves least (i.e. for sinusoidal oscillations the maximum displacement) will be effectively frozen. Other parts of the cycle will produce a 'limited time averaged' fringe system, being the average of the object positions during the on period. When the diameter of the strobe disc holes becomes smaller than the laser beam diameter, the beam must be focused down using additional lenses with some consequent light wastage. However 10kHz object vibrations can be frozen with the unfocused system.

Results are being taken with the double exposure method. The strobe phase is set up using a live fringe hologram. A further hologram is exposed to the strobed vibrating plate for about two seconds and finally re-exposed to the stationary plate for a further $\frac{1}{5}$ second. This method gives clear good contrast frozen stroboscopic fringes up to object frequencies of at least 8kHz.

## ALTERATIONS IN SENSITIVITY

The basic sensitivity of the method, assuming the plate is viewed and illuminated normally (approximately true in the present experiment) is one fringe corresponding to a plate movement of $\frac{1}{2}\lambda$ i.e. $3.164 \times 10^{-5}$cm. This can be increased either by using real time holography, which gives roughly twice as many fringes for the same amplitude of plate oscillation, or by adjusting the strobe phase so that the double exposure is between the two stroboscopically frozen maximum amplitudes. By using a photodensitometer on the frozen fringe hologram sensitivities of up to $\frac{1}{100}$ of a fringe are possible.

Wuerker et al. have shown that by using a frequency doubling crystal in the illumination path, holograms may be taken with ultra-violet and red light simultaneously. On reconstruction with red light alone, the two images are spatially separated and the image corresponding to the ultra-violet exposure has roughly twice as many fringes as the red light exposure.

Metherall & Spinak have described a technique for use when the object vibration is less than a quarter of a wavelength of light. When taking a time averaged exposure a mirror in the object illumination path is vibrated from the same source as the object. Its amplitude and phase are chosen so that points of zero object movement are shifted half way down the side of the central maximum of the $J_0^2$ fringe brightness curve. Points of zero movement are then reconstructed grey and any small movement away from zero causes a brightening or a dimming of the reconstruction. Thus phase information is retained and since the curve is steep in this region, sensitivity is increased. The grey (d.c.) level may be removed by optical filtering effectively amplifying the weak spatial fringes. A similar technique can be applied to stroboscopic experiments.

With increasing angles of illumination and viewing the sensitivity may be reduced at the expense of definition. This technique is applied to advantage in the N.P.L. method for examining the insides of cylinders—here the angles of incidence are very oblique being of the order of 6°. At these angles reflection is almost specular, even from rough surfaces, thus enabling different cylinders to be compared. The low angle of incidence method allows large objects to be viewed with a laser with a small coherence length. This can be seen from the Holodiagram of Abramson.

J.M. Burch (N.P.L.) has been working on an holography-cum-moire method for desensitising the technique. Moire fringes are seen between the distorted object and a hologram containing the original grid. Another method of desentitising described by Hovanesian is the holographic contouring method. A hologram taken using light of one wavelength is illuminated with light of a different wavelength—contour fringes are then produced because of the interference between the illuminated object and the reconstruction, these are then photographed. The object is distorted and the process repeated. The displacement can be deduced from the two sets of contours thus photographed.

## CONCLUSION

A simple and inexpensive system for live stroboscopic holographic interferometry has been developed which gives clear good contrast fringes. The system is in use in the analysis of plate vibrations in the Acoustics group of the Physics Dept, Imperial College.

**Acknowledgement**. Thanks are due to the Admiralty for financial support and to Dr R.W.B. Stephens for his guidance and encouragement.

## REFERENCES

Hallock J.N. Technique to decrease the exposure times for holograms (1968) Amer. J. Phys. **36**. 762.

Powell & Stetson (1965) J. Opt. Soc. Am. **55**. 1593 and 1694.

Watrasiewicz, B.M. Mechanical vibration analysis by holographic methods. (1968) Optics Technology, **1**. 20-3.

Metherall & Spinak. Temporal reference acoustic holography and subfringe holography. (1969) Applied Optics, **8**. 1533 and 1543.

Wuerker, Heflinger & Briones. Interferometry with ultra-violet light (1968) App. Phys. Lett. **12**, No. 9. 302

Metherall. Paper ThF 11, Opt. Soc. Amer. Conference 23 October 1969.

Engineering uses of holography (symposium, 1968). University of Strathclyde.

light. The method need not be restricted to transparent objects or thermal stress. A reflected wavefront and changes due to other causes can equally well be studied. High speed recording techniques other than photography, such as photoelectric detection of the fringe motion, can be used also.

The advantages of the holographic approach with respect to other interferometric techniques are the following:

(1) *Only the change is observed.* Since the hologram compensates for the static distortions of the object under study, only changes in the object made after the hologram is recorded are detected.

(2) *Ease of adjustment.* Alignment of a hologram interferometer is easily accomplished, especially if the hologram is developed in place as was done in the work reported here.

(3) *Low cost.* Because the hologram compensates the wave fronts, relatively large aperture interferometers can be synthesized using inexpensive optics.

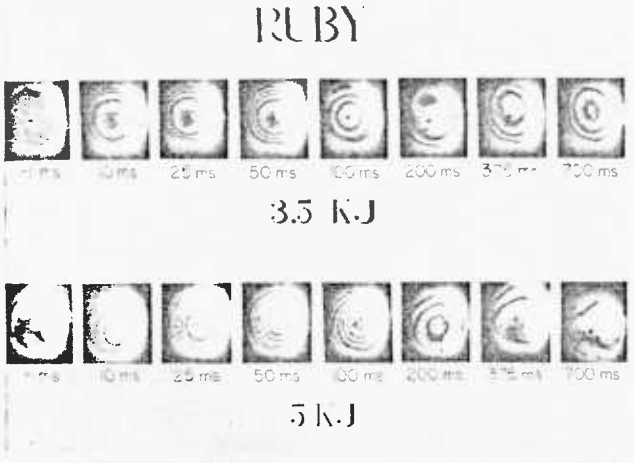



Fig. 2. Selected frames from high-speed recordings for two pump energies, with times elapsed from pumping.

The principal disadvantage of the holographic approach is the low diffraction efficiency (~10%) of the hologram. Thus for good fringe contrast, some light loss is necessary. However, as bleaching methods are improved, blazing of the hologram, thereby increasing the diffraction efficiency, should improve the performance of this method.

## References

1. C. Durou and R. Lefevre, Compt. Rend. Acad. Sci. Paris, **267**, B259 (22 July 1968).
2. This method was devised by L. A. Kersch, C. F. Jacobson, and K. R. Porter at G. C. Optronics Corporation.

# A Scanning Technique for Allowing Whole Vibration Cycles to be Stored on One Hologram

P. A. Fryer

Physics Department, Acoustics Group, Imperial College, London SW7, England.
Received 29 December 1969.

When using conventional stroboscopic holographic double exposure techniques, the laser light is either flashed or interrupted with various devices, ranging from Pockels cells to holes cut into dentists' drill tips. A disadvantage of these techniques is that the phase of the strobing has to be set so that the desired part of the cyclic motion is frozen. When frozen fringes are desired (i.e., most of the time) this necessitates the taking of a live hologram, finding the correct phase for the stroboscopic flashes, exposing the plate to the stroboscopically frozen vibrating object, and finally re-exposing to the stationary object.

With this new technique a strobe disk with an appropriate number of slits is attached to a synchronous motor and situated just in front of the holographic plate. A given slit may be arranged to scan the plate while the object traces through any given fraction, say, a quarter of a cycle (or indeed any number of cycles), and the two exposures may then be taken in the normal way.

The observer, on reconstruction, will see the number of fringes on the reconstructed object increase from zero to the number corresponding to maximum amplitude as he moves his eye along the path taken by the slit across the hologram. Thus whole cycles of movement may be preserved on one hologram, and there is no need to set the phase of the strobe beforehand. To find the maximum amplitude, for instance, the observer moves his eye along the hologram until he observes the maximum number of fringes. Raster scanning techniques may be developed to allow one or several cycles to be stored in greater detail than the simple scanning technique described above.

A technique described by Hallock[1] may be automatically incorporated in this apparatus merely by causing the reference beam *only* to scan the holographic plate, with the light from the vibrating object falling on the hologram at all times. When the object light is unreferenced (as it will be for at least 9/10ths of the time), it merely increases the dc level of the exposure on the photographic plate. This serves to reduce the time needed for the actual holographic exposure, and according to Hallock reduces the contrast by as little as 2% for a reduction of holographic exposure time by as much as 15 times.

The author has had complete success with the technique presented, and as yet only partial success with the technique described by Hallock.

## Reference

1. J. N. Hallock, Amer. J. Phys. **36**, 762 (1968).

# Dual Real Images from Holograms of Transparent Objects

S. K. Dhir and H. A. Peterson

Naval Ship Research and Development Center, Washington, D.C. 20007.
Received 26 September 1969.

Transmission holography has been used by several researchers[1,2] to obtain various kinds of interference fringe patterns related to mechanical and/or optical properties of transparent objects such as photoelastic models for stress analysis. It has been common practice to place a ground glass light diffusing screen just before the object during the formation of such holograms. The purpose served by the diffusing screen is to provide a background for the object. As a result, a clearer and more distinguishable virtual image can be reconstructed. The quality of the real image is not so good, however, and it can be focused only in one plane. Therefore, the virtual image is the one which is chosen for evaluation

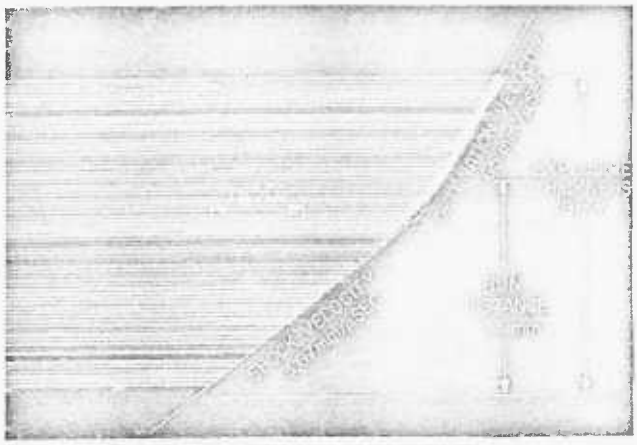


Fig. 2. Test record for a 50-mm diam cylinder of composition *B* impacted by a 6.4-mm thick aluminum flyer plate at 0.914 km/sec.

fibers in the gap are laid out in a row and have the same relative location to each other at both the explosive and the camera's object plane. As the incident shock propagates through the explosive and across the fibers it cuts off the transmitted light, and the displacement history of the shock is recorded by the camera. Since one end of the fiber bundle is presented directly to the light source, and the object plane of the camera remains constant, there is no requirement for any optical alignment of each test. Furthermore, the length of the fiber bundle permits isolation of the light source and camera from the effects of explosive detonation.

A typical test record, Fig. 2, shows the shock and detonation waves in a slab of composition *B* that has been impacted by an aluminum plate. The wave velocity is the slope of a curve through the change in light transmission of each fiber. Figure 2 shows that the shock velocity remained constant for about 60% of the run distance and then changed into a detonation wave within an interval of about 5 mm. As the shock travels through the explosive and becomes a detonation wave, the wavefront emits an increasingly brighter pulse of light. The duration of this pulse is approximately 0.03 μsec and is indicative of the intensity and small size of the reaction zone behind the wavefront.

The fiber optics bundles were made up of 0.25-mm diam Crofon[2] plastic fibers. The fiber bundles were 2.1 m long and had a light transmission of about 15%.[2] The light source was a General Electric FT 503 flashtube operated at full power. The rotating mirror camera had an *f*/4.5 lens, and the image was recorded on Kodak Linograph Shellburst film with a magnification of 1.1.

## References


1. V. M. Boyle, R. L., Jameson, and M. Sultanoff, "Determination of Shock Hugoniots for Several Condensed Phase Explosives," in *Fourth Symposium on Detonation* (Naval Ordnance Laboratory, White Oak, Maryland, 1965), p. 241.
2. "Designing with Crofon Light Guides," Technical Bulletin by E.I. du Pont de Nemours & Company, Inc., Wilmington, Delaware.


# Scanned Holography for Loudspeakers


Peter A. Fryer

Research Department, Rank Leak Wharfedale, Ltd., Idle, Bradford, Yorkshire, U.K.


Received 13 December 1971.

The system of scanned holography whereby whole vibration cycles may be stored on one hologram has been developed for the study of paper loudspeaker cones. With the basic scanned holographic system[1] a disk with an appropriate number of radial slits is placed in front of the holographic plate (Fig. 1). This disk is driven by a synchronous motor fed via a frequency divider from the same source as the vibrating object speaker (Fig. 2). A given slit reaches a given part of the photographic plate at the same phase in each succeeding object cycle. When two exposures are taken on the same plate, one with the object vibrating, the other with the object stationary, a whole series of double exposed stroboscopic holograms is taken along the one photographic plate, and the fringe system corresponding to any object phase may be seen by observing the reconstruction through the appropriate part of the photographic plate.

This system lends itself to the study of paper loudspeaker cone breakup, because paper cones are not dimensionally stable. Not only does the material itself creep over a period of several minutes, but the whole cone moves in and out on its complient suspension in response to the slightest air movement. These facts make live and consequently frozen fringe holographic stroboscopic interferometry very difficult, because the live hologram needed to set the phase of conventional stroboscopic interrupters quickly shows fringes, resembling wood grain, which are due to random cone movement. The loudspeaker chassis, which is rigidly attached to the worktable, does not show any of these fringes, of course. This random movement also prevents the taking of cine films that have been used to demonstrate whole cycles of movement by altering the strobe phase relative to the object. Time averaged holography may be used for low amplitude and high frequency measurements, but the presence of large proportions of piston motion and slight amounts of linear creep limits the usefulness of the unmodified time averaged technique although there are many varients of the basic technique that may be used.[2] Basic time averaged holography yields no information about asymmetrical vibrations.

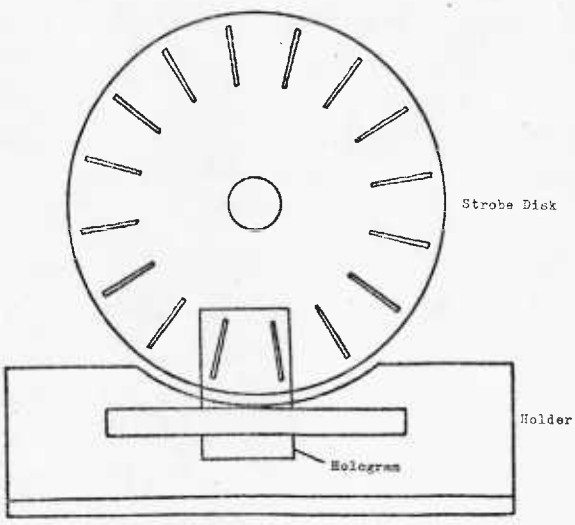



Fig. 1. Scanning disk and holder.

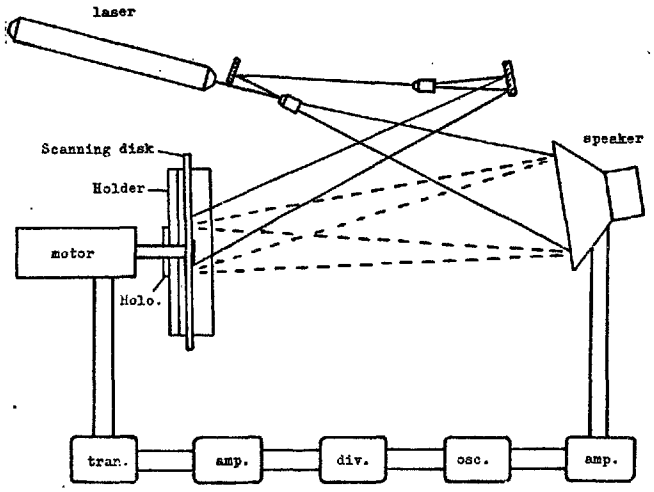



Fig. 2. Basic scanning system.

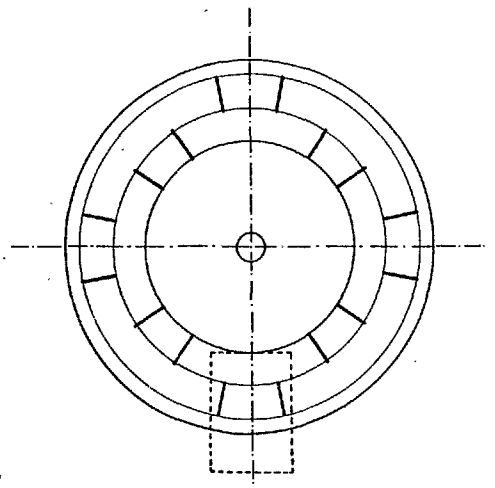


Fig. 3. Disk for single scan II.

The original scanned system is useful for the study of unstable systems in general. No live hologram is needed to set the strobe phase; the two frozen fringe exposures may be taken rapidly one after the other, and the resulting hologram has fringes corresponding to all phases of the object motion. This enables asymmetrical motion to be easily studied, the positions of the nodes to be found (because fringes do not move through them), and weaker fringes to be more easily seen (because the eye is more sensitive to movement), since they move across the loudspeaker image while the observer moves his head along the hologram.

The basic system, however, still requires two sequential exposures. For large speaker cones, or any large object whose dimensional stability lasts for seconds only and does not return to a fixed position when the excitation is removed, a different system is required. Pulsed lasers may, of course, be used, but the scanning system may also be used by altering the strobing rate so that two slits pass in front of the plate during one object cycle—both exposures may then be taken simultaneously in one longer exposure. The fringes seen with this method correspond to the difference in amplitude between different parts of the same object cycle—in fact, between any two parts separated by $\pi$ rad in phase. At one point along the hologram therefore, fringes are seen corresponding to the difference in amplitude between the two peaks of the basic method. The technique allows both exposures to be taken at once, minimizing creep effects and removing doubts about the rest position, but it no longer allows us to observe asymmetry in the vibrations, because positive and negative displacements are effectively added.

This system, called single scan I, has brought to light an unusual feature in the reconstruction of cones moving with medium and large amplitudes. The method allows us to see fringes corresponding to the peak-to-peak cone displacement at one point along the hologram. At this point the fringes seen are very similar (but twice as many) as those seen with the basic method. If, however, we move along the hologram we see that every now and then the cone completely blanks out, obliterating the ordinary fringes. At very high amplitudes this blanking out has the form of one or even two very broad fringes, which move in a manner similar to that of the ordinary fringes. It has been suggested that this effect could be due to linear motion during the exposure, but the fringelike nature of the blanking and other experiments show that this is not so. Theory, in fact, shows that if any linear motion present was sufficiently great to blank out the cone, it would be blanked out at all phases of the object vibration, i.e., the reconstruction would be blank all the way across the hologram.

Another possibility is that the blanking may be due to harmonics of the fundamental. This would explain why the blanking occurs only at certain object phases. Theory shows that odd harmonics would cause no such effect to be observed, and even harmonics are canceled out. It must also be remembered that for a given input level the amplitude of loudspeaker vibrations decreases as the square of the frequency. This means that the vibration amplitudes of any harmonics present are all reduced by the square of their frequency relation to the fundamental. This reduces the amplitude of harmonics, giving even as much as $\frac{1}{10}$ the sound output of the fundamental, to well below that of the observed effect.

Stetson[3] has suggested the more likely possibility that the blanking effect may be due to the presence of subharmonics. In fact for the first subharmonic to give one blanking fringe for every twenty ordinary fringes it need only have $\frac{1}{80}$ of the vibration amplitude of the fundamental—which is entirely possible. The author has not yet had the opportunity to test the subharmonic idea either experimentally or theoretically, but it is known that speakers do indeed produce more than one subharmonic.[4]

A different design of strobe disk gives the same sensitivity as the basic method and allows us to observe asymmetry again while preserving the advantage of a single exposure, but the upper frequency limit of this (single scan II) method is more severely limited. This disk (Fig. 3) has slits that can be made to trace past the hologram at phases corresponding to $\pi/2$ phase differences in the object cycle, and the fringes seen are similar to those seen with the basic method. Asymmetrical vibrations are now recorded, but there are twice as many points along the hologram where no fringes are seen. These correspond to the interference between two identical amplitudes. With the disk shown, two scanned bands are produced on the hologram; the upper band shows fringes that are $\pi$ out of phase with those of the lower band, thus corresponding points in the object cycle 180° out of phase may be directly compared by moving the eye vertically up and down the hologram.

Photography of the reconstruction corresponding to a given object phase may be attempted by illuminating the plate through one given slit when results will be similar, although grainer, to those obtained with normal stroboscopic holography. The system is currently aiding the design of loudspeakers at Rank Wharfedale, Ltd., Bradford.

*Note added in proof:* The 'blanking' fringes *are* due to subharmonics. Fringes due to subharmonics *only* may be produced by causing one slit to trace the hologram per object cycle—resulting in no contribution from the fundamental and (super)harmonics.

## References


1. P. A. Fryer, Appl. Opt. **9**, 1216 (1970).
2. C. C. Aleksoff, Appl. Opt. **10**, 1329 (1971); P. A. Fryer, Rep. Progr. Phys. **33**, No. 5 (1970).
3. K. Stetson, National Physical Laboratory, England; private communication.
4. I. A. Aldoshina, Sov. Phys. Acoust. **17**, 15 (1971).


# Holographic Nondestructive Testing with Impact Excitation


W. P. Chu, D. M. Robinson, and J. H. Goad

W. P. Chu is with Old Dominion University; the others are with NASA Langley Research Center, Hampton, Virginia 23365.


Received 2 February 1972.

The detection of flaws or disbonds in composite material structures using holographic interferometry has recently been reported by a number of workers.[1-5] In most applications of this technique the interferometric fringes that are used to identify the flaws in the material are produced by holographically recording the surface of the sample in various states of excitation or deformation. Generally, this deformation is accomplished by some form of thermal, mechanical, or ultrasonic transducer loading. It is the purpose of this Letter to report some experimental results of a flaw detection scheme in which the sample loading was produced by mechanical impact. The resulting deformation of the sample was then monitored by recording a sequence of double exposure holograms of the sample surface at increasingly longer time intervals after impact.

When an impact is applied to an object, transverse waves originating from the impact center will propagate outward with a velocity that is characteristic of the material structure. Holography can be used to record the transverse wave amplitudes at any time after the impact in the form of an interferometric fringe pattern.[6] If a flaw of sufficient dimension is present in the object, it will create a local disturbance to the propagating transverse wave. This wave disturbance, when recorded holographically, will show up as an anomaly in the reconstructed fringe pattern.

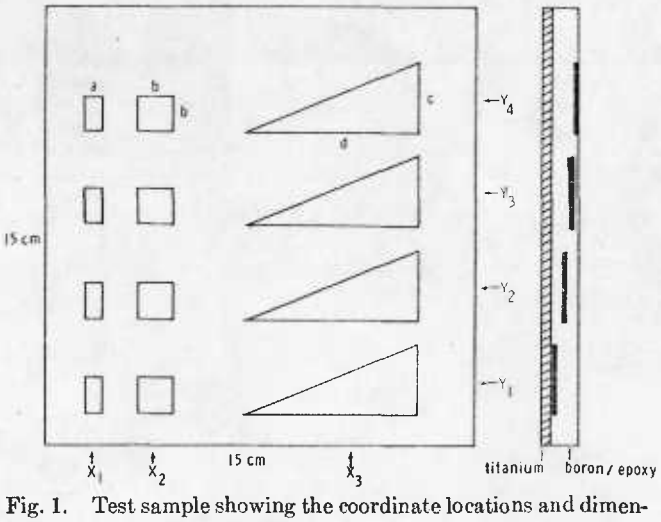



Fig. 1. Test sample showing the coordinate locations and dimensions of the programmed disbonds. For the sample, $a$ = 0.625 cm, $b$ = 1.25 cm, $c$ = 2.5 cm, and $d$ = 6.25 cm.

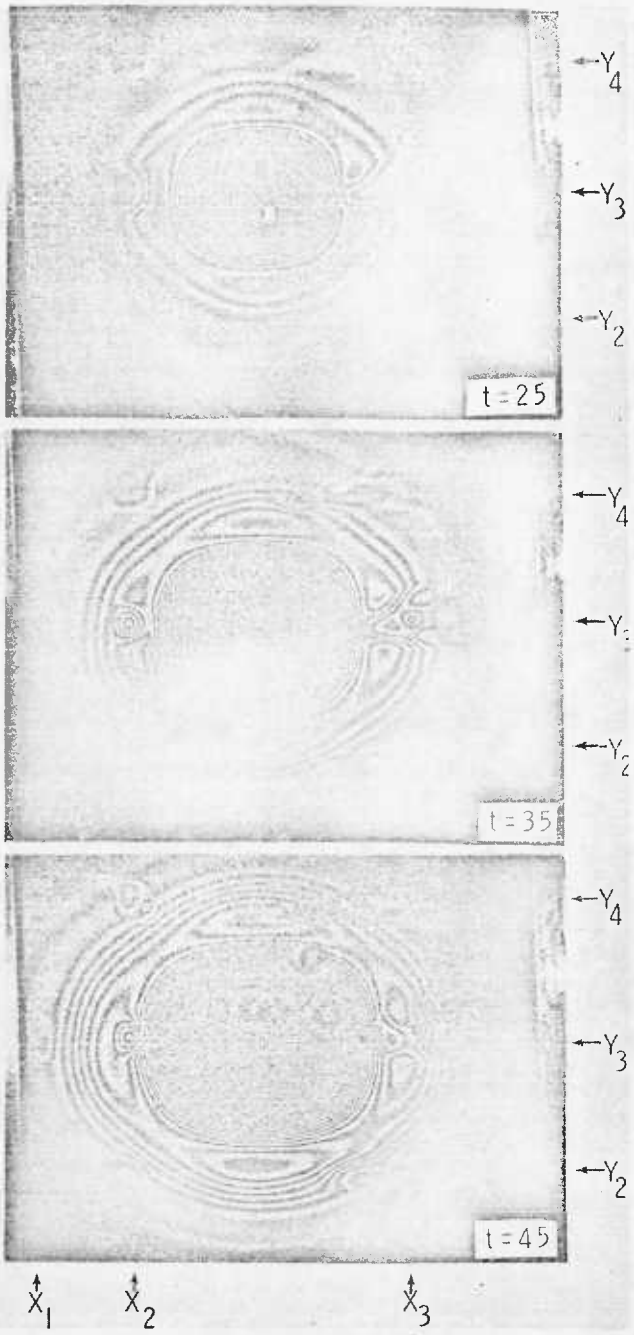



Fig. 2. Photographs of the reconstructions taken from the first sequence of holograms showing the variation of fringe pattern with delay time (given in μsec). For this sequence the sample is unpainted and has stiffeners located along the vertical edges. Coordinates of flaws correspond to those given in Fig. 1.

The experimental apparatus used in the forced impact of the test sample consisted of a pendulum made of a 1.59-cm diam steel ball attached to a string 1.5 m long. The steel ball was released with a magnetic relay system and achieved an impact velocity of approximately 80 cm/sec. Upon contact of the steel ball and the test sample, an electrical signal was generated and was used to synchronize the time of impact with the firing of a Pockels cell $Q$-switched ruby laser.

# Vibration analysis by holography

P. A. FRYER

Acoustics Group, Department of Physics, Imperial College of Science and Technology, London

## Contents


| | Page |
|---|---|
| 1. Introduction | 490 |
| 2. Holography in general | 494 |
| 2.1. Theory | 494 |
| 2.2. General holographic techniques | 495 |
| 2.3. Holographic recording media | 499 |
| 2.4. Techniques for maximum light utilization | 499 |
| 3. The stroboscopic method | 503 |
| 3.1. Theory | 504 |
| 3.2. The basic stroboscopic method and its uses | 505 |
| 3.3. Live and frozen fringe techniques | 507 |
| 3.4. Strobing techniques | 508 |
| 3.5. Advantages of the stroboscopic method | 511 |
| 3.6. Disadvantages of the stroboscopic method | 512 |
| 4. The time-averaged method | 512 |
| 4.1. Theory | 512 |
| 4.2. Advantages and disadvantages of the time-averaged method | 514 |
| 4.3. Modifications | 515 |
| 4.4. An application of time-averaged holography | 516 |
| 5. Alterations in sensitivity, and related methods | 518 |
| 5.1. Methods for increasing sensitivity | 518 |
| 5.2. Methods for reducing sensitivity | 520 |
| 5.3. Related methods of vibration analysis | 523 |
| 5.4. Conclusion | 529 |
| References | 529 |


**Abstract.** This article covers aspects of holography useful to practical workers in the field of vibrational analysis. After an introduction, it is divided into four main sections, the first of which (§ 2) deals with the basic theory and practice of holography. Several ideas which may help to solve particular problems, such as the illumination of long objects, are described, holographic recording media are briefly covered, and the section is concluded with a description of some techniques for the maximum utilization of the available coherent light. The second main section (§ 3) deals exclusively with the technique of stroboscopic holography—its theory and practice—and variations in the basic technique are described with the advantages of 'live' and 'frozen fringe' techniques being discussed in detail. Section 4 covers time-averaged holography in similar detail, with particular attention being given to some of the many modifications to the basic technique which have been devised to overcome some of its disadvantages. The section concludes with a typical utilization of the method of time-averaged holography applied to the study of plate vibrations. The final section (§ 5) covers one or two techniques for altering the fringe sensitivity of the stroboscopic and time-averaged methods and also describes several related methods of vibrational analysis which may have advantages over the holographic system in some experimental situations.

*Rep. Prog. Phys.*, 1970, **33**, 489–531

## 1. Introduction

Holography is a method of photography in which a coherent light wave, coming from an object, is 'frozen' into a photographic emulsion with the aid of a second beam of coherent light. By using the second beam alone the light wave may be 'unfrozen' and reconstructed so exactly that it is indistinguishable from the original by any optical test. It was first called 'wavefront reconstruction' by its inventor Professor Dennis Gabor (Gabor 1948) who developed it in an attempt to increase the resolving power of the electron microscope.

In the original system used by Gabor (figure 1) a divergent light beam strikes a small object and being mainly unaffected by the object passes on to form the

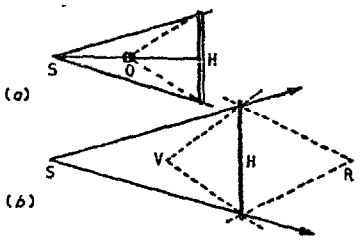



Figure 1. Gabor's original transmission system.

'reference beam'. The light diffracted by the object forms the 'object beam' which interferes with the reference beam at the photographic plate to form coarse interference fringes. If the object is removed and the reference beam only is directed on to the photographically developed plate, the recorded interference fringes act like a diffraction grating and split part of the reference beam into two conjugate beams. One beam appears to come from the original object position and is a reproduction of the light that originally came from the object. The other beam forms a real image on the other side of the plate in line with the virtual image. Light from one image therefore affects the other. In the 15 years following its discovery holography was not used widely because of this difficulty and because of the weakness of coherent light sources then available.

The laser, which is a very powerful source of coherent light, became available in 1961, and Leith and Upatneiks (1962) applied it to holography. They also solved the problem of separating the real and virtual images by using an offset reference system, the simplest of which is shown in figure 2. The object and reference beams now strike the plate at different angles and form a finer interference fringe system. On reconstruction with the reference beam, the virtual image is once again formed at the object position, but the real image is now no longer in line with it (figure 3).

The next significant advance in vibration measurement by holography occurred in 1965 when Powell and Stetson and also independently Burch (at the National Physical Laboratory) observed fringes on the reconstructions of objects that had moved while being holographically recorded. Powell and Stetson then went on theoretically to explain the fringes seen on the reconstruction of an object recorded while executing simple harmonic motion. Other workers have since applied double exposure and stroboscopic techniques to analyse object movements.

Holography offers several advantages over the more traditional methods of vibrational analysis. Strain gauges, accelerometers and position-sensing devices are accurate, but limited to measurement at discrete points and affect the vibrations

being measured. The use of moiré fringes (Ligtenberg 1955) is a technique which in its simplest form compares two reflections of a diffraction grating in the polished, flat surface of the object. The first reflection is photographed with the object stationary and the second is photographed (or double exposed) with the object

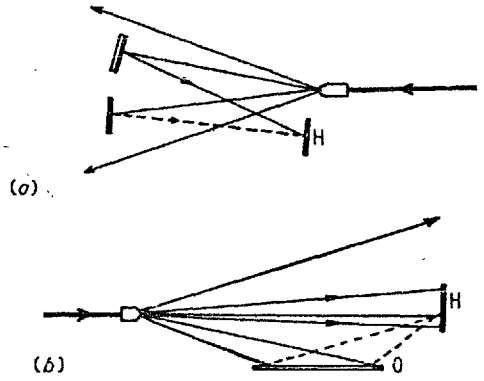



Figure 2. (*a*) Simple reflection system. (*b*) Simplest possible reflection system.

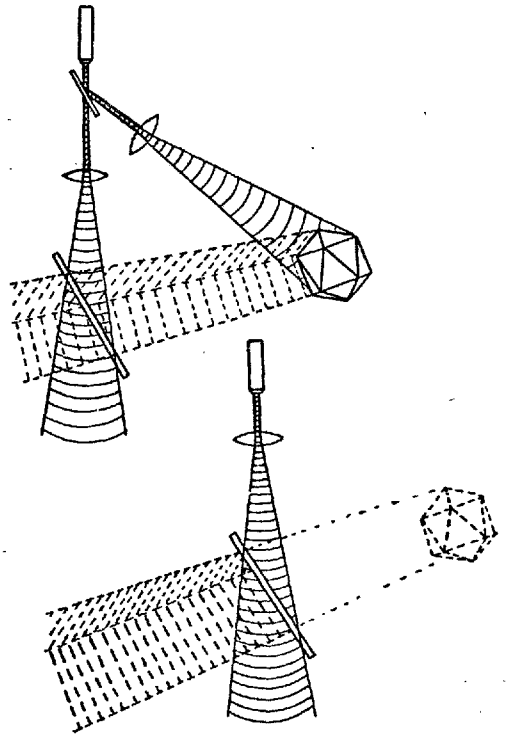


Figure 3. Simple system showing recording and reconstruction.

moving. Moiré fringes can then occur between the two exposures and the motion obtained from these fringes, which are broadened in antinodal regions (Oster *et al.* 1964, Nickola 1966, Theocaris 1967) (figure 4). Shadow moiré where the reflection of a grating is viewed through the original grating, fringes occurring between the original and the reflection, is a similar technique which shares the limited sensitivity and difficulty of interpretation of the former method.

Multiple beam or flatness interferometry can be as accurate as the holographic technique. The vibrating surface is matched against an optical flat and the resulting Fizeau fringes, vibrating with the object (which must be a flat plate), reveal the positions of the surface nodes (Tolansky and Wood 1958). With the two optical surfaces slightly inclined and illuminated with monochromatic light, sharp parallel multiple beam fringes are produced which are broadened in the antinodal

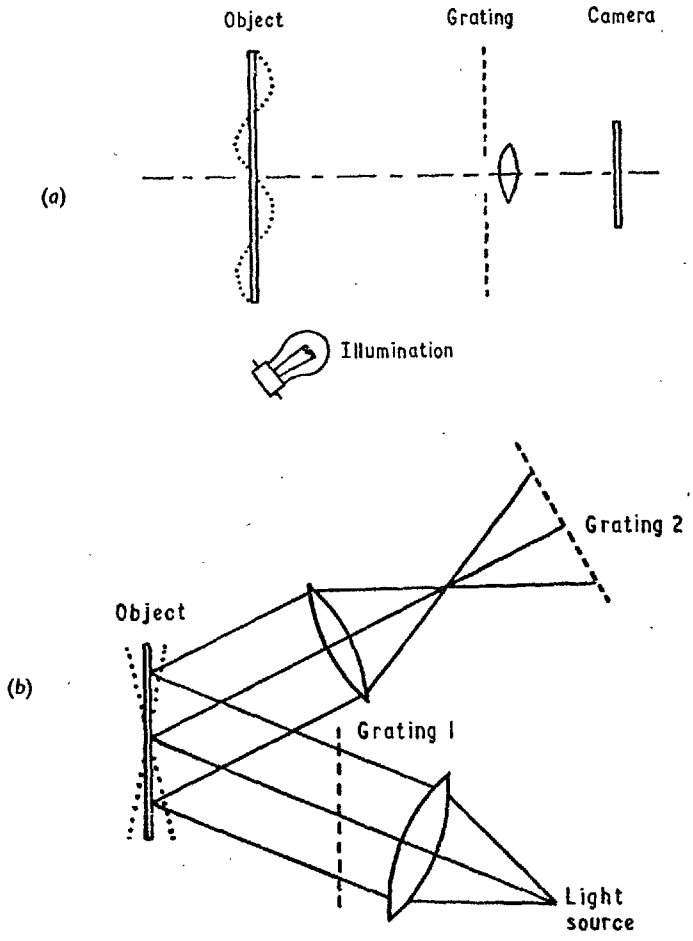



Figure 4. Moiré methods of Ligtenberg (a) and Theocaris (b).

regions. This technique suffers from the disadvantages of requiring a flat object plate and a matching optical flat in close proximity, and is therefore effectively only a laboratory technique. Some powders such as fine sand, licopodium powder and 'bomb dust' have a tendency to collect in the nodal (or antinodal) regions of a vibrating plate, and thus show up the modal pattern (Waller 1961). This technique is insensitive, requires the plate object to be horizontal and gives no information about the amplitude of the vibrations.

Photoelastic materials may be used either to coat existing objects, or to make models representing the behaviour of the original. When these materials are placed under stress they become doubly refracting, the magnitude of this effect being

proportional to the stress magnitude. Polarized monochromatic light, when reflected from a coating or passed through a model, is split into two orthogonally polarized components. Each component is parallel to a direction of principal stress and has a propagation velocity proportional to the magnitude of this stress. On emergence, the light is viewed through a polarizer crossed with the original polarizer which allows only the horizontal component of the two rays to be seen. When the relative retardation is such that the components are in phase, a dark fringe is seen for every point on the object which has a similar principal stress difference. Coloured fringes can also be produced allowing the magnitudes of the principal stresses to be determined (Hollister 1962). High-speed variations may be followed, and even shock waves studied with the aid of high-speed cameras, but the method is relatively insensitive, the coatings may affect the object vibrations, and the method is quite complicated to set up and interpret. Direct stroboscopy where the vibrating object is viewed and photographed under stroboscopic illumination is, of course, very insensitive and may be used only to study large movements. Finally, Schlieren techniques, which show up variations in density caused by stress or the passage of stress waves, may only be used with transparent objects or possibly objects with a transparent coating, and this method suffers from similar disadvantages to those of the photoelastic technique. More recent methods such as the use of laser speckle patterns and laser scanning techniques are described later in this article.

The chief advantages of holography are its simplicity, sensitivity, and the possibility of seeing, and measuring with high accuracy, how the whole surface of the object is vibrating. This may be carried out in real time (using live fringes) or at leisure (utilizing ciné films or frozen fringe holograms). Holography can be used, in general, without special object treatment such as polishing, coating or the making of models, but some treatments will facilitate the process. Measurements can be carried out in the field, especially when pulsed lasers are used, and the technique does not affect the vibrations or movements being measured. It may also be carried out remotely—even with distorting media between the apparatus and the object—is an important consideration in some industrial situations. The sensitivity of the technique may, however, be too high for some applications, although it can be varied within limits, as described in this article. Holography is already being applied in such diverse fields as the measurement of the vibrations of cat's ear-drums (Tonndorf 1970), the measurement of the growth of cacti over 20-minute periods (U.K. Physics Exhibition, 1970) and the determination of particle sizes in aerosol sprays (Thompson and Parrent 1967). The greatest potential use of holography, however, is likely to be in the field of vibration detection and measurement.

Many workers have contributed ideas to the practice of basic holography, the time-averaged (Powell and Stetson) method and the stroboscopic method, and this article will attempt to cover some of the useful developments and related topics in four main sections. Section 2 deals with holography in general, with particular reference to techniques for maximum light utilization; materials, other than the basic silver emulsion, which can be used as holographic recording media are also described. Section 3 deals exclusively with stroboscopic holography, its theory, practice and variations in the basic technique. Section 4 covers time-averaged holography in similar detail, and §4 (the final section) describes techniques for altering the basic sensitivities of the two methods and gives details of a few related methods of vibrational analysis which may prove more useful for some applications.

## 2. Holography in general

This section deals with the basic theory and practice of holography. Several practical ideas that may prove to be useful in setting up a system or helping to solve particular problems such as the illumination of long objects are outlined in §2.2. Some of the many different holographic recording media are described in §2.3 and their particular advantages over ordinary silver halide emulsions are emphasized. Finally, in §2.4 several techniques for the maximum utilization of the available coherent light are described—this may be particularly important when using some of the stroboscopic methods (§3) which cut down the effective object illumination.

### 2.1. *Theory*

Photographic plates are sensitive only to intensity, i.e. to the square of the amplitude of the light waves, so that ordinarily phase information is lost. Gabor *et al.* (1965) have shown that not only amplitude but also phase information about the light wave must be recorded if a three-dimensional image is to be reconstructed. The emulsion may be made to record phase as well as amplitude information by shining on to it another beam, called the reference beam, together with the object beam. Both beams are usually derived from the same laser.

The two beams interfere and the resulting interference pattern is effectively a complicated diffraction grating or (Ferrier 1969, Rogers 1950) a collection of zone plates. When either of the two beams is shone on to the developed emulsion, part of it is diffracted to reconstruct the other beam. In practice the reference beam is usually more intense than the object beam to ensure that it is linearly reconstructed. Mathematically the recording process may be expressed as follows.

The intensity $I$ of the light source may be expressed as the amplitude $a$ times its complex conjugate $a^*$, i.e.

$$I = aa^* \quad (\text{also } I = a^2). \tag{2.1}$$

If $r$ denotes the reference amplitude and $o$ denotes the object beam amplitude, then the intensity at the holographic plate is

$$I_p = (r+o)(r^*+o^*) \tag{2.2}$$

$$= rr^*+oo^*+or^*+ro^*. \tag{2.3}$$

Now $oo^*$ and $rr^*$ are the object ($I_o$) and reference ($I_r$) beam intensities respectively. Hence (2.3) may be written as

$$I_p = I_r+I_o+or^*+ro^*. \tag{2.4}$$

But

$$r = r\exp(i\phi_r) = r(\cos\phi_r+i\sin\phi_r)$$

and

$$r^* = r\exp(-i\phi_r) = r(\cos\phi_r-i\sin\phi_r). \tag{2.5}$$

Thus, (2.4) may also be written as

$$I_p = I_r+I_o+2or\cos(\phi_o-\phi_r). \tag{2.6}$$

Again, if the reference beam of amplitude $r$ illuminates the developed plate, then the transmitted intensity is

$$T = rI_p = rI_r+rI_o+rro^*+rr^*o \tag{2.7}$$

$$= rI_r+rI_o+rro^*+I_ro. \tag{2.8}$$

The term $I_r o$ is the reference intensity modulated by the object amplitude and this is identical to the original object wavefront. For a collimated reference beam, the term $rro^*$ represents the real conjugate image which is in focus at the same distance in front of the hologram as the object and virtual image are behind it.

The theory of double-exposed holograms will be developed from this basis in § 3, and in turn the theory of time-averaged holography will be developed in § 4.

## 2.2. *General holographic techniques*

The practical aspects of holography are well known to workers in the field (Rogers 1966, Lehman 1970) but one or two pointers will be outlined here which may prove useful.

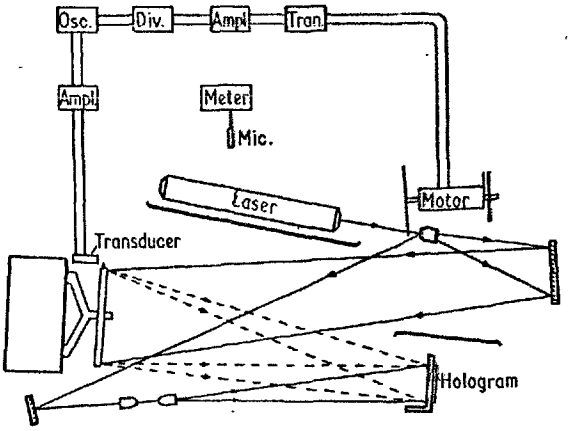



Figure 5. A practical holographic system (after Fryer 1970 a).

(i) The simplest possible optical layout is shown in figure 2 where one beam-expanding lens provides both the object illumination and the reference beam. Each worker in general has his own variation on the same theme. Fryer (1970 a) has an arrangement shown in figure 5 which has a minimum of components in the object beam path and the strength of the reference beam is altered by means of a simple 'zoom lens' system.

When taking reflection holograms, and not using a pulsed laser, if the beam splitter, object and reference beam lenses, hologram and stationary parts of the object are not maintained relative to one another to within $\frac{1}{8}$ of a wavelength of light, then extraneous fringes or time-average effects will result. This desired stability may be achieved by mounting the components on a rigid massive work table which is isolated from the floor by suitable mounts. Commercially available components do the job expensively, and a concrete slab on rubber does the job effectively and cheaply.

The object and reference beam path lengths should not differ by more than the coherence length of the laser, which in most simple helium–neon lasers is roughly equal to the length of the laser and possibly with recurring coherence at multiples of twice the length of the laser (Rose and Pruet 1967). The coherence length may be extended by placing a Fabry–Perot etalon within the laser cavity or by using various mode-locking techniques (Bradley 1970). Wherever possible the temperature of the system should be maintained within fairly close tolerances if any

prolonged work is to be done; this is because fringes may occur as a result of differential expansions in the system. Hot air currents may also cause fringe blurring.

(ii) When very long objects must be analysed, the limited coherence length of lasers that may be available, or the effective coherence length of a ruby laser giving a short pulse (see § 3.4.1), necessitates the use of a device described by Orr *et al.* (1968) and by Abramson (1969, 1970 a) who calls it the 'holodiagram' (figure 6).

The laser and photographic plate are placed at the foci of a system of ellipses. If a point object and a mirror are placed anywhere on one of these ellipses (both reflecting light on to the hologram) the path difference between the two beams is zero. If we now consider two of the ellipses and arrange for the distance between them to equal the coherence length of the laser, the diagram will aid in finding the best position for a long object. If the object can be manœuvred so that it lies in between these two ellipses, the whole length of it will be recorded on the hologram.

If the object is too long to allow this technique to be used, many object beam splitters may be used to illuminate different parts of the object (Melroy 1967), the path differences to each part of the object being then arranged separately to be within the coherence length of the laser.

The holodiagram also has another application when double-exposure techniques (dealt with more fully in § 4) are adopted, as it may be used to help determine, or choose, the amount of movement that each fringe appearing on the object represents. Briefly, the system of ellipses is drawn so that they are separated by half a wavelength of light where they intersect the line joining the foci. When a point object is moved normal to the ellipses, each time one is crossed a complete cycle of light intensity variation occurs at the hologram. The greatest number of cycles, i.e. fringes, for a given object movement occurs along the line joining the foci and to the right-hand side of the hologram; the minimum number occurs when the movement is normal to this line at the centre of the diagram.

(iii) When taking large numbers of holograms it may prove useful to be able to see at a glance, using white light, which holograms have useful information stored in them. The technique of 'image holography' allows this to be accomplished and involves an image of the object being formed on the photographic plate with the reference beam added in the usual way. The resulting hologram (of the image) will be capable of reconstruction by white light. If a double-exposed hologram is made in this way, the resulting image will still keep its interferometric properties, and fringes will be seen on the reconstruction. The image may be formed only on part of the photographic plate, leaving the rest for normal holographic use, and the white light reconstruction may be used only for selection purposes.

A similar technique has been used in holographic microscopy to study the out-of-focus parts of the specimen as well as those parts situated in the focal plane. The technique has been described by Welford (1966), Butters and Denby (1969) and also by many other workers.

(iv) When it is not possible to use either a pulsed laser or an isolated work bench, the vibrational stability requirements of the system may be reduced by a 'scanned reference beam' holographic system described by Palais and Wise (1970). The reference beam is increased in intensity, reduced to spot size and used to scan the hologram during the exposure. Extreme stability must be maintained only for the time needed for the reference beam to illuminate an area of hologram equal to its own spot size. The stability-time reduction is equal to the ratio of the area of the hologram to the area of the reference beam spot. Unreferenced light from the

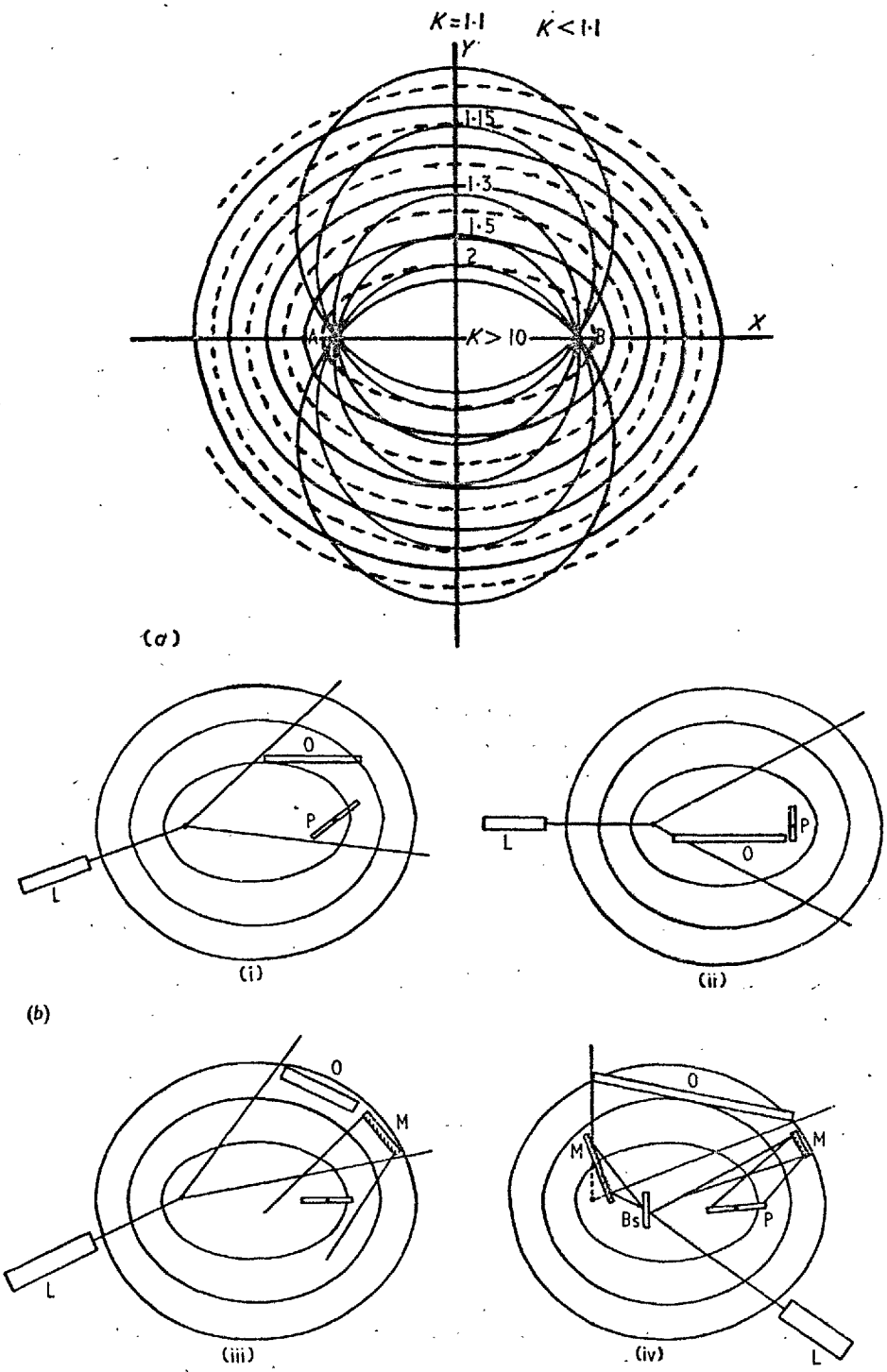



Figure 6. (*a*) The holodiagram (after Abramson 1970). (*b*) Some ways in which the holodiagram facilitates choosing a holographic layout (after Abramson 1970): (i) no mirror for reference beam, (ii) one position for a long object, (iii) hologram with mirror for reference beam, (iv) using a beam splitter and two mirrors. L, laser; O, object; P, photographic plate; M, mirror; Bs, beam splitter.

object will serve to increase the dc level of the exposure as described in §2.4, part (i), and the reduction of contrast caused by this may be troublesome.

(v) By polarizing the reference beam at 90° with respect to the original object beam, specular reflection may be removed from the reconstruction as only diffusely reflected light will be recorded by the hologram. This technique (Rudder 1967) may be useful, for instance, for removing highlights on shiny white objects, or for allowing detail that would otherwise be swamped to be seen on almost perfectly reflecting objects.

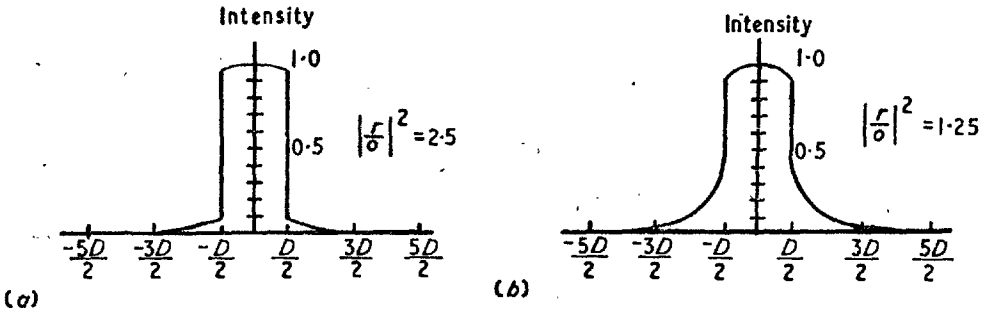



Figure 7. Image blur for two difference reference-object beam ratios (after Goodman and Knight 1968).

(vi) Finally, as described by Urbach and Meier (1969), the choice of the reference beam strength may be important when precision work is to be attempted. Amplitude transmission curves are a nonlinear function of the exposure for all holographic recording media (figure 9). These nonlinearities produce not only higher order images (which need not overlap the first order) but also additional disturbance terms which propagate along the first-order image direction and cause first-order image blurr. If, say, a 5% deviation from linearity is regarded as permissible, the amplitude swing of the fringes will have to be greatly reduced by increasing the reference beam strength and reducing the exposure accordingly. This reduced modulation drastically reduces the diffraction efficiency of the hologram (i.e. the percentage of light incident on the processed emulsion diffracted into the image or images) from the theoretical maximum of 33·9% for thin phase holograms to a mere 9%.

**Table 1**

| Reference object beam ratio | 2·5 : 1 | 1·25 : 1 | 13 : 1 |
|---|---|---|---|
| Fringe modulation | 0·903 | 0·996 | 0·5 |
| Diffraction efficiency (%) | 5·64 | 6·24 | 1·5 |

Goodman and Knight (1968) have computed the amount of image blur for two different references to object beam ratios, as shown in figure 7. Some fringe modulations with the corresponding diffraction efficiencies and reference to object beam ratios are shown in table 1. Ratios of about 5 : 1 are generally used, but when fringe locations are accurately required in relation to surface features, ratios of up to 13 : 1 are sometimes used.

2.3. *Holographic recording media*

Most workers use silver halide emulsions for recording holograms, bleached or unbleached, but there are many other substances that may be used. Urbach and Meier (1969) have presented the theory of some of these, and table 2 shows their diffraction efficiencies.

**Table 2**

| | Amplitude | | | Phase | | |
|---|---|---|---|---|---|---|
| | Thin | Thick | | Thin | | Thick |
| | RT | R | T | RT | | RT |
| Theoretical | | | | sin. | blazed† | |
| Maximum diffraction efficiency (%) | 6·25 | 7·2 | 3·7 | 33·9 | 100 | 100 |
| Measured diffraction efficiency (%) | 4·0 | 3·8 | 3·0 | 33 | 73 | 95 |
| Materials | AB | AB | AB | CDE | C | CF |

R, reflected; T, transmitted.

A, Silver halide, conventional development; B, photochromics; C, bleached silver halides; D, thermoplastics; E, photoresists; F, photopolymers.

† A technique whereby a 'stepped' surface is formed that directs most of the incident light into the desired order image (Sheridon 1968).

After silver halide emulsions, dichromated gelatin is the most commonly used medium, and has a sensitivity and definition similar to 649F film, with the great advantage of a diffraction efficiency of up to 95%. Dichromated gelatin forms thick-phase holograms which transmit effectively all the incident light but whose fringes spatially vary the phase of the transmitted wavefront. Brandes *et al.* (1969) have described the formation and development of dichromated gelatin films and they suggest that the combination of water and isopropanol used on gelatin hardened with ammonium dichromate results in the best photographic speeds with the highest signal to noise ratios, which may, in fact, be up to five times greater than 649F emulsion.

Other media such as thermoplastics, which have a sensitivity comparable with 649F plates, a diffraction efficiency as high as 33%, with the additional advantage of erasure and re-use (Lin 1969) and lithium niobate crystals which are relatively insensitive but which may be used to store up to 1000 holograms in one crystal (*Electronics World*, 22nd January, 1969, from Bell Laboratories) are less commonly used (figure 8).

Photopolymers may be used when rapid dry processing using ultraviolet light is desired, but their disadvantages of low sensitivity, low signal-to-noise ratio, and linearity limit their usefulness (Close *et al.* 1969). Photoresists (Sheridon 1968), photochromics (Kirk 1966), magnetic oxides and liquid crystals have all been used to record holograms, but their disadvantages render them unsuitable for practical use at the present time.

2.4. *Techniques for maximum light utilization*

It is highly desirable in vibration analysis holography for the exposure time(s) to be as short as possible and the reconstructions to be as bright as possible. Short exposures minimize the dimensional and vibrational stability requirements, but the techniques described below may also be used to allow cheaper and therefore weaker lasers to be used, or alternatively may allow much larger areas to be holographically

recorded. $Q$ switched ruby lasers giving two pulses per cycle greatly minimize the stability requirements, but these may not be available on grounds of cost or limited coherence length, and in any case these techniques may be used with pulsed lasers as well as continuous wave lasers with the same advantages.

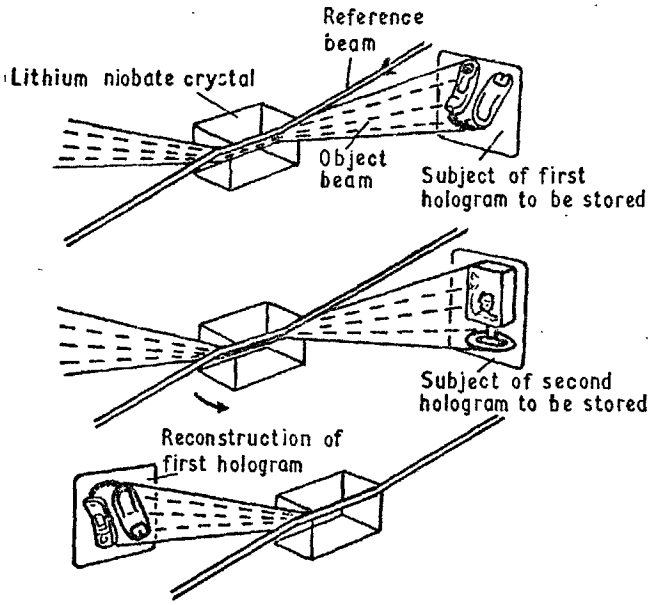



Figure 8. Use of a lithium niobate crystal to store up to 1000 holograms (after *Electronics Weekly*, 22nd January, 1969, from Bell Laboratories).

(i) The choice of photographic plate is important in the maximum utilization of available light. There is little point in having plates whose definition exceeds the experimental requirements, especially when this definition comes at the expense of sensitivity. The number of lines per millimetre needed is $1580 \sin \theta$ for helium–neon lasers (Rogers 1966), where $\theta$ is the maximum angle between object rays and the reference beam. For a maximum angle of 45° for instance, a definition of 1000 lines per millimetre is required. Agfa 10 E 70 and 8 E 75 and Ilford helium–neon plates are satisfactory for this requirement, and have a sensitivity of over an order of magnitude higher than Kodak 649F plates, which have a definition of about 5000 lines per millimetre.

The definition capabilities of a few films are given in table 3 (Upatneiks 1969).

**Table 3**

| Emulsion | Sensitivity (erg $cm^{-2}$) | Resolution (lines $mm^{-1}$) |
|---|---|---|
| Pan X | 0·1 | 150 |
| 10 E 70 | 50·0 | 1800 |
| 649F | 1000·0 | 5000 |
| Dichromated gelatin | 10 000·0† | 10 000 |

† By sacrificing some of this greater speed it is possible to achieve signal to noise ratios of up to five times better than 649F.

It must be remembered when using fast films (which necessitate low object–reference beam angles) that larger film grains will diffract light and cause a bright glow around the reference beam direction. This glow may extend to the reconstruction and swamp parts of it (Urbach and Meier 1969, Lehman 1970).

The effective speed of some emulsions may be increased by hypersensitization (Lin and Lobianco 1967) using triethanol–amine or ammonium hydroxide. Table 4 shows the increases in sensitivity that were obtained for 649F emulsions at different wavelengths, with no apparent decrease in resolution.

**Table 4**

| Agent | Wavelength (Å) | | | Lasting time of hypersensitization |
|---|---|---|---|---|
| | 6328 | 5461 | 4880 | |
| Triethanolamine | ×4·2 | ×2·2 | ×2·1 | 1 month |
| Ammonium hydroxide | ×2·6 | ×1·0 | ×1·0 | 1 h |
| Water | ×2·0 | — | — | — |

The best photographic contrast can usually be obtained with a final neutral density of about 1·0. If it requires $T$ s to obtain unit density, holograms with almost the same final contrast may be made by exposing the photographic plate in the normal holographic manner for $t$ s, then re-exposing the plate to coherent or incoherent light sufficiently to achieve the optimum density. This extra *pre-* or *post*-exposure thus acts as a kind of 'dc bias' bringing the ac fringe information to the central regions of the exposure transmittance curve (figure 9). Though this

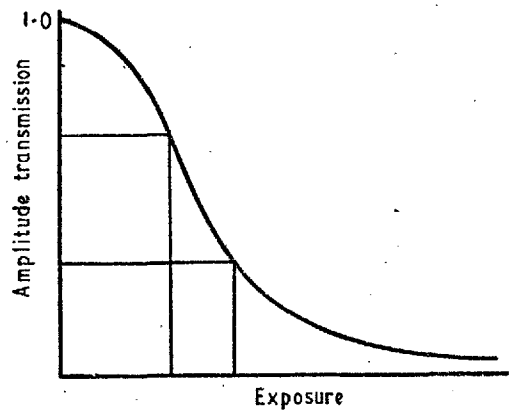



Figure 9. Typical exposure transmittance curve (after Lehman 1970).

technique effectively reduces the fringe modulation, Hallock (1968) has described reductions in the final contrast of as little as 2% for $t = T/15$, i.e. an effective increase of ×15 in the film speed.

Finally in this section on the treatment of the photographic emulsion it is highly desirable that the diffraction efficiency of the hologram should be as high as possible, especially in 'live fringe' work, where it is not possible to direct the whole laser beam on to the hologram for reconstruction.

As has been described above, the diffraction efficiency of phase gratings is higher than simple amplitude (black and white) gratings, and an amplitude grating may be turned into a phase grating by bleaching it (Latta 1968), thus increasing the

diffraction efficiency from about 6% to about 30%. Unfortunately, bleaching increases the light scattered by the emulsion which may cancel out the advantage of increased diffraction efficiency (Wall 1969). This 'flare' light may be reduced by decreasing the low-frequency response of the bleaching process (Lamberts and Kurtz 1970). Bleaching solutions which give increased brightness over ordinary bleaches, such as potassium dichromate, are tabulated below. Bleach (1), being a 'surface' bleach, will not cope with high spatial frequency variations and should therefore only be used on holograms taken with small reference to object beam angles.

(1) One of solution A + $\frac{1}{10}$ B + 10 of water by volume where

A = 500 ml distilled water + 20 g ammonium bichromate + 14 ml concentrated sulphuric acid + distilled water to make 1 l.

B = 45 g sodium chloride + distilled water to make 1 l.

(2) Equal parts of A and B where

A = 10 g $CuBr_2$ per litre.

B = 3% hydrogen peroxide.

Bleach (1) is due to Russo and Sottini (1968) and bleach (2) is due to Leonard and Smirl (1969).

Blazed gratings, dichromated gelatin and dielectric holograms give the maximum diffraction efficiencies but are usually less light sensitive than silver emulsions.

(ii) An equally important method of ensuring efficient light utilization lies in the treatment given to the object. For the formation of a hologram most suitable for holographic interferometry, light should fall on each part of the hologram from each part of the object with equal intensity, i.e. the object when seen from the hologram should appear to be equally bright all over.

Most workers use matt white paint, thus forming an approximation to the perfectly diffusing object; hence, if the hologram is at a realistic distance from the object, *most* of the reflected light is not collected by the hologram. If all this reflected light could be directed to the hologram, this, using a simple comparison-of-areas-argument, would result in a fractional light saving of $2R^2/r^2$, where $R$ is the distance from the object to the hologram and $r$ is the radius of a circular hologram. For example, with a hologram of radius 2 cm at a distance of 1 m there is a 5000-fold saving.

One way of treating the object is to coat it with Scotchlite, a reflecting tape on to which many tiny glass balls have been sprayed; the object then has the property of reflecting back most of the incident light, in a narrow cone around the incident direction. Withrington (1968) has used this preparation to coat bubble chambers and thus provide a bright background for the holography of bubble track (Welford 1966). Jacobson (1969) has described the use of Scotchlite to enable a cylinder to be photographed, and a 35-fold saving in light was obtained. A half-silvered beam splitter is placed at 45° in the object illumination beam path; therefore, 50% of the light is wasted on illumination and collection, but nevertheless there is a considerable saving over the white-painted object.

As mentioned above, the object should not be painted white, nor should it be specularly reflecting. If it were, on reconstruction only a small spot of light would be seen, the location of which would depend on the position of the observer's eye.

This difficulty may be overcome by placing a diffusing screen in the object beam illumination path (after Stroke 1970) but once again this wastes most of the incident light.

By simply roughening the object with a coarse grade of sandpaper some improvement is obtained, but the result is neither perfectly diffusing nor perfectly reflecting, and the image falls off in brightness towards its extremities, although there is a considerable overall improvement. The specular part may be removed using a reference beam polarized at 90° to the object beam, but this again is light-wasting. The Gaussian shape of the fundamental laser mode also reduces the brightness of the outer regions of any object, and this effect is a disadvantage when using Scotchlite.

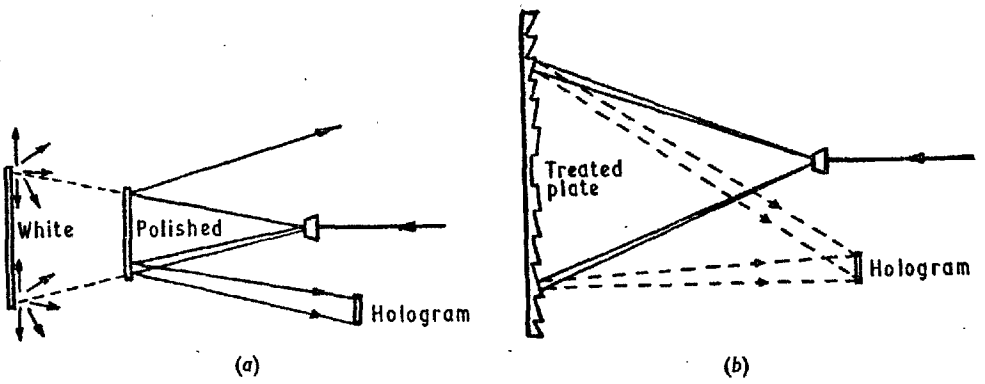



Figure 10. (*a*) The difference between a perfectly diffusing and a perfectly reflecting object. (*b*) Plate treatment directs most of the incident light to the hologram.

When the object is as simple as a flat plate, a kind of 'Fresnel mirror' (i.e. a system of concentric grooves with a saw-tooth profile) may be formed on the plate (Fryer 1970 a, b) and the rising floor of each groove may specularly reflect incident light on to the whole hologram (figure 10). Groove density and floor angle may be arranged to compensate for the various edge-darkening and angle effects mentioned above.

A little more light may be saved by removing the beam splitter from the system. Reflection from the plane surface of the object beam expanding lens may be used to form the reference beam and this has proved (Fryer 1970 a, b) to be of ample intensity for most eventualities. The intensity of the reference beam may be altered with the aid of a simple zoom lens system, rather than filters, and is therefore continuously variable.

Using only a poor approximation to the ideal Fresnel mirror and this last reference beam technique, an exposure time of $\frac{1}{10}$ s has been achieved (Fryer 1970 a, b) for a 30 cm diameter plate when illuminated with a 15 mW laser. This may be considerably reduced by using all the techniques described above.

## 3. The stroboscopic method

As mentioned in the general introduction, holography can offer advantages over other methods of vibrational analysis. The main advantages are its simplicity, sensitivity and the possibility of measuring with high accuracy, either in real time or at leisure, vibration amplitudes over the whole of the object surface. In addition,

measurements may be made in the field, remote from the vibrating object, and through distorting media. Furthermore, when stroboscopic illumination is used the resulting fringes are of equal contrast out to regions of large object movement, and, when moving from nodal regions, each fringe encountered simply indicates that the vibration amplitude has increased by one half wavelength of the laser light used (when illuminated and viewed normally). Further advantages are described in § 3.3.

The basic experimental system is the same as for normal holography (figures 2, 12, 13) with the addition of some method of interrupting the laser light in synchronism with the object vibrations. If a 'strobe-disk' is used, further precautions must be taken to isolate vibrations and air currents caused by the addition of this device. The theory of double-exposure holography, which is the technique effectively used in stroboscopic holography, is described below. Techniques for the interruption of the light and the utilization of the stroboscopic method are discussed, and finally the advantages and disadvantages of the method are listed at the end of this section.

### 3.1. *Theory*

Rewriting (2.4), the intensity at the holographic plate due to the combination of object and reference beams is given by

$$I_p = I_r + I_o + or^* + ro^*. \tag{3.1}$$

On illumination of the developed plate with the reference beam the transmitted intensity is, as before,

$$T = rI_r + rI_o + rro^* + I_r o \tag{3.2}$$

where $I_r o$ is the reference intensity modulated by the object amplitude.

If now two holograms of the same, but slightly displaced, object are recorded sequentially on the same photographic plate using the same reference beam, and if $o_1$ and $o_2$ represent the light amplitudes corresponding to the two object positions, then the hologram effectively superposes the two intensities as follows:

$$I_1 = I_r + I_{o1} + o_1 r^* + o_1^* r \tag{3.3}$$

$$I_2 = I_r + I_{o2} + o_2 r^* + o_2^* r. \tag{3.4}$$

On summation,

$$I_{tot} = 2I_r + I_{o1} + I_{o2} + r^*(o_1 + o_2) + r(o_1^* + o_2^*). \tag{3.5}$$

After development of the plate and reconstruction with the reference beam of amplitude $r$, the term corresponding to $I_r o$ in equation (3.2) is now

$$I_r(o_1 + o_2). \tag{3.6}$$

Neglecting the reference intensity on to which this is modulated, the intensity of this image is

$$I_{image} = (o_1 + o_2)(o_1^* + o_2^*). \tag{3.7}$$

If the displacements of the object are small compared with its distance from the hologram, then $|o_1|$ may be regarded as approximately equal to $|o_2|$; thus

$$\begin{aligned} o_1 &= |o| \exp(i\phi_1) \\ o_2 &= |o| \exp(i\phi_2). \end{aligned} \tag{3.8}$$

Therefore the image intensity may be written as

$$I_{\text{image}} = 2|o|^2\{1+\cos(\phi_1-\phi_2)\}. \tag{3.9}$$

The term $(\phi_1-\phi_2)$ is a direct measure of the object displacement, i.e. if the hologram is illuminated and viewed normally and the object displacement is $d$ at the point in question, the corresponding path difference $\Delta$ is $2d$ and the phase change $(\phi_2-\phi_1) = (2\pi/\lambda)\Delta = (2\pi/\lambda)2d$. Every time the phase changes by $2\pi$ a dark fringe appears on the object reconstruction. This equation therefore represents the contour map obtained with double-exposure techniques where the second position of the object is formed by static displacement or by the stroboscopic freezing of a regularly occurring displacement.

The interferograms obtained are identical to those that would be obtained had classical two-beam interferometry been used, though this would have necessitated a specularly reflecting object. The fringes have the characteristic sinusoidal intensity variation of two-beam interferometry—see also §5.1, part (iii), for a method of forming multiple beam fringes utilizing emulsion nonlinearities.

Advantages and disadvantages of stroboscopic holography are summarized at the end of the section.

### 3.2. *The basic stroboscopic method and its uses*

The most straightforward utilization of the strobe technique either flashes the laser at source, or 'chops' the laser light before it passes through the first component of the actual holographic system. Thus, both the object and the reference beams are chopped together.

Many workers arrange for one flash per object cycle and have an on–off ratio of between 1:10 and 1:20. (Plates 2 and 1 respectively offer a comparison; see also plate 3 illustrating a 1:2·5 ratio and plate 5 showing a more complicated vibration mode.) It is highly desirable that the on–off ratio (duty cycle) should be as low as possible, so that the object does not move appreciably during each illuminating flash. If the light is *on* for too large a fraction of the object cycle time, only that part of the cycle during which the object moves least (e.g. near the maximum displacement for sinusoidal oscillations) can be effectively frozen. Other parts of the object cycle will produce an indistinct 'limited time-averaged' system of fringes which correspond to the average of object positions during the 'on' period. When the duty cycle is as high as 1:2·5, for instance, as shown in plate 3, even the maximum displacement of a sinusoidal oscillation gives indistinct fringes, which are neither truly time-averaged nor stroboscopic and are of limited use for measurement purposes.

The procedure for taking 'live fringe' and 'frozen fringe' holograms is as follows.

A hologram of a stationary object is taken, developed and accurately replaced in its original position. This is known as a 'live fringe' hologram and will be dealt with more fully in §3.3 below. Part of the reference beam is then diffracted to form a virtual image located *on* the object. The reconstructed object beam then interferes with the real object beam, and fringes are seen on the object corresponding to any movement between the object and its virtual image.

If the stroboscopically frozen vibrating object is viewed through this live fringe hologram, fringes are seen which are contour lines corresponding (when illuminated and viewed normally) to half-wavelength increments of object movement. The

phase of the strobe may then be set so that the desired part of the cycle is frozen, and then a fresh photographic plate may be exposed to the vibrating object. This is then re-exposed to the stationary object. The developed plate reconstructs both object states simultaneously, and interference between the two reconstructions results in fringes which are known as 'frozen fringes'.

(i) There are several variations on this theme. For instance, Markova *et al.* (1969) and many other workers use two flashes per cycle, and therefore only one effective exposure need be taken. The fringes that are seen with this method correspond to the difference in object amplitude at the two instances of illumination; these may be at the two peak amplitudes, doubling the number of fringes seen. When integer harmonics are present in the object vibration, assuming that they are

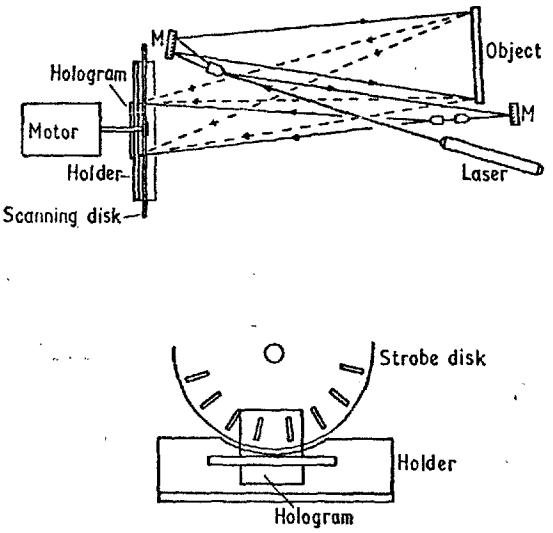



Figure 11. Scanned plate holographic system.

in phase with the fundamental, an exposure between 0 and 90° in the fundamental removes the contribution due to the even-integer harmonics. It is better to have one or more flashes per cycle rather than one flash every few cycles, as this latter method increases the exposure time and puts demands on the mechanical and electrical stability of the system.

Using a $Q$-switched ruby laser, only two flashes are necessary and individual cycles or impulsive events may be studied, provided the flash timing can be accurately adjusted. With this single or double shot illumination there are fewer problems with the stability of the system as a whole, and if the two firings of the laser are within one cycle only, stability problems are rendered virtually non-existent.

(ii) Using a technique which has recently been described by Fryer (1970 b), a whole vibration cycle may be recorded on one hologram and the need for a live hologram and the setting of the strobe phase is obviated.

A strobe disk with an appropriate number of radial slits is attached to a synchronous motor and situated just in front of the holographic plate, see figure 11. A given slit may be arranged to scan the plate while the object traces through any given fraction of a cycle, or indeed any number of cycles. The two exposures may then be taken in the normal way. The observer, on reconstruction, will see the number of fringes on the reconstructed object increase from zero to the number

corresponding to the maximum amplitude of object movement as he moves his eye along the path taken by the slit across the hologram. Tapered slits give differing on–off ratios and the most suitable one used for measurements.

The technique described by Hallock (1968) may be automatically incorporated in this apparatus by causing only the reference beam to scan the photographic plate. The unreferenced light from the object—and it will be unreferenced for at least nine-tenths of the time—increases the dc level of the exposure and effectively decreases the total exposure time. A similar effect may be achieved by increasing the distance between the scanning slits and the photographic plate—the two beams will then fall slightly out of register thus effectively decreasing the slit width while leaving the exposure time unchanged.

Raster scanning or the use of spiralling slits may allow a cycle to be recorded in greater detail. Also, since the formation and dying away of fringes may be observed by moving the eye the location of a node is made apparent by the absence of any fringe movement through it.

### 3.3. *Live and frozen fringe techniques*

If the object is set into vibration and observed through a 'live fringe' hologram (defined in §3.2) weak fringes are seen. These are related to those (time-averaged) fringes seen on the reconstruction of a hologram taken of a steadily vibrating object, but are weaker as a consequence of the integrating time of the eye. Powell and Stetson (1965 a, b, 1966) and Brown *et al.* (1969) have described the theory of these fringes; with time-averaged holography (see §4) the intensity of the reconstruction is

$$I_{\text{image}} = I_0 |\mathrm{J}_0(\Phi)|^2.$$

With real time viewing the intensity of the fringes is

$$I_{\text{image}} = 2I_0\{1 + \mathrm{J}_0(\Phi)\}.$$

This reduction in intensity renders live time-averaged fringes practically useless for all but setting the frequency for a proper time-averaged exposure.

Live fringe arrangements come into their own when used in conjunction with stroboscopic illumination. In this case the fringes seen on looking through a 'live fringe' hologram at the stroboscopically frozen vibrating object are as sharp and clear as those seen on static deformation of the object—assuming, of course, that the stroboscopic flashes are of sufficiently short duration that the object does not move appreciably during the flash.

The main advantage of this method is that the phase of the strobe may be altered while viewing the fringes and whole vibration cycles may be observed. Also, motion pictures may be taken as the phase or frequency are altered and photographs may be taken from the film at the desired points in a cycle or frequency scan and studied at leisure. For measurements to be taken from live fringe holograms there should be no fringe present on relocation of the hologram after development, and no subsequent drifts of either position or frequency during the experiments. Therefore, differential expansions, emulsion shrinkage and other similar effects tend to limit the usefulness of the live fringe technique.

Where good accuracy is desired, frozen fringes are almost invariably used. Because only one or maybe two closely time-related exposures are taken on the same plate, distorting effects are minimized and there is no problem over the

relocation of the photographic plate. Also, in processing, whatever happens to one image will also happen to the other, and thus, good accuracy is assured. The scanning method described above allows whole cycles to be frozen and studied at leisure.

When live fringes are to be utilized, perhaps the most difficult aspect of the technique is the accurate relocation of the developed photographic plate—followed closely by the avoidance of differential expansions, etc. Many ingenious plate holders have been designed both to hold the plate and, should it not be returned to within $\frac{1}{8}$ of a wavelength of its original position, allow it to be moved in any direction or rotated in its own plane. Parallel fringes appear as a result of movement in the plane of the hologram, movement towards or away from the object results in circular fringes appearing (Vienot *et al.* 1970) centred on the line passing through the object parallel to the direction of movement. Usually the initial support is a 'six-point' contact system which completely locates the photographic plate with no redundant supports.

One way of eliminating some of these problems is to hold the plate in a fluid gate (Deelen and Nielsen 1969). The plate is processed *in situ*, and consequently there are no problems of relocation. If the plate is not allowed to dry afterwards there are no problems of emulsion shrinkage either. The hologram is exposed while surrounded with water; this is then drained out and replaced with developer, then stopper, fixer, rinses and finally water again—all at the same temperature. A variation on this theme has been suggested by Castler and Pruet (1967); they first soak the hologram in developer, and during the exposure they occasionally block off the object beam and observe the reconstruction. The exposure is finally terminated when the reconstruction is good enough. With the rapid exposures that can result from the techniques described in § 2.4 this technique may be of limited value.

Neuman and Rose (1967) describe a neat way of eliminating the gradual shift of live fringes due to system creep or warm air currents; in their method they stabilize the fringes by a feedback process. A motor-driven optical wedge is inserted into the reference or object beam to alter the path length. The intensity of the fringes is observed with a photomultiplier, and constancy is maintained by moving the wedge via a servo system. A closely related method has been described by Rose and Pruet (1968), where the length of the laser cavity is adjusted by servo, thereby slightly changing the laser output frequency, which causes a fringe shift owing to unequal object and reference path lengths. Both of these techniques will only guard against effective changes in path length or laser output frequency and will not correct for translations or rotations in the plane of the hologram.

### 3.4. *Strobing techniques*

The essential feature of all stroboscopic methods is that they interrupt the light falling on the vibrating object allowing (say) only one brief flash per cycle. If the flash lasts for a sufficiently small fraction of a cycle and recurs at the same point in succeeding cycles, it seems to the observer that the object so illuminated is stationary.

Many ways have been used for interrupting the laser light for the purposes of stroboscopic holography and they fall into two main groups: causing the laser itself to flash, and chopping the light from a continuous wave laser.

3.4.1. *Causing the laser to emit pulses*

(i) *Q-switched laser.* For 'stroboscopically' recording large objects, ruby and neodymium–glass are the most suitable laser media at present (Bradley 1970, Gates and Hall 1970); it should be noted, however, that these lasers do not usually pulse continuously and may only be used as described in § 3.2. Neodymium–glass lasers emit at 1060 nm, which must be converted to the second harmonic at 530 nm for use in optical holography, the loss of energy in the conversion process being more than made up for by the increased sensitivity of photographic emulsions at this wavelength. The coherence lengths and power outputs of these lasers are being steadily increased—lengths of 1 m are common and peak powers of $10^9$ W for ruby and $10^{13}$ W for neodymium–glass lasers had been achieved by 1969. Sufficient power and coherence length was available as early as 1967 for the first hologram of a living person to be taken (Siebert 1967) using a high coherence pulsed ruby laser, amply demonstrating the reduced stability requirements of pulsed laser holographic systems.

Ruby lasers are typically pumped with a photographic flash lamp, and at the correct instant of maximum storage the Kerr cell shutter between the high reflectivity mirror and the ruby rod is opened by shorting the high-voltage plates to earth, producing a pulse lasting for tens of nanoseconds and with hundreds of kilowatts peak power. Rotating mirrors, Pockel cells and saturable dyes are also used as $Q$ switches, and these are less easily damaged than Kerr cells, but Kerr and Pockel cells are often used because electro-optic initiation may be precisely timed. Pulse duration—normally about 20 transit times between the mirrors—may be made shorter by various techniques such as 'mode-locking' (Bradley 1970), but when it becomes so short that the spatial length of the wave train given out is, for instance, less than the coherence length necessitated by the size of the object, a lower limit has been reached. For example, a pulse duration of 3 ns corresponds to a coherence length of 1 m. Similarly, stroboscopic freezing of moving objects reaches a limit when the shortness of the pulse, which has to be used to arrest the motion, results in an insufficient coherence length or does not allow the object and reference beams to 'overlap' at the hologram.

For stroboscopic work the $Q$-switching Kerr or Pockels cell may be attached to an appropriate pulse generator which in turn is driven in synchronism with the transducer used to drive the object.

(ii) *Altering the continuous-wave exciter.* Some gas laser exciters have a built in facility for modulating the output of the laser within limits; this may only be used to give a rather poor strobing effect because the laser may not be switched completely off. Alternatively, the author has been informed that it is possible to alter the exciter of the continuous-wave laser and cause it to give out pulses which have a greater peak amplitude than the normal steady output of the laser. It is, however, probably easier to use one of the methods of light interruption described below.

3.4.2. *Interrupting the laser light*

(i) One of the most sophisticated methods of interrupting the laser light uses a Pockels cell (Von Winkle, private communication). Figure 12 shows the experimental arrangement. A sinewave generator is used to drive the object plate and to synchronize a pulse generator which produces a pulse variable in phase and duration. This pulse is amplified and drives a Pockel cell with a dc halfwave voltage

of 1300 V. Without any voltage on the cell the polarizer (Glan Thompson polarizing prism) is rotated until minimum transmission is achieved. This is less than 0·5% of the laser output of 70 mW. With the pulse voltage applied, 90% of the incident light is transmitted. Pockel cells have a rapid response time, and therefore pulses of short duration may be used, allowing those parts of a vibration cycle where the object is moving rapidly to be studied. Von Winkle used two exposures per cycle, allowing peak-to-peak double exposures or comparison between any small part of a cycle and any other small part. For the analysis of high amplitudes, the exposure pulses may be moved so that the complete amplitude is covered in small increments.

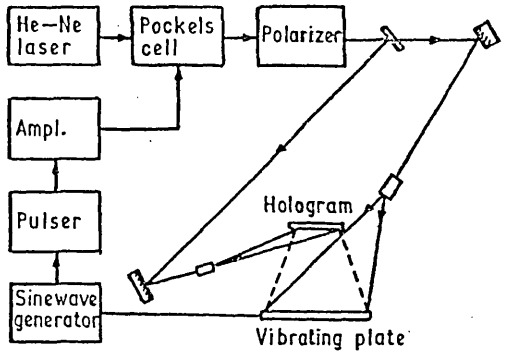



Figure 12. Schematic diagram for stroboscopic holography using a Pockel cell after Von Winkle (U.S. Navy Underwater Sound Laboratory, New London, Connecticut, 06320).

(ii) There are many methods that utilize a disk or plate to interrupt the light from a continuous-wave laser. A particularly elegant one is in use at the National Physical Laboratory at Teddington (Archbold and Ennos 1968, 1970) (see figure 13). The laser beam is focused through a small hole drilled diametrically across a steel spindle attached to a high-speed air turbine of the type used to drive dentists'

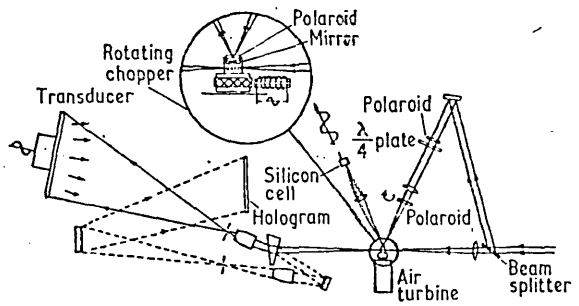



Figure 13. Strobing system in use at the National Physics Laboratory, England (after Archbold and Ennos 1970).

drills. The electrical signal used to drive the object is derived by splitting off part of the laser beam and circularly polarizing it by passing through a filter and quarter-wave plate. The beam is then passed through a second polaroid, and the direction of the resulting plane of polarization may be altered by rotating this polaroid—without altering the amplitude of the light. This light then falls on a polarizing

mirror fixed to the end of the rotating spindle. The reflected light, which varies in synchronism with the transmitted flashes, falls on to a silicon cell whose output is amplified and used to drive the object. The relative phase between the illuminating pulses and the electrical signal may be altered by rotating the second polaroid, thereby allowing any part of the vibration cycle to be studied.

When this system is used to examine objects having sharp resonances (0·5 Hz bandwidth), small variations in turbine frequency have to be overcome by building a small magnet into the spindle and placing a solenoid close to it. The turbine locks on when the solenoid is supplied with the object excitation frequency.

(iii) A less complicated system has been used by several authors (Watrasiewicz *et al.* 1968 a, b, Markova *et al.* 1969, and Fryer 1970 a, b). This utilizes a strobe disk attached to a synchronous motor supplied with the frequency used to excite the object. These systems in their basically simple form are limited to frequencies of around 2 kHz by the tendency of the strobe disk to fly apart under rotational forces. If the laser is focused down, the size of the holes, and hence of the strobe disk, may be reduced for a given on–off ratio, and the upper frequency limit increased accordingly.

Fryer (1970 a, b) has used an integrated circuit frequency divider to supply the strobe motor—this preserves synchronism and allows the motor to run at a lower frequency than the object. By chopping only the reference beam at its focus, a smaller disk may be used and the method of Hallock (1968) may be automatically incorporated.

This section is completed with a list of the advantages and disadvantages of the stroboscopic method.

### 3.5. *Advantages of the stroboscopic method*

(i) The greatest single advantage is the ease of fringe interpretation. If the object is illuminated and viewed normally, each fringe corresponds to an object movement of one half-wavelength of the laser light.

(ii) The sensitivity may be changed slightly by exposing either peak-to-peak or peak-to-zero amplitudes.

(iii) Fringes are of equal contrast up to regions of high object amplitude (plates 1 and 4).

(iv) Motions that are not sinusoidal or symmetrical, i.e. that have a large harmonic content, may be studied either by a scanning method or by taking many exposures at different phases and building up a picture of the amplitude variation during a cycle.

(v) If two flashes per cycle are allowed, some harmonics may be automatically removed and/or two separate exposures may no longer be necessary.

(vi) When pulsed lasers are used, stability requirements are very greatly reduced as only one cycle need be investigated.

(vii) Live fringes may be easily seen, facilitating the setting up of the experiment and allowing ciné films of the live fringes to be taken.

(viii) By use of the techniques of Varner and der Hovanesian (see § 5), the phases of different parts of the object may be determined (with difficulty) from the moiré fringes produced.

(ix) Progressive waves due to the combination of two close frequencies may be seen with the 'live' and 'scanned' systems.

3.6. *Disadvantages of the stroboscopic method*

(i) The apparatus is more complicated.

(ii) The position of nodes and antinodes may not be apparent and may have to be deduced. The scanning method described in part (ii) of § 3.2 allows this to be done more easily however.

(iii) Phase information may not be evident, but it can be deduced.

(iv) Longer exposure times are necessary with continuous-wave lasers, although the method of Hallock may be incorporated by strobing the reference beam only, and this minimizes the increase in the exposure time. With pulsed lasers this disadvantage does not apply.

(v) There may be the need, when using some variations of the method, for two separate exposures which increases the long-term stability requirements of the system.

## 4. The time-averaged method

The experimental arrangement for the basic method is the same as for the holographic recording of a stationary object, although perhaps some extra precautions may be necessary to ensure that the object vibrations do not communicate themselves to the optical components. The photographic plate is simply exposed to the light from the vibrating object and also to a reference beam. The exposure time is the same as that used for stationary objects, although some modifications to the technique may require different exposures. The theory of time-averaged fringes is described below, and some of the many modifications to the basic technique, evolved mainly to overcome its disadvantages, will be discussed.

4.1. *Theory*

When two holograms are taken successively on one emulsion, we have seen that the result is the superposition of the two reconstructed images, so that they appear to occur simultaneously (§ 3). If the emulsion is exposed to a vibrating object, the resulting hologram is the superposition of a large number of separate holograms corresponding to each instantaneous position of the object. The hologram will simultaneously reconstruct the superposition of all these object positions weighted by the relative exposure time occupied by each of them (Powell and Stetson 1965 a, b).

Let $\bar{o}(rt)$ (more accurately) represent the amplitude of a light field from the object at position $r$ and time $t$. If a position $r_1$ lasts for a fraction $\Delta t/T$ of the total exposure time, then the image amplitude $\bar{i}(r_1)$ resulting from this is

$$\bar{i}(r_1) = \bar{o}(r_1 t)\Delta t/T \tag{4.1}$$

and therefore the total amplitude of the image is the sum of these individual contributions, i.e. the time average, in the limit

$$\bar{i}(r) = \frac{1}{T}\int_0^T \bar{o}(rt)\,\mathrm{d}t. \tag{4.2}$$

Now when the object displacement is small compared with its distance from the hologram,

$$\bar{o}(rt) = |o|\exp\{i\phi(rt)\}. \tag{4.3}$$

Where $\phi(rt)$ is the 'phase difference' due to object movement $d$. Therefore, substituting (4.3) into (4.2), we have

$$\bar{i}(r) = |o|\frac{1}{T}\int_0^T \exp\{i\phi(rt)\}\,dt \tag{4.4}$$

and the corresponding virtual image intensity on reconstruction is

$$\bar{I}(r) = |o|^2\left|\left(\frac{1}{T}\int_0^T \exp\{i\phi(rt)\}\,dt\right)\right|^2. \tag{4.5}$$

Expressions may be derived for the way in which the phase difference $\phi$ varies when the object movement $d$ is known, and the corresponding fringe systems may therefore be interpreted. For instance, if the object is illuminated and viewed normally and is vibrating sinusoidally, then the object distortion $d$ at any point (corresponding to the coordinates $(r, t)$) is

$$d = d_0 \sin \omega t \tag{4.6}$$

where $\omega$ is the circular frequency of the object vibration. The corresponding phase variation is:

$$\phi(rt) = \left(\frac{2\pi}{\lambda}\right)2d = \left(\frac{2\pi}{\lambda}\right)2d_0 \sin \omega t. \tag{4.7}$$

On substituting (4.7) into (4.5), we have

$$\bar{I}(r) = |o|^2\left|\left(\frac{1}{T}\int_0^T \exp\left\{i\left(\frac{2\pi}{\lambda}\right)2d_0 \sin \omega t\right\}dt\right)\right|^2. \tag{4.8}$$

Writing

$$\Phi(r) = \left(\frac{2\pi}{\lambda}\right)2d_0 \quad \text{and} \quad \psi = \omega t$$

(in the more general case $\Phi(r)$ will be a more complicated expression carrying information about different angles of illumination and viewing), then

$$I(r) = |o|^2\left|\left(\frac{1}{T}\int_0^T \exp\{i\Phi(r)\sin\psi\}\,dt\right)\right|^2. \tag{4.9}$$

Now it is known that

$$\exp\{i\Phi(r)\sin\psi\} = J_0(\Phi(r)) + \sum_{n=1}^{\infty} J_{2n}\{\Phi(r)\cos 2n\psi\}$$

$$+ \sum_{n=0}^{\infty} J_{2n+1}\{\Phi(r)\sin(2n+1)\psi\}. \tag{4.10}$$

When $T$ is much larger than any individual cycle time, as is usually the case in time-averaged work, $T$ may be regarded as tending to infinity. All the Bessel functions under the integral then tend to zero except the zero order. Therefore in the limit

$$\bar{I}(r) = |o|^2\left|\left(\frac{1}{T}\int_0^T \exp\{i\Phi(r)\sin\psi\}\,dt\right)\right|^2$$

$$= |o|^2|J_0\Phi(r)|^2 \quad \text{as} \quad T\to\infty \tag{4.11}$$

$$= |o|^2 J_0\left(\frac{2\pi}{\lambda}\right)2d_0|^2. \tag{4.12}$$

Therefore, the object reconstruction will be covered with fringes whose intensity follows a (zero-order Bessel function)$^2$ law (see figure 14). The amplitude $d_0$ will vary across the surface of the vibrating object and, for instance, when the term $(2\pi/\lambda)2d_0$ has the values 2·4, 5·52, 8·634, etc. the intensity of the object reconstruction will be zero—i.e. there is a dark fringe on the reconstruction. A more complete table of these zeros and the corresponding object movements is to be found in Brown *et al.* (1969).

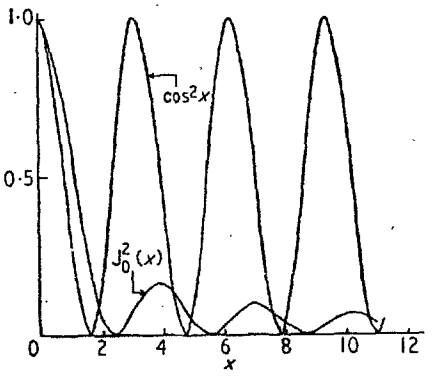



Figure 14. Comparison of (Bessel function)$^2$ fringes and cos$^2$ fringes.

Similar expressions may be derived for the fringes corresponding to other simple object movements, but the presence of harmonics makes the analysis more difficult!

The advantages and disadvantages of the time-averaged method will be listed first, as most of the techniques described in this section are methods of countering the disadvantages.

### 4.2. *Advantages and disadvantages of the time-averaged method*

#### 4.2.1. *Advantages*

(i) The experimental arrangements are as simple as those for the basic holographic system.

(ii) Exposure times necessary are, in general, shorter than for stroboscopic holography.

(iii) The positions of the nodes, being brighter than the rest of the reconstruction, are easily found (plates 4 and 6).

(iv) The basic technique may be modified in many ways—eliminating some of the disadvantages.

#### 4.2.2. *Disadvantages*

(i) The technique necessitates averaging over several cycles, and therefore demands more mechanical and electrical stability than 'pulsed laser' stroboscopy, though less stability than 'interrupted laser' stroboscopy.

(ii) The vibration amplitude cannot be simply obtained, even for sinusoidal vibrations.

(iii) If the oscillations contain harmonics the analysis becomes difficult (Wilson 1970) and the intensity of succeeding fringes falls off very rapidly.

(iii*a*) Asymmetric vibrations may not be studied at present.

(iv) The intensity of succeeding fringes for sinusoidal oscillations falls off as a (zero-order Bessel function)$^2$, making high amplitude oscillations difficult to study (plates 4 and 6).

(v) Phase information is ordinarily lost.

(vi) No information about the freqeuncy of the oscillations is recorded (Powell 1970).

(vii) Live fringe viewing is difficult (§ 3.3).

(viii) A linear motion superimposed on the vibration completely erases the fringe pattern.

4.3. *Modifications*

(i) One of the disadvantages of the time-averaged method is that phase information is ordinarily lost. However, Aleksoff (1969) has described a method whereby some phase information may be retained.

With his procedure the reference beam is phase modulated with the function $b\cos(\omega t+\beta)$, so that a point on the object will reconstruct with a brightness proportional to $J_0^2(c)$, where

$$c^2 = a^2+b^2-2ab\cos(\alpha-\beta).$$

This means that fringes are not formed around the zero vibrational amplitude, but about a vibrational amplitude determined by the modulation depth and phase of the reference beam.

The reference beam may be modulated by sending it through or reflecting it from any part of the object. Indeed, the reference beam may be formed by *imaging* the object or part of the object on to the photographic plate. Any desired reference phase and amplitude may be obtained by reconstruction from the appropriate part of the hologram.

For example, by modulating the reference beam with the amplitude and phase of the maximum amplitude of the object vibration, this amplitude then becomes the most brightly reconstructed part of the object, and adjacent lobes that are 180° out of phase are less brightly reconstructed.

(ii) The sub-fringe technique of Metherell described in § 5 may allow some phase information to be obtained as follows. Vibrations whose amplitudes are less than half a wavelength of light are made visible by using an oscillating reference mirror; information about the phase of the object vibrations may be obtained by noting the changes in the fringe pattern seen on inverting the phase of the reference mirror with respect to the object vibrations.

(iii) Another disadvantage of the time-averaged method is that the intensity of the fringes falls off with increasing amplitude of movement and soon becomes difficult to record on film and use for measurements. For example, the fringe intensity varies from 1 at zero amplitude position to 0·006 at fringe number 30, i.e. a ratio greater than 100 : 1. However, from fringe number 10 to fringe number 40 the ratio is only 5 : 1 (i.e. 0·0225 to 0·0040). If the zero-amplitude fringe could somehow be shifted to correspond to the 10 order fringe, much higher relative vibration amplitudes could be recorded and more easily studied. This effect would be achieved if the object were given piston motion or effective piston motion of the appropirate amplitude and phase (Fein and Green 1968). This piston motion may actually be imparted to the object, but the author suggests that the equivalent difference in phase may be applied anywhere in the object or reference beam paths

by using a vibrating mirror as in Metherell's sub-fringe technique (Metherell *et al.* 1969), but with a greater vibrational amplitude imparted to the vibrating mirror. Then a correspondingly larger number of fringes should be capable of reproduction.

(iv) Collins (1968) has shown that by altering the relative phase between the object beam and the reference beam by 180° between the two exposures necessary for a frozen fringes hologram, those parts of the object which remained undistorted or stationary will vanish on reconstruction. This phase shifting may be accomplished by varying the pressure in an air cell; by utilization of this device, wide variations in the relative phase may be produced if necessary. The theory is as follows. Let the amplitude of the first reference beam be

$$r = |r| \exp(i\phi_r)$$

and that of the second be

$$r_1 = |r| \exp\{i(\phi_r + \beta)\}.$$

Then the two image intensities are

$$I_1 = I_r + I_o + or^* + o^* r \tag{4.13}$$

$$I_2 = I_{r_1} + I_{(o+\Delta)} + (o+\Delta) r_1^* + (o+\Delta)^* r_1 \tag{4.14}$$

where $o$ is the amplitude of the light from the unchanged object and $o+\Delta$ is the amplitude of the light from the distorted object, on summation we have

$$I_{tot} = I_r + I_{r_1} + I_o + I_{(o+\Delta)} + r^*\{o + (o+\Delta)\exp(i\beta)\} + r\{o^* + (o^*+\Delta^*)\exp(i\beta)\}. \tag{4.15}$$

On developing the plate and reconstructing with the reference beam amplitude $r$, from equations (3.6) and (4.15) the new image amplitude is

$$I_r\{o + o\exp(i\beta) + \Delta\exp(i\beta)\}$$

and its intensity is, neglecting the reference beam intensity,

$$I_{image} = |o\{1 + \exp(i\beta)\} + \Delta\exp(i\beta)|^2. \tag{4.16}$$

Now let the phase of the reference beam change by 180° between exposures, i.e. $\beta = \pi$; the resulting image exposure is than $|\Delta|^2$, $\Delta$ being the change in the amplitude of the object light between exposures.

Some other alterations to the basic time-averaged method will be described in the next section, notably Metherell's subfringe technique in § 5.1 which greatly increases the sensitivity of the method.

### 4.4. *An application of time-averaged holography*

This section on time-averaged holography concludes with a description of how Molin and Stetson (1969) have applied the time-averaged method to the study of combination mode patterns. The experiment illustrates some of the advantages of holography (and time-averaged holography in particular) over more traditional methods of analysis.

Firstly a flat glass plate was used to test the theory of combination modes at one frequency. If the plate were isotropic, the angular orientation of a mode would depend only on the position of the exciter. The test plate was investigated with real time interferometry and corrected with pieces of wax until it was reasonably isotropic. Next, various combinations of two transducers excited at various relative phases and situated physically 90° apart were tried. With the exciters phased at

180° apart the component modes were easily compared with the combination patterns by overlaying photographic negatives of the time-averaged reconstructions. These experiments confirmed the theoretical predictions and showed that only the points of intersection of the component nodes remain (see below).

Experiments were then carried out at two different frequencies. The solenoid exciters were placed at the centre and right of the plate exciting the first radial and second diameteral modes respectively. Time-averaged holograms were taken of the two separate modes and their combination. Comparison of the negatives shows that the combination has nodes only at the intersection of component nodes as above, but also has black fringes where either of the component holograms has a black fringe.

As was shown in the theory of this section the image intensity, which may also be regarded as a fringe function, is

$$I(r) = |o|^2 \left| \frac{1}{T} \int_0^T \exp(io \sin \omega t)\, dt \right|^2 \tag{4.9}$$

$$= |o|^2 |J_0(\Phi(r))|^2. \tag{4.12}$$

When $\Phi(r)$, which describes the geometry of the motion of the object, is composed of two vibrations 90° out of phase, the resulting fringe function is, neglecting $|o|^2$,

$$I(r) = J_0\{(\Phi_1^2(r) + \Phi_2^2(r))^{1/2}\}. \tag{4.13}$$

This indicates that the argument of the fringe function is the vectorial sum of the component arguments. If they are 180° out of phase they will add algebraically and if there is an arbitrary phase difference between them they may be resolved into in-phase and quadrature components giving

$$I(r) = J_0(|\Phi_1(r) + \Phi_2(r)|) \tag{4.14}$$

where $\Phi_1(r)$ and $\Phi_2(r)$ are now phasor functions of the object vibration. Equation (4.14) shows that the Bessel function can be zero only when both phasor amplitudes are zero and all that will remain of the component nodal lines will be their points of intersection.

If there is sufficient amplitude, these points are circled with elliptical fringes which may be used to compute the phase difference between the two component vibrations by use of the following formula:

$$\cos \Delta = \frac{\Phi_2^2 \sin 2(\phi + \theta) + \Phi_1^2 \sin 2\theta}{2\Phi_1 \Phi_2 \sin(\phi + 2\theta)} \tag{4.15}$$

where $\Delta$ is the relative phase difference, $\phi$ is the angle between the node contours of the two component vibrations and $\theta$ is the angle between the major axis of the ellipse and the node line of the larger vibration magnitude (described here by $\Phi_1$)—this does imply some prior knowledge of the component vibration modes, however.

It may be shown (Stetson 1969) that if the object motion can be regarded as a number of separate time functions, statistically independent during the exposure time, the joint fringe function is the product of the separate functions. The joint function is therefore

$$I(r) = J_0(\Phi_1(r))\, J_0(\Phi_2(r)) \tag{4.16}$$

for a combination of two modes at different frequencies. This function has nodes

only at the intersection points of the component nodes, and black fringes where either component has a black fringe. Rational frequencies have been treated partially theoretically by Powell (1970).

## 5. Alterations in sensitivity, and related methods

This section covers one or two techniques for altering the number of fringes, seen on the object reconstruction, for a given amount of object movement. For precision work more fringes may be desirable, and for engineering inspection work far fewer fringes are necessary. Holographic interferometry as such may give more information than is necessary for some applications, and perhaps one of the related methods described later in this section may give the answer more rapidly and with less calculation. Some methods may indeed provide a more accurate and more readily displayed result in some experimental situations.

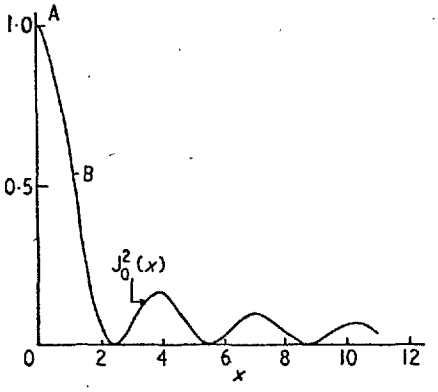



Figure 15. (Bessel function)$^2$ fringes showing region of small intensity change for small object movement at A and large intensity change at B.

### 5.1. *Methods for increasing sensitivity*

(i) The powerful technique of sub-fringe holography has recently been described by Metherell *et al.* (1969). This technique may be applied to both time-average and stroboscopic methods, and can increase the sensitivity to allow movements of as little as 3 Å to be recorded.

With the time-averaged technique the image intensity (figure 15) follows the well-known (Bessel function)$^2$ relation. If the object vibrations are less than a wavelength of light in amplitude, the brightness of the reconstruction at points of object movement is only slightly less than the brightness at points of no object movement—point A in figure 15. As may be seen, the steepness of the curve of image intensity against object movement in the neighbourhood of A is slight, and very little change in image brightness will occur for movements of up to $\frac{1}{10}$ of a wavelength. What is needed is some way of pushing the zero-movement datum down the slope to the approximately linear region of the central peak at B. This may be achieved by imparting a 'pseudo-movement' to the object of just the right amplitude, frequency and phase to shift the real zero-amplitude datum by the required amount. This is accomplished by placing a mirror in the object or reference beam paths, and vibrating it with the required amplitude and phase. The amplitude in

this case is less than a wavelength. In § 4 dealing with the disadvantages of the time-averaged method, a similar technique is described involving a vibrating mirror whose amplitude of vibration is several wavelengths in magnitude.

By changing the phase of the oscillating mirror, certain parts of the object become dark and other parts become light and thus, information about the relative phases of various regions of the object may be extracted. With very small movements, the contrast of the fringes may be improved by coherent optical filtering using a dc stop in the Fourier transform plane of a lens imaging the fringes. The overall grey background is then removed and the spatially varying parts of the image (the fringes) are more clearly seen.

(ii) A method described by Wuerker *et al.* (1968) effectively doubles the sensitivity of the stroboscopic technique by recording holograms in ultraviolet light.

Red light from a $Q$-switched ruby laser is passed through a crystal of potassium dihydrogen phosphate (KDP). This crystal generates second-harmonic ultraviolet light of wavelength 3471 Å. Two holograms are then simultaneously recorded using one 50 ns pulse on an ordinary 649F plate, and the resulting two virtual images are reconstructed with helium–neon laser light of wavelength 6943 Å. The two images may easily be spatially separated because the 'ultraviolet' hologram diffracts light at twice the angle of that diffracted by the 'red' hologram.

The reconstruction from the ultraviolet exposure will have approximately twice the number of fringes as that from the red exposure, which may be used as a check. The intensities of the red and ultraviolet illuminating beams were balanced by inserting glass windows to absorb sufficient of the ultraviolet light. For good quality ultraviolet holograms special lenses should be used where necessary. It is also interesting to note that because of gelatin absorption at ultraviolet frequencies, the effective emulsion thickness is reduced from 11 $\mu$m to 2·5 $\mu$m, and this results in a reduced angular orientation sensitivity of $\pm 23°$ compared with $\pm 11°$ for red light.

(iii) A method which does not actually increase the fringe sensitivity but which may make two-beam (i.e. stroboscopic) fringes more easily seen and hence easier to use for measurement purposes has been described by Matsumoto (1969). This technique allows the advantages of multiple beam interference fringes to be utilized in stroboscopic holography.

These multiple beam effects may be produced by the nonlinear characteristics of the photographic material and its processing. If the hologram is recorded in a nonlinear way, then many ghost or higher order images will be formed, and each propagates in different though related directions. If these could all be superimposed, sharper multiple beam fringes would result.

Nonlinear reconstruction produces the following wave fronts from the hologram:

$$a_0 \quad a \pm \exp(\pm ixy) \quad a \pm 2\exp(\pm 2ixy) \quad a_m \exp\{mi\psi(xy)\}$$

where $m$ is an integer and

$$\psi(xy) = \frac{2\pi}{\lambda x}\sin\theta + \xi(xy)$$

and where $a_m$ is the amplitude of the $m$th-order diffracted wave, that is

$$a_m = |a_m| \exp(i\delta_m)$$

and $\delta_m$ is the phase retardation of the $m$th wave front. On superposing with

some phase variation $\xi_m$ the total irradiance produced is

$$I_{xy} = \left| \sum_{-\infty}^{\infty} a_m \exp\{mi\xi(xy)\} + (\delta_m + \xi_m) \right|^2$$

where $a_m$ and $(\delta_m + \xi_m)$ are properly chosen so that the interference fringes are sharper than a sinusoidal profile.

One way of superposing the orders by using a diffraction grating is shown in figure 16. The grating is chosen to diffract each wave front generated by the hologram in the same direction. These wave fronts are then focused by a lens, and if the hologram is viewed from a given direction through a small orifice, multiple beam fringes are seen. Orders up to $m = \pm 6$ are observed with the naked eye.

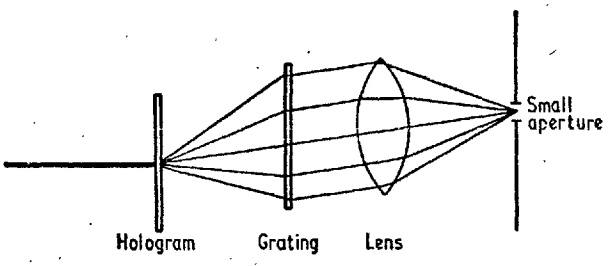



**Figure 16.** Optical system for multiple beam interferometry from a hologram.

The phase $\xi_m$ is related to the spacing between the hologram and the grating. (See also the laser spot scanning methods of Korpel *et al.* in §5.3 which are more sensitive than any straightforward holographic technique.)

5.2. *Methods for reducing sensitivity*

(i) The first method relies on the use of oblique illumination and viewing. The most famous example of this technique has been described by Archbold and Ennos (1968, 1970) where it has been used for the inspection of cylinder bores with the added advantage that similar cylinders may be directly compared.

With their technique (figure 17) an expanded laser beam passes through an annular conical lens which redirects it as a collimated conical beam on to the cylinder walls at an angle of 6° off grazing incidence. The reference beam is derived from the central part of the beam, which is expanded by a spherical concave lens. Contour spacings of $\frac{1}{2}$ $\mu$m have been demonstrated with this method. By inverting the illuminating annulus (figure 17) the fall in illuminating intensity with increasing initial beam radius may be compensated for by the reduced area that the beam has to fill after inversion.

(ii) A method which has a considerably lower sensitivity is the method of 'non-holography' (Redman *et al.* 1969). This technique is limited to small objects or objects whose extremities or gross motions are of interest. The object moves by such a large amount during the exposure that no hologram of it is reconstructed. However, if the bright background is sufficiently stationary the moving object leaves a three-dimensional holographic shadow against the stationary background. This shadow trajectory may then be studied as if it were an actual hologram. Surface features and movements of the object will be lost but the gross movements and movements of extremities will be preserved, allowing low-frequency oscillations of the whole object to be followed as the object moves along its trajectory.

(iii) *Moiré techniques.* The majority of desensitization techniques rely on the formation of moiré fringes between a set of lines connected in some way with the undistorted object, and a corresponding set connected with the distorted or vibrating object. The techniques differ in the ways in which the grilles are formed on, or related to, the object, and all are more complicated and therefore more difficult to carry out than straightforward time-averaged or stroboscopic holography.

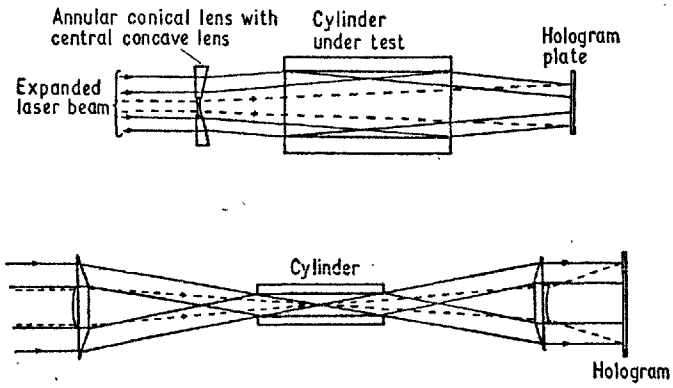



Figure 17. Two systems for making holograms of cylinder bores (after Archbold and Ennos 1970).

Der Hovanesian and Varner (1970) use the moiré fringes formed between the two sets of 'contour fringes' formed on the object. The object is first holographically recorded by use of light of wavelength $\lambda$. The photographically processed plate is returned exactly to its former position, and the reference mirror is rotated to position $M_2$. The object and hologram are then illuminated with light of wavelength $\lambda_2$, and real time contour fringes are seen on the object when viewed through the hologram. Each fringe occurs at a constant distance from the hologram, and the distance between fringes depends on the wavelength difference and, of course, the shape of the object. A photograph is taken of the object plus fringes, the object is distorted and the whole procedure is repeated. Finally, the two photographs are superposed and the object strain (or frozen vibrational amplitude) is computed from moiré fringe theory (Theocaris 1967). Alternatively, quadruple exposures will result in frozen fringes being seen. The sensitivity depends on the contour pitch and therefore on the wavelength difference (figure 18).

Another method of forming the contours necessary for this method has been described by Tsuruta and Shiotake (1967). In this case fringes are formed firstly by exposing the photographic plate to the object immersed in one gas and then re-exposing with the object immersed in a gas of a different refractive index. For instance, if air and $SF_6$ are used, the 1% difference in their refractive indices produces beats (fringes) between their wavelengths, separated by about 0·58 mm. Almost any contour spacing may be achieved within a given range by using different gases or mixtures of gases.

Varner (1969) has shown that by using two liquids or a liquid and a gas, wide variations in contour spacing may be achieved, i.e. from 0·75$\lambda$ to 300$\lambda$; these allow a correspondingly large variation in sensitivity.

The advantage of the two wavelength technique is that it allows the objects to be 'contoured' in their own environment. The contour spacings, however, are limited

to the laser lines available—the liquid gas techniques allow almost any desired contour spacing to be achieved.

(iv) Brooks and Heflinger (1969) utilize the moiré technique in a different way; 'light sheets' formed by the interference between two coherent beams of light are projected on to the object. A laser beam is directed into a Twyman–Green interferometer and then passed through a beam expansion telescope which projects the resulting sheets on to the object. The object is then viewed by a combination of telecentric lens and camera, the telecentric lens maintaining the apparent direction

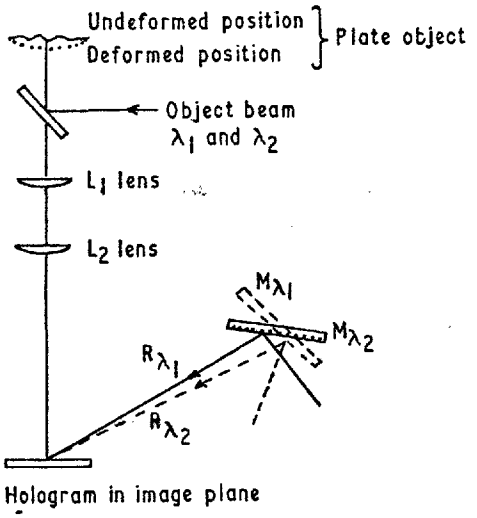



Figure 18. Apparatus for forming contours (after der Hovanesian and Varner 1970).

of view constant over the whole object. A master negative is taken (by the camera) of the whole object 'covered' with its light sheets, and returned to its original position. When the object is viewed through this master negative it appears to be uniformly dark. Only positions of object movement are then seen as the projected light sheets move out of register with the master negative. If the distance between the light sheets is $d$ and $\phi$ is the angle between the normal to the light sheets and the viewing axis, then the contour spacing is $\delta = d/\cos\phi$. For example, with $d = 0{\cdot}33$ mm and $\phi = 40°$ a shift of one fringe means an object movement of 0·43 mm in the direction of view.

(v) Burch (1970) has been working on a technique involving the formation of a grille on the object by utilizing photoresist. This substance, when exposed to light, becomes resistant to chemical attack.

The object is coated with resist, and a fine grid, formed by the interference between two laser beams, is projected on to it; diffraction effects limit the grids to about 1000 lines per inch. The resist is developed and etched, leaving the grid on the object, and a hologram of this is taken. This hologram is then used to 'back project' the real image on to the object. Holographic back projection works as follows: a conjugate reference beam is shone on to the hologram (from the direction opposite to the original reference beam); the real image is consequently reversed in polarity and falls on the object. The object then scatters the light, and the real image may be seen in much the same way as a cinema screen scatters a focused image. If the object is distorted, moiré fringes occur between the original fringes

and the projected ones. A second hologram may be taken of the object with its resist fringes together with its projected fringes. Practical problems involved with this method have until now proved difficult to resolve.

(vi) Several variations on the straightforward double exposure holographic technique involving moiré fringes have been suggested by der Hovanesian and Varner (1970); in their first technique a grille is formed on the object by rotating it, or the hologram, between two holographic exposures.

The photographic plate is exposed to the object, which is then rotated through a small angle about an axis in its surface (say). The photographic plate is then re-exposed. On reconstruction the object image has a linear fringe system superimposed in or near its surface; the spacing of these fringes (grille lines) is determined by the angle of rotation but may not be made arbitrarily great. A photograph can be taken of this master grille on high-contrast film. A second photographic plate is then exposed to the undistorted object and re-exposed to the distorted object rotated through the same angle as before (the hologram itself may be rotated about an axis in its plane with the same result), a photograph is taken of the new fringes produced. When the two photographs are superposed, moiré fringes are seen from which the distortion may be computed.

A triple exposure technique using two reference beams allows frozen moiré fringes to be produced. The first exposure is taken with two reference beams, the object is rotated and the second exposure is taken with one reference beam; finally, the object is distorted and the third exposure is taken with the other reference beam. Reconstruction with both reference beams produces the frozen moiré fringes. The third exposure may, of course, be of the stroboscopically frozen vibrating object.

By studying their local curvature, moiré fringes may be used to find positive and negative displacements of the object surface, i.e. the relative phases between various parts of the object.

### 5.3. *Related methods of vibration analysis*

The following methods do not rely on holography directly, but they all use a laser and some property of coherent light to render movement and vibration visible and measurable. Some may aid the experimenter because they give less (confusing) information about a particular experimental situation and therefore allow him to achieve results more quickly. Others, although they may be more complicated to set up experimentally, may provide increased sensitivity.

(i) A surface illuminated with coherent light and viewed through a limited aperture, such as the eye pupil, exhibits a mottled or speckled appearance. Any speckle pattern contains information about the light wave front, the position of the scatterer relative to the source and the observer, and the scattering properties of the illuminated object. A wide variation in any of these three properties causes the speckle pattern to change, and this change may be measured by comparison with the pattern recorded earlier, or by direct observation.

If an object vibrating with an amplitude of more than a few wavelengths of light is illuminated by dispersed laser light, the laser speckle pattern will be blurred at the antinodes, and it may be seen only at the nodal regions (Mottier and Eliasson 1970), the patterns seen are thus analogous to the Chladni sand patterns of Waller (1961). The sensitivity of the method may be altered within limits by changing the geometrical parameters of the experimental system (see the method

due to G Groh below). If the vibration amplitude is lower than that required to blur the speckle pattern, Fernelius and Tome (1970) have suggested that an object having a moderately rough surface produces a pattern in the antinodal regions which has more dark areas interspersed with brighter light areas. This pattern is thus complementary to most Chladni patterns (most powders collect at nodes though a few powders will collect at the antinodes).

Normally, in fact, if the illuminated surface moves towards or away from the observer, relatively little change in the appearance of the speckle patterns will occur unless a component of tilt is also present (Massey 1968). Detection of surface motion can be made more sensitive by adding a coherent reference beam, at the viewing aperture, which has a similar intensity to the speckle pattern (Archbold *et al.* 1969). Interference between the two beams causes the speckles to undergo cyclic brightness variations (twinkles) every time the object displacement in the line of sight changes by one quarter wavelength. Faster motion blurs the speckles at all but the nodal regions, as described above.

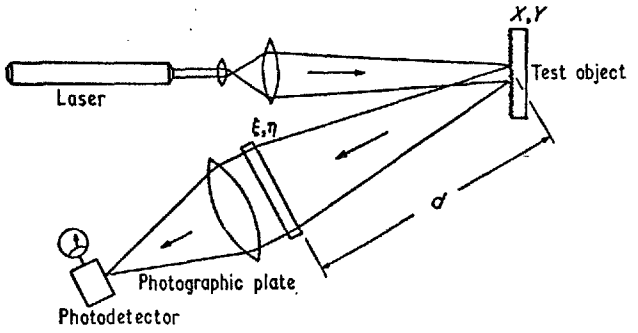



Figure 19. Apparatus for photographic laser speckle patterns (after Groh 1970).

Archbold *et al.* use a telescope with an iris diaphragm at the entrance pupil to observe the speckles. If the effective eye pupil is reduced to 0·5 mm the resulting speckle size of about 5 min of arc allows the antinodal blurring to be easily seen, but necessitates the use of as powerful a laser as possible. The reference beam is obtained by splitting off a small fraction of the illuminating laser light and focusing it into the telescope aperture. The speckle and reference intensities are balanced with polarizing filters. The twinkle effect due to slow movements—which would completely obliterate holographic fringes—aids the observation of nodal regions. Indeed, if there is not sufficient natural twinkle it can be introduced by varying the pressure in a gas cell placed in one of the beams. This speckle technique provides a quick method of assessing the nature of the vibrations, and indicates whether the conditions are sufficiently stable for the recording of a hologram. Archbold and Ennos' most recent development, 'speckle correlation interferometry', involves the superposition of two incoherent speckle patterns and can be used to give 'in plane' object movement fringes.

Another technique utilizing speckle patterns has been described by Groh (1970) who uses the experimental system shown in figure 19. The laser beam may be made convergent, divergent or parallel before illuminating the test object. The scattered light falls on to a photographic plate which may be returned to its original position after processing. Since it is a photographic negative the plate will blot out the bright parts of the speckle pattern and the transmitted intensity will be at a

minimum. The object may be viewed either through the negative, with the aid of a diffuser placed behind it, or the light passing through may be focused on to a photodetector.

If the object is slightly displaced a 'moiré' pattern is observed between the recorded and actual speckle patterns. A rotational disturbance causes the outer regions of the negative to brighten up, and the greater the rotation the greater is the encroachment of brightness towards the dark central regions. If the object is laterally displaced as well, the position of the dark area moves in the direction of the displacement.

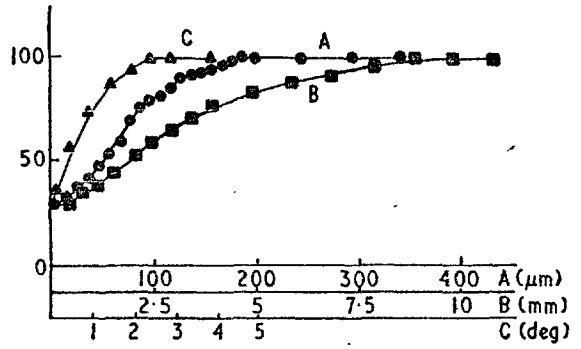



Figure 20. Intensity of light passing through the negative of the speckle pattern as a function of (A) lateral, (B) longitudinal and (C) rotational displacements. The rotation is about an axis normal to the surface of the object.

Figure 20 shows the total intensity passing through the plate as a function of the lateral and rotational displacements. With collimated illumination the displacement sensitivity is relatively low, but when the object is illuminated with a converging beam the sensitivity is increased. The measuring range is increased if the size of the illuminated area is reduced, table 5 gives a few examples; for a 1·5 mm diameter illuminated area, 0·6 mm displacements and for a 3·8 mm diameter illuminated area, 0·3 mm displacements are measurable.

**Table 5. Movement for maximum transmission**

| Illumination (2 mm dia.) | Lateral | Depth | Rotation 1 | Rotation 2 |
|---|---|---|---|---|
| Parallel beam | 0·2 mm | 8 mm | 2·5° | 5° |
| Converging to 50 mm behind | 0·02 mm | 0·3 mm | — | 1° |
| Converging to 5 mm behind | 0·01 mm | 0·06 mm | — | — |

Rotation 1, about an axis normal to the surface; rotation 2, about an axis in the scattering surface.

When the object is vibrating, the transmitted intensity variations may be displayed on an oscilloscope screen as shown in figure 21. The minimum corresponds to the rest position. The minimum to maximum transmission is denoted as $a$, maximum to zero as $b$ and minimum to zero as $c$. If the ratios of $a/b$ and $c/b$ are plotted against the number of cycles undergone by the object, they show in a

highly sensitive manner when fatigue has altered the surface characteristics, as shown in figure 22. The changes in these curves occur well before either changes in the resonance frequency or microscopic surface changes become visible.

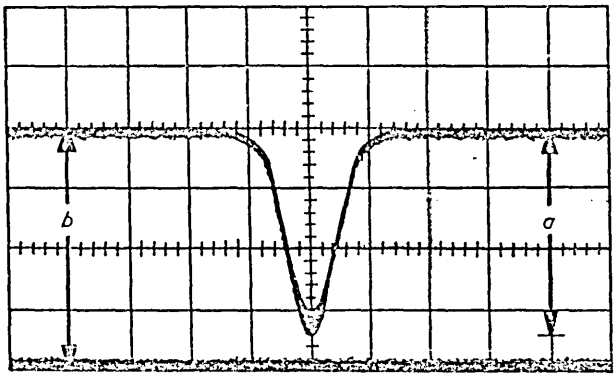



Figure 21. Photodetector signal when the test object is vibrating.

If two laser beams are shone onto a surface at equal angles to the normal but from opposite directions, the speckle pattern will not change as the object moves towards the observer. It will only change as the object moves in its own plane (Butters and Denby 1969). Korpel *et al.* have described several techniques for rendering visible and for measuring the amplitude of surface waves. They all use a probing coherent light beam and differ in the size of the beam and the way in which the vibrational information is 'decoded' from the reflected beam.

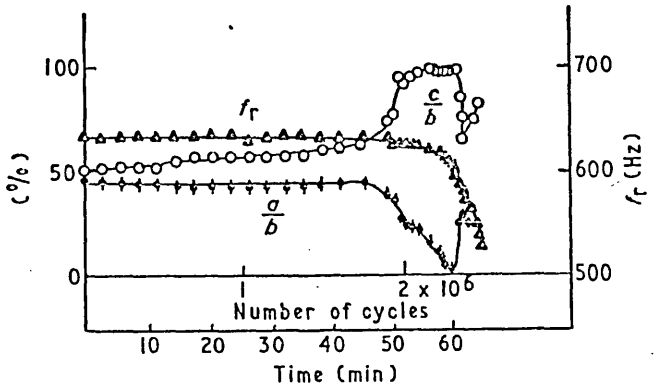



Figure 22. Ratios of $a/b$, $c/b$ and the resonance frequency of a steel plate spring as a function of time during a fatigue test.

(ii) The first of the Laser scanning methods (Korpel and Whitman 1968) has been later called the 'knife-edge technique' (Korpel and Whitman 1969), and the experimental arrangement is as follows.

Light from a laser is passed through a scanner and lens $L_1$ and comes to a focus at the specimen (which must be flat and specularly reflecting—figure 23). The spot then traverses the surface when the scanner angle is changed, and the reflected light passes through lens $L_2$ to fall subsequently on the knife edge and photodetector. Since the object lies in the Fourier transform plane of the scanner, and the detector

in the Fourier transform plane of the object, the detector is therefore in the image plane of the scanner. Because of this, the light beam always strikes the knife edge and detector in the same place, whatever the scan angle and position of the spot on the object surface.

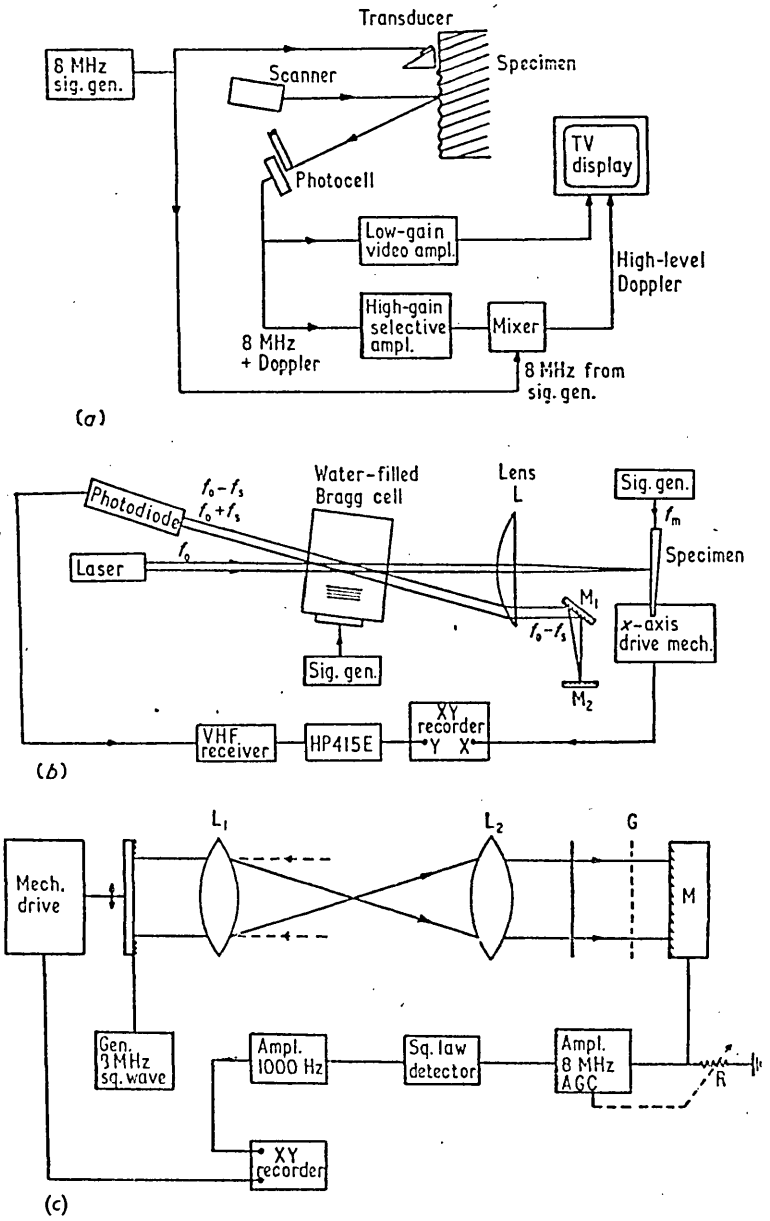



Figure 23. (*a*) Schematic diagram of laser spot scanning system for surface wave visualization; (*b*) heterodyne; (*c*) amplitude grating technique. (After Korpel and Whitman 1969).

In one particular system the light beam scans across the surface at 240 m s$^{-1}$, which is about 8% of the velocity of the type of surface wave being studied. This corresponds to a Doppler shift of $\pm 640$ kHz on an 8 MHz signal and the photodetector has an output of 8 MHz together with the two Doppler shifted frequencies.

The Doppler shift may have any intermediate value, depending on the angle of the surface wave propagation with respect to the scanning beam.

The photodetector output may then be fed to a television system where the spot is scanned in synchronism with the laser scanning mechanism. A picture would be seen on the screen, the brightness of which would be proportional to the local surface amplitude—which, since this is rapidly varying, would not be visible. To make the surface wave visible they must be strobed in some way, and this may be accomplished by heterodyning one or other or both of the Doppler shifted signals with the orginal from the signal generator. By using only one Doppler signal, surface waves travelling in one direction may be preferentially selected.

This may be interpreted as a synchronous detection process where the acoustic phase at each point is compared with the reference phase. Depending on the acoustic phase at any given point, the detector gives an output which is either black or white on the screen. Before the Doppler frequency is selected, some signal is split off and used to give an ordinary television background of surface features against which to observe the vibrations. The weakest signals observable with this technique correspond to about 0·1 Å of object movement.

(iii) The second technique is an optical heterodyning method having a similar sensitivity to the knife-edge technique. It differs from the above system in that the light reflected from the surface (and acoustically perturbed at a frequency $f_m$) is heterodyned with a reference beam at the frequency $f_0+f_s$ (where $f_s \neq f_m$). The additional frequency $f_s$ is added by passing the light through a Bragg cell filled with water and excited at the appropriate frequency. The frequencies $|f_s \pm f_m|$ are produced by this process, and their amplitudes are proportional to the amplitude of the surface waves. These signals may ultimately be used to modulate either the amplitude of an oscilloscope trace in a one-dimensional scanning system, or the brightness as in the previous method. Two different ways of achieving the superposition of the reference and probing beams have been described by Korpel and Whitman (1969).

(iv) The final method is called the amplitude grating technique. Again the sensitivity is similar to the above techniques, but uses a probing beam which is several acoustic wavelengths wide. The surface waves impress a moving phase ripple on to the reflected light beam, which may be regarded as a zero-order beam together with two first-order beams having an apparent phase velocity. Whenever the zero order differs in phase by multiples of 90° with respect to the other beams, the phse ripple becomes an 'amplitude ripple'. If a grating of the correct spatial frequency is placed at an optimum position, a time-varying light power will pass through it. This can be detected by a photodetector and used as in the above two methods.

The above three methods have a similar sensitivity but do have differences which may make one or other more suitable for a given application. For instance, the knife-edge technique is more readily adapted to three-dimensional display, and the superheterodyne technique is the best one for measuring long surface wavelengths, and also has no directional sensitivity. The three techniques require more sophisticated equipment than the most complicated holographic system, but they are more sensitive than even the subfringe technique of Metherell *et al.* (1969).

(v) Finally, another related superheterodyne system has been described by Avsec, Botcherby and Davis C.L.E.A. conference, Washington, 1969). The frequency off-set between the two beams is achieved by vibrating a reference

mirror $M_1$ (figure 24) sinusoidally with a much greater amplitude than that of the object $M_2$. The output signal of the photodetector has a series of Bessel function related sidebands (since this is a carrier wave, frequency modulated by both the reference mirror and the object). The first sideband may be frequency doubled and combined with the second sideband which is in quadrature with the first. The phase-modulated wave produced has a deviation proportional to the movement of the object and the amplitude related to the light intensity falling on the photodetector. This method has the advantage of relative simplicity when compared with the other similar methods.

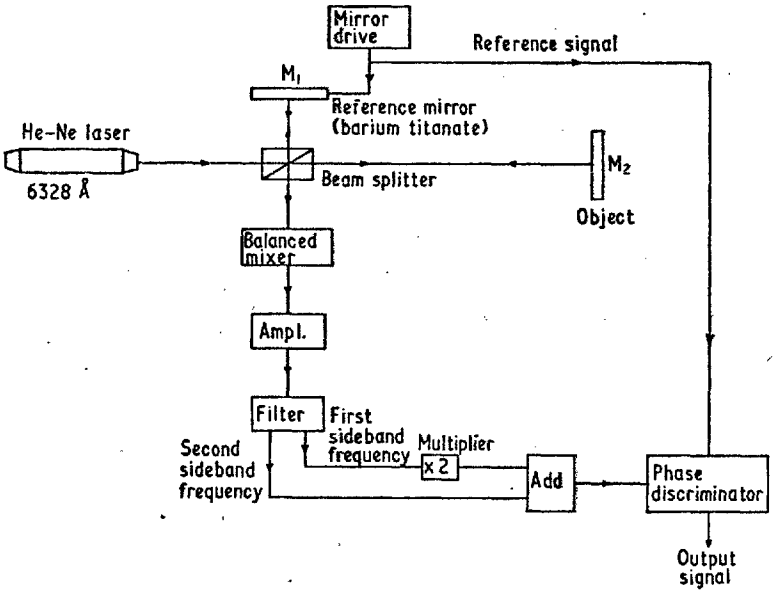



Figure 24. Vibration measurement using an optical superheterodyne system (after Avsec *et al.* C.L.E.A. conference 1969).

### 5.4. *Conclusion*

Some techniques useful to workers in the field of vibrational analysis have been described. The technology of holography and related fields is expanding rapidly and the author recommends that readers wishing to keep up to date with new developments should consult the following journals: *Applied Physics Letters*; *Applied Optics*; *Journal of the Optical Society of America*; *Nature*.

## References

ABRAMSON, N., 1969, *Appl. Opt.*, **8**, 1235–40.

ABRAMSON, N., 1970 a, *Engineering Uses of Holography*, Ed. J. M. Harvey and E. R. Robertson (London: Cambridge University Press).

ABRAMSON, N., 1970 b, *Appl. Opt.*, **9**, 97–102.

ALEKSOFF, C. C., 1969, *Appl. Phys. Lett.*, **14**, 23–4.

ARCHBOLD, E., and ENNOS, A. E., 1968, *Laser Focus*, October Edition.

ARCHBOLD, E., and ENNOS, A. E., 1970, *Engineering Uses of Holography*, Eds J. M. Harvey and E. R. Robertson (London: Cambridge University Press).

ARCHBOLD, E., ENNOS, A. E., BURCH, J., and TAYLOR, P. A., 1969, *Nature, Lond.*, **222**, 263–5.

BRADLEY, D. J., 1970, *Phys. Bull.*, **21**, 116–22.
BRANDES, R. G., SHANKOFF, T. A., and FRANÇOIS, E. E., 1969, *Appl. Opt.*, **11**, 2346–8.
BROOKS, R. E., and HEFLINGER, L. O., 1969, *Appl. Opt.*, **8**, 935–9.
BROWN, G. M., GRANT, R. M., and STROKE, G. W., 1969, *J. Acoust. Soc. Am.*, **45**, 1166–79.
BURCH, J. M. L., 1970, *Engineering Uses of Holography*, Eds J. M. Harvey and E. R. Robertson (London: Cambridge University Press).
BUTTERS, J. N., and DENBY, D., 1969, *Proc. Conf. on Photography in Engineering* (London: Institution of Mechanical Engineers).
CASTLER, D. H., and PRUET, H. D., 1967, *Appl. Phys. Lett.*, **10**, 341–2.
CLOSE, D., *et al.*, 1969, *Appl. Phys. Lett.*, **14**, 159–60.
COLLINS, L. F., 1968, *Appl. Opt.*, **7**, 203–5.
DEELEN, W. VAN, and NIELSEN, P., 1969, *Appl. Opt.*, **8**, 951–5.
DEVELIS, J. B., and REYNOLDS, G. O., 1967, *Theory and Application of Holography* (London: Addison Wesley).
FEIN, M. O., and GREEN, E. L., 1968, *Appl. Opt.*, **7**, 1864–5.
FERNELIUS, N., and TOME, C., 1970, *J. Opt. Soc. Am.*, **60**, 739.
FERRIER, W. G., 1969, *Contemp. Phys.*, **10**, 413–36.
FRYER, P. A., 1970 a, *Opt. Technol.*, **2**, 36–9.
FRYER, P. A., 1970 b, *Appl. Opt.*, **9**, 1216.
GABOR, D., 1948, *Nature, Lond.*, **161**, 777–8.
GABOR, D., *et al.*, 1965, *Phys. Lett.*, **18**, 116–8.
GATES, J. W. C., and HALL, R. G. N., 1970, *Engineering Uses of Holography*, Eds J. M. Harvey and E. R. Robertson (London: Cambridge University Press).
GOODMAN, J. W., and KNIGHT, G. R., 1968, *J. Opt. Soc. Am.*, **58**, 1276–83.
GROH, G., 1970, *Engineering Uses of Holography*, Eds J. M. Harvey and E. R. Robertson (London: Cambridge University Press).
HALLOCK, J. N., 1968, *Am. J. Phys.*, **36**, 762–3.
HOLLISTER, G. S., 1962, *Appl. Mater. Res.*, **1**, 149–59.
DER HOVANESIAN, J., and VARNER, J., 1970, *Engineering Uses of Holography*, Eds J. M. Harvey and E. R. Robertson (London: Cambridge University Press).
JACOBSON, A. D., 1969, *J. Opt. Soc. Am.*, **59**, 1529.
KIRK, J. P., 1966, *Appl. Opt.*, **5**, 1684–5.
KORPEL, A., and WHITMAN, R. L., 1968, *IEEE Transonics and Ultrasonics*, **SU-15**, 157.
KORPEL, A., and WHITMAN, R. L., 1969, *Appl. Opt.*, **8**, 1567–76.
LAMBERTS, R. L., and KURTZ, C. N., 1970, *J. Opt. Soc. Am.*, **60**, 724.
LATTA, J. N., 1968, *Appl. Opt.*, **7**, 2409–16.
LEHMAN, M., 1970, *Engineering Uses of Holography*, Eds. J. M. Harvey and E. R. Robertson (London: Cambridge University Press).
LEITH, E. N., and UPATNIEKS, J., 1962, *J. Opt. Soc. Am.*, **52**, 1123–30.
LEONARD, C., and SMIRL, A., 1969, *J. Opt. Soc. Am.*, **59**, 1530.
LIGTENBERG, F. K., 1955, *Exp. Stress Analysis*, **12**, 82–97.
LIN, L. H., and BEAUCHAMP, H. L., 1969, *J. Opt. Soc. Am.*, **59**, 1529.
LIN, L. H., and LOBIANCO, C. V., 1967, *Appl. Opt.*, **6**, 1255–8.
MARKOVA, G. V., *et al.*, 1969, *Sov. Phys.–Tech. Phys.*, **13**, 1470–3.
MASSEY, G. A., 1968, *U.S. Department of Commerce* document no. N 68-14070.
MATSUMOTO, K., 1969, *J. Opt. Soc. Am.*, **59**, 777–8.
MELROY, D. O., 1967, *Appl. Opt.*, **6**, 2005.
METHERELL, A. F., *et al.*, 1968, *Appl. Phys. Lett.*, **12**, 340–3.
METHERELL, A. F., *et al.*, 1969 a, *Appl. Oot.*, **8**, 1533–6.
METHERELL, A. F., *et al.*, 1969 b, *Scientific American*, October issue, pp. 36–44.
METHERELL, A. F., *et al.*, 1969 c, *J. Opt. Soc. Am.*, **59**, 1534–5.
MOLIN, N. E., and STETSON, K. A., 1969, *J. Phys.* E: *Sci. Instrum.*, **2**, 602–12.
MOTTIER, F. M., and ELIASSON, B., 1970, *J. Opt. Soc. Am.*, **60**, 739.
NEUMAN, D. B., and ROSE, H. W., 1967, *Appl. Opt.*, **6**, 1097–104.
NICKOLA, W., 1966, *Exp. Mechanics*, December issue, pp. 593–602.
ORR, L. W., *et al.*, 1968, *Appl. Opt.*, **7**, 202–3.
OSTER, G., WASSERMAN, M., and ZWERLING, C., 1964, *J. Opt. Soc. Am.*, **54**, 109–75.
PALAIS, J. C., and WISE, J. A., 1970, *J. Opt. Soc. Am.*, **60**, 714.

POWELL, R. L., 1970, *Engineering Uses of Holography*, Eds J. M. Harvey and E. R. Robertson (London: Cambridge University Press).
POWELL, R. L., and STETSON, K. A., 1965 a, *J. Opt. Soc. Am.*, **55**, 1593–8.
POWELL, R. L., and STETSON, K. A., 1965 b, *J. Opt. Soc. Am.*, **55**, 1694–6.
POWELL, R. L., and STETSON, K. A., 1966, *J. Opt. Soc. Am.*, **56**, 1161–7.
REDMAN, J. D., *et al.*, 1969, *J. Opt. Soc. Am.*, **59**, 1545.
ROGERS, G. L., 1950, *Nature, Lond.*, **166**, 237.
ROGERS, G. L., 1966, *J. Sci. Instrum.*, **43**, 677–84.
ROSE, H. W., and PRUET, H. D., 1968, *Appl. Opt.*, **7**, 87–9.
RUDDER, C. L., 1967, *Appl. Phys. Lett.*, **10**, 270–2.
RUSSO, V., and SOTTINI, S., 1968, *Appl. Opt.*, **7**, 202.
SHERIDON, N. K., 1968, *Appl. Phys. Lett.*, **12**, 316–18.
SIEBERT, L. D., 1967, *Appl. Phys. Lett.*, **11**, 326–8.
STETSON, K. A., 1967, *Appl. Phys. Lett.*, **11**, 225–6.
STETSON, K. A., 1969, *Optik*, **29**, 386–400.
STROKE, G. W., 1970, *An Introduction to Coherent Optics and Holography*, 2nd edn (New York: Academic Press).
STROKE, G. W., BROWN, G. M., and GRANT, R. M., 1969, *J. Acoust. Soc. Am.*, **45**, 1166–80.
THEOCARIS, P. S., 1964, *Proc. Soc. Exp. Stress Analysis*, **21**, 153–9.
THEOCARIS, P. S., 1967, *Br. J. Appl. Phys.*, **18**, 513–19.
THOMPSON, B. J., and PARRENT, G. B., 1967, *Science J.*, **2**, 42–9.
TOLANSKY, S., and WOOD, A. F. B., 1958, *Physica*, **24**, 508–18.
TONNDORF, J., 1970, *J. Acoust. Soc. Am.*, **47** (part 1), 60.
TSURUTA, T., and SHIOTAKE, J., 1967, *Jap. J. Appl. Phys.*, **6**, 1166.
UPATNIEKS, J., 1969, *J. Opt. Soc. Am.*, **59**, 1539.
UPATNIEKS, J., and LEONARD, C., 1970, *J. Opt. Soc. Am.*, **60**, 297–305.
URBACH, J. C., and MEIER, R. W., 1969, *Appl. Opt.*, **8**, 2269–91.
VARNER, J., and ZELENKA, J. S., 1969, *Appl. Opt.*, **8**, 1431–4.
VIENOT, J. CH., *et al.*, 1970, *Engineering Uses of Holography*, Eds J. M. Harvey and E. R. Robertson (London: Cambridge University Press).
WALL, M., 1969, *Optics Technol.*, **1**, 266–70.
WALLER, M. D., 1961, *Chladni Figures* (London: G. Bell).
WATRASIEWICZ, B. M., *et al.*, 1968 a, *Nature, Lond.*, **217**, 1142–3.
WATRASIEWICZ, B. M., *et al.*, 1968 b, *Optics Technol.*, **2**, 20–3.
WELFORD, W. T., 1966, *Appl. Opt.*, **5**, 872–3.
WILSON, A. D., 1970, *J. Opt. Soc. Am.*, **60**, 1068–71.
WITHRINGTON, R. J., 1968, *Engineering Uses in Holography*, Eds J. M. Harvey and E. R. Roberston (London: Cambridge University Press).
WUERKER, R. F., and HEFLINGER, L. O., 1970, *Engineering Uses of Holography*, Eds J. M. Harvey and E. R. Robertson (London: Cambridge University Press).
WUERKER, R. F., HEFLINGER, L. O., and BRIONES, R. A., 1968, *Appl. Phys. Lett.*, **12**, 302–3.

# A New Technique for the Measurement of Sound Transmission Through Plates

P. Fryer, A.T. Fry and R.W.B. Stephens

## INTRODUCTION

An acoustic duct is used as a waveguide in which various pressure distributions are developed across the specimen plate occupying a cross-section of the duct. The latter was of square section bounded on the sides and bottom by concrete walls set into the basement floor of the building and which was below ground level. The sound source consisted of a 5 x 5 array of loudspeakers which permitted modes up to (4.0) to be exclusively excited.

FROM: The International Symposium on
The Damping of Plates by Means of a Layer
Leuven 14-16.9.1967.

## THEORY

### Source Configurations for Mode Excitation in Waveguides of Rectangular Cross Section.

#### Wave Equation

For a rectangular waveguide with dimensions 2b and 2d in the x and y directions, the z axis being located centrally, the wave equation, in terms of velocity potential, may be written:-

$$\frac{\partial^2\phi}{\partial x^2} + \frac{\partial^2\phi}{\partial y^2} + \frac{\partial^2\phi}{\partial z^2} = \left[-\frac{\omega}{C_d}\right]^2 \phi \qquad (1)$$

The solution to this equation is

$$\phi = A\begin{bmatrix}\cos\\ \sin\end{bmatrix} J(k_x x)\begin{bmatrix}\cos\\ \sin\end{bmatrix} J(k_y y)\exp(-ik_o z)\exp(i\omega t) \qquad (2)$$

with

$$(\omega/C_d)^2 = k_x^2 + k_y^2 + k_o^2 \qquad (3)$$

$k_x$ and $k_y$ are evaluated by application of the boundary conditions

$u_y = u_x = 0$, at $x = \pm b$, $y = \pm d$ respectively.

Since $\dot{u}_x$ is proportional to $(\partial\phi/\partial x)$, we have for modes which are:-

Symmetrical in x

$$k_x b = \frac{m\pi}{2}, \text{ m being zero or even} \qquad (4)$$

Asymmetric in x

$$k_x b = \frac{m\pi}{2}, \text{ m being odd} \qquad (5)$$

A similar analysis applies to y.

#### Relative Amplitudes Excited by Symmetrical and Asymmetrical Sound Sources.

(a) By a Symmetrical Source

Assuming a symmetrical source and neglecting variations in the y direction, the potential function which represents all the modes excited will be:-

$$\phi(x,z,t) = \sum_m A_m \cos\left[\frac{m\pi}{2b}\right]x.\exp(ik_{mo}z)\exp(i\omega t) \qquad (6)$$

Where m is even and only symmetrical modes are excited. $A_m$ is the amplitude of the mode (m,0).

Using the usual techniques for evaluating amplitudes in Fourier series it follows that:

$$A_m = \frac{2}{b}\int_0^{+b} \phi(x,0)\cos\frac{m\pi}{2b}x.dx, \qquad (7)$$

where $\phi(x,0) = \sum_m A_m \cos \frac{m\pi}{2b} x$ is the potential at z = 0 (8)

due to the source.

(b) By an Asymmetrical Source

A similar analysis to the above yields

$$A_m = \frac{2}{b} \int_0^{+b} \phi(x,0) \sin \frac{n\pi}{2b} x \cdot dx \qquad (9)$$

Exclusion of Modes of Order n for Symmetrical Sources

For a source configuration to exclude the mode of order n, $A_n$ must be zero. Hence for symmetrical modes with n zero or even

$$\int_0^b \phi(x,0) \cos \frac{n\pi}{2b} x.dx = 0 \qquad (10)$$

Calculation of Relative Source Amplitudes for a 5 by 5 Loudspeaker Array

The discussion in this section involves three major considerations

(1) To find a general formula for the amplitudes and positions of the speakers needed to exclude specific modes.

(2) To determine the effect of the source width on the modes excited, and

(3) To calculate the specific relative amplitudes of the loudspeaker cones needed to excite modes up to (4,0)

General Formula

Even-mode Excitation (i.e. m = 2n)

Distribution of Loud Speakers (each of source width 2D)

Line source at $\pm$ fb excited at amplitude A,

Line source at $\pm$ gb excited at amplitude B,

Central line source at 0 excited at amplitude C.

Each line comprises five speakers.

Assuming that the speakers produce a uniform pressure over their cone width the amplitude of the mth order mode (even) is:-

$$A_m = \frac{2}{y} \int_0^{y} \phi(x\ 0) \cos \left(\frac{n\pi}{y}\right) x.dx$$

On substitution of the speaker configuration $\phi(x,0)$ and integrating

$$A_m = \frac{2A}{n} \left[ \sin \frac{n\pi}{y}(fb-D) - \sin \frac{n\pi}{y}(fb+D) \right] +$$

$$\frac{2B}{n} \left[ \sin \frac{n\pi}{y}(gb-D) - \sin \frac{n\pi}{y}(gb+D) \right] +$$

$$\frac{2C}{n} \left[ - \sin \frac{n\pi}{y}(D) \right],$$

whence

$$A_m = \frac{-2}{\pi} \left[ \sin \frac{n\pi D}{D} \right] \left[ C + 2B \cos (n\pi g) + 2A \cos (n\pi f) \right]$$

For $A_m$ to be zero therefore

$$\sin \frac{n\pi D}{D} = 0 \qquad (11)$$

$$C + 2B \cos (n\pi g) + 2A \cos (n\pi f) = 0 \qquad (12)$$

Use of the General Formula

Equations (11) and (12) are the component equations of the general formula. For a given mode the choice of either amplitude or location of a line of speakers is quite arbitrary but by choosing one, the other is then defined by equation (12).

It would be convenient for the excitation of plane waves if all the speakers were given the same amplitude and the speaker location found from equation (12). Assuming $A = B = C = 1$, and that $f = 2g$, by substituting these conditions into equation (12) in order to find the speaker positions for the exclusion of modes (n) greater than 0, it follows

$$4 \cos^2 (n\pi g) + 2 \cos (n\pi g) - 1 = 0$$

Hence

$$\cos (n\pi g) = \cos \frac{2\pi}{5} \text{ or } = \cos \left\{ \pi \pm \frac{\pi}{5} \right\}$$

i.e. $$n\pi g = 2m\pi \pm \frac{2\pi}{5} \text{ or } = 2m\pi \pm \left\{ \frac{\pi}{5} \pm \pi \right\} \qquad (13)$$

In order to exclude the (2,0) mode, substituting $n = 1$, $m = 0$ in (13) gives

$$g = \frac{2}{5} \text{ and } f = \frac{4}{5}$$

To ascertain the other modes excluded by equation (12), substitution of $g = 2/5$ in equation (13) gives

$$\frac{2n}{5} = 2m \pm \frac{2}{5} \text{ or } \frac{2n}{5} = 2m \pm \left[ \frac{1}{5} \pm 1 \right] \qquad (13a)$$

(9) chose position ∴ amp fixed by (12)

(10) turns out that speakers spaced evenly IF ALL TO HAVE SAME AMP for (00)

In order for a mode 'n' to be excluded, equation (13a) must be satisfied by integer m. The following table shows which values of n are in fact satisfied by integer m.

| n = | m = | $\frac{n+1}{5}$ | $\frac{n-1}{5}$ | $\frac{n-2}{5}$ | $\frac{n-3}{5}$ | $\frac{n+2}{5}$ | $\frac{n+3}{5}$ |
|---|---|---|---|---|---|---|---|
| n = 1 | m = | - | 0 | - | - | - | - |
| n = 2 | m = | - | - | 0 | - | - | 1 |
| n = 3 | m = | - | - | - | 0 | 1 | - |
| n = 4 | m = | 1 | - | - | - | - | - |
| n = 5 | m = | - | - | - | - | - | - |
| n = 6 | m = | - | 1 | - | - | - | - |
| n = 7 | m = | - | - | 1 | - | - | 2 |
| n = 8 | m = | - | - | - | 1 | 2 | - |
| n = 9 | m = | 2 | - | - | - | - | - |
| n = 10 | m = | - | - | - | - | - | - |

From this table it is seen that all modes will be excluded by equation (12) except those that are multiples of 10, i.e. n is a multiple of 5.

When D is $y/5$, equation (11) is satisfied if n is also a multiple of 5; all modes other than (0,0) are then excluded.

Summary of Deductions from General Formula

(a) From equation (12) for $g = 2/5$ all even modes will be excluded which are not multiples of 10.

(b) From equation (11) for $g = 2/5$ all even modes will be excluded which are multiples of 10 when $D = y/5$. That is, only the zero order mode is excited.

(c) The width of the speaker, assuming that the pressure output is constant over this width, does not affect the exclusion conditions except in the case where D is a multiple of $y/5$. The speaker width, when it is not a multiple of $y/5$, does affect the amplitude of modes not excluded by the speaker positioning or amplitudes.

Calculation of Relative Amplitudes (even modes)

Restating equation (12)

$$C + 2B \cos(n\pi g) + 2A \cos(2n\pi g) = 0$$

From this equation values of A, B and C can be found by solving, TWO at a time, the three equations obtained by putting n = 0, 1, 2. Values can be found by this means that will specifically:-

(i) excite (0,0), excluding (2,0) and (4,0)

(ii) excite (2,0), excluding (0,0) and (4,0)

and (iii) excite (4,0), excluding (0,0) and (2,0)

Similar analysis to the above yields, for odd modes, the following equation

$$A_m = \frac{-8}{m\pi} \left[\sin \frac{m\pi D}{y}\right] \left[B \sin \frac{m\pi}{5} + A \sin \frac{2m\pi}{5}\right] \qquad (14)$$

From equations (12) and (14) the following table has been derived

| Amplitude and Position / Mode | A, $\frac{4}{5}y$ | B, $\frac{2}{5}y$ | C, 0 |
|---|---|---|---|
| only (0,0) | 1 | 1 | 1 |
| only (1,0) | 1 | .618 | 0 |
| only (2,0) | -.809 | .309 | 1 |
| only (3,0) | -.618 | 1 | 0 |
| only (4,0) | .309 | -.809 | 1 |

Summary and Comments

Similarly as for the (0,0) mode the upper frequency limits may be found for the other modes.

| Mode | Upper frequency limit | Frequency at 22°C |
|---|---|---|
| (0,0) | (10,0) cut-off frequency | 2830 Hz |
| (1,0) | ( 9,0) cut-off frequency | 2547 Hz |
| (2,0) | ( 8,0) cut-off frequency | 2264 Hz |
| (3,0) | ( 7,0) cut-off frequency | 1981 Hz |
| (4,0) | ( 6,0) cut-off frequency | 1698 Hz |

This is interesting since the calculations were only concerned with the pure excitation of modes up to the (6,0) cut-off for even modes, and (5,0) cut-off for the odd modes. It is seen that the upper frequency limit is extended upwards as the mode number is reduced.

Effective Angle of Incidence upon Specimen

Each mode may be thought of as a synthesis of plane waves travelling along the guide in a zig-zag path. The sinusoidal distribution of pressure across the width of the duct is a result of the interference between these waves as they intersect. These plane waves will strike the boundaries at a characteristic angle of incidence $\phi$. The angle of incidence of waves on a partition across the guide will be $90 - \phi = \theta$, where $\theta$ is given by $\theta = 1 - \frac{mv^2}{4yv} \cdot m$ is the mode number, $v$ is the sound velocity in free air and $\nu$ is the frequency.

Properties of Modes Influencing Experiments in Waveguides

(1) Associated with each mode of propagation at a given frequency there is a definite angle of incidence attributed to sound waves impinging on a specimen panel placed at right angles to the axis of the guide.

(2) The angle of incidence decreases as the frequency is increased. This means that for a number of different angles of incidence at any given frequency, the same number of modes will have to be excited. It will not be possible in general to have the same angles of incidence at the different frequencies used in a single waveguide.

(3) Each mode possesses a cut-off frequency below which it will not be propagated.

At low frequencies, therefore, the number of angles attainable is limited by the number of modes that are capable of excitation. In the present experiments only the (m,0) mode was excited as this proved easier to excite. This meant that a new mode and corresponding angle of incidence was introduced for every increase of 283 cycles per second. Below 283 c/s only the (0,0) mode was excited, giving a constant zero angle of incidence.

(4) The excitation of a given mode in a guide of square section required a minimum number of sources: To excite a given mode in a frequency region where the highest mode that is capable of excitation is (n,n) requires the use of $(n+1)^2$ sources appropriately placed and excited. If the frequency is increased beyond this region other modes will be excited by the source configuration - along with the desired mode - giving amplitudes at other angles of incidence and causing some uncertainty in measurement.

(5) Each mode possesses a characteristic pressure pattern across the duct, this property enables the experimenter to check the purity of a given mode.

Details of Mechanical System

The apparatus was constructed with simple components consistent with ease of assembly and attainment of appropriate accuracy of experimental measurement.

(1) Microphone Carriage

This system had necessarily to be silent and smooth in operation with freedom of movement in three directions within the duct, and acoustically to be as small as possible. The control section displayed an exact analogue of the location of the microphone within the duct and is depicted in Fig.(1), where the cross pieces attached

to the various cords controlling the position of the microphone (m) are indicated.

(2) Sound Source System

Twenty-five loudspeakers, each of 4½" diameter, were fixed to a plywood panel to form a symmetrical five x five assembly. A framework was bolted to the back of the panel so that it was quite massive and rigid. The 'specimen' side of the duct was rendered as 'anechoic' as possible by the suitable disposition of glass fibre.

(3) Specimen Holder

The frame carrying the specimen panel was fixed with mastic to the sides and bottom surfaces of the duct. The upper surface of the frame was 'tailored' with quick setting 'plastic padding' to the undersurface of the appropriate concrete block forming the roof of the duct. (see Fig. 2).

Experimental Procedure

(1) The (0,0) Mode

(a) The control unit was set so that all the speakers had the same amplitude and the same phase.

(b) The frequency analyser (No.2), into which was plugged the fixed microphone r on the 'specimen' side of the duct was set for 'frequency analysis', and the variable pass band was set to the maximum selectivity. This not only excluded most of the unwanted noise found over the audio frequency band but also allowed the frequency to be accurately measured.

(c) The moveable microphone was hung with its axis pointing along the central axis of the duct, and was moved as close to the specimen as possible.

Readings were taken at one cycle intervals up to 50 Hz then two cycle intervals up to about 200 Hz. For frequencies below about 200 Hz it was not found necessary to move the microphone 'm' on the speaker side to a maximum in the duct because at very low frequencies the pressure was at a maximum near the specimen. At medium low frequencies the second maximum was a long way down the duct and did not differ appreciably from the first.

At medium frequencies, however, the fact that it was not possible

to move the microphone up to the surface of the specimen, meant that even though this microphone could be moved close to the specimen it was not in fact measuring the maximum pressure. After about 200 Hz had been reached, the microphone r was therefore moved to the first maximum from the specimen and this was taken to represent the pressure at the surface of the specimen.

Above about 200 Hz readings were taken at longitudinal resonances in the duct. These were spaced at about 40 cycle intervals. In regions where the tranemission was found to be varying rapidly more readings were taken at points other than the duct resonances.

For all even-mode runs the specimen microphone was located centrally within the duct. It was thought that little modal propagation would occur in the heavily damped specimen side of the duct but to ensure that the microphone would be at a maximum, should any occur, it was placed at the centre for even modes and at the edge (or as close to the edge at the absorbent allowed) for the odd modes.

(2) Other Modes

The oscillator was set to a frequency above the cut-off of the mode considered. The control unit was set to the combination of amplitude and phase for the particular mode and the voltage across each speaker column was checked. The oscillator was then swept below the cut-off frequency when a large drop in sound level on the speaker side of the duct was observed. The oscillator was then set by ear to the first resonance for the mode being excited. The travelling microphone was then moved both along and across the duct to a maximum, for the first maximum of any mode this was found to be quite a distance away from the specimen. Readings were taken at duct resonances, as in theplane wave case, up to the highest frequency at which the mode could be excited purely. It was found that close to the cut-off frequency, corresponding to high anglee of incidence, duct resonances were separated by only a few Hz. The difference between successive resonances gradually increased to the 40 Hz of the plane wave case ((1) above) as the frequency was raised and the corresponding angle of incidence decreased. Before each run on a panel the velocity of sound in the duct was measured in order to calculate the angles of incidence for the modes. In practice the temperature and humidity was found to be almost constant in the duct and

so a velocity correction was found to be unnecessary.

(3) Modal Purity

The oscillator was tuned to a modal resonance and the travelling microphone was moved along the duct to a maximum and then across the duct. The recorded pressure pattern was plotted with particular attention being given to the cusps. For each mode two maxima were used for the cross-section plots in each frequency interval of 283 Hz this was because a new mode became capable of excitation each time the frequency was increased by 283 Hz and it was desired to see how effectively the speaker excitation excluded unwanted modes. Finally the pressure patterns were plotted for frequencies above those of the last excluded mode.

The following paper will describe preliminary measurements made on various forms of panel, using the waveguide technique.

## REFERENCES TO LITERATURE

### BOOKS


| | |
|---|---|
| Mechanical Waveguides | Martin Redwood |
| Sound Insulation and Room Acoustics | Per V Bruel |
| The Handbook of Noise Control | Harris |
| Acoustics and Building Materials | Parkin & Humphrey |
| Vibration Problems in Engineering | Timoshenko |
| The Measurement and Supression of Noise | King |


### RESEARCH PAPERS


The Acoustic Wave Guide E.A.G. Shaw JASA 25 224

Transmission of Reverberant Sound through Single Walls, A. London J. Res. Nat. Bur. Stds. U.S.A. 42 688

Excitation of Flat Panels by the Coincidence Effect J. Sound & Vib 2, 2

Use of Turbulent Model to calculate the Radiation and Vibration Responses of a Panel with practical suggestions for reducing the Sound Level. L. Maestrello J. Sound, Vib 5 407

Bond Stresses in a Randomly Vibrating Sandwich Plate: Multi modal Theory A.J. Pretlove J. Sound, Vib 2 Z

On the Interaction Between Plate Bending Waves and their Radiation Load G. Kurtze and R.H. Bolt Acustica 9, 288

Fig 1

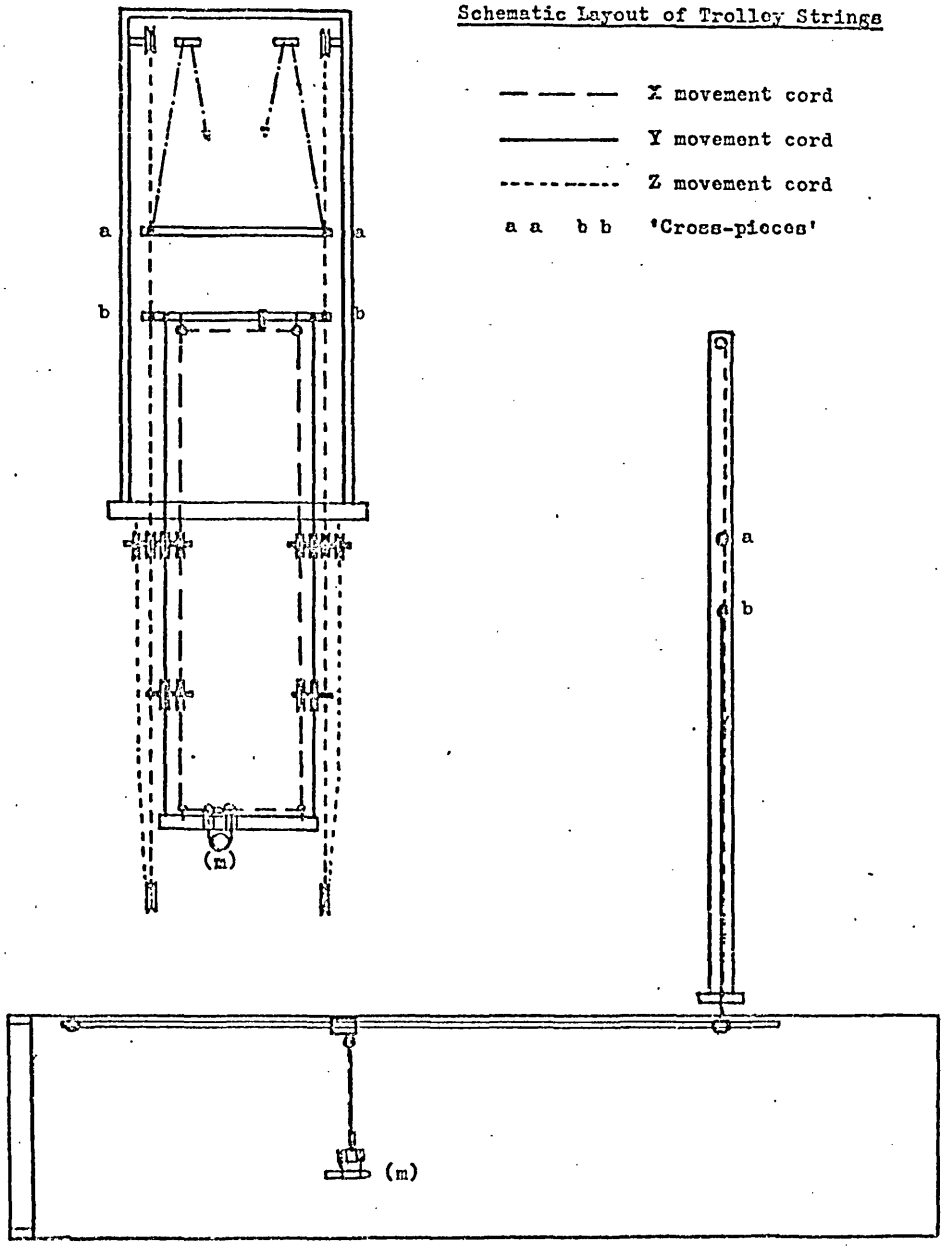
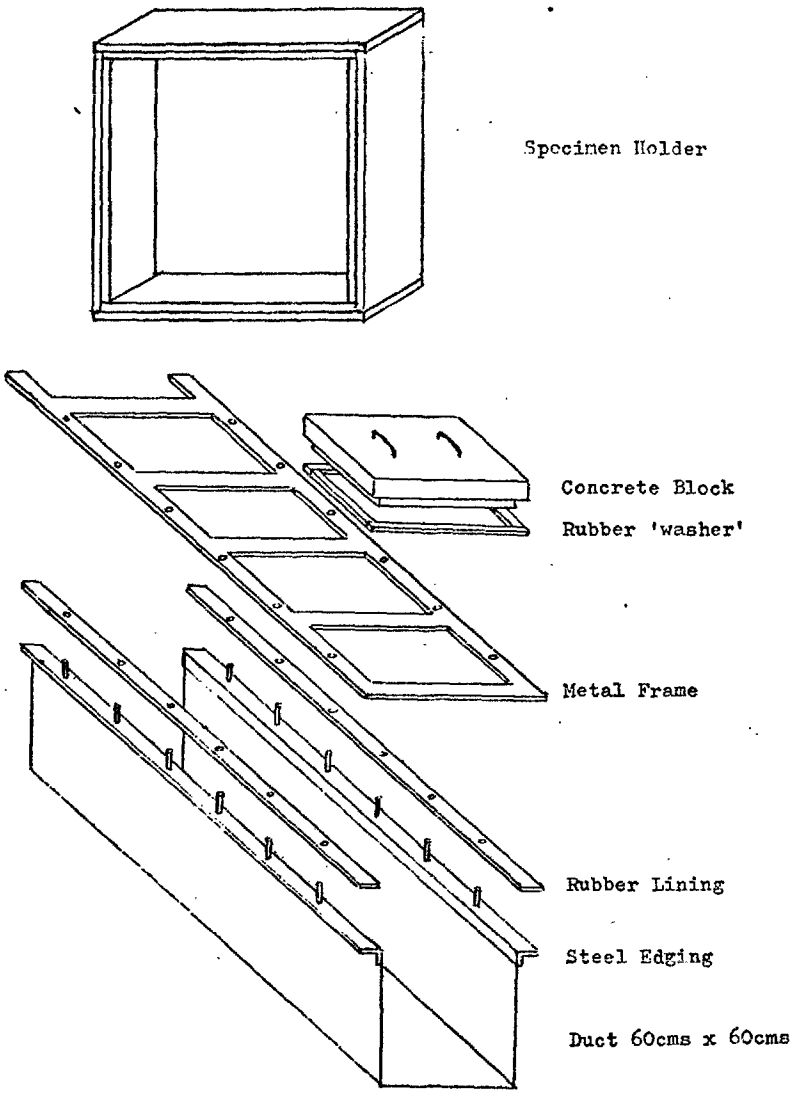

Schematic Layout of Trolley Strings
X movement cord
Y movement cord
Z movement cord
a a b b 'Cross-pieces'
a
a
b
b
(m)
a
b
(m)

Fig 2

Specimen Holder and Exploded View of the Duct




Exploded view of duct roof

# SOUND TRANSMISSION THROUGH PLATES OF VARIOUS STRUCTURES

A.Fry, P.Fryer and R.Stephens (Imperial College-London)

The object of this paper is to demonstrate the use of the acoustic wave-guide as an experimental tool to study sound transmission through panels embodying specific features. Results are presented to demonstrate the effects of varying these features.

## MODES:

When sound is incident at an angle on a panel a discrete pressure pattern is established across the incident face. The pattern due to a single wave train moves across the face at the speed of the projected wave, $\frac{c}{\sin\theta}$, where $\theta$ is the angle of incidence of the wave. ($\theta$ = angle between the normals to the wave-front and to the panel).

Except at the "coincidence frequency" this velocity does not equal the natural speed of the corresponding bending wave train in the plate. However if two waves are incident from opposite edges of equal amplitude and at the same angle $\theta$, a standing air wave pattern will be formed across the face of the panel. This may coincide with a flexural standing resonance mode of the panel. The resonant frequencies for these modes will be given by equation (1), when the panel is not rigidly supported at its perimeter.

$$f = \frac{\pi}{2}\sqrt{\frac{E\,h^3}{12(1-\sigma)}\cdot\frac{1}{M}}\cdot\left(\frac{m^2}{a^2}+\frac{n^2}{b^2}\right) \quad \ldots\ldots\ldots \quad (1)$$

where E and $\sigma$ are Young's Modulus and Poisson's ratio respectively of the panel material

h = panel thickness

M = mass per unit area

a and b are the panel dimensions

m and n are integers

Depending on the source configuration at the end of the duct these standing air wave patterns may be formed across the face of the panel, which form the discrete duct modes. The (0,0) mode represents a plane wave in the duct with uniform pressure amplitude across the duct. For any one chosen configuration (discussed in another paper) of the source elements, the mode pattern generated will be the same at all frequencies above the cut-off frequency for this mode. This contrasts with the angle of incidence of the two intersecting wave fronts which may be considered

frequency is varied in order to keep the resultant wave pattern constant. This variation of angle with frequency is shown in Figure 1.

The facility to vary the mode pattern was only applied across the width of the duct, the vertical pressure pattern remaining constant. That is the (n,0) modes were used where n = 0, 1, 2, 3, 4.

The theoretical mode patterns are illustrated in Figures 2, 3, 4 and 5 together with the measured values obtained across the duct at several frequencies. The root mean square pressure values are plotted in dB, phase correction being shown by the broken line. The vertical pressure pattern and that of the (0,0) mode were flat to within $\pm\frac{1}{2}$dB below 2000 Hz.

It will be noted that the minima in the pressure plots are not absolutely zero, due to the presence of other modes. It was verified that the contribution to the transmission loss curves by these spurious modes was negligible. In Figure 6 the (0,0) and (1,0) transmission loss curves are plotted and it can be seen that at 400 Hz there is a dip in the (0,0) mode. The (0,0) mode was found (Figure 2) to be at a level of 66 dB in the presence of the (1,0) mode excited at 100 dB.

From the transmission graph (full line) for the pure (0,0) mode the loss at 400 Hz should be 28 dB reducing the 66 dB level of the (0,0) mode to 38 dB. The nett transmitted sound level was 53 dB. Thus the predicted contribution of 38 dB from the (0,0) mode may be neglected assuming negligible coupling between modes.

In general the transmission loss recorded for each mode will be representative for that mode if the measured separation between the (0,0) and the (n,0) loss curves is less, by 10 dB or more, than the difference between the maximum and minimum pressures of the (n,0) modal pressure pattern.

The evidence for coupling between the duct modes and the flexural standing modes in the test panels is inconclusive. For example, when the (0,0) plane wave mode is used with the 12 mm resin bonded chip board panel, (Figure 7), the expected resonance at 100 Hz for the (1,1) panel mode is evident by a dip in the isolation curve. However, anomalous dips in this curve also occur at 400 Hz and 900 Hz corresponding to the (2,2) and (3,3) modes of the panel.

Also anisotropic panels were used to see if the modal transmission varied with their relative orientation. A material used is illustrated in Figure 8. This consisted of 40 mm thick resin-bonded chip board faced with veneer and pierced with 25 mm diameter holes set in one direction, the holes being regularly spaced at 32 mm between centres.

The transmissions were measured with holes "running" vertically and then horizontally, the modal pressure pattern variation always being only across the width of the duct, i.e. (n,0) modes. With plane waves (0,0) the isolation was virtually the same for both orientations at all frequencies. However with the (1,0), (2,0), (3,0) and (4,0) modes it can be seen from Figure 9 that no consistent isolation trends can be demonstrated.

The special case of the "Coincidence Effect"

For free space the conventional "coincidence effect" occurs only when the projected wave length of the incident sound wave and the panels' flexural wave length are equal at the same frequency, (f.), i.e.

$$\lambda_b = \frac{\lambda_a}{\sin \theta}$$

$\lambda_a$ = air wave length

$\lambda_b$ = flexural wave length in panel

This condition also implies,

$$C_b = \frac{C_a}{\sin \theta}$$

where $C_a$ = speed of sound in air

$C_b$ = speed of flexural waves in the panel

Since $\lambda_a \propto \frac{1}{f}$ and for a given panel $\lambda_b \propto \frac{1}{\sqrt{f}}$, it follows that the coincidence condition, $\lambda_a = \lambda_b \sin \theta$ can only be satisfied for one angle of incidence at any given frequency. The lower frequency limit, called the "coincidence cut-off frequency" occurs when $\theta = 90°$.

The value of wave length of the flexural waves is given by

$$\lambda_b = \sqrt{(1.8h \sqrt{\frac{E}{\rho}})} \cdot \sqrt{\frac{1}{f}} \quad \ldots\ldots (2) \text{ (c.g.s. units)}$$

where h = panel thickness

E = Young's Modulus for the panel material

$\rho$ = density of material

and $\lambda_a = \frac{c_a}{f}$ ..... (3)

In order to solve the coincidence condition a graph is plotted of calculated values of $\left(\frac{\lambda_a}{\sin\theta}\right)$ against (frequency)$^{-i}$ for a wide range of values of $\theta$. These are combined with $\lambda_b$ against (frequency)$^{-\frac{1}{2}}$ curves for appropriate values of the material and panel dimensions (Fig.10).

The two sets of curves limit the region in which coincidence may occur. Thus coincidence cannot occur for frequencies to the right of the 90° curve and the point where this curve cuts any particular $\lambda_b$ line (Equation 2) is the "coincidence cut-off frequency".

By way of illustration consider Figure 10 for which the curve for 12 mm thick glass has its "coincidence cut-off frequency" at point Y. The coincidence condition will be satisfied along YX as frequency, f, and angle, $\theta$, are varied.

When excited by the air waves in the duct, trains of flexural waves moving in opposite directions in the plane of the panel can give rise to a standing wave system. The appropriate condition occurs when the breadth of the panel is equal to $\frac{n}{2}\lambda_b$, where n is an integer, and is referred to as "coincidence resonance".

For the (1,0) mode $\lambda_b$ = 60 cm,

(2,0) $\lambda_b$ = 30 cm,

(3,0) $\lambda_b$ = 20 cm,

(4,0) $\lambda_b$ = 15 cm etc.

These conditions are included on Figure 11 as horizontal lines superimposed on the previous conditions for coincidence for a travelling wave (Fig.10). Thus the generality of obtaining coincidence for various frequencies and angles is now eliminated. Only special cases will be allowable where the three sets of curves intersect. This occurs for

($\lambda$= 15 cm) at about 1250 Hz. should occur with the 'equivalent' angle of incidence at 70°.

Figure 12 shows the measured transmission curve for normal coincidence (solid line) and the (4,0) air mode (broken line). This coincidence is seen to occur at about 1250 Hz. as predicted. Also this particular feature does involve correlation between the velocities in the (4,0) duct and panel modes.

Low Frequencies

The duct is well suited to experiments down to 20 Hz. when sound pressures of 90 dB can be obtained. Below 300 Hz, only the plane wave (0,0) is excited and this will be very pure. The fundamental panel resonances to be studied usually exist within this frequency range.

The use of continuously variable pure sine tones

The use of single sine wave tones rather than one third octave bands of noise is of particular value when the effects of minor panel modifications are to be investigated. An added advantage of the duct technique is that it is possible to make a change of frequency and yet to maintain a particular air mode pattern. Hence any small yet possibly significant departure of the experimental transmission curve from a smooth line may be carefully studied, whereas such deviations could lose their full significance in third octave analysis. It follows that sharp panel resonances, which are often associated with selective frequency transmissions, can be located and investigated.

In Figure 13 a comparison is made between the results obtained using third octave noise analysis and the results obtained using pure sine wave tone excitation for a plate with and without damping. It can be seen that the considerable improvements accruing from damping are not fully revealed when third octave bands of noise are used.

Resonant frequency location

The effect of mounting conditions was investigated and Figure 14 shows the transmission loss through a 3 mm steel plate, firstly mounted flexibly on a soft mastic to provide an adhesive seal, and then rigidly mounted with screws. Again the discrimination inherent with pure sine tone analysis facilitated easy detection of the shift of the (1,1) panel resonance from 58 Hz. to 70 Hz. resulting from the stiffening of the plate system. The (2,2) resonance has shifted from 240 Hz to 250 Hz,

indicating that the particular mounting employed has a greater percentage effect on the lower fundamental mode.

Discussion of some experimental results

A number of single and double panel transmission features have been studied and some of these are presented to illustrate the application of the duct technique.

1. Panel Damping: In Figure 15 the isolation of a 3 mm steel plate is presented, before damping treatment (upper curve) and after damping treatment. The damping consisted of wet mastic distributed over about 25% of the area as lines and discs. A thin aluminium plate was pressed firmly on to the mastic, to act as a shear reference plane.

The damping effect is most marked at the (1,1) and (2,2) mode resonances of the plate and the smoother damped curve has a slope of about 7 dB/octave.

2. Double Panels with Thin Air Gaps: As a forerunner to tests on plastic interlayered glass (i.e. safety glass) and on vacuum separated panels, some comparison tests were carried out on double glass panels separated by thin air gaps.

Apart from the panel mode resonances, to be associated with each individual panel, there will be an extra coupling resonance across the enclosed air space. The two panes with surface mass $m_1$ and $m_2$ form, together with the air space of thickness h, a system with characteristic resonance frequency $f_m$, which is given by equation 4:-

$$f_m = \frac{1}{2\pi} \sqrt{\left(\frac{\rho c^2}{h}\right) \cdot \left(\frac{m_1 + m_2}{m_1 - m_2}\right)} \qquad (4)$$

In Figure 16 are plotted the transmission curves for two sheets of 3 mm thick glass initially separated by 0.3 mms (full curve) and then by 0.6 mm (dotted curve). The calculated values of the "air spring resonance" are 1600 Hz. and 1120 Hz. respectively for the 0.3 mm and 0.6 mm air gaps. These resonances are indicated on the transmission graph as dips at 1550 Hz. and 1200 Hz.

It is also to be noted on this Figure 16 that the (1,1) mode and (2,2) mode resonances at about 50 Hz. and 200 Hz. (1:4) are not affected, and

the repeatability when remounting the same type of panel is very good.

In Figure 17 the compound glass - air - glass panel (0.3 mm air gap) used alone is compared with solid 6 mm thick glass. The air gap resonance at 1550 Hz. is of course no longer apparent for the 6 mm thick glass, and the (1,1) and (2,2) mode resonances occur at higher frequencies. However, the overall isolation, apart from these resonances, is very similar for the two cases.

In Figure 18 the two panes are of different thicknesses, 4 mm and 3 mm, with an air space of 0.3 mm (dotted curve) and this trace is compared with the double 3mm/0.3 mm panel used in the above graphs (15) and (16). The strong (1,1) and (2,2) resonances of the two panes are now different and the combined effect is to smooth out the corresponding resonances, especially the (2,2) mode. The air space resonance for the thicker pane combination is reduced to a lower frequency due to the increased surface mass of the glass.

3. Double Plastic Sheet: A compound panel of two thin ($20 \times 10^{-3}$ cm) plastic sheets separated by 15 cm was investigated filled with air, and filled with hydrogen at atmospheric pressure. The results are shown in Figure 19.

A simple calculation of the air gap resonance showed a significant disparity with the observed value and this effect is receiving further investigation. The respective resonance values were, observed 1300 Hz. and predicted 1100 Hz., for a 15 cm air gap. On substituting hydrogen for air the resonance (4500 Hz.) moved beyond the experimental range.

At about 350 Hz. the impedance of the plastic sheet and that of the air are equal. Above this frequency each sheet impedance should be seen to obey the "mass law", i.e. transmission loss doubles with each octave increase in frequency. It follows that the two sheets should yield a combined increase in transmission loss of 12 dB per octave about 350 Hz. This deduction is followed by the observations on the hydrogen filled panel up to 1600 Hz.

4. Air-edge Damping for 15 cm Double Steel Panel: A compound double panel was constructed of two 3 mm thick steel plates separated by 15 cm of air. The transmission through this panel was measured without and with air-edge damping. This damping was supplied by 6 cm of fibre-glass. The results are shown in Figure 20 where a large damping occurs i

in the region 160 Hz. to 400 Hz. The height-width resonance of the enclosed chamber, corresponding to a half wave length resonance of 60 cms, will occur at about 280 Hz. within this damped region. Also an increase in insulation is to be noted in the 400 Hz. to 1200 Hz. region.

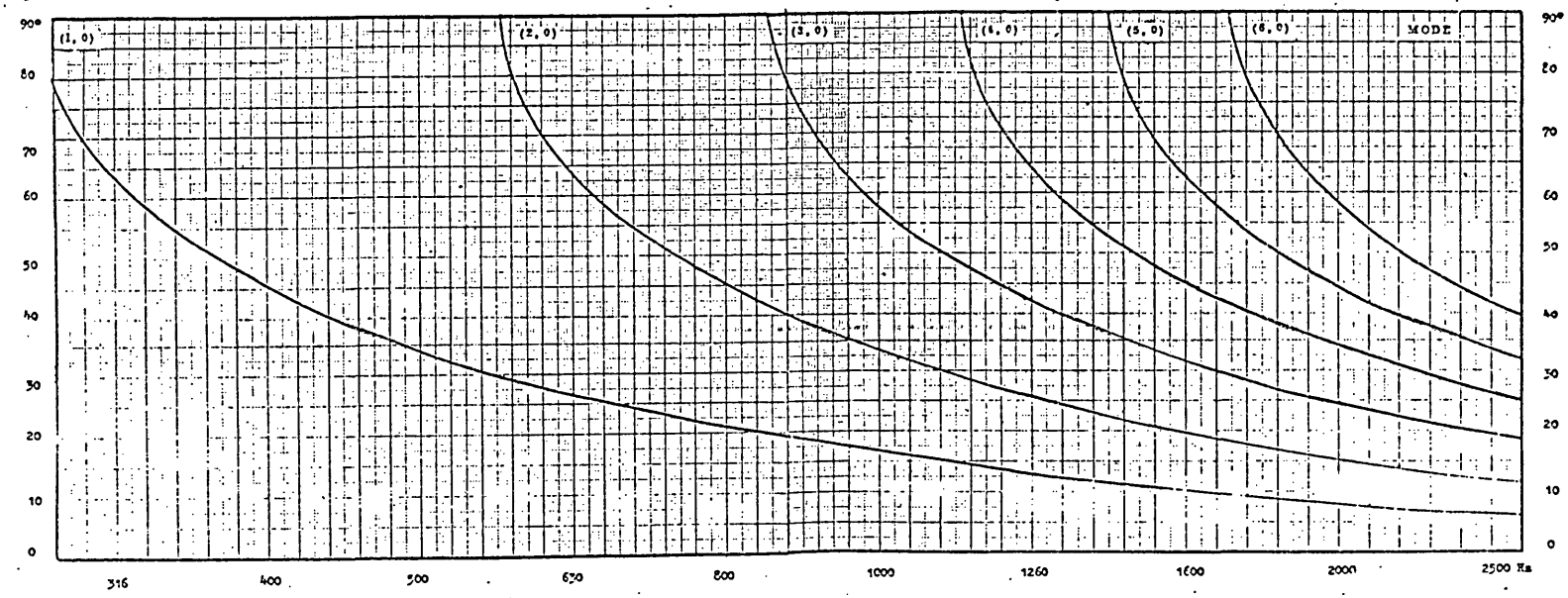
## CONCLUSION

Evidence has been given to confirm that the duct technique can be used as a useful tool for panel transmission studies. It is hoped to correlate these measurements with those performed on large panels by more conventional methods.

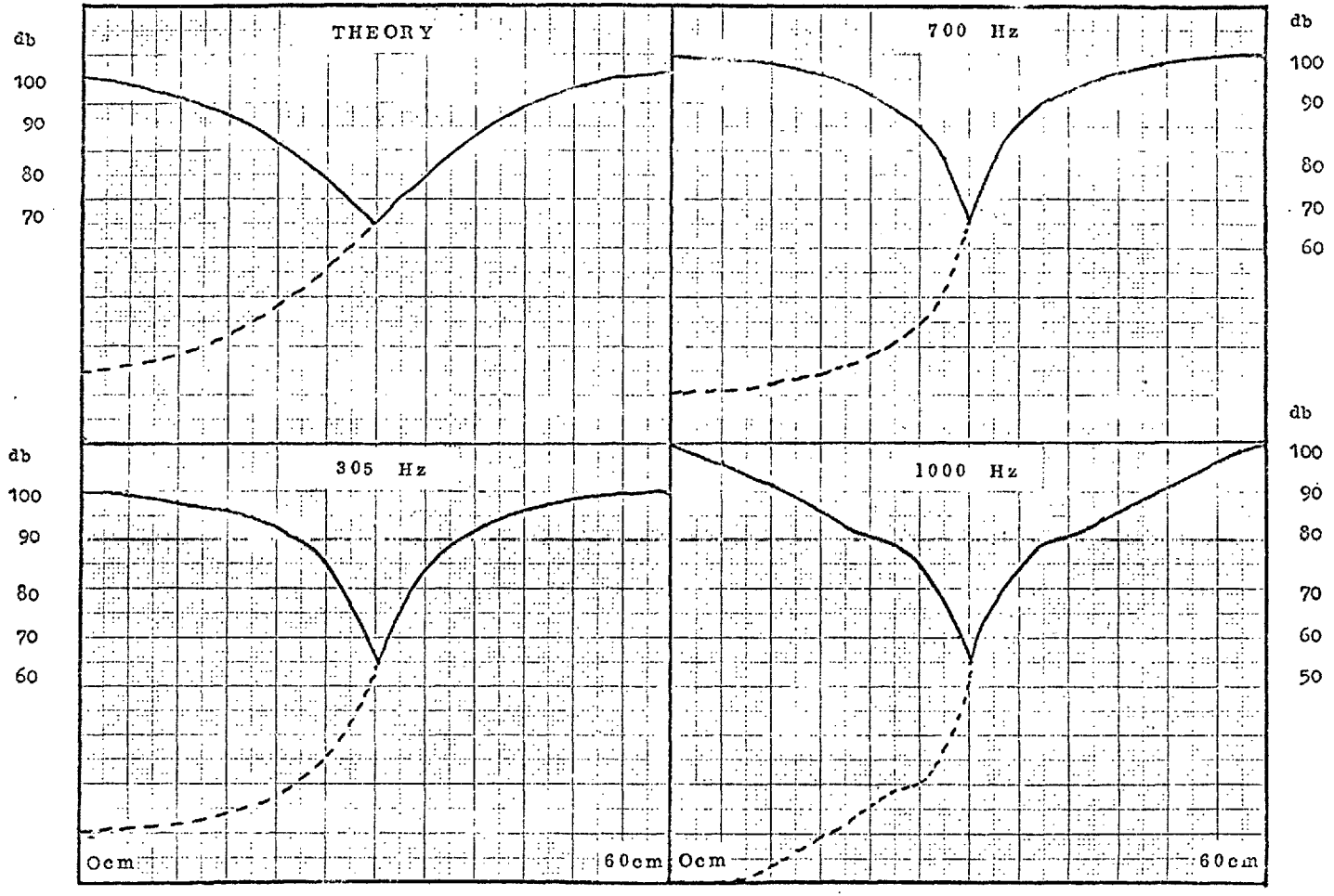
It is hoped that these papers have also provided basis for future workers in this field.

A.FRY, P.FRYER, R.STEPHENS(Imperial College - London)

FIG. 1 FREQUENCY/ANGLE VARIATION FOR MODES

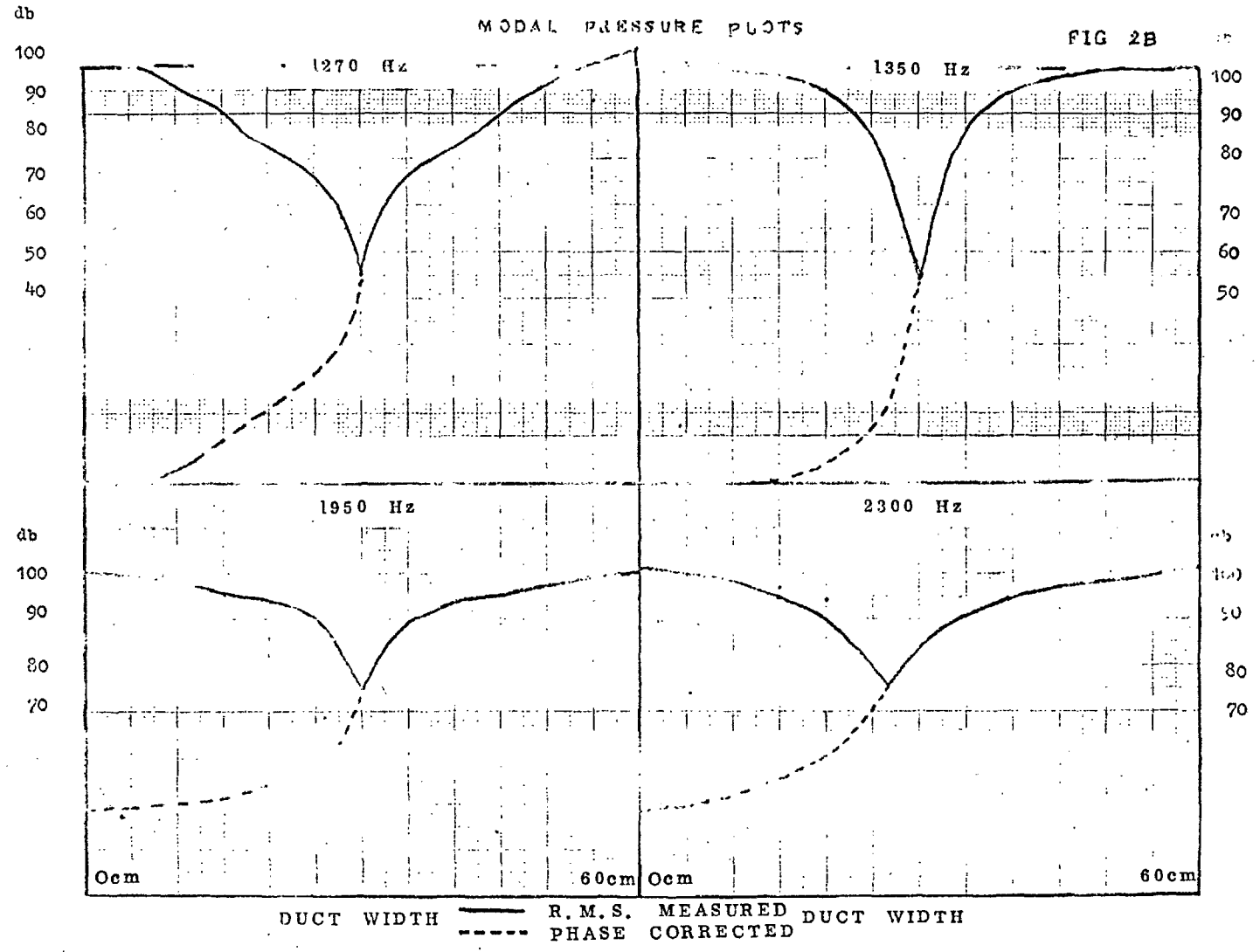


MODAL PRESSURE PLOTS FIG. 2 A



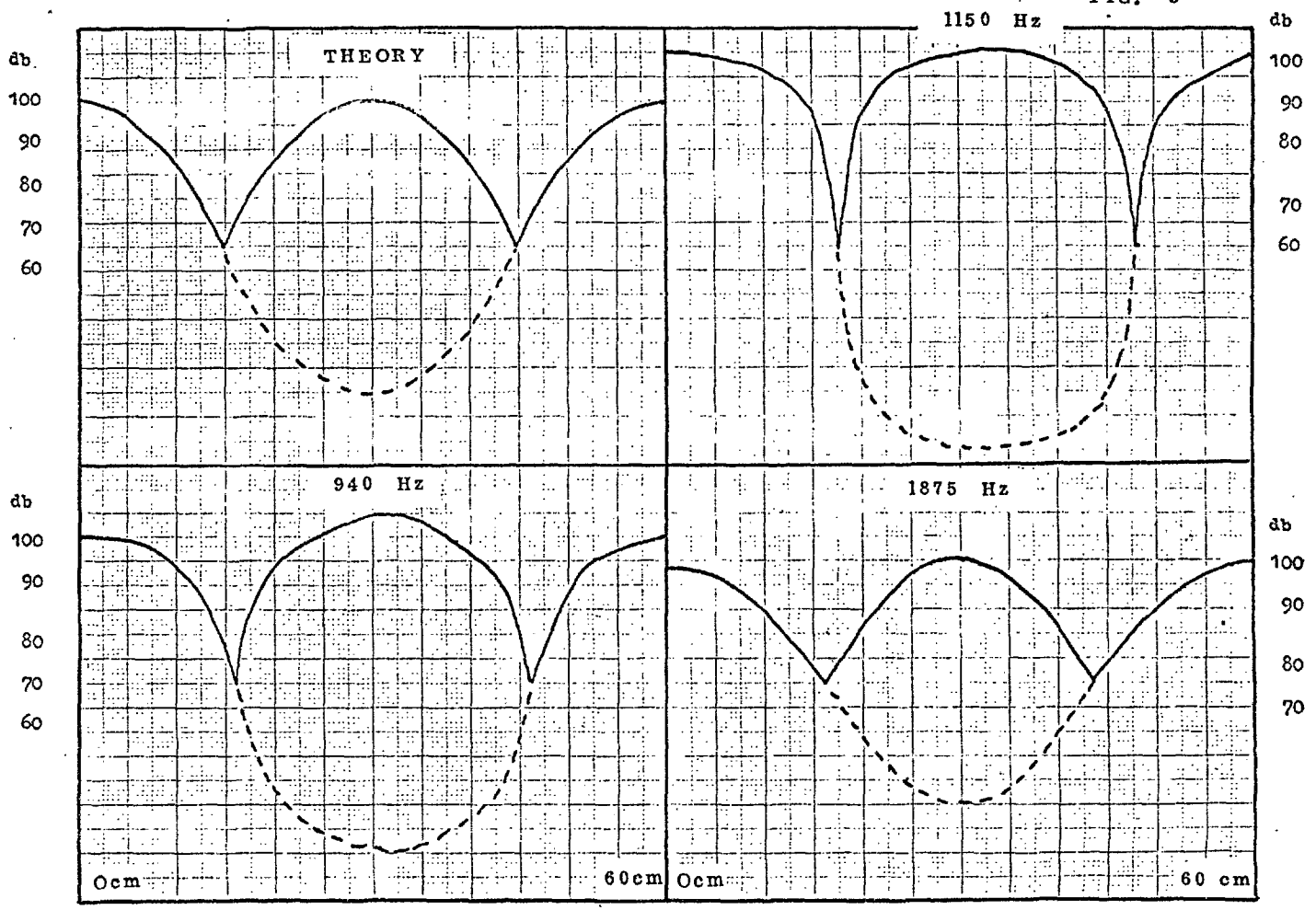

DUCT WIDTH —— R.M.S. MEASURED DUCT WIDTH

- - - - - PHASE CORRECTED


MODAL PRESSURE PLOTS
FIG 2B
db
1270 Hz
1350 Hz
1950 Hz
2300 Hz
100
90
80
70
60
50
40
Ocm
60cm
DUCT WIDTH
R.M.S. MEASURED
PHASE CORRECTED

MODAL PRESSURE PLOTS

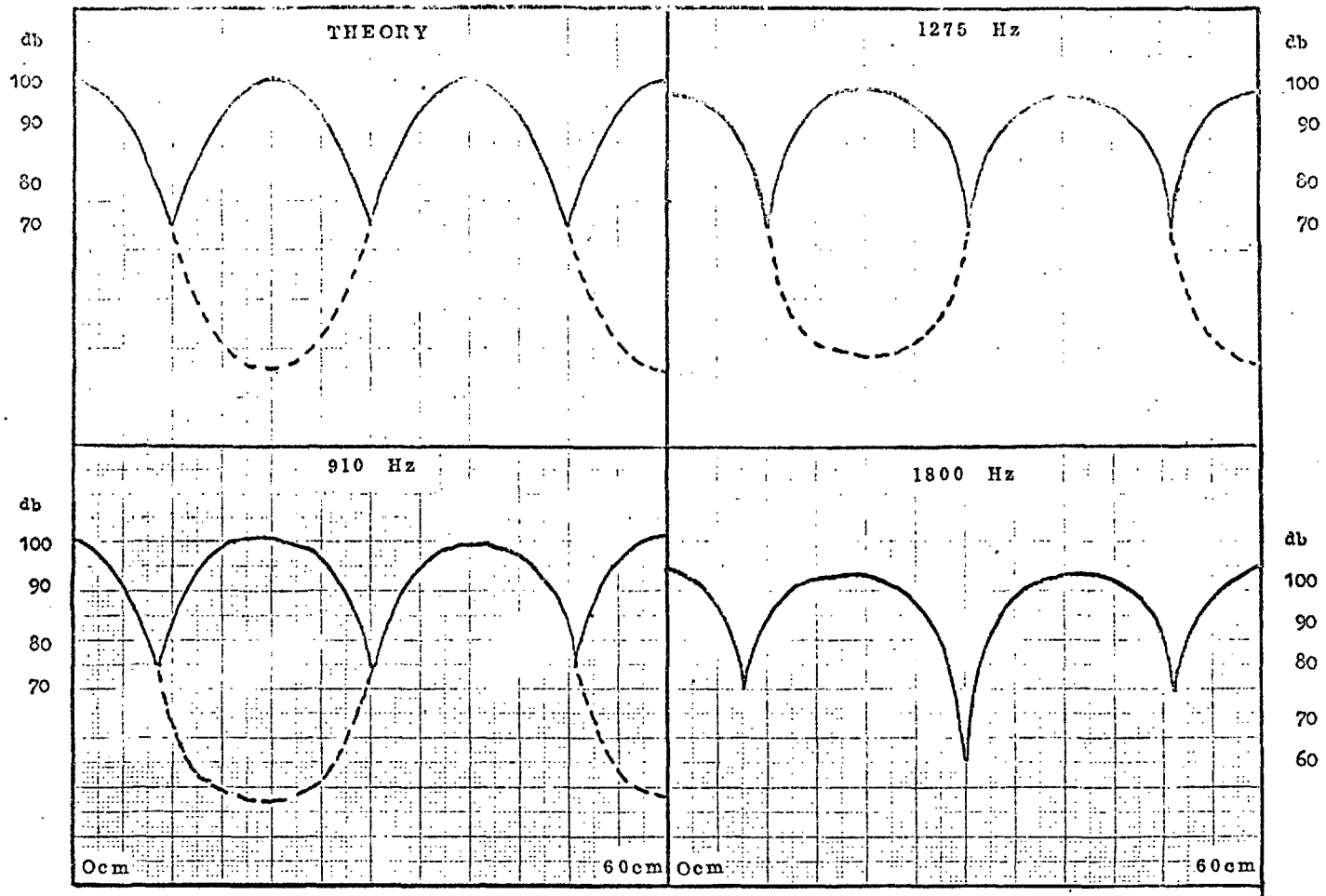
FIG. 3




DUCT WIDTH —— R.M.S. MEASURED DUCT WIDTH

- - - - - PHASE CORRECTED

MODAL PRESSURE PLOTS FIG. 4

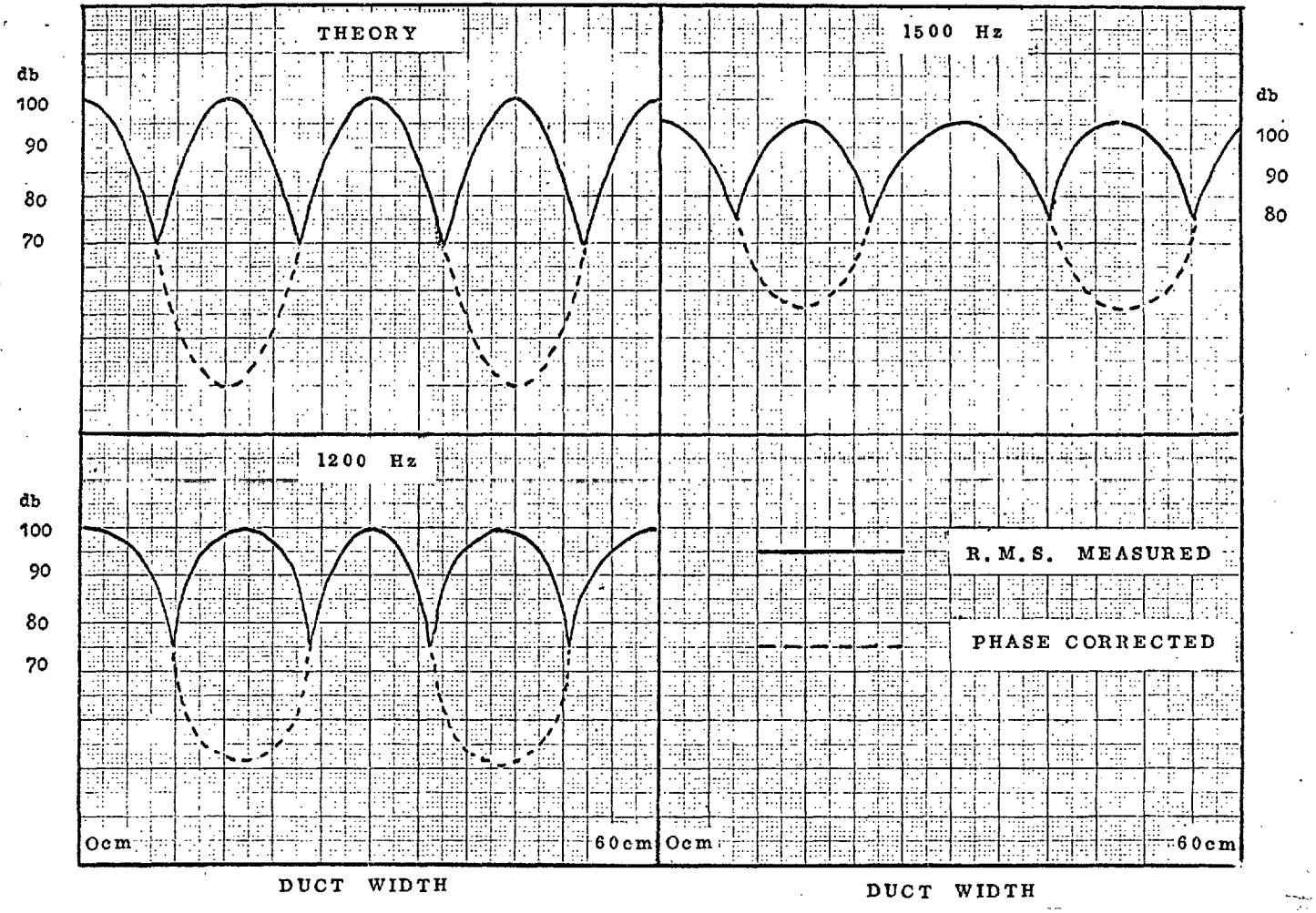


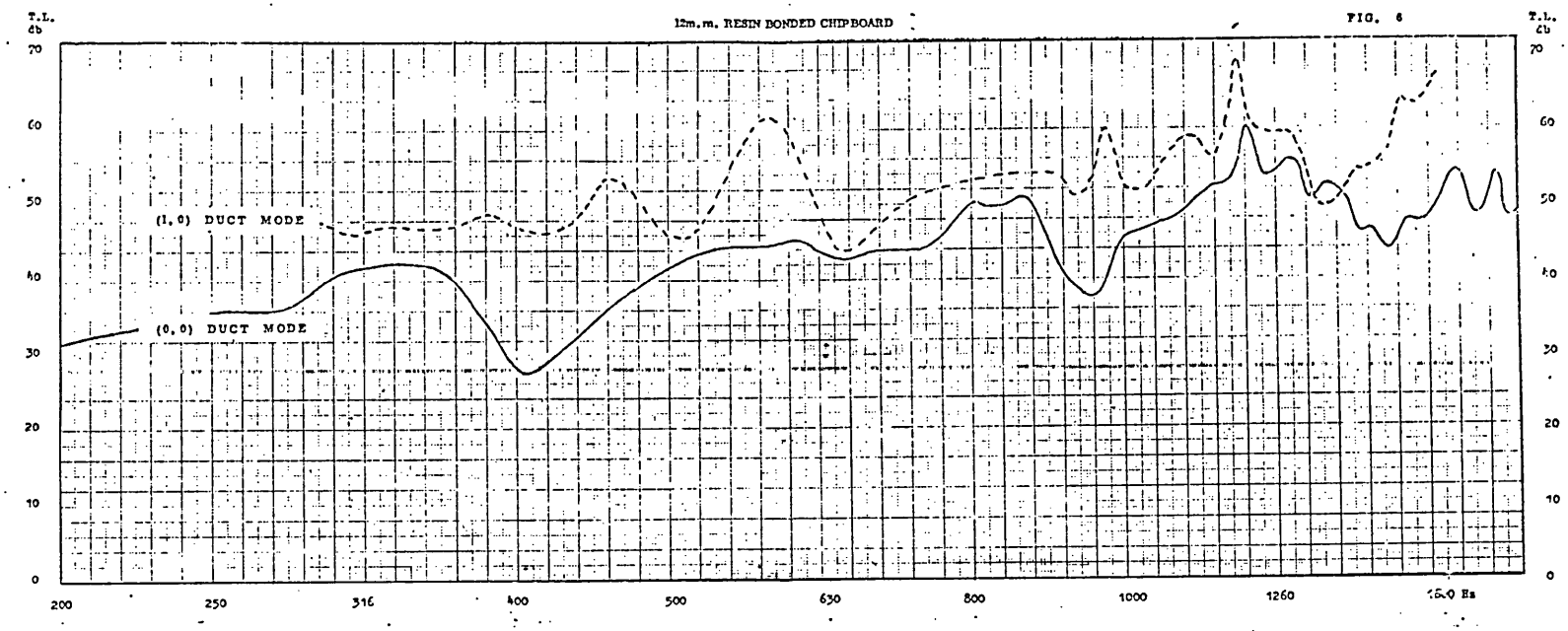

DUCT WIDTH —— R.M.S. MEASURED DUCT WIDTH

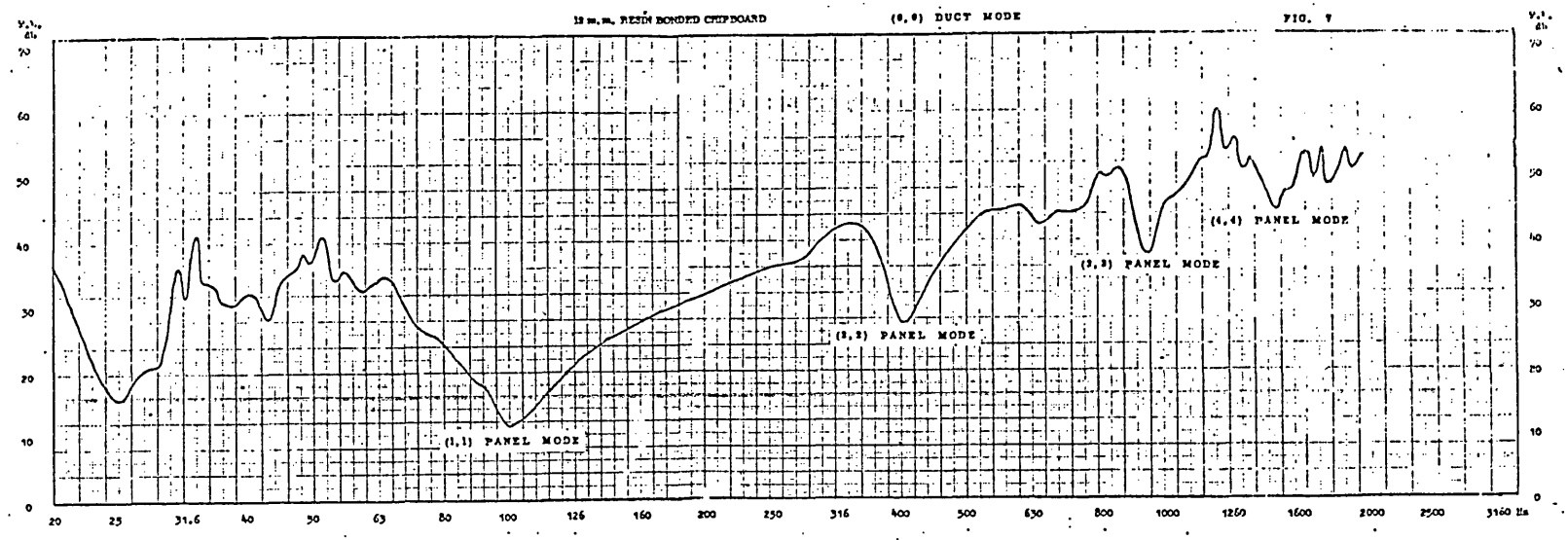
----- PHASE CORRECTED

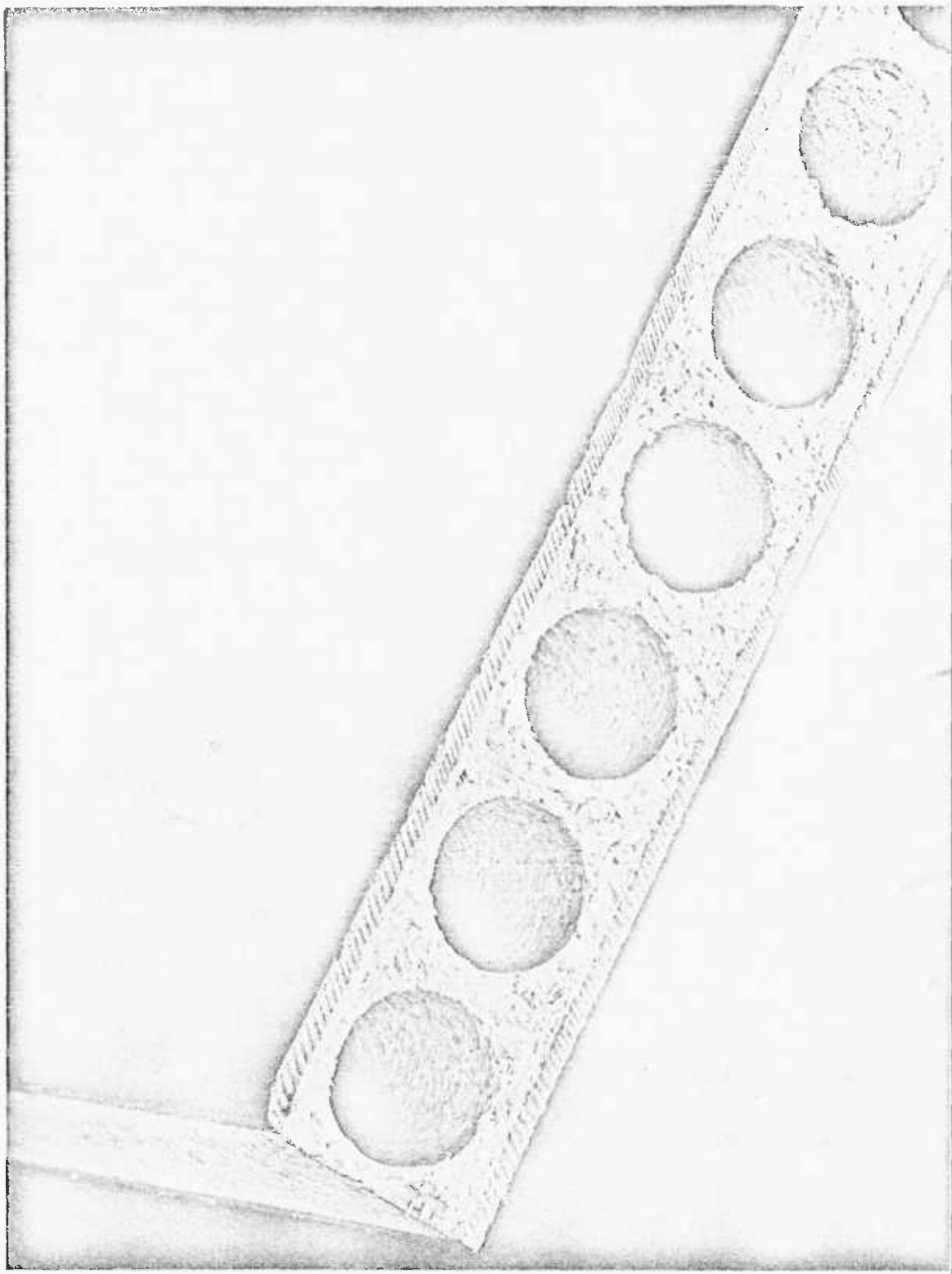
MODAL PRESSURE PLOTS

FIG. 5




12m.m. RESIN BONDED CHIPBOARD
FIG. 6
T.L. db
70
60
50
40
30
20
10
0
(1, 0) DUCT MODE
(0, 0) DUCT MODE
200
250
316
400
500
630
800
1000
1260
1600 Hz


12 m.m. RESIN BONDED CHIPBOARD
(0, 0) DUCT MODE
FIG. 9
(1, 1) PANEL MODE
(2, 2) PANEL MODE
(3, 3) PANEL MODE
(4, 4) PANEL MODE
0
10
20
30
40
50
60
70
20
25
31.5
40
50
63
80
100
125
160
200
250
315
400
500
630
800
1000
1250
1600
2000
2500
3150 Hz



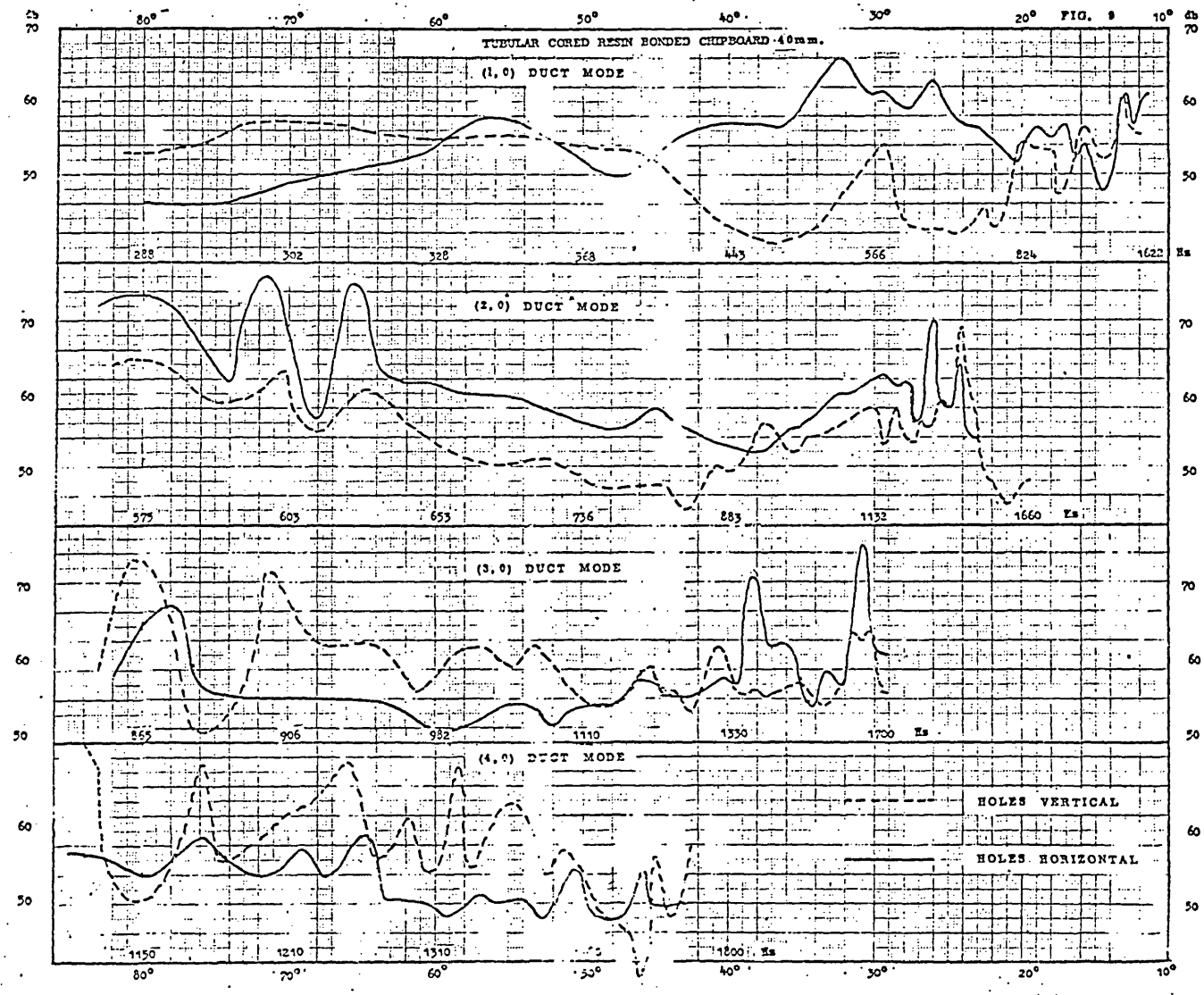
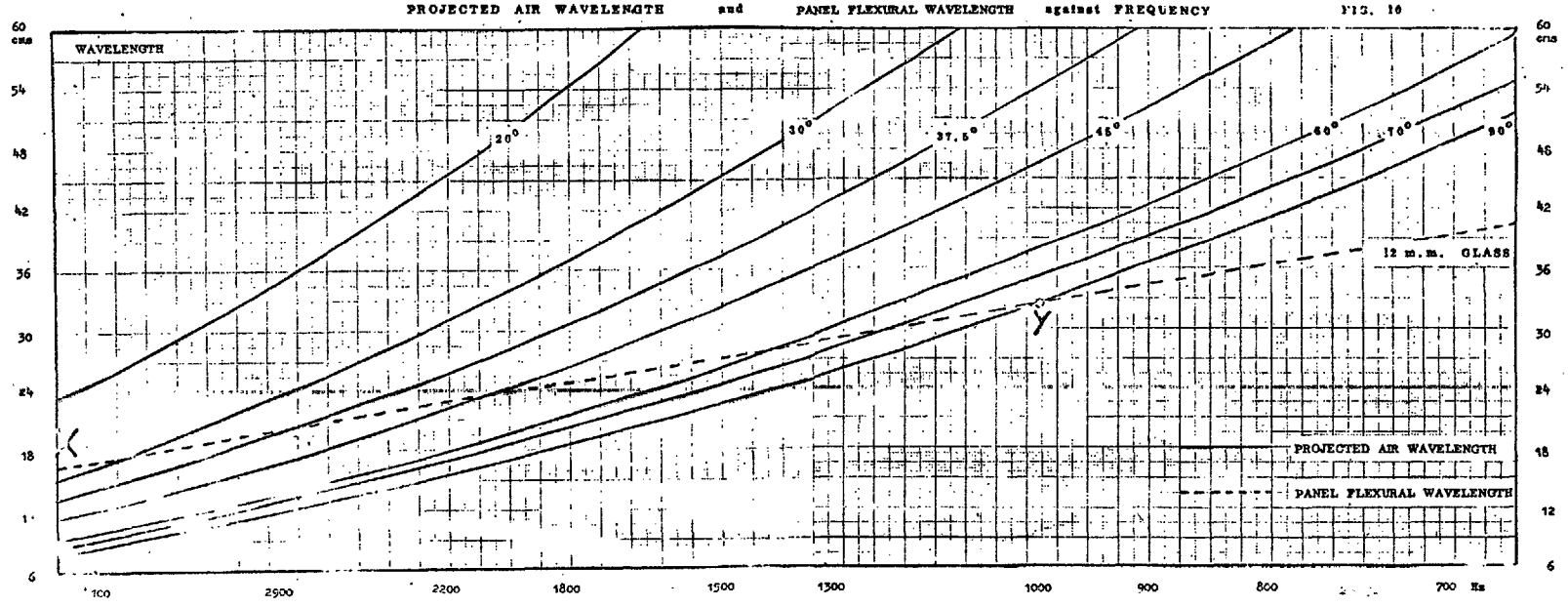

TUBULAR CORED RESIN BONDED CHIPBOARD 40mm.
(1, 0) DUCT MODE
(2, 0) DUCT MODE
(3, 0) DUCT MODE
(4, 0) DUCT MODE
HOLES VERTICAL
HOLES HORIZONTAL
db
Hz

FIG. 9

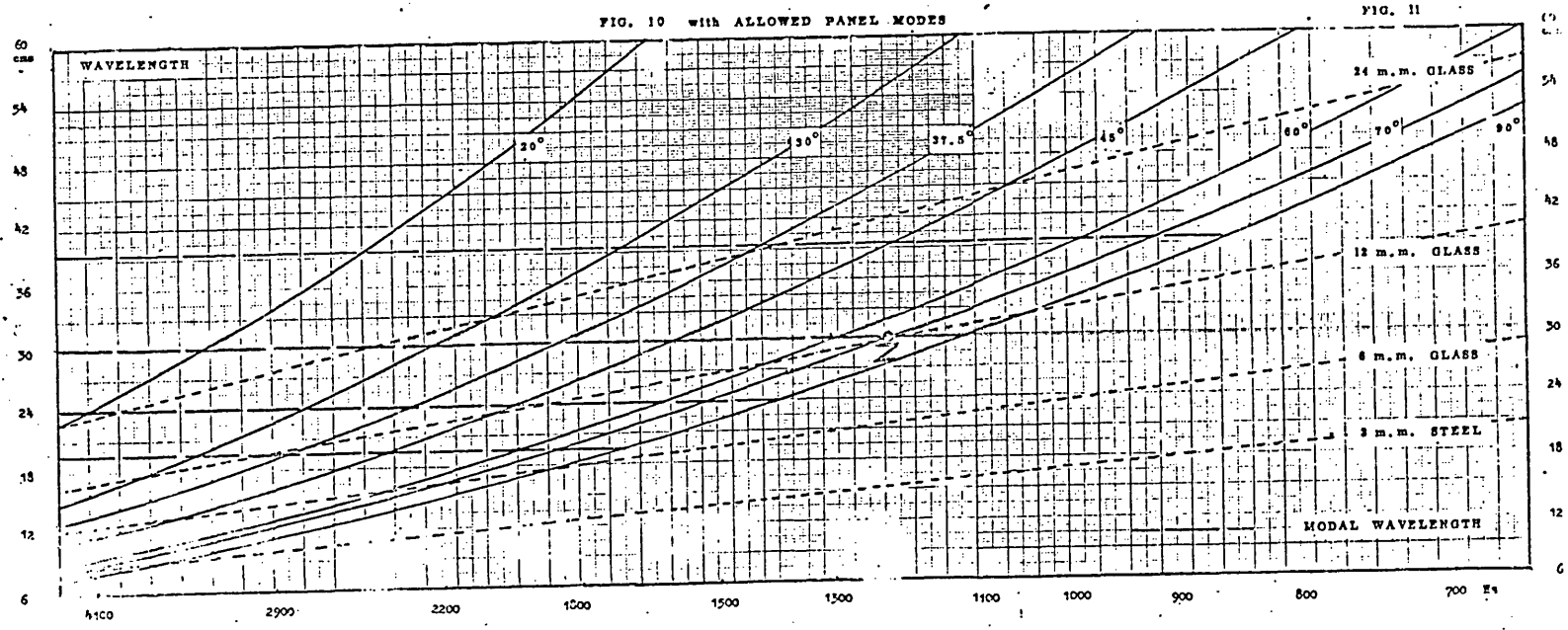
PROJECTED AIR WAVELENGTH and PANEL FLEXURAL WAVELENGTH against FREQUENCY FIG. 10




$\frac{1}{\sqrt{f}}$ scale factor

FIG. 10 with ALLOWED PANEL MODES

FIG. 11

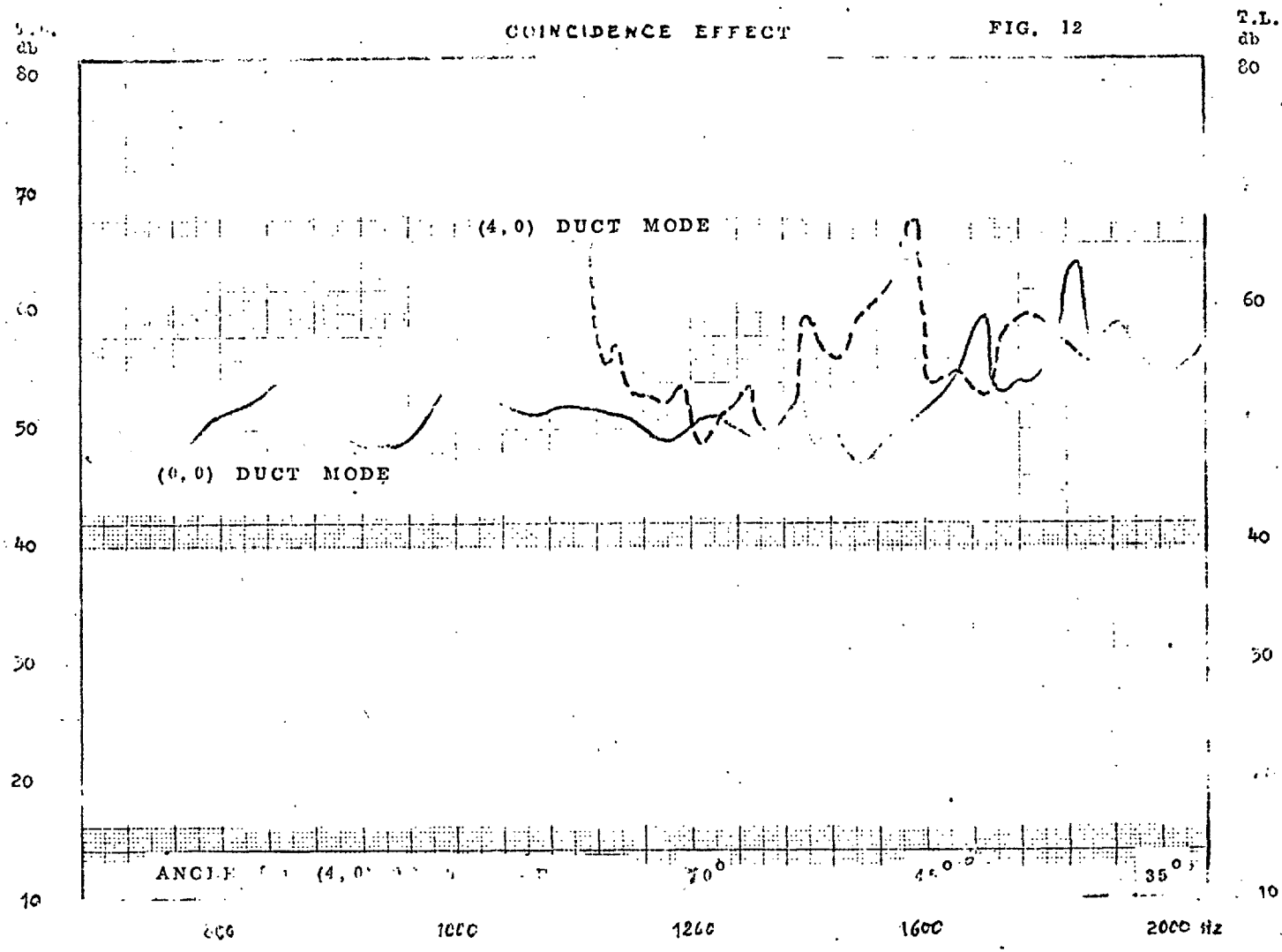



(3,0)

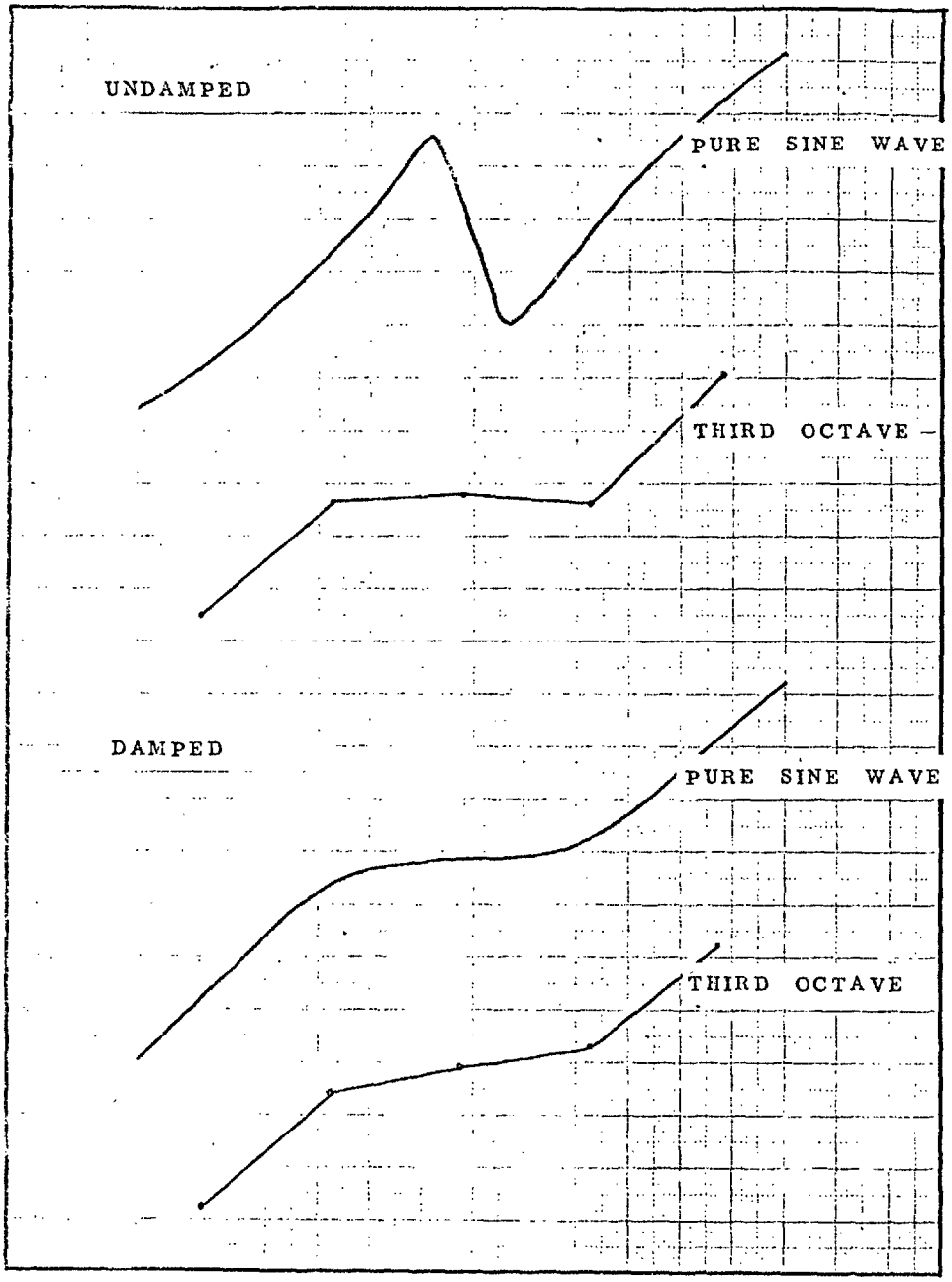
(3,0)

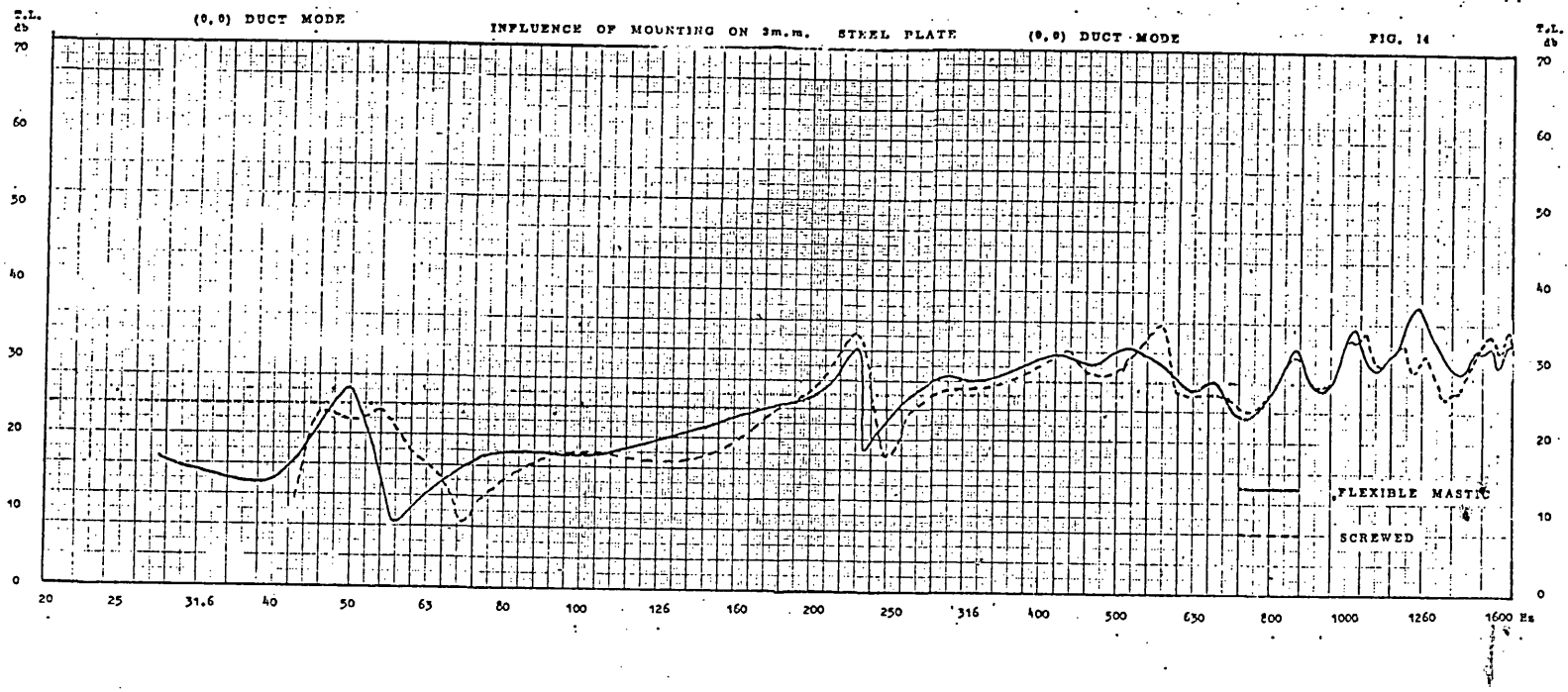
(4,0)

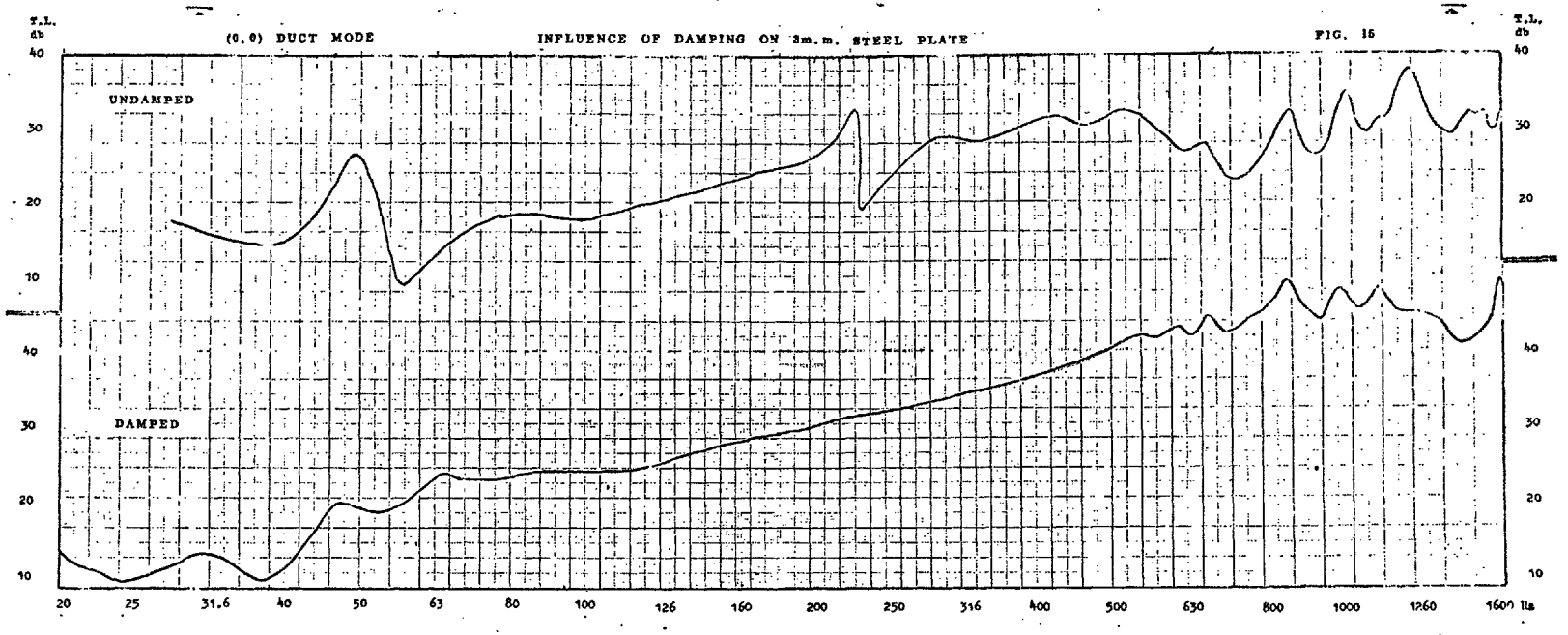
COINCIDENCE EFFECT FIG. 12

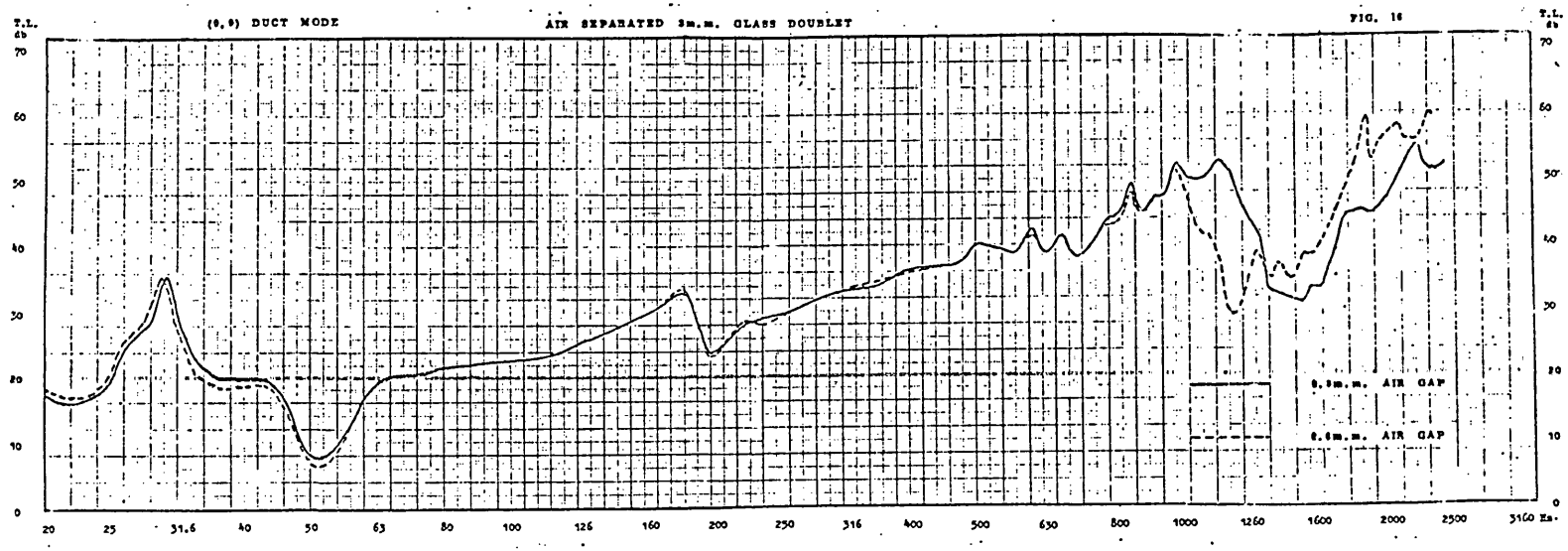


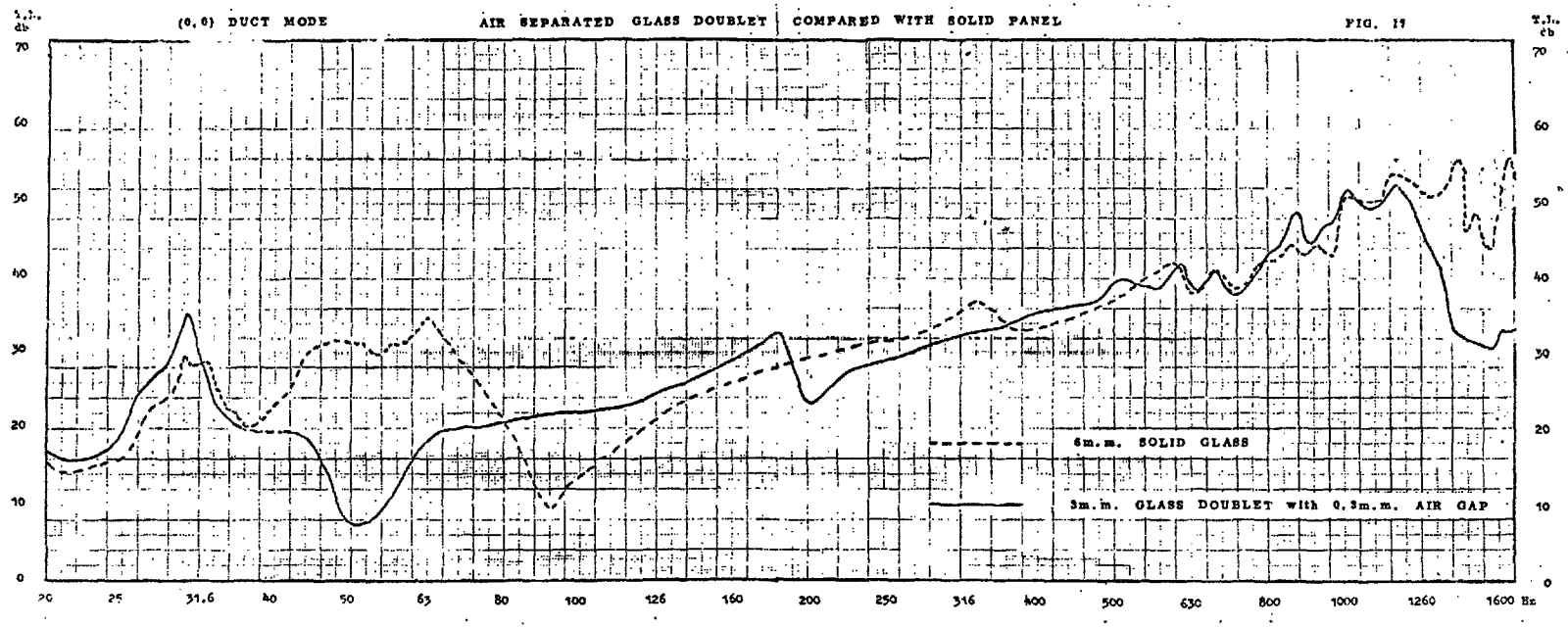
COMPARISON OF PURE SINE WAVE AND THIRD OCTAVE TECHNIQUE FIG. 13

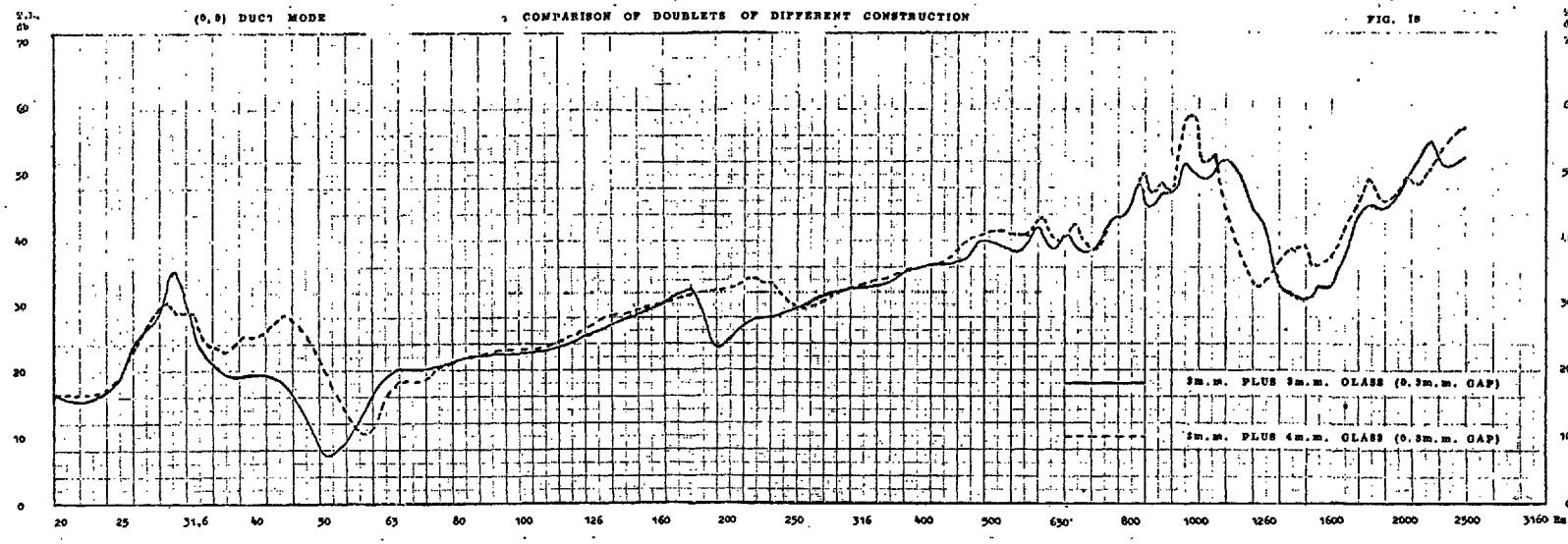


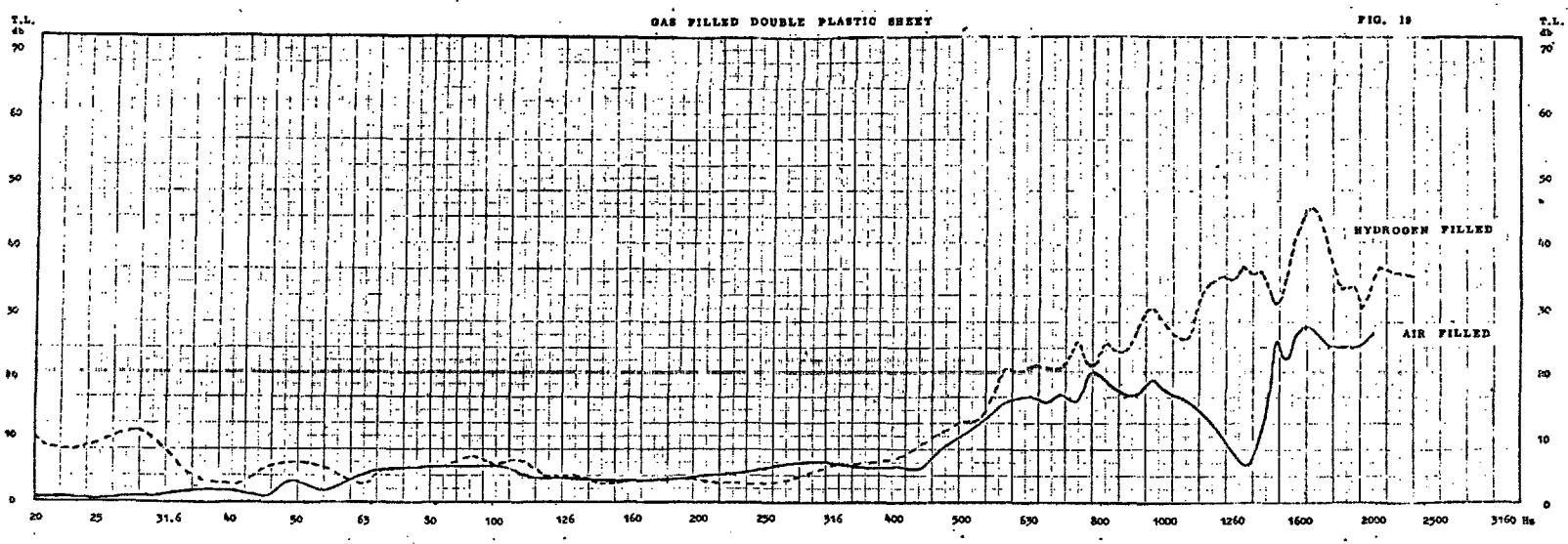

T.L. db
(0,0) DUCT MODE
INFLUENCE OF MOUNTING ON 3m.m. STEEL PLATE
(0,0) DUCT MODE
FIG. 14
70
60
50
40
30
20
10
0
20
25
31.6
40
50
63
80
100
126
160
200
250
316
400
500
630
800
1000
1260
1600 Hz
FLEXIBLE MASTIC
SCREWED

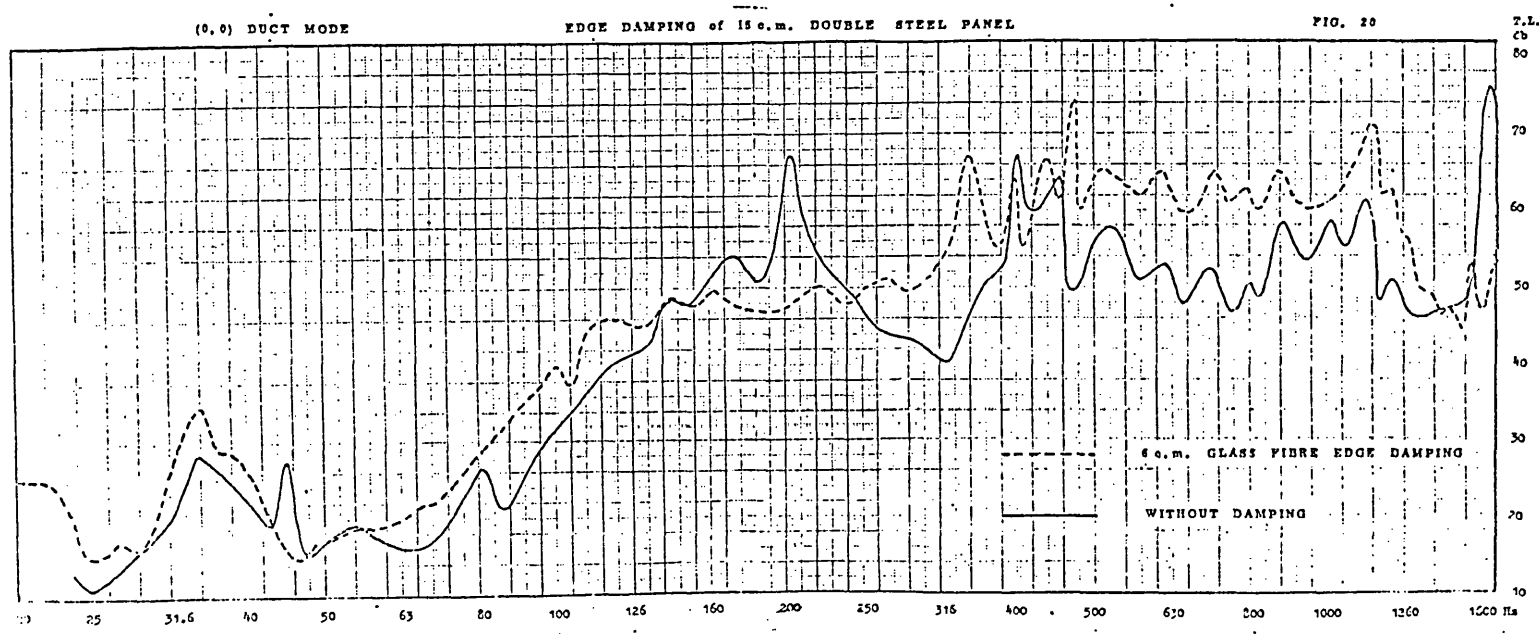

T.L. db
(0, 0) DUCT MODE
INFLUENCE OF DAMPING ON 3m.m. STEEL PLATE
FIG. 16
UNDAMPED
DAMPED
40
30
20
10
20
25
31.6
40
50
63
80
100
126
160
200
250
316
400
500
630
800
1000
1260
1600 lls


(0,0) DUCT MODE
AIR SEPARATED 3m.m. GLASS DOUBLET
FIG. 16
T.L. db
70
60
50
40
30
20
10
0
20
25
31.5
40
50
63
80
100
125
160
200
250
315
400
500
630
800
1000
1250
1600
2000
2500
3150 Hz.
3.3m.m. AIR GAP
6.6m.m. AIR GAP


(0,0) DUCT MODE
AIR SEPARATED GLASS DOUBLET COMPARED WITH SOLID PANEL
FIG. 17
T.L. db
70
60
50
40
30
20
10
0
20
25
31.6
40
50
63
80
100
125
160
200
250
316
400
500
630
800
1000
1250
1600 Hz
6m.m. SOLID GLASS
3m.m. GLASS DOUBLET with 0.3m.m. AIR GAP


S.I. db
(0, 0) DUCT MODE
COMPARISON OF DOUBLETS OF DIFFERENT CONSTRUCTION
FIG. 18
70
60
50
40
30
20
10
0
20
25
31.5
40
50
63
80
100
125
160
200
250
315
400
500
630
800
1000
1250
1600
2000
2500
3150 Hz
3m.m. PLUS 3m.m. GLASS (0.3m.m. GAP)
3m.m. PLUS 4m.m. GLASS (0.3m.m. GAP)


GAS FILLED DOUBLE PLASTIC SHEET
FIG. 18
T.L. db
HYDROGEN FILLED
AIR FILLED
20
25
31.5
40
50
63
80
100
125
160
200
250
315
400
500
630
800
1000
1250
1600
2000
2500
3150 Hz


(0, 0) DUCT MODE
EDGE DAMPING of 15 c.m. DOUBLE STEEL PANEL
FIG. 20
T.L.
Cb
80
70
60
50
40
30
20
10
6 c.m. GLASS FIBRE EDGE DAMPING
WITHOUT DAMPING
25
31.5
40
50
63
80
100
126
160
200
250
315
400
500
630
800
1000
1260
1600 Hz